



MONASH University

Millennial Perspectives on Tropical Climate Variability from the Last Glacial through to the Holocene: a palaeoecological analysis from Lynch's Crater, northeast Queensland, Australia.

Susan Rule

A thesis submitted for the degree of *Doctor of Philosophy* at

Monash University in 2020

School of Earth, Atmosphere and Environment

Faculty of Science

Copyright notice

© Susan Rule (2020).

I certify that I have made all reasonable efforts to secure copyright permissions for third-party content included in this thesis and have not knowingly added copyright content to my work without the owner's permission.

Abstract

The terrestrial sedimentary sequence from Lynch's Crater provides a key record of late-Quaternary environmental change in tropical north-east Queensland and the Southern Hemisphere more generally. The long palynological record extending back to 230,000 years ago provides the contextual vegetation history for the present study by providing a baseline of the vegetation patterns and likely climatic conditions prior and up to ~54 ka, the starting point of this study. Importantly, the resolution of the full record is relatively coarse, limiting the level of detail and interpretation that can be undertaken. This is of concern particularly for the last 50,000 years, a critical time-period likely covering the arrival and period of occupation of Aboriginal people within the study site region. The present study uses a high resolution, multi-proxy approach supported by intensive radiocarbon dating to provide a comprehensive analysis of local and regional scale changes within the environment. This multi-proxy approach has allowed better understanding of the local environment through the inclusion of plant macrofossils often allowing for identification to species level and confirming that generally inorganic phases were indicative of wetter conditions with the proliferation of aquatic hydrophytes (pollen and macrofossils) at these times. This analysis has been complemented by the availability of more precise dating, allowing the calculation of pollen influx, which provides insight on changes in vegetation density through time but also changes in local catchment processes.

Spectral analysis has identified millennial and notably, semi-precessional cycles in the record, consistent with previous work at Lynch's Crater. This study reports an assessment of the sometimes-conflicting conclusions of conditions present during North Atlantic iceberg-rafting Heinrich events (H-events), which has allowed the revision of the nature and timing of millennial-scale events in tropical northeast Queensland. Through the Last Glacial Maximum, there is strong evidence of extreme environmental variability, with a discrete event centred on 20 ka suggesting a previously unidentified period of warm and wet conditions. Complementing the above, comprehensive charcoal analysis of both microscopic and macroscopic fragments, enabled the identification of changes in fire type and origin (local and regional). This is especially significant from 32 ka through to 28 ka when both elevated inorganics and increased local fire activity are indicated. These results suggest that fire was used to manipulate the vegetation for the purpose of attracting remaining large herbivores, i.e. extant kangaroos. Macroscopic charcoal also provides evidence of changing fuel type through the separation of macroscopic charcoal particles into morphological types 'elongated' (herbaceous) and 'blocky' (tree and shrub). This was particularly evident in the middle Holocene (6 ka) when wet conditions were present, and the fuel source changed from herbaceous taxa to tree and shrub taxa on the swamp which could suggest human activity in the landscape. This study demonstrates the value of high-resolution, multi-proxy analyses supported by comprehensive dating to better understand the

interaction of environmental (including landscape) processes and human interactions and should be adopted more widely in the future.

Declaration

This thesis is an original work of my research and contains no material which has been accepted for the award of any other degree or diploma at any university or equivalent institution and that, to the best of my knowledge and belief, this thesis contains no material previously published or written by another person, except where due reference is made in the text of the thesis.

Signature:

Print Name: Susan Rule

Date: 9th September 2020

Publications during enrolment

Turney, CSM, Haberle, S, Fink, D, Kershaw, AP, Barbetti, M, Barrows, T, Black, M, Corregge, T, Hua, Q, Hesse, P, Johnston, R, Moss, P, Morgan, V, Nanson, G, van Ommen, T, Rule, S, William, NJ, Zhao, FX, Cohen, TJ, D'Costa, D, Feng, Y-X, Gagan, M, Mooney, S and Xia, Q (2006). Integration of ice core, marine and terrestrial records for the Australian last glacial maximum and termination: A contribution from the OZ Intimate Group. *Journal of Quaternary Science*, vol 21, Issue 7, pp. 751-761.

Turney, CSM, Kershaw, AP, Lowe, JJ, van der Kaars, S, Johnston, R, Rule, S, Moss, P, Radke, L, Tibby, J, McGlone, MS, Wilmshurst, JM, Vandergoes, MJ, Fitzsimons, SJ, Bryant C, James, S, Branch, NP, Cowley, J, Kalin, RM, Ogle, N, Jacobsen, G & Fifield, LK (2006). Climatic variability in the southwest Pacific during the last Termination (20 – 10 kyr BP). *Quaternary Science Review*, vol. 25, pp. 886-903.

Kershaw, AP, van der Kaars, S, Opdyke, B, Guichard, F, Rule, S & Turney, C (2006). Environmental change and the arrival of people in the Australian region. *Before Farming*, issue 1, pp. 1-24. (online).

Coulter, SE, Turney, CSM, Kershaw, P & Rule, S (2009). The characterization and significance of a MIS 5a distal tephra on mainland Australia. *Quaternary Science Reviews*, vol. 28, pp. 1825-1830.

Acknowledgements

I would like to thank my supervisor Professor (Emeritus) Peter Kershaw for his ongoing support, wisdom and guidance throughout this very long thesis. His deep knowledge of my topic provided many stimulating conversations and without his insightful advice and constant feedback during the writing stage, this PhD would not have been achieved, and I am eternally grateful. I would also like to thank my co-supervisor, Professor Chris Turney for providing his expertise on radiocarbon dating and help during the writing stage. I have always valued his advice but also his boundless energy. Many thanks to my co-supervisor, Professor Simon Haberle, for his ongoing support which has been massive and who got me interested in the dark side, charcoal, and all the complexity that is involved in studying this inert material. Thank you to Professor Nicholas Branch (University of Reading) who did the humification analysis for this study, which was utilized in the statistical analyses. Monash University awarded me a Monash Graduate Research Scholarship at the initial stage of my PhD and allowed me to finish my PhD once my candidature had gone beyond lapsed. I am extremely grateful that they had the confidence in me to complete my PhD.

The two coring seasons on the Atherton Tableland provided the means for this PhD but also provided the opportunity to discover this beautiful region. Fieldwork was supported by a National Geographic grant to Dr Chris Turney and Prof Peter Kershaw and an Australian Research Council Discovery grant to Dr Raphael Wust, Prof Peter Kershaw and Dr William Anderson and the rotary drilling rig was provided by the ANU. However, the people involved in the coring was what made it a memorable journey. To Jono, Damien, Malin, Raphael, William, Chris and Peter but especially Sarah and Jo, both also doing PhDs, it was a great team but not always dry. My knowledge of all things pollen was greatly advanced with Peter's knowledge but the pollen team at Monash, Merna, Barbara and Sander, gave of their time and expertise and introduced me to the weird and wonderful world of Non-Pollen Palynomorphs (NPPs) while Urszula provided me with the skills to be competent in the lab, thank you. In the squashed confines of the PhD and Post-doctoral office I shared with Cecilia, the two Nicks and Kale there was always interesting conversations maybe not always relevant to anyone's PhD or work but always stimulating. Fieldwork was a constant at Geography and Environmental Science, and everyone was involved, so thanks to all who allowed me to be part of their project and fieldwork but especially Alex, Tibby, Chris, Nick, Merna and Tara. Many thanks to Tara Lewis who put me on the path to macrofossils her vast knowledge and

skills in botany and macrofossil identification as well as being a great friend helped me tremendously, the addition of this proxy in my study added so much to this thesis, and I am ever grateful. In addition, thanks to Jo Palmer at the National Herbarium Canberra, who allowed me to harvest seeds from the collection that greatly helped in my identifications. I would also like to thank Sophie Lewis who helped me understand the workings of spectral analysis and Mark Burrows another Atherton Tableland convert for his help in understanding humification .

Last but definitely not least to my family and friends who were always positive and encouraging and always knew I would finish. They may not have known or understood my topic but they knew it was important to me and that was all that matter. This thesis is dedicated to my sister, Kathleen, who would be very pleased.

Table of Contents

Copyright Notice	ii
Abstract	iii
Declaration	v
Publications during enrolment	vi
Acknowledgements	vii
Chapter 1 Introduction	1
1.1. Background to the Project	2
1.2. The Climate Factor.....	2
1.2.1. Milankovitch and non-Milankovitch cycles	3
1.2.2. Internal forcing factors	6
1.2.3. El Niño-Southern Oscillation (ENSO) phenomenon	7
1.3. The Human Factor.....	12
1.4. Fine Resolution Palynology.....	14
1.4.1. Pollen.....	16
1.4.1.1. <i>Pollen Production and Dispersal</i>	16
1.4.1.2. <i>Pollen Influx across stratigraphical sequences</i>	17
1.5. Macrofossils and Non-pollen Palynomorphs	18
1.5.1. Sediment type and transport	18
1.5.2. Production and Preservation	19
1.5.3. Non-Pollen Palynomorphs.....	20
1.5.3.1. <i>Fungal Spores</i>	20
1.5.3.2. <i>Algal Remains</i>	21
1.5.3.3. <i>Biogenic Silica</i>	22
1.6. Project Aims	22
1.6.1. Thesis structure	23
Chapter 2 Humid Tropics of northeast Queensland	24
2.1 Geology	25
2.1.1. Atherton Basalt Province.....	27
2.2. Physiography	28
2.3. Soils.....	30
2.4. Drainage	31
2.5. Climate	31
2.5.1. The local climate influences	34
2.5.1.1. <i>Atherton Tableland</i>	36
2.6. Vegetation.....	37
2.6.1. Rainforest Structural Classification	37
2.6.2. Rainforest Floristics	38
2.6.3. Sclerophyll Floristics.....	41
2.6.4. The present-day vegetation of Lynch's Crater.....	43

Chapter 3 Palaeoenvironmental and Archaeological Studies on the Atherton Tableland	46
3.1. Palaeoenvironmental Research	46
3.1.1. Local Pollen Representation	46
3.1.2. Modern Pollen Influx Studies across the area.....	49
3.1.3. Analysis of modern pollen spectra from rainforest plots.....	51
3.2. Fossil pollen and related studies	54
3.2.1. The late Pleistocene from Lynch's Crater	55
3.2.1.1. <i>Redating the Holocene record of Lynch's Crater</i>	57
3.2.2. Macrofossil evidence of swamp rainforest on Lynch's Crater	58
3.2.3. Correlation of Strenekoff's Crater and Lynch's Crater	59
3.2.4. The stand dynamics of Lake Barrine during the Holocene	59
3.2.4.1. <i>Hydrological patterns at Lake Barrine</i>	60
3.2.5. The correlation of marine and terrestrial records	61
3.2.6. The soil charcoal record of north Queensland	61
3.2.7. A higher resolution and multiproxy record from Lake Euramoo.....	63
3.2.8. A refinement of the Lynch's Crater chronology and the humification record	65
3.2.9. The geochemistry and the presence of wet Heinrich events on Lynch's Crater	67
3.2.10. Spectral analysis on the long Lynch's Crater record	69
3.2.11. Fire, people and megafauna	70
3.3. The Archaeological Record	71
3.3.1. Intensification or climate variability during the Holocene?	70
3.3.2. Adaptation to a rainforest environment during the late Holocene	73
3.3.3. The early European contact period.....	75
3.3.4. The Ngadjon-Jii People of Atherton Tableland	76
3.3.5. The creation of Lake Eacham and Lake Barrine.....	77
3.3.6. Lynch's Crater-Djilan bora.....	80
 Chapter 4 Fire and Charcoal	 81
4.1. Global Fire and its impact	81
4.1.1. Fire History.....	82
4.2. Fire in the Environment.....	83
4.2.1. Fire ignition	83
4.2.2. The presence and effects of fire within peat environments	84
4.2.3. Effects of fire on soil chemistry and microbial activity	84
4.2.4. Fire and vegetation succession.....	85
4.3. By-products of fire	87
4.4. Charcoal.....	89
4.4.1. Charcoal representation and deposition.....	89
4.4.2. Charcoal preparation	91
4.4.3. CharAnalysis.....	93
4.4.4. Macro-charcoal Morphotypes	94
4.5. Fire in Australia during the late Pleistocene and Holocene	98
4.5.1. Long terrestrial and marine records of fire in Australia	100
4.5.1.1. <i>Long terrestrial records of fire in Australia</i>	101
4.5.1.2. <i>Long marine records of fire in Australia</i>	102
4.5.2. The early contact period	103
4.5.3. Local fire and environmental relationships	105
4.5.4. Fire in northern Australia	106

Chapter 5 Materials and Methods	109
5.1. Field methods.....	109
5.2. Laboratory methods	113
5.2.1. Sediment sampling	113
5.2.2. Sediment description	113
5.2.3. Moisture content and Loss on Ignition (LOI)	113
5.2.4. Pollen and microcharcoal preparation	114
5.3. Pollen.....	115
5.3.1. The Pollen Sum and Identification.....	115
5.3.2. Myrtaceae Identification.....	116
5.3.3. Moraceae and Urticaceae Identification.	118
5.3.4. Non-pollen palynomorphs	119
5.4. Microscopic charcoal	119
5.4.1. Microscopic charcoal counting	119
5.4.2. Calculation of pollen and charcoal concentration and influx	120
5.5. Macrocharcoal reference materials	120
5.5.1. Macrocharcoal reference burn preparation	120
5.5.2. The macrocharcoal reference burn methods	123
5.5.3. The macrocharcoal reference burn results	124
5.6. Macrocharcoal and macrofossils.....	126
5.6.1. Macrocharcoal preparation	126
5.6.2. Fossil macrocharcoal identification and counting.....	126
5.6.3. Macrofossil identification and counting.....	128
5.7. Pollen, charcoal and macrofossil diagrams.....	129
5.8. Statistical analysis	129
 Chapter 6 Developing a Chronology for Lynch's Crater	 131
6.1. Radiocarbon Dating	131
6.1.1. Contamination.....	133
6.2. Dating of Lynch's Crater.....	134
6.2.1. Lynch's Crater's original chronology	135
6.3. Establishment of a combined sedimentary sequence	135
6.3.1. Radiocarbon dating of core sequence.....	137
6.3.2. Comparison of Lynch's Crater core chronologies	140
6.3.3. Overview of the Bayesian Model.....	142
6.3.4. Establishment of a chronology.....	143
 Chapter 7 Palaeoenvironmental Results	 150
7.1. Sediment Description	150
7.2. Palynological and macrofossil results	154
7.2.1. Zonation of Lynch's Crater Aquatic and Swamp Pollen Sum Taxa (LCA)	155
7.2.2. Zonation of Lynch's Crater Dryland Pollen Sum Taxa (LC1)	169
7.2.3. Charcoal representation	192
7.2.3.1. <i>Macrocharcoal representation</i>	192
7.2.3.2. <i>Microcharcoal representation</i>	196
7.2.4. Influx patterning.....	198
7.2.4.1. <i>Aquatic and swamp taxa influx patterning</i>	198

7.2.4.2. <i>Dryland taxa influx patterning</i>	199
7.2.4.3. <i>Charcoal influx patterning</i>	200
7.2.5. Non-quantified observational data and target counts	201
Chapter 8 Statistical Analysis	203
8.1. Principle Component Analysis (PCA).....	203
8.1.1. PCA of the aquatic and swamp percentage data (Full record 54,000 yrs BP–3,000 yrs BP).....	205
8.1.2. PCA of the dryland percentage data (Full record 54,000 yrs BP–3,000 yrs BP).....	208
8.1.3. PCA of the aquatic and swamp percentage data (Pleistocene record 54,000 yrs BP–11,800 yrs BP).....	210
8.1.4. PCA of the aquatic and swamp percentage data (Humification record 37,900 yrs BP–28,500 yrs BP).....	213
8.1.5. PCA of the aquatic and swamp percentage data (Holocene record 11,700 yrs BP–3,000 yrs BP)	216
8.1.6. PCA of the dryland percentage data (Pleistocene record 54,000 yrs BP–11,800 yrs BP)	218
8.1.7. PCA of the dryland percentage data (Holocene record 11,700 yrs BP–3,000 yrs BP)	221
8.2 Spectral Analysis	224
8.2.1 Methods.....	226
8.2.2 Spectral analysis dryland taxa results.....	228
8.2.2.1. <i>Red-noise analysis</i>	231
8.2.3. Spectral analysis aquatic and swamp results	235
8.2.4. Spectral analysis humification results	239
8.2.5. The precessional and semi-precessional frequency.....	241
8.2.6. Millennial frequencies	242
Chapter 9 Discussion	248
9.1. Climatic conditions during MIS 3 to 1 within and around the northeast Australian region	248
9.1.1. Araucarian Vine Forest – 54–41 ka.....	250
9.1.1.1. <i>Local environment</i>	252
9.1.2. The rainforest to sclerophyll transition 41–32ka	254
9.1.2.1. <i>Local changes and fluctuating water levels 41–32 ka</i>	255
9.1.2.2. <i>The impact of drier conditions regionally and locally 32–27 ka</i>	256
9.1.2.3. <i>Local and regional representation of Poaceae through the sequence</i>	257
9.1.3. An extended Last Glacial Maximum.....	260
9.1.3.1. <i>Regional influences at a local level from 20–12 ka</i>	266
9.1.4. Sclerophyll to rainforest dominance.....	269
9.2. Orbital and sub-orbital frequencies in the Lynch’s Crater record	276
9.2.1. Precessional and semi-precessional influence	276
9.2.2. ‘Heinrich Events’	279
9.2.3. The presence of Heinrich Events at Lynch’s Crater.....	281
9.3. Fire patterns: the role of climate variability and potential human influence	286
9.3.1. From low to high intensity fire	287
9.3.2. Changing trends in regional and local fire.....	293
9.3.3. Fires of the Last Glacial Maximum.....	295
9.3.4. Fire in an ever increasing humid environment.....	296
Chapter 10 Conclusion	301
10.1. Vegetation and Environment Overview	301

10.2. Sclerophyll Phase	302
10.3. Regional to Global Variability	303
10.4. Transitioning into Tropical Rainforest	304
10.5. General overview, contributions and limitations.....	305
References	308
Appendices	357
Appendix A-Map, reference pollen and charcoal material.....	357
Figure 1. Map of the WTWHA region (after Prideaux and Falco-Mammone 2007).	357
Section 1. Pollen Reference Material Myrtaceae.....	358
Section 2. Pollen Reference Material Urticaceae/Moraceae	359
Plate 1. Reference burn photos.....	360
Table 1. Reference Burn Counts.....	361
Appendix B (1) Table 1 Ecological Information on taxa represented in the pollen fossil spectra of this study (Kershaw 1976, 1983a; Stephen and Dowling 2002; Hyland et al. 2010)	362
Appendix B (2) -Observations and Statistical Analyses	369
Section 1. Non-quantified observational data and target counts dryland sum.....	369
Section 2. Tables generated from STATISTICA	373
2.1. Aquatic and Swamp percentage data (Full record 3–54 ka).....	373
2.2. Eigenvalues for the Aquatic and Swamp (Full record 3–54 ka) Error! Bookmark not defined.	
2.3. Aquatic and Swamp percentage (Pleistocene 11.8–54 ka)..... Error! Bookmark not defined.	
2.4. Eigenvalues for the Aquatic and Swamp (Pleistocene 11.8–54 ka) Error! Bookmark not defined.	
2.5. Aquatic and Swamp percentage (Humification 28.5–37.9 ka)	376
2.6. Eigenvalues for the Aquatic and Swamp (Humification 28.5–37.9 ka)..... Error! Bookmark not defined.	
2.7. Aquatic and Swamp percentage data (Holocene 3–11.7 Ka)	3786
2.8. Eigenvalues for the Aquatic and Swamp percentage data (Holocene 3–11.7 ka)	376
2.9. Dryland percentage data (Full record 3–54 ka)	377
2.10. Eigenvalues for percentage Dryland (Full record 3–54 ka)	377
2.11. Dryland percentage data (Pleistocene 11.8–54 ka)	378
2.12. Eigenvalues for percentage Dryland (Pleistocene 11.8–54 ka)	378
2.13. Dryland percentage data (Holocene 3–11.7 ka)	379
2.14. Eigenvalues for percentage Dryland (Holocene 3–11.7 ka)	380
Section 3. Tables for Spectral Analysis	380
3.1. Tables 3.1–3.6 Spectral analysis peaks for Full, Pleistocene and Holocene sequences	380
3.2. Tables 3.7–3.12 Spectral analysis peaks after filter from Red noise (ARI) for Full, Pleistocene and Holocene sequences	390
Section 4. Plates for spectra and red-noise spectra plots.....	396
Plates 4.1-4.5. Dryland percentage data full sequence (3–54 ka).....	396
Plates 4.6-4.8. Dryland influx data full sequence (3–54 ka)	401
Plates 4.9-4.13. Dryland percentage data Pleistocene sequence (11.8–54 ka).....	404
Plates 4.14-4.19. Dryland influx data Pleistocene sequence (11.8–54 ka)	409

Plates 4.20-4.22. Aquatic/swamp (inc, charcoal) percentage data Full sequence (3–54 ka)	415
Plates 4.23-4.24. Aquatic/swamp (inc. charcoal) influx data Full sequence (3–54 ka)	418
Plates 4.25-4.27. Aquatic/swamp (inc. charcoal) percentage data Pleistocene sequence (11.8–54 ka)	420
Plates 4.28–4.30. Aquatic/swamp (inc. charcoal) influx data Pleistocene sequence (11.8–54 ka)	423
Appendix C- Distribution map (<i>Nymphoides</i> and <i>Liparophyllum</i>), calibration of ages (Kershaw 1976, 1983a)	426
Figure 1. Distribution map of <i>Nymphoides indica</i> (red circle) and <i>Liparophyllum exaltata</i> (blue circle) in the present-day Australia and nearby (Atlas of Living Australia, 2017)	4266
Table 1. 14C Age and calibrated age for Kershaw (1976, 1983a), ‘+’ 14C Age from core 1 (1976), ‘*’ 14C Age from core 2 (1983a).	4266

List of Figures

Figure 1.1. Lynch’s Crater, Atherton Tableland, northeastern Queensland	1
Figure 1.2. Schematic of the Earth’s orbital changes (Milankovitch cycles) that drive the ice age cycles. ‘T’ denotes changes in the tilt (or obliquity) of the Earth’s axis. ‘E’ denotes changes in the eccentricity of the orbit (due to variations in the minor axis of the ellipse), and ‘P’ denotes precession, that is, changes in the direction of the axis tilt at a given point of the orbit (after Rahmstorf and Schellnhuber 2006).	4
Figure 2.1. Location of Lynch’s Crater and ODP site 820 in relation to major environmental features of the humid tropics, northeast Queensland (after Kershaw et al. 2007a).	24
Figure 2. 2. Geology of the Humid Tropics and location of Lynch’s Crater and other major pollen sites on the Atherton Tableland. Rainfall isohyets are illustrated (adapted with permission from Burrows et al. 2016).	26
Figure 2. 3. The Atherton Basalt Province, Basalt lava flows – grey, Shield volcanoes – yellow diamonds (B: Bones Knob, H: Hallorans Hill, M: Malanda, J: Jensenville, W: Windy Hill, L: Lamins Hill). Scoria Cones – orange triangles, with associated flows outlined in red. Maars – blue circles with Lynch’s Crater – red star, Hypipamee Crater – red circle (after Whitehead 2008).	27
Figure 2. 4. Cross-section of the major physiographic features of the Humid Tropics of northeast Queensland, Australia (adapted from Nix and Switzer 1991).	29
Figure 2. 5. Walker Circulation pattern during neutral (typical) and El Niño type conditions (after Bureau of Meteorology 2020).	32
Figure 2. 6. Schematic of circulation in the Pacific- location of the intertropical convergence zone (ITCZ) and the South Pacific convergence zone (SPCZ) in the South Pacific region along with the main sea level pressure contours and surface wind streamlines (arrows) (after Australian Bureau of Meteorology & CSIRO 2011; McGree et al. 2016).	33
Figure 2. 7. Isohyetal map of the Atherton Tableland showing position of Lynch’s Crater and other pollen analytical sites along rainfall gradient (after Hiscock and Kershaw 1992).	35

Figure 2. 8. Aerial scan of Lynch's Crater showing peripheral and parallel drainage lines and stream outlet in the southeast of the crater marked by treeline with breached eastern section marked by red arrows (Dept of Natural Resources and Mines 2006).	43
Figure 2. 9. Swamp vegetation on Lynch's Crater with <i>Lepironia articulata</i> , tall sedge, and grass <i>Ischaemum australe</i> in the foreground and secondary rainforest taxa on the crater slope in the background (Photo S.Rule 2003).	45
Figure 3. 1. Major habitat types of Lake Euramoo, Quincan Crater and Bromfield Swamp derived from the vegetation analyses of Kershaw (after Kershaw 1978).	47
Figure 3.2. Ordination diagram of the sites on pollen data and related environmental variables. Numbers in brackets are values of correlation between each of the environmental variables and the ordination axes' scores for each site – annual mean temperature (TANN), annual mean temperature range (TSPAN), mean temperature of the wettest quarter (TWETQ), mean temperature of the driest quarter (TDRYQ), annual mean precipitation (RANN), mean rainfall of the wettest quarter (RWETQ), mean rainfall of the driest quarter (RDRYQ) (adapted from Kershaw and Bulman 1994).	53
Figure 3.3. Selected attributes of the Lake Euramoo pollen diagram and derived palaeoclimatic estimates. Diagonal hatching indicates the total range envelope while cross hatching indicates the 25-75 percentile range envelope (after Kershaw and Nix 1988).	55
Figure 3.4. Selected features of the initial Lynch's Crater pollen record including a summary diagram of ratios of dryland vegetation types, selected taxa and the microscopic charcoal record (after Kershaw 1983b).	56
Figure 3.5. Selected attributes of the pollen record from Lynch's Crater extending down to 60 m, estimated to approximately 190,000 years BP (Kershaw 1984, 1986).	57
Figure 3.6. Selected pollen taxa which relate to the identified swamp forest: 1. fossil <i>Dacrydium</i> , 2, extant New Caledonian <i>Dacrydium guillauminii</i> ; 3. <i>Oraniopsis</i> ; 4 and 5. fossil <i>Syzygium</i> types; 6. extant New Guinean <i>Xanthomyrtus</i> ; 7. fossil <i>Xanthomyrtus</i> ; 8. fossil <i>Rapanea</i> . All magnification X1000 (Bohte and Kershaw 1999).	59
Figure 3.7. The seventeen districts (numbered) from which <i>in situ</i> charcoal fragments were collected. Black arrows show where charcoal may have been transported considerable distances from source. 1 Cape Tribulation, 2 Windsor Tableland, 3 Half Ton Creek, 4 Mt Lewis, 5 Macalister Range, 6 Mt Haig, 7 Mt Edith, 8 Breach Creek, 9 Mt Nomico, 10 West Bartle Frere, 11 Upper Russell R, 12 Downey Creek, 13 Maple Creek, 14 Longlands Gap, 15 Wallaman falls, 16 Jourama, 17 Mt Spec (after Hopkins et al. 1993).	63
Figure 3. 8. Lake Euramoo pollen diagram – Summary diagram with rarefaction analysis, principal components analysis results and charcoal accumulation rates (after Haberle 2005).	64
Figure 3.9. Summary of palaeoenvironmental data from Lynch's Crater showing Turney et al. (2001) chronology, the Cyperaceae/Poaceae ratio, charcoal and humification (absorption) values. Grey shading bands indicate inferred dry periods (after Turney et al. 2004).	65

Figure 3.10. A-Cross-spectral (a) and wavelet analysis (b and c) of the Lynch's Crater and GISP2 records for the past 50 kyr. B-Comparison of Lynch's Crater 1,490-yr and 11.9-kyr trends in absorption values. GISP2 $\delta^{18}\text{O}$ values and the precessional component of the orbital forcing with Heinrich events indicated. Grey shading indicate inferred dry periods (after Turney et al. 2004). 66

Figure 3. 11. Trophic status of deposit – minerotrophic peat (Mn) with transitional zone (Tr) into ombrotrophic peat (Om) in upper layers and identified dust source change points are indicated on the ages vs. $(\text{Eu}/\text{Eu}^*)_{\text{PAAS}}$ and $^{206}\text{Pb}/^{207}\text{Pb}$ profiles with the four wet events indicated by grey shading (P1-P4), (after Kylander et al. 2007). 68

Figure 3.12. Summary diagram for Lynch's Crater with spectra shown in relation to age and including the SPECMAP stack oxygen isotope values and stages, insolation values for January and July at 17°S , relative to selected forest taxon groups, aquatic taxa, Poaceae and charcoal concentrations (after Kershaw et al. 2007a). 69

Figure 3.13. Lynch's Crater summary diagrams including *Sporormiella* for A-Kershaw (adapted from Kershaw 1994, Kershaw et al. 2007a) and B-Present study, red arrows indicate same time-periods, red highlighted grey shade area covers period where *Sporormiella* decreases followed by increased charcoal (adapted from Rule et al. 2012). 70

Figure 3.14. Radiocarbon date curves for regions in tropical Australia for human occupation; Kimberley; Kakadu; Southeast Cape York Peninsula (adapted from Lourandos and David 2002). 72

Figure 3.15. The Atherton-Cairns-Innisfail region showing the extent of present-day rainforest and areas where rainforest has been cleared. The locations of the archaeological sites discussed in *sub-section 3.3.2* are also shown, red star Lynch's Crater (after Cosgrove et al. 2007). 74

Figure 3.16. Ngadjonjii tribal area ★ Lynch's Crater, ▲ Lake Eacham, ▲ Lake Barrine and ☆ Bromfield Swamp (adapted from Pannell 2005). 76

Figure 3.17. Lake Eacham *Yidyam/Wiinggina* (after Pannell 2005). 77

Figure 3.18. Lake Barrine *Barriny* (after Pannell 2005). 78

Figure 4.1. The relationship of fire with rainforest and sclerophyll vegetation. Building an alternative state where vegetation types correspond to alternative stable states along an axis of "effective wetness". (a) Rainforest vegetation – wet conditions/monostable system, drier conditions increase and a "pyrophobic threshold" is reached. (b) Pyrophytic vegetation where "ombrophobic threshold" is reached (no longer can compete with rainforest vegetation). (c) When (a) and (b) overlap, vegetation types co-exist, compete and dominance shifts between them, and wet sclerophyll forests become "momentarily" stable (after Warman and Moles 2009). 86

Figure 4.2. The pyrogenic (black) carbon combustion continuum and the corresponding techniques of quantification (modified from Thevenon et al. 2010). 88

Figure 4.3. Silhouettes of grass (A), leaf (trees) (B) and wood (C) charcoal magnified at 20x (after Umbanhowar and McGrath 1998). 95

Figure 4.4. Wood combustion particles from domestic fireplace burning mixed hardwood and softwood. A – irregular, rounded and angular features present taken under polarized light; reddish rounded particle in the centre due to the presence of anisotropic organic compounds such as resin. B and C – irregular and angular features present as well as cell wall structure/lacy pattern retained due to the presence of more resistant molecules containing less volatile material. D – close-up of lacy structure which is only partial charred/brown charcoal (for full results see Doubleday and Smol 2005, Plate 1, p. 403).	96
Figure 4.5. Charcoal morphotypes identified in the sediments of Prosser Lake: Type C (a,b); Type S (c-e); Type D (f); Type F (g,h); Type M (i-k); Type B (l,m); and Type P (n) (after Enache and Cumming 2006).	97
Figure 4.6. Geographic location of sedimentary charcoal records in the Australasian region mentioned in text (modified from Mooney et al. 2011).	100
Figure 5.1. Drill rig on Lynch’s Crater, 2003 prior to inclement weather (Photo S.Rule 2003). ...	110
Figure 5.2. Coring on Lynch’s Crater 2003 (Photo S.Rule 2003).	111
Figure 5.3. Schematic drawing of Lynch’s Crater showing drainage lines and positions of cores taken in 1998 and field seasons 1 and 2 (2003 and 2004), (modified from Coulter 2007).	112
Figure 5.4. Retrieval of the core LYE(LIV) used in this study using a livingstone corer (Photo S.Rule 2003).	112
Figure 5.5. Some of the Myrtaceae pollen morphological types found in the study site area. (a) <i>Acmena smithii</i> (now <i>Syzygium smithii</i>), (b) <i>Acmena graveolens</i> (now <i>Syzygium graveolens</i>), (c) <i>Syzygium leuhmannii</i> (formerly <i>Eugenia leuhmannii</i>); (d) <i>Syzygium kuranda</i> (formerly <i>Eugenia kuranda</i>); (e) <i>Syzygium cormiflorum</i> (formerly <i>Eugenia cormiflora</i>); (f) <i>Austromyrtus dallachiana</i> (now <i>Gossia dallachiana</i>); (g) <i>Rhodomyrtus trineura</i> ; (h) <i>Syncarpia glomulifera</i> ; (i) <i>Melaleuca dealbata</i> ; (j) <i>Melaleuca leucadendra</i> ; (k) <i>Tristaniopsis exiliflora</i> (formerly <i>Tristania exiliflora</i>) high focus and (l) <i>T. exiliflora</i> low focus; (m1) <i>Leptospermum wooroonooran</i> (cluster of pollen grains), (m2) <i>L.wooroonooran</i> polar view, (m3) <i>L.wooroonooran</i> equatorial view; (n) <i>Corymbia intermedia</i> (formerly <i>Eucalyptus intermedia</i>); (o) <i>Eucalyptus tereticormis</i> ; (p) <i>Eucalyptus macta</i> (formerly <i>E.resinifera</i>); All photographs were taken by the author except for (b) and (p) which were sourced from the Australasian pollen and spore atlas and all pollen reference slides photographed, including those from the Australasian pollen and spore atlas, were from the Australian National University pollen reference collection with full details given in Appendix A, Section 1.	117
Figure 5.6. Genera and species from the Moraceae/Urticaceae family that are found in the study site area (a) – <i>Ficus rubiginosa</i> , (b) – <i>F.virens</i> , (c) – <i>F.coronata</i> and (d) – <i>F.macrophylla</i> , (e) – <i>Streblus glaber</i> , (f) – <i>Dendrocnide photinophylla</i> (formerly <i>Laportea photinophylla</i>), (g) – <i>Pipturus argenteus</i> and (h) – <i>Urtica incisa</i> . All photographs were taken by the author and all pollen reference slides photographed were from the School of Geography and Environmental Science, Monash University pollen reference collection with full details given in Appendix A, Section 2.	119

Figure 6.1. Schematic of radiocarbon production and decay in the atmosphere. ^{14}C is produced in the atmosphere by cosmic neutrons colliding with nitrogen atoms. The newly formed ^{14}C is oxidized to $^{14}\text{CO}_2$ when it enters the biosphere. Following an organism's death, radioactive decay occurs, converting the ^{14}C back to ^{14}N (after Radiocarbon Laboratory, ANU 2020).....	132
Figure 6.2. Comparison between (A) the originally-reported loss-on-ignition (LOI) values obtained from Lynch's Crater (Kershaw 1976, 1986) and (B) LOI from the D-section and Livingstone cores used in this study. The blue star indicates the presence of lake sediments, suggesting near permanent water conditions below.....	136
Figure 6.3. Age-depth plot with radiocarbon dates obtained from Lynch's Crater (Table 6.2). Red circle indicates the dates taken from core LY(3)Liv1 which were reversed: The green circle indicate those ages below 776 cm that appear to have reached the radiocarbon dating limit.....	139
Figure 6.4. Correlation of LOI values (A to C) and (D) carbon content (%) across cores taken from Lynch's Crater. A-present study; B-Muller et al. (2006, 2008a,b,); C-Kershaw (1973, 1976); D-Turney et al. (2001b). Solid orange lines indicates what are considered to be confident points of correlation between the cores; the dashed orange lines indicate a relatively good fit. AMS ^{14}C dates before and after high inorganic phases are shown with full details in Table 6.3. Blue Star marks the transition from lake to peat sediments. Sequence B did have the transition from lake to peat sediment at approximately 13 m but LOI data was not available.	141
Figure 6.5. Age-depth plot of combined radiocarbon dates prior to calibration and modelling, circled area are ages from 158 198 cm from the present study included in the age model.	142
Figure 6.6. Bayesian modelled age-depth plot (M1) with the radiocarbon date number to the left; the radiocarbon date can be found in Table 6.2. Ages were calibrated using SHCal13 (Hogg et al. 2013). Bayesian model utilised using the deposition model P-Sequence with a k parameter of 0.2 cm (Oxcal 4.3).	145
Figure 6.7. Bayesian modelled age-depth plot (M2) with the radiocarbon date number to the left; the radiocarbon date can be found in Table 6.5. Ages were calibrated using SHCal13 (Hogg et al. 2013). Bayesian model utilised using the deposition model P-Sequence with a k parameter of 0.2 cm (Oxcal 4.3).	146
Figure 6.8. Bayesian modelled age-depth plot with the radiocarbon date number to the left; the radiocarbon date can be found in Table 6.8. Ages were initially calibrated using SHCal04 and IntCal04 and against the Cariaco Basin comparison curve in OxCal v4.2. Bayes theorem was utilised using the deposition model P-Sequence with a k parameter of 0.2 cm (Oxcal 4.2).....	148
Figure 7.1. Field photos for LYE(LIV) cores 1-8 m (amended depth 2.02-9.02 m), red circled area indicates primarily organosilicate layer at 380 cm (amended depth 482 cm), (see Table 7.1 and Chapter 6 for more detail).	151
Figure 7.2. Lithology, Moisture loss (ML) and Loss on Ignition (LOI), Magnetic Susceptibility (low and high frequency) and Sedimentation rate per $\text{cm}^{-2}\text{yr}^{-1}$ for the 9.02 m record from Lynch's Crater.	153

Figure 7.3. Aquatic and Swamp percentage pollen, charcoal (conc.) and local observations diagram with Coniss (detrended correspondence analysis) used for zoning based on the percentage aquatic and swamp pollen sum.	166
Figure 7.4. Aquatic and Swamp influx pollen, charcoal (influx) and local observations diagram, zoning based on percentage aquatic and swamp pollen sum.	167
Figure 7.5. Macrofossil (count data) and macrocharcoal total and macrocharcoal types diagram with zoning based on percentage aquatic and swamp pollen sum.....	168
Figure 7.6. Dryland percentage summary diagram with charcoals, with Coniss (detrended correspondence analysis) used for zoning based on the percentage dryland pollen sum.	180
Figure 7.7. Dryland percentage rainforest canopy taxa diagram with percentage dryland pollen sum zoning.....	181
Figure 7.8. Dryland percentage rainforest secondary and vine taxa diagram with percentage dryland pollen sum zoning.	182
Figure 7.9. Dryland percentage rainforest understorey taxa diagram with percentage dryland pollen sum zoning.....	183
Figure 7.10. Dryland percentage sclerophyll taxa, Poaceae, shrub and herb taxa diagram with percentage dryland pollen sum zoning.	184
Figure 7.11. Dryland percentage pteridophyte taxa diagram with percentage dryland pollen sum zoning.	185
Figure 7.12. Dryland influx summary diagram including charcoals with percentage dryland pollen sum zoning.....	186
Figure 7.13. Dryland influx rainforest canopy taxa diagram with percentage dryland pollen sum zoning.	187
Figure 7.14. Dryland influx rainforest secondary and vine taxa diagram with percentage dryland pollen sum zoning.	188
Figure 7.15. Dryland influx rainforest understorey taxa diagram with percentage dryland pollen sum zoning.	189
Figure 7.16. Dryland influx sclerophyll taxa, Poaceae, shrub and herb taxa diagram with percentage dryland pollen sum zoning.	190
Figure 7.17. Dryland influx pteridophyte taxa diagram with percentage dryland pollen sum zoning.	191
Figure 7.18. Microcharcoal and macrocharcoal concentration and influx diagram with percentage dryland pollen sum zoning.	197

Figure 8.1. Scree plot of the eigenvalues of the correlation matrix of the active taxa for the aquatic and swamp percentage data (Full record 3–54 ka)	206
Figure 8.2. Projection of the taxa on F1 and F2 for the aquatic/swamp percentage data, full record. Abbreviations are given for supplementary variables (red line and pointer) :- MaE-macrocharcoal ‘elongated’, MaB-macrocharcoal ‘blocky’, MaL-macrocharcoal ‘lattice’, MaO-macrocharcoal ‘other’, Micro-microcharcoal, In-inorganics, M-moisture, <i>Gelas=Gelasinospora</i> , <i>Neuro-Neurospora</i> , SS-Sponge spicules.....	207
Figure 8.3. Projection of samples on F1 and F2 for the aquatic and swamp percentage data, full record.....	208
Figure 8.4. Scree plot of the eigenvalues of the correlation matrix of the active taxa for the dryland percentage data (Full record)	209
Figure 8.5. Projection of the taxa on F1 and F2 for the dryland percentage data, full record. <i>Cas-Casuarinaceae</i> , <i>Euc-Eucalyptus</i> , <i>Pet-Petalostigma</i> , <i>Aga-Agathis</i> , <i>Arau-Araucaria</i> , <i>Pod-Podocarpus</i> , <i>Dac-Dacrydium</i> , <i>Argy-A.peralatum</i> , <i>Syz-Syzygium</i> , <i>Elaeo-Elaeocarpus</i> , <i>CunT-CunoniaceaeTricolpate</i> , <i>CunD-CunoniaceaeDicolpate</i> , <i>Fic-Ficus</i> , <i>Mall-Mallatus</i> , <i>Celt-Celtis</i> , <i>Olea-O.paniculata</i> , <i>Trem-Trema</i> , <i>Leg-Leguminosae</i> , <i>U/M-Urticaceae/Moraceae</i> , <i>Gloc-Glochidon</i> and supplementaries In-inorganics, Micro-microcharcoal, Macro-macrocharcoal, M-moisture and <i>MeA-Melastoma affine</i>	209
Figure 8.6. Projection of samples on F1 and F2 for the dryland percentage data, full record.	210
Figure 8.7. Scree plot of the eigenvalues of the correlation matrix of the active taxa for the aquatic and swamp percentage data (Pleistocene record 11.8 ka–54 ka)	211
Figure 8.8. Projection of the taxa on F1 and F2 for the aquatic and swamp percentage data, Pleistocene record. The red circle encloses all the macrocharcoal components (‘blocky’, ‘elongated’, ‘lattice-type’ and ‘other’), <i>Halo-Haloragis</i> , <i>Hydro-Hydrocotyle</i> , <i>Cyp-Cyperus</i> , <i>C/S-Carex/Schoenplectus</i> , <i>Anth-Anthoceros</i> IN-inorganics, M-moisture, <i>Bo-Botryococcus</i> , <i>Pers-Persicaria</i> , <i>Eleo-Eleocharis</i> , <i>Nym-Nymphoides</i> , <i>Poa-Poaceae</i> , <i>Bau-Baumea</i> , <i>Lip-Liparophyllum</i> , <i>Poa-Poaceae</i> and Micro-microcharcoal.	211
Figure 8.9. Projection of the samples on F1 and F2 for the aquatic and swamp percentage data, Pleistocene record.	213
Figure 8.10. Scree plot of the eigenvalues of the correlation matrix of the active taxa for the aquatic and swamp percentage data (Humification record 37.9–28.5 ka)	214
Figure 8.11. Projection of the taxa on F1 and F2, for the aquatic and swamp percentage data, humification record. <i>C/S-Carex/Schoenplectus</i> , <i>Pers-Persicaria</i> , <i>Bau-Baumea</i> , <i>Eleo-Eleocharis</i> , M-Moisture, Macro‘O’-macroOther, Macro‘L’-macroLattice, Macro‘E’-macroElongated, Macro‘B’-macroBlocky, <i>Cyp-Cyperus</i> , Hum-humification, IN-inorganics, <i>Halo-Haloragis</i> , <i>Poa-Poaceae</i> , <i>Anth-Anthoceros</i> , <i>Lip-Liparophyllum</i> , Micro-microcharcoal.	214

Figure 8.12. Projection of samples on F1 and F2 for the aquatic and swamp percentage data, humification record.	215
Figure 8.13. Scree plot of the eigenvalues of the correlation matrix of the active taxa for the aquatic and swamp percentage data (Holocene record)	216
Figure 8.14 Projection of the taxa on F1 and F2 for the aquatic and swamp percentage data, Holocene period. Macro'L'-macroLattice, Poa-Poaceae, M-Moisture, <i>Bau-Baumea</i> , <i>Nym-Nymphoides</i> , <i>C/S-Carex/Schoenplectus</i> , <i>Eleo-Eleocharis</i> , <i>erio-Eriocaulon</i> , <i>Halo-Haloragis</i> , <i>Hydro-Hydrocotyle</i> , <i>Anth-Anthoceros</i> , <i>Cyp-Cyperus</i> , Macro'E'-macroElongated, Macro'O'-macroOther, Macro'B'-macroBlocky, IN-inorganics, Micro-microcharcoal.	216
Figure 8.15. Projection of the samples on F1 and F2 for the aquatic and swamp percentage data, Holocene period, shaded area depicts zone B cases aligned with zone A cases.	217
Figure 8.16. Scree plot of the eigenvalues of the correlation matrix of the active taxa for the dryland percentage data (Pleistocene record)	219
Figure 8.17. Projection of the taxa on F1 and F2 for the dryland percentage data, Pleistocene record. <i>Cas-Casuarina</i> , <i>Mela-Melaleuca</i> , <i>Euc-Eucalyptus</i> , <i>Cint-Corymbia intermedia</i> , <i>Pet-Petalostigma</i> , IN-inorganics, Micro-microcharcoal, Macro-macrocharcoal, M-moisture, <i>Aga-Agathis</i> , <i>Arau-Araucaria</i> , <i>Pod-Podocarpus</i> , <i>Dac-Dacrydium</i> , <i>Ap-A.peralatum</i> , <i>Syz-Syzygium</i> , <i>Mall-Mallatus</i> , <i>Celt-Celtis</i> , <i>Mel-Melicope</i> , <i>Dod-Dodonea</i> , <i>Call-Callitris</i> , <i>Op-O.paniculata</i> , <i>Trem-Trema</i> , Leg-Leguminosae, U/M-Urticaceae/Moraceae.	219
Figure 8.18. Projection of the samples on F1 and F2 for the dryland percentage data, Pleistocene record.	220
Figure 8.19. Scree plot of the eigenvalues of the correlation matrix of the active taxa for the dryland percentage data (Holocene record)	221
Figure 8.20. Projection of the taxa on F1 and F2 for the dryland percentage data, Holocene record. M-moisture, IN-inorganics, Macro'L'-macroLattice, Macro'E'-macroElongated, Macro'B'-macroBlocky, Macro'O'-macroOther, Micro-microcharcoal, U/M-Urticaceae/Moraceae, <i>Syz-Syzygium</i> , <i>Cint-C.intermedia</i> , <i>Cas-Casuarina</i> , <i>Euc-Eucalyptus</i> , <i>Mela-Melaleuca</i> , <i>Dod-Dodonea</i> , <i>Call-Callitris</i> , <i>Celt-Celtis</i> , <i>Trem-Trema</i> , <i>Op-O.paniculata</i> , <i>Acm-Acmena</i> , <i>Gloc-Glochidion</i> , <i>Rap-Rapanea</i> , Leg-Leguminosae, <i>Frey-Freycinetta</i> , <i>CunT-Cunoniaceae(tricolpate)</i> , <i>CunD-Cunoniaceae(dicolpate)</i> , <i>Fic-Ficus</i> , <i>Elae-Elaeocarpus</i> , <i>Maff-M.affine</i> , <i>Oran-Oraniopsis</i> , <i>Arch-Archontophoenix</i> , <i>Mall-Mallotus</i>	222
Figure 8.21. Projection of the samples on F1 and F2 for the dryland percentage data, Holocene record, shaded area depicts zone 3b samples aligned with zones 1 and 2 samples.	223
Figure 8.22. Spectral analysis of the mid-January insolation record (15°S) over the last.....	225
Figure 8.23. Red-noise spectra of <i>Celtis</i> (%Full), frequencies noted on plot	231
Figure 8.24. Spectra plot of Casuarinaceae (%Full), frequencies noted on plot	231
Figure 8.25. Spectra plot of Poaceae (%Full), frequencies noted on plot	232

Figure 8.26. Spectra plot of Sclerophyll total (Influx Full), frequencies noted on plot	232
Figure 8.27. Spectra plot of Chenopodiaceae (Influx Full), frequencies noted on plot	232
Figure 8.28. Spectra plot of <i>Dodonaea</i> (%Pleistocene), frequencies noted on plot	233
Figure 8.29. Red-noise spectra plot of Urticaceae and Moraceae (%Pleistocene), frequencies noted on plot	233
Figure 8.30. Red-noise spectra plot of Asteraceae (tubuliflorae), (%Pleistocene), frequencies noted on plot	233
Figure 8.31. Spectra plot of Chenopodiaceae (Influx Pleistocene), frequencies noted on plot	234
Figure 8.32. Spectra plot of Poaceae (Influx Pleistocene), frequencies noted on plot	234
Figure 8.33. Spectra plot of Sclerophyll total (Influx Pleistocene), frequencies noted on plot	234
Figure 8.34. Spectra plot of microcharcoal (Conc. Full), frequencies noted on plot	237
Figure 8.35. Spectra plot of macrocharcoal (Influx Pleistocene), frequencies noted on plot	237
Figure 8.36. Red-noise spectra plot of Cyperaceae/Poaceae ratio (Pleistocene), frequencies noted on plot	237
Figure 8.37. Spectra plot of Haloragis (% Pleistocene), frequencies noted on plot	238
Figure 8.38. Spectra plot of <i>Typha</i> (% Pleistocene), frequencies noted on plot	238
Figure 8.39. Spectra plot of Cyperaceae (Influx Pleistocene), frequencies noted on plot	238
Figure 8.40. Spectra plot of humification (28.5 ka–37.9 ka sequence), frequencies noted on plot	239
Figure 8.41. Spectra plot of Cyperaceae/Poaceae ratio (28.5 ka–37.9 ka sequence), frequencies noted on plot	240
Figure 8.42. Red-noise spectra plot of Poaceae (%28.5 ka–37.9 ka sequence), frequencies noted on plot	240
Figure 8.43. Red-noise spectra plot of Poaceae (Influx 28.5 ka–37.9 ka sequence), frequencies noted on plot	240
Figure 8.44. Spectra plot of macrocharcoal (Influx 28.5 ka–37.9 ka sequence), frequencies noted on plot	241
Figure 8.45. Red-noise spectra plot of <i>Elaeocarpus</i> (%Pleistocene), frequencies noted on plot	243
Figure 8.46. Red-noise spectra plot of <i>Elaeocarpus</i> (Influx Pleistocene), frequencies noted on plot	243
Figure 8.47. Red-noise log-linear spectra plot of Menispermaceae (%Pleistocene), frequencies noted on plot	243
Figure 8.48. Red-noise spectra plot of <i>Celtis</i> (Influx Pleistocene), frequencies noted on plot	244
Figure 8.49. Spectra plot of <i>Argyrodendron peralatum</i> type (Influx Full), frequencies noted on plot	244

Figure 8.50. Red-noise log-linear spectra plot for <i>Mallotus</i> and <i>Macaranga</i> (influx Pleistocene record) with both the 21.7 kyr (precessional) and 1.31 kyr (millennial) frequency at 99% confidence level.	246
Figure 8.51. Spectra plot of <i>Trema</i> (%Holocene and LGM) indicating the centennial frequency, 725 yr, at 99% confidence level.	247
Figure 9. 1. Selected pollen and charcoal from Lynch's Crater dryland percentage data	251
Figure 9. 2 Selected aquatic and swamp and dryland taxa, and charcoal from Lynch's Crater percentage data.	253
Figure 9.3. Microcharcoal and macrocharcoal top graph; Cyperaceae/Poaceae ratio middle graph; Cyperaceae and Poaceae (y-axis) and Inorganics (y2-axis) full influx record with blues lines (inc. dashed) and letters denoting the aquatic/swamp pollen zones and the orange lines with diamond arrow (inc. dashed) and numbers denoting the dryland pollen zones.	256
Figure 9.4. Cyperaceae versus Poaceae influx on the full record biplot	259
Figure 9.5. Cyperaceae versus Poaceae percentage on the full record biplot.	259
Figure 9.6. Major vegetation types and groups for the period 12 ka through to 28.9 ka for (A) Percentage data for major sclerophyll taxa, Casuarinaceae and <i>Eucalyptus</i> , (y2-axis), rainforest gymnosperms, rainforest angiosperms and <i>Syzygium</i> (y-axis), (B) Influx data for major sclerophyll taxa, Casuarinaceae and <i>Eucalyptus</i> , (y2-axis), rainforest gymnosperms, rainforest angiosperms and <i>Syzygium</i> (y-axis), (C) Microcharcoal. Shaded areas indicate periods of high influx for pollen....	260
Figure 9.7. Selected macrofossil taxa from Lynch's Crater, <i>M.affine</i> , <i>N.indica</i> and <i>L.exaltatum</i> have been exaggerated x10 and <i>Azolla</i> *=megasporocarps and <i>Azolla</i> + =microsporangia. Shaded area show major inorganics where aquatic hydrophytes are present.....	267
Figure 9.8. Percentages of major rainforest elements and microcharcoal (concentration) for the period 3 – 13 ka, <i>Syzygium</i> and <i>M.affine</i> were not included in the dryland pollen sum.....	270
Figure 9.9. Influx data for the pteridophytes, Poaceae and macrocharcoal for the period 3 – 13 ka.	271
Figure 9.10. Red-noise log-linear spectra plot for <i>Elaeocarpus</i> . Frequencies noted on plot.....	278
Figure 9.11. Red-noise log-linear spectra plot for <i>Celtis</i> . Frequencies noted on plot.	278
Figure 9.12. Major dryland summary types for period ~ 10-40 ka - A-Percentage, B-Influx, C-Inorganics (concentration and Influx) and Cyperaceae/Poaceae ratio, D-Charcoal (micro). Grey shaded areas indicate H-events (1-4) and ACR and YD.	281
Figure 9.13. Comparison of LC macrocharcoal and microcharcoal (B), LC Cyperaceae/Poaceae ratio and inorganics (C), with Flores, Indonesia (Lewis et al. 2011) (A), and Hula Cave, China, and Botuvera, Brazil (Wang et al. 2001, 2006; Zhao et al 2010). Shaded areas indicate time of climate anomalies, H – Heinrich, YD – Younger Dryas and ACR – Antarctica Cold Reversal for time sequence 40-10 ka.	283

Figure 9.14. Percentage (A) and influx (c) values of Eucalyptus, Casuarinaceae, Swamp Myrtaceae 1, Poaceae, Cyperaceae, Sporormiella and Sordaria and (B) micro- and macro-charcoal concentration s shown in relation to the zonation based in the dryland pollen sum. Both micro- and macro-charcoal truncated with actual values indicated at the end of each relevant sample 289

Figure 9.15. Macrocharcoal types and total alongside inorganics and microcharcoal as well as the Elongated/Blocky macrocharcoal ratio, brown charcoal abundance on a 0-5 scale, *Neurospora* and *Gelasinpora* (present/absent) and charred seeds on a 0-2 scale). Both microcharcoal and macrocharcoal are expressed as concentrations with highest values truncated and macrocharcoal types have been exaggerated x2. Zonation is based on the aquatic/swamp pollen sum..... 291

List of Plates

Plate 2.1. Rainforest features Atherton Tableland, (A)-Epiphytic ferns; (B)-Lianes; (C) Lake Barrine MVF; (D)-Lake Eacham MVF (Photos S.Rule 2003). 40

Plate 2.2. (A)-Strangler *Ficus* (Moraceae) present in MVF and CNVF; (B)-MFT with *Leptospermum wooroonooran*; (C)-Ecotonal transition between rainforest and sclerophyll woodland; (D)-Tall eucalypt forest (WSF) *E.grandis* emergent (Photo (A) S.Rule; Photos (B), (C) and (D) Webb 2007)..... 42

Plate 5.1. *Carex fascicularis* (a) *C. fascicularis* (sample 6) tested at 400°C for 10 minutes with outer blade completely charred but inner part/epidermis still with a brown/coppery tinge indicating that it is not completely charred, (b) *C. fascicularis* (sample 7) completely charred but distinct venation structure still visible. 122

Plate 5.2. Burn samples (Grid size 1 mm); (1a) > 500 µm Poaceae, (1b) > 250 µm Poaceae, (2a) > 500 µm *Carex fascicularis*, (2b) > 250 µm *Carex fascicularis*, (3a) > 500 µm *Typha*, (3b) Epidermis of *Typha* prior to burning, (3c) Charred epidermis of *Typha*, (3d) Charred epidermis of *Typha*, (4a) > 500 µm *Eucalyptus regnans*, (4b) > 250 µm *Eucalyptus regnans* 125

Plate 5.3. (a) Charred remains of *Nymphoides* seed; (b) Partially charred remains of *Liparophyllum* (*Villarsia*) seed; (c) unknown charcoal type (red circled area) x 10; (d) likely charred remains of flower/seed component from a sedge; (e) unknown charcoal type (red circled area); (f) charred remains of unknown seed and sedge component. 127

Plate 7.1. Macrofossils present in zone LCA-F. (a)-woody fragment, (b)-*Gonocarpus cf. chinensis* subsp. *verrucosus*, (c)- *Carex cf. appressa* (d)- Mericarps of *Hydrocotyle*, (e) – cf. *Passiflora* type seed, (f)- inner seed linings..... 156

Plate 7.2. Macrofossils and organosilicates from subzone LCA-E2, (a) – eroded silicates, (b) – *Azolla pinnata* megasporangia, (c) – *A.pinnata* micro sporocarps, (d) – *Nitella* sp., (e) – *P.tricarinatus* carpel, (f) – *Liparophyllum exaltatum* (formerly *Villarsia exaltata*) seed. 158

Plate 7.3. Macrofossils from subzone LCA-E1, (a) – <i>Eleocharis</i> cf. <i>sphacelata</i> , (b) – <i>Persicaria strigosa</i> , (c)- <i>Typha domingensis</i> , (d) – <i>Rorippa</i> sp., (e) – <i>Elatine gratioloides</i> , (f) – <i>Chara</i> oospore	160
Plate 7.4. Macrofossils and algal remains present in LCA-C, (a) – the algal spore <i>Pseudoschizaea</i> , (b) – <i>Nymphoides indica</i> , the light coloured seed (fertile), the darker seed infertile, (c) – <i>N.indica</i> seed coating without spines, (d) – Size differences of <i>N.indica</i> and <i>L.exaltatum</i> – <i>N.indica</i> (centre small seed) and <i>L.exaltatum</i> (large seed to the left and right). The seed samples for <i>L.exaltatum</i> were taken from subzone LCA-E2 as <i>L.exaltatum</i> seeds were not found in zone LCA-C.....	163
Plate 7.5. Macrofossils present in zone LCA-B and LCA-A, (a) – <i>Cyperus polystachyos</i> , (b) – <i>Melastoma affine</i> , (c) - <i>Axonopus</i> cf. <i>affinis</i> , (d) – Fern scales.....	164
Plate 7.6. Podocarpaceae types found through subzone <i>LC1-9b</i> . (a) – Smaller variant of the Podocarpaceae pollen type; (b) – The more common Podocarpaceae pollen type, which shows a close affinity to the pollen of <i>Podocarpus amarus</i> (now <i>Sundacarpus amarus</i>). This pollen type is found throughout the Lynch’s Crater record.	169
Plate 7.7. Charred remains recorded in zone LCA-F, sub-zone LCA-E1, sub-zone LCA-E2 and LCA-D. (a) - charred <i>Schoenoplectus</i> nut with other charred plant remains, (b) - <i>Nymphoides indica</i> , (c) - <i>Liparophyllum exaltatum</i> , (d) - ? <i>Carex</i> spp., nuts, (e) – sedge plant remains, (f) – peat, (g) - <i>A.pinnata</i> fragment, (h) – a number of different sedge species (<i>Schoenoplectus</i> , <i>Carex</i> , <i>Cyperus</i>) and <i>Typha/Lipocarpa</i> (364 cm).....	193
Plate 7.8. Lattice-type charcoal zone LCA-B, (a) – Lattice-type charcoal single epidermis layer, (b) – Lattice-type charcoal double epidermis layer, (c) - Woody/sedge fragments, (d) - Sedge stem, (e) - Epidermis ? <i>Typha</i> (see Figure 5.10 3b), (f) - Woody/Sedge remains, (g) - Woody remains, (h) - Flowering and/or seed head of sedge.	195

List of Tables

Table 2.1. Bioclimatic estimates for present-day conditions for pollen sites on the Atherton Tableland, northeast Australia, MAT-mean annual temperature, MAP-mean annual precipitation, PDQ-precipitation driest quarter (Busby 1991).	36
Table 2.2. Classification of main rainforest types (1–11) mixed communities (12–13) and sclerophylls communities (14–16) for north Queensland in relation to rainfall, altitude, and soil materials (Tracey & Webb 1975; Tracey 1982).	39
Table 3. 1. Model fitting results from pollen influx data from Lake Barrine (after Chen 1986)	60
Table 5.1. Myrtaceae groupings used in this thesis and their ecological habitat and local attributes (taken from Tracey 1982; Webb <i>et al.</i> 1984; Hyland <i>et al.</i> 2003).	118
Table 5.2. Reference material used for experimental burns	121
Table 5.3. Testing of <i>Carex fascicularis</i> with temperatures, times and degree of charring given. .	122

Table 5.4. Percentage average results across 3 counts for >2:1 L:W ratio for herbaceous (Poaceae/Sedges/ <i>Typha</i>) and woody taxa (<i>Eucalyptus</i> spp. and <i>Acmena</i>).	124
Table 6.1. A list of the previous studies from Lynch's Crater with detail of the number of radiocarbon dates and source material.	134
Table 6.2. Complete list of radiocarbon dates from the present study. The amended sample depth is the depth that is used in this study across all diagrams. 'DS' – denotes samples taken from D_Section core LYB; 'LY3' – refers to samples taken from LY(3)Liv1 core, and 'LYE' – samples taken from LYE(LIV) core (see section 6.3 for more details).	138
Table 6.3. Depositional models that can be used for Bayesian modelling (after Bronk Ramsey 2008).	143
Table 6.4. List of ages selected from Lynch's Crater cores for combined chronological model (M2) construction prior to calibration. All ages are from the present study except B-Muller et al. (2008a, b), C-Kershaw (1973, 1976) and D-Turney et al. (2001b, c). List of ages in M2 that returned an agreement index of <60% and were discarded.	144
Table 6.5. List of ages M1 that returned an agreement index of <60% and were discarded.....	145
Table 6.6. List of ages selected from Lynch's Crater cores for chronological model construction used in this study prior to calibration. All ages are from the present study except B-Muller et al. (2008a, b), C-Kershaw (1973, 1976) and D-Turney et al. (2001b, c). List of ages from model used in this study that returned an agreement index of <60% and were discarded.....	147
Table 7.1. General sediment description	152
Table 7.2. Non-quantified observational data and target counts (TC), N/O-nil observed (for full details see Appendix B).....	202
Table 8.1. Critical spectral analysis frequencies, precessional, semi-precessional, 15–17 kyr and millennial, using Siegel's significance test for the dryland percentage, concentration, and influx data for the full record (3 ka–54 ka). X – primary frequency (99% confidence level), X – secondary frequency (99% confidence level), X – frequency within Fisher 99% and Siegel's 95% critical confidence levels.....	229
Table 8.2. Critical spectral analysis frequencies, precessional, semi-precessional, 15–17 kyr and millennial, using Siegel's significance test for the dryland percentage, concentration and influx data for the time-period 11 ka–54 ka, X – primary frequency (99% confidence level), X – secondary frequency (99% confidence level) and X – frequency within Fisher 99% and Siegel's 95% critical confidence levels.....	230
Table 8.3. Critical spectral analysis frequencies, precessional, semi-precessional, 15–17 kyr and millennial, using Siegel's significance test for the aquatic and swamp inc. macrocharcoal and microcharcoal percentage, concentration and influx data for the full record (3 ka–54 ka), X –	

primary frequency (99% confidence level), X – secondary frequency (99% confidence level) and X – frequency within Fisher 99% and Siegel’s 95% critical confidence levels. 235

Table 8.4. Critical spectral analysis frequencies, precessional, semi-precessional, 15–17 kyr and millennial, using Siegel’s significance test for the aquatic and swamp inc. macrocharcoal and microcharcoal percentage, concentration and influx data for the time-period (11 ka–54 ka), X – primary frequency (99% confidence level), X – secondary frequency (99% confidence level) and X – frequency within Fisher 99% and Siegel’s 95% critical confidence levels. 236

Table 8.5. Significant spectral frequency, 1.2–1.7 kyr, using Fisher and Siegel’s significance test for selected components across all time-series and percentage, concentration and influx data. 245

Chapter 1

Introduction



Figure 1. 1. Lynch's Crater, Atherton Tableland, northeastern Queensland (Photo S.Rule)

Lynch's Crater on the Atherton Tableland, northeast Queensland (Figure 1.1.) has provided one of the longest and most continuous late Quaternary records of environmental change in the low altitude tropics. It has yielded multi-proxy datasets that have made important contributions to the understanding of Australian palaeoclimates and rainforest ecology as well as being influential in debates over the time of arrival of Aboriginal people on the continent and their degree of impact on the landscape through their burning activities (Kershaw 1986; Kershaw et al. 2002; Turney et al. 2001*b*; Rule et al. 2012). One of the outstanding attributes of these data is that they present a picture of a highly dynamic landscape, sensitive to climate change variability on orbital to millennial timescales. However, there is still little known about how the landscape responded to changes that occurred at millennial to sub- millennial timescales including centennial and decadal timescales within which critical tropical climate systems such as the Southern Oscillation phenomenon are known to operate (Sturman and Tapper 2006).

In this project I will examine sediment cores from Lynch's Crater at higher resolution than has been achieved previously in an attempt to understand the response of tropical ecosystems to high frequency environmental change as well as provide a detailed examination of the possible concurrent role of Aboriginal people within the environment. The proxies chosen for this study, including pollen, charcoal (microscopic and macroscopic), macrofossils and other components of the sediment record, will each provide their own unique record through time but together will give a more comprehensive representation of both local and regional scale environment change.

1.1. Background to the Project

Instrumental records document changes in the earth's atmosphere over periods of decades to centuries. These timescales are significant as they cover the time-period of greatest human population growth and the ensuing economic activity that has been necessary to sustain this growth. These records also provide baseline data for climate models, which may then be able to provide a practical predictive outcome of the impact of human activity on the climate system (Randall et al. 2007; Hausfather et al. 2019). However, whatever anthropogenic effects there are on climate, from pre-historical societies through to the present-day and future, they will be superimposed on "natural" climate variability which varies on all timescales in response to different forcing factors (Bradley 2000; Sturman and Tapper 2006;). It is important to document and explain this natural variability in order to fully assess the degree and impact of anthropogenically-induced change and to examine the potential for any 'surprises' in future climate, evident on scales longer than those covered by the instrumental record.

1.2. The Climate Factor

Natural forcing factors can be external to the earth due to variation in the solar output at interannual to decadal timescales such as sunspot activity or long-term variations in solar activity due to astronomical changes in the Earth's orbit in relation to the Sun. A reduction in sun-spot activity during the 17th and 18th centuries termed the 'Maunder minimum' has been linked to the Little Ice Age (1430-1850 AD), a climatic deterioration especially prevalent in Europe (Sturman and Tapper 2006). Such variations in sun spot activity have now been documented over longer periods. In eastern Qinghai-Tibet plateau, China, for example, it has been inferred that temperature variation within the region during the past

6000 years was mainly due to a quasi- 100 year fluctuation of solar activity (Xu et al. 2006) while sunspot activity and variations in solar insolation maybe responsible for multi-centennial fluctuations of the East Asian winter monsoon in the eastern Mu Us desert, China during the early Holocene (Wen et al. 2016).

1.2.1. Milankovitch and non-Milankovitch cycles

Long-term variations result from the gravitational effects that cause the Earth's orbit around the Sun to change over many thousands of years. This in turn causes variation in the amount and distribution of insolation received at the Earth's surface. The three cycles within this astronomical theory of climate are known collectively as the Milankovitch mechanisms, see Figure 1.2.

They are:-

- 1) Eccentricity of the Earth's orbit – Earth's orbit varies from being almost circular to being highly elliptical, over a cyclic period of about 100,000 years. At present, it is almost circular.
- 2) The obliquity of the ecliptic – the degree of tilt of the Earth's axis of rotation. Obliquity varies from about 21.8° to about 24.4° over a period of about 42,000 years. At present it is 23.5° . When obliquity is high, the seasonal range of solar radiation intensity in the respective hemispheres is high.
- 3) Precession of the equinox – the earth's axis of rotation is not upright and wobbles like a spinning top with one revolution completed in about 26,000 years and is known as the precession of the equinox. But as precession is in the opposite direction to the rotation of the earth's orbit, precessional cycles occur less than 26,000 years, averaging about 20,600 years with periodicities of 23,000 and 19,000. Perihelion is when the earth is closest to the sun while aphelion is when it is furthest away from the sun. At present the earth is closest to the sun (perihelion) during the Southern Hemisphere summer (austral summer) with aphelion occurring during the Northern Hemisphere summer (boreal summer). When perihelion occurs during the summer months there is greater seasonal variation with hotter summers and cooler winters and when aphelion occurs during the summer months, summers are cooler with less seasonal variation.

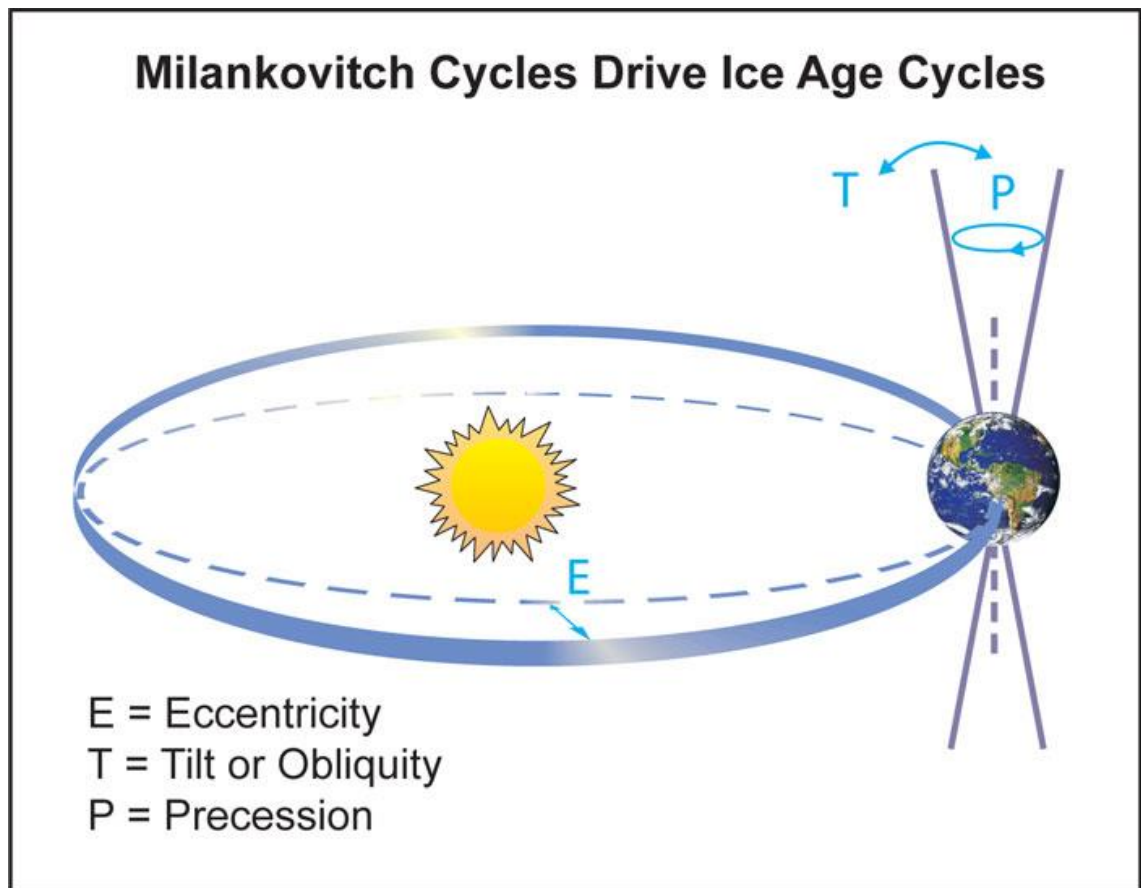


Figure 1. 2. Schematic of the Earth's orbital changes (Milankovitch cycles) that drive the ice age cycles. 'T' denotes changes in the tilt (or obliquity) of the Earth's axis. 'E' denotes changes in the eccentricity of the orbit (due to variations in the minor axis of the ellipse), and 'P' denotes precession, that is, changes in the direction of the axis tilt at a given point of the orbit (after Rahmstorf and Schellnhuber 2006).

These cycles are believed to be the principle mechanism driving glaciation during the Pleistocene epoch (Berger 1978, 1989; Williams, M et al. 1998; Sturman and Tapper 2006; Pittock 2009). The changing oxygen isotope ratio (O^{18}/O^{16}) derived from ice cores in the Arctic and Antarctica provides information on the presence and/or absence of ice sheets which can then be chronologically divided into cold and warm periods referred to as Marine Isotope Stages (MIS) (Martinson et al. 1987; Bintanja et al. 2005; Hodgson et al. 2006; Bintanja and van der Wal 2008). The expansion and retreat of ice-sheets is most clearly defined on the Northern Hemisphere continents (Imbrie et al. 1993; Petit et al. 1999; Lisiecki and Raymo 2005; de Vernal and Hilliard-Marcel 2008; Lang and Wolff 2011) although ice sheets in Antarctica have been both bigger and more extensive than any in the Northern Hemisphere. In areas with limited or no ice-sheet presence, other indicators are used to signify changes in the climate system such as variations in sea-level and sea-surface temperature, altered land:sea ratios and changed continental connections which impact on ocean currents, regional climates and vegetation distributions (Barrows

and Juggins 2005; Reeves et al. 2013a,b; Woodroffe and Webster 2014; Hinestrosa et al. 2016).

Alongside the principal astronomical cycles are millennial scale variations of irregular periodicity. Studies from ice and marine sediment cores from the northern North Atlantic showed significant changes in regional climate characterized by rapid temperature excursions that have been found to be a characteristic feature of Greenland climate during the last glacial period. These excursions are now known as Dansgaard-Oeschger events (D-O events) and occur approximately every 1500 years with abrupt warming followed by a more gradual return to cold glacial conditions (Dansgaard et al. 1984, 1993; Clement and Peterson 2008). During the coldest phases of groupings of D-O cycles, layers of ice-rafted debris were found in sub-polar North Atlantic sediments and are referred to as Heinrich events (H events) (Heinrich 1988; Bond et al. 1993). The time frame of this thesis places it partially within MIS 3 (59.4 ka–29.8 ka) which is characterized by frequent Dansgaard-Oeschger events and MIS 2 (29 ka–15 ka) which are characterized by cooler conditions than MIS 3 and contains the Last Glacial Maximum (LGM) and meltwater pulse (MWP) 1A, 14.6–14.3 ka. MWP 1A is a period where abrupt post glacial sea level rise occurs due to rapid release of meltwater from collapsed continental ice sheets. MWP 1A is the most well-known and least disputed MWP with the highest known rates of postglacial, eustatic sea level rise (Cronin 2012), although the source (Northern Hemisphere or Southern Hemisphere) of this meltwater pulse has not been resolved completely (Deschamps et al. 2012; Golledge et al. 2014). MIS 1 (14 ka – continuing to the present) comprises the late Pleistocene-Holocene transition (MWP 1B and 2) through to the Holocene (Lisiecki and Raymo 2005; Van Meerbeeck et al. 2009).

The best known and studied cold phase during the warming climate of the last deglaciation is the Younger Dryas (YD), an abrupt return to near glacial conditions and identified by some as Heinrich event (H0), lasting approximately a millennium (~12,900–11,700 years BP), and recorded in the high-latitude North Atlantic region (Pearce et al. 2015; Schenk et al. 2018). Within the Southern Hemisphere the most well known deglacial event is the Antarctic Cold Reversal (ACR) which occurs prior to the YD and is defined in Antarctic ice cores as cooling or the termination of deglacial warming ~15 to 13 ka (Jouzel et al. 1995; Pedro et al. 2016).

The causes of these millennial-scale variations and whether they are globally present is not fully understood but there are a number of mechanisms that are thought to play a key role in their initiation. Changes in the internal oscillations of the ocean-atmosphere systems are thought to be a key cause, primarily the thermohaline circulation of the North Atlantic, which transports warm water from the equator towards the North Pole, with this system periodically interrupted by ice-sheet melting and calving and subsequent channeling of continental runoff (Elliot et al. 2002; Schulz et al. 2004; Pearce et al. 2015). It has also been suggested that changes in the tropical Pacific coupled ocean-atmosphere system may also be important with orbitally driven changes fixing the seasonal cycle for several centuries resulting in changes in the sea surface temperature of the tropical Pacific Ocean and these changes would have a global impact (Clement et al. 2001; Turney et al. 2004; Clement and Peterson 2008; Chung et al. 2019) while others suggest it is a combination of changes in the ocean-atmosphere system alongside solar forcing (Bond et al. 2001; Dima and Lohman 2009).

It has been suggested that there is a millennial bipolar seesaw relationship through the latter part of the last glacial period with antiphase temperature anomalies in the two poles. This bipolar seesaw response is considered due to changes in the Atlantic meridional overturning circulation (AMOC), causing a redistribution of heat to the Southern Hemisphere and thereby advocating a Northern Hemisphere origin (Broecker 1998; Alley and Clark 1999; Blunier and Brook 2001; Clark et al. 2002). Alternative suggestions involve atmospheric forcing or that local insolation in the Southern Hemisphere as well as enhanced Southern Ocean convection may be primary causes for these Antarctic deglacial events thereby negating a Northern Hemisphere origin (Moreno et al. 2001; Broecker 2003; Vandergoes et al. 2005; Laepple et al. 2011; Skinner et al. 2020). It is also likely that the combination of these variations and interaction with the atmosphere-hydrosphere-lithosphere collectively or individually changed the frequency, phase and amplitude of the weak astronomical input (Rial and Anaclerio 2000).

1.2.2. Internal forcing factors

Internal forcing factors include the geometry and movement of the lithosphere plates (continental plates) and volcanic events. Although continental movement is a slow process, the drift northward of the Australian continent into subtropical latitudes, that has taken place over several hundred millions years, may have induced threshold changes in

climate through, for example, alternation of atmospheric and oceanic circulations with progressive constriction of the Indonesian Throughflow (Krebs et al. 2011; Auer et al. 2019). Volcanism on the Atherton Tableland commenced at 7.1 Ma and continued into the Early Holocene and, although climate conditions are not known from these early time periods, they would have had a significant impact on regional climate, topography and vegetation. The earliest and largest eruptions involved extensive flows from shield volcanoes (Malanda shield volcano, 3.14 Ma) which filled valley floors and overflowed the escarpment to the east, (see Chapter 2, sub-section 2.1.1). In the last million years the volcanic landscape saw reduced lava flow characterized by cinder cones (<0.5 Ma and 1–0.5 Ma) and maars (<0.5 Ma), see Chapter 2, sub-section 2.1.1 (Kershaw 1980; Whitehead et al. 2007).

Specific volcanic events may trigger short-term climatic fluctuations like the ‘year without summer’ in 1816 experienced in the Northern Hemisphere when Mt Tambora in Indonesia exploded in 1815 and more recently the eruption of Mt Pinatubo (Philippines) in 1991 which caused a temporary cooling over several years. In both these cases the radiative influence of the injected particulate content caused low solar irradiance and circulation anomalies (McCormick et al. 1995; Bradley 2000; Kitzberger et al. 2001; Pittock 2009).

These forcings, Milankovitch and internal, are superimposed on, or modulate "internal" variations of the climate system such as the circulation systems of the Polar regions and oscillations within the Pacific region. These circulatory and oscillating systems work at an interannual and decadal time-scale alongside longer-term time-scales and are the primary source of "natural" climate variability (Bradley 2000).

1.2.3. El Niño-Southern Oscillation (ENSO) phenomenon

Critical to the documentation and understanding of climate variability over much of the Australian region, as well as over a large part of the globe, is the El Niño-Southern Oscillation (ENSO) phenomenon, one of the earth's most dynamic interactions between atmosphere, oceans and continents. This phenomenon is a global scale irregular pressure fluctuation, which particularly affects the tropics (Yang et al. 2018). The Southern Oscillation Index (SOI) is calculated from the pressure difference between Tahiti and

Darwin and is an indication of the strength of the Walker circulation, a major circulation cell that moves air zonally between eastern and western sides of the South Pacific. When the SOI becomes low (negative), El Niño dominates; a strong positive SOI is called La Niña. An El Niño phase is when a weakening of the Walker circulation produces a reduction in the intensity of the trade winds, which decreases ocean water circulation across the Pacific. This, in turn, results in warm water that is normally transported to the western Pacific warm pool (WPWP) region moving back eastwards to the Peruvian coast (Dijkstra and Neelin 1995; Santoso et al. 2019). A La Niña phase occurs when there is a strengthening of the Walker circulation causing heat to concentrate in the western tropical Pacific resulting in an increase in convection within this area. There is also a normal or neutral phase where the Walker circulation is weaker than during La Niña phases and although still functioning other climate phenomena such as the Indian Ocean Dipole (IOD) maybe influential (BOM 2019). At a regional scale, SOI correlates with changes in the location and strength of the South Pacific convergence zone (SPCZ) and the Intertropical convergence zone (ITCZ) which are both important energy sources for the Walker circulation. The SPCZ shifts (diagonally) from the more central position in the Pacific during the warm phase of ENSO (El Niño) to the eastern Australian coast during La Niña (Salinger et al. 2014), while the ITCZ shifts further south (north) during austral summer when La Niña (El Niño) is present although other factors such as the strength of the IOD and sea surface temperatures may also contribute to these latitudinal shifts (Zhang et al. 2009; Freitas et al. 2017).

Within the last few decades, ENSO has been recognised as the single most important determinant of variability in global precipitation fields (Dai et al. 1997; Dai and Wigley 2000; Santoso et al. 2019). Within the Australasian region 30–60% of the annual precipitation variance is explained by ENSO and there is a positive link to the Australian summer monsoon and tropical cyclone activity. El Niño events see the late onset of the monsoon while early onset tends to precede El Niño events, and El Niño is also responsible for extended drought periods in Australia that contribute greatly to an increased incidence of bush fire. During high positive phases of the SOI (La Niña), tropical cyclones develop closer to the northeastern coast of Australia (Sturman and Tapper 2006).

It has been suggested that phase activity of the Southern Oscillation includes a quasi-periodicity in the range of two to ten years with ENSO events lasting from 18 to 24 months (Sturman and Tapper 2006). However, recent protracted El Niño events suggest that ENSO periodicity has varied throughout the time-period covered by the historical instrumental record. Research has found that 'persistent' El Niño events are not rare and there is a decadal-multidecadal signal in the ENSO record (Allan and D'Arrigo 1999; McGree et al. 2016). It is considered that these frequency fluctuations are poorly understood and most likely to be linked to other features of the global climate system and that recourse to reconstructions based on longer proxy records is necessary for reliable predictive outcomes in the future.

To date there have been relatively few investigations of longer term or palaeo ENSO variability in Australia, and most of these have been focused on the Holocene period, although Tudhope et al. (2001) suggests evidence of ENSO for the past 130,000 years indicated from annually banded corals from Papua New Guinea. Decadal to annual resolution has been achieved from fossil corals within tropical regions where changes in sea-surface temperature (SST) and salinity (precipitation) can be attributed to single ENSO events. This has made it possible to interpret discontinuous fossil coral records from the Great Barrier Reef dating from 6200 years ago with results suggesting that the mid-Holocene El Niño events in the Greater Barrier Reef were ~20% weaker than the present-day strong El Niño events (Gagan et al. 2000, 2004). However, the discontinuous nature of these records does not allow for the full expression of climate variability.

Although most palaeoclimate records from the Australasian region are of a relatively coarse resolution, some climatic conditions within the Holocene period may be suggestive of ENSO-like activity (Beck et al. 2017; Barr et al. 2019). McGlone et al. (1992) suggest that drier conditions within Australasia for the early Holocene may indicate a more negative phase for the Southern Oscillation although other factors such as lower sea-levels and therefore greater continentality would have also contributed at this time. However drier conditions have been suggested for the mid-Holocene (5000–7000 yr BP) for northern Australia with McGowan et al. (2012) suggesting that a 1500 yr mega-drought during this period was caused by ENSO resulting in the collapse of the Australian summer monsoon. In arid south-central Australia speleothems indicate that precipitation was more effective during the early Holocene (c. 11.5 and c. 8–5 ka) (Quigley et al. 2010).

A more extensive analysis of data from the Northern and Southern Hemispheres found that ENSO was generally dampened during the early to mid-Holocene (White et al. 2018). From 5000 years B.P. variability within records are evident (Moy et al. 2002; Gagan et al. 2004; Turney and Hobbs 2006; Donders et al. 2007, 2008; Rees et al. 2015) and from 3000 years B.P. factors that coincide with present-day ENSO activity become apparent (Shulmeister and Lees 1995; Barr et al. 2019) although spatio-temporal variability is evident (Turney et al. 2017).

Within the Australasian region, millennial scale changes have been suggested from a marine sediment core taken from the eastern edge of the Indonesian archipelago where temperature and salinity were reconstructed from planktonic foraminifera for the past 70,000 years (Stott et al. 2002). Results suggest that the ENSO mode may have been active throughout this time with El Niño-like conditions, which correlate with stadials and La Niña-like conditions correlating with interstadials at high northern latitudes. It is further suggested that millennial scale changes within the ENSO mode are similar to high latitude Northern Hemisphere records which may indicate that climate forcing leading to marked temperature variation in the North Atlantic originated from the tropical Pacific region. Turney et al. (2004) found that millennial-scale dry periods based on the degree of peat humification and the ratio of sedges to grasses, taken from a continuous sediment core from Lynch's Crater north-east Queensland spanning 45,000 years, may indicate periods of frequent El Niño events. They suggest that climate variations in the tropical Pacific Ocean on millennial and orbital scales are likely to have had a global influence on climate in the past and could do so well into the future.

Orbital scale variability in ENSO activity has also been suggested from the study of long marine records in the Australasian region. Although the main Milankovitch frequencies have an overall importance in terrestrial proxies recorded in four marine cores taken around the northern perimeter of Australia spanning the last 100–300 ka, there is a 30 ka cyclicity reported in charcoal particles as well as pollen of those taxa susceptible to burning (Kershaw et al. 2003). This frequency has also been reported from nine deep-sea cores taken along the equator in the Indian and Pacific oceans and, as with the marine cores from Australia, an ENSO driven modification of the precession cycle is seen as the likely cause (Beaufort et al. 2001). The longevity of ENSO-like activity has also been demonstrated in annually banded coral from raised reef terraces on the Huon Peninsula,

Papua New Guinea, dated from 2.5 ka through to 130 ka intermittently (Tudhope et al. 2001). All fossil corals showed well preserved seasonality and all showed, in varying degrees, typical ENSO-like frequency bands. The results suggest that ENSO has been a persistent component of the climate system over the past 130 ka and Tudhope et al. (2001) consider that the precession cycle of orbital forcing may determine the degree of ENSO variability. Clement et al. (1999) used a coupled ocean atmosphere system with precessional forcing to model ENSO activity over the past 150 kyr using the present day frequency of ENSO events in the tropical Pacific region. The results reinforced interpretations of the proxy studies that ENSO has been in existence over at least the last glacial cycle and that there may have been up to 150 El Niño type events in any given 500-year period over this interval. The coupled ocean atmosphere model is relatively simplistic and limited to the Pacific region which limits its interpretation to the broader region. More recent Earth System models provide a more total environment outcome as they can stimulate multiply cycles, carbon, nitrogen, atmospheric chemistry, ocean ecology and changes in vegetation and land use as well simulating soil microbial processes, providing more realistic outcomes both regionally and globally (Wieder et al. 2015; Hausfather et al. 2019).

However, the complexity across the climate systems (atmosphere, hydrosphere, cryosphere, lithosphere and biosphere) and climate forcing mechanisms are not uniform and may differ across marine and continental environments. A review by Leduc et al. (2009) compared marine sediment cores from key areas in the northeast and northwest tropical Pacific Ocean with the continental record from Lynch's Crater, in the southwest Pacific. There was synchronicity between the marine records with wetter conditions during D-O interstadials and drier periods during D-O stadials and H events. The response from the terrestrial record, Lynch's Crater, surmised from Muller et al. (2008b), was the opposite to that found in the marine records, with wetter conditions found during D-O stadials and H events and drier conditions found during D-O interstadials. Leduc et al. (2009) suggest that it is the positioning of the ITCZ that is a key component of climate variability within the area and conclude that it is this latitudinal reversal which indicates that changes in the ITCZ seasonal cycle maybe a greater contributor to millennial-scale climate changes than ENSO (Leduc et al. 2009).

Studies on fossil corals from Indonesia and Papua New Guinea also found that the ITCZ is an important component of climate variability in the region (Abram et al. 2009). The positioning of the ITCZ dictated whether the Indo-Pacific Warm Pool (IPWP) expanded or contracted within the southeastern and southwestern margins of the IPWP and had a major influence on the three climate systems, ENSO, Asian-Australian monsoon and the Indian Ocean Dipole (IOD), operating within this region. The IOD produces upwelling events which can produce cool SST anomalies greater than 4°C (Chen et al. 2016). Interaction between the Asian-Australian monsoon and the IOD and the Asian-Australian monsoon and ENSO are well known. However, there is also an interaction between ENSO and the IOD and, like the other climate interactions, these influences are likely found on both centennial and millennial scales (Webster et al. 1998; Liu et al. 2003; Ashok et al. 2004; Kumar et al. 2006; Abram et al. 2007).

1.3. The Human Factor

Within northern Queensland, the earliest known human occupation sites are west of the Great Dividing Range with the oldest at Ngarrabullgan Cave dated to $35,460 \pm 750$ /-690 ^{14}C yrs BP ($40,540 \pm 650$ yr cal BP). This site is 80 km northwest of the Atherton Tableland, and although occupation was limited, it is suggested that even a small number of people through their use of fire may have had a catalytic impact on the vegetation (David et al. 1998). Around Lynch's Crater and possibly nearby Strenekoff's Crater, the replacement of araucarian forest by sclerophyll vegetation from about 45,000 years ago is attributed to human burning (Kershaw 1994; Kershaw et al. 1997). A fine resolution study was undertaken at Lynch's Crater within the time-frame 35,000 to 45,000 years B.P. in an attempt to decouple the relative influences of climate and people on the vegetation change at this site (Rule 2001). The study established that there was marked variability in climate as deduced from variation within the swamp community, not detected previously (Kershaw 1986) that may have initiated change, but a human cause could not be ruled out. Recent research from Lynch's Crater found that from ~41,000 ka the increased fire activity was most likely due to human influence and was related to the demise of the megafauna (Rule et al. 2012; Johnson et al. 2015). These dates are consistent with current generally accepted archaeological dates for the arrival of people on the continent (O'Connell et al. 2018) and therefore provide support for these scenarios. Although a much earlier date, 65,000 years ago, for human arrival has been given for Madjedbebe rock shelter in northern Australia (Clarkson et al. 2015, 2017). It has been

suggested that downward movement of the dated artifacts could have occurred and thereby the radiometric (OSL) ages are older than the artifacts they contain (O'Connell et al. 2018).

Palynological research on the marine palynological record of ODP Site 820, east of Cairns, does support the Lynch's Crater evidence, in general, for a decline in araucarian forest relative to sclerophyll vegetation and an increase in burning around 40,000–45,000 years ago but, in contrast, suggests that the araucarian forest decline had began long before the time of human arrival. It is suggested that the development of the WPWP north of this region and an associated increase in ENSO variability may have been influential in this decline (Kershaw 1994; Thunell et al. 1994; Zhang et al. 1997; Moss and Kershaw 2000). The study from ODP Site 820 clearly implies that a complex relationship exists between climate, vegetation and fire within the region.

Some indication of the spatial pattern of representation of sclerophyll vegetation on the Atherton Tableland in relation to fire is provided by the study of the presence, age and identification of soil charcoal in present-day rain forest areas (Hopkins et al. 1990). All charcoal was identified as *Eucalyptus* occurring between 27,000 and 8,000 years ago. Although no ages approach 40 ka, this is not unexpected as it was drier araucarian forest at Lynch's Crater rather than the wetter forests that was being replaced by sclerophyll vegetation in the Hopkins et al. (1990) study. The survival of sclerophyll vegetation in such areas as late as 8 ka supports also the proposal from the palynological records on the Tableland that human activity resulted also in the retardation of Holocene rainforest expansion within this region (Ash 1988). The suggestion of Aboriginal influence on the Tableland extends to palynological evidence from more recent times with the destruction of swamp forest on the surface of Lynch's Crater about 4500 years ago (Kershaw (1983a), an event that corresponds with evidence for increased intensification of human settlement at Ngarrabullgan and, in fact, at many other Australian archaeological sites (Lourandos and David 2002). However, there is still uncertainty as to whether Indigenous peoples were able to exploit rainforest environments at this time (Yen 1995; Cosgrove 1996). The timing of these mid-late Holocene changes also correspond with evidence for increased climatic variability, attributed to ENSO (McGlone et al. 1992; Turney and Hobbs 2006; Donders et al. 2007, 2008; Rees et al. 2015; Barr et al. 2019) and it has been suggested that this was the trigger for social change, which saw populations forming into territorial

regional groups and a broadening of the range of foodstuffs consumed (Haberle and David 2004).

1.4. Fine Resolution Palynology

A short summary of the proxies that will be used in this study and their attributes will follow this introduction to fine-resolution palynology. Fine-resolution palynology arose out of the need to bridge the gap in time scale between palaeoecology and field ecology with sampling intervals reduced from then conventional millennial scale down to centennial to sub-centennial and further down to decadal, or even sub-decadal scales (Green and Dolman 1988; Green et al. 1988). This may have allowed for key landscape processes at a local scale to be detected such as stand dynamics within a tropical rainforest. Chen (1988) found in his study on a pollen record from Lake Barrine on the Atherton Tableland, that canopy angiosperm trees and emergent gymnosperms have a turn-over rate above 100 years. However, most secondary species, which utilise gap openings, have a turn-over rate of less than a hundred years and in some cases only several decades. This would suggest that sub-centennial to decadal sampling is needed to detect changes in secondary species. However, it does imply that centennial sampling should make it possible to verify or quantify stand dynamics within a tropical rainforest through changes seen in key canopy and emergent species. Although the aim of fine resolution palynology is to bridge the temporal gap between palaeoecology and actuoecology, many studies have focused instead on simply reducing the sediment sampling interval with timescales being of secondary importance. The value of this approach, especially if sediment sequences are sampled contiguously, is that temporal information gaps are avoided. This is the approach adopted in this thesis.

Common obstacles inherent in coarse resolution studies also apply to fine resolution studies (Green 1983; Ritchie 1995; Birks and Birks 2000, 2006) such as:-

- random errors from sampling, processing and counting
- changes in pollen production
- changes in the sedimentation rates and patterns
- spatial diversity of the pollen sources

The presence of sediment mixing becomes more likely the finer the resolution. However, sediment re-working is usually not substantial in catotelm peat (bottom layer) but maybe present in acrotelm peat (upper layer) which allows water and pollen to move vertically within little decomposed vegetation (Ivanov 1981; Joosten and de Klerk 2007). But sustain climate variability, varying sediment accumulation rates and complex hydrological and depositional conditions may present problems (La Moreaux et al. 2009; Leng et al. 2019). However, it has been suggested that the amorphous humic- and pectin-rich gel constituents formed by the decomposition of plants on a swamp provide an efficient particle-trapping mechanism (Green et al. 1988). This allows pollen grains in peat to maintain their stratigraphic position under relatively constant climate conditions irrespective of subsequent changes in the water table (Malmström 1923; Rowley and Rowley 1956; Godwin and Willis 1959; Polach and Singh 1980; Clymo and Mackay 1987).

Improved dating techniques provide the means for good chronological control which has certainly been the case for Lynch's Crater which has been found to have stratigraphic integrity with generally continuous and constant (well dated) deposition through long periods of time (Kershaw 1976, 1983*a*, 1985; Turney et al. 2001*b*; Muller et al. 2006, 2008*a*). Once a robust chronology has been established then more detailed statistical analyses becomes possible. Relationships between and across different plant communities can be verified with multivariate analyses such as Principle Component Analysis (PCA), while Milankovitch and sub-Milankovitch and millennial to centennial scale cycles can be verified with time series analyses.

The stronger ecological signal that is achievable with these refinements can be further enhanced when a multi-proxy approach is employed. The benefits of combining both biotic and abiotic elements allows for a more multi-dimensional approach with each proxy having its own unique position in the ecosystem and therefore used to reconstruct different facets in the palaeoenvironment (Birks and Birks 2006). The next section will give a brief summary of the proxies that will be used in this study and their attributes except for macroscopic and microscopic charcoal which will be discussed in more detail in Chapter 4.

1.4.1. Pollen

Palynologists analyse fossil pollen and spore assemblages as their primary means for reconstruction of palaeoenvironments, increasingly with the addition of charcoal analysis in order to investigate the role of both natural and anthropogenic fire in the explanation of vegetation and climatic variability and change (Bradley 1999; Conedera et al. 2009; Power et al. 2010; Scott 2010; Graves et al. 2019). The analysis of charcoal is an important component of this thesis and will be looked at in more detail within its own chapter. In a simplistic version of events, pollen is dispersed from local and regional sources and, where deposited on swamp or lakes surfaces, becomes incorporated into accumulating sediments. Samples of it are then extracted at intervals through a sediment sequence, identified, counted and results portrayed on a pollen diagram and interpreted basically in terms of the vegetation that produced it and inferences made about the causes of vegetation change (Faegri and Iversen 1975; Moore et al. 1991).

1.4.1.1. Pollen Production and Dispersal

In analysing fossil pollen records the palynologist must be aware of the disparity between the proportion of species contributing pollen and the final representation of those taxa in the pollen rain. The mode of transport, the number of grains produced by each species, the size of each grain and its degree of robustness influence the outcome of final representation in the pollen record. Although these factors are fairly well understood in temperate floras, in the tropics much less is known about pollen representation. The very factors that make a tropical setting unique—huge species diversity, complex canopy structure, evergreen growth habit and the dominance of entomophily (insect pollination)—has led to the assumption that the feasibility of determining evolutionary, palaeoclimatic and biogeographical outcomes from tropical fossil pollen spectra is problematic but not insurmountable (Faegri and Iversen 1975; Bush 1995, Bush and Rivera 1998).

Extensive research undertaken on modern pollen influx in north-east Queensland has greatly alleviated some of the uncertainties in the research of tropical fossil pollen within the study site area. Lake surface trapping studies, studies within rainforest plots to assess pollen transport within the canopy and trunkspace and also a pollen trapping study traversing herbaceous/woodland through to rainforest to assess the degree of pollen transport through these vegetation types have greatly improved our understanding of

pollen dispersal and deposition within rainforest areas (Kershaw 1973; Kershaw and Hyland 1975; Kershaw and Strickland 1990; Kershaw and Bulman 1994; Walker 2000; Walker and Sun 2000). Although the outcome of these studies found that pollen production and dispersal for rainforest is generally low, it did find that some top canopy and emergent taxa carried much of the information needed for community classification and establishment of environmental relationships, see Chapter 3, section 3.1 for details (Kershaw and Bulman 1994). As proposed by Bush (1995) and Bush and Rivera (1998), it is likely that these taxa utilize small generalist insect pollinators that are essentially the equivalents of the anemophilous (wind pollinated) taxa that have largely been responsible for the successful application of palynology within traditional temperate environments. It has also been suggested that the smooth exine surface of the pollen of some rainforest taxa, such as some *Syzygium* spp., (Myrtaceae family) which are primarily insect/animal pollinated may be facultatively wind pollinated (Boulter et al. 2005) a feature that is shared with myrtaceous sclerophyll eucalypts.

1.4.1.2. Pollen Influx across stratigraphical sequences

In tracing vegetation composition through time, palaeoecologists look at the variation in the vegetation usually indicated by the percentage (relative abundance) of each pollen taxon through the time sequence studied (Hicks and Hyvärinen 1999). However, if one wants to track the absolute abundance of a particular species i.e. the number of pollen grains falling on a unit area of sediment in a given time or its pollen influx (Davis 1969), may be able to do this more accurately (Desprat et al. 2003). Although fossil pollen influx values from stratigraphical samples are more susceptible to uncertainties in pollen recruitment and time dimension a relatively reliable sedimentation rate (well dated) provides more confidence in the resulting pollen influx (Hicks and Hyvärinen 1999; Wilmhurst and McGlone 2005a). The relative heterogeneity of peat sediment, change in peat type, compaction or change in outside input, may present particular problems with changes in sedimentation rate especially at annual to decadal resolution although this is likely to be averaged out as the temporal resolution is lowered (Hicks and Hyvärinen 1999; Grindean et al. 2019).

1.5. Macrofossils and Non-pollen Palynomorphs

Plant macrofossils comprise diaspores (seeds, fruits, spores), and vegetative parts including, leaves, buds, flowers, rhizomes, roots, tissue fragments, bark and wood and lower-plant remains include sporangia, megaspores and Characeae oospores. The identification of fossil plants by their macroscopic remains goes back to the late 19th Century when Heer and others published detailed descriptions and drawings of fossil plant remains with the earliest detailed studies of fossil floras from the Quaternary based on plant macrofossils (Heer 1862; Dawson 1866, Warner 1988). However, with the publication of Von Post (1916) which showed that pollen could not only be used as a stratigraphic tool but could also track the immigration of plant species and their relative numbers, stand-alone studies on plant macrofossils declined. Although both techniques were used in studies, pollen analysis became the more prominent technique (Warner 1988; Birks and Birks 2000). However, by the 1970s there was resurgence in macrofossil analysis as some limitations of pollen analysis became evident and, with improvements in macrofossil quantitative techniques which allowed a more detailed and precise interpretation, stratigraphic presentation alongside pollen data was possible (Grüger 1972; Van Zant 1979; Spicer 1989; Birks 2003). From these works many have concluded that the two techniques should be used in a complementary manner in palaeoecological reconstructions (Birks 1973; Birks and Birks 2000, 2006). Like pollen the modern processes of dispersal, deposition and sedimentation of macrofossils within lakes and swamps are important considerations but, unlike the majority of pollen grains especially in a tropical environment, it is frequently possible to identify plant macrofossils to species level allowing for a more precise ecological interpretation (Birks and Birks 2000, 2006; Birks 2003, 2017; Vălıranta 2006, Vălıranta et al. 2015; Bennion et al. 2018). The relatively large size of plant macrofossils also determines that transport is usually limited and presence indicative of local origin. However other factors such as sediment type, lake sediments or peat deposits, climate conditions as well as the robustness of the plant itself and seed production may also influence whether macrofossils will be present (Collinson 1983; van Bergen et al. 1994; Kidwell 2001; Davidson et al. 2005; van den Broek et al. 2005; Cadd et al. 2018; Clarke 2019).

1.5.1. Sediment type and transport

In a peat deposit, macrofossils are usually indicative of local presence although, depending on the size and area of the deposit, transport across different habitats within

the peat deposit itself is possible (Singer et al. 1996; Alexander et al. 1999; Pisaric 2002; Vogt et al. 2004; Ferguson 2005). Transport potential is also influenced by the size and unique characteristics of the macrofossils. Like pollen, most seeds or fruit components have adaptations that aid dispersal; wings and parachutes for wind dispersal, burrs and spines for external dispersal by animals; succulent parts for internal animal dispersal (Cappers 1993; Birks 2007). In wetlands, wildfowl are important agents for dispersal while in tropical Australia the Cassowary (*Casuarius casuarius*) is the only frugivore that is large enough to effectively disperse many of the rainforest plants in northern Australia (Stocker and Irvine 1983), while sculpture and size of seed and density of tissue dictate the potential for water dispersal (van den Broek et al. 2005). The main dispersal vector for the Cyperaceae family is water, with many species having buoyant seeds, while animals are a secondary dispersal agent (Leck and Schütz 2005).

1.5.2. Production and Preservation

Different plant organs have differing preservation potentials depending on chemical and tissue composition and the structure of their physical, chemical and biological environment at the time of deposition with sampling methods then having a further impact on the final result. Taxa with more soft or perishable parts are likely to be under-represented, for example the fragile spikelets of *Poa* spp., while over-representation is likely for taxa that have many components which break into numerous identifiable fragments. Like pollen there is a great deal of variability in seed production. The robust nuts of some Cyperaceae species such as *Eleocharis* may suggest that preservation should be high, however seed production in some rhizomatous species is low (Holyoak 1984; van Bergen et al. 1994; Beaudoin 2007).

While *Typha* has both abundant pollen ($174\text{--}420 \times 10^6$) and seed production ($363\text{--}682 \times 10^3$), the pappus and lightness of the seed means that it is easily carried by wind and may be transported many kilometres (Finlayson et al. 1983; Parsons and Cuthbertson 2001). This could suggest the presence of *Typha* seeds may not guarantee local deposition, but both the high predation and success rate of seed germination may limit the presence of fossil *Typha* seeds (Finlayson et al. 1983). Palynological studies suggest that the consistent presence and high values of *Typha* pollen would indicate a local presence (Head and Stuart 1980; Bickford and Gell 2005). A common denominator for some aquatic/swamp plants, especially the large monotylenous species, is the change

to vegetative reproduction which may have impacts on the fossil record as both pollen, seeds and nuts could be underestimated or absent during these periods (Leck and Schütz 2005).

1.5.3. Non-Pollen Palynomorphs

Non-pollen palynomorphs (NPPs) or extra microfossils composed of organic material include fungal remains, especially spores, algal remains, testate amoebae, invertebrates (appendages, eggs and casings) and remains of vascular plants. Peat sediment is an ideal environment for NPPs especially fungal and algal remains, with particular genera indicative of hydrological conditions on the surface and, in the case of dung fungi, allows quantity estimates of mammalian herbivores (Davis and Shafer 2006; Raper and Bush 2009; Etienne et al. 2013; Gill et al. 2013; Baker et al. 2016; Johnson et al. 2015, 2016). Extensive studies by van Geel (1978, 1986; van Geel and van der Hammen 1978; van Geel et al. 1981, 1989, 1995) in the Netherlands and Colombia has provided a ready reference guide for palaeoecologists for NPPs. These studies have provided baseline information of NPPs with descriptions and illustrations of the NPP types and suggested indicator value, including morphological descriptions along with stratigraphic information (van Geel 2001). The list of NPPs has continually been updated as new studies provided both a greater geographical distribution of NPPs but also provided information on new NPP types (Richardson 2001; Rumes et al. 2005; Medeanic 2006; Limaye et al. 2007; Mumbi et al. 2008; Rull et al. 2008; Gelorini et al. 2011; van Geel et al. 2011). Although there are many taxa that have not been properly identified, ecological information can be inferred from the co-occurrence (curve matching) with identified taxa and other microfossils such as pollen (van Geel 1978, 1986, 2006). The majority of NPPs can be counted alongside pollen although there may be a differential resistance against decomposition with the outcome that the more robust and resistant types dominate as is seen with pollen (Havinga 1984; Campbell and Campbell 1994; Prager et al. 2006).

1.5.3.1. Fungal Spores

Most fungi live as either parasites of plants or animals where they frequently cause disease or as saprophytes where they obtain nutrition from dead or decaying organic matter. They can have a symbiotic relationship with certain plants but the vast majority live as saprobes, that is, along with bacteria and animals, they break down the complex plant and animal remains in the soil. Various studies have found that fungal spores are

predominately of strictly local occurrence, being fossilized at, or near where they were produced (van Geel et al. 1989, 1995, 2011; Medeanic and Silva 2010). Fungal spores and fruiting bodies exhibit great diversity and therefore are useful structures for distinguishing different species. The spores of dung fungi, *Sporormiella*, *Podospora* spp., and *Sordaria* spp., have been increasingly used to verify the presence of domesticated livestock but also the presence and absence of megafauna (Davis 1987; Burney et al. 2003; Davis and Shafer 2006; Graf and Chmura 2006; Gill et al. 2009, 2013; Raper and Bush 2009; Rule et al. 2012).

An important aspect of the present study is the role of fire in the fossil record. The spores of *Neurospora* (Sordariaceae) have found to be a local fire indicator (see Chapter 4, subsection 4.2.3) with germination occurring after induction by fire and are primary colonisers of trees and shrubs killed by forest fire. They are universally found in both cold and dry temperate regions as well as humid tropical and sub-tropical regions (Turner 2001; Turner et al. 2001). Another member of the Sordariaceae family, *Gelasinospora*, has been primarily found in highly decomposed peat under relatively dry conditions and often found in layers with charred material. *Gelasinospora* species are predominantly found in the soil (terricolous) with a few fruiting on burnt areas (carbonicolous) or wood (lignicolous) and are frequently collected from tropical and subtropical regions (Krug et al. 1994). All *Gelasinospora* species have been recently re-classified and are now included in the genus *Neurospora* (García et al. 2004). The record of these two fungal spores, *Neurospora* and *Gelasinospora*, have been noted in this thesis and for practical purposes these two will be separated as there are distinct ornamentation differences between them and, from the current literature it is suggested that there may be ecological differences (Lundqvist 1972; van Geel 2006) although a more recent study has suggested that both fungal ascospores are indicators of fire (Stivrins et al. 2019).

1.5.3.2. Algal Remains

Algal remains have been found to be useful for the reconstruction of temperature, depth, salinity, pH and nutrient status of past aquatic environments. The most commonly encountered in fossil records are the coccal green algae, *Pediastrum* and *Botryococcus*, but the zygospores of *Zygnema*, *Spirogyra* and *Mougeotia* as well as *Pseudoschizaea* (*Concentricystis*) may also be encountered (Jankovská and Komárek 2000; Medeanic 2006; Medeanic and Silva 2010; Medeanic et al. 2010; Montoya et al. 2010).

Botryococcus is the only algae counted alongside the pollen in this thesis. *Botryococcus* can be found in both deep and relatively shallow water and its ability to store large amounts of food and its resistant to desiccation allows it to withstand changing environmental conditions (Guy-Ohlson 1992; Medeanic 2006). Studies have found that, when there have been extremely low counts of pollen and spores, *Botryococcus* has dominated indicating the presence of drought (Medeanic and Silva 2010; Medeanic et al. 2010). Although *Pseudoschizaea* was not counted here, its presence was noted. It has been suggested the presence of *Pseudoschizaea* could be an indicator of warm climates with seasonal drying (Scott 1992; Mudie et al. 2010).

1.5.3.3. Biogenic Silica

Wetlands are abundant in amorphous silica with diatoms (unicellular eukaryotic organisms), phytoliths (opal-silica bodies) and sponge spicules (skeletons of freshwater sponges) the most well-known silica containing materials. Diatoms, phytoliths and sponge spicules can all be found in peat sediment but the higher aluminium content found in sponge spicules make them significantly more resistant to dissolution (Conley and Schelske 1993; Schwandes and Collins 1994). Although phytoliths, diatoms and sponge spicules were not counted in this thesis their presence was noted (see Chapter 5 Materials and Methods for detail). Peat formed from grasses and sedges contain up to 30% phytoliths and a minor component of diatoms and sponge spicules (McCarthy et al. 1989). Studies in peat wetlands of the Swan Coastal Plain (Western Australia) found that sponge spicules and fragments may constitute up to 10% of wetland sediment (Semeniuk and Semeniuk 2004). It has also been found that concentrations of phytoliths and diatoms in the uppersoil/sediment layer make them susceptible to entrainment by fluvial and aeolian processes (Street-Perrott and Barker 2008).

1.6. Project Aims

The aims of this high resolution record are :-

- 1) primarily to reconstruct a detailed vegetation and environmental history from pollen, charcoal and associated analyses of contiguous samples from a peat sediment core from Lynch's Crater, north-east Queensland through a substantial period of the last glacial/interglacial cycle.

- 2) to investigate cycles of orbital to sub-millennial frequency and identify those that may be significant in forcing vegetation, biomass burning and climate changes in tropical north-east Queensland through the last c. 50,000 years.
- 3) to determine nature and extent of fire, as determined from micro- and microcharcoal analysis, in order to assess the potential human influences on the landscape that include testing previous suggestions of marked impact causing or associated with the demise of moist rainforest at the expense of sclerophyll, vegetation, and possible retardation of the Holocene expansion of present dominant wet rainforest.

1.6.1. Thesis structure

Chapter 2 provides the geographic setting of the study area and incorporates the geology, physiography, soils, climate and vegetation. Chapter 3 summarises previous palynological and sedimentological research as well as relevant archaeological studies on the Tableland. Chapter 4 examines fire and its by-products especially charcoal and how charcoal is interpreted in the fossil record within the Australasian region. Chapter 5 is the materials and methods chapter and includes all field, laboratory and statistical methods used in this study. It includes some results from the experimental burns as these results dictate the methods to be used for the macrocharcoal analysis. Chapter 6 presents the chronology and the methods used to produce it. Chapter 7 focuses on the pollen, macro- and microcharcoal, macrofossils, sedimentary and lithological results and also includes observational data. Chapter 8 includes all results from the statistical analyses, and some preliminary discussion of them. Chapter 9 and Chapter 10 present the major discussion and conclusions respectively.

Chapter 2

Humid Tropics of north-east Queensland

Introduction

The humid tropics region of north-east Queensland, (Figure 2.1) lies within the bounds of latitudes 15° and 19°S and longitudes 145° and 146°E. It contains the largest and most diverse expanse of rainforest in Australia (Williams et al. 1998) and encompasses the Wet Tropics, an area designated as a World Heritage Site. The study site, Lynch's Crater (17°37'S, 145°70'E), is located on Atherton Tableland, within the humid tropics, which has been greatly transformed due to extensive agricultural land use during historical times although small pockets of remnant rainforest are protected in national parks. This chapter will examine the diverse geological, physiological, climate and vegetation features of the humid tropics especially those that are deemed to be influential as indicated from past palynological studies on Atherton Tableland.

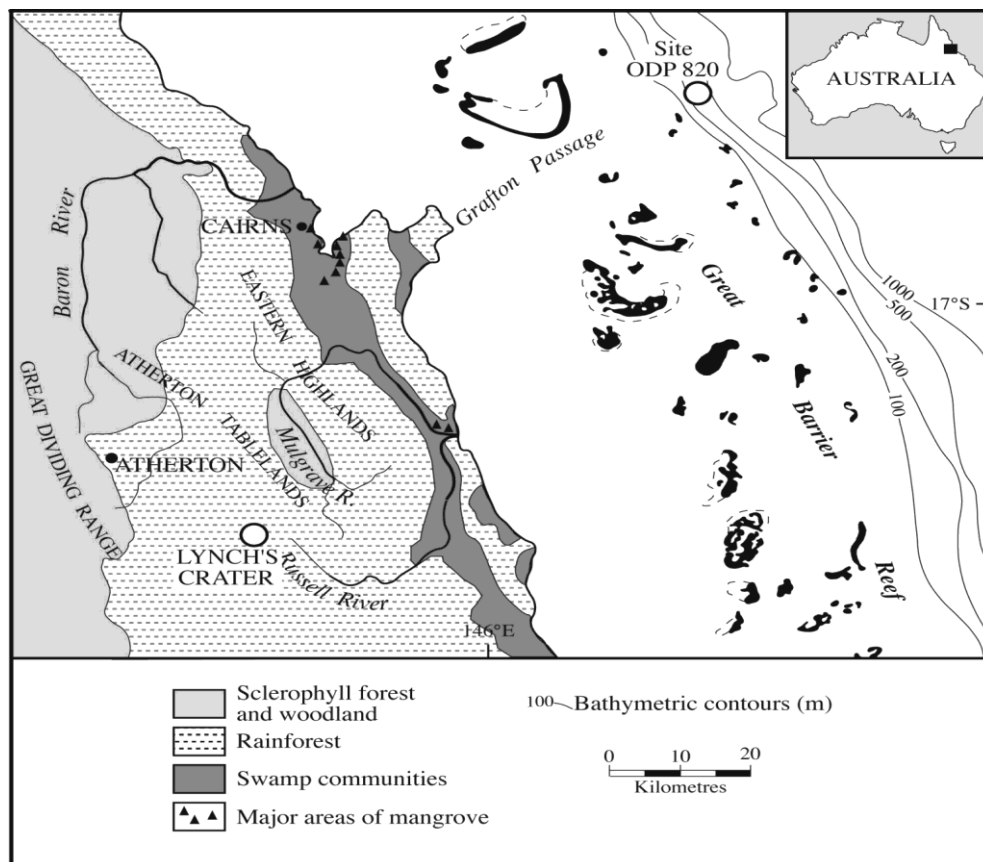


Figure 2. 1. Location of Lynch's Crater and ODP site 820 in relation to major environmental features of the humid tropics, northeast Queensland (after Kershaw et al. 2007a).

2.1 Geology

The geology of the humid tropics is shown in Figure 2.2. The oldest rocks within this area are the Barron River and Bernard metamorphics in the Hodgkinson Basin and are part of the Palaeozoic Tasman Geosyncline that was active during the Middle Devonian to Early Carboniferous. During the Carboniferous orogeny massive to thin-bedded arenites with intercalated bedded cherts, basic volcanics, conglomerate, inter-formational breccias and rare limestone lenses were folded and metamorphosed with igneous masses intruded during the Carboniferous and Permian. Volcanic activity was also active along Precambrian faults that were rejuvenated during the Palaeozoic and formed what are now known as the Glen Gordon Volcanics. The collision of the Australian and Asian continental plates during the middle Tertiary resulted in uplift and warping which resulted in major faulting in the late Tertiary. Further uplift and warping resulted in Atherton Tableland and the subsidence of the continental shelf and coastal plains (Best 1960; Best et al. 1960; Morgan 1968; Stephenson et al. 1980; Bultitude et al. 1997).

The dominant rock types are basalt, granite, low-grade metamorphics (mainly schist and phyllite) and acid volcanics (mainly Rhyolite). While basalt is the most extensively occurring rock type across Atherton Tableland, it is underlain by Lower Permian/Upper Carboniferous metamorphics. Middle Palaeozoic granites dominate the Bellenden Ker Ranges (eastern/central highlands) while a mixture of Lower Permian/Upper Carboniferous metamorphics and Tully and Mareeba granites dominate the Herberton Highlands. Quaternary alluvium dominates the coastal plains but occurs throughout the area with beach sands eroded from the highlands and outcrops of Tully and Mareeba granites forming the coastal ranges (Kershaw 1973; Stephenson et al. 1980; Bultitude et al. 1997).

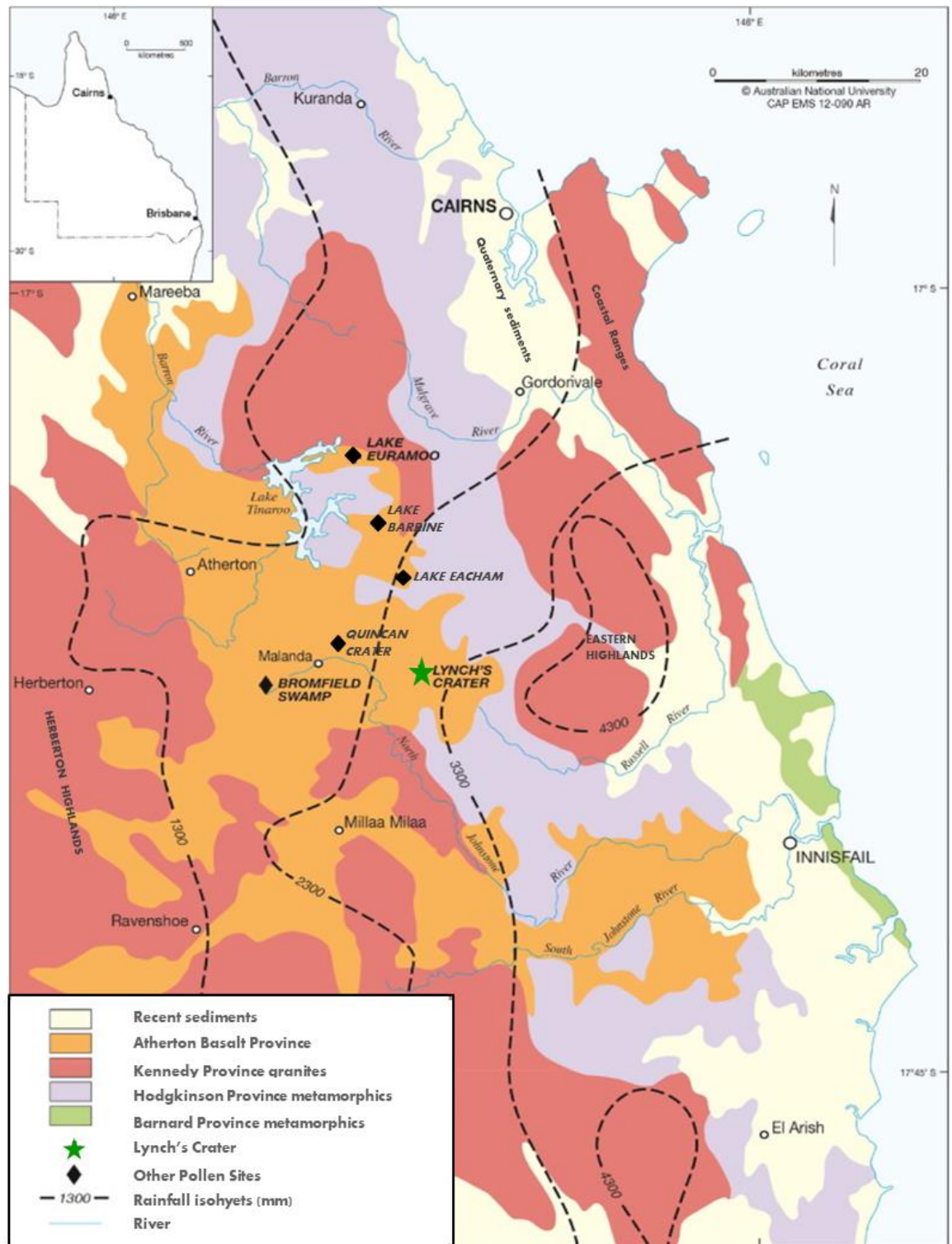


Figure 2.2. Geology of the Humid Tropics and location of Lynch's Crater and other major pollen sites on the Atherton Tableland. Rainfall isohyets are illustrated (adapted with permission from Burrows et al. 2016).

2.1.1. Atherton Basalt Province

The distinct basalt-capped plateau of the Atherton Basalt Province on Atherton Tableland covers nearly 2500 km², (Figure 2.3) with 65 eruptive centres identified in the Province (Whitehead et al. 2007; Whitehead 2008). Basaltic flows occurred during the late Tertiary, but the dominant phase of volcanism was during the Quaternary. The reactivation of strong faults, during the Cainozoic, underlying the Atherton Tableland tapped uncontaminated basic magma that then erupted to the surface. The Atherton basalt lavas that erupted during this period, Pliocene to Quaternary, are dominated by subaerial basaltic lava flows sourced from shield volcanoes that can be extensive with some flanks extending up to 10 km. A diatreme, Hypipamee Crater, is found 12 km southwest of Herberton and was formed due to an explosive incident which instigated 55 m high vertical walls above a crater lake 87 m deep. The younger lavas are associated with cinder cones comprising gravely scoriaceous basalt with basaltic and terrigenous bombs. Cinder cones occur throughout the region with Mt Quincan being an example (Stephenson et al. 1980; Bultitude et al. 1997; Whitehead et al. 2007).

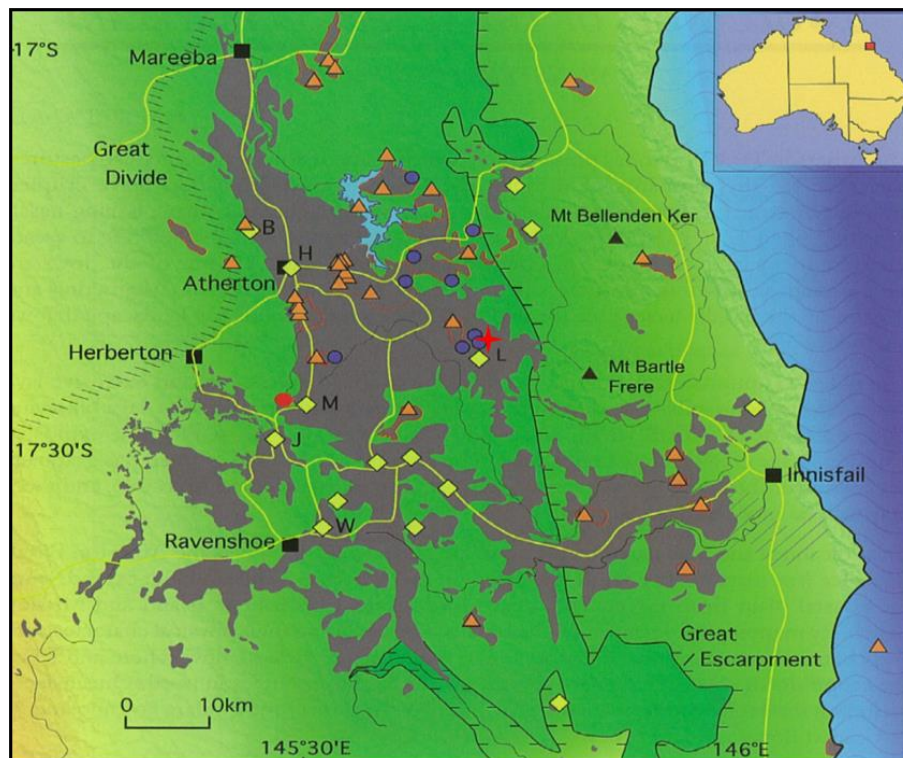


Figure 2.3. The Atherton Basalt Province, Basalt lava flows – grey, Shield volcanoes – yellow diamonds (B: Bones Knob, H: Hallorans Hill, M: Malanda, J: Jensenville, W: Windy Hill, L: Lamins Hill). Scoria Cones – orange triangles, with associated flows outlined in red. Maars – blue circles with Lynch's Crater – red star, Hypipamee Crater – red circle (after Whitehead 2008).

The Atherton Basalt Province is the only province in north-east Queensland in which maars have developed. A maar is a monogenetic volcano formed in a phreatomagmatic eruption with a low rim and a broad flat crater. The centre of the crater lies below the surrounding ground surface and therefore, depending on the initial and subsequently changing drainage factors for surface water in the crater, a lake may form, a swamp may develop, or the crater is left dry (Whitehead et al. 2007, Whitehead 2008). Erosion gradually increases the crater diameter and decreases its depth while the steeply outwardly dipping layers present in the initial development over time only remain around the rim of the crater. Other factors such as high rainfall can also be influential in their development (Ollier 1967; Lorenz 1986; Bultitude et al. 1997; Whitehead et al. 2007). There are both young and old maars with Lakes Barrine, Eacham, and Euramoo being examples of the younger maars which date to the late Pleistocene and Holocene while Lynch's Crater extends back to over 200,000 years (Kershaw 1986; Kershaw et al. 2007a). These crater lakes and swamps in most cases have a continuous accumulation of sediment, making them ideal for palynological, geochemical and sedimentological investigations (see Chapter 3).

2.2. Physiography

The major physiographic features of the Humid Tropics are given below and illustrated in Figure 2.4.

- The Herberton Highlands,
- The Atherton Tableland
- The Eastern Highlands (also known as the Central Highlands)
- The Coastal Plains and Ranges
- Coral Sea
- The Continental Shelf
- The Great Barrier Reef
- The Continental Slope

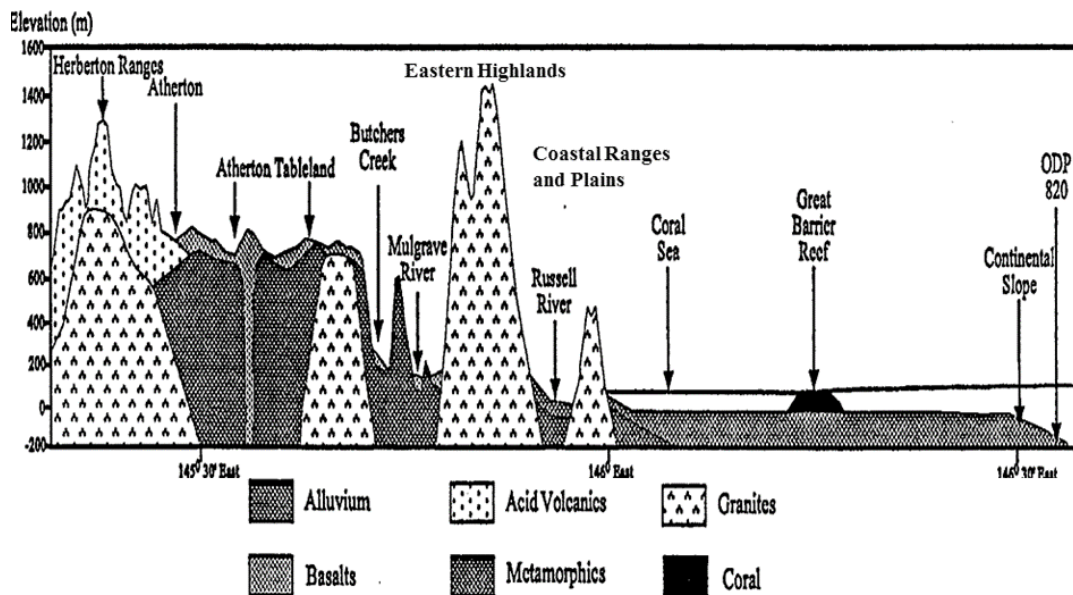


Figure 2.4. Cross-section of the major physiographic features of the Humid Tropics of north-east Queensland, Australia (adapted from Nix and Switzer 1991).

The main physiographic features (Figure 2.4) formed through block faulting that resulted in uplift and subsidence at the end of the Tertiary. The Atherton Tableland is the principle block of uplift and the main subsidence is the continental shelf. Narrower horst and grabens formed between these two features with differential erosion facilitating the development of relief. These more prominent features are superimposed on a 400 m high escarpment. The majority of the fault block coastal hills and ranges are aligned parallel to the coast that is separated from the escarpment by a coastal plain of Quaternary sediment, varying in width up to 50 km (Nott et al. 2001, Nott 2003). To the east is the Coral Sea and approximately 30 km offshore the Great Barrier Reef. The Quaternary deposits of the coastal plain are due to the erosion of the main escarpment and coastal ranges from climatic and eustatic conditions while the deposits of the adjacent continental shelf are the result of changing carbonate production on the outer shelf of the Great Barrier Reef in response to fluctuating sea levels (Nott 2003).

Further south in the Innisfail region (Figure 2.1 and Figure 2.2) the coastal plain is subdivided into the Mulgrave River Corridor and the Innisfail Plain and is composed of alluvium, swamp deposits and beach sands. To the west are the Eastern Highlands that are deeply incised valleys, with steep mountainsides and narrow spurs. Metamorphics and intruded granites are the dominant rock types with the erosional resistance of granite evident in the massifs of Mt Bartle Frere (1608 m) and Bellenden Ker (1593 m) the

highest mountains in Queensland. Basalts have partially filled valleys along the margins of the granite (Laffan 1988).

West of the Eastern Highlands is the Atherton Tableland which extends from Mareeba in the north to south of Millaa Millaa. The average altitude of the tableland is 700 m with the fossil pollen sites indicated in Figures 2.2. Topography on the tableland is variable but relief generally increases from north to south. Flat to undulating lavas predominate in the north where rainfall is least, with steep to very steep land occurring on lavas and other rocks in the south and east where rainfall is highest. Further west are the Herberton Highlands that reach a maximum altitude of 1300 m, and represent the Great Dividing Range (see Figure 2.2). The deeply divided valleys of Palaeozoic sediments and acid volcanics are interrupted by Cainozoic basalt flows, which have partially filled some of the valleys draining westward (Stephenson et al. 1980; Bultitude et al. 1997).

2.3. Soils

Soils formed from basalt cover some 56% of the tableland and are mainly red friable earths (Krasnozems). With a decrease in rainfall, the soils derived from basalt become shallower and there is a change from red earths to tropical black earths between 650 and 1000 mm of rainfall (Isbell et al. 1976; McKenzie et al. 2004). Red earths also form on granites, but, with decreased rainfall, there are greater structural and textural changes; soils become shallower, loams replace earths and below 1000 mm of rainfall, sandy soils dominate. On metamorphics, yellow friable loams give way to shallow loamy hardsetting duplex soils with clayey subsoils under lower rainfall and to gravelly loams on steep slopes (Isbell et al. 1976). The soils derived from basalt have very high clay contents (60-80%) in the median and high rainfall areas with lower clay content (40-50%) in the drier regions. Kaolin dominates the clay fraction of basaltic soils although in the higher rainfall areas it is lower in the upper solum; other minerals present are haematite and goethite with gibbsite more prevalent in the higher rainfall sites. Quartz grains are common in the sand fraction of most soils and it is believed that soil quartz is largely residual derived from the parent basalt (Isbell et al. 1976; Isbell 1994). Soils derived from basaltic parent materials in the higher rainfall areas of north Queensland are much deeper and acidic than those from drier areas with soil depths exceeding 5 m where mean annual rainfall ranges between 1000–4000 mm (Pillans 1997).

2.4. Drainage

Most of the region is drained by major rivers sourced or flowing through the Atherton region (Figure 2.2). The Russell River is sourced in the southern part of the tableland and exits just north of Cairns while the headwaters of the Mulgrave River are in the Eastern Highlands but the river flows through a section of the Atherton basalts. The Barron River is sourced just near Atherton and exits just north of Cairns. The breached south-east corner at Lynch's Crater where an outlet stream forms directly south forming a tributary maybe the source of the North Johnstone River that drains the northern part of the tableland and exits as the Johnstone River south of Cairns, see Figure 2.2 and 2.8 (Kershaw 1980a; Thomas et al. 2001; Page et al. 2003). Most rivers show evidence of diversion due to volcanic activity and basalt flows on the Tableland or due to sedimentation and sea level changes on the coastal plains (Nott et al. 2001; Whitehead and Nelson 2014). Diversions are enhanced by tropical climatic conditions with intense seasonal rainfall and deeply weathered uplifted hinterland making it ideal for the production of large fluvial sediment yields with the major rivers associated with extensive deltaic or estuarine infill deposits (Nott 2003; Thomas et al. 2007).

2.5. Climate

North-east Queensland has considerable spatial climate variability due to topographical diversity and the varying influence of major climate circulation systems such as the Walker circulation and the Australian summer monsoon (see Chapter 1 sub-section 1.2.3). The summer monsoon in Australia is characterised by a seasonal reversal of wind regime with a pronounced wet summer and dry winter. These two systems represent atmospheric teleconnections that see conditions in one part of the globe closely linked to other far-removed areas. The differences in the intensity of these circulation systems result in the phenomenon called the Southern Oscillation (SO), which is a global scale irregular pressure fluctuation that is responsible for much of the variability seen in Australia's climate but particularly the tropics (Cobb et al. 2003). A weakening of the Walker circulation produces a reduction in the intensity of the trade winds, as shown in Figure 2.5. This decreases ocean water circulation across the Pacific, with the waters off the Peruvian coast and the central and eastern Pacific, which are normally ~20°C, being as warm, 28°C–30°C, as the western Pacific during El Niño events (Rasmusson and Wallace 1983; Sturman and Tapper 2006).

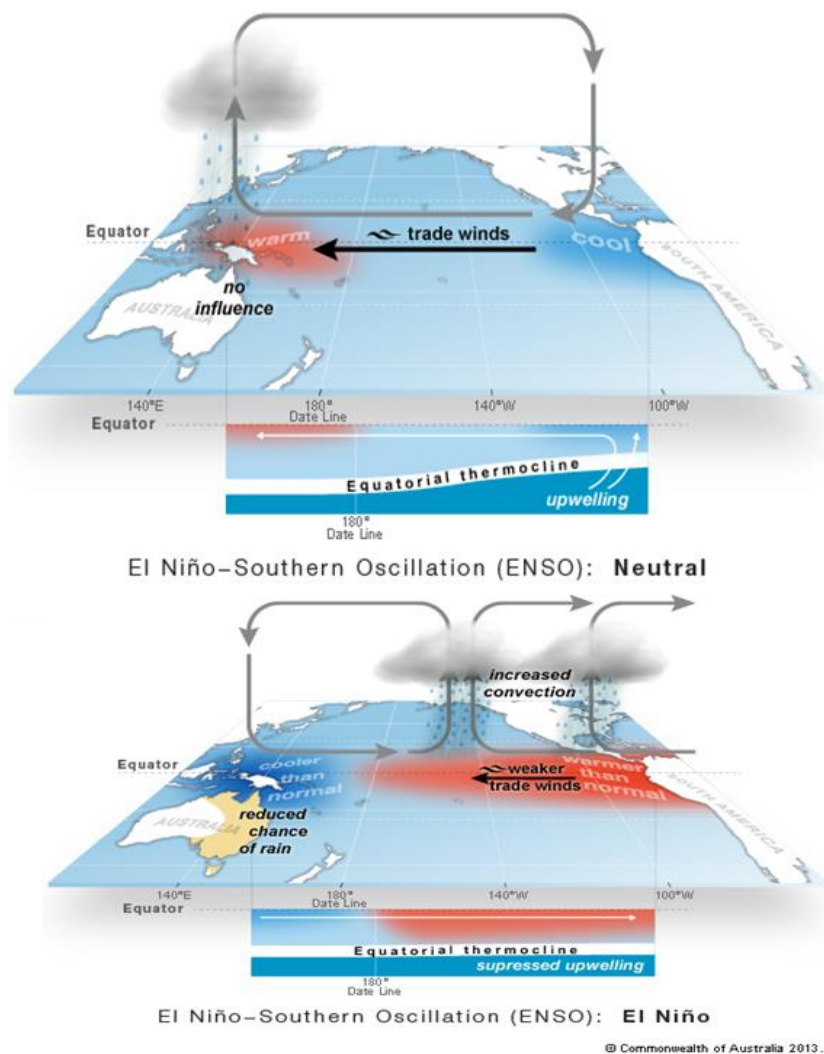


Figure 2.5. Walker Circulation pattern during neutral (typical) and El Niño type conditions (after Bureau of Meteorology 2020).

El Niño recurs every three to eight years but there is variability in the duration of each event and research has shown there is also a decadal and multi-decadal signature in the El Niño–Southern Oscillation (ENSO) record (Diaz et al. 2001). The Interdecadal Pacific Oscillation (IPO) is also associated with decadal climate variability over parts of the Pacific Basin, mainly the south-west Pacific, and modifies interannual ENSO-related climate variability over Australia. The IPO maybe a Pacific-wide expression of the Pacific Decadal Oscillation (PDO) which together may be part of a continuous spectrum of low frequency modulation of ENSO (Salinger et al. 2001; Mantua and Hare 2002).

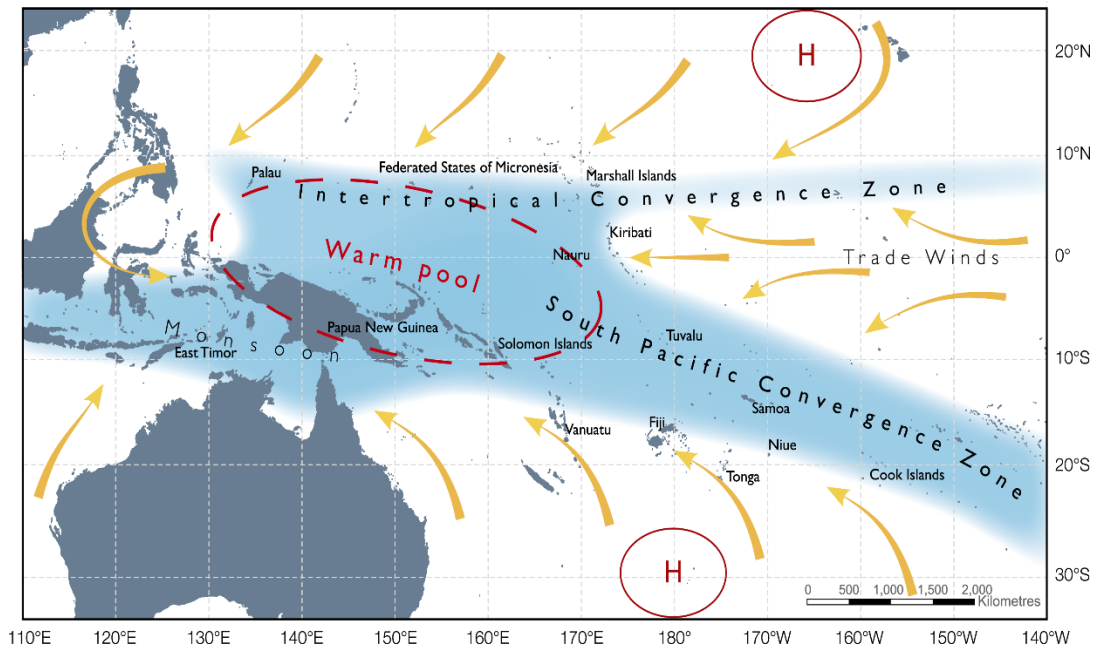


Figure 2.6. Schematic of circulation in the Pacific - location of the intertropical convergence zone (ITCZ) and the South Pacific convergence zone (SPCZ) in the South Pacific region along with the main sea level pressure contours and surface wind streamlines (arrows) (after Australian Bureau of Meteorology & CSIRO 2011; McGree et al. 2016).

While both the SPCZ and ITCZ (Figure 2.6) are energy sources for the Walker circulation, the SPCZ shows little seasonal change, although during La Niña (El Niño) events it can be displaced 1°–3° west (east) of the mean position on average (Salinger et al. 2014). Conversely the ITCZ shows marked latitudinal shifts north and south of the equator and in austral summer the ITCZ can be located just north of Cairns (Sumner and Bonell 1986). This is largely due to the seasonal shift in continental heating and the weak Coriolis deflection of airflow in the tropics that also allows the Walker circulation and the Australian monsoon to operate. The surface winds in the tropics are influenced by the south-east and north-east trade wind systems with the convergence of trade winds favoured by warmer water > 27°C (Trenberth 1991; Salinger et al. 2014; McGree et al. 2016; Brown et al. 2020).

The Australian monsoon circulation is linked at a broader scale to the Asian-Australian monsoon. Its onset is linked to inland heat lows and in austral summer the lower-tropospheric flow over northern Australia (equatorward ~15°S) switches from a dry south-easterly trade regime to a moist north-westerly monsoon flow (Berry and Reeder 2016). The monsoon can either be in an ‘active’ or ‘inactive/break’ phase. The active phase may see monsoon depressions located over northern Australia which form on the

monsoon shear line between the trade-wind easterlies and the monsoon westerlies and are associated with large-scale convection and heavy rainfall. During an inactive phase the monsoon trough is weakened and is located equatorward and light winds and reduced rainfall prevail. An active phase of the monsoon can see the breaking of droughts in Australia with the potential of monsoon depressions transforming into tropical cyclones that although potentially destructive, do bring much needed rain to inland areas (Suppiah 1992; Sturman and Tapper 2006; Berry and Reeder 2016).

The positive association of the SO and Australian rainfall especially over eastern Australia is also linked to the Australian summer monsoon and tropical cyclone activity. The late onset of the monsoon is associated with El Niño events while early onset tends to precede El Niño events. During high positive phases of the SOI (La Nina) tropical cyclones develop closer to the north-eastern coast of Australia (Sturman and Tapper 2006). Alongside, these global and synoptic scale circulation systems are meso- and local scale systems that not only act alongside the larger systems but also may influence the degree of impact from these systems due to prevailing surface conditions such as coastal and orographic proximity.

2.5.1. The local climate influences

The position of the subtropical high-pressure belt and the movement of the ITCZ dominate the weather patterns in this area. The south-east trade winds dominate throughout most of the year and these moisture-laden winds blow onto the elevated escarpment and Great Dividing Range producing substantial orographic rainfall (Bonell et al. 1991). During the summer months the north-west monsoon is influential as the ITCZ moves south over northern Australia. Although the SPCZ, a band of heavy rainfall, is relatively stationary it does move closer to the Queensland coast during La Niña events (Klingaman 2012). The majority of rainfall, in excess of up to 60%, falls during the summer months (December to March) and maybe supplemented by high prevailing rainfall intensities during active monsoonal conditions from either monsoonal depressions or cyclones, although the south-east trade winds still contribute rainfall during this period (Bonell and Callaghan 2008). There is a steep rainfall gradient along the coast (Figure 2.7) which is influenced by several synoptic and local factors (Bonell and Gilmour 1980; Connor and Bonell 1998).

Orographic effects result in higher rainfall on the peaks of the Eastern Highlands, Mt Bartle Frere and Mt Bellenden Ker, where annual totals of 10,000 mm have been recorded (Connor and Bonell 1998). These upland forested areas have a hidden precipitation component derived from ‘cloud stripping’ that is due to interactions between cloud fog droplets and vegetation. Cloud stripping only occurs in forested areas above 600 m asl. This component may contribute up to 70% of total water input in the drier months and up to 31% of annual gross precipitation (McJannet et al. 2007a, b).

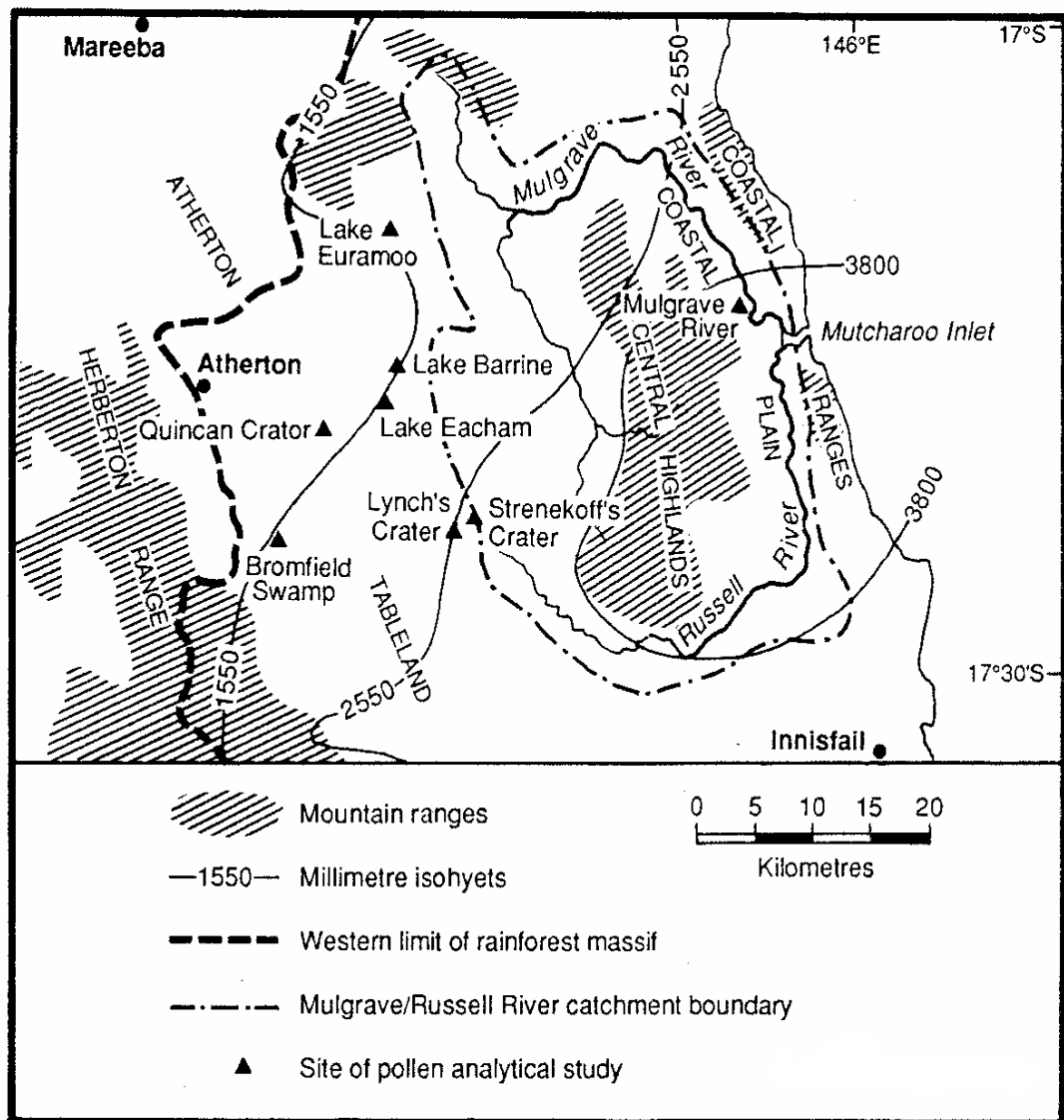


Figure 2.7. Isohyetal map of the Atherton Tableland showing position of Lynch's Crater and other pollen analytical sites along rainfall gradient (after Hiscock and Kershaw 1992).

Monthly and annual rainfall are affected by the status of ENSO with differences up to and over 1000 mm in some regions between El Niño and La Niña periods. This interannual

variability may lead to areas being severely affected by both drought and fire (Balston and Turton 2005; Edwards and Krockenberger 2006).

2.5.1.1. Atherton Tableland

The Atherton Tableland with an average altitude of 760 m lies obliquely in a steep rainfall gradient decreasing from southeast to northwest, with Figure 2.7 showing the position of Lynch's Crater and other palynological sites along this rainfall gradient. The majority of rainfall falls during the summer months sourced from either the south-east trade winds, the positioning of the ITCZ and SPCZ and their influence on ENSO and monsoonal and cyclonic events (Klingaman 2012). There is no weather station at Lynch's Crater but estimates of both present-day and past climate conditions have been generated from the bioclimatic predictive system BIOCLIM, see Table 2.1 (Kershaw and Nix 1989; Busby 1991).

Table 2.1. Bioclimatic estimates for present-day conditions for pollen sites on the Atherton Tableland, north-east Australia, MAT-mean annual temperature, MAP-mean annual precipitation, PDQ-precipitation driest quarter (Busby 1991).

Pollen Sites	Latitude	Longitude	Elevation (m)	MAT (°C)	MAP (mm)	PDQ (mm)
Quincan Crater	17.3	145.58	720	20.6	1625	99
Bromfield Swamp	17.38	145.55	760	20.4	1794	128
Lake Euramoo	17.17	145.63	660	20.9	1675	99
Lake Barrine	17.25	145.63	743	20.6	1748	125
Strenekoff's Crater	17.33	145.70	694	20.7	2092	164
Lynch's Crater	17.37	145.70	760	20.4	2570	210

Both Lynch's and Strenekoff's Craters lie on or near the 2550 mm isohyetal line (Figure 2.7) respectively which is the result estimated for Lynch's Crater from the bioclimatic predictive system BIOCLIM (Kershaw and Nix 1989; Moss and Kershaw 2007). These

estimates show the influence of the rainfall gradient across the Atherton Tableland. It is likely the close proximity of both Lynch's and Strenekoff's Crater to Mt Bartle Frere in the south-west of the Eastern Highlands, would result in frequent cloud cover and drizzle in the south-east of the Tableland ensuing less seasonal rainfall than at lower altitudes or further west. It is also likely that areas that have not been deforested within the Atherton Tableland and are above 600 m may also have a contribution from 'so-called' hidden precipitation (McJannet et al. 2007*a, b*). Frosts can occur on the Atherton Tableland and are more common on non-forested areas and higher altitudes usually in July and August with rare frosts also occurring on the coastal lowlands (Kershaw 1976; Stocker et al. 1995).

2.6. Vegetation

The humid tropics of northeast Queensland as stated in the introduction of this chapter encompasses the Wet Tropics which contains a diverse expanse of rainforest and sclerophyll elements and will provide the background to this section. The Wet Tropics of north-east Queensland was designated as the Wet Tropics World Heritage Area (WTWHA) in 1988. It lies along the tropical north-east coast of Queensland between Cooktown (north) to Townsville (south) and comprises approximately 1.8 million hectares with approximately one million hectares of rainforest (Appendix A, Figure 1). The WTWHA protects nearly 900,000 hectares of the region, primarily rainforest. The crater lakes (Barrine and Eacham) were gazetted for national park status in 1934 and are included within the WTWHA. The listing of WTWHA is based on the region being an outstanding example of major stages in the earth's evolutionary history; as an outstanding example representing significant ongoing ecological and biological processes, superlative natural phenomena and containing important and significant habitats for in situ conservation of biological diversity (Department of Sustainability 2008).

2.6.1. Rainforest Structural Classification

Webb (1959) undertook a detailed classification of the three main Australian rainforests divisions, Tropical, Sub-tropical and Temperate based on their physiognomic and structural features as well as the influence of climate, altitude and soil material. This resulted in twelve sub-formations for the three rainforest divisions based on leaf size (macrophyll, mesophyll, notophyll, microphyll and nanophyll), height and continuity of tree layers, species dominance, proportion of evergreen, semi-evergreen, deciduous or

araucarian emergents, presence of other emergents and the prominence of special growth forms (lianes, vascular epiphytes, palms, tree ferns, plank buttresses, leaf form). The rainforest classification of the humid tropics by Webb (1963, 1968, 1978) also includes the other major vegetation components, the sclerophylls (specifically *Eucalyptus*, *Acacia*, *Melaleuca* and *Allocasuarina*) (Table 2.2). The ecological relationship between rainforest and the sclerophylls is complex with soil fertility, moisture and temperature dictating their relative distributions. The classification and terminology used in the following sections is based on the Webb and Tracey (1984) and Tracey (1982) publications that follow the structural and floristic types established in the earlier works of Webb (1959, 1968 and 1978), Tracey and Webb (1975*a,b*) and Webb et al. (1967, 1976) with the addition of mixed rainforest and sclerophyll types as well as sclerophyll dominated types.

2.6.2. Rainforest Floristics

The structural complexity of the vegetation of the humid tropics indicated in Table 2.2 is also combined with floristic diversity, although there is some floristic variation along environmental gradients such as rainfall and geology and this can be seen where the western limit of rainforest lies at a mean annual rainfall of ~1250 mm on basalt soils, 1500 mm on granite soils, and about 1600 mm on metamorphic soils (Kershaw 1973).

Complex Mesophyll Vine Forest (CMVF) in the lowlands is characterised by an uneven canopy and multiple layers with the families, Araliaceae, Myrtaceae (*Syzygium* spp.), Lauraceae (*Cryptocarya mackinnoniana*), Meliaceae (*Dysoxylum pettigrewianum*), Elaeocarpaceae (*Elaeocarpus*), Moraceae (*Ficus* spp.), Protaceae (*Musgravea heterophylla*) and Apocynaceae are typically present in the canopy layer while in swampy areas where *Archonotophoenix* (Arecaceae) dominates, Myrtaceae, Moraceae, Rubiaceae (*Nauclea orientalis*), Rutaceae (*Melicope* spp.) and Sapindaceae (*Mischocarpus*) feature with the Rhizophoraceae family prominent in coastal areas. Macrophyllous vines, (*Faradaya*, *Flagellaria* and *Calamus*) and epiphytic ferns are present in both lowland and upland CMVF (Plate 2.1) and become more common in areas where cyclones are frequent (Tracey 1982; Webb et al. 1984). CMVF (1b) at higher altitude sees a reduction in the diversity of species in comparison to lowland CMVF but the canopy layer is much taller. There is some commonality with lowland CMVF with Lauraceae, Myrtaceae, Meliaceae,

Moraceae, Elaeocarpaceae and Proteaceae present in the canopy layer but some canopy species, such as *Argyrodendron peralatum* (Malvaceae) are more conspicuous.

Table 2.2. Classification of main rainforest types (1-11) mixed communities (12-13) and sclerophylls communities (14-16) for north Queensland in relation to rainfall, altitude, and soil materials (Tracey and Webb 1975, Tracey 1982).

<p>1. Complex mesophyll vine forest (CMVF) 1a. Very wet and wet lowlands and foothills; basalts, basic volcanics, mixed colluvium on foot-slopes and riverine alluvia. 1b. Very wet and wet cloudy uplands, basalts 1c. Moist and dry lowlands; riverine levees (gallery forests)</p>
<p>2. Mesophyll vine forest (MVF) 2a. Very wet and wet lowlands and foothills, granites and schists 2b. Very wet and wet lowlands, beach sands</p>
<p>3. Mesophyll vine forest with dominant palms (MFPVF) 3a. Very wet lowlands, feather-leaf palm (<i>Archontophoenix</i>) swamps, basaltic and alluvial soils 3b. Very wet lowlands and lower foothills; fan-leaf palm (<i>Licuala</i>), seasonally impeded drainage, schists and granites</p>
<p>4. Semideciduous mesophyll vine forest (SDMVF) Moist and dry lowlands and foothills; granites and basalts</p>
<p>5. Complex notophyll vine forest (CNVF) 5a. Cloudy wet highlands; very limited areas of basalt and basic rocks 5b. Moist and dry lowlands; foothills and uplands, basalt</p>
<p>6. Complex notophyll vine forest (with emergent <i>Agathis robusta</i>) (CNVF + emergent <i>Agathis robusta</i>) Moist foothills and uplands; granites and schists</p>
<p>7. Notophyll vine forest (rarely without <i>Acacia</i> emergent) (NVF + <i>Acacia</i> emergents) 7a. Moist lowlands and foothills along coast including islands; granites and schists 7b. Moist and dry lowlands; beach sands</p>
<p>8. Simply notophyll vine forest (often with <i>Agathis microstachya</i> (SNVF + <i>Agathis microstachya</i>)) Cloudy wet and moist uplands and highlands; granites, schists and acid volcanics</p>
<p>9. Simply microphyll vine-fern forest (often with <i>Agathis atropurpurea</i>) (MFF + <i>Agathis atropurpurea</i>) Cloudy wet highlands; granites</p>
<p>10. Simply microphyll vine-fern thicket (MFT) Cloudy wet and moist wind-swept top-slopes of uplands and highlands; granites</p>
<p>11. Deciduous microphyll vine thicket (DVT) Dry lowlands and foothills; granite boulders</p>
<p>12. Vine forest with <i>Acacia</i> - emergents and co-dominants Very wet to wet locations; foothills, uplands and highlands, granites and metamorphics</p>
<p>13. Vine forest with Eucalypt – emergent and co-dominants Moist to wet locations, granites, metamorphics and acid volcanics</p>
<p>14. Tall Open-forest and Tall Woodland inc. Wet Sclerophyll Forest (WSF) Cloudy, moist uplands and drier more fire prone situations on granites and on basalts</p>
<p>15. Medium Open-forest and Medium Woodland <i>Eucalyptus</i> with <i>Acacia</i> and <i>Allocasuarina</i> found after fire; Poorly drained lowland sites (<i>Melaleuca</i>)</p>
<p>16. Medium and Low Woodland (Eucalypts) Found west of Type 15 on dry uplands and highlands; granites and metamorphics and found on acid volcanics and basalts Atherton and Mareeba region. Fire common</p>

These typical canopy families surround the crater lakes, Barrine and Eacham, today, where Euphorbiaceae (*Mallotus/Macaranga* spp, *Aleurites* spp.), Urticaceae (stinging trees *Dendrocnide moroides* and *Dendrocnide photinophylla*), Elaeocarpaceae (*Sloania australis*), Sapindaceae and Sapotaceae are common as secondary or understory trees. Numerous epiphytic ferns, lianes and vines (Plate 2.1) are present and were important plants in Aboriginal culture with *Calamus* spp. (Arecaceae) used for medicinal purposes (headaches) as well as basket making (Tracey 1982; Hyland et al., 2003).



Plate 2.1. Rainforest features Atherton Tableland, (A)-Epiphytic ferns; (B)-Lianas; (C) Lake Barrine MVF; (D)-Lake Eacham MVF (Photos S.Rule 2003).

Away from the optimal conditions where CMVF presides, the floristic composition is simplified and coniferous emergents (*Agathis* spp.) are present in some CNVF, SNVF and MFF (Table 2.2) with Cunoniaceae, Monimiaceae, Moraceae, Lauraceae,

Sapindaceae, Rutaceae, Myrtaceae and Elaeocarpaceae also represented in these forest types. There can be an overlap of MVF and NVF type related to sediment type or a reduction in moisture due to a more pronounced dry season which sees an opening up of the canopy layer with an increase in semi-deciduous/deciduous species, such as *Brachychiton acerifolius* (Malvaceae) and *Terminalia* spp. (Combretaceae). SNVF sees a more even canopy layer with Rhamnaceae, Rutaceae and Alangiaceae present usually on metamorphic sediment while CNVF is found on basalt in high rainfall uplands where Cunoniaceae, Myrtaceae, Proteaceae and relict populations of *Araucaria bidwillii* (Araucariaceae) are present. Podocarpaceae and tree ferns become more common at higher altitude in the understory and vines such as *Calamus* become rare. High altitude wind-swept MFT found at the top of Mt. Bartle Frere and the Bellenden Ker Range displays sees abundant *Cyathea* sp., reduced canopy height and the sclerophyllous species *Leptospermum wooroonooran* (Myrtaceae) (Plate 2.2).

2.6.3. Sclerophyll Floristics

Tall eucalypt forest on soils derived from granite are found less than a km from Lake Euramoo where NVF is present on similar mixed sediment type. Along with the emergent, *Eucalyptus grandis* which can exceed 55 m, *Corymbia intermedia*, *Eucalyptus pellita*, *Eucalyptus tereticornis*, *Eucalyptus tessellaris* *Lophostemon confertus* and *Syncarpia glomulifera* from the Myrtaceae family can be frequently found along rainforest/sclerophyll ecotones. *Acacia* spp. as well as *Allocasuarina torulosa* (Casuarinaceae) can be recorded below this canopy layer along with rainforest species (Table 2.2 12-14, Plate 2.2). The composition of the ground layer is dependant on moisture availability and fire frequency with an increase in sedges, grasses and wiry vines when fire is frequent but when absent there is an increase in rainforest seedlings and woody taxa such as *Maesa dependens* var. *dependens* (Myrsinaceae), *Hibbertia melhanioides* (Dilleniaceae) and *Alpinia caerulea* (Zingiberaceae) in these wet sclerophyll forest (WSF) types (Tracey 1982; Harrington et al. 2005). Medium Open Forest and Open Woodland (Table 2.2, type 15) are dominated by *Eucalyptus* species in the canopy layer, especially *E. acmeniodes*, *E. alba* and *E. tereticornis*, alongside *Corymbia intermedia* while *Acacia* spp. and *Allocasuarina littoralis* and *A. torulosa* are commonly found after disturbance, especially fire.



Plate 2.2. (A)-Strangler *Ficus* (Moraceae) present in MVF and CNVF; (B)-MFT with *Leptospermum wooroonooran*; (C)-Ecotonal transition between rainforest and sclerophyll woodland; (D)-Tall eucalypt forest (WSF) *E. grandis* emergent (Photo (A) S.Rule 2003; Webb (B), (C) and (D) 2007).

Vines become more common when fire is less frequent while grasses (*Themeda australis* and *Imperata cylindrica*) form a dense ground layer with an increase in fire. Fire is a common occurrence in Medium and Low Woodland where eucalypt complexes are present but pure stands are not unusual and actual patterns depend on annual rainfall, topography and degree of disturbance. *E. papuana*, *E. tereticornis*, *E. alba* and *C. intermedia* are more common in higher rainfall areas or on basaltic soils with a lower rainfall. Grasses form a dense understorey in high rainfall areas which are subjected to a

high fire frequency, usually annual, while sclerophyllous shrubs become more common further west, away from rainforest with a reduced fire frequency.

2.6.4. The present-day vegetation of Lynch's Crater

The area surrounding Lynch's Crater was initially cleared by the timber-getters and then for dairy cattle grazing and minor agricultural products (Figure 2.8). At present tea plantations and tropical fruits along with both beef and dairy cattle grazing continue within the area with a small section near the breached south-east section of the crater now planted with black bamboo for cropping (species unknown). The slope on the northern side of the crater is at $\sim 45^\circ$ while there is a reduction to $\sim 20^\circ$ along the west and south crater walls. The crater is approximately 350 m in diameter with a recent botanical survey estimating the total floor area at just under 21 ha (Kahler 2005). Although subdued by erosion there have also been multiple attempts at hydrological reconfiguration of the crater floor for grazing purposes.

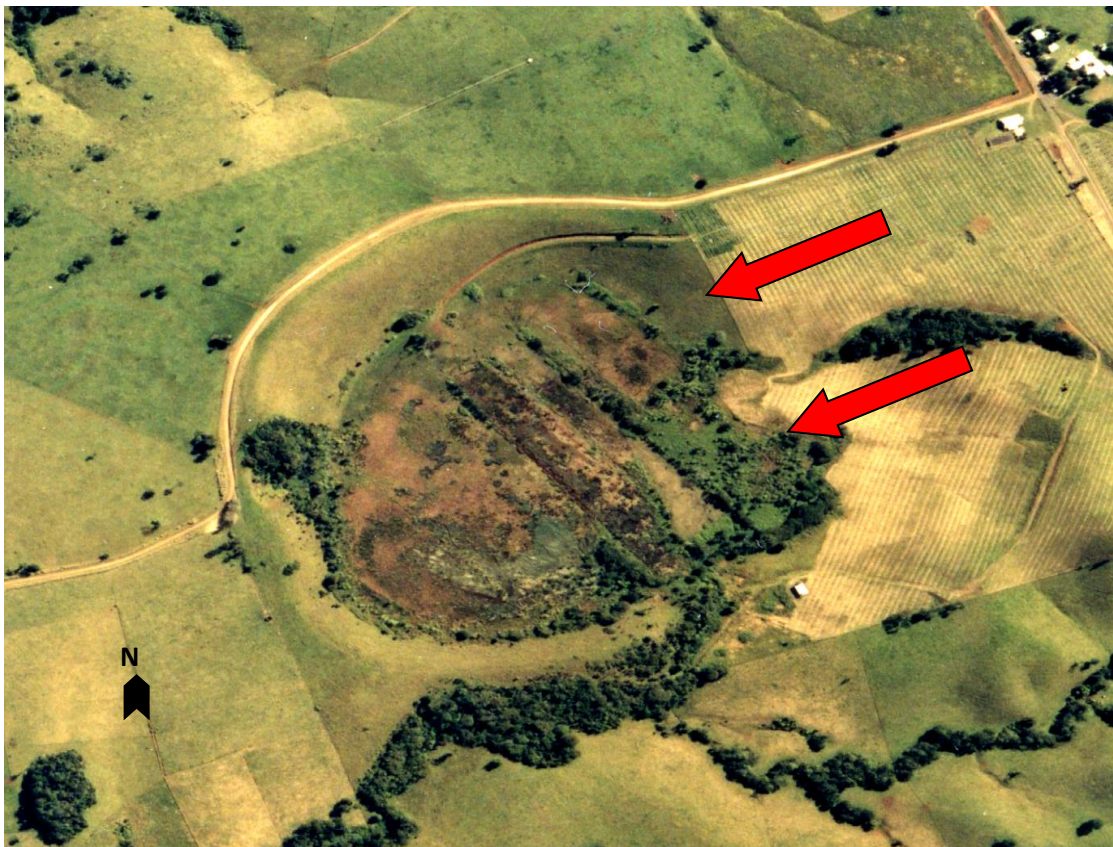


Figure 2.8. Aerial scan of Lynch's Crater showing peripheral and parallel drainage lines and stream outlet in the southeast of the crater marked by treeline with breached eastern section marked by red arrows (Dept of Natural Resources and Mines 2006).

In the 1940s a ring drain round the periphery of the swamp was dug to lower the water table and provide pasture for cattle in the dry season. Lowering of the water table continued into the 1960s with parallel drains 1 m deep and 80 m apart constructed across the swamp so that exotic grasses, *Panicum maximum* var. *triglume*, could be planted for pasture. These attempts were not particularly successful with severe winter frost and competition from the local swamp vegetation the main adversaries (Kershaw 1973). Peat strip mining from the 1970s and up to the 1990s has resulted in leaving half of the estimated 21 ha of the crater floor scarred (Kahler 2005). Both beef and dairy cattle grazing have continued sporadically to the present-day.

But despite all this modification of the vegetation and hydrology, a botanical survey undertaken in 2005 suggests that about half of the area contained within the rim of the crater supports remnant vegetation (Kahler 2005) which is classified under the Queensland Herbarium remnant grassland definition (Neldner et al. 2004). The native sedge *Lepironia articulata* and the native grass *Ischaemum australe* (Figure 2.9) dominate the swamp surface. At the margins of the swamp *Lepironia articulata* dominates, rising to 3 m with *Blechnum* spp. conspicuous and *Cyclosorus gongylodes*, *Oenanthe javanica*, *Rhynchospora corymbosa* and *Cyperus lucidus* restricted to the wetter parts of the swamp where shallow open water is sporadically present. On the drier margins *Ischaemum australe* dominates interspersed with *Fimbristylis dichotoma*, and *Persicaria* spp. which become common where fire and other disturbances have occurred. Other rarer components interspersed within the grassland/sedgeland communities are *Drosera* sp. (*D. burmanni*), *Kyllingia brevifolia*, *Phylidrum lanuginosum*, *Ludwigia* spp. and the fern *Lygodium*. Remnants from past introductions, meadow grasses, and opportunistic weedy shrubs such as *Lantana camara*, are still present on the swamp surface. Along the drainage lines and above the crater rim secondary rainforest trees, particularly the secondary species *Alphitonia petriei* and *Euodia elleryana* are present with understorey tree ferns, ground ferns and orchids (Kershaw 1973, 1976).



Figure 2.9. Swamp vegetation on Lynch's Crater with *Lepironia articulata*, tall sedge, and grass *Ischaemum australe* in the foreground and secondary rainforest taxa on the crater slope in the background (Photo S.Rule 2003).

Chapter 3

Palaeoenvironmental and Archaeological Studies on the Atherton Tableland

Introduction

Palaeoenvironmental research on the Atherton Tableland has involved predominantly palynological and associated studies, spanning over 50 years and has been integral to understanding the dynamic nature of vegetation change through glacial and interglacial periods, as well as the influence that fire has exerted whether from a climate or anthropogenic source. This has been possible because of a relatively large number of suitable sites, such as maar lakes and swamps, formed by volcanic activity. All Tableland pollen sites are located on Figure 2.1. Other techniques including geochemistry and anthracology, have also been undertaken on some sites to assist palaeoenvironmental reconstruction. Archaeological sites extending back to the Pleistocene are limited but have provided an approximate arrival period for Aboriginal people in the region. The majority of archaeological sites are restricted to the late Holocene and European contact periods from both rainforest and sclerophyll environments and they provide some insight into potential management practices especially in regards to fire.

3.1. Palaeoenvironmental Research

Palynological studies on the Atherton Tableland began in the 1960s with Prof. D. Walker making exploratory trips to the rainforest areas of north Queensland and seeing the potential of the crater lakes and swamps on the Atherton Tableland for pollen analysis. Following on from this Kershaw (1973) undertook an extensive investigation on the Atherton Tableland incorporating modern studies on both local and regional pollen representation and construction of late Quaternary palynological records. Subsequently, research has continued and broadened in scope until the present day.

3.1.1. Local Pollen Representation

Initial studies at Lynch's Crater (Kershaw 1973, 1986) showed that pollen representation fluctuated greatly from swamp to lake conditions suggesting significant hydrosere vegetation variation in relation to changes in water depth. Both present-day aquatic

vegetation and modern pollen representation of three sites on the Atherton Tableland were analysed to aid interpretation of past local aquatic communities in the region (Kershaw 1978, 1979). The study sites included a small crater lake, Lake Euramoo, a small swamp infilled crater, Quincan Crater, and a larger swamp infilled crater, Bromfield Swamp (Figure 3.1). Several transects from the edge to the centre of each site were sampled across different vegetation types and after numerical analyses four main floristic types were recognised which could be related to different environmental conditions (Kershaw 1978).

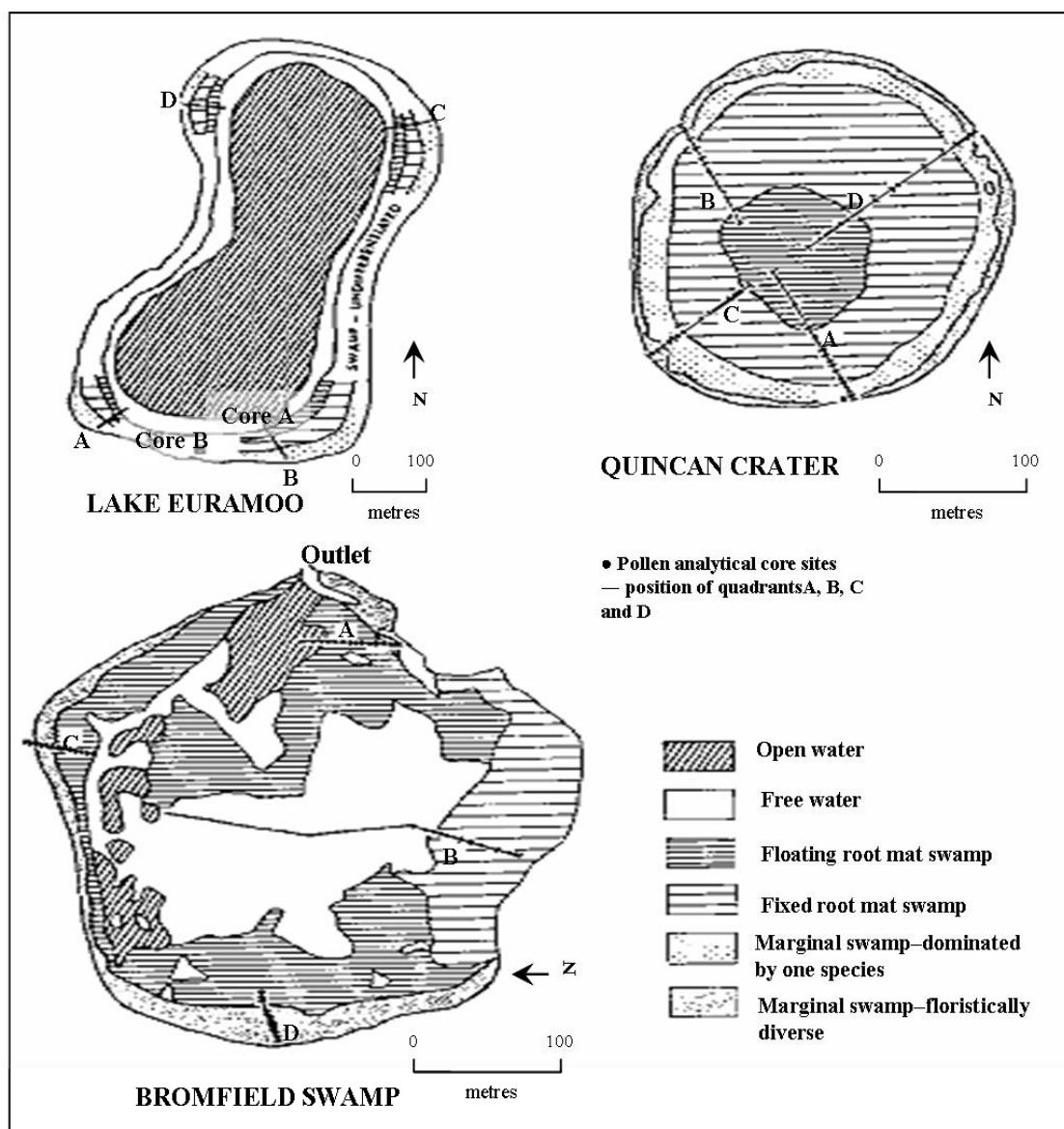


Figure 3.1. Major habitat types of Lake Euramoo, Quincan Crater and Bromfield Swamp derived from the vegetation analyses of Kershaw (after Kershaw 1978).

These floristic types are:-

1. a free water group determined by the presence of the floating leaved aquatic *Nymphoides*; chemical and physical environment homogenous with water depths varying from 50 cm to 250 cm.
2. a floating mat community with little or no sediment, not recorded over a water depth greater than 2–3 m; taxa present included the swamp fern *Cyclosorus*, the aquatic grass *Leersia* and *Polygonum strigosum* (*Persicaria strigosa*) with *Cyperus platystylis* and *Sparganium* sp. present on less stable mats and *Machaerina* (*Baumera*) dominant on more stable mats.
3. a type including the ground fern *Blechnum* and Cyperaceae species and characterised by a fixed mat substrate often above water level displaying a high degree of decomposition, low pH and high potassium ion concentrations. At the present time Lynch's Crater is dominated by this habitat.
4. a type not characterised by any particular species; open water above a fixed root mat; mud or soil substrate, indicative of marginal swamp situations with a high degree of decomposition; the possibility of chemicals and inorganic material being washed in from the crater slope; structurally both complex vegetative mosaics with a variety of species and simple communities usually with a single dominant monocotyledonous species, such as *Lepironia* or *Phragmites*.

Type representation within the sites, as shown in Figure 3.1, shows that Bromfield Swamp has a greater variety of habitat types and greater floristic diversity than the small sites. However, Kershaw (1978) suggests that, overall, free water, floating mat swamp and fixed mat swamp represent stages in hydrosere succession resulting from recent site disturbance and, if the pollen taxa *Nymphoides*, *Cyclosorus* and *Blechnum* are found in accumulated sediments, systematically changing water levels would be indicated.

These proposed dynamic relationships were tested by taking surface sediment samples from each vegetation quadrat followed by pollen analysis to examine the relationship between aquatic vegetation and the modern pollen spectra and then comparing the modern pollen samples with fossil pollen spectra from the sites (Kershaw 1979). It was found that identifying pollen types to species level was difficult especially for the large monocotyledonous families, Cyperaceae and Poaceae that are often dominant. It was also

suggested that most aquatic pollen was of very local origin, presumably because of the low stature of most swamp vegetation, although it does appear that the taller monocotyledonous species, especially *Typha*, tended to have a wider distribution because of the likelihood of wind dispersal (Finlayson et al. 1983). *Nymphoides* pollen was a reliable indicator of its free-water habitat which if recorded in fossil deposits, would suggest that a similar environment was present (Kershaw 1979). An important gauge of whether swamp or lake conditions prevailed in the past was also devised by using the ratio between aquatic and dryland pollen, with a ratio of 1:1 indicating a transition between swamp and open water and, where the local aquatic pollen sum was less than the dryland pollen sum, then free or open water conditions prevailed. Some of the problems identified in this local pollen aquatic study, including taxonomic precision, have been attempted to be overcome in this study by the analysis of plant macrofossils.

3.1.2. Modern Pollen Influx Studies across the area

Within the project area, research has been undertaken on studies of modern pollen influx. These include lake-surface trapping (Kershaw 1973; Kershaw and Hyland 1975; Walker 2000) a 10-year pollen trapping programme within rainforest (Kershaw and Strickland 1990) and a 2-year trapping programme across 11 localities from herbaceous to woodland to rainforest designed to determine the extent and abundance of pollen transport through the different vegetation types (Walker and Sun 2000).

Kershaw and Hyland (1975) found, from a 14-month study of pollen trapping on Lake Euramoo, that the pollen from rainforest vegetation did not travel far in general. However, there were exceptions such as the presence of *Balanops* (Balanopsidaceae) whose nearest source sub-montane rainforest above 900 m is, several kilometres away. Walker's (2000) longer trapping period (over an 8 year period) across the crater lakes Barrine and Eacham, recorded a pollen fall-out (influx) of 509 kgr m⁻² wk⁻¹ in contrast to Kershaw and Hyland results of 39 kgr m⁻² wk⁻¹ for the smaller crater lake, Euramoo. Both studies used the pollen trap sampler designed by Tauber (1965, 1967) although refinements were made by Walker to inhibit perching birds which contributed a large amount of extraneous matter to the pollen traps at Lake Euramoo limiting the pollen counts at this site.

It is also likely that the longer trapping period by Walker, in comparison to Kershaw and Hyland's shorter trapping period (14 months), would have allowed for both the variability of seasonal variation (wet and dry seasons) to be recorded but also the variability present in flowering periodicity which varies between species and years (Boulter et al. 2008). Walker also suggested that the smaller size of Lake Euramoo may have limited the potential pollen fall out for this site. However, in both studies key canopy and secondary taxa, *Elaeocarpus* (Elaeocarpaceae), *Trema* (Ulmaceae) and *Mallotus* and *Macaranga* (Euphorbiaceae), dominated the rainforest component which in total comprised approximately 40% to 70 % for Lake Eacham and Lake Barrine respectively and 50% for Lake Euramoo. In both results the sclerophyll component varied between 10 and 20% of the total pollen.

Walker and Sun's (2000) transect across a vegetation mosaic found that pollen is carried between vegetation types but much less from rainforest than from the other vegetation types (sclerophyll woodland and herbaceous vegetation) although there were exceptions with the secondary tree taxon, *Mallotus* or *Macaranga* contributing extraordinarily high values (900 and 1100 grains $\text{cm}^{-2} \text{a}^{-1}$ respectively) in a sclerophyll forest trap. Often non-rainforest tree pollen (NRF) exceeded the rainforest tree pollen (RF) in its own environment. For example, the rainforest locality, Curtin Fig, had an influx value of 858 grains $\text{cm}^{-2} \text{a}^{-1}$ for RF but 1203 grains cm^{-2} for NRF primarily consisting of Casuarinaceae and *Eucalyptus* (Myrtaceae) and overall NRF ranged from 10 to 65% of the total pollen in rainforested sites. The mean influx for RF in rainforested localities was found to be > 600 grains $\text{cm}^{-2} \text{a}^{-1}$ and all traps within rainforest registered > 25% RF with greater values in the larger stands of rainforest. The authors suggest that uncertainty could prevail on the proximity of certain individual taxa such as the large pollen producers, *Casuarina* and *Eucalyptus*, which can appear > 1 km from their nearest source in large quantities. The authors also suggest that the size of the habitat, especially the rainforest component, would influence pollen capture from outside sources.

A 10-year pollen trapping record from Kershaw and Strickland (1990) was undertaken within a lower montane/Simple Notophyll Vine forest plot on Mt Lewis at 1000 masl. The local woody component accounted for two-thirds of the pollen total, while 19% was accounted for from extra-local plants with the remainder from a regional pollen source including woody taxa, herbs and pteridophyte spores. Within the local component,

canopy and emergent tree taxa were the main contributors especially *Acmena* (Myrtaceae), Sapotaceae, and *Elaeocarpus* (Elaeocarpaceae) although the understorey genus *Symplocos* (Symplocaceae) had the highest individual total. Moderate representation was found for *Ceratopetalum* (Cunoniaceae), *Flindersia* (Rutaceae), *Sloanea* (Elaeocarpaceae) and *Cardwellia* (Proteaceae) while *Diospyros* (Ebenaceae) and *Endiandra* (Lauraceae) were a couple of the genera present but not recorded. *Balanops* (Balanopsidaceae) was the main contributor to the extralocal component with *Halfordia* (Rutaceae), *Podocarpus* (Podocarpaceae), *Argyrodendron* (Malvaceae) and Sapindaceae also having relatively high representation. The regional component was dominated by Casuarinaceae and *Eucalyptus* type with *Trema* (Ulmaceae) the only rainforest regional component with significant values. Kershaw and Strickland (1990) concluded that many taxa will be invisible in a pollen record while some will only be represented if close to the pollen site, 10–20 m. The study of Walker and Sun (2000) also found that other taxa with regional dispersal will be present even if growing several kilometres away. This later study (Walker and Sun 2000) and the more recent findings of Boulter et al. (2009) suggest that a high degree of annual variation in rainforest pollen influx is due to periodic mass flowering of a number of tree taxa.

3.1.3. Analysis of modern pollen spectra from rainforest plots

In order to facilitate pollen identification and provide the basis of a direct floristic comparison with the fossil pollen from Atherton Tableland, samples were collected from beneath the rainforest canopy across 14 sites that covered a range of existing rainfall, altitude and soil nutrient status variation (Kershaw and Bulman 1994). It was found that rainforest canopy trees reached maximum proportions in medium to high altitude forests away from edge disturbances, and that understorey taxa had a similar distribution but at lower values while secondary trees became more prominent near the drier rainforest margins. Several taxa were good indicators of forest type and environmental conditions. The palm *Archontophoenix alexandrea* (Arecaceae), *Argyrodendron peralatum* (Malvaceae), *Dysoxylon* (Sapotaceae), *Elaeocarpus* (Elaeocarpaceae), and *Trema* (Ulmaceae) had their greatest representation in sites from the humid coastal areas while Cunoniaceae types, *Halfordia scleroxyla* (Rutaceae), and *Stenocarpus* comp. (Proteaceae) were indicative of high altitude forests and *Blepharocarya involucrigera* (Anacardiaceae) and *Mallotus* and *Macaranga* (Euphorbiaceae) indicated drier forests. *Schefflera actinophylla* (Araliaceae), *Sloanea* comp (Elaeocarpaceae), *Symplocos*

(Symlocaceae), *Melicope broadbentiana* comp. (Rutaceae) and Cyatheaceae had a broader representation primarily in the wetter forests of any altitude while *Balanops australiana* (Balanopsidaceae) and *Podocarpus* (Podocarpaceae) were absent from lowland forests. As in Kershaw and Strickland's (1990) study, many taxa were not present or recognisable in the pollen fall-out with the most noticeable being the absence of pollen from the Lauraceae family whose component species are dominant or conspicuous in the majority of rainforest types. Its delicate pollen may initially be present in the pollen fall-out but disappear during the preparation process (Kershaw and Bulman 1994).

The pollen data and the key bioclimatic parameters estimated in BIOCLIM (Busby 1991) for each site were then ordinated using principle components analysis (PCA) and principle co-ordinate correlation (PCC) respectively (see Figure 3.2). The first axis was found to be related to rainfall, with a clear separation of the more complex forests from the drier and lower fertility sites while the second axis was associated with temperature with correlations for pollen variation found across all temperature parameters. The two sites outside their likely forest type, 4 (Simple Notophyll Vine Forest) and 8 (Mixed Mesophyll Vine Forest), (Figure 3.2) were thought to be intermediate in nature and the positioning of site 8 with the tall open forest was due to the close proximity of an extensive stand of *Casuarina*.

Both the pollen influx studies and the modern pollen study found that pollen deposition from rain-forest is low, but it was of regional significance and dominated by pollen of the top canopy species (Kershaw and Hyland 1975; Kershaw and Strickland 1990; Kershaw and Bulman 1994; Walker 2000; Walker and Sun 2000). Kershaw and Strickland conclude that these results support conclusions from the floristic analysis of rainforest plots that "the big tree species" carry the whole of the classificatory information (Webb et al. 1967; Webb 1968).

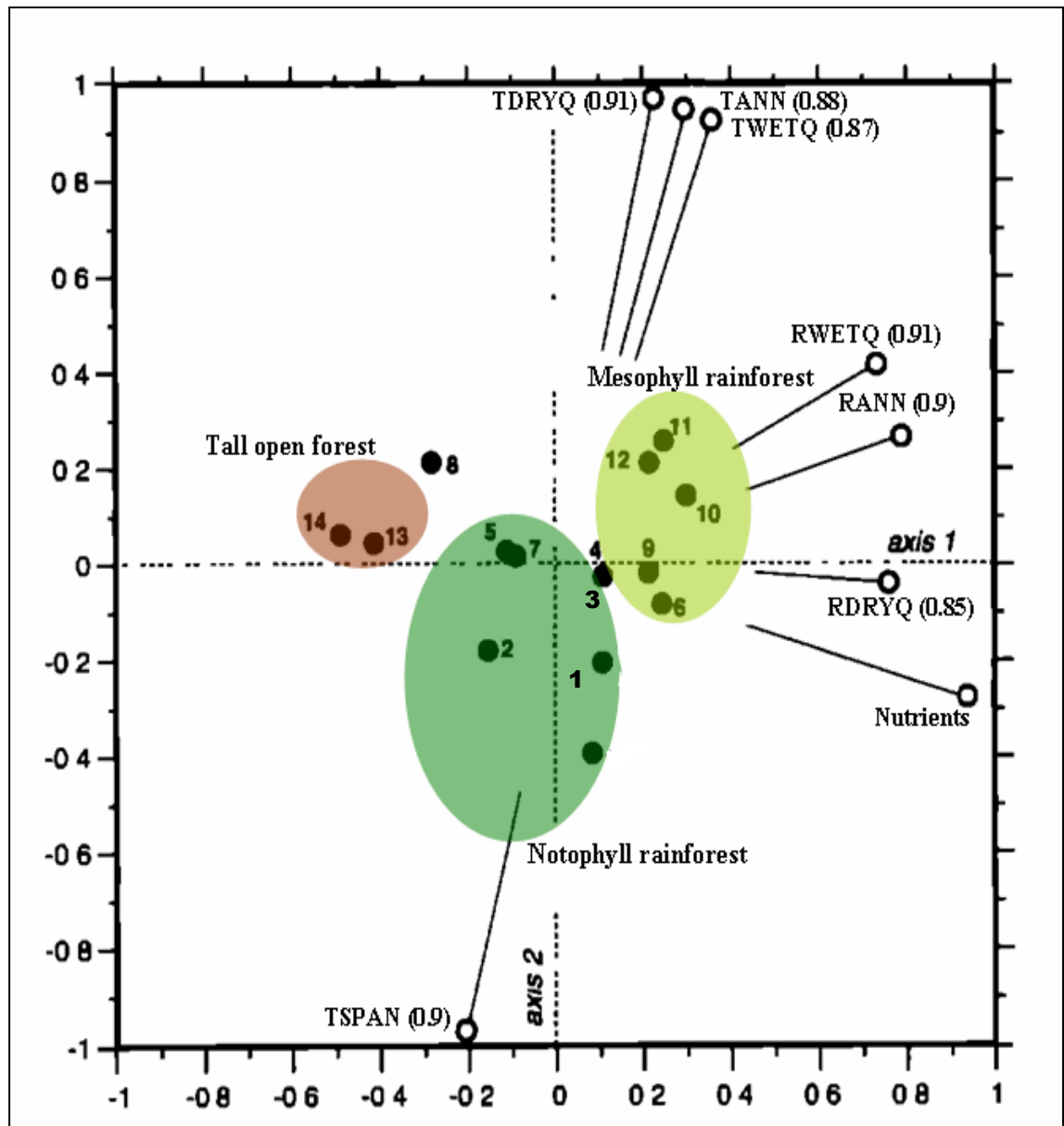


Figure 3.2. Ordination diagram of the sites on pollen data and related environmental variables. Numbers in brackets are values of correlation between each of the environmental variables and the ordination axes' scores for each site – annual mean temperature (TANN), annual mean temperature range (TSPAN), mean temperature of the wettest quarter (TWETQ), mean temperature of the driest quarter (TDRYQ), annual mean precipitation (RANN), mean rainfall of the wettest quarter (RWETQ), mean rainfall of the driest quarter (RDRYQ) (adapted from Kershaw and Bulman 1994).

3.2. Fossil pollen and related studies

Palynology and related studies from Atherton Tableland have recorded significant vegetational changes at both local and regional scales. Pollen records from Bromfield Swamp, Lake Euramoo and Lynch's Crater and subsequently at Lake Barrine covering at least the whole of the Holocene show major changes in dryland pollen from sclerophyll and grassland dominated vegetation to rainforest indicating an increase in precipitation from 8,000 to 6,000 years BP although not uniform across sites (Kershaw 1970, 1973, 1975; Chen 1986, 1987). Differences of timing of this rainforest expansion across the Tableland was considered dependant on topography, incidence of fire and soil type as well as position along the rainfall gradient by these authors and possibly also the distance away from rainforest refugia during the last glacial period (Ash 1988).

Furthermore, a shift to drier rainforest components from around 4,500 years BP through to the present suggested a likely decrease in precipitation and/or increase in temperature (Kershaw 1973). Refinement of Holocene climates was provided by the application of bioclimatic analysis (BIOCLIM) of key rainforest taxa from the substantial rainforest data set (644 sites x 1422 species) of Webb et al. (1984) to the Lake Euramoo pollen (Kershaw and Nix 1988). The results were found to give realistic quantitative climatic estimates and in some cases a refinement of estimates in comparison to other evidence (Figure 3.3). Of particular note was the suggestion that proposed drier conditions after about 4500 years BP probably resulted from an increase in seasonal rainfall variation, although this signal was later considered also to perhaps indicate the onset of an increase in interannual variability or ENSO (McGlone et al. 1992). Kershaw and Nix (1988) suggested that more refined estimates would be possible if there was a higher level of taxonomic identification for the pollen.

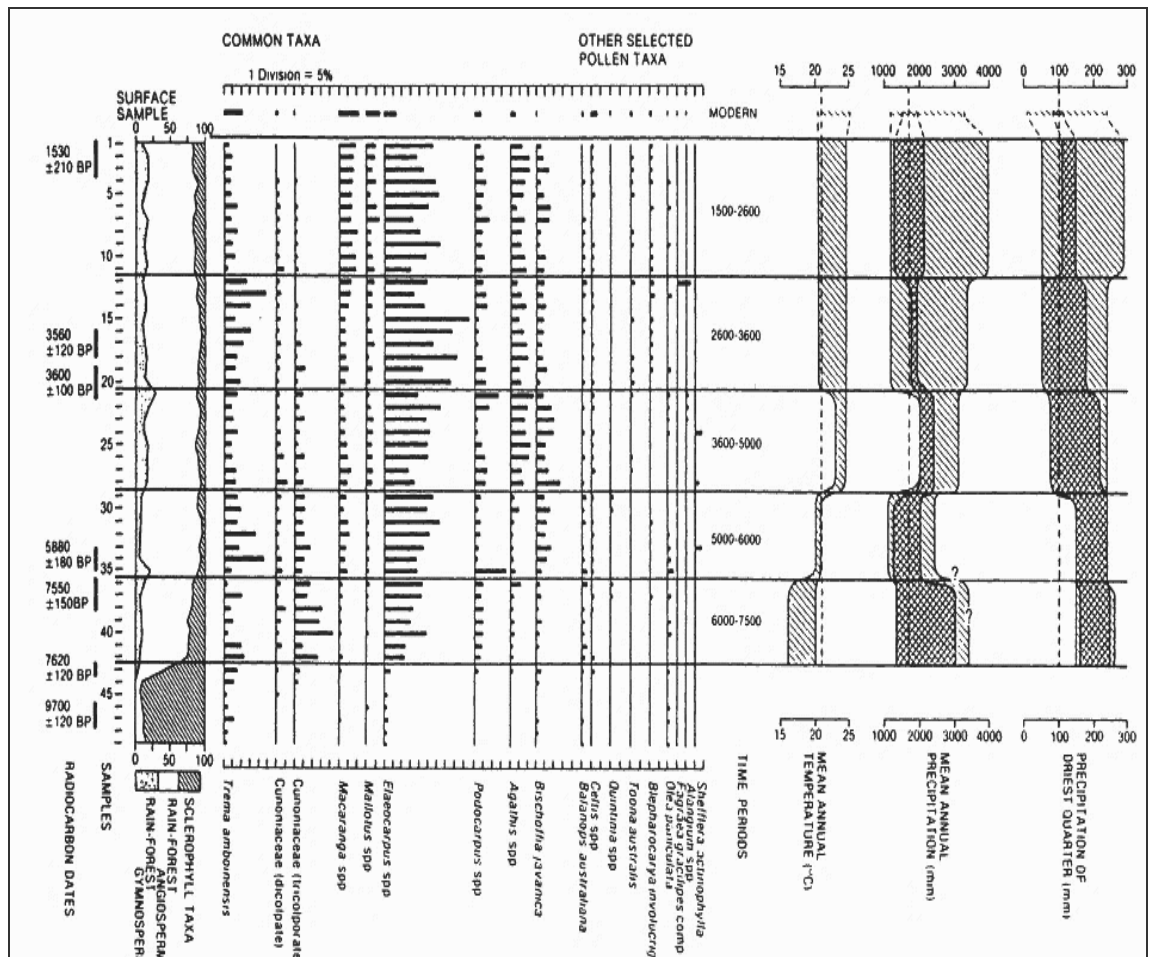


Figure 3.3. Selected attributes of the Lake Euramoo pollen diagram and derived palaeoclimatic estimates. Diagonal hatching indicates the total range envelope while cross hatching indicates the 25-75 percentile range envelope (after Kershaw and Nix 1988).

3.2.1. The late Pleistocene from Lynch's Crater

In the early 1970s only the Lynch's Crater record extended far beyond the Holocene and this provided evidence of vegetational shifts into the last glacial period. Dry rainforest dominated by *Araucaria*, which was a major component of the vegetation from 60,000 yrs BP until progressively replaced by sclerophyll vegetation from about 38,000 to 26,000 radiocarbon years BP. Initially this change was attributed to Aboriginal burning (Kershaw 1976) and this interpretation was reinforced by the inclusion of a charcoal curve (Figure 3.4) (Singh et al. 1981). However, it was considered that Aboriginal burning was insufficient to prevent re-expansion of wetter rainforest in the early Holocene that was attributed to increased rainfall.

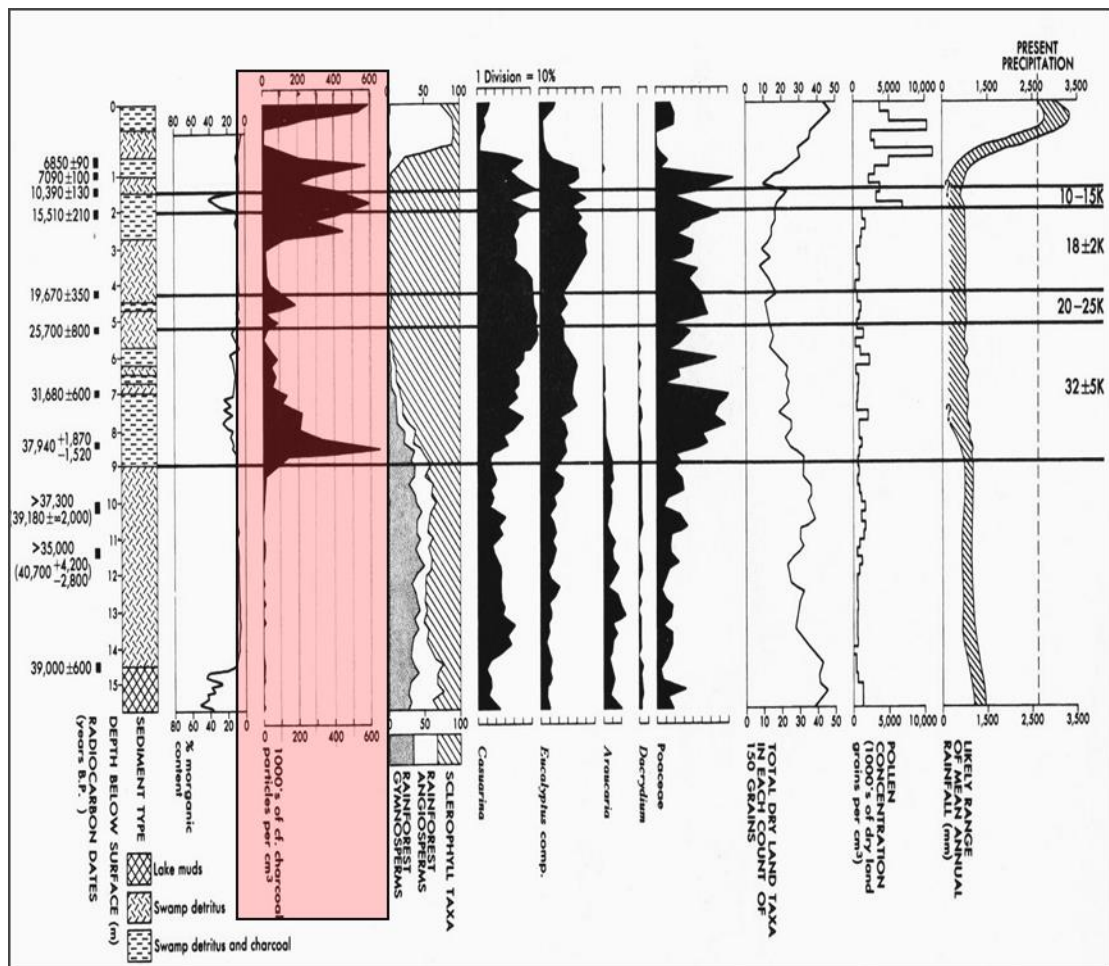


Figure 3.4. Selected features of the initial Lynch's Crater pollen record including a summary diagram of ratios of dryland vegetation types, selected taxa and the microscopic charcoal record, highlighted in red box (after Kershaw 1983b).

Further cores were obtained from Lynch's Crater, progressively extending the palynological core record down to 60 m (Figure 3.5) with the premise that it covered the last 2 glacial-interglacial cycles, approximately the last 190,000 years (Kershaw 1994). It showed that clear systematic shifts from high pollen values for drier rainforest dominated by *Araucaria* during the glacial periods to wetter rainforest during the interglacials were due to changing climatic conditions and confirmed that the mid last glacial shift from approximately 38,000 years BP to total sclerophyll domination was unrelated to the orbitally-induced climate pattern. This change also saw a decline in taxon diversity. The dry rainforest communities prior to 38,000 years BP would fit into either or a combination of *Araucarian* Notophyll Vine Forest and *Araucarian* Microphyll Vine Forest. The pollen record during these araucarian periods also shows a diverse group of secondary rainforest angiosperms, such as *Urticaceae*/*Moraceae*, *Mallotus*/*Macaranga* and *Trema*/*Celtis* as well as the canopy species *Olea paniculata*, *Elaeocarpus* and *Argyrodendron*. Sclerophyll

components are represented during these periods but the more widely dispersed pollen of *Casuarinaceae* is more prominent than *Eucalyptus*. During the last interglacial (115,000–126,000 yrs BP), Complex Notophyll/Mesophyll Vine Forest was dominant which, like the early to mid-Holocene period, was characterised by high values of Cunoniaceae, *Elaeocarpus*, *Freycinetia* and a high diversity of rainforest angiosperms species with near complete absence of the rainforest gymnosperms and sclerophyll taxa as well as a reduction in the drier rainforest canopy species *Arygradendron* and *Olea paniculata*. Of interest in this study is whether the replacement by sclerophyll taxa from 38,000 radiocarbon years BP diverges from this direction prior to the advance of rainforest during the Holocene.

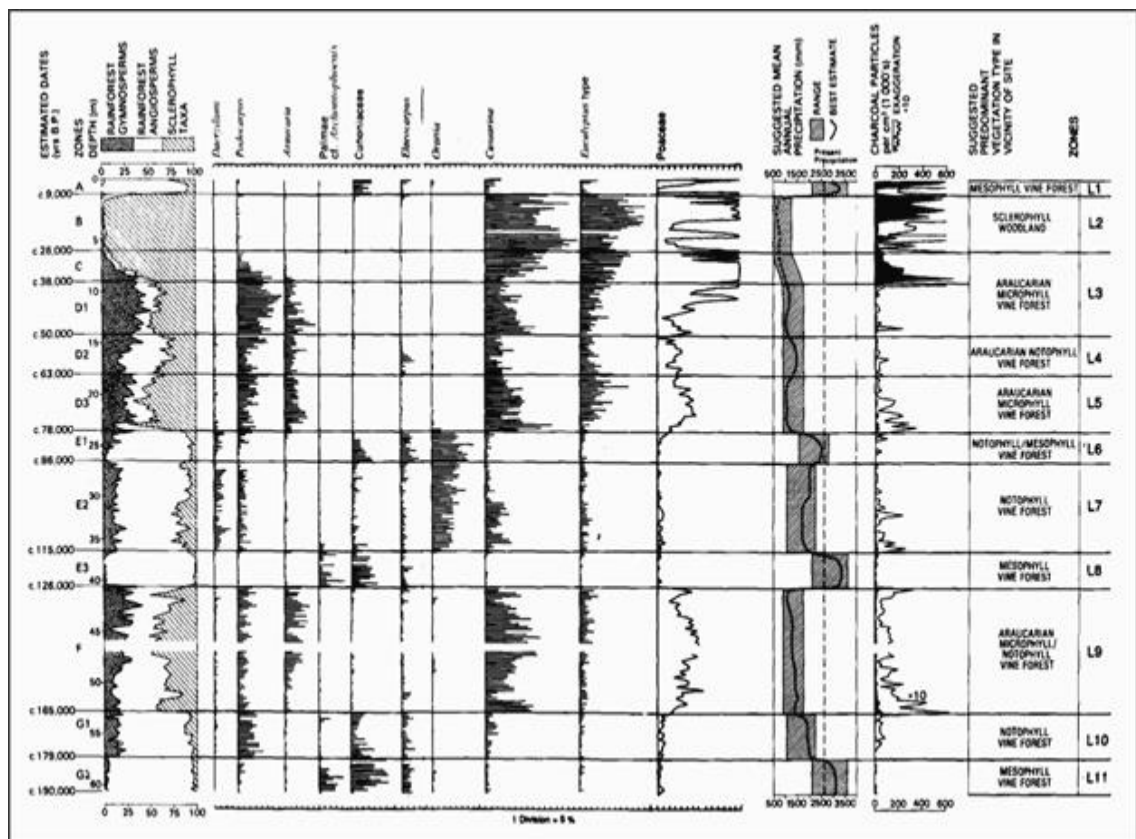


Figure 3.5. Selected attributes of the pollen record from Lynch's Crater extending down to 60 m, estimated to approximately 190,000 years BP (Kershaw 1984, 1986).

3.2.1.1. Redating the Holocene record of Lynch's Crater

There were problems in dating the younger rainforest phase at Lynch's Crater with the suggestion that contamination by soluble organic material moving down the profile maybe the problem (see Chapter 6, *sub-section 6.2.1*). A more continuous Holocene record was obtained and further dating undertaken across the rainforest/sclerophyll

boundary and within the rainforest period to make it possible to compare Lynch's Crater with other Holocene pollen diagrams from Atherton Tableland and so provide a more unified record of regional vegetation and change. Unaltered *in situ* wood, *Flindersia*, found on Lynch's Crater was also selected for dating and provided evidence of the local presence of swamp forest. The results suggest that dryland vegetation is broadly similar across the sites but timing of rainforest advancement did vary and that close proximity to highland refugia as well the presence of fire was likely to be influential (Kershaw 1983a).

3.2.2. Macrofossil evidence of swamp rainforest on Lynch's Crater

Pollen and plant macrofossils from a discontinuous record (Bohte 1994; Bohte and Kershaw 1999) along the margin of Lynch's Crater confirmed an earlier suggestion (Kershaw 1983a) that swamp forest was present on the site during the early Holocene but also confirmed its presence prior to the height of the glacial period. Within this earlier period, estimated to have dated from 85,000 to 95,000 years ago, plant cuticular material was identified to the understorey rainforest species *Rapanea howittia* and *R. asymetrica* with an unidentified *Syzygium* sp. also present, while wood specimens were identified to the myrtaceous genus *Xanthomyrtus*, a genus no longer present in Australia. Further confirmation of the presence of *Xanthomyrtus*, on the swamp was provided by the presence of fossil pollen and its match with an extant *Xanthomyrtus* sp. from New Guinea. Reference pollen material for the New Caledonian species *Dacrydium guillauminii* also showed a good match for the fossil *Dacrydium* found at Lynch's Crater. These two genera, *Dacrydium* and *Xanthomyrtus*, (Figure 3.6) were part of the peat swamp forest, which also included the endemic palm *Oraniopsis*, during the glacial period. *Dacrydium* and *Xanthomyrtus* are now extinct on the Australian continent with Lynch's Crater being the sole fossil record for *Xanthomyrtus* presence with Bohte (1994) suggesting that the crater swamp itself may have been a refugium for selected rainforest taxa during the glacial period.

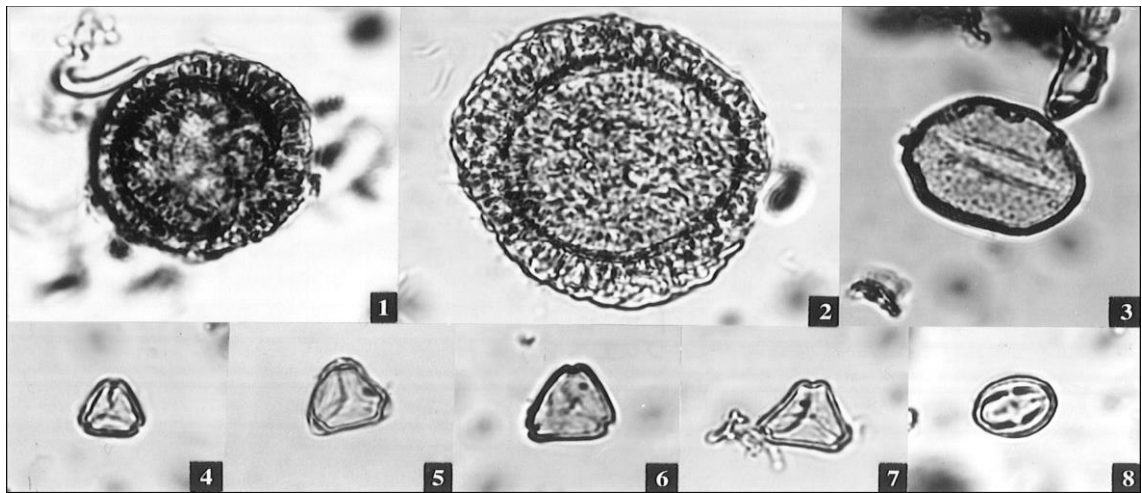


Figure 3.6. Selected pollen taxa which relate to the identified swamp forest: 1. fossil *Dacydium*, 2. extant New Caledonian *Dacrydium guillauminii*; 3. *Oraniopsis*; 4 and 5. fossil *Syzygium* types; 6. extant New Guinean *Xanthomyrtus*; 7. fossil *Xanthomyrtus*; 8. fossil *Rapanea*. All magnification X1000 (Bohte and Kershaw 1999).

3.2.3. Correlation of Strenekoff's Crater and Lynch's Crater

A nearby record from Strenekoff's Crater (Kershaw et al. 1991; Kershaw 1994) covers approximately the same length of time as Lynch's Crater (Kershaw 1994) but features of the pollen record and the complex sediment stratigraphy prevent the construction of a reliable, independent chronology through much of the core. However, there is some commonality with Lynch's Crater with the suggestion that, when key rainforest angiosperm taxa, Cunoniaceae and *Eleaocarpus*, are present, it indicates the penultimate and last interglacial periods in both records. The major difference between the two records is the representation of the palms, *Archonotophoenix* and *Oraniopsis*, that correlate at Strenekoff Crater but have largely separate representation at Lynch's Crater and it is suggested that the differences in the extent of the swamps and spring activity within the craters could be the reason for these differences. There is also a marked increase in charcoal at Strenekoff's Crater but this increase is dated to approximately 23,000 years BP, some 15,000 years after that at Lynch's Crater. This could suggest a lag in human influence but it is most likely that the radiocarbon dating is inaccurate because of the condensed and discontinuous nature of the record (Kershaw et al. 1991; Kershaw 1994).

3.2.4. The stand dynamics of Lake Barrine during the Holocene

The stand dynamics of rainforest and sclerophyll taxa from Lake Barrine was examined by Chen (1986) and Walker and Chen (1987) from pollen and charcoal to elucidate the

transitional phases that occurred in the early Holocene (see Figure 2.1 in Chapter 2). The fine-resolution pollen study of selected indicator taxa tracked the initial arrival of rainforest trees in the area at 9.3 ka BP suggesting the time of change to more humid conditions. However, pioneer rainforest trees were not established at Lake Barrine for another 2500 years, a time which coincided with a reduction in burning and sclerophyll vegetation with an estimated fire interval return at this time to approximately 220 to 240 years (Chen 1986). It is suggested that fire was the factor inhibiting the forest's development with site specific conditions the likely explanation for this result. This study also allowed model fitting estimates to be made of the doubling times for individual taxa from the pollen influx data, for different periods (Table 3.1).

Table 3. 1. Model fitting results from pollen influx data from Lake Barrine (after Chen 1986)

Taxa	Period BP	Model	IRI #	DT *(years)
<i>Agathis</i>	5200-5000	Exponential	0.003481	199
<i>Podocarpus</i>	6700-6200	Exponential	0.002937	236
<i>Podocarpus</i>	4500-4100	Exponential	0.001950	355
<i>Eugenia (Syzygium)</i>	6000-5300	Exponential	0.003748	185
<i>Elaeocarpus</i>	6800-6500	Exponential	0.004192	165
<i>Elaeocarpus</i>	6100-5500	Logistic	0.006518	106
Cunoniaceae	6700-6200	Exponential	0.005852	118
Cunoniaceae	6700-6200	Logistic	0.010937	63
<i>Rapania</i>	6500-6100	Exponential	0.004621	150
<i>Balanops</i>	6600-6200	Exponential	0.004060	171
<i>Blepharocarya</i>	4600-3800	Logistic	0.004760	146
<i>Macaranga/Mallotus</i>	6900-6400	Exponential	0.006517	106
<i>Macaranga/Mallotus</i>	5100-4700	Logistic	0.008085	86
Moraceae/Urticaceae	6800-6500	Exponential	0.006504	107
Moraceae/Urticaceae	5300-5000	Exponential	0.008797	79
<i>Trema</i>	6800-6500	Exponential	0.006498	107
<i>Trema</i>	5200-5000	Exponential	0.008839	78

Intrinsic rate of increase * Doubling time

3.2.4.1. Hydrological patterns at Lake Barrine

Further extensive work was undertaken at Lake Barrine by Walker (1999, 2007), Walker and Owen (1999), and Walker et al. (2000). The lake sediments exhibited contrasting hydrological conditions in the late Pleistocene with the lake basin often dry but also subjected to intense rainfall events. Walker (2007) suggests a monsoon-related climate at this time or a climate producing severe tropical storms. However, because of the complex nature of the lake bathymetry, little sustained organic accumulation occurred. During the

early Holocene due to an increase in rainfall or a decrease in seasonality, areas within the lake basin began to accumulate organic sediment along with an expansion of the lake itself. Walker (2007) suggests that the origin of winter time-dry season finely non-annual laminated organic rich muds in the last 5000 years was due to changes in the climate system with more regular rainfall and the dominance of the Trade winds in the region, similar to the present-day, providing a relatively stable period which saw greater lake depth enabling laminations to develop.

3.2.5. The correlation of marine and terrestrial records

Although not derived from the Atherton Tableland but of relevance to interpretation of Tableland records, especially Lynch's Crater, is a palynological marine record from the ODP 820 core (Moss 1999; Moss and Kershaw 2000, 2007) located off the coast of north-east Queensland. Both records cover approximately the same period of time and, as there are general similarities in patterns of change in pollen representation, it has been possible to confirm the chronology of Lynch's Crater through comparison with the much more firmly dated, ODP record derived through oxygen isotope analysis on the core. One significant difference is that the single, sharp *Araucaria* decline dated around 38,000 years BP at Lynch's Crater is not evident from the ODP 820 record. Instead, a more step-wise reduction in *Araucaria* is indicated from approximately 140,000 years BP. Originally it was suggested that the initial decline in *Araucaria*, combined with a peak in charcoal at this time, could have indicated an earlier human presence (Kershaw et al. 1993; Moss and Kershaw 2000) but a subsequent interpretation is that this event may have been related to an increase in ENSO variability with the development or expansion of the West Pacific Warm Pool (WPWP) to the north of this region (Kershaw 1994; Thunell et al. 1994; Zhang et al. 1997; Moss and Kershaw 2000, 2007). Another anomaly between the records is that the charcoal increase at Lynch's Crater dated to 38,000 radiocarbon years ago was dated to about 45,000 years BP at the ODP 820 site.

3.2.6. The soil charcoal record of north Queensland

Independent of the palynological studies, soil charcoal analysis (Hopkins et al. 1990) revealed that charcoal fragments identified as *Eucalyptus* spp. and dated between 27,000–12,000 years BP were found in a soil profile under moist tropical rainforest on the Windsor Tableland, northwest of Mossman (Figure 3.7). The authors concluded that this

present-day rainforested site was occupied by sclerophyll forest during this period which is within the sclerophyll dominated period around Lynch's Crater.

A more extensive charcoal analysis was then carried out within the present-day distribution of rainforests in north Queensland between latitudes 15°30'S and 19°15'S and longitudes 145°E and 146°30'E (Figure 3.7) with all positively identified charcoal particles assignable to the genus *Eucalyptus* (Hopkins et al. 1993). They found that charcoal was common and often locally abundant. However, there were few records prior to 20,000 BP and suggest that fire would have penetrated some rainforest areas with the subsequent *Eucalyptus* colonisation a lot later than in the original study site of the Windsor Tableland. The maximum geographic distribution of charcoal fragments was found during the period 13,000–8000 BP and, although not positively identified, charcoal fragments with similarities to *Lophostemon* and *Alstonia* were also found in the Macalister Range Massif area. They were not dated but the *Astonia* charcoal type was found directly above positively identified dated *Eucalyptus* charcoal (12,230±250 kyr BP). This large pioneer rainforest species, *Astonia*, can be one of the first rainforest trees to establish under sclerophyll forests. Although the majority of charcoal fragments dated were within the period 13,000–8000 BP, positively identified *Eucalyptus* charcoal persisted until c. 6000 years BP in some areas (Macalister Range Massif area/Mt Formartine and Mt Nomico). The period 13,000–8000 BP clearly coincides with the latter part of the period of sclerophyll domination around Lynch's Crater with the subsequent decline of charcoal fragments after this period consistent with the re-establishment of rainforest taxa and reduction in fire frequencies found at Lynch's and the other crater lakes. This broader spread of sites does allow us to see that the extent of sclerophyll dominated landscapes was not confined to the palynological sites but it also demonstrates that fire and the encroachment of sclerophyll vegetation was not uniform. This is clearly seen when a comparison is made with the charcoal record from Lynch's Crater (Figure 3.5) which has high values at 38,000 yrs BP as per Kershaw's (1994) record well before the 27,000 yrs BP date from the Windsor Tableland.

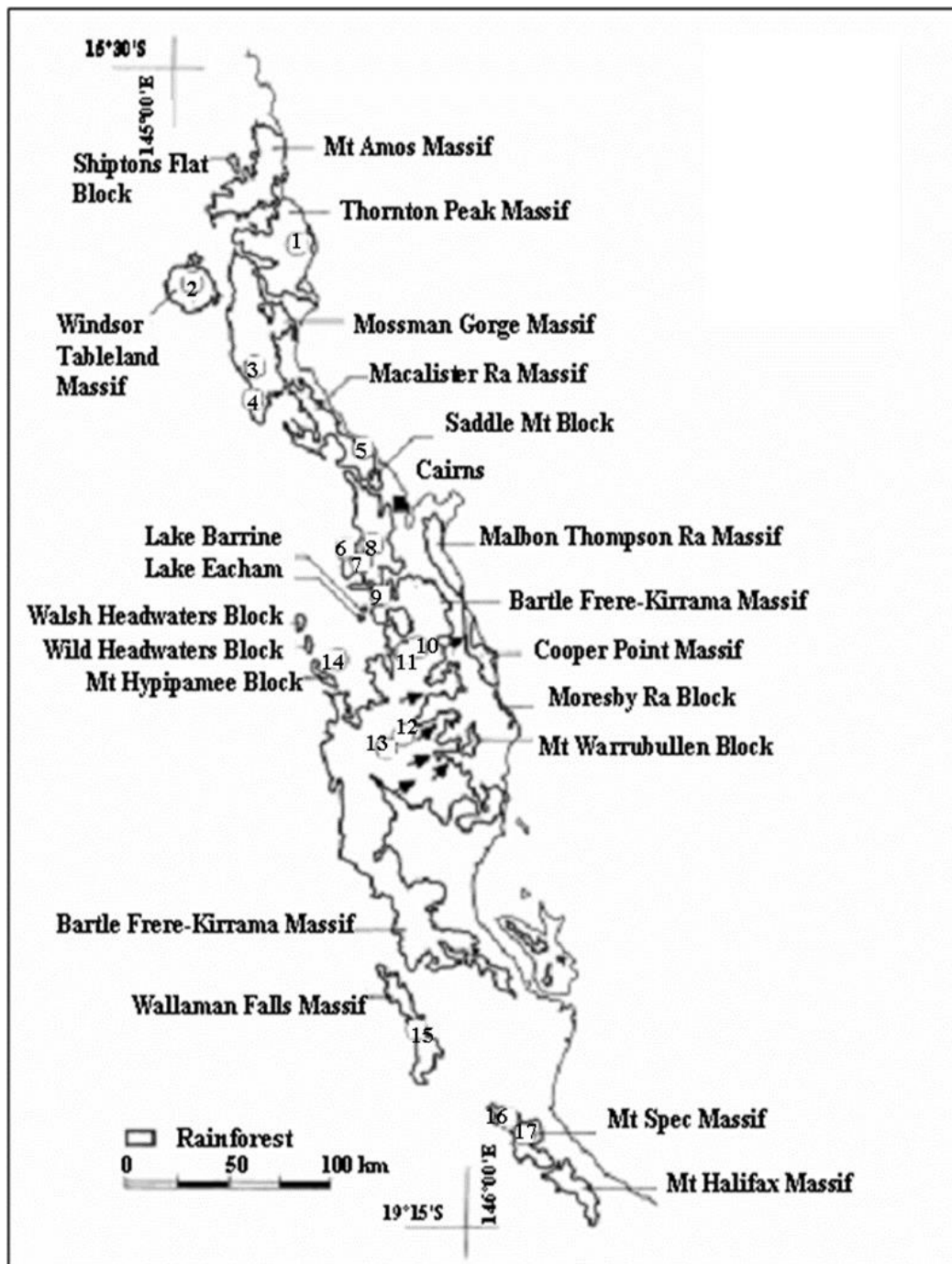


Figure 3.7. The seventeen districts (numbered) from which *in situ* charcoal fragments were collected. Black arrows show where charcoal may have been transported considerable distances from source. 1 Cape Tribulation, 2 Windsor Tableland, 3 Half Ton Creek, 4 Mt Lewis, 5 Macalister Range, 6 Mt Haig, 7 Mt Edith, 8 Breach Creek, 9 Mt Nomico, 10 West Bartle Frere, 11 Upper Russell R, 12 Downey Creek, 13 Maple Creek, 14 Longlands Gap, 15 Wallaman falls, 16 Jourama, 17 Mt Spec (after Hopkins et al. 1993).

3.2.7. A higher resolution and multiproxy record from Lake Euramoo

In 1999 a new core was taken from Lake Euramoo extending the record of this lake from the base of the Holocene to the Last Glacial Maximum (LGM) which provided detail of the causes and roles of disturbance within tropical rainforests. This palynological study

also included a contiguous record of macroscopic charcoal (Figure 3.8) and found that rainforest expansion was a complex process with climate change, topography and anthropogenic input all contributing to the picture (Haberle 2005). Prior to 9,000 cal. yr BP fire was seen as a dominant factor which retarded rainforest expansion and thereby provided a competitive advantage to fire-tolerant and pioneer species in the early Holocene. The rainforest expansion and ensuing sclerophyll decline after ~ 9,000 cal. yr BP is the major variable on axis 1 of the PCA (Figure 3.9) and is also indicated by an increase in palynological diversity (rarefaction analysis). Subsequent diatom studies covering the last 15,000 years, found that there was a lowering of lake levels between 13,800 and 11,500 cal. yr BP which did not correspond to large-scale climate events such as the Antarctic Cold Reversal or Younger Dryas but was more likely linked to changing climate regimes in the south-west Pacific during the transitional phase of the late glacial (Tibby and Haberle 2007).

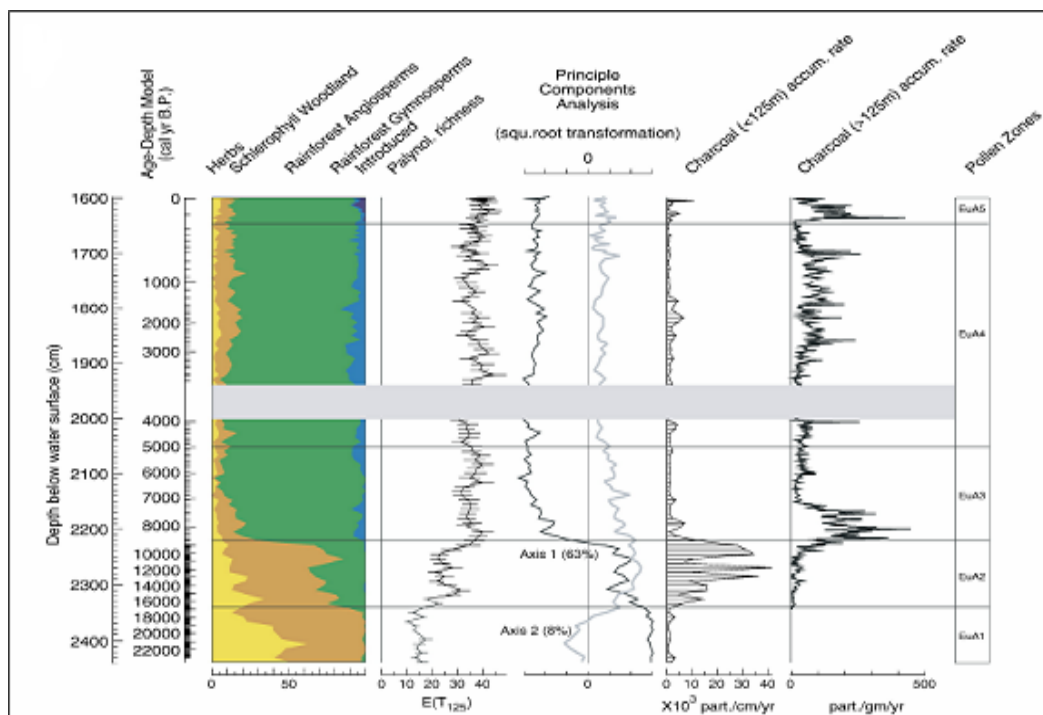


Figure 3.8. Lake Euramoo pollen diagram – Summary diagram with rarefaction analysis, principal components analysis results and charcoal accumulation rates (after Haberle 2005).

3.2.8. A refinement of the Lynch's Crater chronology and the humification record

A study of the last 50,000 years at Lynch's Crater was undertaken to refine the chronology and, particularly, redate the timing of charcoal increase to determine the degree of synchronicity with current archaeological ages for human arrival in Australia (Turney et al. 2001*a,b*). A rigorous pre-treatment (ABA-Acid Base Acid) was applied to samples for radiocarbon dating and results extended the time of increase in fire frequency from 38,000 to 45,000 radiocarbon years BP, more consistent with existing evidence for human arrival (Turney et al. 2001*c*). With the establishment of this robust chronology that demonstrated a fairly constant sedimentation rate, further analysis was undertaken to explore the nature and causes of variability within the record (Turney et al. 2004). It was found that a high *Cyperaceae*/*Poaceae* ratio, indicative of wetter conditions, alternated with high sediment humification or absorption and charcoal levels, which were indicative of drier conditions (Figure 3.9). Spectral analysis was undertaken on the peat humification data and two significant spectral frequencies were produced, a millennial-scale cycle at 1,490 yr and a semi-precessional cycle at 11.9 kyr.

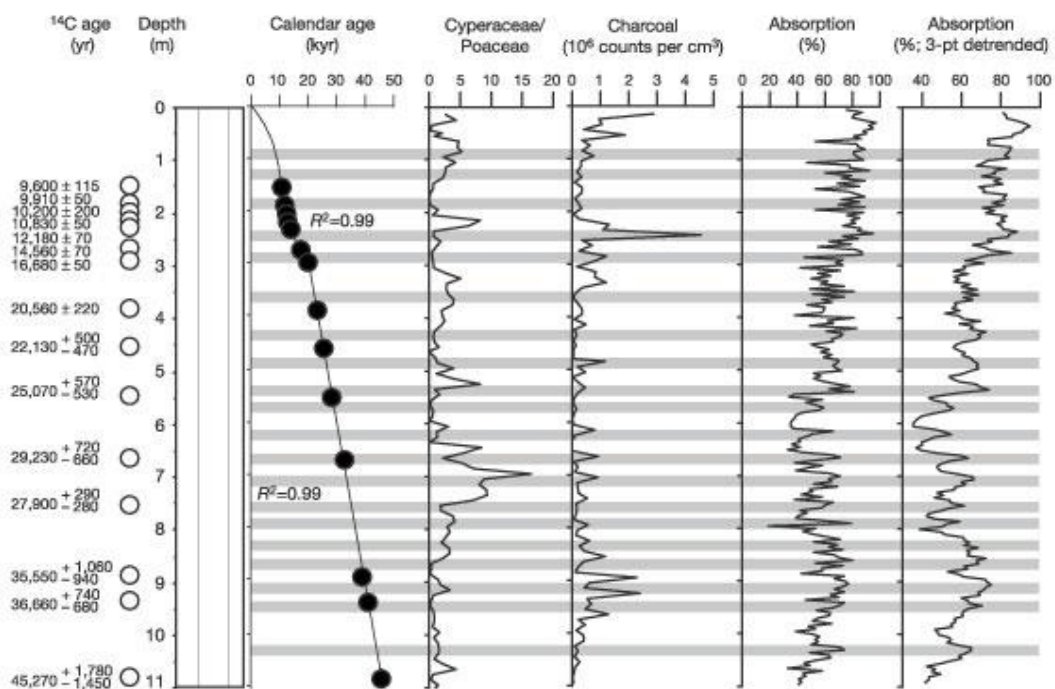


Figure 3.9. Summary of palaeoenvironmental data from Lynch's Crater showing Turney et al. (2001) chronology, the *Cyperaceae*/*Poaceae* ratio, charcoal and humification (absorption) values. Grey shading bands indicate inferred dry periods (after Turney et al. 2004).

The millennial scale cycle was linked to changes in precipitation associated with long-term changes in ENSO in the tropical Pacific Ocean and matched Dansgaard-Oeschger (D-O) events in the North Atlantic. Cross-spectrum analysis of Lynch's Crater (Figure 3.10) with the GISP2 record shows that these two records are in phase. Wavelet analysis of both records showed that the maximum amplitude of the 1,470-yr cycle was the period between 35 and 25 kyr ago when the most conspicuous alternating periods of drying and wetting cycles occurred in the crater record. Both wavelet plots show the semi-precessional cycle but unlike the GISP2 record, the cycle at Lynch's is strong and is the dominant frequency for the whole sequence, see Figure 3.10 A(a).

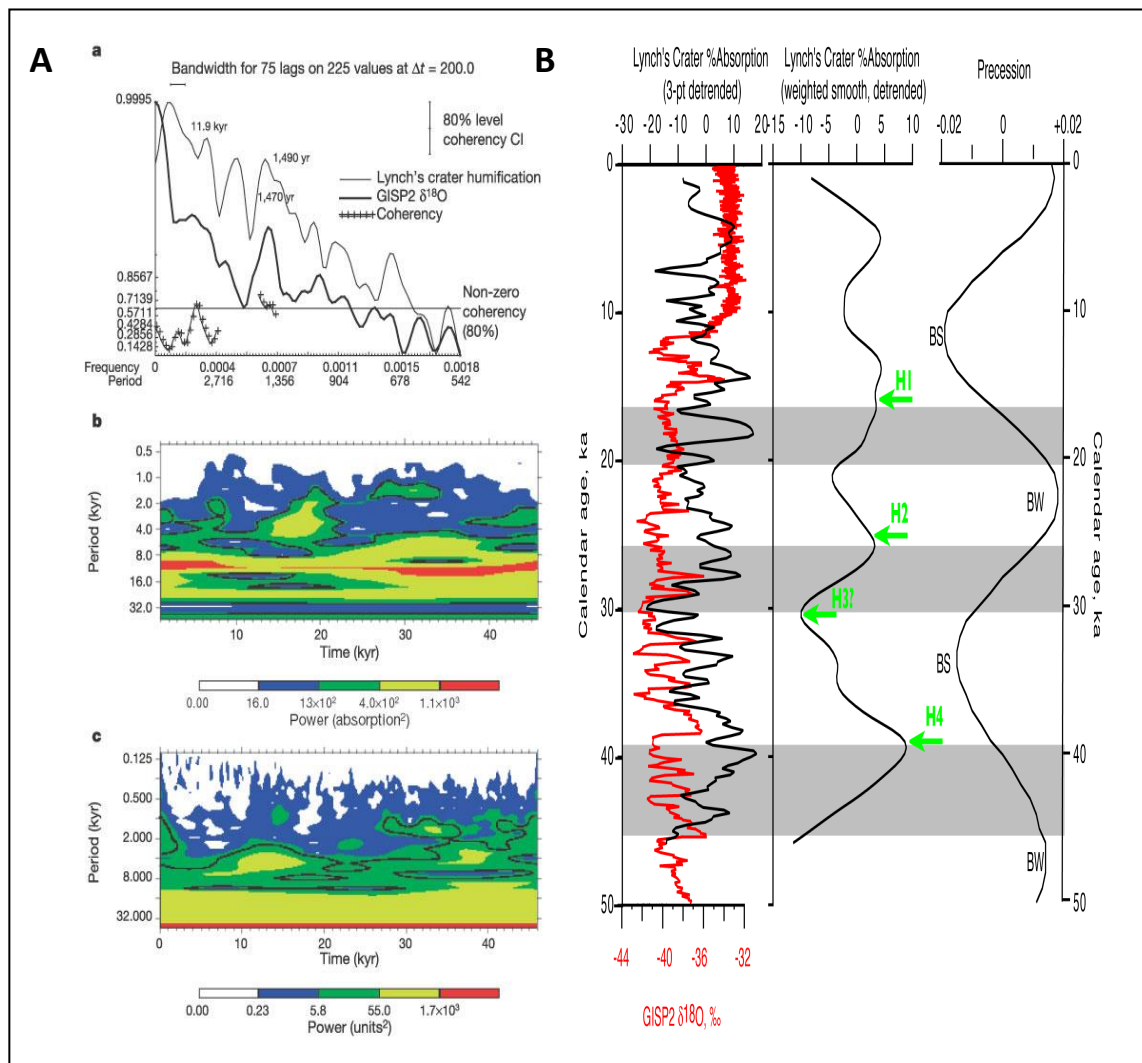


Figure 3.10. A – Cross-spectral (a) and wavelet analysis (b and c) of the Lynch's Crater and GISP2 records for the past 50 kyr. B – Comparison of Lynch's Crater 1,490-yr and 11.9-kyr trends in absorption values. GISP2 $\delta^{18}\text{O}$ values and the precessional component of the orbital forcing with Heinrich events indicated. Grey shading indicate inferred dry periods (after Turney et al. 2004).

This would suggest that, even though there are wetter periods on the crater during stadials, the semi-precessional cycles indicate longer-term changes in drying which may be linked to the North Atlantic ‘Bond’ cycles. Turney et al. (2004) suggest that this drying indicates longer term changes in ENSO independent of the monsoonal system and therefore of the North Atlantic. These ‘warm’ ENSO events, represented as drying conditions in north Australia, are particularly strong at 40, 25 and 15 kyr ago while ‘cold’ events, expressed as wetter conditions in north Australia, are strong at 30 and 21 kyr ago.

These ‘warm’ ENSO events coincide with Heinrich –1, –2 and –4 in the GISP2 $\delta^{18}\text{O}$ data set (Figure 3.10B) but there is no correlation with Heinrich–3. Turney et al. (2004) suggest that, when there is a correlation it could be due to a larger latitudinal temperature gradient during ENSO activity which would allow more moisture to be carried to the high latitudes increasing the possibility of an ice surge, or that during these warm El Niño events there is a north-west to south-east transect across North America with the possibility of ice melting. These findings suggest that the tropical Pacific Ocean is a crucial component of the Earth-ocean-atmosphere operating at millennial and semi-precessional timescales (Turney et al. 2004). However, Kaal et al. (2014) suggests that humification analysis may be problematic on older material, > 12 ka, as the signal could reflect degradation of organic material rather than humification.

3.2.9. The geochemistry and the presence of wet Heinrich events on Lynch’s Crater

More recent work on the last 50,000 years at Lynch’s Crater has focused on the geochemistry of the crater. Initial research provided some interesting results on patterns and sources of windblown dust (Muller et al. 2006; Kylander et al. 2007). It was suggested that between about 52.5 and 41 ka the Lynch’s Crater dust component was derived predominantly by long distance transport (>1500 km) from south-east Australia, from 41 to 8.5 ka from regional sources (100-1500 km) and between about 8.5 and 2 ka the dust signal was local (<100 km) (Kylander et al. 2007). However, these longer-term changes were interrupted by more easily interpreted shorter distinct phases indicated by high inorganic levels characterised by abundant biogenic silica, sponge spicules and diatoms (Figure 3.11) which displayed varying degrees of weathering.

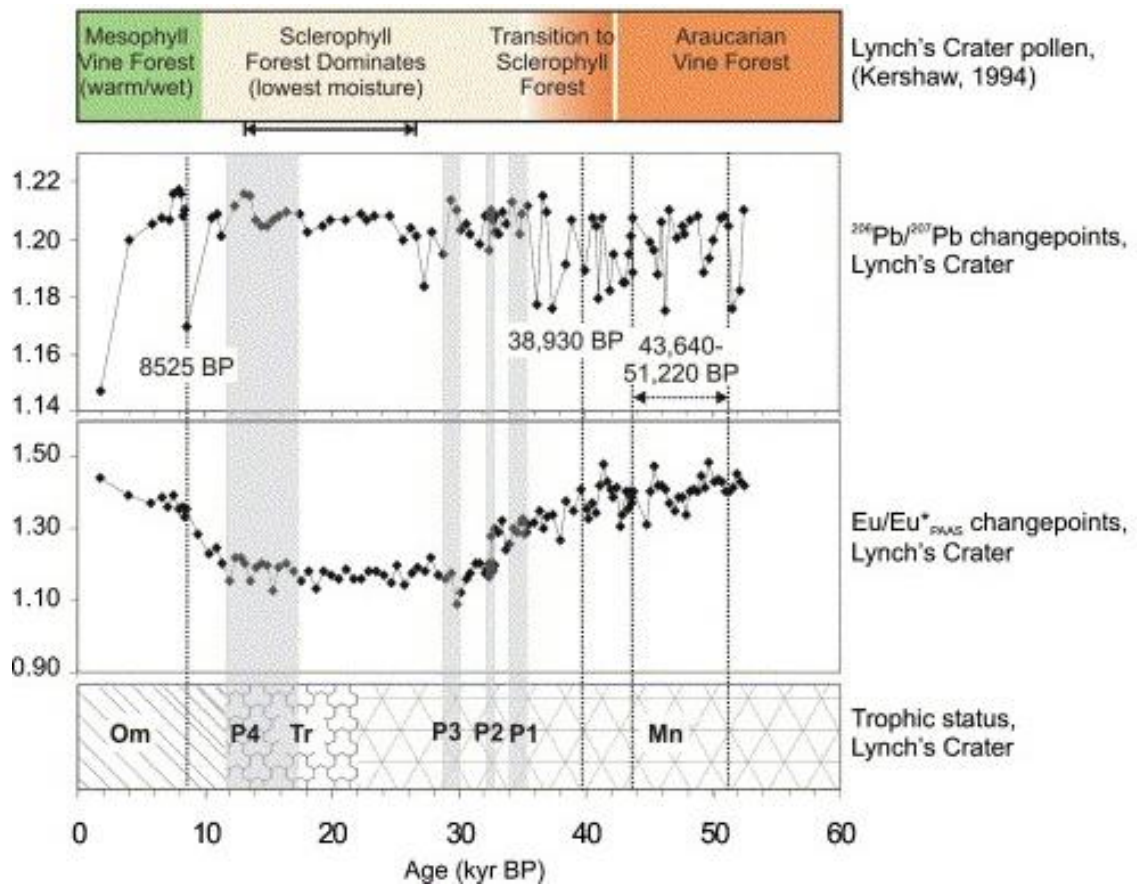


Figure 3.11. Trophic status of deposit – minerotrophic peat (Mn) with transitional zone (Tr) into ombrotrophic peat (Om) in upper layers and identified dust source changepoints are indicated on the ages vs. $(\text{Eu}/\text{Eu}^*)_{\text{PAAS}}$ and $^{206}\text{Pb}/^{207}\text{Pb}$ profiles with the four wet events indicated by grey shading (P1-P4), (after Kylander et al. 2007).

Corresponding to these phases there is enrichment in silicon, aluminum, lead and copper which are likely to be sourced from local clay minerals. The local input of these minerals and the abundant weathered biogenic silica suggest local flooding events and erosional activity with the likelihood of shallow ponding or lake conditions present during these episodes (Muller et al. 2008a), a suggestion supported more recently from analyses of Kaal et al. (2014). Kaal et al. (2014) looked at both humification and the molecular composition of organic matter at Lynch's Crater using pyrolysis-GC-MS. They suggest, like Muller et al. (2008b), that these wet phases represent the last three Heinrich events which coincide with a more southward migration of the ITCZ. The southward displacement of the ITCZ was considered likely driven by increased temperature gradients between the Northern and Southern Hemisphere with triggers originating in the low latitudes. Kaal et al. (2014) also suggest that the Cyperaceae/Poaceae ratio may not always indicate wet or dry conditions as Poaceae may also be a wetland taxa. All studies discussed above, sub-section 3.2.8 and 3.2.9, were sampled at similar intervals and it is

hoped that the more high-resolution contiguous sampling of the present study will provide some insight to these conflicting findings.

3.2.10. Spectral analysis on the long Lynch's Crater record

In 2004 a full sediment core, 64.05 m in length, was retrieved from Lynch's Crater enabling construction of the basal part of the palynological record and providing material for geochemical analysis. A summary diagram of the complete palynological record, estimated to cover the last 230,000 years, is shown in Figure 3.12. Spectral analysis demonstrated that the strongest response was to eccentricity with a diminished response to obliquity and no significant precessional signal. It was suggested (Bretherton 2006; Kershaw et al. 2007a) that vegetation and climate on the Atherton Tableland is largely forced by Northern Hemisphere insolation and ice volume, probably operating through sea level and sea surface temperature changes.

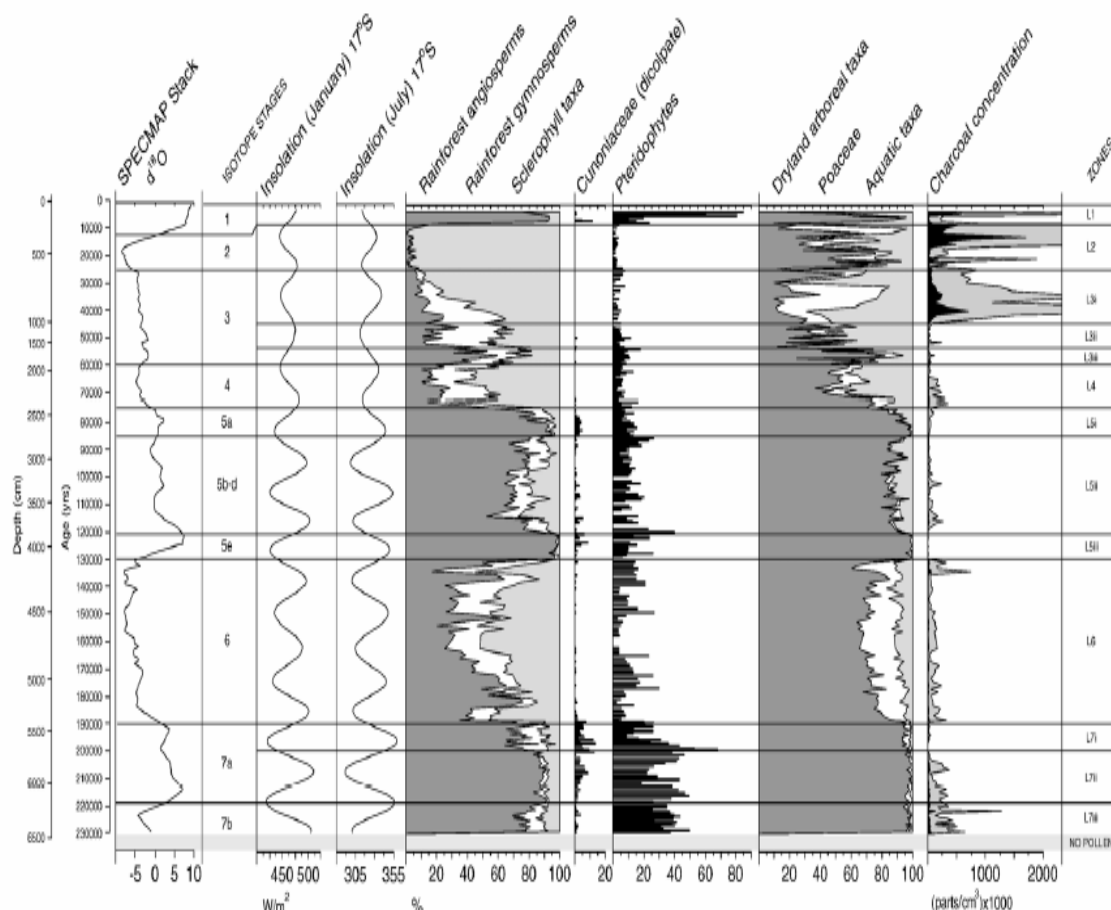


Figure 3.12. Summary diagram for Lynch's Crater with spectra shown in relation to age and including the SPECMAP stack oxygen isotope values and stages, insolation values for January and July at 17°S, relative to selected forest taxon groups, aquatic taxa, Poaceae and charcoal concentrations (after Kershaw et al. 2007a).

However, as for the ODP 820 record and other Pacific and Indian Ocean records, a 30,000-year frequency was also present at Lynch's Crater that may relate to longer term ENSO activity although the cause of this signal has not been determined for certain (Beaufort et al. 2001; Kershaw et al. 2003).

3.2.11. Fire, people and megafauna

To resolve the relationship between humans, fire and megafauna, research was undertaken at Lynch's Crater by utilizing the ascospore *Sporormiella* and other dung fungi (Rule et al. 2012) which provide a proxy for large herbivore biomass and therefore activity (Davis 1987; Burney et al. 2003; Davis and Shafer 2006; Wood et al. 2011; Gill et al. 2013; Johnson et al. 2016). Both the present record and Kershaw's record (1994) were included in the study (Figure 3.13).

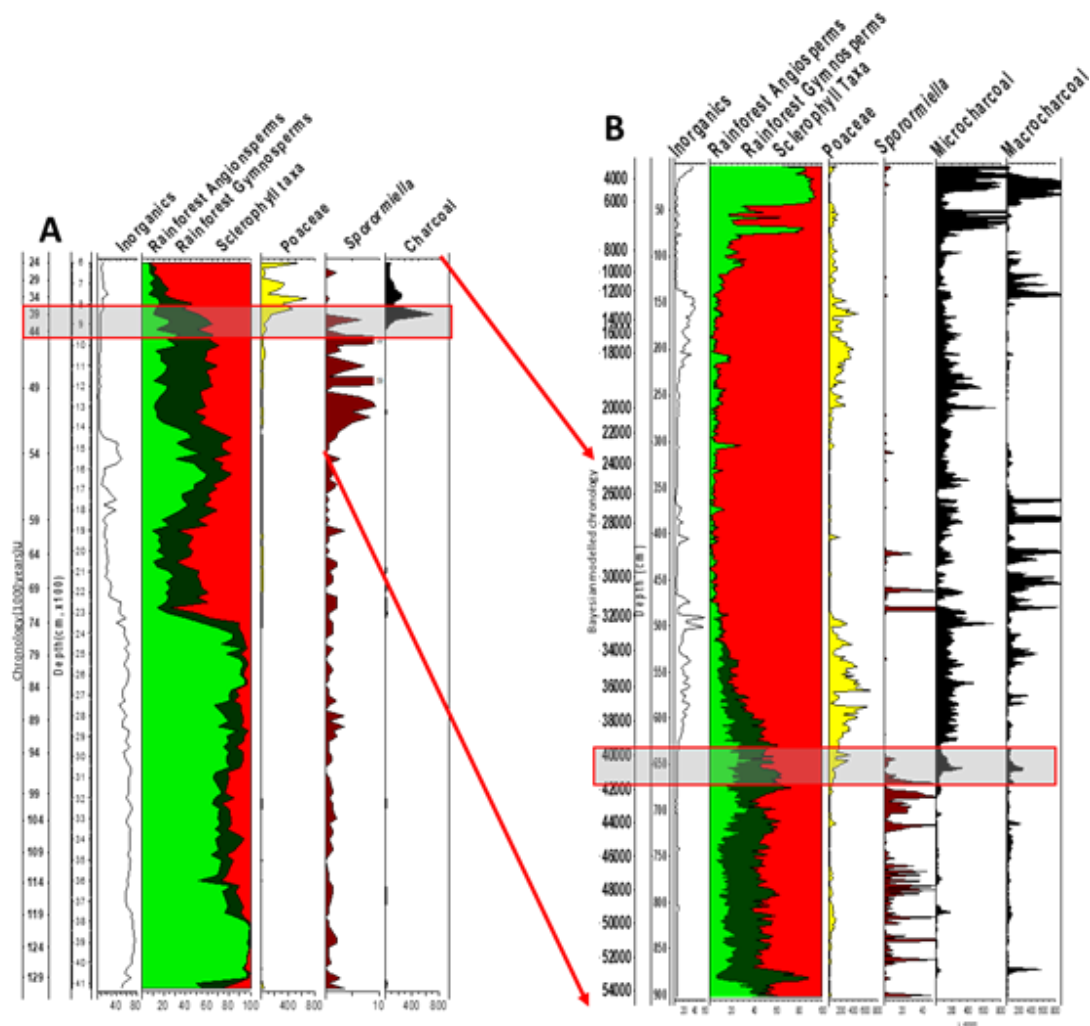


Figure 3.13. Lynch's Crater summary diagrams including *Sporormiella* for A-Kershaw (adapted from Kershaw 1994, Kershaw et al. 2007a) and B-Present study, red arrows indicate same time-periods, red highlighted grey shade area covers period where *Sporormiella* decreases followed by increased charcoal (adapted from Rule et al. 2012)

Standardized estimates of the magnitude of ecological changes following megafaunal decline after ~41 ka in comparison to earlier climate-driven shifts from 74 and 120 ka, on *Sporormiella*, charcoal and sclerophyll vegetation found that megafaunal extinction was not driven by an increasingly arid climate. Regression analysis also indicated that vegetation changes lagged *Sporormiella* and charcoal changes at ~ 41 ka therefore ruling out fire as a cause for megafaunal extinction. It was concluded that human arrival caused megafaunal extinction at this site which was followed by the replacement of dry rainforest dominated by *Araucaria* with sclerophyll vegetation, triggered by the reduction in herbivory and increased fire (Rule et al. 2012; Johnson et al. 2015).

3.3. The Archaeological Record

Within the general region of northern Queensland, the earliest known human occupation sites are mainly west of the Great Dividing Range with the oldest at Ngarrabullgan Cave (40,540±650 yr cal BP). This site is 80 km north-west of Atherton Tableland, and it is suggested that, due to the sparsity of cultural materials from this time period, limited levels of occupation would have occurred until the middle to early Holocene when artifacts increase two-fold (David et al. 1998). However, Fern Cave in the Chillagoe area of north Queensland, where marginal use is recorded prior to 29,000 ¹⁴C yrs BP, indicates that between 17,000 and 13,000 ¹⁴C yrs BP the site was used intensively but abandoned at the end of the Pleistocene. It is suggested that the higher rainfall in the Holocene may have made the cave uninhabitable (David 1990; David 1991; Morwood and Hobbs 1995). In the limestone karst region of Laura on the Cape York Peninsula, north-east of the study site, earliest human occupation, dated from rock art friezes, starts from approximately 24,600 ¹⁴C yrs BP (Sandy Creek 2) with a more continuous presence from the early Holocene (Cole and Watchman 2005).

3.3.1. Intensification or climate variability during the Holocene?

From the early Holocene an increasing trend of human occupation is found in south-east Cape York in common with many other Australian archaeological sites (Figure 3.14). This trend across tropical Australia in particular shows a threefold increase from around 4000 years BP which continues through the late Holocene until recent times. The “intensification” model centered on this period, the middle to late Holocene, proposes

that socio-economic and demographic changes were the key components for this change which ultimately saw a more dynamic participation of Australian Aborigines within both the natural and socio-cultural environments (Lourandos and David 2002).

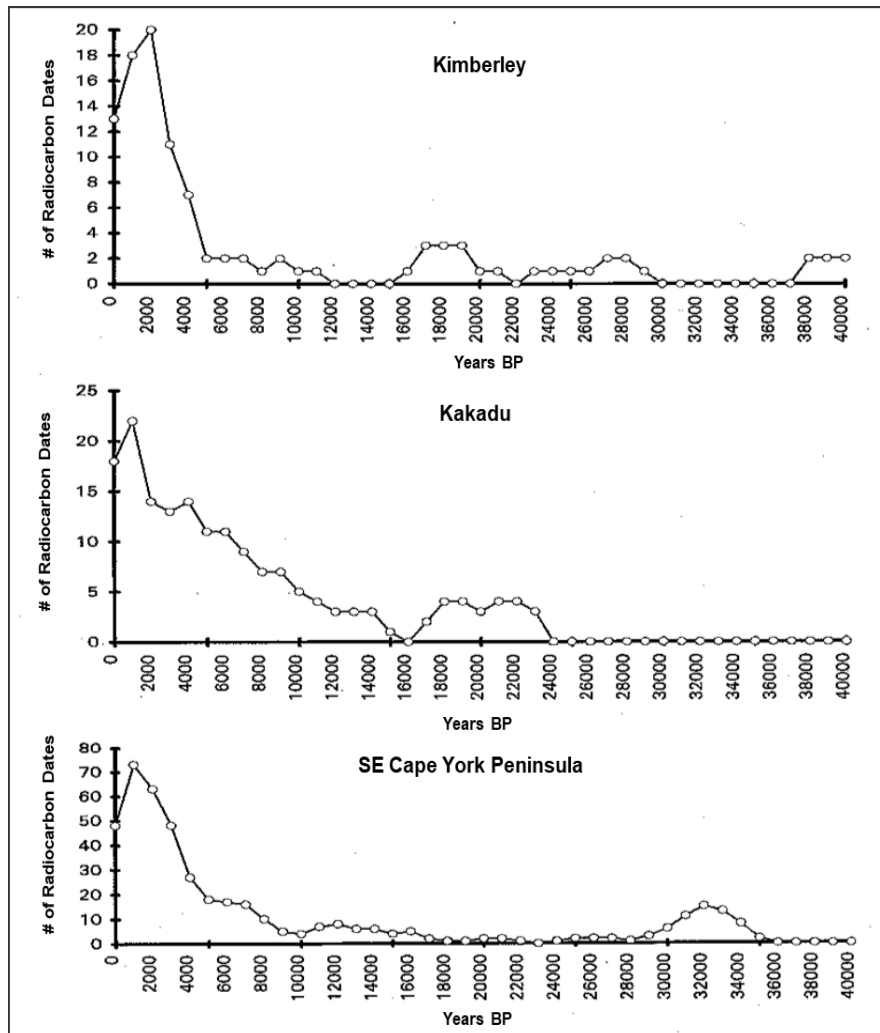


Figure 3.14. Radiocarbon date curves for regions in tropical Australia for human occupation; Kimberley; Kakadu; Southeast Cape York Peninsula (adapted from Lourandos and David 2002).

However, the intensification model is hotly debated as the proposed period of peak activity in the landscape during the middle to late Holocene corresponds with increased climate variability attributed to ENSO (McGlone et al. 1992; Lourandos and Ross 1994; Shulmeister and Lees 1995; Turney and Hobbs 2006; Holdaway et al. 2008; Johnson and Brook 2011). The latter has been suggested to be the trigger for social change that saw populations forming into territorial regional groups with a broadening of the range of foodstuffs consumed (Haberle and David 2004).

3.3.2. Adaptation to a rainforest environment during the late Holocene

This broadening of foodstuffs consumed has been the emphasis of archaeological investigations in the wet tropics of north-east Queensland, especially evidence of the preparation of toxic plants for human consumption. Jiyyer Cave located in the lowland rainforest about 50 km south of Cairns (Figure 3.15) has initial human occupation dated at 5,000 years BP with identified charred toxic nutshells dated to approximately 1000 years BP, while the nearby Mulgrave River site has toxic nutshells dated to approximately 2,000 years (Horsfall 1987). Recent research at Jiyyer Cave has reaffirmed Horsfall's original chronology in the area (Cosgrove and Rayment 2002). Three archaeological sites, Urumbal Pocket, Goddard Creek and Murubun Shelter near Koombooloomba Dam south of Ravenshoe, (Figure 3.15) reiterated findings from Jiyyer Cave.

The Mulgrave River site has provided additional information gained from starch analysis and phytoliths which verified the processing of toxic starchy seeds, *Beilschmedia bancroftii* (Yellow walnut) and *Endiandra palmerstonii* (Black walnut) (Cosgrove et al. 2007). Cosgrove et al. (2007) suggest that, within the rainforest and its western margins, there are three phases of occupation within the rainforest; the first two 8200 to 8000 cal. BP and 6000 to 5000 cal. BP have low discard rates suggestive of only occasional use which coincides with re-establishment of rainforest in the area as suggested by palynological results. By contrast, the third phase between 3300 and 2100 cal BP signifies more intensive settlement of the region with extremely high levels of activity recorded after 2000 cal. BP indicating permanent occupation of the north-east Queensland rainforest. This is in contrast to the western margins of the rainforest where archaeological evidence suggest at least limited occupation at > 35 ka (Ngarrabullgan Cave) with intermittent usage and at times more extensive usage in some areas from 30,000 cal. yr BP (Fern cave) (David 1991, 1993, 1998: David and Lourandos 1997).

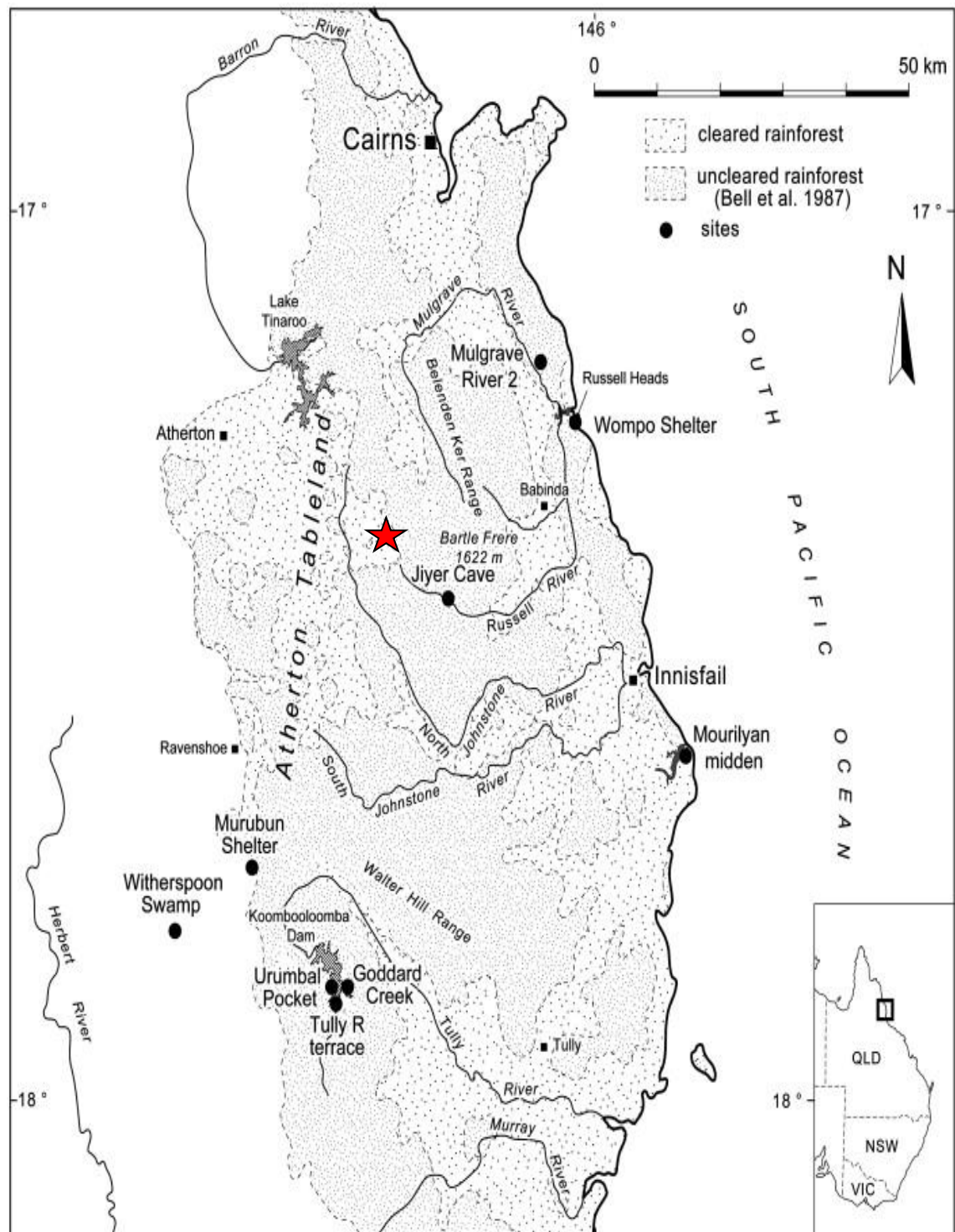


Figure 3.15. The Atherton-Cairns-Innisfail region showing the extent of present-day rainforest and areas where rainforest has been cleared. The locations of the archaeological sites discussed in *sub-section 3.3.2* are also shown, red star Lynch's Crater (after Cosgrove et al. 2007).

3.3.3. The early European contact period

Observations by early explorers Palmerston and Lumholtz included reference to an abundant Aboriginal diet from rainforest flora and fauna (Birtles 1997). Christie Palmerston noted the detailed preparation needed for the toxic nut *Beilschmiedia bancroftii* by Aborigines while traversing the Atherton Tableland in 1883 (Savage 1992). Both Palmerston and the Norwegian ethnologist Carl Lumholtz as well as others did note that, although there was a distinctive Aboriginal rainforest culture, their overall perception that they were primitive savages or a doomed race unfortunately meant that only brief accounts of Aboriginal customs are given or, in the case of Lumholtz, were only available to a limited scientific community, and not available in English (Lumholtz 1889; Savage 1992).

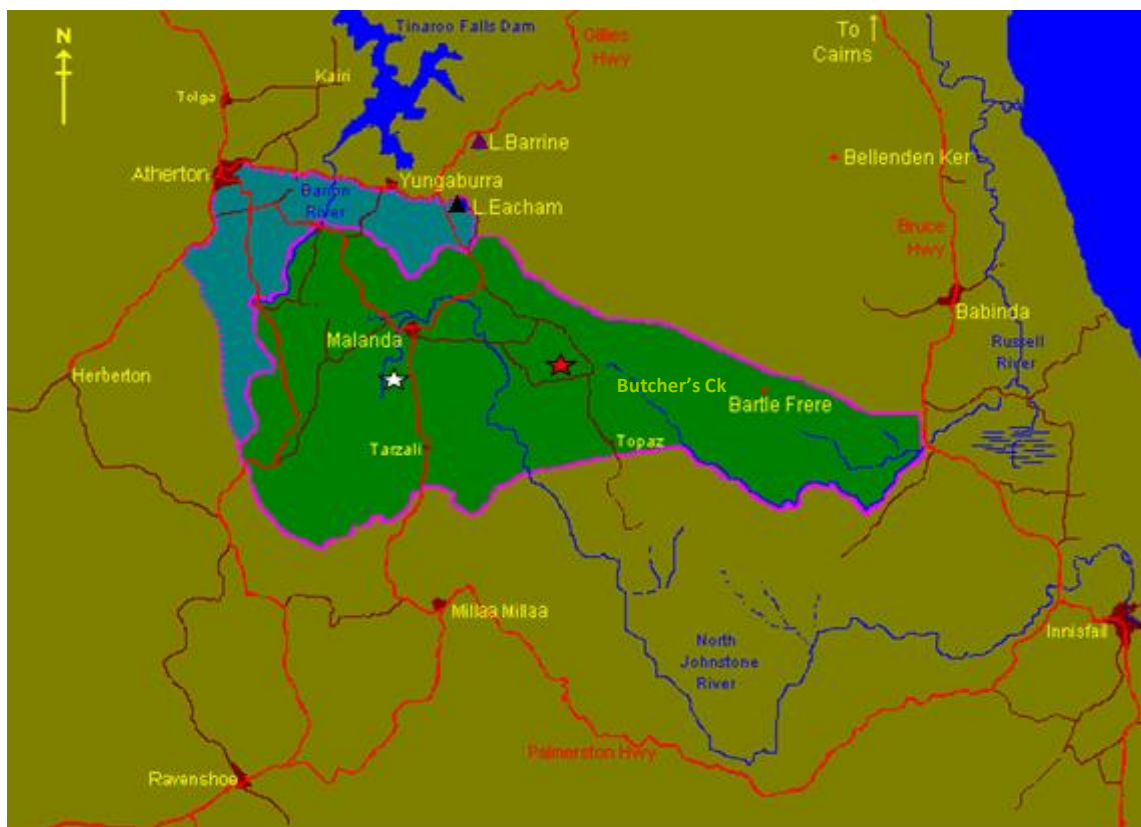
Palmerston and Lumholtz also noted the preference of some Tableland Aborigines for travel to the coast during the dry season (June to August) not only to escape the drizzle and frosts but also because food was more plentiful along the coast at this time. By contrast during the wet season (December to February) coastal Aborigines came inland not only to escape the extreme humidity but because of abundant nut crops from rainforest trees. Throughout their accounts they mention the presence of fire both as-a-tool-for obtaining food and clearing pathways in the rainforest; the upland Aborigines burnt the grass in early February in order to hunt wallabies (Lumholtz 1889, p. 265) and, as a weapon against unwanted presence on their land, setting fires around the camp sites of the European intruders (Lumholtz 1889; Savage 1992; Birtles 1997).

Uncontrolled logging in the Cairns lowlands saw the loss of prime cedar (*Toona cilita*) stands as the establishment of European settlement (1877-80) progressed. Settlements within the Tableland rainforest were established in cleared sites and along paths that the earlier European explorers and later timber-cutters followed. These sites later became known as “pockets” and were originally Aboriginal camp sites which were relatively permanent and linked to well-beaten tracks related to a seasonal cycle of migration (Birtles 1982). The influx of settlers to the Atherton Tableland taking up land under freehold and leasehold conditions meant that increasing tension occurred between the settlers and the local Aborigines and in many cases the locals were forcibly removed from their land or their access was limited. However, it was not unusual for settlers to allow

the locals to stay, on the proviso that they help clear the land or, in the case of the women, help domestically (Pannell 2005).

3.3.4. The Ngadjon-Jii People of Atherton Tableland

Despite this aggressive encroachment on their lands, local Aborigines on Atherton Tableland continued their customs and cultural links to their land. The descendants of the Indigenous people in the Malanda District at European contact time refer to themselves, their culture, their language and their country as “Ngadjon-Jii”. The district includes Malanda, Yungaburra, Peeramon (north of Malanda), Butchers Creek, Topaz and Tarzali and includes the highest peak in Queensland, Mt Bartle Frere (Figure 3.16) as well as Bromfield Swamp and Lynch’s Crater with Lakes Eacham and Barrine near the disputed and district boundaries (Pannell 2005).



■ Traditional tribal area of the Ngadjon-Jii ■ Lands disputed with other tribes

Figure 3.16. Ngadjonjii tribal area ★ Lynch’s Crater, ▲ Lake Eacham, ▲ Lake Barrine and ☆ Bromfield Swamp (adapted from Pannell 2005).

Pannell (2005) points out that we see the history of the Tableland through the settlers and explorers eyes which are those of newly explored territories transformed and conformed into a “passive planisphere” (Carter, 1996, p. 9). To the Ngadjon-Jii they and the landscape are collaborative and active participants in their culture and customs.

3.3.5. The creation of Lake Eacham and Lake Barrine

Lake Eacham and Lake Barrine have great significant to the Ngadjon-Jii. On the outskirts of Malanda, on a patch of relic rainforest, there is a mosaic-tiled mural that tells of the creation of Lake Eacham (Figure 3.17) through Ngadjonjii eyes. It tells of the Yamani or rainbow serpent which according to the Ngadjon-Jii inhabits many of the waters of the region, Dixon (1972, pp. 24–25) notes that Dyirbal speakers regard this spirit as dangerous and therefore do not leave camp at night or bathe in dangerous pools. The story of the eruption at Lake Eacham also hints of the vegetation at this time the ‘flame tree’ that was hit by a spear is likely to be *Brachychiton (acerifolius)* a deciduous tree indicative of dry rainforest but is also a common species in sclerophyll forest.



Figure 3.17. Lake Eacham Yidyam/Wiinggina (after Pannell 2005).

“...Those young fellas were trying to spear that kangaroo. But they missed and hit a flame tree. That’s a sacred tree for Ngadjon-Jii mob. Those young fellas not supposed to be out hunting. They’d just gone through Law. Their elders told them they had to stay put, not go hunting. But they didn’t listen. When they pulled their spear out, a grub fell out, a witchetty grub. They started cutting down that tree to get more grubs. When they cut down that tree, the ground began to shake. Those two fellas had made that Yamani angry. Then the sky grew dark, than all these people here, back at the camp, the earth went from underneath them, sucked them in, whoosh, they all got drowned. Where they were camped became Lake Eacham, Bana Wiingina. (Warren Canendo (Wundadijila) Ngadjon-Jii man and one of the artists of the mural telling the story to Pannell 2005, pp. 7-8).

Lake Barrine has been known to Europeans since 1889 and has been a popular tourist spot since the early 1920s with boat tours around the lake giving a commentary on the history and the natural wonders of the lake, but little is indicated about the significance it holds to the Indigenous people of the area except for a single painting located downstairs of the Lake Barrine tea-room. The commentary of the painting by Vanessa Gertz (Gundja) (Figure 3.18), is given by Warren Canendo, cousin of Vanessa Gertz.



Figure 3.18. Lake Barrine *Barriny* (after Pannell 2005).

“There is that black bird, that story-bird now, that Spotted Drongo. That’s Lake Barrine, this here [pointing to another lake-like feature] is that swamp, not Hasties, the one up there behind Butchers Creek. On that dairy farm. Nan, what the name of that water? That’s where that water moved from there now. Where that waterhole is, where that swamp there is now, years and years ago, back in the old Dreaming, it used to be real cold and lot of storms and lightening must have hit a log and lit the log up for fire. All these birds were all cold sitting on the edge of the swamp. They see that big Yamani there and he’s all warm. They all shivering because they cold. They used to fly down there and try and get a bit of fire-stick to get warm and every time they did he would chase them away. And this Spotted Drongo came there one time. All the birds reckoned they were cold and told him that the Yamani asleep. Spotted Drongo grabbed that firestick, and as he was coming out of the swamp the Yamani woken up and got wild with him. He flipped his tail and when he did this he hit the back of the bird’s tail and split it. That’s how come got that fork in that tail of the Spotted Drongo. He managed to get up to the top with that fire-stick and all the birds were singing out, real happy they got that fire-stick. That Yamani got the shits with them mob, with those birds then and that is when he moved to Lake Barrine. Early in the morning. They reckon if you see it from an aeroplane you can see that the trail of the lava flow, where he come all the way to here. He went through the earth and made that track, and the water follow him here, and he bin come here, to Lake Barrine, he left early in the morning. Barriny, ‘early morning’. When those birds woke up that water was gone, but they didn’t worry because they all warm. They got their firestick.....” (Pannell 2005, p. 9-10).

Although Aborigines were often seen fishing and hunting on the crater lakes they would never approach them at night and the early settlers knowing of these stories intentionally camped at these taboos areas so as to avoid confrontation with the locals (Toohey 2001; Pannell 2005). This does suggest that the stories have been passed on from generation to generation, how long is unknown. Dixon (1991) suggests that the account of the origin of the crater lakes (Lake Barrine and Lake Eacham) given by the Ngadjon-Jii people is a plausible account of a volcanic eruption, and studies in Papua New Guinea have found that oral tradition and stories regarding volcanic eruptions have been reliable and go back many hundreds if not thousands of years (Blong 1982).

3.3.6. Lynch's Crater-Djilan bora

The destruction of swamp forest on the surface of Lynch's Crater about 4500 years ago has been attributed to the activities of Indigenous people (Kershaw 1983*a*) and this corresponds with evidence for increased intensification of human settlement in many Australian archaeological sites suggested earlier in this chapter, *sub-section 3.3.1*. Unlike the taboos assigned to the crater lakes, the swamps, especially the older and drier ones were bora grounds used for camping as well as meeting places for larger gatherings for ceremonial purposes. The swamp mentioned in the Lake Barrine story is most likely to be Lynch's Crater. Unfortunately both Lynch's Crater (Djilan bora) and Bromfield Swamp (Bundjabili bora), feature in the Butcher Creek massacre where many Aboriginal people were killed (Pannell 2005) and we know that Lynch's Crater was used and visited by the local Aborigines prior to European and post-European period as stone tools were exposed when peat mining commenced in the 1970s (Kershaw *pers comm.*).

Chapter 4

Fire and Charcoal

Introduction

When charcoal is found in the fossil record, the presence of biomass burning is presumed. However, to understand the nature and impact of biomass burning, it is necessary to examine both fire and its by-products especially charcoal. This chapter first looks at fire impacts at a global scale and then how fire has been detected in early history. The physical and biogeochemical properties of fire are then examined and are followed by the basics of charcoal taphonomy with special emphasis on macroscopic charcoal and charcoal morphotypes. This chapter concludes with an examination of selected fire/charcoal studies within Australia.

4.1. Global Fire and its impact

Fire is a global phenomenon; it is present in all vegetated regions of the world. It is both a regenerative mechanism and a destructive force which means there have been and continue to be diverse approaches to understanding this phenomenon from the molecular level through to global satellite tracking systems (Levine 1991; Garstang et al. 1997; Spessa et al. 2005; Thevenon et al. 2010; Belcher 2013; Doerr and Santin 2016). It is known that some areas are more fire-prone than others due to the presence of flammable vegetation in combination with conducive climatic conditions. However, it has become evident over the last few decades that vegetation formations such as rainforest, usually thought to have been relatively impervious to fire, can and will burn at some frequency. In Central and Latin America and south-east Asia, slash and burn agricultural practices and the deforestation of areas for agricultural and plantation expansion have been influential in increasing fire within rainforest, but it is becoming apparent that climatic phenomena such as El-Niño, which can generate episodic megadrought conditions, are an important component of the equation and very likely to have been so in the past. Within the 1997–1998 period, El-Niño drought conditions prevailed throughout south-east Asia where 8 million hectares burned in Indonesia; while in America 3 million hectares burned in Bolivia; 2.5 million hectares burned in Central America and 5.8 million hectares burned in one Amazonian state of Brazil (Andreae 1991; Goldammer 1991, 1993; Cochrane 2003).

4.1.1. Fire History

Fire has been present from well before anthropogenic influence. Fossil charcoal has been recorded frequently from Late Palaeozoic deposits in the Northern Hemisphere and in the Southern Hemisphere from Permian Gondwana coals in South Africa and New South Wales, Australia (Glasspool 2000, 2003). One aspect that has been problematic from these earliest records to the present day, is the evidence we use to identify fire presence. Initially the pyrogenic origin of the inertinite macerals, sub-groups fusinite and semifusinite, from Permian coal-bearing deposits of the Southern Hemisphere had been questioned but Scott (2000) and Scott and Glasspool (2007) demonstrated that these sub-groups, which have a higher reflectance in comparison to the macerals of the vitrinite and liptinite groups, are products of charcoalification. Macerals are the constituents of coal and both the vitrinite and liptinite groups of macerals are primarily formed from humified plant material although fungal material may also be present, while the sub-groups, fusinite and semifusinite, of inertinite macerals are primarily sourced from charred plant material (Jones and Chaloner 1991; Scott 2000; Scott et al. 2000; Scott and Glasspool 2007).

The earliest signs of human use and control of fire is a contentious issue in archaeological research. Cultural data including hearths, burned flint artifacts and burned bones from the Upper Pleistocene have been found in Africa (McBrearty and Brooks 2000) whereas in European sites it has been suggested that exploitation and use of fire by hominins may have been as early as the Middle Pleistocene (~500,000 years ago) (Dennell et al. 2011). Earlier Pleistocene records suggestive of fire use by hominins from Africa have been fragmentary and only based on sediment coloration. However, from Benot Ya'aqov in Israel the presence of burned seeds, wood and flint suggests hominins had control of fire nearly 790,000 years ago (Goren-Inbar et al. 2004). They came to this conclusion by being able to eliminate both peat fires and volcanic activity, while the more likely candidate, natural wildfires by lightning strikes, was also eliminated because the limited amount of burned material recovered, less than 2% of the total excavated, as well as its clustered distribution was not considered characteristic of material burnt by natural fires.

However, our knowledge of early geologic time-periods is limited and sporadic and consequently palaeo-records have focused on the late Quaternary where records are more frequent and, of course, where humans have become a more important ignition source.

Once humans had fire then their whole existence became reliant on its presence. It made once unpalatable foodstuffs edible, enabled the preservation of food by smoking techniques, it could be used as a tool for hunting purposes and as an aid to clear and cultivate land. It aided the development of weaponry and tool making and of course provided warmth and finally it became the central focus for gatherings and therefore facilitated gathering of humans into cohesive groups that ensured their longevity (Pausas and Keeley 2009; Gowlett 2016). The Quaternary period also experienced dramatic climatic changes in relatively short succession that would have influenced fire behaviour and, consequently, although humans were able to use and control fire to a certain extent, wildfires would have still been present whether originating from a natural or human source. Fire continues to be an important factor in the landscape in the present-day from both wildfires and human induced fires

4.2. Fire in the Environment

4.2.1. Fire ignition

Initial ignition is a kinetically controlled process that can terminate due to temperature and moisture before smoldering or flaming starts. As soon as the surface temperature of a twig reaches 100°C, the twig starts outgassing its water as steam; after this occurs temperatures rise rapidly (Lobert and Warnatz 1993; Novakov et al. 1997). Degradation of lignins and hemicellulose of wood begin at relatively low temperatures, 130–190°C, and between 200–280°C depending on the minerals present, cellulose undergoes a chemical dehydration process. Exothermic reactions predominate at >280°C and ignition will occur if fuel is insulated from external cooling. Above 320°C low molecular weight gases such as methane and ethane as well as complex tars are formed and this continues until surface temperatures reach 500–600°C, when methane, ethane and the complex tars are expelled and glowing combustion or smouldering commences if oxygen is not excluded from the char surface. At temperatures below 1000°C carbon is consumed at the surface as rapidly as char is produced (Chandler et al. 1983; Lobert and Warnatz 1993; Novakov et al. 1997). Thin fuels ignite more easily than thick fuels as they have less mass to be heated as will fuels with a larger surface and volume ratio than those of the same size with a smaller ratio because they will intercept more radiant heat (Chandler et al. 1983; Bradstock et al. 2012). Consequently, the type of fire, fuel type and behaviour play a major role in the amount of fuel consumed (Bradstock et al. 2012; Cruz et al. 2018).

4.2.2. The presence and effects of fire within peat environments

The potential of fires in peat sediment increases if there has been prolonged drying or drought conditions either through natural conditions or by draining of the peat surface. Surface fires can ignite peat, usually through smouldering, and the extent of fire penetration to lower layers is dependent on the difference in the density of filtration conditions and the ratio between the fuel and the oxidizer. The minimum energy for ignition depends on the botanical composition of the peat, its density (porosity), moisture content and ash content (Fransden 1997; Subbotin 2003; Grishin et al. 2006). Peat fires once established are difficult to extinguish and may burn for several years surviving rainfall and destroying the rooting systems of most plant species (Chandler et al. 1983; Knicker 2007). The effect of peat drying can extend to > 2 m depth; Hope et al. (2005) found that in Kalimantan, Indonesia, although rare, peat loss from burning and drought conditions could be as great as 8.5 m.

4.2.3. Effects of fire on soil chemistry and microbial activity

Severe burns can sterilize the upper soil and change soil properties. Even temperatures between 40° and 70°C can start biological tissue disintegration and result in a more friable, less cohesive and more erodible soil (Humphreys et al. 1981; Shakesby and Doerr 2006). The increase in pH after fires has a fertilising effect that provides a positive impact on the biological recovery of soils (Bäath and Arnebrant 1994; Chambers and Attiwill 1994; Pyne 2001), but this increase in pH only takes effect at high temperatures (> 450°C) with increases up to 3 pH units in acid top soils which may persist up to 3 years or more (Giovannini et al. 1990; Kutiel and Inbar 1993; Knicker 2007). An increase in pH favours bacterial population growth over fungal population growth although this is dependent on fire intensity with heterotrophic bacteria, filamentous fungi and algae not suffering long term effects when moderate intensity fires, > 400°C, occur (Renbuß et al. 1973; Certini 2005; McMullan-Fisher et al. 2011). However, with more intense fires fungal survival is limited except for the fungus *Neurospora* which is present shortly after a fire when all other fungi have expired. *Neurospora* is a cosmopolitan genus found in tropical, sub-tropical and temperate regions. It readily germinates after induction by fire and when present indicates a local fire origin although its absence does not negate the presence of local fire (Turner 2001; Turner et al. 2001; Innes and Blackford 2003; Jacobson et al. 2006).

4.2.4. Fire and vegetation succession

In the humid tropics of north-east Queensland and the more humid temperate forests of southern Australia, the relationship between rainforest and sclerophyll forest and woodlands is complex and the vegetation present is dependent on topography, rainfall gradients, soil type and fertility, site history, seasonal water stress and particularly fire for their presence or absence (Jackson 1968, 1977; Webb and Tracey 1981; Ash 1988; Hopkins et al. 1993). Lightning ignited fires are more common prior to the wet season but are generally only small and along the humid northern eastern coast conditions are generally too wet during the wet season although further west they may continue to be a fire ignition source (Stanton 1995). In the open grassy forest to the west of the WTWHA fires are usually lit after the first storm at the beginning of the wet season for pasture productivity for cattle. While there is also a continuing effort by the Indigenous people who have land rights within the WTWHA to continue their own fire management practice (Hill et al. 1999; Hill and Baird 2003).

Jackson's "Ecological Drift" theory (1968, 1977) based primarily on southern Australian forests, especially wet sclerophyll forest (WSF), found that vegetation succession was primarily dictated by the fire-frequency interval. Ash (1988) suggests that the local distribution of rainforest and pyrophytic vegetation in north-east Queensland is primarily due to the interactions between climate, substrate and topography. However, the varied structure and composition of rainforest, 27 different rainforest community types and complexes, means that the interaction across these factors, climate, substrate and topography, and fire activity varies significantly.

In the humid tropics, WSF is mainly restricted to the western edge of rainforest with dry sclerophyll on the opposing side and, generally, although not exclusively, occurs on granite protusions through the surrounding basaltic lava flows. However, unlike its southern counterparts where regeneration is characterized by high intensity crown fires, a more low-moderate intensity fire is common (Harrington et al. 2000, 2005; Murphy et al. 2013; Peeters and Butler 2014). Fires may rapidly extinguish on the rainforest side of WSF where availability of rainforest seeds provides a ready source for rainforest establishment while grass advancement is more common on the dry sclerophyll side where fire may be more extensive and hotter (Harrington et. al. 2000). Warman (2011)

suggests that, rather than WSFs being purely ecotonal (Ash 1988), they could be considered as stable in time but move as the boundary between vegetation types advances and retreats (Figure 4.1).

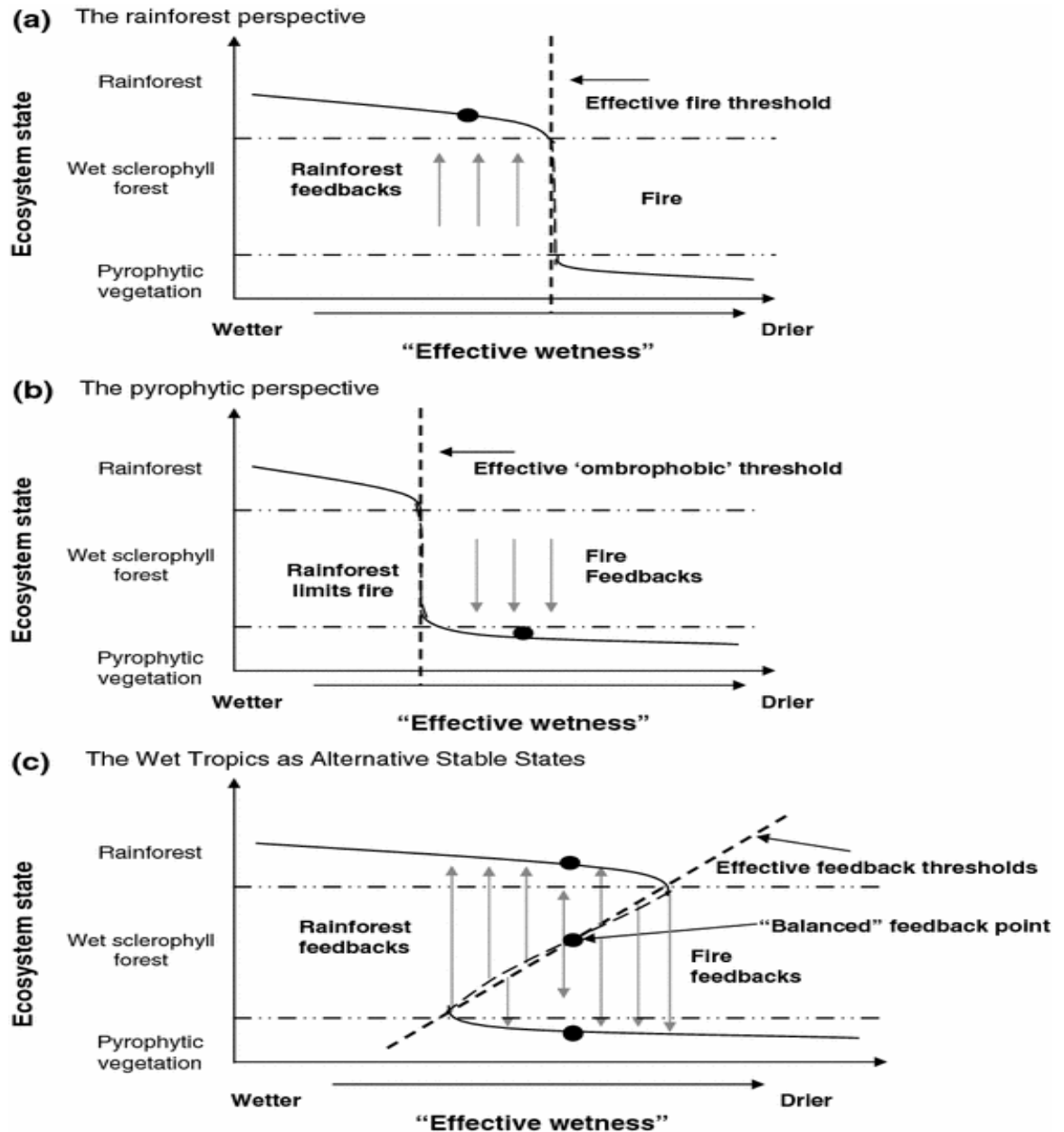


Figure 4.1. The relationship of fire with rainforest and sclerophyll vegetation. Building an alternative state where vegetation types correspond to alternative stable states along an axis of “effective wetness”. (a) Rainforest vegetation – wet conditions/monostable system, drier conditions increase and a “pyrophobic threshold” is reached. (b) Pyrophytic vegetation where “ombrophobic threshold” is reached (no longer can compete with rainforest vegetation). (c) When (a) and (b) overlap, vegetation types co-exist, compete and dominance shifts between them, and wet sclerophyll forests become “momentarily” stable (after Warman and Moles 2009).

However, in north-east Queensland where sharp boundaries exist between basalt and granite and metamorphics, there is no WSF and a sharp transition is—found between rainforest and open sclerophyll forest and woodland. Here, frequent grassy understorey fires are common and may burn to the rainforest margin (Ash 1988). These fire types are more common in the dry season and their ability to escalate is reliant on rainfall deficiencies (Figure 4.1). Fire impact and advancement is also dependant on the threshold capacity of the vegetation community which may be able to withstand single events such as impacts from cyclones but, when there are also prolonged rainfall deficiencies and drought conditions become common, then fire is likely to have a greater impact (Ash 1988; Warman and Moles 2009, Warman et al. 2013). Warman and Moles (2011) suggest that in north-east Queensland there is a non-linear system present where rainforest and pyrophytic vegetation occur as alternative stable ecosystem states and are not independent systems. They also suggest that, rather than a simplistic analogy of pyrophytic vegetation versus pyrophobic vegetation, both vegetation types actively modify environmental parameters with both fire and water availability acting as external parameters (Warman et al. 2013). Tng et al. (2012) suggest that though eucalypts, especially giant eucalypts, may be dependant on or advantaged by fire for regeneration, they should not be considered as an alternative state from rainforest ecosystems but as a long-lived ‘rainforest’ pioneer species dependant on fire for regeneration.

4.3. By-products of fire

The carbon-rich material produced from the incomplete combustion of organic material during fires may be seen a component of a combustion product continuum, see Figure 4.2, with black carbon the general type used to encompass this continuum of slightly charred material and charcoal to soot (Schmidt and Noack 2000; Bruun et al. 2008; Thevenon et al. 2010). While some fire by-products may be difficult to recognise or find in the environment, all can be used for reconstructing past fire regimes and are considered direct indicators of palaeo-fire.

Although there is also the possibility that all these fire by-products could be present within the same sediment-accumulating basin, as shown in Figure 4.2 they indicate quite different fire types and fire origin. The vast majority of palaeo-fire research has been concentrated within the terrestrial environment and generally the term “charcoal”

(microscopic or macroscopic) is used to denote fire by-products found in soil and sediments (Thevenon et al. 2010). The advantage of terrestrial records is that charcoal is relatively easy to find and identify in soil and sediment. While terrestrial records provide local to regional scale records, marine records can provide a more continent-wide to global scale record of biomass burning with the smaller size fraction, sub-micron (Figure 4.2), of black carbon (BC) the combustion by-products in marine records, generally quantified (Conedera et al. 2009). However, because BC in marine sediments is usually derived from long-distance derived transport processes (rivers, winds and ocean currents) which are likely to involve various erosion-redeposition cycles as well as a life span which may range from short, medium to long-storage periods, identification of fire events or their location is generally not possible (LaRowe et al. 2020).

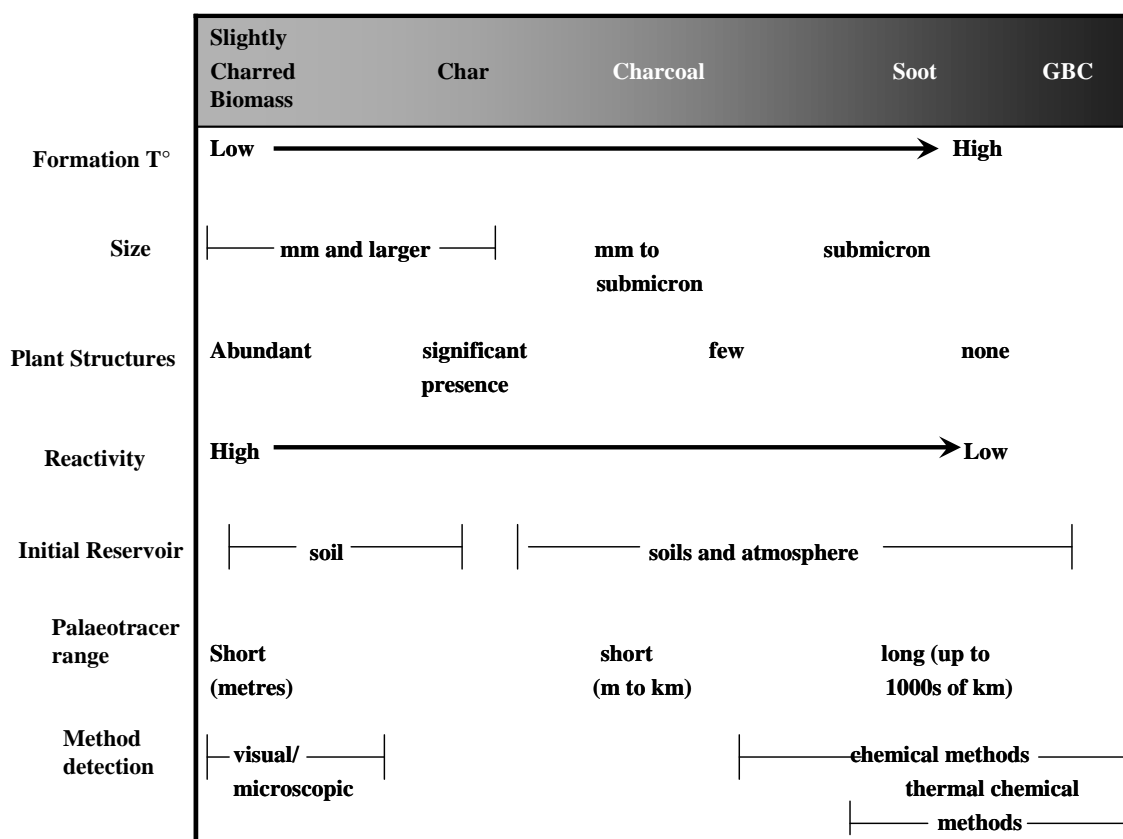


Figure 4.2.The pyrogenic (black) carbon combustion continuum and the corresponding techniques of quantification (modified from Thevenon et al. 2010).

There may also be problems in quantifying BC in marine sediments because of the chemical changes that may occur to BC from both the transport processes and the extended storage periods (Schmidt and Noack 2000; Currie et al. 2002; Schmidt et al. 2003; Masiello 2004; Hammes et al. 2006; LaRowe et al. 2020). However, the advantage of utilising the smaller fraction of the BC continuum not only provides a record of biomass burning at a global scale but the methods used for isolation of combustion-derived carbon can be further analysed for isotopic and spectroscopic properties providing information on fuel consumption and combustion conditions (Haberstroh et al. 2006; Conedera et al. 2009).

4.4. Charcoal

Charcoal is a substance generally identified as black, opaque and angular particles. It is a relatively inert substance and, in most cases, not altered by chemical or biochemical processes which makes it ideal for preservation in sediments, (see section 4.3 and Figure 4.2) (Conedera et al. 2009). The preservation of charcoal in lakes and peat bogs provides the opportunity to reconstruct fire histories over varying time spans and the form that the charcoal analysis takes is dependent on the background of the researcher and what questions they want charcoal to answer (Coffey et al. 2012; Hawthorne et al. 2018). An important aspect of this project is to see whether it is possible to separate “natural” fire from human fire activity. For this reason, it was considered important that both microscopic (micro) and macroscopic (macro) charcoal were analysed as it maximises insight into the different fire types represented.

4.4.1. Charcoal representation and deposition

Charcoal is produced in discrete events of short duration and at intervals of a few to many years (Clark 1983). Variation in representation is because charcoal is the outcome of varying fire regimes that may be vegetation specific or the outcome of changing environmental and climatic conditions in addition to human activities (Wolf et al. 2013; Leys et al. 2015). Furthermore, there may not be a direct relationship between the timing of a fire and representation of charcoal in the fossil record, as charcoal can be blown into a site at the time of the fire or washed in from the soil surface subsequent to it. If a fire occurs under relatively drier conditions, surface runoff or stream flow may be delayed, in which case the fire may be under-represented in, or missing from, the sedimentary

charcoal record. In areas where runoff is increased following fire and, depending on the deposition site and the degree of erosion, the fire may be over-represented in the sedimentary charcoal record (Clark 1988; Bradbury 1996; Whitlock and Millspaugh 1996; Scott 2010). These erosion-induced sequences may be identified by layers of charcoal and mineral matter found at the foot of slopes or near the outlet of creeks or inlet streams (Patterson et al. 1987). This fact was exploited in a study undertaken in the Sydney region where sediment cores taken from the bottom of a steep slope were used to investigate recent fire history that was then compared to known historic fire events (Mooney et al. 2001).

Though charcoal deposition is usually rapid, redeposition, sediment mixing or delayed transport of charcoal to a suitable site can result in a single fire episode spanning many years (Bradbury 1996) and, although microscopic charcoal may travel further than macroscopic charcoal, research suggests that, in large floodplain wetlands, macro-charcoal source is variable (Graves et al. 2019). Whitlock and Millspaugh (1996) found that lakes in both burnt and unburnt catchments received charcoal during and after a fire although, after a given number of years, the burnt catchment sites had greater charcoal abundance than that in the unburnt catchment. The charcoal was supplied at this stage by secondary sources such as resuspension and redeposition of littoral and sublittoral charcoal as well as inwash from burned slopes and burned trees falling into the lakes. This suggests that charcoal accumulation may lag several years behind the fire event, and abundance may vary with lake and watershed characteristics making it difficult to correlate charcoal directly with a particular fire regime attribute such as fire size or intensity. However, Clark et al. (1998) found that, based on an experimental burn, particle distribution could identify the type of burn. They found that high intensity crown fires contributed charcoal particles to many lakes in a region and therefore the local representation is less pronounced than it would be for lower-intensity burns. This is because strong turbulence associated with intense convection can sustain a wider range of particle sizes in the air, allowing wider dispersion and a conservative particle size distribution. They suggest that burns with lower intensity would show a more marked decline in accumulation with distance and lakes would allow for better spatial resolution of nearby burns. However, subsequent research has shown that, even in high-intensity crown burns, charcoal accumulation declines sharply outside the fire with only about 1%

of the measured charcoal particles deposited beyond 20 m from the burn edge (Lynch et al. 2004).

4.4.2. Charcoal preparation

Charcoal preparation is dependant on the aims of the analyst and the site characteristics (Clark 1982; Rhodes 1998). Some of the techniques used for quantification of charcoal are:-

- 1) Microfossil charcoal counting on pollen slides (Iversen 1941)
- 2) Chemical digestion-assay methods (Winkler 1985)
- 3) Petrographic thin section methods (Clark 1988*b*)
- 4) Macrofossil charcoal estimation using the Petri dish method (Simmons and Innes 1981)
- 5) Sediment slurry preparation procedure (Clark 1986)
- 6) Rhodes bleached method (Rhodes 1998)

The chemical digestion-assay method was developed to quantify the elemental carbon content of sediments. It calculates the weight of the charcoal relative to the dry weight of the sample, which is then expressed as a percentage (Winkler 1985). There are problems with this method with fibrous peat samples not sufficiently digested and small-scale changes in carbon content in cores not being able to be resolved by this method (Rhodes 1998). The petrographic thin section method is primarily used for high-resolution fire histories of annually laminated lake sediments and can be used for quantifying both macroscopic and microscopic charcoal particles. The complex and time-consuming nature of the preparation procedures for this method are a quite significant drawback, admitted by the original proponent (Clark 1988*b*). The estimation of macro-charcoal using the 'petri dish method' (Simmons and Innes 1981) is where sediment samples are mixed with water in gridded petri dishes and percentage charcoal cover is estimated under a binocular microscope. Although this method is quick and avoids problems caused by pollen preparation, the accuracy of charcoal estimation and identification is based on subjective quantification and therefore errors maybe compounded (Rhodes 1998). The sediment slurry preparation procedure developed by Clark (1986) is a quick easy method

whereby volumes of standardised sediment slurry not treated with chemical analyses are mounted on microscope slides under sealed cover slips. This method avoids the problems of charcoal-pollen slide quantification but also may have problems of differentiation between charcoal and other organic matter.

However, the vast majority of fossil microscopic charcoal analyses over the past six decades have quantified charcoal on pollen slides (No.1) thereby reducing both sample preparation and sample counting time by quantifying the charcoal and pollen at the same time (Rhodes 1998). Although the chemical and mechanical procedures involved in pollen preparation may alter the original fossil charcoal population, Clark (1984) found that all processing steps reduced the area of charcoal by about the same amount. Therefore, the most important factor for quantifying charcoal is consistency of preparation procedures for all samples within a sedimentary core and between cores if comparative studies are undertaken. Size distribution at the microscopic level is not routinely evaluated but a number of studies (Blackford 2000; Duffin et al. 2008; Rucina et al. 2009) have suggested that it may be possible to assess fire type as well as the likely fire distance if this was estimated. Duffin et al. (2008) looked at both micro- and macrocharcoal in their study of present-day fires in the savannas of Kruger National Park, South Africa, where microcharcoal particles were divided into four size classes (3–12 μm , 13–25 μm , 26–50 μm and $> 50 \mu\text{m}$) and $> 150 \mu\text{m}$ for macrocharcoal. They found that microcharcoal particles $< 50 \mu\text{m}$ were indicative of more regional fires, while the larger microcharcoal particle size, $> 50 \mu\text{m}$, was a more reliable indicator of fires within an area of 20 km radius and that the larger microcharcoal particle size, 51–150 μm , was positively correlated with the macrocharcoal.

Macroscopic charcoal is generally quantified by Rhodes bleached (No.6) method that requires any preparation needed to separate charcoal from the sediment to be minimal (Rhodes 1998). This is to limit fragmentation and breakage beyond that which may have occurred prior to deposition. Carcaillet et al. (2001) found that, from testing sieving techniques, breakage was not a problem if sieving was done gently. A study by Schlachter and Horn (2010) tested the validity of using chemical pre-treatments on macroscopic charcoal from both modern and fossil samples. They found that statistically there was no loss from the modern samples but there was a marked reduction in the fossil samples

suggesting that the bleaching agent used, hydrogen peroxide (H_2O_2) applied at different strengths, was bleaching or removing particles not fully charred and suggesting that analysts should be aware of this effect.

They also recommended that the sample size used should be significantly greater than that commonly used for microscopic charcoal analysis (1 cm^3) as they found charcoal concentration varied horizontally across adjacent samples from the same core. This was also noted by McKenzie (1989) when working in the central highlands of Victoria, Australia. Although observed partially charred material or brown charcoal is not usually considered, it could indicate widespread fire of low intensity and therefore provide additional information in macrocharcoal studies especially when counts are low (Clark 1988*b*; MacDonald 1991). However, in view of the study by Schlachter and Horn (2010), one needs to take into account that, if brown charcoal is to be assessed, the chemical pre-treatment step of either hydrogen peroxide (H_2O_2) or sodium hypochlorite (NaOCl), used to bleach or dissolve non-charred remains, may adversely affect these results.

4.4.3. CharAnalysis

Statistical analysis 'CharAnalysis' is also now used in some studies as a way to estimate fire frequency and intensity (Long et al. 1998; Higuera et al. 2005). This analysis removes the background charcoal component that consists of charcoal that remains in the watershed for a length of time prior to transportation and subsequent deposition. It also removes the regional component from the local watershed component leaving the peak component that primarily represents charcoal produced by a single fire event within the local watershed and therefore gives a more accurate estimate of fire frequency and intensity (Long et al. 1998; Lynch et al. 2011). One pre-requisite for this type of analysis is that the sampling interval must be less than the fire frequency. The sampling should preferably be contiguous and to a certain extent the resulting fire frequency produced should be able to be validated against historical records and/or other proxies such as dendrochronology which does not have the taphonomic problems that are present for charcoal. The majority of studies using CharAnalysis have been located in North America (Mensing et al. 1999; Hallett and Walker 2000; Brunelle and Anderson 2003; Whitlock et al. 2004; Higuera et al. 2005; Power *et al.* 2006; Briles et al. 2008) where both historical

archives and proxies, such as dendrochronology, have been used to test and validate the charcoal records.

There has been limited use of CharAnalysis other than in North America (Pitkänen et al. 1999; Kaniewski et al. 2008; Vanni  re et al. 2008), and even less so in the Southern Hemisphere except for South America where dendrochronology has been used to validate the charcoal record (Markgraf et al. 2009, 2013; Holz et al. 2012). Initially within Australia the use of CharAnalysis with validation was limited to the studies of Mooney and Maltby (2006) and Mooney et al. (2007) for southeast Australia with the former study utilising both historical and fire scar information and the later study utilising historical information. However, in recent years, studies in Tasmania have incorporated CharAnalysis into multi-proxy reconstructions on fire activity and climate with Beck et al. (2017) comparing CharAnalysis results from Paddy’s Lake with a charcoal composite derived from two lakes in south-west Tasmania, and Stahle et al. (2017) using the fire and vegetation history for the Cradle Mountain region to compare with the CharAnalysis results from Cradle Mountain sites.

4.4.4. Macro-charcoal Morphotypes

Attempts have been made to identify pieces of charcoal to source plant taxa or vegetation synusaie. Initial studies focused on the cellular structural differences between grass and sedge epidermis and woody tissues (Patterson et al. 1987). This meant that ‘only charcoal exhibiting obvious cellular structure was included in the counts’ (Byrne et al. 1977, p. 36) and severely under-estimated charcoal abundance (Patterson et al. 1987). Research has found that, during experimental burns, grass charcoal particles (Figure 4.3) are longer and narrower than charcoal from leaves or wood and that charcoal morphology using a length:width ratio may be a useful indicator of vegetation type especially across forest-grassland ecotones (Umbanhowar and McGrath 1998).

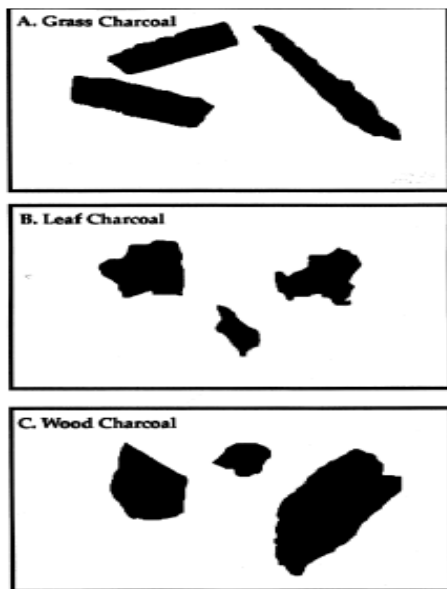


Figure 4.3. Silhouettes of grass (A), leaf (trees) (B) and wood (C) charcoal magnified at 20x (after Umbanhowar and McGrath 1998).

However, Umbanhowar and McGrath (1998) did find that, in their open control burns (control field burn) the length:width ratio was less than in the closed control burns (laboratory control burn) although the ratio was still valid. They suggested that, in the field, other factors such as fire intensity, temperature, turbulence, abrasive activity and fragmentation may impact and/or distort charcoal size and shape. McGinnes et al. (1971), Bryden and Hagge (2003) and Njankouo et al. (2005) found the opposite, with the length and width of material burnt in natural fire greater than that found in laboratory control fire with the greater shrinkage found in the laboratory control fire due to less oxygen and greater burn time. Although this may not affect the ability to separate woody from more herbaceous grass charcoal, it does show that structural alteration does occur whether it is a natural or laboratory controlled fire. This would suggest that, besides the plant epidermis being altered by fire, identification of other macrofossils such as seeds and nutlets, may also be structurally altered and impacted by fire. Fine ornamental features, such as hairs or appendages, that maybe diagnostic are usually destroyed by fire leaving only the shape and size of the seed and nutlet for identification so caution is needed if charred seeds and nutlets need to be identified to species level (Wright 2003).

The use of charcoal morphotypes in the form of charred grass cuticles has been used in southern Africa to understand grassland communities and their response to fire (Mworia-Maitima 1997; Wooller et al. 2000, 2003). Grass cuticle analysis is usually done in

conjunction with phytoliths and is used to address the lack of taxonomic resolution that occurs in the Poaceae family when using pollen. The analysis can provide identification in some instances to genus or species level and can also provide information on what fire type, low or high intensity, is associated with a particular grass type. The separation of charred Poaceae has also been successfully utilized in studies by Lynch et al. (2006) and Walsh et al. (2008) giving information on the fuel type and severity of fire events. They suggest that, although Poaceae is identified by the arrangement and shape of epidermal cells, caution is needed as other monocotyledons such as the sedge, *Carex*, have similar cell arrangements and therefore comparison with the pollen record would be advised. These studies usually incorporate a burned reference collection from the study site which enables a more accurate identification of charred material. Doubleday (1999) and Doubleday and Smol (2005) took an assemblage approach to describe and classify particles linked with combustion processes. This extensive study encompassed as far as possible all combustion types including those from wood charcoal, soot from wood and coal burning chimneys, ash from wood combustion, fossil fuel burner soot, gas, oil and diesel-burning stoves and fly ash. They surmise that the morphological features used to distinguish particles results from the original fuel type, the type of combustion and the combustion process itself.

Their results from the wood combustion fire found that there was a range of particle types, including rectangular (blocky), irregular shape, both angular and rounded shapes as well as the preservation of woody vessel walls, early and late wood cell walls (lacy structure) and resin ducts. Details of some of these features are shown on Figure 4.4.

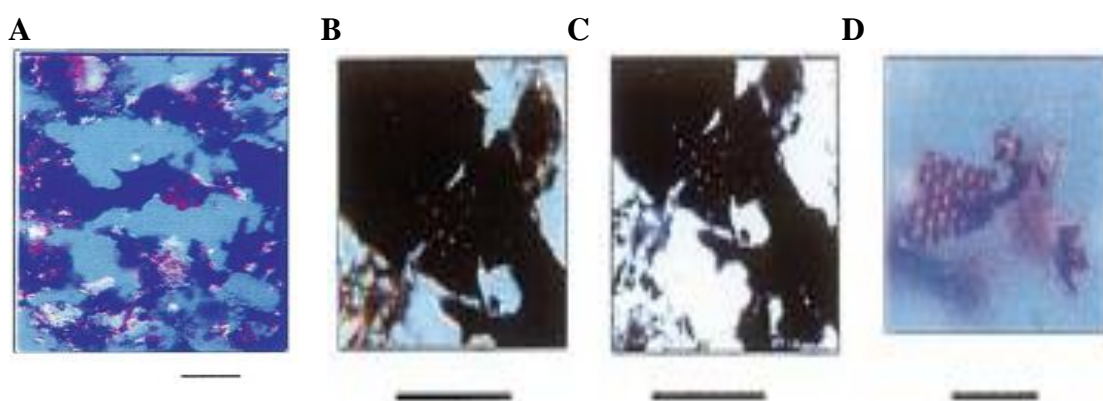


Figure 4.4. Wood combustion particles from domestic fireplace burning mixed hardwood and softwood. A – irregular, rounded and angular features present taken under polarized light; reddish rounded particle in the centre due to the presence of anisotropic organic compounds such as resin. B and C – irregular and angular features present as well as cell wall structure/lacy pattern retained due to the presence of more resistant molecules containing less volatile material. D – close-up of lacy structure which is only partial charred/brown charcoal (for full results see Doubleday and Smol 2005, Plate 1, p. 403).

A comprehensive study by Enache and Cumming (2006) found that variations in morphological features of charcoal showed a distinct relationship to recorded area burned by fire. They divided charcoal particles into groups based on shape and porosity. Figure 4.5 shows the charcoal morphotypes found in sediments of Prosser Lake.

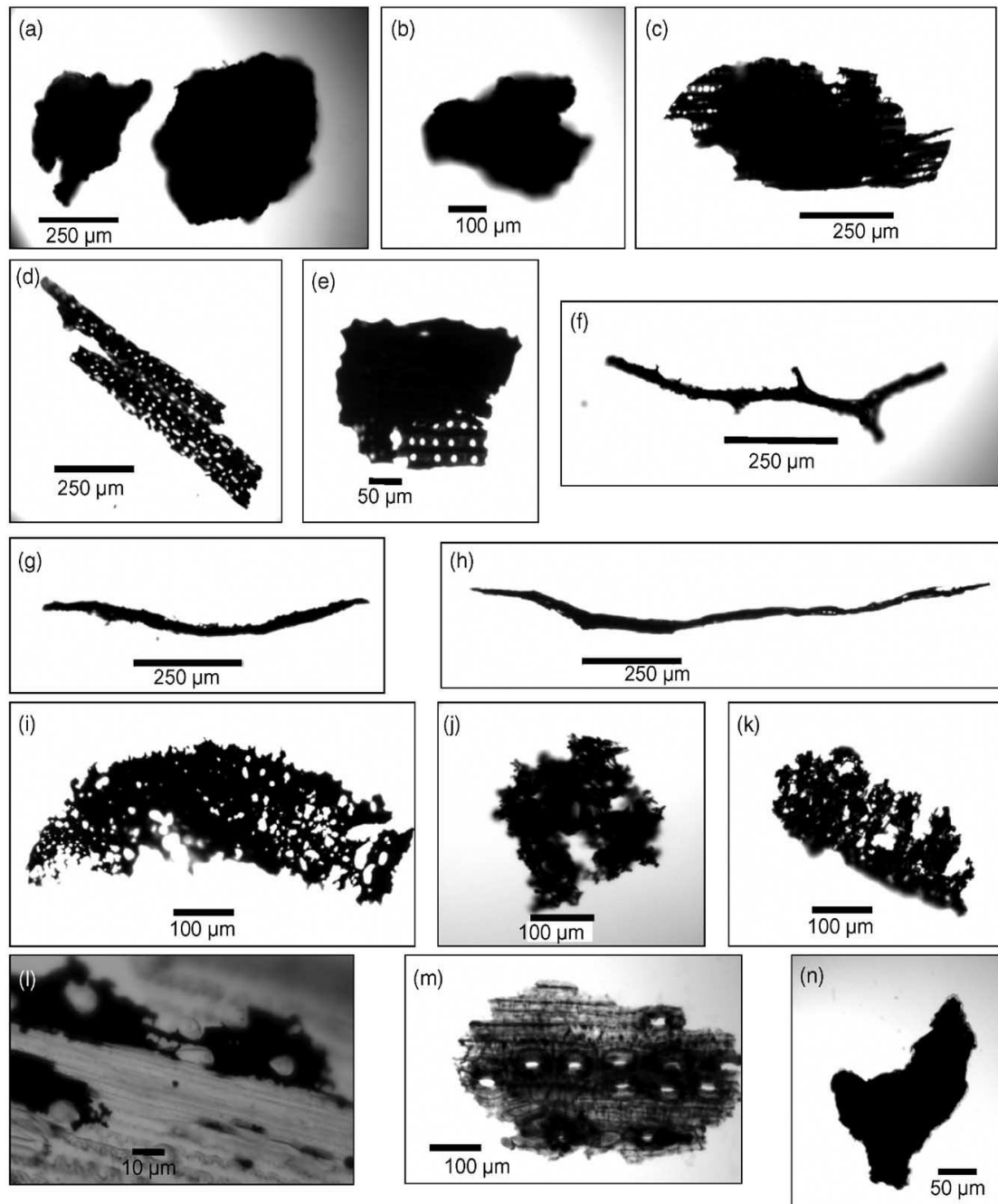


Figure 4.5. Charcoal morphotypes identified in the sediments of Prosser Lake: Type C (a,b); Type S (c-e); Type D (f); Type F (g,h); Type M (i-k); Type B (l,m); and Type P (n) (after Enache and Cumming 2006).

Enache and Cumming (2006) found that these divisions could allow identification of fuel types such as bark, trunk, branches and leaves as well as fire severity. They suggest that

particular types, for example Type M, Figure 4.5, which were highly porous and “light” may lend themselves to transportation outside the immediate watershed and therefore be more indicative of a regional fire signal. The more robust Type C is likely to be aerially transported short distances and therefore be more indicative of local fire events (Enache and Cumming 2006, 2009). Further work on macrocharcoal morphological types hopes to link fuel types with charcoal morphotypes across a number of ecosystems to understand both biomass burning and long-term fire ecology (Mustaphi and Pisaric 2014; Crawford 2015).

Jensen et al. (2007) also found that using charcoal morphotypes allowed them to track the change from a surface fire regime to the less frequent crown fire regime by the identification of charred particles with distinct bordered pits. All the above studies had burn reference material collections which helped with the identification of source and type of fire and were particularly helpful in mixed vegetation where charcoal morphotypes did not fit the usual criteria of black, opaque and angular.

4.5. Fire in Australia during the late Pleistocene and Holocene

An important aspect of this project has been to see whether it was possible to separate ‘natural’ fire from ‘anthropogenic’ fire activity and, although charcoal is used fairly routinely in palaeoecology to understand past fire regimes, it has been suggested that the lack of uniformity in charcoal methods and analysis makes it difficult to make comparisons across sites let alone regions (Harrison and Sanchez-Goñi 2010; Power et al. 2010).

Early reviews on long-term history of fire in Australia (Kershaw et al. 2002; Lynch et al. 2007) were considered to be limited by a lack of data quantification. This limitation was corrected to some degree by Mooney et al. (2011) in their compilation of 223 sedimentary charcoal records from the Australasia region. Data was standardised and a composite charcoal record was constructed for the whole of Australia as well as various sub-regions with a focus on the last 70 ka. Mooney et al. (2011) found that, within the composite charcoal record for Australasia, there was an increase in biomass burning during the latter part of MIS 4 (MIS 4 extending from 71 ka to 59 ka). Fire remained high through MIS 3

(59.4 ka to 27.8 ka) with lower levels during of MIS 2 (29 ka to 14 ka) and higher levels returning during the Holocene. However, a number of sub-regions showed contrasting patterns. In the tropics, biomass burning gradually increased after the LGM and through to the early Holocene especially at 15 ka and 8 ka with a decrease at 6.5 ka. Regions at latitudes between 25°S and 45°S showed no marked trend during the deglacial period but there was an increase during the first part of the Holocene around 6 ka but a decrease during the late Holocene. Most sites across Australia had relatively low biomass burning during the LGM and low biomass burning during the Antarctic Current Reversal (ACR) for sites in south-eastern Australia and New Zealand in contrast to high biomass burning at many sites in the tropics.

Mooney et al. (2011) found no evidence of a change in fire regimes at a continental scale at the time of Aboriginal colonization of Australia (50 ± 10 ka) and also no relationship between surmised Aboriginal populations and mid-late Holocene intensification (Lourandos 1980, 1983; Turney et al. 2004). Mooney et al. (2011) conclude that fire regimes were controlled by changing climate conditions which then resulted in vegetation changes and that, though the composite nature of the sedimentary charcoal record itself may not be ideal in distinguishing small-scale or low intensity fires that may be characteristic of Aboriginal burning, climate is the dominant factor in fire activity. They also found that some charcoal peaks appear to occur around the time of the Dansgaard-Oeschger (D-O) warming events and suggest that there was an increase in biomass burning in the Australasian region during Greenland Interstadials and reduced during Greenland Stadials. Though climate maybe the key driver, there are distinct variations across the Australian continent with an analysis undertaken by Bird et al. (2019) on 19 lakes across savannas in northern Australia finding that, although external climate forcing is likely to have been important, more indirect changes such as indigenous fire management and local factors such as soil type, soil fertility and topography may also have been influential, especially at a local scale.

The following section presents a selection of fire records to exemplify those providing a relatively clear climate signal regarding fire activity, those records where fire activity has been related to human activity, and those where a combination of climate and human forcing of fire activity are suggested. The records to be examined are limited to Australia

except for nearby marine records, those that cover at least the last 50 ka, shorter records in northern Australia and records that have utilized macrocharcoal in their studies in an effort to separate natural from anthropogenic burning. Figure 4.6 provides the location of sites discussed in the following sub-sections.

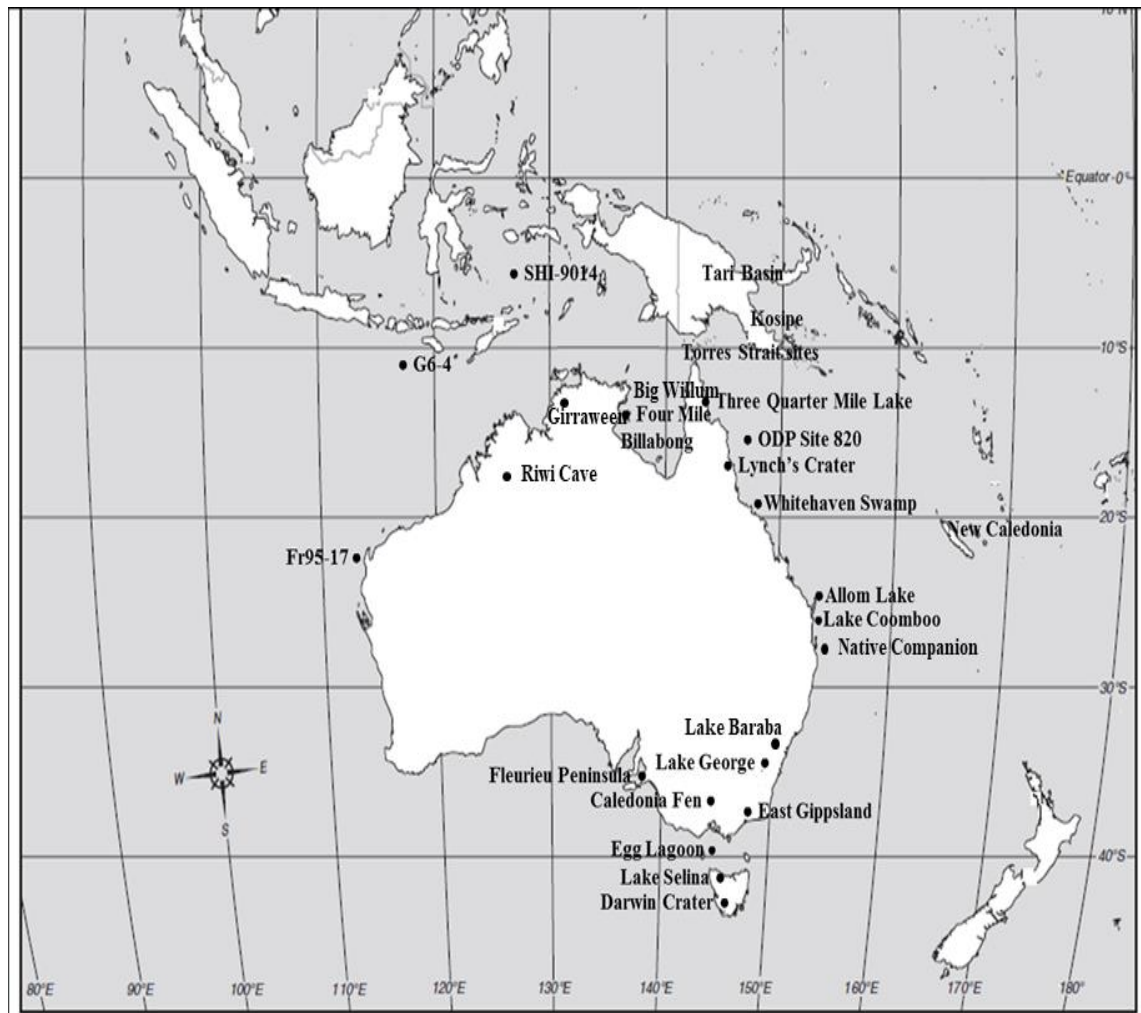


Figure 4.6. Geographic location of sedimentary charcoal records in the Australasian region mentioned in text (modified from Mooney et al. 2011).

4.5.1. Long terrestrial and marine records of fire in Australia

It is important to have, as far as possible, baseline information on fire presence and variability prior to the arrival of people and long terrestrial and marine records can provide this insight. However, there are few long terrestrial and marine records on the Australian mainland and surrounding marine environment and those that exist generally have poor chronological control so correlation is problematic (Singh and Geissler 1985; McKenzie 1989; Longmore 1997; Harle et al. 2002; Kershaw et al. 2007b). A notable

exception is the combination of the long terrestrial record of Lynch's Crater and marine record ODP Site 820 that together provide insight into both local and a more generalized regional record of fire activity in the region (Chapter 3, see sub-sections 3.2.1, 3.2.5 and 3.2.7).

4.5.1.1. Long terrestrial records of fire in Australia

Early low resolution records from Lake Coomboo (Fraser Island) found that fire was present from at least 600 ka but drier conditions from 350 ka saw the expansion of sclerophyllous forest accompanied by a significant increase in charcoal in comparison to the earlier part of the record but no increase in charcoal at around 50 ka–40 ka (Longmore 1997; Longmore and Heijnis 1999). The dry rainforest component, *Araucaria*, was still present but from 22 cal. kyr BP pollen frequencies declined and, even with a return to more mesic conditions after the LGM, it never fully recovered to its former status. The Tasmanian Lake Selina record extends to 130 ka (Colhoun et al. 1999) and records relatively high charcoal values from 70 ka through to 20 ka in a landscape dominated by herbs, alpine and sub-alpine taxa and myrtaceous trees and shrubs at a time of relative cool dry conditions. Prior to 70 ka the presence of cool temperate rainforest and relatively wet conditions preclude fire activity but a return to wetter conditions during the Holocene sees the return of high charcoal values in the presence of higher values for sclerophyll vegetation.

At the central Victorian highland site, Caledonia Fen, the highest charcoal values are found in the earliest part of the record (170 ka–190 ka) likely due to a greater fuel availability, within a forested catchment, primarily sclerophyll Myrtaceae. Through the rest of the record charcoal peaks are generally associated with warmer periods and the subsequent increase in woody taxa, especially *Eucalyptus*, and therefore a climate control is suggested for this increase in fire activity. There is no increase of charcoal at ~50 ka although there is an increase at ~31 ka which has been attributed to anthropogenic influence with this later date of Aboriginal influence due to both the altitude and isolation of the site (McKenzie 1989; Kershaw et al. 2007b). While the timing of fire presence differs between Lake Coomboo (drier conditions), Lake Selina (cool drier conditions) and Caledonia Fen (warmer conditions), the common denominator is the presence of sclerophyll vegetation (Colhoun et al. 1999; Kershaw et al. 2007b).

4.5.1.2. Long marine records of fire in Australia

The broad regional to global scale record of biomass burning in marine records does provide a more generalized record of fire activity in the region. Marine core records from the north of Australia in the Indonesian region indicate that there is both an Indonesian and northern Australian signal within the pollen records and that there is general correspondence between these two regions with regard climate but also the likely impact of anthropogenic influence. The pollen and charcoal record from the Banda Sea core SH-9014 (Figure 4.6) that includes micro-charcoal, elemental carbon and also stable carbon isotopes, provides a regional picture of vegetation, fire and climate over the last 180,000 years (van der Kaars et al. 2000). Drier conditions and increases in burning were found in northern Australia and eastern Indonesia during oxygen isotope stages 6, 4 and 2 while there were increased values for rainforest taxa from eastern Indonesia and increased values for wetter sclerophyll taxa from northern Australia during oxygen isotope stage 5 and the Holocene. Fire was an important component during the drier period MIS 6 with $\delta^{13}\text{C}$ values indicating that woodland and herbaceous vegetation were likely sourced mainly from the exposed Sunda shelf area. But the highest values for both microcharcoal and elemental carbon are recorded after 37 ka accompanied by a substantial increase in grassland and a decline in *Eucalyptus* with $\delta^{13}\text{C}$ values indicating the prime source was C4 plants. Drier climates are not indicated at this time as there is a concurrent increase in pteridophytes suggesting slightly wetter conditions so an anthropogenic source is indicated.

The importance of fire is also evident from the eastern Indian Ocean marine core G6-4 (Figure 4.6) which covers the last 300,000 years with increases in Poaceae in the earlier part of the record related to lower rainfall levels and accompanied by an increase in fire activity, likely to be climate related. Although a section of oxygen isotope stage 3 (59.4 ka–27.8 ka) is missing in this record the greatest sustained increase in both charcoal and elemental carbon occurs through this stage and it was suggested that this is likely related to the burning activities of people (Wang et al. 1999).

Fire is also an important component of the 100 ka marine core GC-17 off the Cape Range Peninsula, Western Australia (van der Kaars and De Deckker 2002). There is some similarity between GC-17 and the above mentioned marine cores with high charcoal

values correlating with lower *Eucalyptus* values but, unlike the other marine cores, there are no corresponding higher Poaceae values. Although relatively high charcoal values are present at 46 ka, a major vegetation shift at ~40 ka is accompanied by low charcoal values. Van der Kaars and De Deckker (2002) suggest that the presence of a much more sparse vegetation at 40 ka would have reduced the available biomass for burning and, although there may have been a human influence, the low charcoal values at 40 ka would suggest otherwise. They suggest that there was a northward shift of the summer/winter rainfall boundary and that this was more likely responsible for this vegetation change. These long terrestrial and marine records provide valuable information on both the longevity of fire and the impact of human influence within the Australasian region but in most cases their resolution is low (greater than 1500 yrs) and therefore the timing of changes within the suggested 'early contact period' is somewhat limited. The next sub-section will look at those records that cover that suggested 'early contact period' but at a relatively high resolution.

4.5.2. The early contact period

There are few high resolution records on the Australian mainland that cover the 'early contact period' although, in the last decade, a number have been produced from south-east Queensland (Donders et al. 2006; McGowan et al. 2008; Petherick et al. 2008, 2011). These sub-tropical sites lie close to the summer-winter rainfall boundary and have been found to be extremely sensitive to changes in precipitation and the impacts of ENSO, and provide an important link between the tropics and temperate climate regions (Moss et al. 2013). The high resolution study of Lake Allom (Fraser Island) covering the last 57 ka recorded significant declines in Araucariaceae ~52 ka which Donders et al. (2006) suggested is in sequence with the Araucariaceae decline seen at Lynch's Crater (Kershaw 1994). Charcoal values do increase at this time but are variable and it is suggested that cooler and drier conditions were responsible for the decline of Araucariaceae and that changing local hydrological conditions which saw an increase in aquatic and swamp taxa were responsible for the higher charcoal values.

Charcoal values are variable through the Holocene with maximum values recorded during the early Holocene when sea-levels were low and conditions were drier due to increased continentality. From 5.5 cal. ka BP rising sea-levels were accompanied by more mesic

conditions and a decrease in charcoal. There is a further rise in rainforest taxa at 3 cal. ka BP but charcoal values also increase; this increase is mainly recorded in the microscopic charcoal and therefore a regional source, considered not likely to have had a significant effect on the local taxa. Donders et al. (2006) conclude that the vegetation and fire changes through the record are due to climatic changes amplified by changing sea-levels and the strengthened ENSO conditions during the Holocene and that an anthropogenic cause is not evident either from ~52 ka or during the Holocene. A recent study from this site incorporating palynological proxies and organic proxies (levoglucosan and its isomers and long chain *n*-alkanes) found that biomass burning at 4 ka could have been caused by human-lit fires correlating to archaeological evidence of their presence on the island (Schreuder et al. 2019).

A record from Native Companion Lagoon on North Stradbroke Island (~45 ka) indicates the climate was relatively warm and wet from 45 ka–32 ka, with a Casuarinaceae and eucalypt forest dominant and a rainforest community including *Araucaria* and palms nearby. High charcoal values through this period would suggest fire was present and could be linked to human arrival. Drier conditions existed through the early glacial period (32 ka–22ka) with a shift to eucalypt forest but *Araucaria* still had relatively high values and it is suggested the existence of a rainforest refugium. Charcoal values are lower through this time until 22 ka when charcoal peaks, thought to be associated with an increased fuel-load derived mainly from the sclerophyll Casuarinaceae. Casuarinaceae returns to prominence during the early deglacial (18 ka–15 ka) and there is also a suggested increase in climatic variability towards the early Holocene with peaks in charcoal at 13.7 ka and 10.5 ka. Wetter conditions prevailed through the early to the mid Holocene with low charcoal abundance in contrast to the late Holocene when drier conditions prevailed and increased fire activity is evident (Petherick et al. 2008, 2011; Moss et al. 2013). More recent research on these large off-shore sand islands in south-east Queensland suggest there is great potential to further understand the complexities of past climate variability and the role of fire (Barr et al. 2017; Tibby et al. 2017).

Lake Baraba situated 100 km southwest of Sydney extends to ~54.6 ka and shows considerable variability in the charcoal record (Mooney et al. 2011; Black et al. 2006). Casuarinaceae woodland was dominant until the early Holocene with low but variable

macroscopic charcoal values. Myrtaceae expanded from ~8.5 ka but charcoal values did not increase until ~6.7 ka. The archaeological record from this region shows an increase in habitation during the Late Glacial period to the early Holocene with a further substantial increase from ~8 to 7 ka. Black et al. (2006) suggest that the increased charcoal values at ~6.7 ka could be due to climatic instability, ENSO, and the availability of flammable *Eucalyptus*. However, they also suggest that a change in the sedimentary environment, lake to swamp, could have resulted in an increase in charcoal delivery due to fires impacting the site itself. This does not exclude an anthropogenic contribution as the authors suggest that the low charcoal values prior to ~6.7 ka could indicate a degree of landscape management.

Although not a continuous sediment record, archaeological wood charcoal analysis at Riwi cave, Gooniyandi country, Western Australia provides information on shifts in woody vegetation over the last 45,000 years alongside human usage of woody sp. and likely fire activity. The wood charcoal assemblage during the Holocene reflects the present day modern vegetation while shifts from *Eucalyptus* to *Corymbia* dominated savanna between c. 38,000–35,000 cal BP could suggest a change in water availability or a disturbance event such as fire (Whitau et al. 2017).

4.5.3 Local fire environmental relationships

Of particular interest to this study, based on a swamp sequence, is records that illustrate relationships between local swamp environments and fires, whether ‘natural’ or anthropogenic. Bickford and Gell (2005) looked at both micro- and macrocharcoal and suggested that the low and constant levels of microscopic charcoal found in a cyperaceous swamp on the Fleurieu Peninsula, South Australia could reflect high-frequency, low-intensity fires of Aboriginal origin but finer resolution sampling frequency would be needed to confirm this premise. However, the high amounts of macroscopic charcoal at times of maximum swamp wetness they suggest, is more concrete evidence of deliberate Aboriginal wetland burning.

The abundance of *Typha* pollen, which is generally thought to be poorly represented in pollen records unless beneath very large stands (Head and Stuart 1980), suggests it was

ubiquitous in the swamp at these times. The roots of *Typha* are known to be a staple food for southern Aborigines with specific fire regimes implemented to sustain this staple with ethnographic records substantiating this claim (Gott 1999, 2005). The palynological and macrofossil investigation of Kenyon (1989) within a swamp in the East Gippsland rainforest of eastern Victoria perhaps provides more compelling evidence for Aboriginal management of the local swamp environment. The complimentary use of light and scanning electron microscopes (SEM) allowed examination of surface and cellular structures from both reference and fossil material (mainly charcoal) with identification to species level made possible. From 11,500 to 7,000 years BP mesic conditions prevailed and wet sclerophyll forest expanded with a corresponding decrease in fire (micro-charcoal) regionally. However, the continual presence of charred *Typha* remains and other monocots suggests Aboriginal management of the *Typha* resource.

4.5.4. Fire in northern Australia

The palaeoecological studies by Kershaw (1983a, 1986, and 1994), Kershaw et al. (2007a), Haberle (2005) and the soil charcoal studies of Hopkins et al. (1990, 1993), (see Chapter 3) confirm that fire was an important part of the landscape throughout Atherton Tableland and nearby areas in the late Quaternary. Further north the charcoal record (~10,000 yrs BP) from Three-Quarter Mile Lake, Cape York Peninsula, shows a sustained increase at 8,000 ¹⁴C yr BP coinciding with an increase in woody taxa in comparison to the more open grassy landscape of the late Pleistocene where charcoal values are low (Luly et al. 2006). Luly et al. (2006) suggest two scenarios are possible; the increase in charcoal could be due to the increased woody vegetation which may have left a greater charcoal signal or that anthropogenic firing of the landscape was occurring, but found there was no conclusive result at this site.

Conversely, the vegetation and fire changes recorded in a 5.7 m core taken from Whitehaven Swamp on Whitsunday Island, off the central coast of Queensland, is thought to have emanated from both natural and anthropogenic ignition sources (Genever et al. 2003). The earliest human occupation on the island dates to 2720 BP but there is archaeological evidence of human occupation back to 9000 BP on nearby Hook Island. Although marine resources would have been paramount, Genever et al. (2003) suggest that the swamp environment would have also been utilised and this is inferred from the

persistent representation of charcoal through both dry and moist conditions from ~7000 ka to the present. They suggest that anthropogenic fire use was established prior to the suggested time of human “intensification”, ~3 cal. kyr BP (Lourandos 1985).

It is in the northern monsoonal parts of Australia especially Arnhem Land in the Northern Territory, the nearby offshore islands and the Torres Strait Islands directly north of Cape York Peninsula that Indigenous fire use is still practiced, to a degree. However, there is considerable variation in fire practice across vegetation types, floodplain, woodland, open forest and closed forest, as well as varying fire usage between different clans (Haynes 1985). Therefore, numerous studies have tried to assess the ecological impact of Aboriginal landscape burning in the present-day environment (Bowman et al. 1988, 1998; Gill et al. 1996; Russell-Smith et al. 1997; Crowley and Garnet 2000).

A detailed study from a freshwater lake, Four Mile Billabong, on Groote Eylandt (off-shore from Arnhem Land) extending to ~10,000 yrs BP analysed the role of climate in this region and also whether there was correspondence to the Atherton Tableland sites (Shulmeister 1992; Shulmeister and Lees 1995). It was found there was correspondence during the early Holocene where there was an increase in precipitation but there were also regional differences that were likely responses to both local geomorphic process as well as possible climatic signals. There was an effective precipitation (EP) maximum at roughly 5000–4000 BP due to enhanced monsoonal activity with a decline in EP after 4,000 yrs BP because of increased variability resulting from changes in the Walker Circulation and the dominance of ENSO conditions. There was no significant change in the vegetation communities at this time (4000 yrs BP) although an increase in grasses and charcoal does suggest a more open environment with this increase in fire likely related to anthropogenic activity.

However an increase in effective precipitation proposed for the last 1000–2000 yrs BP, not found from the Atherton Tableland sites, is accompanied by the puzzling increase in both grass and charcoal which could be the result of increased variability but also could be a direct result of anthropogenic activity. Shulmeister (1992) suggests that an increase

in burning in the last 1000 years could be more directly related to the use of so-called cool burning undertaken in the early part of the dry season.

Moisture availability has been found to be the key driver of vegetation composition at Girraween, Northern Territory, during the Holocene, which subsequently influenced the extent of fire and its impact. However, changes in the late Holocene to what is suggested to be a more managed human landscape is indicated by a change or an intensification in resource-sourcing c. 3750 cal. yr BP that corresponds to a change in fire regime and vegetation transformation (Rowe et al. 2019).

A comprehensive study of inland sites from the Torres Strait Islands (Rowe 2007a,b) reveals maximum, rainforest and Myrtaceae forest from the early to mid-Holocene in line with northern mainland Australia records (Woodroffe et al. 1985, 1986; Hiscock 1999). Drier, more variable conditions are evident in the late Holocene as indicated by a decline in tree abundance and diversity and an increase in fire with a more substantial increase recorded in the last 1000 years. This increase in charcoal in the last 1000 years also corresponds to the increase found at Four Mile Billabong, on Groote Eylandt (Shulmeister 1992) and also at Big Willum Swamp, Weipa, Queensland where it is suggested it signals a more permanent expansion to inland locations (Stevenson et al. 2015).

Chapter 5

Materials and Methods

Introduction

This chapter contains all the material and methods that were used in this study except for those relating to dating and establishment of a stratigraphy that are treated in Chapter 6. A brief description of the fieldwork undertaken in 2003 and 2004 is given and this is followed by description of collected sediment cores, sampling methods and the technique used for Loss on Ignition (LOI) that includes moisture loss (water content). Details of the microfossil analyses, including preparations, identification and counting, then follow. As a component of this study was to look at charcoal morphology, burns and counts on plant material were carried out for reference purposes to aid the identification of charcoal morphotypes prior to preparation and analysis of macrofossils and macrocharcoal. Graphing techniques and statistical analyses used for proxies are then given.

5.1. Field methods

Fieldwork was conducted in July 2003 and September and October 2004 to collect a continuous core through at least the last 50,000 years from Lynch's Crater for high resolution, multiproxy analysis and to undertake associated activities that included collection of plant material for experimental burns to allow recognition of the sources of fossil charcoal. The field trips were undertaken in association with a broader project aim of collecting a complete sediment core from Lynch's Crater to allow extension of the existing pollen record to the base of the sediments. Field work was supported by a National Geographic grant to Dr. Chris Turney and Prof Peter Kershaw and by an Australian Research Council Discovery grant to Dr. Raphael Wüst, Prof Peter Kershaw and Dr William Anderson.

In 2003 an attempt was made to position a rotary drilling rig, hired from the Australian National University (ANU), in the middle of the swamp as close as possible to the location of the core collected in 1998 for the previous study of the last 50,000 years (Turney et al. 2001*b,c*, 2004, 2006a). Achievement of the location failed because inclement weather caused the truck supporting the drill rig to bog well before reaching that position (Figure 5.1). Having established the rig as far as possible onto the swamp

(Figure 5.2), cores were extracted in 1m length stainless steel barrels, extruded into split PVC tubes and described and photographed. Coring continued to a depth of 20 m before a combination of hole collapse due to penetration of very unconsolidated sediment that continuously filled the hollow augers and prevented collection of new sediment material, and equipment failure caused coring to be abandoned. In addition, percentage core recovery was poor in places and unsuitable for this study. In its place, a 10.72 m core, LYE(LIV), was taken alongside the rig core, with a Livingstone piston corer except for the compacted top metre that was recovered with a Russian D-section corer. Because sediments were disturbed around the coring position, in addition to the D-section (LYE) and LYE(LIV), D-section cores (LYA and LYB) were taken several metres distant from the drill rig and Livingstone cores.



Figure 5.1. Drill rig on Lynch's Crater, 2003 prior to inclement weather (Photo S.Rule 2003).



Figure 5.2. Coring on Lynch's Crater 2003 (Photo S.Rule 2003).

This meant that the D-section core component was extended to 150 cm to allow for any possible gap in the record. An additional 2 metre livingstone core, LY(3)Liv1, was also taken in the same area to cover the depth 100 cm to 300 cm, and cover the cross-over between the D-section and Livingstone cores. In addition, D-Section and Livingstone cores were taken to various depths over the crater to determine the degree of variation in sediment type (Figure 5.3). Each Livingstone core was extruded into a split PVC tube, wrapped in cling wrap and then a PVC lid was attached to secure the core and avoid distortion and contamination. The D-section cores were placed in split PVC tubes and wrapped in cling wrap. All collected cores were taken back to Monash University and stored in the cold store at 4°C. My analyses were restricted to the combined D-Section and Livingstone cores, LY(3)Liv1 and LYE(LIV) (Figure 5.4), taken near the main rig-core. Sections of the main rig-core and appropriate Livingstone and D-section cores were provided to Joanne Muller (PhD student at James Cook University, Queensland) for geochemical analysis and Sarah Davies (PhD student at Queens University, Belfast) for tephra analysis.

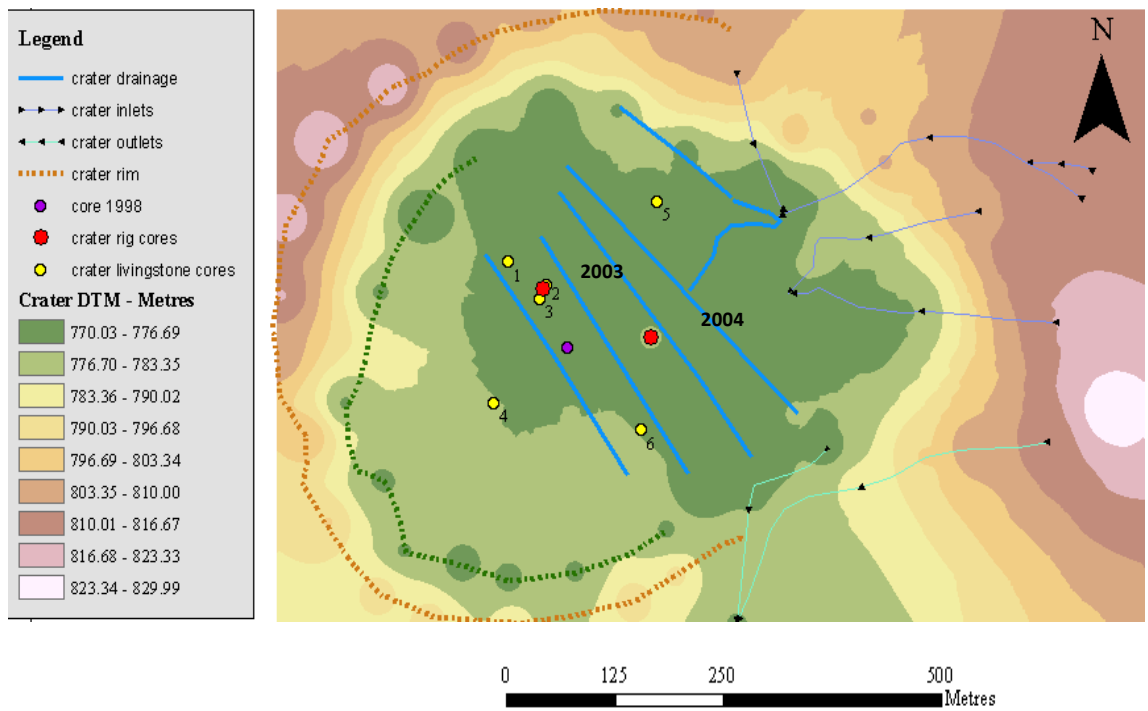


Figure 5.3. Schematic drawing of Lynch's Crater showing drainage lines and positions of cores taken in 1998 and field seasons 1 and 2 (2003 and 2004), (modified from Coulter 2007).



Figure 5.4. Retrieval of the core LYE(LIV) used in this study using a livingstone corer (Photo S.Rule 2003).

5.2. Laboratory methods

5.2.1. Sediment sampling

In order to achieve a high resolution record, a strategy of contiguous sampling at 2 cm intervals for the various proxies was implemented. Initially pollen sub-samples of 1 cm³ were taken from the central part of each 2 cm slice, while 5cm³ samples were taken initially for magnetic susceptibility measurement and, subsequently divided into sub-samples for calculation of moisture content LOI (1 cm³) and for macrocharcoal and other macroremain analysis (4 cm³) except on the D-section cores where 4 cm³ was used for both LOI and macrocharcoal due to the limited material available. A smear from each sample depth was taken to determine whether diatoms were present. Later, 2 cm³ samples from selected parts of the core were taken for accelerator mass spectrometry (AMS) radiocarbon dating while 1 cm³ samples for sediment absorption (humification) calculation were selected based on the findings of Turney et al. (2004) that showed humification picked up periods of high variability.

5.2.2. Sediment description

A detailed, semi-quantitative description of the sediment, using a modified Troels-Smith system (Kershaw 1997), was carried out at the same time as sampling for pollen, LOI and macroscopic charcoal as the interior of the core was now visible and descriptive analysis of sediment properties and elements possible.

5.2.3. Moisture content and Loss on Ignition (LOI)

Moisture content is a useful guide to the degree of sediment drying and/or saturation level. Each sample was weighed then oven dried at 105°C overnight and reweighed to determine the moisture content of the sample with calculation details given below.

Moisture Loss (ML) is calculated as:

$$ML = ((WS - DW_{105}) / WS) * 100$$

WS = wet sample

DW₁₀₅ = dry weight of sample after oven dried at 105°C

LOI is a simple method used to estimate organic matter; in this study procedures set out in Dean (1974) and Heiri et al. (2001) have been followed. Once the moisture loss had been calculated (see above) samples were placed in the muffle furnace at 550°C, left for 2 ½ hours, and reweighed to allow calculation of the loss on ignition, i.e. organic content of the sample, as shown below.

LOI content is calculated as:

$$\text{LOI} = ((\text{DW}_{105} - \text{DW}_{550}) / \text{DW}_{105}) * 100$$

DW_{105} = dry weight of sample after oven dried at 105°C

DW_{550} = dry weight of sample after combustion of organic matter at 550°C

5.2.4. Pollen and microcharcoal preparation

Each sample taken for pollen analysis, including microcharcoal analysis, was initially dispersed in tetra sodium pyrophosphate, $\text{Na}_2\text{P}_2\text{O}_7$, (10%), in a waterbath for ½ hour at 100°C after which a *Lycopodium* spore tablet (10,679 spores) was added to enable the calculation of pollen and charcoal concentrations, see Chapter 4 sub-section 4.4.2. It was found that, due to the high concentration of charcoal, and in some cases pollen, on a number of slides, two *Lycopodium* tablets had to be added to ensure reliable statistical estimates of concentrations to be determined. As samples were highly organic, they were then treated with potassium hydroxide, KOH, (10%), which breaks down and dissolves organic material before being sieved through a 210 µm mesh sieve, to remove larger sediment fragments. Routinely in the laboratory, samples are also sieved through a 7 µm sieve to remove the fine fraction. However, as there was concern that this may result in the loss of some pollen types especially from the families Cunoniaceae and Elaeocarpaceae that fall at or just below this size fraction and as they have been shown to be important indicator taxa in previous palaeoecological studies, this step was not undertaken.

Acetolysis (acetic anhydride/sulphuric acid) was then undertaken on each sample to remove cellulose and darken the pollen to assist morphological recognition. Heavy liquid separation using sodium polytungstate, (specific gravity 2.0) then followed in order to separate mineral matter from the pollen residue. Further separation was achieved by

treatment with hydrofluoric acid (HF) that digests silica, including siliceous microfossils such as diatoms and phytoliths. Hydrochloric acid, HCl, (10%) was then used to remove any silicofluorides produced during HF treatment. Finally, each sample was dehydrated by addition of absolute ethanol ready for mounting onto microscope slides. Glycerol was the preferred mounting medium, and this was mixed into the sample on a 1: 1 ratio and aided in dispersing the sample across each slide. Paraffin wax was used to seal the cover slips on the slides.

5.3. Pollen

5.3.1. The Pollen Sum and Identification

The prepared pollen slides were examined under a Zeiss Axioskop light microscope at X630 magnification. The target count was a pollen sum of 150-200 dryland arboreal taxa, which excluded pteridophytes and bryophyte spores and pollen of Poaceae, Chenopodiaceae, Asteraceae (tubuliflorae and liguliflorae), other sclerophyll herbs and shrubs, aquatics and swamp taxa, *Leptospermum* and other apparent locally-derived Myrtaceae, for each depth. Previous studies from Lynch's Crater (Kershaw 1973, 1984) omitted, the Cupressaceae genus *Callitris* due to uncertainty in recognition of this morphologically indistinctive grain, but subsequent greater certainty in identification has resulted in its inclusion within the pollen sum. The aquatic and swamp taxa and pteridophytes and bryophytes were excluded from the sum because of the likelihood of over-representation of local taxa on dryland pollen percentages. However, as the local environment can be informative of both local and regional changes, a separate pollen sum was constructed for aquatic and swamp taxa including the swamp fern *Cyclosorus* (Thelypteridaceae) and the hornwort (bryophyte) *Anthoceros*. The herbs and shrub category, composed largely of Poaceae, was excluded from the dryland pollen sum because of the difficulty in separating dryland and local swamp sources while *Leptospermum* was excluded because of the likelihood of a very local source and therefore over-representation, a situation also considered to be the case for other Myrtaceae taxa at varying depths.

Pollen identification was facilitated with the aid of reference photographs of pollen types from northeast Queensland fossil pollen samples (Kershaw *unpublished*) and the reference slide collection housed at the School of Geography and Environmental Science,

Monash University where pollen floras from northern Queensland were targeted. A general separation to sub-family level of Myrtaceae pollen and taxa within the Urticaceae and Moraceae families was attempted as key indicator taxa are contained within these families, (see following sub-sections). Publications of pollen types from Australia and from different parts of the world possessing relevant rainforest taxa were also utilised. These included the 'Pollen flora of Taiwan' (Huang 1972), 'Spore atlas of New Zealand ferns and fern allies' (Large and Braggins 1991), 'A pollen flora of the native plants of South Australia and southern Northern Territory, Australia' (Boyd 1992), the 'Pollen and spores of Chile' (Heusser 1971) and 'Pollen and spores of Barro Colorado Island' (Roubik and Moreno 1991).

5.3.2. Myrtaceae Identification

The Myrtaceae family has a largely uniform pollen type with differences between many genera and species minute or obscure making it hard if not impossible to identify grains to a refined taxonomic level under the light microscope (Pike 1956; Gadek and Martin 1981, 1982; Thornhill et al. 2012*a, b, c* and *d*). But separation into loose groupings is possible. Here, separation was aided by the publications of Pike (1956), Gadek and Martin (1981, 1982) and Thornhill et al. (2012*a, b, c* and *d*) which provided information on separation by sculpture, the presence (*Melaleuca*) or absence (*Syncarpia*) of the apocolpial island, the endopore size (*Eucalyptus* large) as well as general size (*Syzygium* small) and shape (concave or convex) of the pollen sides with some of these pollen characteristics shown in Figure 5.5.

This allowed separation of the main Myrtaceae types based on discrete but consistent morphological characteristics and the Myrtaceae groupings used in this thesis and their likely ecological habitat and attributes are given in Table 5.1. The composition of the pollen sum has been given in sub- section 5.3.1 and, although *Syzygium* pollen grains are generally small, on examination of available pollen reference slides not all conformed to this characteristic so it was decided to exclude the *Syzygium* grouping from the pollen sum alongside the *Leptospermum* grouping. *Acmena* has now been placed within the *Syzygium* genus but, on examination of available pollen reference slides, it was possible to distinguish it from *Syzygium* and therefore it is separated from *Syzygium* in this thesis. All other Myrtaceae groupings, including *Acmena*, were included in the dryland pollen sum and, although there may be some overlap between the *Eucalyptus*, *Melaleuca* and

Corymbia groupings in particular it is considered that these groups generally provide a good indication of open sclerophyll communities.

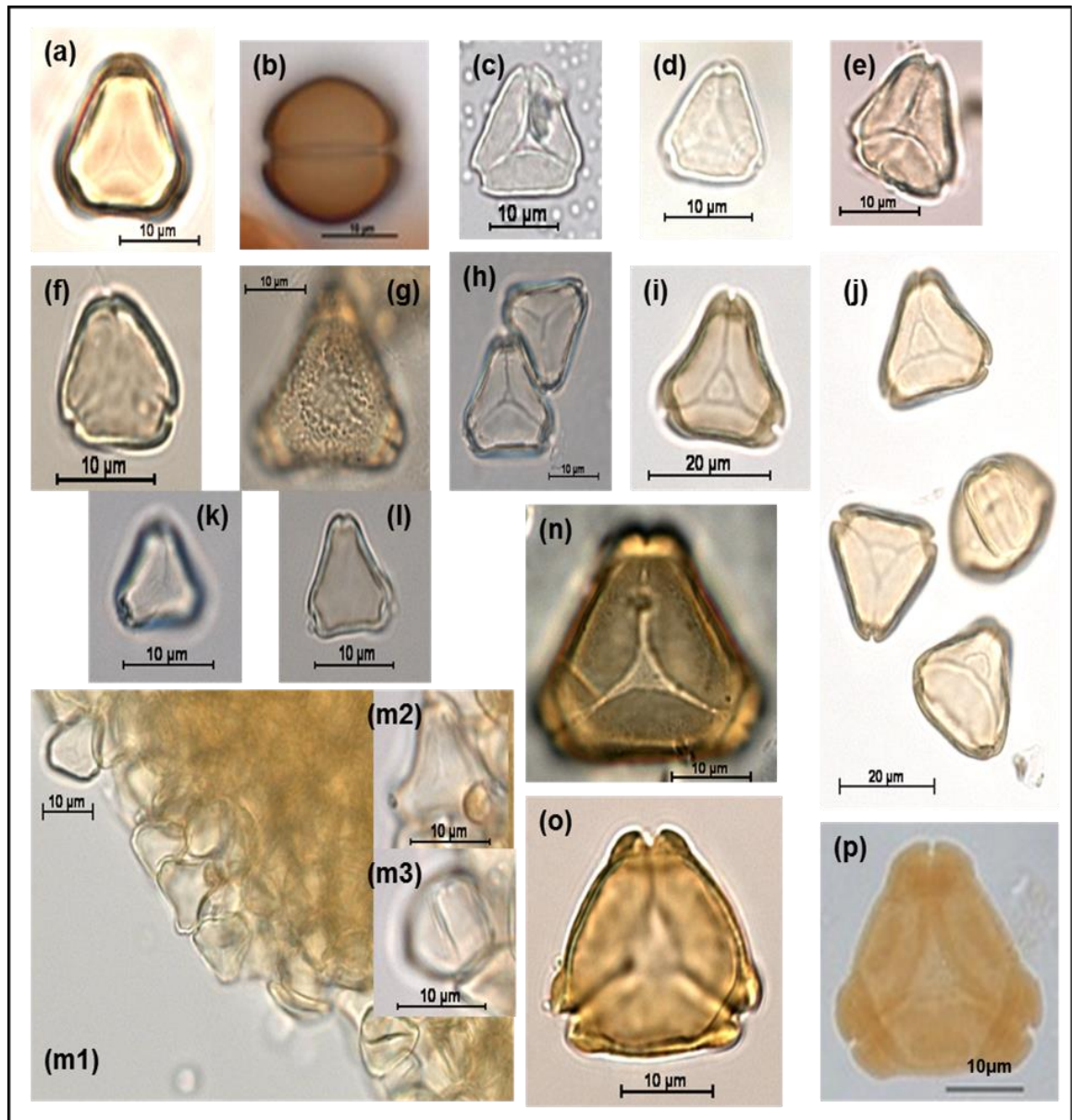


Figure 5.5. Some of the Myrtaceae pollen morphological types found in the study site area. (a) *Syzygium smithii* (formerly *Acmena smithii*), (b) *Syzygium graveolens* (formerly *Acmena graveolens*), (c) *Syzygium leuhmannii* (formerly *Eugenia leuhmannii*); (d) *Syzygium kuranda* (formerly *Eugenia kuranda*); (e) *Syzygium cormiflorum* (formerly *Eugenia cormiflora*); (f) *Gossia dallachiana* (formerly *Austromyrtus dallachiana*); (g) *Rhodomyrtus trineura*; (h) *Syncarpia glomulifera*; (i) *Melaleuca dealbata*; (j) *Melaleuca leucadendra*; (k) *Tristaniopsis exiliflora* (formerly *Tristania exiliflora*) high focus and (l) *T. exiliflora* low focus; (m1) *Leptospermum wooroonooran* (cluster of pollen grains), (m2) *L.wooroonooran* polar view, (m3) *L.wooroonooran* equatorial view; (n) *Corymbia intermedia* (formerly *Eucalyptus intermedia*); (o) *Eucalyptus tereticormis*; (p) *Eucalyptus macta* (formerly *E.resinifera*) All photographs were taken by the author except for (b) and (p) which were sourced from the Australasian pollen and spore atlas and all pollen reference slides photographed, including those from the Australasian pollen and spore atlas, were from the Australian National University pollen reference collection with full details given in Appendix A, Section 1.

Table 5.1. Myrtaceae groupings used in this thesis and their ecological habitat and local attributes (taken from Tracey 1982; Webb et al. 1984; Hyland et al. 2003).

Myrtaceae Grouping	Ecological habitat and local attributes
<i>Syzygium</i> type	Mainly rainforest taxa
<i>Acmena</i> type	Rainforest taxa (some <i>Acmena</i> are rheophyte)
<i>Leptospermum</i>	Local taxa most likely derived from swamp surface based on limited pollen dispersal; and ecologically perhaps high altitude (low temperature). <i>Tristaniopsis</i> pollen type is similar in size but is not likely to be found on swamps under relatively cool conditions. .
<i>Eucalyptus</i> type	Predominantly open forest and woodland but can also be found in wet sclerophyll forest and on the margins of rainforest.
<i>Melaleuca</i>	Woodland species but can tolerate impeded drainage as on swamp surfaces. It is possible that <i>Syncarpia</i> may also be present but ecologically it is more variable than <i>Melaleuca</i> and can be in woodland, rainforest and wet sclerophyll forest.
<i>Corymbia</i> type	Bloodwood species, found in woodlands but also in wet sclerophyll forests and on rainforest margins.

5.3.3. Moraceae and Urticaceae Identification.

In previous studies from Lynch's Crater the families Moraceae and Urticaceae have generally been grouped together in pollen counts because of the similarity in pollen morphology across this grouping. Initially Kershaw (1973, 1976) did not separate the genus *Ficus* from the Moraceae family but with the extension of the Lynch's Crater record (Kershaw 1984) *Ficus* was included in the extended section of the record to indicate its importance within the rainforest assemblage (Kershaw et al. 2007a). The *Ficus* genus was separated from other Urticaceae and Moraceae pollen types in this thesis but it was found that further separation was not possible within the Urticaceae and Moraceae grouping. Figure 5.6 shows some of the genera and species from the Moraceae and Urticaceae family that are found in the study site area.

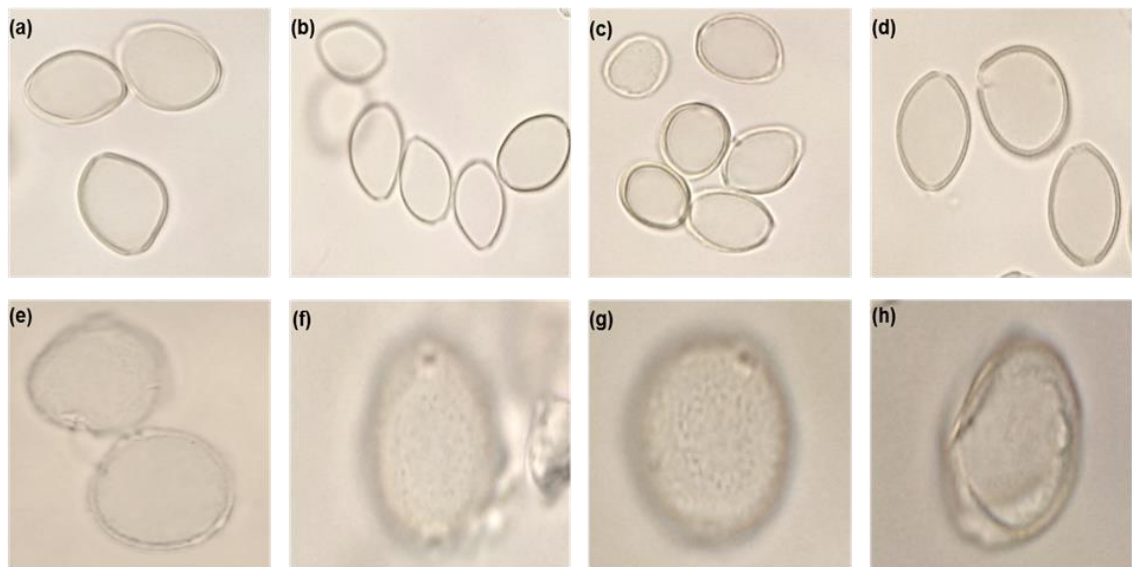


Figure 5.6. Genera and species from the Moraceae and Urticaceae family that are found in the study site area (a) – *Ficus rubiginosa*, (b) – *F. virens*, (c) – *F. coronata* and (d) – *F. macrophylla*, (e) – *Streblus glaber*, (f) – *Dendrocnide photinophylla* (formerly *Laportea photinophylla*), (g) – *Pipturus argenteus* and (h) – *Urtica incisa*. All photographs were taken by the author and all pollen reference slides photographed were from the School of Geography and Environmental Science, Monash University pollen reference collection with full details given in Appendix A, Section 2.

5.3.4. Non-pollen palynomorphs

Several non-pollen palynomorphs were included in the counts. *Botryococcus* was the only algal palynomorph with counts included along with pollen, presence was noted for the fungal spores *Gelasinospora* and *Neurospora* throughout the entire sequence, while large peaks in some fungal and algal spore types were also noted. The general state of preservation in pollen was also noted.

5.4. Microscopic charcoal

5.4.1. Microscopic charcoal counting

The microscopic charcoal counts (see sub-section 5.2.4) were undertaken on the prepared pollen slides. The size distribution of charcoal, see Chapter 4 for more detail, is expected to reflect source distance with microcharcoal generally considered to be mainly locally sourced (Lynch et al. 2004) although some suggest it will reflect a combination of local, extra-local and regional sources (Clark and Hussey 1996; Ohlson and Tryterud 2000). Studies have also suggested that assessing the size distribution of microscopic charcoal particles can give a good estimate of both fire intensity and relevant charcoal size area, see sub-section 4.4.2 (Morrison 1994; Blackford 2000; Duffin et al. 2008; Rucina et al.

2009). Microcharcoal recognition here was based on the criteria of black, opaque and angular particles and particles were divided into five size categories, 10–52 µm, 53–104 µm, 105–156 µm, 157–208 µm and > 208 µm.

5.4.2. Calculation of pollen and charcoal concentration and influx

Charcoal and pollen concentrations (per cm³) were calculated using the number of charcoal particles and pollen grains in relation to the volume of sediment and added *Lycopodium* spores (10679x2). Pollen/charcoal concentration values (Pn), grains/particles per cm³ are determined according to the following formula: -

$$Pn = \frac{N \times Lyct}{V \times Lycf}$$

Pn = number of charcoal or pollen particles or grains per cm³

Lyct = total *Lycopodium* added (1 tablet = 10679)

Lycf = counted *Lycopodium* spike spores

V = the sample volume (cm³)

N = number of charcoal/pollen particles counted on slide

Having a good chronology allowed for influx to be calculated for both pollen and charcoal and is defined by the number of pollen grains (charcoal particles) accumulated per unit area of sediment surface per unit time presented here as cm⁻² yr⁻¹.

5.5. Macrocharcoal reference materials

5.5.1. Macrocharcoal reference burn preparation

Experimental burns were undertaken to see whether structural integrity and morphological features were preserved in macrocharcoal. Initially material collected in the field was to be utilised but deterioration of the swamp and aquatic samples meant that it was not possible to use these for the reference burns. However, the cosmopolitan nature of the aquatic/swamp taxa meant that most of these or similar taxa were able to be sourced from the Monash University grounds or nearby environments. Wood pieces and fragments for the woody component were made available courtesy of a wood reference collection at Monash University (see Table 5.2).

Table 5.2. Reference material used for experimental burns

Aquatic/Swamp Taxa	Poaceae/Herb Taxa	Pteridophytes	Sclerophyll Taxa	Rainforest Taxa
<i>Typha domingensis</i>	<i>Danthonia</i>	<i>Pteridium</i>	<i>Eucalyptus regnans</i>	<i>Acmena</i>
<i>Eleocharis dulcis</i>	<i>semiannularis</i>	<i>Blechnum</i>	(wood and leaf)	<i>smithii</i>
<i>Carex fascicularis</i>	<i>Dianella</i> sp.	<i>Cyathea</i>	<i>Eucalyptus pauciflora</i>	(wood and leaf)
<i>Carex appressa</i>			<i>Casuarina</i>	<i>Petalostigma</i>
<i>Myriophyllum</i> sp.			<i>cunninghamii</i>	<i>banksii</i>
			<i>Melaleuca viridiflora</i>	

Umbanhowar and McGrath (1998) carried out both open burns and muffle furnace burns to replicate as far as possible natural burns and experimental burns within the laboratory to assess the comparability of the two fire types. It was not possible to carry out natural burns for this project and so burns were limited to experimental burns using a muffle furnace within the laboratory. However, Umbanhowar and McGrath did find that a key measure, Poaceae and sedge to woody taxa ratio, was still valid across both burn types (natural and experimental) see sub-section 4.4.4.

All non-woody samples were dried at 70°C, any higher and it is likely that initial degradation of lignin and hemicellulose components would have begun to char (Scotter 1970; Chandler et al. 1983). Testing was carried out for the temperature and duration needed for the experimental burns on the Cyperaceae species *Carex fascicularis*. *C. fascicularis* was used as its wide blade (leave) and distinct venations is similar to some grasses and also to the (semi) aquatic perennial *Typha* and it would be of interest to see whether these distinct venations remain after the temperature testing. All test samples were tightly wrapped in foil and placed in a porcelain crucible and then placed in the muffle furnace. Although there are varying methods for experimental burns on plant material (Orvis et al. 2005) the methods used in this project were based on the methods of Umbanhowar and McGrath (1998) with adaptations when needed. All regimes and results are shown in Table 5.3.

Table 5.3. Testing of *Carex fascicularis* with temperatures, times and degree of charring given.

Sample	Temperature	Time (minutes)	Degree of Charring
1	300*	20	Outer blade charred only
2	300	10	Outer blade charred only
3	300	15	Outer blade charred and partial charring of epidermis
4	300	20	Outer blade charred and partial charring of epidermis
5	350	20	Outer blade charred and near complete charring of epidermis
6	400	10	Outer blade charred and near complete charring of epidermis
7	400	20	Outer blade and epidermis completely charred

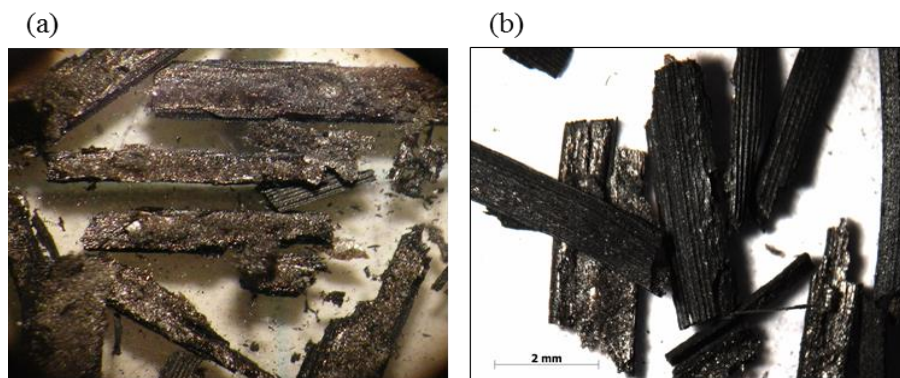


Plate 5.1. *Carex fascicularis* (a) *C. fascicularis* (sample 6) tested at 400°C for 10 minutes with outer blade completely charred but inner part (epidermis) still with a brown-coppery tinge indicating that it is not completely charred, (b) *C. fascicularis* (sample 7) completely charred but distinct venation structure still visible.

Plate 5.1 shows the result for Sample 6 (a) from Table 5.3 where there is incomplete charring of the epidermis and Sample 7 (b) where charring is complete but the distinct venations of *C. fascicularis* are still visible. From the results in Table 5.3 a standard procedure was established for all non-woody taxa. All samples were dried at 70°C then wrapped in foil and placed in porcelain crucibles. Samples were then placed in the muffle furnace, which had been preset to 400°C, for 20 minutes. Samples were then taken out and, once they had cooled, and been checked, were left in the foil but placed in paper envelopes with burn details. Samples were then ready to be sieved and reviewed.

Control burns for woody taxa had to be modified due to differences in structure and mass. Initial drying was at 70°C but excess smoke on burning meant samples needed to be dried at a higher temperature. Excess smoking is due to high moisture content which limits flaming and therefore ignition which will prolong the charring process (Chandler et al. 1983). Therefore, it was decided that all samples would be dried at 105°C. This temperature is when moisture is outgassed as steam and charring may commence, and unlike Cyperaceae and Poaceae, structural damage would be limited in woody samples due to the lower surface to mass ratio (Hammes et al. 2006). An initial burn at 400° C on the woody taxa suggested that 20 minutes would not be long enough for complete charring so all woody taxa, following the same regime as for non-woody taxa with muffle furnace preset to 400°C, but for 1 hour. They were then cooled, kept in the foil and placed in paper envelopes.

5.5.2. The macrocharcoal reference burn methods

Prior to sieving, all charcoal had to be broken down. Although there was breakage of charcoal from the control burns, especially for the more fragile components, it was necessary for moderate force to be applied to enable a more extensive review of the structural components of the charcoal. This was achieved for nearly all non-woody components with a gentle press down with a probe while all woody components needed relatively more pressure achieved by gently tapping using a mortar and pestle. Samples were sieved under gently flowing water. Once this was completed, samples were placed in nested meshed sieves of different size categories to facilitate counting and examination. Each size component was then transferred to a petri dish. Initially it was decided that image analysis (Scion) be used for the counting but the problem of bleeding and the degree of heterogeneity in the shape of the charcoal meant that this was not appropriate. Consequently, quantification of area was not possible so statistical analysis was not performed on these samples. However manual counts were undertaken on selected Poaceae, sedges and *Typha* alongside woody samples to see whether the ‘elongated’ and ‘blocky’ L:W ratio applied. Umbanhowar and McGrath (1998) found that grass charcoal had a L:W ratio of 3.62 - muffle furnace (4.83 open burn) while wood charcoal had a L:W ratio of 2.13 - muffle furnace (2.23 open burn) while a mix burn of grass and leaf saw a significant drop in the L:W ratio.

In view of these results it was decided that a >2:1 L:W ratio would be used to separate elongated (Poaceae and sedge) charcoal from woody charcoal. A gridded (mm) mat divided into 4 sections was placed under the petri dish for easy of counting and a >2:1 L:W ratio was used to designate ‘elongated’ charcoal while a <2:1 L:W was used to designate ‘blocky’ charcoal. It is unlikely that every single Poaceae, sedge and *Typha* charcoal particle and woody charcoal particle would comply with this scenario but the aim of this exercise was to see whether the reference burn material generally complied with this outcome. If it did so then this separation of ‘elongated’ from ‘blocky’ should provide a guideline of Poaceae, sedge and *Typha* dominated fire over woody taxa dominated fire.

5.5.3. The macrocharcoal reference burn results

The results of the reference burn counts found that there was a clear difference in the ratio of ‘elongated’ to ‘blocky’ charcoal for grass and sedge charcoal and wood charcoal (see Table 5.4), and the majority of the grass and sedge charcoal samples had a markedly elongated shape and in most cases much greater than a 2:1 ratio with a 4:1 ratio more common (Plate 5.2). This would suggest that separation of ‘blocky’ and ‘elongated’ charcoal could provide not only information about the source material burnt but also the fire intensity (see Appendix A, Table 1 for full details of reference burn results).

Table 5.4. Percentage average results across 3 counts for >2:1 L:W ratio for herbaceous (Poaceae, sedges and *Typha*) and woody taxa (*Eucalyptus* spp. and *Acmena*).

Size μm	Poaceae	<i>Carex appressa</i>	<i>Carex fascicularis</i>	<i>Typha</i>	<i>Eucalyptus regnans</i>	<i>Eucalyptus pauciflora</i>	<i>Acmena</i> sp.
> 500 μm	81.1	80.3	75.2	80	14.7	16.5	17.5
> 250 μm	78	81.6	78.7	79	16.2	15.8	21.9
> 125 μm	77	83.1	78.8	79.7	18.8	19.9	21.1

Not all charcoal material could be allocated so clearly to ‘elongated’ and ‘blocky’ and on examination of the base section of *Typha*, a great deal of porosity was found in the charcoal (Plate 5.2 (3c and d)).

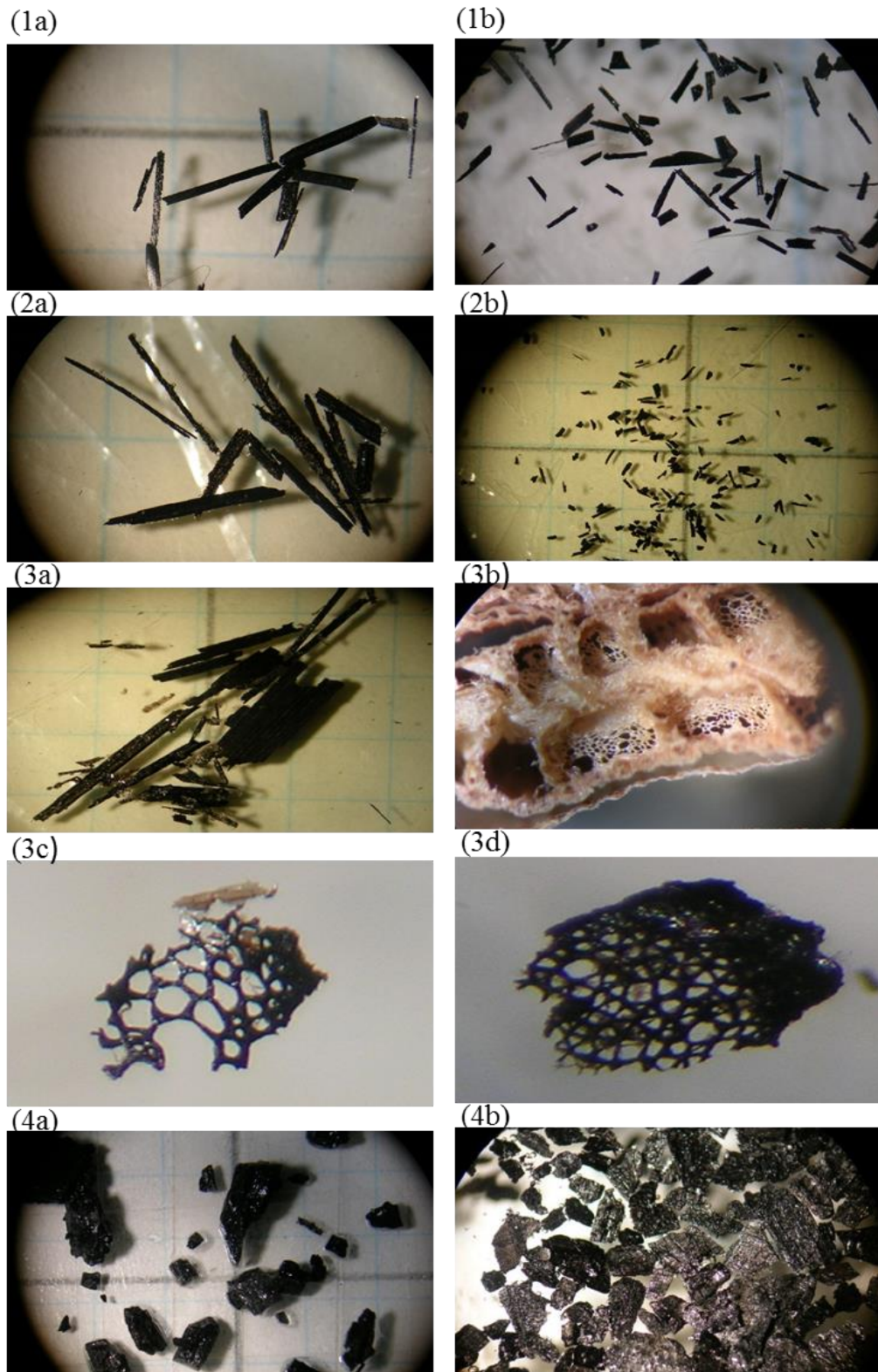


Plate 5.2. Burn samples (Grid size 1 mm); (1a) > 500 μ m Poaceae, (1b) > 250 μ m Poaceae, (2a) > 500 μ m *Carex fascicularis*, (2b) > 250 μ m *Carex fascicularis*, (3a) > 500 μ m *Typha*, (3b) Epidermis of *Typha* prior to burning, (3c) Charred epidermis of *Typha*, (3d) Charred epidermis of *Typha*, (4a) > 500 μ m *Eucalyptus regnans*, (4b) > 250 μ m *Eucalyptus regnans*

As Umbanhowar and McGrath (1998) had found for their study, the leaf material used for this study, was consistently more polyhedral, except for *Melaleuca* and *Casuarina*. This was also found for the fronds of pteridophytes, *Cyathea*, *Pteridium* and *Blechnum*, which showed some similarity to the leaf material but there was a consistent presence of a curved and pointed shape which was also found in the leaf material of *Melaleuca* and *Casuarina* (see Appendix A, Plate 1). These results suggest that there may be a significant group of charcoal morphotypes outside the ‘elongated’ and ‘blocky’ groupings. These were not included in the reference burn counts but do suggest that another grouping is warranted if encountered.

5.6. Macrocharcoal and macrofossils

The > 210 µm coarse fraction obtained from the sieving for pollen analysis was found to contain a number of macrofossils, such as seeds and nuts, and so it was decided that the greater volume (4 cm³) used for the macrocharcoal analysis (McKenzie 1989; Schlachter and Horn 2010) would provide additional material for a limited study on plant macrofossils prior to their use for the macrocharcoal analysis.

5.6.1. Macrocharcoal preparation

Samples were dispersed in distilled water and Na₂P₂O₇ (10%) in a waterbath for ½ hour at 100° C followed by KOH (10%) and distilled water in a waterbath for ½ hour at 80°C. Samples were then sieved at 125 µm under gently flowing water to remove KOH residue. Macrofossils were then removed before the addition of 5–10 ml of NaCl (12.5%) to each sample in order to bleach the organics but not the charcoal. The high dilution of NaCl (12.5%) used in this study meant that samples were regularly checked until bleaching occurred usually within 3 hours (Schlachter and Horn 2010).

5.6.2. Fossil macrocharcoal identification and counting

As noted in sub-section 5.5.3 and 5.5.4, the macrocharcoal reference burns showed a high degree of heterogeneity in porosity for some burns (see Plate 5.2 (3c and d)) and a degree of heterogeneity in shape for the pteridophytes and leaf burns (see Appendix A, Plate 1). The highly irregular porosity noted in sub-section 5.5.4, hereby termed lattice-type, is likely to have a number of sources but at least 1 source could be verified from the

reference burns and that is the epidermis of *Typha* (Plate 5.2 (3c and d)). Initial observations prior to the macrocharcoal counts also found that the outer coatings of the aquatics *Nymphoides* and *Liparophyllum* (formerly *Villarsia*) (Plate 5.3(a) and (b)) had a similar patterning minus their ornamental spikes and nodes, although the patterning was more uniform than that of the *Typha* epidermis. It maybe informative to include ‘lattice-type’ as a third category. The fourth category ‘other’ included components that did not fit into the other three categories but were clearly charcoal (Plate 5.3(c), (d), (e) and (f)).

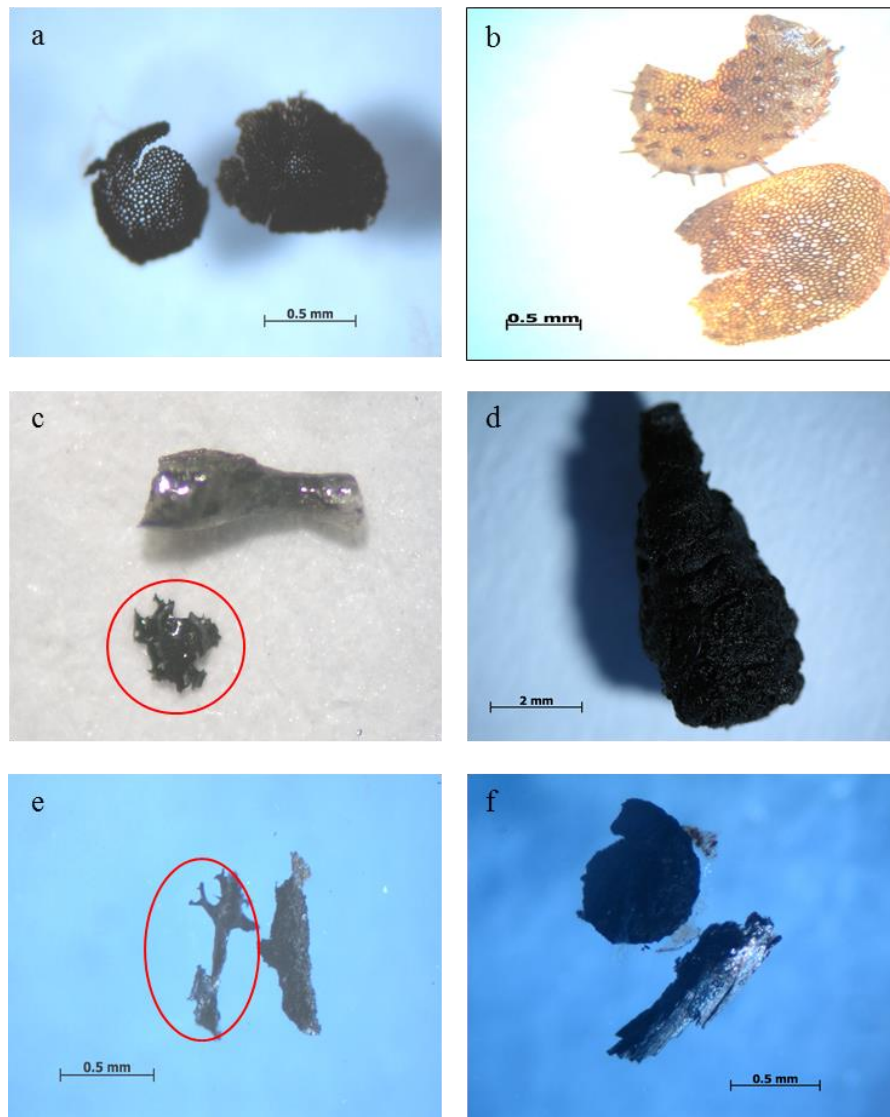


Plate 5.3. (a) Charred remains of *Nymphoides* seed; (b) Partially charred remains of *Liparophyllum* (formerly *Villarsia*) seed; (c) unknown charcoal type (red circled area) x 10; (d) likely charred remains of flower (seed) component from a sedge; (e) unknown charcoal type (red circled area); (f) charred remains of unknown seed and sedge component.

It was also decided that if 'brown charcoal' was present during the counts it would be noted and, if numbers allowed, a ranking of abundance would be included. In addition to these categories and observations any other consistent findings would be recorded. These categories and observations will be in place across all size categories. Once all samples had been sized sieved under gently flowing water to remove any residue of NaCl, they were transferred to a petri dish placed on a gridded mat and manually counted using a binocular AIS-OPTICAL microscope at X40 magnification. All photographs of macroscopic charcoal and macrofossils were taken on a binocular Zeiss Stemi 2000-c microscope and attached KL 1500 LCD Canon Power Shot A620 digital camera.

5.6.3. Macrofossil identification and counting

In most macrofossil studies, size separation is used (Birks 1973; Tiffney 1990; Beaudoin 2007), but it was decided, because of the limited material available that size separation was not possible and only the initial sieve size $> 125\ \mu\text{m}$ would be used to separate the very fine fraction. Once the samples were sieved at $> 125\ \mu\text{m}$ under gently flowing water to remove KOH residue, the macrofossils were ready to be counted. The emphasis was placed on retrieving seed and nut remains although any other fragment that was visible and could be identifiable was also retrieved. Initially all macrofossils were picked out of the sample under a binocular AIS-OPTICAL microscope X40 magnification and placed in a small plastic vial containing distilled H_2O . Once all samples had been processed, macrofossils were counted and grouped into identifiable types and photographed.

In comparison to pollen identification, macrofossil analysis in Australia is very much in the preliminary stage, and therefore resource and reference material is limited. Field based collection is the ideal method for comparison of modern and near surface fossil specimens however there were problems in achieving this aim. Time was a major drawback in establishing a comprehensive field herbarium and previous records from Lynch's Crater suggest that compaction and/or loss of material through the top 2 metres may mean that the modern samples are not directly comparable to the fossil record. However, the limited number of samples collected by the author together with material collected and identified previously from Lynch's Crater and other swamps in the Atherton Tableland region proved surprisingly rich in seeds and nuts. Identification of fossil seeds was aided by a number of online seed databases and literature.

5.7. Pollen, charcoal and macrofossil diagrams

All pollen, charcoal, macrofossil and information on sediment stratigraphy are illustrated on pollen diagrams, produced using the programmes TILIA and TGView 2.02 (Grimm 2004). Both percentage (percentage of the pollen sum) and influx (absolute) diagrams have been produced. Influx was possible due to the relatively good chronological control, see Chapter 6, but changes in the sedimentation rate need to be viewed alongside the influx results (Hicks Hyvärinen 1999), see Chapter 7. Macrofossil data (excluding macrocharcoal) are only shown as count data or in some cases in the form of presence or absence. The stratigraphically constrained classification CONISS (Grimm 2004) was used for zonation in conjunction with significant changes in the pollen sum data.

5.8. Statistical analysis

The main statistical analyses used in this study are Principle Component Analysis (PCA) and Spectral Analysis. PCA is an ordination technique which has been widely used in palaeoecology and is effective in deciphering the underlying structure and relationship between taxa especially when large data sets are used. In PCA a new set of axes are provided in a lower dimensional space (vector space) which the original taxa and samples can be projected. Therefore the aim of the ordination technique PCA used in this study is to reduce the data to a number of taxa which accounts for the majority of the variance in the data and also, if possible, detect any hidden alignments and divergents not readily visible in the original data (Jambu 1991). PCA was undertaken using the statistical software programme, STATISTICA (StatSoft, Inc. 2011).

Spectral Analysis is a statistical technique which identifies underlying periodicities in time-varying data which is a specific modification of Fourier analysis (Chatfield 1989). Fourier analysis is limited to deterministic functions whereas spectral analysis is able to decipher information from stochastic or chaotic processes. The specialized SPECTRUM programme (Schulz and Statteger 1997) was used for the spectral analysis. SPECTRUM uses a Lomb-Scargle Fourier Transform for unevenly spaced series in combination with a Welch-Overlapped-Segment-Averaging procedure. This method allows direct analysis of unevenly spaced time-series without preceding interpolation, which amounts to reddening, or a bias, in the low frequency spectral components. The statistical significance of harmonic components detected by SPECTRUM was determined by

REDFIT (Schulz and Mudelsee 2002). Palaeoclimatic data display a red-noise background that is a continuous decrease of spectral amplitude with increasing frequency which artificially enhances the spectrum of low frequency components of a time-series. REDFIT uses an autoregressive (ARI) process to test whether a palaeoclimatic time-series is distinguishable from a red-noise background. Both spectra data plots, red-noise spectra and log-linear red-noise data plots were plotted in Gnuplot 4.0 (Williams and Kelley 2004).

Chapter 6

Developing a Chronology for Lynch's Crater

Introduction

This chapter describes the methods used to construct a chronology for the Lynch's Crater sequence. Ages obtained from radiocarbon dating peat sediments by Accelerator Mass Spectrometry (AMS) during this study are compared to previously reported ages by precise correlation between sequences. From these data and with the use of Bayesian statistics, a robust geochronological timescale is reported for the Lynch's Crater sequence.

6.1. Radiocarbon Dating

Carbon 14 (^{14}C) is continually formed in the upper atmosphere by cosmic neutrons which rapidly oxidizes in air to form carbon dioxide. Plants and animals integrate ^{14}C from carbon dioxide throughout their lifetime and when they die they no longer take in radiocarbon which subsequently radioactively decays. The half-life (the period of time required for half a radioactive isotope to decay) of ^{14}C is 5730 ± 40 years. The practical outcome is the older the sample analysed the less ^{14}C is present (Figure 6.1) with a dating range of up to ~50,000 years (Bowman 1990; Turney et al. 2001a; Bronk Ramsey et al. 2012).

There are three methods for the measurement of ^{14}C concentration: gas proportional counting, liquid scintillation counting and AMS. Decay counting by either gas proportional counting or liquid scintillation counting measure the emission of β^- particles during the radioactive decay of ^{14}C . In contrast, AMS directly measures the ratio of ^{14}C atoms in a sample relative to ^{12}C and ^{13}C (Figure 6.1). AMS has advantages over decay counting including relatively fast measurement time (minutes/hours compared to days) and the substantially smaller sample size required (0.1–2 mg compared to 0.5–> 2 g of carbon). The smaller amount of material that can be dated by AMS means that a wider variety of materials can be dated, including amino acids extracted from bones, pollen and macrofossils from lakes and peat sediments and sub-annual layers from trees and corals (Olsson 1986; Hua 2009).

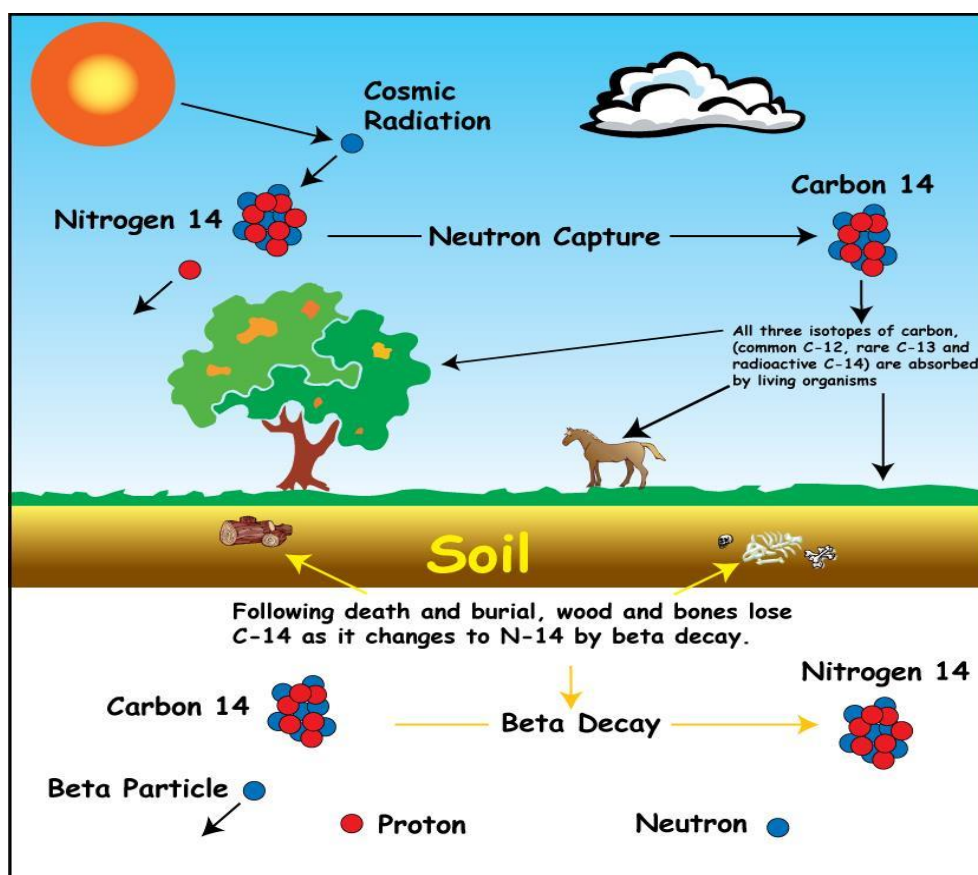


Figure 6.1. Schematic of radiocarbon production and decay in the atmosphere. ^{14}C is produced in the atmosphere by cosmic neutrons colliding with nitrogen atoms. The newly formed ^{14}C is oxidized to $^{14}\text{CO}_2$ when it enters the biosphere. Following an organism's death, radioactive decay occurs, converting the ^{14}C back to ^{14}N (after Radiocarbon Laboratory, ANU 2020).

Radiocarbon ages are reported in years before present (BP) with present defined as AD/CE 1950 (Millard 2014). However, a radiocarbon year does not directly equate to a calendar year as the concentration of ^{14}C in the atmosphere has not been constant through the ages. Variations in the rate of radiocarbon production in the atmosphere are caused by changes to the cosmic ray flux (solar wind and solar magnetic field) and to variations in the Earth's magnetic field as well as fluctuations in the Earth's carbon reservoirs such as increased burning of fossil fuels which may affect the ratio of ^{14}C to ^{12}C (Merrell and McElhinny 1983; Post et al. 1990; Balco 2011). While a reduction in deep ocean ventilation may allow enhanced accumulation of respired carbon in the ocean interior, for a suggestion made for the Last Glacial Maximum (Skinner et al. 2017). Long term changes (10^3 – 10^4 yrs) are due to the Earth's magnetic field while short term changes (10^1 – 10^2 yrs) are mainly due to solar activity. The biological carbon cycle is rapid from yearly to centennial while the long-term cycling of the geological carbon cycle, which includes fossil fuels, can take millions of years (Haig 1996; Willeit et al. 2014; Brown et al. 2018

Due to this variability, radiocarbon and calendar ages are not identical and therefore radiocarbon ages have to be converted to a calendar timescale via a calibration curve.

The internationally-accepted calibration curve (IntCal) is developed from precisely and independent dated materials such as dendrochronologically-dated tree rings for the period 0–12,400 cal BP, and from 12,400–26,000 cal BP the curve is derived from dated marine samples, such as foraminifera, and corals (Reimer et al. 2013). The deep sea has a much lower ^{14}C content than the atmosphere and therefore carbon material from the deep ocean has a smaller ^{14}C concentration than carbon from a terrestrial origin, resulting in ages that appear older. Organisms that live in the surface waters, such as corals and shells, have ^{14}C concentration that is intermediate between deep-ocean and terrestrial. Importantly there is also a difference between the Southern and Northern Hemispheres, with the south on average having lower ^{14}C concentration equivalent to some 40 ^{14}C years pre-AD 1900 (Godwin 1962; van der Plicht and Hogg 2006; Hua 2009). The IntCal series of calibration curves started in 1998 with updates based on new data from tree rings, varves and corals. To address the generally older ages in the south, there is also a Southern Hemisphere calibration curve (SHCal13; Hogg et al. 2013) which has been used here in combination with the IntCal curve and Bayesian modelling. Full details are given in sub-section 6.3.3.

6.1.1. Contamination

The Lynch's Crater sediments spanning the radiocarbon timescale are primarily peat but also contain some wood material. The following section summarises some of the possible sources of contamination of material and the pretreatment methods undertaken. Pretreatment methods used in previous studies from Lynch's Crater are given in Table 6.1. Before samples are processed for dating, contaminants need to be removed through pretreatment to provide the most accurate ages possible. For wood, charcoal and sediment samples, both physical and chemical means are employed to remove extraneous rootlets and surface sediment. Studies have found that there may be a significant variation in the radiocarbon content of the different fractions of peat, with contamination from humic acids playing a significant role (Piotrowska et al. 2011). In most cases, pre-treatment of samples minimizes contamination from these sources (Olsson 1986; Shore et al. 1995; Piotrowska et al. 2011).

Pre-treatment methods are particularly important for samples older than seven half-lives, containing 0.7–1% of the original radiocarbon carbon, equivalent to approximately 40,000 yrs BP (Bird et al. 1999; Turney et al. 2001c; Higham 2011). The conventional pre-treatment for contaminants is an acid-base-acid (ABA-SC) pre-treatment with the development of a wet oxidation, stepped-combustion (ABOX-SC) procedure recommended for dating “old” charcoal (Bird et al. 1999). These two pre-treatments have been used previously on Lynch’s Crater sediments and it was found that the ABOX-SC pre-treatment results were variable likely due to the scarcity of charcoal in the older sediments. Consequently, ABOX-SC pre-treatment may not be reliable in removing contaminants from lake and peat sediments (Turney et al. 2001c). Pre-treatments used on previous Lynch’s Crater records are provided in Table 6.1.

6.2. Dating of Lynch’s Crater

The previous studies at Lynch’s Crater have all provided ^{14}C dates and chronologies, with Table 6.1 providing summary information on these studies.

Table 6.1. A list of the previous studies from Lynch’s Crater with detail of the number of radiocarbon dates and source material.

Studies at Lynch’s Crater	Core Details (m)	Pre-treatment	Number of radiocarbon dates	Source material
Kershaw (1973, 1976)	0-20 Central area of crater		10 radiocarbon dates	Peat
Kershaw (1983a)	0-3 Central area of crater	Sieved > 700µm	7 radiocarbon dates	6 peat 1 wood
Bohte (1994), Bohte and Kershaw (1999)	0-3 Edge of crater		2AMS radiocarbon dates	Peat
Turney <i>et al.</i> (2001b, 2001c)	0-16 Central area of crater	Removal coarse plant material, sieved >500 µm ABA-SC 1 st batch ABOX-SC 2 nd batch	11 AMS radiocarbon dates 18 AMS radiocarbon dates	Peat Peat
Muller <i>et al.</i> (2006) Muller <i>et al.</i> (2008a, 2008b) Kylander <i>et al.</i> (2007)	0-7 Central area of crater 0-13 Central area of crater	Removal coarse plant material, sieved >250 µm ABA-SC (all samples)	15 AMS radiocarbon dates 28 AMS radiocarbon dates	Peat Peat

6.2.1. Lynch's Crater's original chronology

Kershaw's 1973 and 1976 chronology extended beyond the limit of radiocarbon dating and was based on 10 radiometric dated samples (Kershaw 1973). A subsequent sedimentary core was taken to focus on the sclerophyll and rainforest boundary within the Holocene given the ages obtained from the original core were considered to be anomalously young (Kershaw 1983a). There was no conclusive outcome as the ages produced from the peat sediment with this subsequent dating were both younger and older than the initial dates. The presence of well-preserved wood stumps, which were exposed by the peat mining operations, did provide an opportunity for relatively contaminant free material for dating. The wood sample used belonged to a species of *Flindersia* (Kershaw 1973, 1984) and although the actual depth of the wood sample could not be verified, it did provide evidence that rainforest in some form was present on the swamp by at least 7270 ± 80 years BP. Although there was no definitive conclusion regarding the validity of the ages of the young dates, several plausible scenarios were suggested related to the complex nature of the swamp and ongoing agricultural and mining activities. It was suggested that the presence of swamp forest could be the source of the contamination due to deep root penetration of the sediments (see Chapter 3 for more details). This problem has been found in swamp forests in Indonesia where root penetration can extend down to 20 m (Wust et al. 2008). It was also suggested that past agricultural activities and the more recent peat mining would have resulted in both a loss of sediment as well as sediment mixing (Kershaw 1983a).

6.3. Establishment of a combined sedimentary sequence

Before undertaking a comprehensive radiocarbon dating program, the sequential order of the cores used in this study was established (Figure 6.2). It was estimated that the Livingstone (LYE(LIV)) core, starting from 1 m depth, used in this study would extend to at least 45,000 years BP as the lowermost metre contained lake muds that had previously been dated by Kershaw (1976) and Turney et al. (2001b) to around this time. A D-section core 'LYA' taken approximately 10 metres distance from the drain provided the top 1.5 m of sediments but, as there was no obvious overlap with the start of the Livingstone LYE core, a short (2 m) Livingstone core, LY(3)Liv1, was taken (see Chapter 5 for more detail). The latter core overlapped with Livingstone LYE core 1–2 m as demonstrated by the LOI results (Figure 6.3). Further sampling down the LYE(LIV) cores encountered no significant problems. As a result, these three cores were spliced together

to provide a continuous sequence for this study with the D-section LYA comprising 0–150 cm, LY(3)LIV1 152–202 cm and LYE(LIV) comprising 204 cm–902 cm (Figure 6.3).

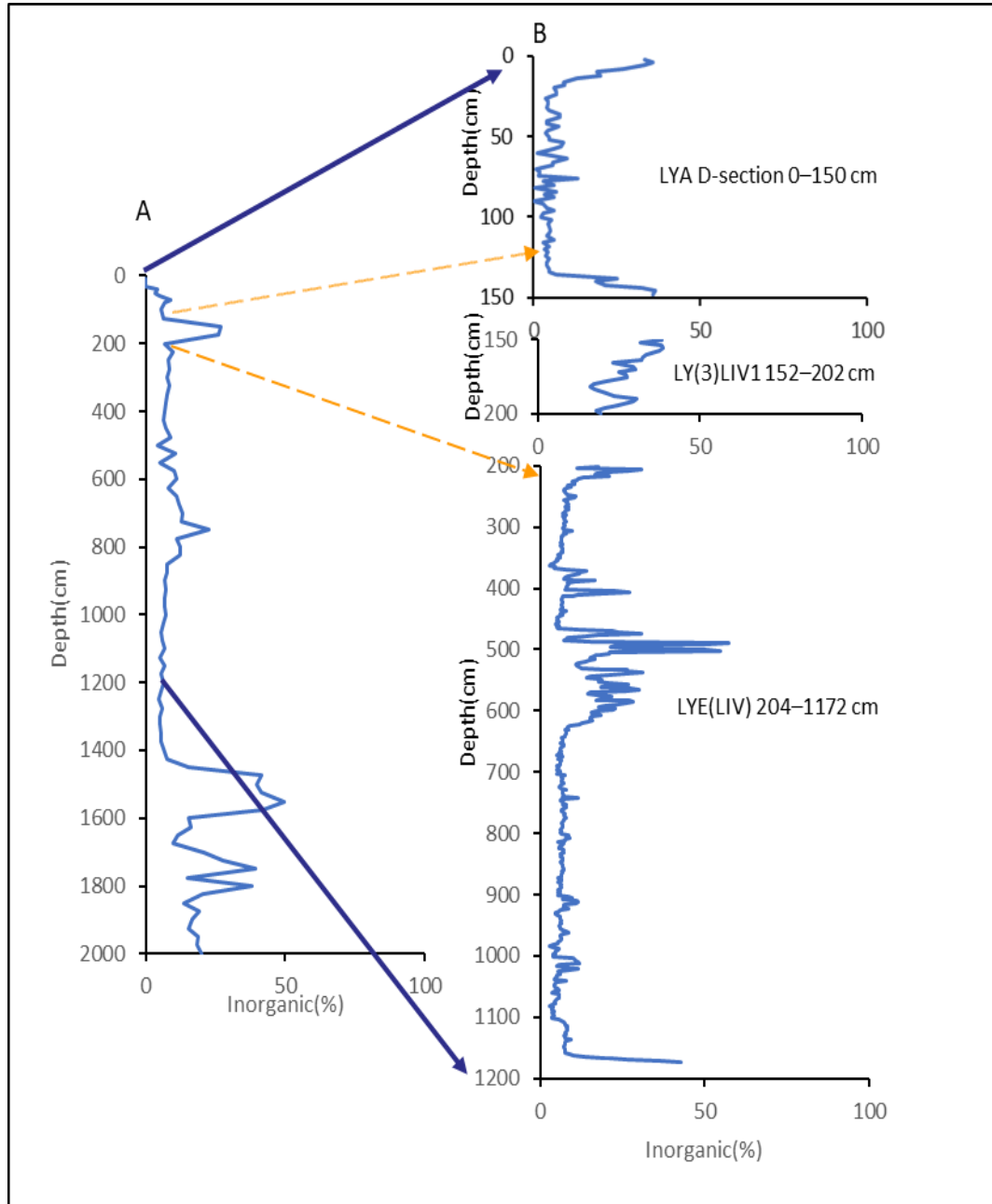


Figure 6.2. Comparison between A the originally-reported inorganic (%) values obtained from Lynch's Crater (Kershaw 1976, 1986) and B inorganic(%) from the D-section and Livingstone cores used in this study. The dark blue arrows indicate the same depth for A and B; and the dashed orange arrows indicate the corresponding top inorganic (%) section for A and B.

6.3.1. Radiocarbon dating of the core sequence

A total of 30 AMS ^{14}C dates, were funded by two ANSTO grants (AINSE Grant 05/166P and 06/180) in support of this work with most of the ages obtained on 3 cm³ from the same cores used for the palynological and macrofossil study. Unfortunately, the D-section core (LYA) did not have sufficient material available for dating and instead it was necessary to use material from another D-section core (LYB) taken adjacent to LYA. Samples were taken, as far as possible, evenly along the entire sequence but also taking into account significant changes in the LOI and pollen data, a strategy similar to that proposed by Bennett (1994). All samples were pretreated by Prof C Turney in the Department of Earth and Environmental Science the University of Wollongong, following the procedures outlined in Turney et al. (2001*a, b*). Samples were sieved through a 500 micron mesh to remove rootlets and other coarse plant fragments and then left overnight in HCl. The samples then had 2 treatments of 1M NaOH to remove humic acids before being placed in HCl for 1.5 hours. In between each step, samples were centrifuged and thoroughly washed in distilled water. The resulting fine-fractions were then sent to ANSTO for AMS ^{14}C dating. Results are given in Table 6.2.

The age-depth model shown in Figure 6.3, shows a relatively linear relationship but there are reversals and the ages at and below 776 cm have probably reached, or are beyond, the dating limit. There are relatively minor reversals within the top part of the core (6930 yrs BP at 66 cm and 6260 yrs BP at 78 cm) which may be due to soluble organic matter moving down the core profile (but see sub-section 6.2.1), a similar situation to that recorded in the original chronology of Kershaw (1976). The top 50 cm of the sequence is highly fibrous, primarily from sedge roots; the next 50 cm (0.5 to 1 m depth) grades into more decomposed material but remains relatively coarse which could influence the AMS dating through this section. There is also a large gap between the youngest ^{14}C date of 1520 yrs BP at 16 cm, and the next ^{14}C date of 6060 yrs BP at 48 cm. This could be explained by erosion or, more likely, peat wastage as suggested by the high inorganic values from 20 cm to the surface most likely resulted from a combination of the initial clearing and subsequent pasture improvement and drainage of the swamp for cattle grazing; a situation exacerbated by recent peat strip mining over part of the swamp surface (see sub-section 6.2.1 and Chapter 2 sub-section 2.6.4).

Table 6.2. Complete list of radiocarbon dates from the present study. The amended sample depth is the depth that is used in this study across all diagrams. ‘DS’ – denotes samples taken from D_Section core LYB; ‘LY3’ – refers to samples taken from LY(3)Liv1 core, and ‘LYE’ – samples taken from LYE(LIV) core (see section 6.3 for more details).

ANSTO code	Amended	Submitter ID	$\delta(^{13}\text{C})$ per mil	Percent Modern		Conventional ¹⁴ C age	
	Depth (cm)			Carbon			
				pMC	1 σ error	yrs BP	1 σ error
OZI171*	16 DS	Peat LC1a	-25.7	82.75	0.61	1520	60
OZI172*	48 DS	Peat LC2a	-27.8	47.03	0.40	6060	70
OZI173	66 DS	Peat LC3a	-28.7	42.23	0.32	6930	70
OZI174*	78 DS	Peat LC4a	-26.3	45.89	0.31	6260	60
OZJ222*	92 DS	Peat LC1b	-27.0	41.30	0.39	7100	80
OZI175*	116 DS	Peat LC5a	-27.1	33.23	0.29	8850	70
OZJ223*	136 DS	Peat LC2b	-26.1	32.18	0.34	9110	90
OZJ224	158 LY3	Peat LC3b	-27.6	15.19	0.22	15140	120
OZI176*	182 LY3	Peat LC6a	-27.4	19.11	0.24	13290	100
OZJ225	198 LY3	Peat LC4b	-25.8	37.49	0.42	7880	100
OZJ226	238 LYE	Peat LC5b	-26.5	22.95	0.29	11820	110
OZI177*	260 LYE	Peat LC7a	-27.7	12.85	0.20	16480	130
OZJ227*	286 LYE	Peat LC6b	-27.2	10.22	0.20	18320	160
OZI178	306 LYE	Peat LC8a	-27.3	13.85	0.21	15880	130
OZJ228*	328 LYE	Peat LC7b	-27.0	8.03	0.19	20260	190
OZI179	360 LYE	Peat LC9a	-28.4	8.02	0.15	20270	160
OZI180*	388 LYE	Peat LC10a	-26.9	5.42	0.16	23420	240
OZJ229*	414 LYE	Peat LC8b	-26.9	4.91	0.14	24210	240
OZJ230*	462 LYE	Peat LC9b	-27.2	4.33	0.11	25210	220
OZJ231*	510 LYE	Peat LC10b	-26.8	2.76	0.10	28840	290
OZJ232*	534 LYE	Peat LC11b	-26.5	2.41	0.11	29910	370
OZJ233*	574 LYE	Peat LC12b	-27.2	1.80	0.08	32260	370
OZJ234*	624 LYE	Peat LC13b	-26.2	1.42	0.09	34170	520
OZJ235*	648 LYE	Peat LC14b	-25.3	1.21	0.10	35430	660
OZJ236*	676 LYE	Peat LC15b	-26.0	0.96	0.08	37340	700
OZJ237*	720 LYE	Peat LC16b	-22.2	0.74	0.10	39400	1200
OZJ238*	776 LYE	Peat LC17b	-27.5	0.63	0.07	40710	880
OZJ239*	792 LYE	Peat LC18b	-26.8	0.60	0.10	41100	1600
OZJ240*	822 LYE	Peat LC19b	-27.1	0.59	0.11	41300	1800
OZJ241	862 LYE	Peat LC20b	-27.4	0.58	0.07	41300	1100

The most significant reversal in radiocarbon ages is observed between 157 and 238 cm. The three dates contributing to this reversal were from the 2 m Livingstone core, LY(3)Liv1 (see section 6.3 for details and Fig 6.2): the oldest age was obtained at 158 cm

(15,140±120 yrs BP) with the youngest age (7880±100 yrs BP) at 198 cm, and the intermediate age (13,290±100 yrs BP) at 182 cm. The sediment from this core was finely decomposed peat with only isolated extraneous root or rootlet fragments present.

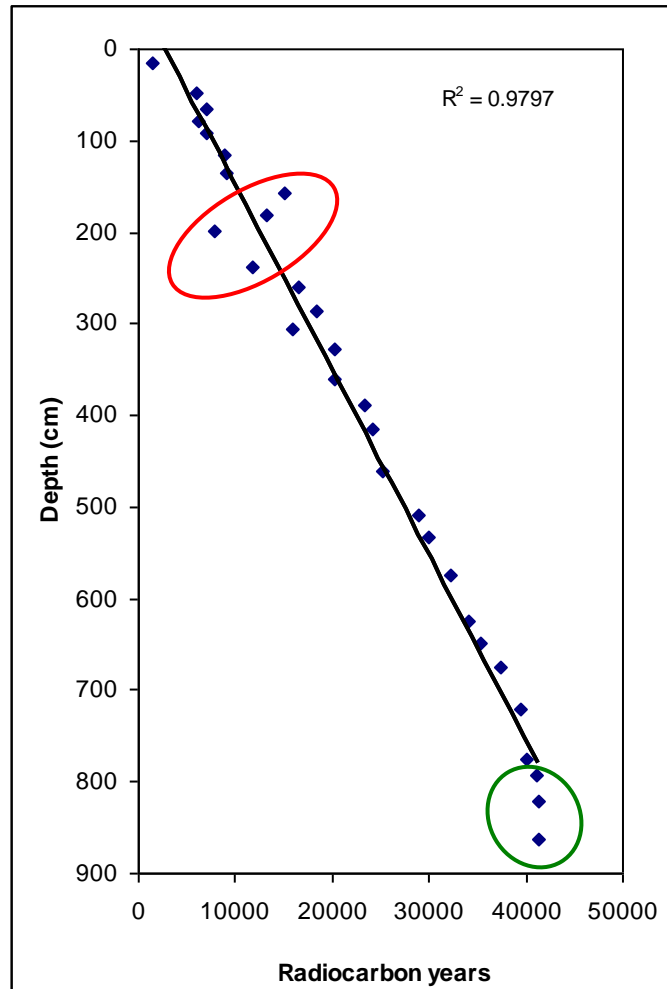


Figure 6.3. Age-depth plot with radiocarbon dates obtained from Lynch’s Crater (Table 6.2). Red circle indicates the dates taken from core LY(3)Liv1 which were reversed: The green circle indicate those ages below 776 cm that appear to have reached the radiocarbon dating limit.

The cause of this age reversal is not immediately apparent. There is the possibility that human error was the cause, either from incorrect labeling in the field due to the inclement weather or in the laboratory when processing samples for AMS ^{14}C dating. However, the high inorganic values through this section could suggest that erosional and/or flooding events were responsible. The latter scenario would suggest that conditions of deposition through this period are highly variable. Although previously reported radiocarbon dates from Lynch’s Crater have not been obtained from the highly inorganic sediments, there

are a number of radiocarbon dates from other sections that can be utilized. The details of these other ages are provided in the following sub-section.

6.3.2. Comparison of Lynch's Crater core chronologies

The development of a chronological model for Lynch's Crater was undertaken over two stages of data selection. Ages were initially selected from the present study on the basis of details given in the above section. The basal two ages (see Table 6.2) were not included as it is likely that a radiocarbon background was reached. Even though the uppermost age (1520 yrs BP) at 16 cm may have been affected by artificial drainage for pasture grazing and peat mining, it was included in the model as were reversals found through the remainder of this sequence.

The second stage of developing a chronological model for Lynch's Crater involved an assessment of previously reported radiocarbon dates in order to assess whether it might be possible to incorporate some of these into a grand chronological scheme for the late Pleistocene and Holocene part of the sequence. A common feature of these studies was the similarity in the LOI pattern within the sediments (Figure 6.4), particularly the peaks in inorganic matter (low LOI and carbon content values) that have been suggested to relate to globally-significant and independently dated Heinrich events (Muller et al. 2008*b*). The ages obtained from previous studies relating to the inorganic peak identified in this study at 140–206 cm are particularly valuable inclusions as they relate to depths of substantial age variability in the present study (see Table 6.2 and Figure 6.3). The ^{14}C date WK-266 4550 ± 60 yrs BP from the chronology of Kershaw (1983*a*) was included as it was located just below extremely high charcoal (micro) values which were also present in the record of Turney et al. (2001*b*) as well as the present core. Figure 6.4 shows the locations and degree of confidence in correlation points between the sequences where dates could be utilised and Figure 6.5 shows the age-depth relationship of these ^{14}C dates; the calibration is described below. However, as it was likely that sedimentation varied across the different cores (Figure 6.4), initially a calibration model was run utilizing just the ^{14}C dates obtained from the present study (Table 6.2).

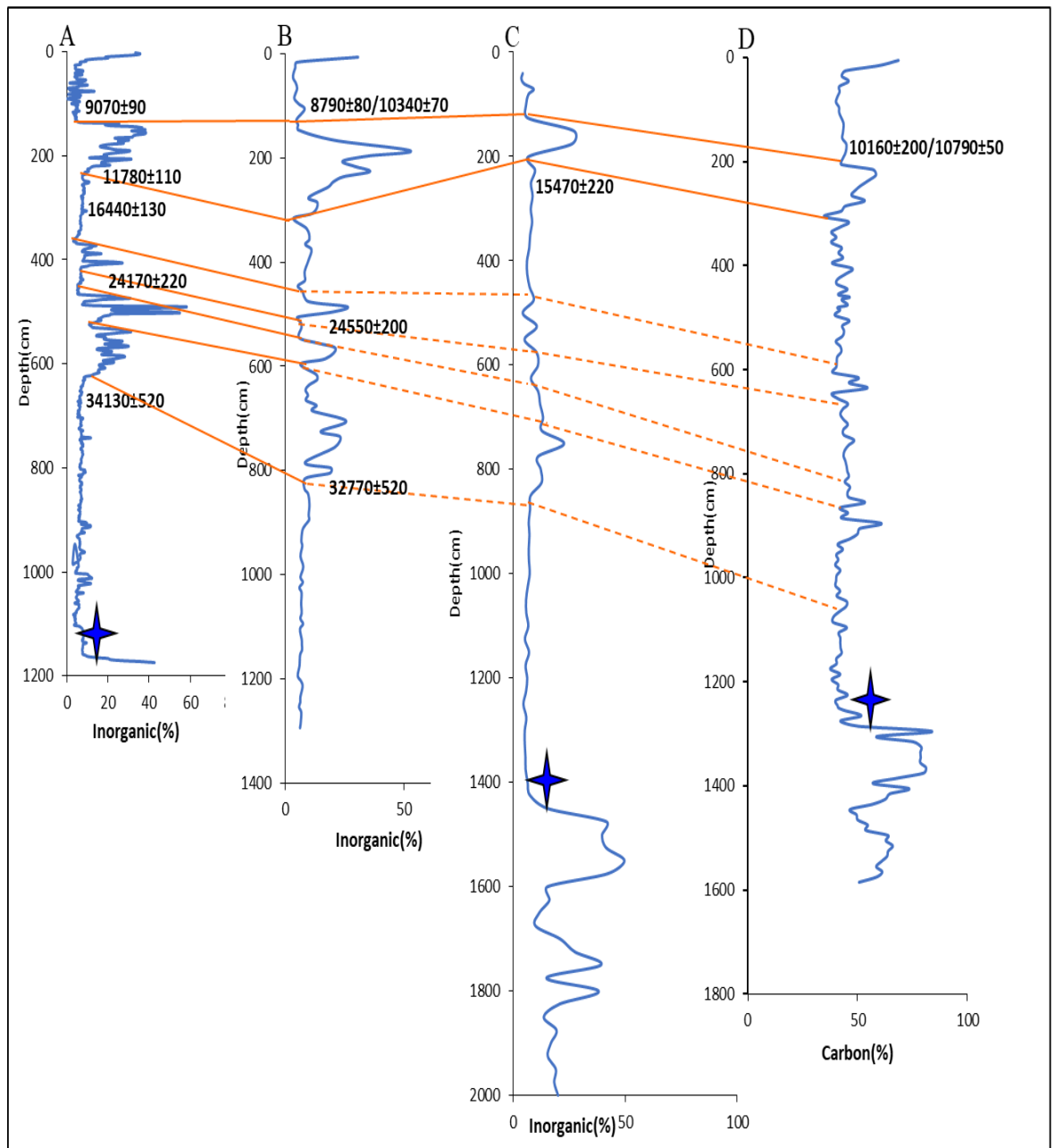


Figure 6.4. Correlation of LOI values (A to C) and (D) carbon content (%) across cores taken from Lynch's Crater. A-present study; B-Muller et al. (2006, 2008a,b,); C-Kershaw (1973, 1976); D-Turney et al. (2001b). Solid orange lines indicates what are considered to be confident points of correlation between the cores; the dashed orange lines indicate a relatively good fit. AMS ^{14}C dates before and after high inorganic phases are shown with full details in Table 6.3. Blue Star marks the transition from lake to peat sediments. Sequence B did have the transition from lake to peat sediment at approximately 13 m but LOI data were not available

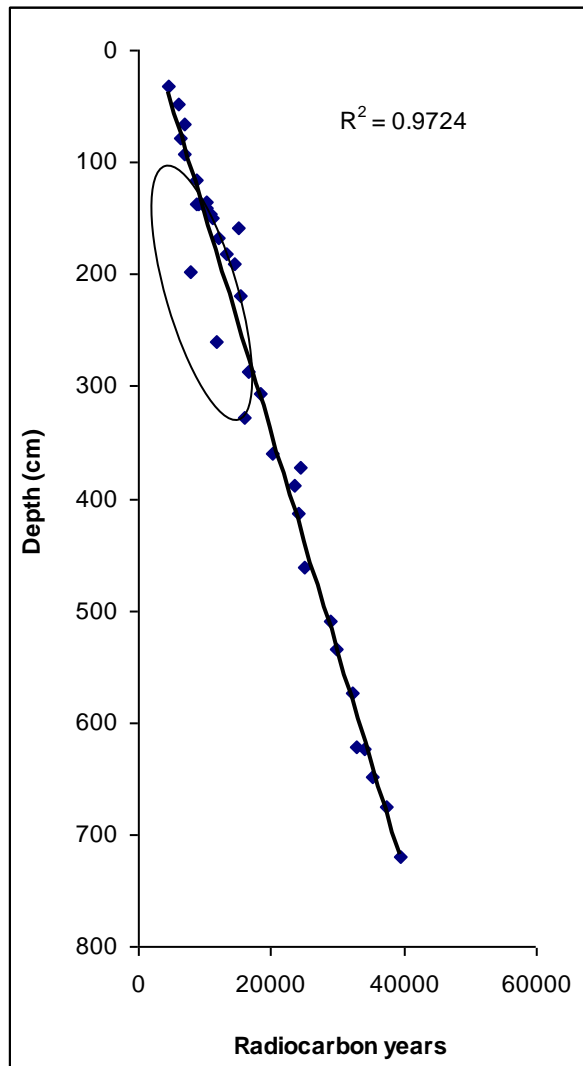


Figure 6.5. Age-depth plot of combined radiocarbon dates prior to calibration and modelling, circled area are ages from 158–198 cm from the present study included in the age model.

6.3.3. Overview of the Bayesian Model

To produce a reliable chronology, Bayesian modelling of the ages was undertaken. The mathematical basis for Bayesian analysis is Bayes' Theorem which ultimately aims to find a representative set of possible ages for each depth point in a sedimentary sequence. Initially Markov Chain Monte Carlo (MCMC) sampling provides a distribution of possible solutions. Bayes' theorem then supplies a number of possible solutions with a probability which is a product of the *prior* and *likelihood* probabilities. Relative age information can be very precise, such as for annually laminated ice cores or can be obtained from assumptions about the deposition rate of the sediment, and within the Bayesian framework is referred to as *prior*

(Bronk Ramsey 2003). While absolute age information can be sourced from historical documents, in most cases it is derived from scientific dating methods and within the Bayesian framework is referred to as *likelihood*. The *posterior* probability densities are the resulting distributions which include both the deposition model and the actual radiocarbon ages (Bronk Ramsey 2003, 2009).

There are different modes of deposition and in some cases actual deposition rates are known for example, from varved lake sediments and ice cores for which there is an independent timescale. In these cases a defined deposition rate, *D_Sequence* (Table 6.3), can be applied in the model (Bronk Ramsey 2008). Here, the deposition rate is unknown so it was necessary to use a *P_Sequence* model (details below).

Table 6.3. Depositional models that can be used for Bayesian modelling (after Bronk Ramsey 2008).

OxCal key word	Description
<i>D_Sequence</i>	Age gap between points known (e.g. tree-rings, varved sediments, ice layers)
<i>V_Sequence</i>	Age gaps between points known approximately with normally distributed uncertainty
<i>U_Sequence</i>	Deposition assumed to be a function of another parameter <i>z</i> (usually depth)
<i>P_Sequence</i>	Deposition assumed to be random giving approximate proportionality to <i>z</i> (usually depth): more flexible than <i>U_Sequence</i> but less than <i>Sequence</i>
<i>Sequence</i>	Ages of specified events assumed to be in correct order but no use made of depth information.

6.3.4. Establishment of a chronology

Two calibrated age models were produced in this study using SHCal13 (Hogg et al. 2013). The first calibrated age model relied solely on the ¹⁴C dates from the present study (M1 - Table 6.2). The second calibrated age model comprised new and previously reported ¹⁴C dates for the combined model (M2, see Table 6.4). All ages were calibrated using SHCal13. The *P_Sequence* and the *k* parameter with an increment size *k* = 0.2 cm, was used as this is the suggested deposition unit for peat growth (Bronk Ramsey 2008; Bronk Ramsey and Lee 2013) and outlier (general) analysis with a probability of (0.05) was also incorporated into the model (Bronk Ramsey 2009). In both (M1) and (M2) ages that had a very small overlap with the likelihood probability distribution returned an agreement index of <60% and were discarded (see Table 6.4 and 6.5). There was a discrepancy between the two models

especially when reviewing the interpolation results with M1 being relatively younger (~4000 yrs) than M2. Figures 6.6 (M1) and Figure 6.7 (M2) show the Bayesian modelled ages plotted against depth.

Table 6.4. List of ages selected from Lynch's Crater cores for combined chronological model (M2) construction prior to calibration. All ages are from the present study except B-Muller et al. (2008*a, b*), C-Kershaw (1973, 1976) and D-Turney et al. (2001*b, c*). List of ages in M2 that returned an agreement index of <60% and were discarded (red).

Depth(cm)	¹⁴ C Lab code	¹⁴ C age	¹⁴ C error
16	OZI171	1520	60
32	WK266	4550 ^C	60
48	OZI172	6020	70
66	OZI173	6890	70
78	OZI174	6220	60
92	OZJ222	7060	80
116	OZI175	8810	70
136	OZJ223	9070	90
138	OZH074	8790 ^B	80
140	OZI164	10340 ^B	70
150	OZI463	11180 ^B	90
168	OZG095	12140 ^D	70
182	OZI176	13250	100
190	OZG094	14520 ^D	70
198	OZJ225	7840	100
220	ANU961	15470 ^C	210
238	OZJ226	11780	110
260	OZI177	16440	130
286	OZJ227	18280	160
306	OZI178	15840	130
328	OZJ228	20220	190
360	OZI179	20230	160
388	OZI180	23380	240
414	OZJ229	24170	240
462	OZJ230	25170	220
510	OZJ231	28800	290
534	OZJ232	29870	370
574	OZJ233	32220	370
622	OZH591	32770 ^B	520
624	OZJ234	34130	520
648	OZJ235	35390	660
676	OZJ236	37300	700
720	OZJ237	39360	1200
792	OZJ239	41100	1600

Table 6.5. List of ages M1 that returned an agreement index of <60% and were discarded

Depth(cm)	¹⁴ C Lab code	¹⁴ C age	Sigma
78	OZI174	6260	60
158	OZJ224	15140	120
198	OZJ225	7880	100
238	OZJ226	11820	110
306	OZI178	15880	130
720	OZJ237	39400	1200
776	OZJ238	40710	880
792	OZJ239	41100	1600

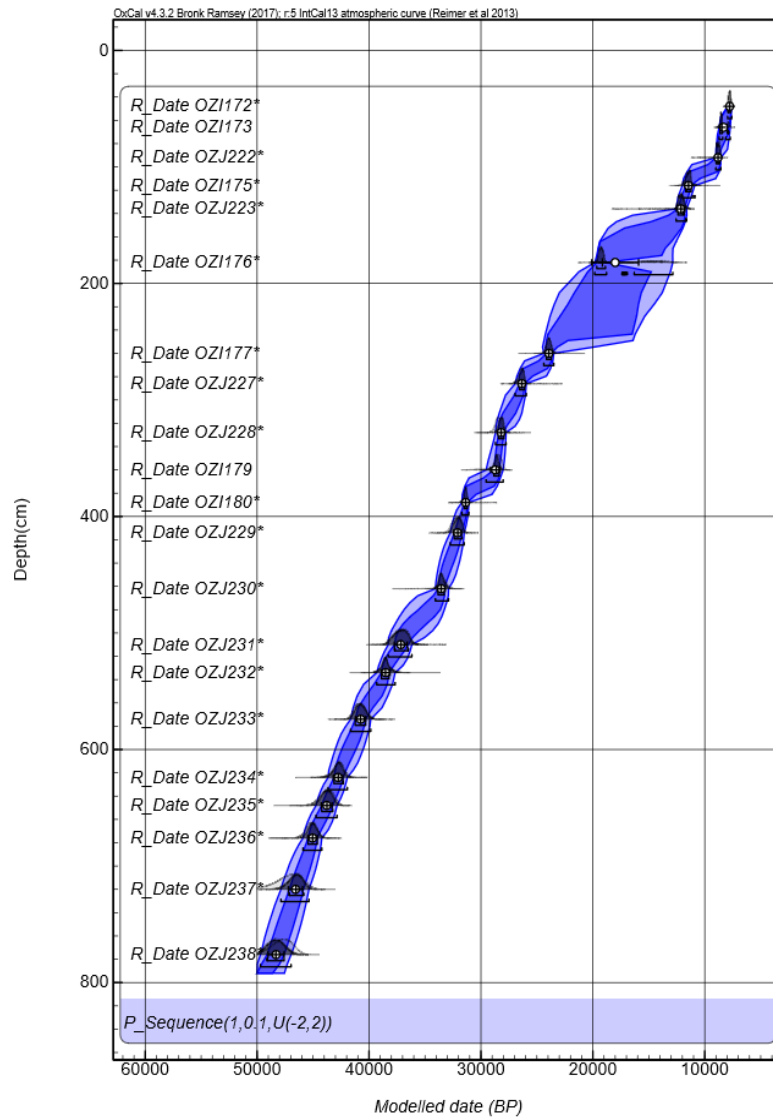


Figure 6.6. Bayesian modelled age-depth plot (M1) with the radiocarbon date number to the left; the radiocarbon date can be found in Table 6.2. Ages were calibrated using SHCal13 (Hogg et al. 2013). Bayesian model utilised using the deposition model P-Sequence with a k parameter of 0.2 cm (Oxcal 4.3).

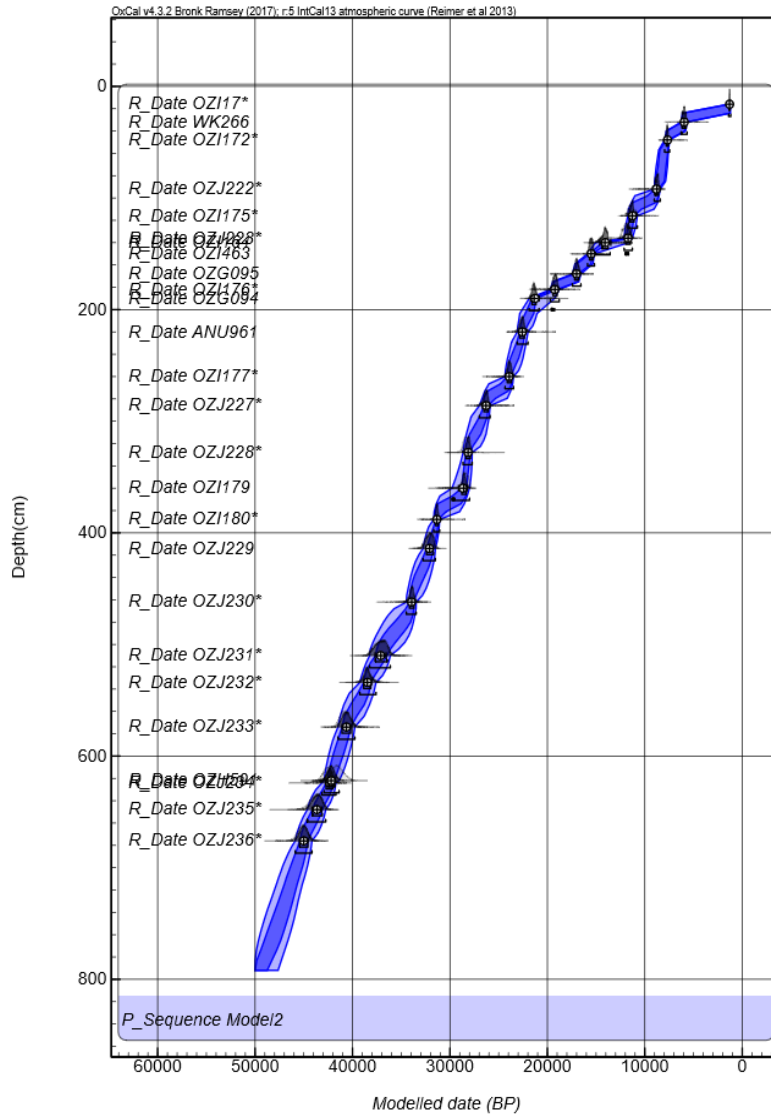


Figure 6.7. Bayesian modelled age-depth plot (M2) with the radiocarbon date number to the left; the radiocarbon date can be found in Table 6.5. Ages were calibrated using SHCal13 (Hogg et al. 2013). Bayesian model utilised using the deposition model P-Sequence with a k parameter of 0.2 cm (Oxcal 4.3).

M2 (Figure 6.7) provides good control through to 20 ka which is lacking in M1 (Figure 6.6) although, as suggested earlier, there was a possibility of human error from either incorrect labeling or processing of samples through 20–3 ka, sub-section 6.3.1. which may have impacted on the modelled results. It was decided because of the uncertainty of ages through the period (0-20 ka) and the difference in sedimentation rate across the cores used for M2, the chronology in Rule et al. (2012) would be utilized (M3). The dates used for this chronology also utilized previous dates from Lynch’s Crater (Table 6.6).

Table 6.6. List of ages selected from Lynch's Crater cores for chronological model construction (M3) used in this study prior to calibration. All ages are from the present study except B-Muller et al. (2008a, b), C-Kershaw (1973, 1976) and D-Turney et al. (2001b, c). List of ages from model used in this study that returned an agreement index of <60% and were discarded (red)

Depth(cm)	¹⁴ C Lab code	¹⁴ C age	¹⁴ C error
16	OZI171	1520	60
32	WK266	4550 ^C	60
48	OZI172	6020	70
66	OZI173	6890	70
78	OZI174	6220	60
92	OZJ222	7060	80
116	OZI175	8810	70
136	ANU11524	10160 ^D	200
136	OZJ223	9070	90
138	OZH074	8790 ^B	80
140	OZI164	10340 ^B	70
146	OZG096	12842 ^D	50
150	OZI463	11180 ^B	90
158	OZJ224	18495	120
168	OZG095	12140 ^D	70
182	OZI176	13250	100
190	OZG094	14520 ^D	70
198	OZJ225	7840	100
220	ANU961	15470 ^C	210
238	OZJ226	11780	110
260	OZI177	16440	130
286	OZJ227	18280	160
306	OZI178	15840	130
328	OZJ228	20220	190
360	OZI179	20230	160
372	OZH603	28626	200
388	OZI180	27643	240
414	OZJ229	24170	240
462	OZJ230	25170	220
510	OZJ231	28800	290
534	OZJ232	29870	370
574	OZJ233	32220	370
622	OZH591	32770 ^B	520
624	OZJ234	34130	520
648	OZJ235	35390	660
676	OZJ236	37300	700
720	OZJ237	39360	1200
792	OZJ239	41100	1600

The methods and model (M3) used for Rule et al. (2012) were the same as M1 and M2 except the earlier version SHCal04 (McCormac et al. 2004) and IntCal04 (Reimer et al. 2004) were used for calibration. The age that had a very small overlap with the likelihood probability distribution returned an agreement index of <60% and was discarded (see Table 6.6) and Figure 6.8 shows the Bayesian modelled ages plotted against depth. All models suggest a fairly constant rate of sedimentation over the long-term and interpolation of the ages in OxCal allowed influx to be calculated on the pollen and charcoal concentration data. The average sediment accumulation rate was approximately 120 years per sample (across 2 cm).

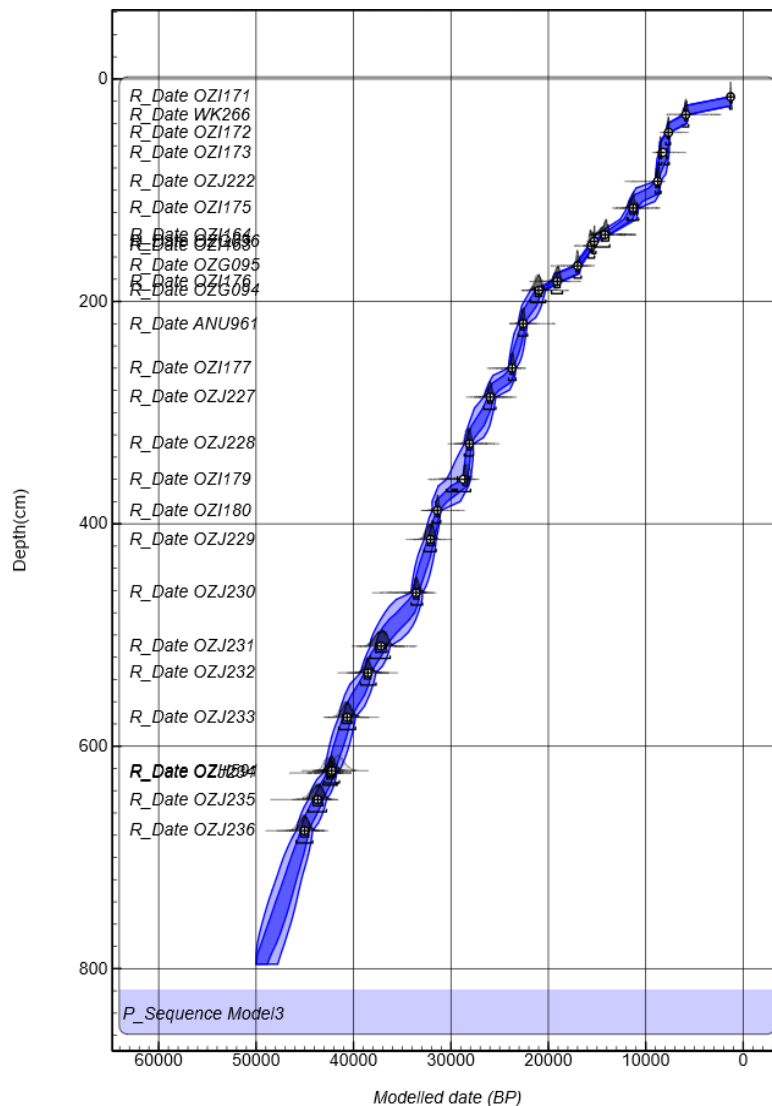


Figure 6.8. Bayesian modelled age-depth plot with the radiocarbon date number to the left; the radiocarbon date can be found in Table 6.8. Ages were initially calibrated using SHCal04 and IntCal04 and against the Cariaco Basin comparison curve in OxCal v4.2 (McCormac et al. 2004; Reimer et al. 2004). Bayes theorem was utilised using the deposition model P-Sequence with a k parameter of 0.2 cm (Oxcal 4.2).

However, it is important to note, that in the upper 200 cm, and particularly between 100 and 200 cm, there is a significantly greater variability than in the rest of the sequence. This does suggest that, although the Bayesian model allows for a more precise outcome statistically, it still relies on the accuracy of the radiocarbon dates and the implied deposition rate and suggests caution when interpreting across critical climate events especially those that are abrupt.

Chapter 7

Palaeoenvironmental Results

This chapter incorporates all palaeoenvironmental results. Sediment description and results of moisture loss (ML) and loss on ignition (LOI) are first presented. These are followed by the percentage results for the swamp/aquatic pollen sum (including the macrofossil results) and the dryland pollen sum. The results of the macroscopic charcoal (macrocharcoal) and the microscopic charcoal (microcharcoal) are then presented followed by results for influx data and its relationships to percentage data. Non-quantified observations not previously presented, such as pollen clumping, pollen target count outcome, degree of oxidation and the presence of degraded grains, are then given in a summarized form.

7.1. Sediment Description

The 9 metres sampled from the 10.72 m Livingstone E core LYE (LIV), Figure 7.1, D-Sections LYA 0-150 cm, and LY (3) Liv (1) core, consist largely of peat sediment with variations in colour from brown, through dark brown to black. Table 7.1. provides a general sediment description of the 9 m sequence. Photos taken in the field (Figure 7.1) are the primary source for the darkness element in the sediment description as all sediment had oxidized once opened in laboratory conditions, although photos were not available for the D-Sections and LY(3)Liv(1) cores. The lithology column, moisture loss, loss on ignition, magnetic susceptibility (low and high frequency) and sedimentation rate are shown alongside the depth and the Bayesian modelled chronology, in Figure 7.3. The lithology patterns used are Troels-Smith vector patterns provided in TGView (Grimm 2004).



Figure 7.1. Field photos for LYE(LIV) cores 1-8 m (amended depth 2.02–9.02 m); red circled area indicates primarily organosilicate layer at 380 cm (amended depth 482 cm), (see Table 7.1 and Chapter 6 for more detail).

Table 7.1. General sediment description

Depth (cm)	Sediment Description
0–50 cm	Brown partially decomposed (primarily) <i>Turfa herbacea</i>, with <i>Substantia humosa</i> and small amounts of <i>Detritus lignosus</i> and <i>Detritus herbosus</i> with sedge and graminoid material in growing position; woody fragments and charred wood, sedge and fern stem present.
50–150 cm	Dark brown partially decomposed (primarily) <i>Detritus herbosus</i>, with <i>Turfa herbacea</i> and small amounts of <i>Substantia humosa</i> with fragments > 2 cm present. Charred herbaceous and woody fragments up to 1 cm also present.
150–204 cm	Dark brown decomposed (primarily) <i>Detritus herbosus</i> followed by <i>Substantia humosa</i> with small amounts of <i>Detritus granosus</i>.
204–402 cm	Dark brown to black <i>Substantia humosa</i> then <i>Detritus herbosus</i> and small amounts of <i>Detritus granosus</i> with charred fragments of peat, herbaceous material and woody fragments up to 0.5 cm.
402–481 cm	Dark brown to black (primarily) <i>Substantia humosa</i> and <i>Detritus lignosus</i> and small amounts of <i>Detritus granosus</i> and <i>Detritus herbosus</i>.
481–482 cm	Grey and brown material <i>Limnus siliceous</i> with a small amount of <i>Substantia humos</i>, very gritty texture with white siliceous material visible.
482–602 cm	Black decomposed <i>Substantia humosa</i> with small amounts of <i>Detritus lignosus</i> and <i>Detritus granosus</i> with charred peat, herbaceous and woody fragments near the top.
602–902 cm	Dark brown to black decomposed <i>Substantia humosa</i> with small amounts of <i>Detritus lignosus</i> and <i>Detritus granosus</i> and with woody fragments up to 5 cm.

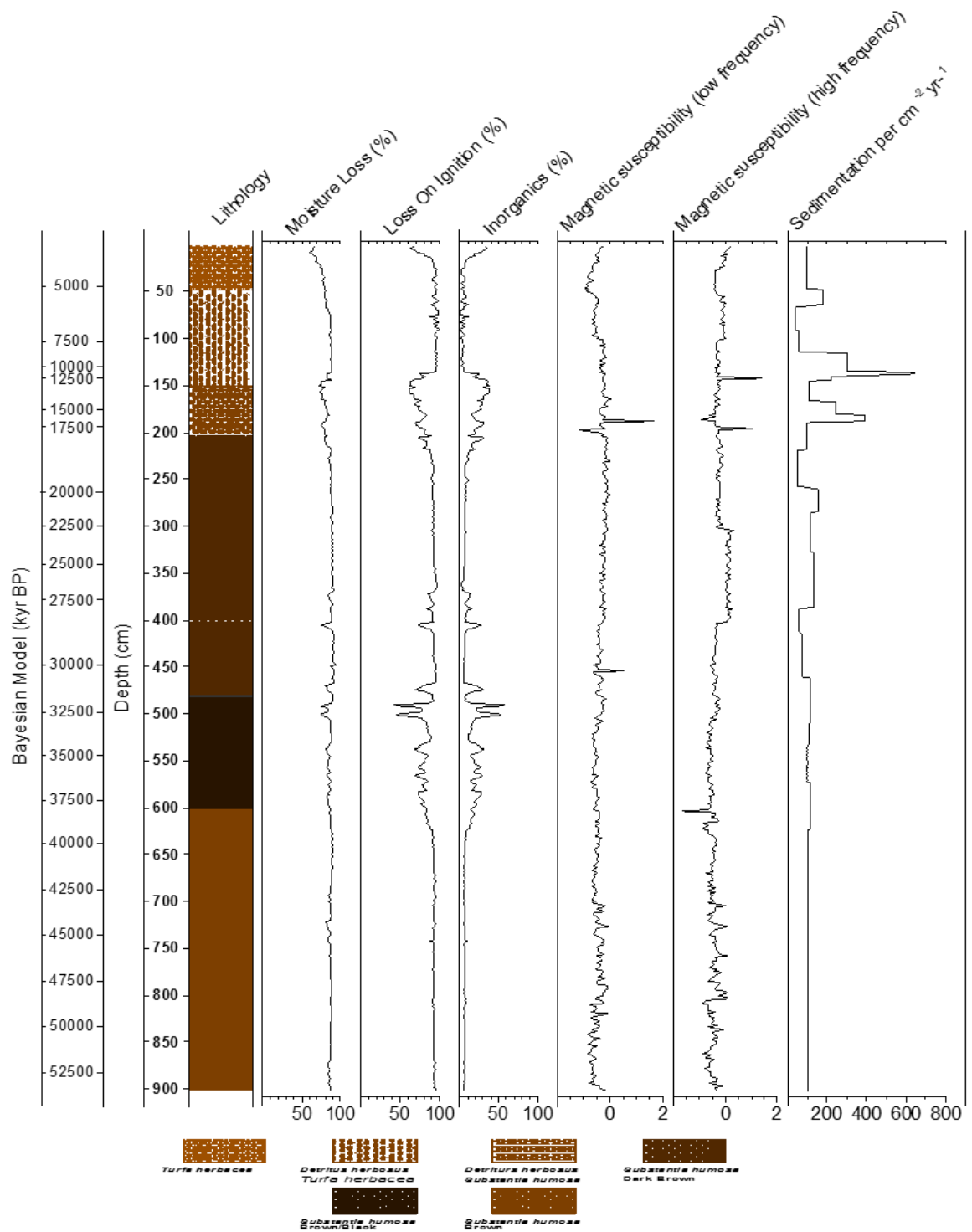


Figure 7.2. Lithology, Moisture loss (ML) and Loss on Ignition (LOI), Magnetic Susceptibility (low and high frequency) and Sedimentation rate per $2 \text{ cm}^2 \text{yr}^{-1}$ for the 9.02 m record from Lynch's Crater.

7.2. Palynological and macrofossil results

Following Kershaw (1976, 1984) separate pollen sums were adopted for the dryland and swamp and aquatic pollen taxa. However, Kershaw (1994), Bohte (1994) and Bohte and Kershaw (1999), found that certain taxa considered to be predominantly dryland were present on the swamp surface, at least at times. Several of these taxa, *Leptospermum*, and Myrtaceae type 1 and 2, whose erratic but temporally limited representation suggests strongly that they grew on the swamp surface and have been included on the swamp and aquatic pollen diagrams though excluded from that sum. Poaceae, considered to be a major component of both dry land and swamp vegetation is included on both diagrams but excluded from both sums. Appendix B (1) Table 1 provides some ecological information on taxa represented in the pollen fossil spectra of this study, informed by Kershaw (1976, 1983a; Stephens and Dowling 2002; Cooper and Cooper 2004; Hyland et al. 2010). The refined chronology (see Chapter 6) presented the opportunity for companion influx diagrams for all taxa. Influx dryland diagrams have been zoned according to their respective pollen sum (%) diagrams as have the influx aquatic and swamp diagrams. The chronology is included in all diagrams and the moisture loss (ML) and inorganic content (IN) curves are included in the summary diagrams, percentage and influx, for the dryland taxa and for both the aquatic and swamp diagrams, percentage and influx, and macrofossil diagram.

The full diagrams (Figures 7.3–7.4) for the percentage and influx of the swamp and aquatic taxa include all taxa that were included in the aquatic and swamp pollen sum, as well as microcharcoal and macrocharcoal, presence and absence data and observational data related to the local environment, Poaceae, *Leptospermum* and the two (swamp) Myrtaceae. Exaggeration (x5) has been included for Poaceae to highlight the extent of variation in places; *Botryococcus* and charcoals (micro- and macrocharcoal) have been truncated with high values shown at the end of each graph. A summary diagram of the macrofossils alongside the macrocharcoal total and individual types is given in Figure 7.5 and the macrofossil results are provided in the aquatic and swamp pollen percentage results (sub-section 7.2.1) while all influx results (aquatic and swamp and dryland) are found in sub-section 7.2.4.

Dryland percentage and influx summary diagrams are given in Figure 7.6 and Figure 7.12 respectively which also include all rainforest gymnosperms, while Figures 7.7–7.11 provide detail of all other dryland taxa percentages, including rainforest angiosperms, grouped according to most likely synusiae, canopy, secondary and vine, and understorey (Figures 7.7–7.9), sclerophyll taxa, Poaceae, dryland herbs and shrubs (Figure 7.10) and pteridophytes (Figure 7.11). Influx diagrams follow the percentage diagram lay-out; rainforest canopy, secondary, vine and understorey (Figures 7.13–7.15), sclerophyll taxa, Poaceae, dryland herbs and shrubs (Figure 7.16), and pteridophytes (Figure 7.17). The full results for microcharcoal and macrocharcoal concentration and influx, are given in Figure 7.18. Although *Syzygium* is not included in the dryland pollen sum, it is included in the rainforest angiosperm canopy section for both percentage and influx results as its percentage curves suggest a close affinity to this element. Although Poaceae has been included in the aquatic and swamp diagram it will also be included in dryland discussion because of the likely input from dryland grasses.

7.2.1. Zonation of Lynch's Crater Aquatic and Swamp Pollen Sum Taxa (LCA)

Zone LCA-F. Depth 902–628 cm (samples 451–314) c. 54,390–39,360 yrs B.P.

This zone is characterized by consistently high values for loss on ignition (> 90%) and moisture loss (>80%). Wet smears taken before pollen preparation indicated the occasional presence of intact diatoms, *Pinularia* sp., near the base of the zone. *Pinularia* sp. can be found in freshwater, moist sediments and peat (Sonneman et al. 1999; Taffs et al. 2012). The sediment consists of highly humified brown peat with some woody fragments (Plate 7.1a), especially near the base. Cyperaceae was separated into generic groupings based on the pollen morphology. Some additional perspective and refinement is provided by the macrofossils. *Schoenoplectus* and *Carex* are the dominant pollen taxa on the swamp while there are high although variable nut counts of *Carex appressa* and *Carex fascicularis* (Figures 7.3 and 7.5 and Plate 7.1c) while *Eleocharis* and *Cyperus* have low but consistent pollen representation through this zone without macrofossil representation.

Haloragis and *Gonocarpus*, *Stylidium* and *Hydrocotyle* have their highest values through this zone especially when Cyperaceae values are low, and local presence is also indicated for

Gonocarpus (*Gonocarpus chinensis* subsp. *verrucosus*) and *Hydrocotyle* by seed and mericarp presence (Plate 7.1 b and d). Other notable features are the high values (up to 46% of the pollen sum) for the swamp fern *Cyclosorus* (Thelypteridaceae) through the middle of this zone and high values (up to 50% of the pollen sum) for the hornwort, *Anthoceros*, towards the top of this zone. Other aquatic taxa present in descending order of abundance are *Oenanthe*, Brassicaceae, *Typha*, *Myriophyllum*, *Persicaria* and *Eriocaulon* with the occasional presence of *Potamogeton* (pollen and *P. tricarinatus* carpel), *Utricularia*, *Nymphoides* (pollen and *N. indica* seed), *Geraniaceae* and *Ranunculus*.



Plate 7.1. Macrofossils present in zone LCA-F. (a)-woody fragment, (b)-*Gonocarpus* cf. *chinensis* subsp. *verrucosus*, (c)-*Carex* cf. *appressa* (d)-Mericarps of *Hydrocotyle*, (e) –cf. *Passiflora* type seed, (f)-inner seed linings.

Poaceae values through the zone are comparable to those Cyperaceae. The woody taxa, *Leptospermum* and swamp Myrtaceae 2 have their only effective representation of the diagram in this zone with both taxa displaying a large spike followed by a smaller one near the base of the zone and then *Leptospermum* alone continues with relatively consistent representation into the upper part of the zone. Swamp Myrtaceae 1 has a single large spike near the middle of the zone with values of up to 900% of the aquatic/swamp sum but it is absent from the rest of the diagram. Considering the paucity of *Leptospermum* species regionally and the likely cooler conditions than today within this ‘glacial’ period, the most likely candidate for *Leptospermum* is *L. wooroonooran* a long-lived species in the present-day restricted to mountain rainforest above 1200 m although the variability in the pollen identified as *Leptospermum* could also suggest a taxon which is now extinct.

The fungal spore, *Gelasinospora* has a sporadic presence mainly near the base and top of the zone, while the algal spore, *Botryococcus*, has values of 1% or less through this zone. There are also a number of unknown seeds in this zone, including *Passiflora* type seed (Plate 7.1e) and a high number of intact inner seed linings (Plate 7.1f) but further taxonomic identification for these components is not possible as they have no distinctive features to align them with any of the reference seeds and nuts.

Zone LCA-E. Depth 628–404 cm (samples 314–202) c. 39,360–28,540 yrs B.P.

This zone is characterized by relatively high, fluctuating inorganic values (20-60%) and moisture loss. Broken and dissolved sponge spicules and diatoms are present at the base and in the middle of the zone and correspond to the high inorganic values especially at 481–482 cm where there is an organosilicate band (Figure 7.1 and Plate 7.2a). Intact diatoms are present and are, as previously recorded, *Pinularia* sp. Charred peat is evident at the base and in the middle of this zone as are woody charcoal fragments up to one1 cm in length. At the base and towards the top of this zone brown humidified peat predominates with darker brown/black peat present through the middle of this zone (Figure 7.1). Although the high but fluctuating inorganic values and high Cyperaceae values characterize this zone, there are distinct changes within the swamp community which justify dividing this zone into two subzones.

Subzone LCA-E2. Depth 626–494 cm (samples 313–247) c. 39,260–32,290 yrs B.P.

Schoenoplectus and *Carex* dominates this subzone although macrofossil presence is limited to the base and middle of this subzone for *C. appressa* and *C. fascicularis*; *Eleocharis* and *Cyperus* values have increased while *Baumea* (formerly *Machaerina*) is consistently present through this subzone. Cyperaceae (other) has substantially higher values through to the middle and then is absent from the rest of the diagram. Cyperaceae (other) was separated from *Schoenoplectus* and *Carex* due to its large size and thick exine but it is possible that it is just a large pollen grain variant of *Schoenoplectus* or *Carex*.

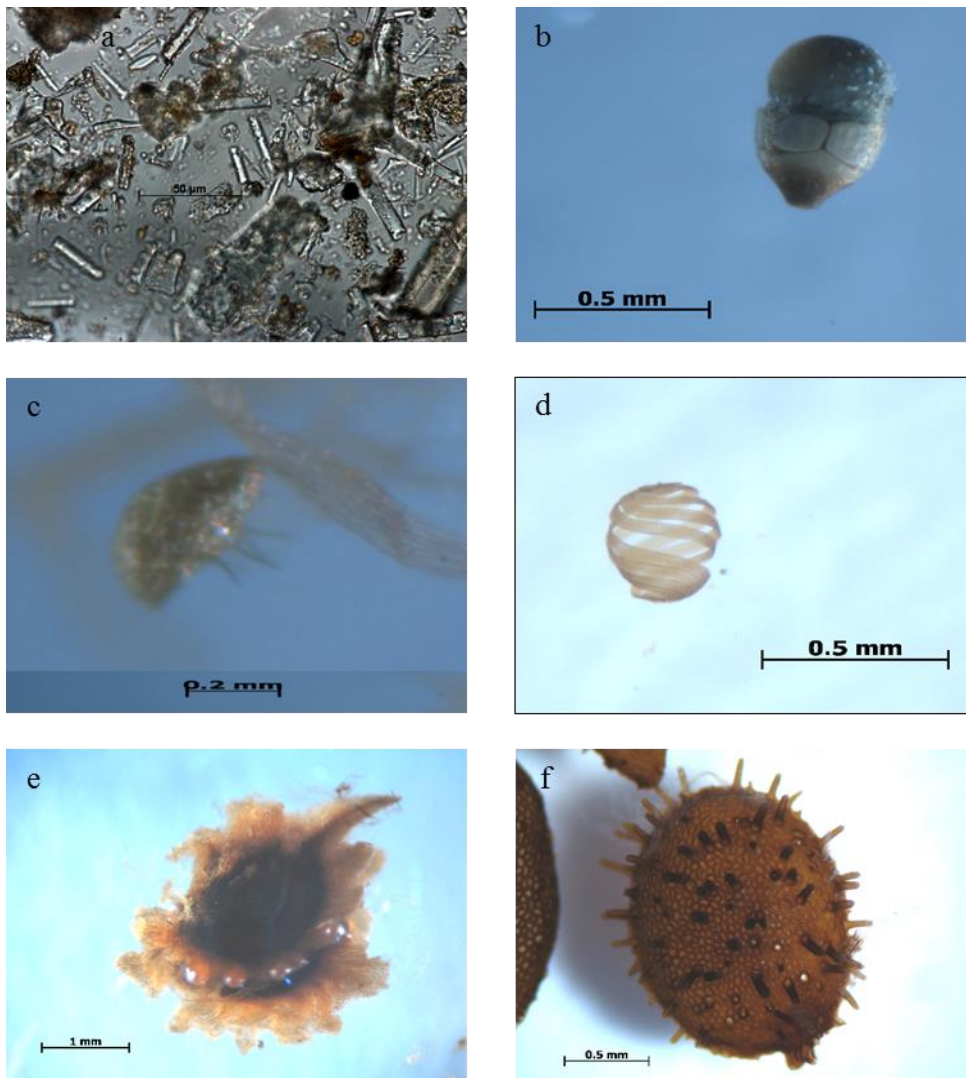


Plate 7.2. Macrofossils and organosilicates from subzone LCA-E2, (a) – broken and dissolved silicates, (b) – *Azolla pinnata* megasporgania, (c) – *A. pinnata* micro sporocarps, (d) – *Nitella* sp., (e) – *P. tricarinatus* carpel, (f) – *Liparophyllum exaltatum* (formerly *Villarsia exaltata*) seed.

Although *Liparophyllum* (formerly *Villarsia*) is absent from the base of this subzone and has sporadic representation towards the top, it is a key element through the rest of this subzone aligning with the high inorganics and its macrofossils (seed) *Liparophyllum exaltatum* (Plate 7.2f). *Haloragis* and *Gonocarpus*, *Stylidium*, *Hydrocotyle* and *Oenanthe* values are greatly reduced although *Oenanthe* does have higher values towards the middle of this subzone, while values for *Persicaria*, Brassicaceae, Geraniaceae and *Anthoceros* are considerably higher in this subzone. Other notable taxa present are *Typha*, *Ludwigia*, *Eriocaulon*, *Elatine* and *Ranunculus* with *Philydrium* and *Nymphoides* present towards the top of this subzone. The macrofossils follow their pollen namesake trend with a reduction in *G. chinensis* seeds and *Hydrocotyle* mericarps while there are abundant macrofossils for *Philydrium lanuginosum* and *Elatine gratioloides* and to a lesser extent for *P. tricarinatus* (Plate 7.2e), *Rorippa* sp. and *N. indica*. Poaceae from the middle to the top of the zone consistently registers higher values when Cyperaceae values are lower. There is a consistent presence of the macro-remains (Plate 7.2b and c) of the aquatic fern *Azolla pinnata* (plant material, megasporangia and micro sporocarps) as well as the oospore, *Nitella* (Plate 7.2d). Inner seed linings have counts consistently above 30 while wasp parts and other insect fragments are present throughout the zone. *Botryococcus* continues to have low values while *Gelasinospora* makes only one appearance.

Subzone LCA-E1. Depth 492–404 cm (samples 246–202) c. 32,180–28,540 yrs B.P.

The inorganic values through this sub-zone are more variable than in the previous *subzone LCA-E2*, but the sedges are still the dominant taxa, although only *Schoenoplectus* and *Carex* has consistently high values through this zone. All other sedges have only minimal values except towards the top where they all spike. The nuts of *C. appressa*, *C. fascicularis*, *Lipocarpha microcephala* and several unknown types are present from the bottom through to the middle of this subzone while the nuts of *Eleocharis sphacelata* (Plate 7.3a) have a greater representation than the other Cyperaceae macrofossils especially in the middle of this sub-zone. Poaceae values are mainly on par with Cyperaceae although there is variability at times with high values corresponding to lower values for Cyperaceae. *Utricularia* is the other key element through this zone although *Persicaria* is consistently present while both *Typha* and Brassicaceae have high values near the base and towards the middle of this subzone. Seeds of *Persicaria strigosa*, *Typha domingensis*, *Rorippa* sp., and *E. gratioloides* are

relatively abundant and are mainly present from the bottom to the middle of this subzone (Plate 7.3 b-e). Seeds of *G. chinensis*, *N. indica* and *P. tricarinatus* are also represented but to a much lesser degree. *Stylidium* is found at the base and has a single occurrence at the very top while *Liparophyllum*, *Philydium* and *Eriocaulon* are restricted to the base and no macrofossils are present for these taxa while *Ludwigia* and Geraniaceae are absent from this subzone. *Botryococcus* follows the previous subzone values while *Gelasinopora* is present from the middle to the top of this subzone.

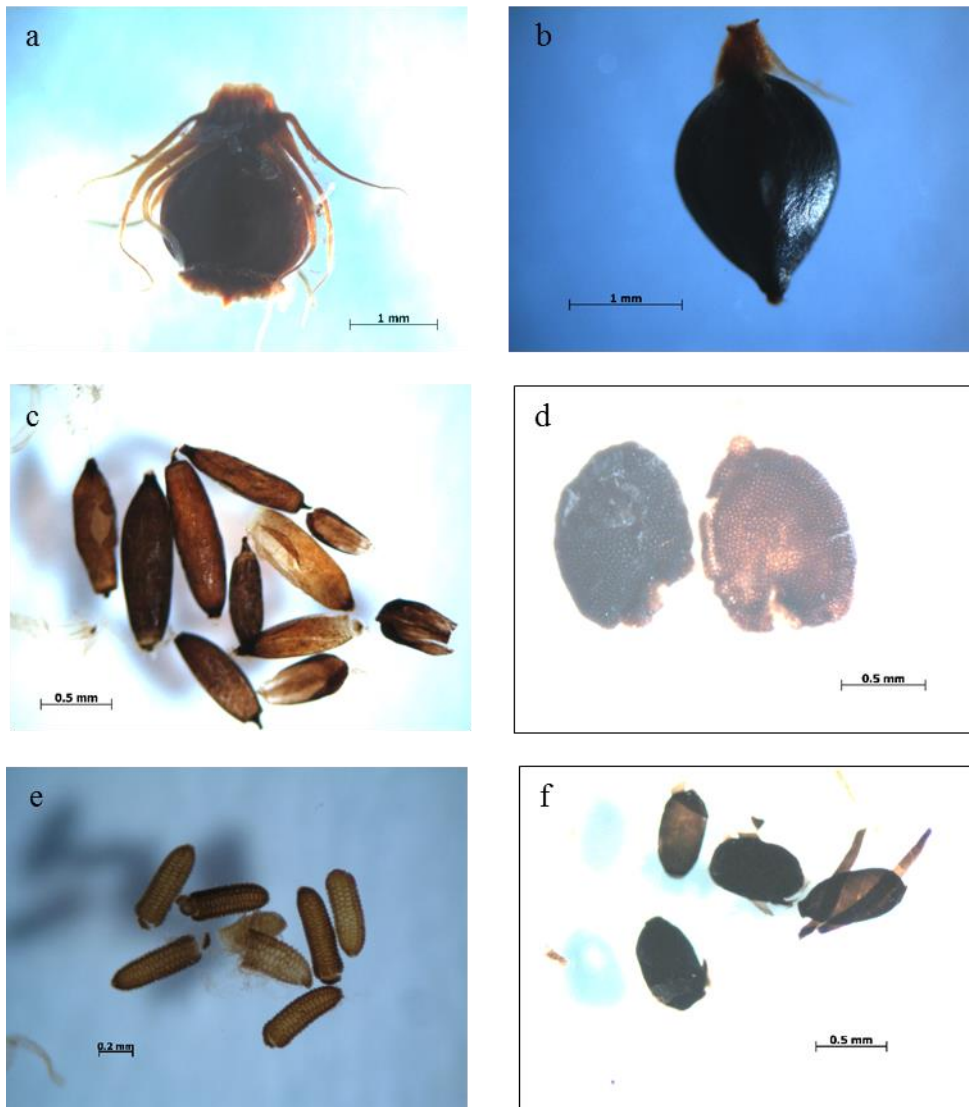


Plate 7.3. Macrofossils from subzone LCA-E1, (a) – *Eleocharis* cf. *sphacelata*, (b) – *Persicaria* *strigosa*, (c)- *Typha domingensis*, (d) – *Rorippa* sp., (e) – *Elatine gratioloides*, (f) – *Chara* oospore

A. pinnata remains (megasporgina, plant material and micro sporocarps) are only present at the base but *Nitella* is present throughout this zone with high counts from the middle to the top of this subzone. The oospore, *Chara*, has its only representation in this subzone (Plate 7.3 f) with high counts in the middle of the subzone while extremely high counts for inner seed linings are also recorded in this subzone.

Zone LCA-D. Depth 402–244 cm (samples 201–122) c. 28,480–19,320 yr B.P.

This zone is characterized by low inorganics (3-10%) although near the base values are slightly higher (8-16%), moisture loss is high and consistent (86-89%) while the sediment is uniform dark brown highly humified peat. There is some increase in damaged and/or corroded pollen. Cyperaceae still dominates the swamp, especially *Eleocharis*, *Schoenoplectus* and *Carex*, with alternating higher values. However, the macrofossil representation for these taxa, *C. appressa*, *C. fascicularis* and *E. sphacelata*, and other Cyperaceae taxon, *L. microcephala* and other *Carex* spp. are low. *Cyperus* and *Baumea* are present through most of the zone but with relatively low values. *Persicaria* has its highest values through this zone although by the top values are greatly reduced. *Typha*, *Utricularia*, *Lemna* and Brassicaceae are mainly present from the base to the middle of the zone with fluctuating values. Other taxa present are *Haloragis* and *Gonocarpus*, *Myriophyllum*, *Hydrocotyle*, and *Anthoceros* with the occasional presence of *Potamogeton*, *Eriocaulon*, *Nymphoides*, Liliaceae and the swamp fern, *Cyclosorus*.

Seeds of *P. strigosa*, *T. domingensis*, *Lemna*, *Rorippa*, *E. gratoiloides* and a number of unknown seeds and nuts are intermittently present while *N. indica* and *Hydrocotyle* mericarps are especially abundant near the top of the zone. *A. pinnata* megasporgia are only present near the base as are its microsporocarps although counts are extremely high. *Nitella* is present throughout this zone but counts are greatly reduced. Inner seed coatings and unidentified seeds fragments have high counts near the base while insect fragments are scattered throughout this zone. *Gelasinospora* is present through most of the zone except from ~28 ka to 26 ka while *Neurospora* makes its first appearance just after the middle of the zone. *Botryococcus* spikes near the base of the zone and high values continue through to just after the middle where values are low or the taxon is absent. Poaceae values are relatively

low in comparison to the aquatic and swamp pollen sum except high values, well above the aquatic and swamp pollen sum, are recorded at the base and in the middle of the zone.

Zone LCA-C. Depth 242–142 cm, (samples 121–71) c. 19,270–12,390 yrs B.P.

Inorganic values are low (7%) at the base of this zone but higher values (20-35%) are recorded through the rest of the zone. Moisture loss values are around 80% with mild perturbations corresponding to the higher inorganic values. As with previous zones with high inorganics, there is a greater component of eroded diatoms, sponge spicules and phytoliths. There is a slight change in sediment through the zone with dark brown highly humified peat through to the middle and a slightly more fibrous (*detritus herbosus*) peat continuing to the top. There is also a slight reduction in damaged and corroded grains. Although not included in the counts or diagrams, the algal spore, *Pseudoschizaea* (Plate 7.4 a) was consistently found in this zone as was the floating liverwort, *Riccia*. Cyperaceae taxa still dominant with *Schoenoplectus* and *Carex* the most prominent composing 50-95% of the aquatic and swamp pollen sum. However, it is the prominence of the submerged aquatic taxa, *Nymphoides* and to a lesser extent *Myriophyllum*, that are the key element of this zone. Other taxa present are *Hydrocotyle*, *Oenanthe*, *Stylidium*, Brassicaceae, *Ranunculus* and, for the first time, Liliaceae is prominent in the record. There is also the occasional presence of *Potamogeton*, *Typha*, and *Eriocaulon* while values for *Persicaria* are significantly lower through this zone and *Anthoceros* only makes an appearance at the top of the zone. *Gelasinospora* has a single occurrence and *Neurospora* is present at the top of the zone and, while *Botryococcus* spikes near the base, relatively minor values are recorded through the rest of the zone.

The seeds of *N. indica* (Plate 7.4 b-d), dominate the macrofossils through this zone with medium counts near the base, higher counts past the middle and then lower counts at the top of the zone following the *Nymphoides* pollen percentage representation. Other seeds and nuts are rare and they are the sedge nuts *Cyperus polystachyos* and *Carex* spp., *E. gratioiloides*, *P. tricarinatus* and a number of unknown seed types. *A. pinnata* megasporangia has low counts from the middle through to the top but high counts are recorded for the microsporocarps in the middle of the zone. *Nitella* has relatively lower counts than previous and is only present at the base and top of the zone while inner seed linings have high counts from the middle

through to the top of the zone. Unidentified seed fragments are found throughout the zone as are wasp and other insect fragments. Poaceae continues with high values well above the aquatic and swamp pollen sum through to the middle of this zone but relatively low values occur towards the top of the zone.

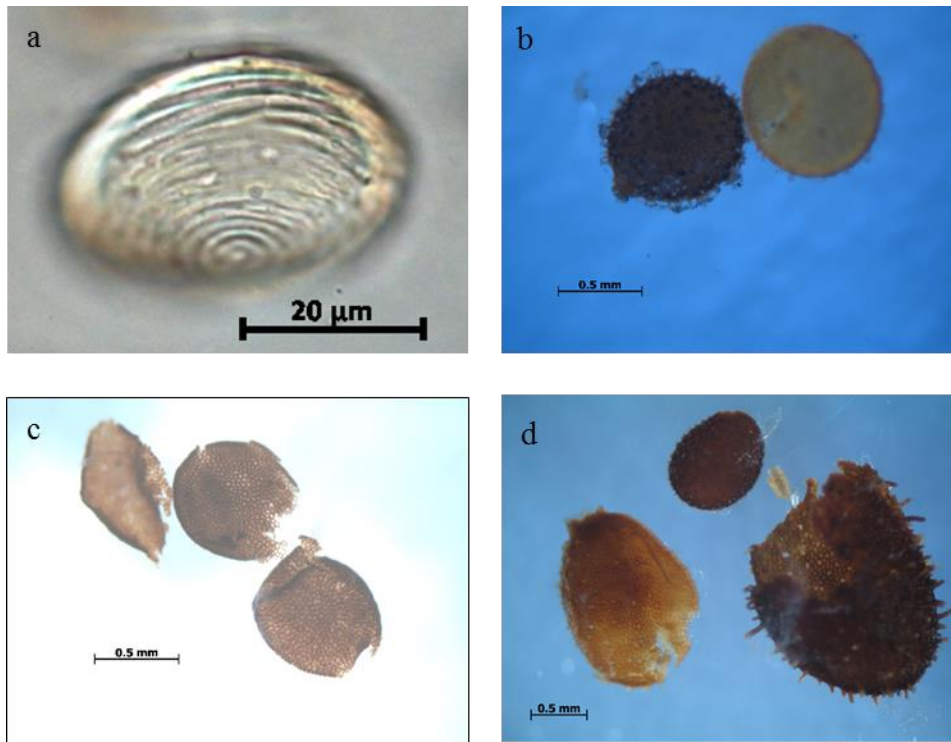


Plate 7.4. Macrofossils and algal remains present in LCA-C, (a) – the algal spore *Pseudoschizaea*, (b) – *Nymphoides indica*, the light coloured seed (fertile), the darker seed infertile, (c) – *N. indica* seed coating without spines, (d) – Size differences of *N. indica* and *L. exaltatum* – *N. indica* (centre small seed) and *L. exaltatum* (large seeds to the left and right). The seed samples for *L. exaltatum* were taken from subzone LCA-E2 as *L. exaltatum* seeds were not found in zone LCA-C.

Zone LCA-B. Depth 140–46 cm (samples 70–23) c. 12,170–6640 yrs B.P.

There is a return to very low inorganics (2-6%) in this zone, except for the base and the occasional higher value (10%) through the middle of the zone, while moisture loss is slightly higher than in the previous zone (80-88%). Brown fibrous peat composes the sediment through this zone. Cyperaceae dominates throughout most of the zone, especially *Schoenoplectus* and *Carex*, although *Cyperus* (*C. polystachyos*) is the one with large nut counts (Plate 7.5 b) especially from the base to the middle while lower nut counts are found

for *Carex* spp., and *E. sphacelata*. *Typha* is a dominant element near the base of zone with values lower through to the middle and absent by the top of the zone.

Both *Haloragis* and *Gonocarpus* and *Hydrocotyle* have a more consistent representation in this zone with mericarps of *Hydrocotyle* near the base and *G. chinensis* seeds towards the top of the zone. The seeds of *Melastoma affine* make their first appearance near the base of this zone (Plate 7.5 a). Other taxa present are *Nymphoides*, *Potamogeton*, *Persicaria* and *Oenanthe* with the occasional presence of *Eriocaulon*, *Utricularia* and *Drosera*, while seeds of *N. indica* are scattered throughout the zone with high counts at the top and carpels of *P. tricarlinatus* found near the base of the zone.

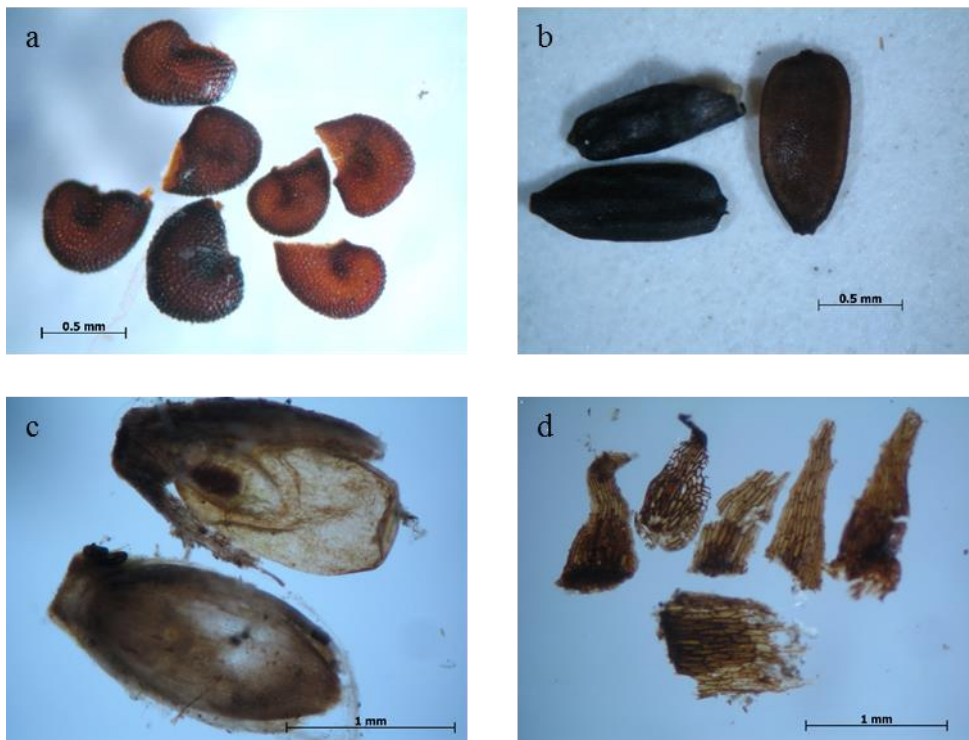


Plate 7.5. Macrofossils present in zone LCA-B and LCA-A, (a) – *Cyperus polystachyos*, (b) – *Melastoma affine*, (c) - *Axonopus* cf. *affinis*, (d) – Fern scales

Nitella has high counts near the base and florets of the exotic grass cf. *Axonopus* makes its first appearance at the top of the zone. *Gelasinospora* has a sporadic presence but *Neurospora* has its greatest presence of the diagram near the base of this zone. *Botryococcus* has medium values at the base but only minor values are found through this rest of the zone. Although

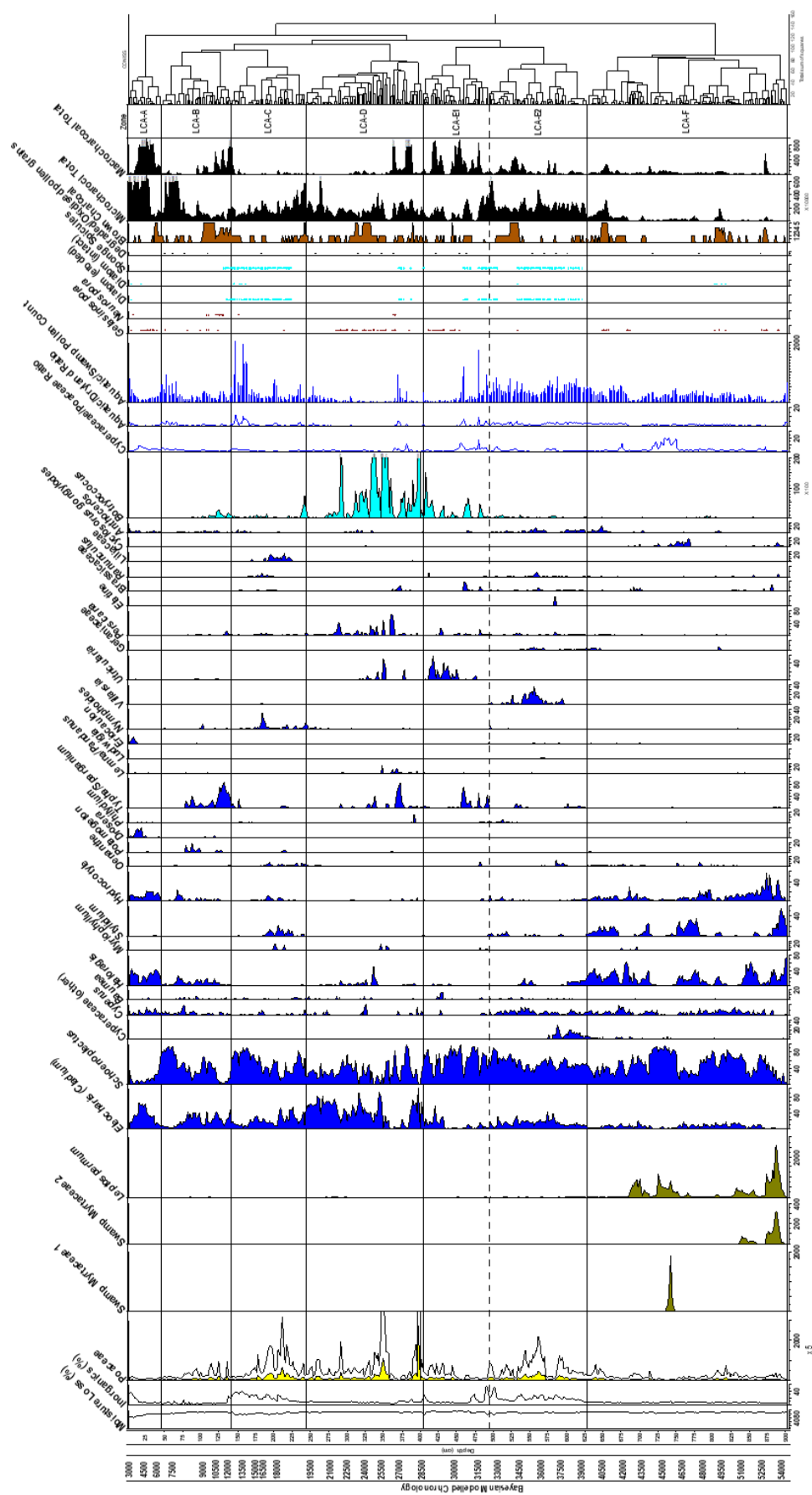
there are intermittent high values for Poaceae through this zone, values are generally low in comparison to the aquatic and swamp pollen sum.

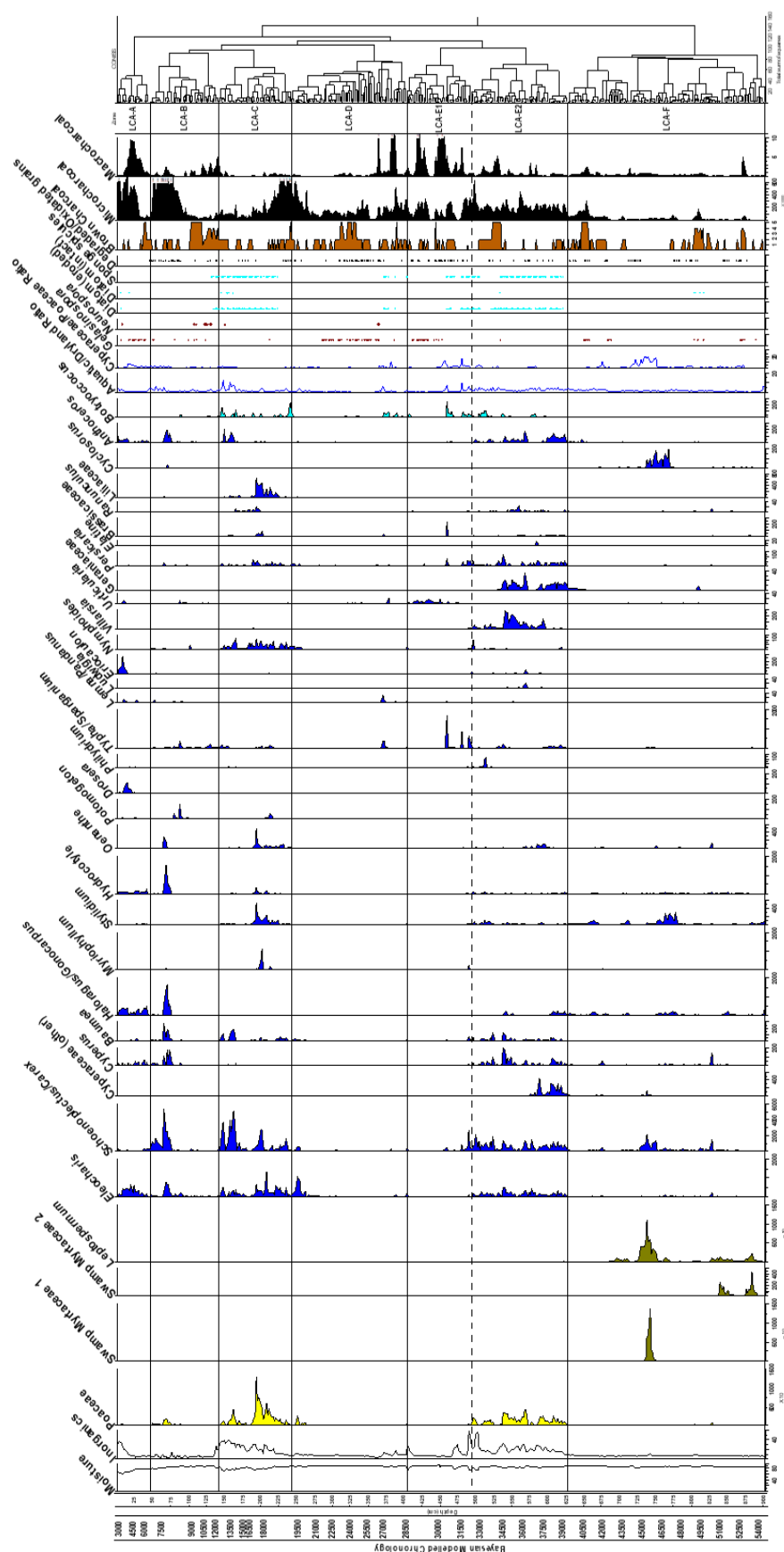
Zone LCA-A. Depth 44–0 (samples 22–1) c. 6430–~3000 yrs .B.P.

This zone is characterized by a relatively low inorganic content (4–8%) from the base to the middle with a higher contribution (12–35%) towards the top of the zone in line with lower moisture content. The sediment consists of very fibrous brown peat with graminoid material in growing position especially towards the top of the zone with woody fragments, charred wood and sedge and fern stem also present. This zone is unusual as it's the first time in the diagram where *Schoenoplectus/Carex* are not the dominant sedge with *Eleocharis* and *Cyperus* being the dominant sedges in this zone. The macrofossils follow this trend with only a single nut of *C. fascicularis* recorded while *Eleocharis dulcis* nuts are found at the base and top and *C. polystachyos* nuts are present throughout and are especially abundant towards the top of the zone. Poaceae values are predominantly less than 20% of the aquatic and swamp pollen sum with a minor increase towards the top of the zone.

Both *Haloragis* and *Gonocarpus* and *Hydrocotyle* have consistently high values through this zone with *G. chinensis* seeds present throughout, while *Anthoceros* also is consistently present but at lower values. *Drosera* has high values (10%) towards the top of the zone but then declines significantly whereas *Eriocaulon* values are high (20%) at the very top of the zone. There is also the occasional representation of *Myriophyllum*, *Stylidium*, *Potamogeton* and *Pandanus* or *Lemna*. *Gelasinospora* is consistently present with *Neurospora* present at the top of the zone.

The seeds of *M. affine* occur throughout the zone with large counts especially near the base of the zone. Grass florets, likely to be from the introduced species *Axonopus* cf. *affinis*, are sporadically present from 20 cm with large counts at the top of the zone (Figure 7.12a). *A. pinnata* megasporangia have medium counts near the base while *Nitella* has low counts in the middle of the zone. Fern parts and fern scales are present near the top of the zone and insect and wasp fragments are present throughout the zone (Plate 7.5 d). This zone has the largest number of unknown seed.





7.2.2. Zonation of Lynch's Crater Dryland Pollen Sum Taxa (LC1)

Zone LC1-9 Depth 902–578 cm (samples 451–288) c. 54,390–36,660 yrs B.P.

This whole zone is characterized by a much more even distribution across the three major dryland components (rainforest angiosperms and gymnosperms and sclerophyll taxa) than what is seen through the rest of the record (Figures 7.6–7.10). However, the increased sclerophyll presence towards the top of the zone provides the basis for dividing this zone into subzones, 9*b* and 9*a*.

Subzone LC1- 9b 902–658 cm (samples 451–329) c. 54,390–40,960 yrs B.P.

The sclerophyll component has values on average 40% to 50% of the dryland pollen sum through most of this subzone with Casuarinaceae having slightly higher values, on average, than *Eucalyptus* type. Other sclerophyll taxa *Callitris*, *Dodonaea*, *Banksia*, *Myoporum*, Gyrostemonaceae, *Bursaria*, *Exocarpus* and *Acacia* have relative minor representation although, *Acacia* does have high values (28% of the dryland sum) in the middle of the subzone. This is prior to the high values of swamp Myrtaceae type 1, details of which are given in sub-section 7.2.1/Zone LCA-F. *Podocarpus* is the dominant rainforest gymnosperm with values on average 15–29% of the dryland sum except near the base where extremely high values (60–80%) are recorded. These high values also coincide with high counts for a smaller variant of the Podocarpaceae pollen type (Plate 7.6). *Araucaria* is consistently present with values ranging from 5–28% of the pollen sum while *Dacrydium* and *Agathis* are also consistently present but with values under 5%.

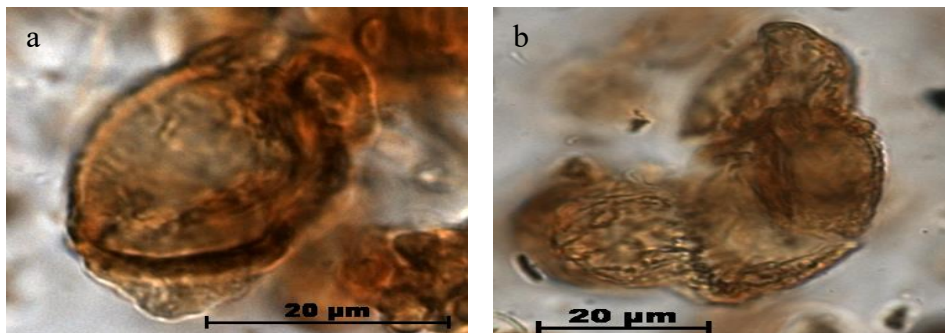


Plate 7.6. Podocarpaceae types found through subzone LC1-9*b*. (a) – Smaller sacculus variant of the Podocarpaceae pollen type; (b) – The more common Podocarpaceae pollen type, which shows a close affinity to the pollen of *Sundacarpus amarus* (formerly *Podocarpus amarus*). This pollen type is found throughout the Lynch's Crater record.

High values (30–40%) are recorded for the rainforest angiosperms near the base and towards the top of the subzone with values of 10–20% through the rest of the subzone. The canopy component is the dominant element through most of the subzone although towards the top the secondary component has equal values. *Argyrodendron peralatum* is the dominant canopy species but also present are *Syzygium* comp., *Olea paniculata*, *Longetia* (*Austrobuxus*), Sapindaceae (syncolpate), *Flindersia*, *Acmena*, *Elaeocarpus*, *Balanops* and *Cardwellia* with another 22 known taxa present with minor values.

Key elements for the secondary taxa are *Macaranga* and *Mallotus*, Urticaceae and Moraceae, *Homalanthus* (formerly *Omalanthus*), *Melicope*, *Euodia*, *Celtis* and *Trema* with a further nine taxa present with minor values. Like the canopy component there is a great deal of diversity within the understorey component with *Elaeodendron*, *Zanthoxylum*, *Oraniopsis*, *Dissilaria*, *Helicia* and *Acalypha* the main contributors with *Symplocos*, Acanthaceae, *Austromuellera* and *Rapanea* frequently present while *Tasmannia* (formerly *Drimys*) has its greatest representation in this subzone. Menispermaceae and *Cissus* are the most consistent vines present.

Poaceae values are relatively low (20–40%) near the base but higher values (60–100%) are recorded towards the top of the subzone. Of other ‘herbaceous’ or small shrub taxa Asteraceae (tubuliflorae) and Chenopodiaceae are present throughout this subzone as are *Monotoca*, *Plantago* and Asteraceae (liguliflorae) with Epacridiaceae (Ericaceae) only present near the base. The pteridophytes have generally low values through this subzone although monolete (psilate) ferns record values up to 10% throughout this subzone and *Cyathea* and *Platyserium* consistently record values up to 5% while the sclerophyll fern, *Pteridium*, records values of 5% towards the top of this subzone. The swamp fern *Cyclosorus* has high values, in the middle of this subzone (see sub-section 7.2.1, Zone LCA-F).

Subzone LC1-9a Depth 656–578 cm (samples 328–289) c. 40,850–36,660 yrs B.P.

This subzone sees increasing percentages for the sclerophyll component with values of 66% achieved by the top of the subzone with Casuarinaceae and *Eucalyptus* type the main contributors. All other sclerophyll components follow this trend except for *Callitris* and

Dodonaea which have higher values near the base of the subzone. Rainforest gymnosperm values have decreased through this subzone although *Podocarpus* still contributes 15% to the dryland pollen sum at the top of the subzone and *Dacrydium* has its highest values (11%) towards the top but values are under 2% at the very top of the subzone, similar to the percentage here for *Araucaria*.

Like the rainforest gymnosperms, the rainforest angiosperms initially have high values (43%) but are reduced to ~17% (excluding *Syzygium*) by the top of the subzone. The rainforest canopy is the main component affected, especially *A. peralatum*, *Longetia*, *Flindersia*, *Balanops* and Proteaceae, although more than 20 taxa are present including *Elaeocarpus* but by the top of the subzone they record only minor values. The more seasonal drier rainforest canopy element *O. paniculata* initially has the high values previously recorded for *A. peralatum* but values are reduced to < 5% by the top of the subzone. The rainforest secondary taxa, initially like *O. paniculata* have higher values, and as in the previous subzone *Macaranga* and *Mallotus*, Urticaceae and Moraceae, *Homalanthus*, Leguminosae, *Melicope*, *Celtis* and *Trema* are the dominant taxa present with a further eight more taxa present with minor values. The understorey component has slightly higher values through this subzone but it is only *Oraniopsis* and *Elaeodendron* that are significantly contributing to this increase. The vine taxa also have slightly higher values through this subzone with Menispermaceae and *Morinda* the main contributors.

Poaceae values are extremely high (600%) through most of this subzone but are reduced to 150% by the top of the subzone. Chenopodiaceae and Asteraceae (tubuliflorae) and the pteridophytes also have higher values through this subzone with the monolete (psilate) ferns the main contributor for the pteridophytes although *Platyserium*, Davalliaceae, Ophiolossaceae and the sclerophyll ferns, *Pteridium* and *Pteris*, are also consistently present.

Zone LC1-8 Depth 576–484 cm (samples 288–242) c. 36,550–31,740 yrs B.P.

The sclerophyll component is dominant through this zone with values up to 88% towards the top of the zone. The sclerophyll Myrtaceae, especially *Eucalyptus* type, are the main contributors although Casuarinaceae still contributes at times up to 40% of the dryland pollen

sum. *Corymbia*, *Callitris* and *Dodonaea* record their highest values for the diagram in this zone. All rainforest gymnosperms have declined substantially although *Podocarpus* has values of 14% near the base of the zone. The rainforest angiosperms fluctuate between 5–14% with the canopy taxon *O. paniculata* and the secondary taxa *Macaranga* and *Mallotus*, *Trema* and *Celtis* the major contributors. The main contributor for the understorey taxa is *Petalostigma* while *Morinda* is the only vine taxon with a consistent presence.

Poaceae values in places are on par with the high values (600%) recorded in the subzone *LC1-9a* but values are highly variable and by the top of the zone are reduced to 24%. Asteraceae (tubuliflorae) and Chenopodiaceae have slightly lower values through this zone as do the pteridophytes except for the sclerophyll ferns, *Pteridium* and *Pteris* which have slightly higher values.

Zone LC1-7 Depth 482–412 cm (samples 241–206) c. 31,620–28,800 yrs B.P.

Values up to 98% of the dryland sum are recorded for the sclerophyll component with Casuarinaceae the dominant taxon while the sclerophyll Myrtaceae fluctuate between 18–45% through the zone with *Eucalyptus* type the dominant component. All rainforest gymnosperms have only minor values. The rainforest angiosperms have values of 8% near the base but are less than 2% at the top of the zone. *O. paniculata* is the only consistent canopy element through this zone whereas the secondary taxa have several consistent elements, *Macaranga* and *Mallotus*, Leguminosae and *Trema*, although with reduced values. As in the previous zone, LC1-8, only the understorey taxon *Petalostigma* has values above 1% while the vine taxa have only occasional representation.

Poaceae continues with the low values (20%) from the previous zone. Asteraceae (tubuliflorae) has values under 3% but Chenopodiaceae values are higher but more variable through this zone. Pteridophytes have minor values throughout the zone with only the epiphytic fern, *Platyserium*, and the sclerophyll ferns, *Pteridium* and *Pteris* present through most of the zone.

Zone LC1-6 Depth 410–220 cm (samples 205–110) c. 28,740–18,730 yrs B.P.

The sclerophyll component continues with the high values from the previous zone. Casuarianaceae values fluctuate between 50–70% while the sclerophyll Myrtaceae fluctuate between 25–55%. *Callitris* and *Dodonaea* have lower values through this zone except in the middle in line with higher values for the sclerophyll Myrtaceae. The rainforest gymnosperms continue with minor values through this zone. The rainforest angiosperms have values mainly under 10% with *O. paniculata* the most consistent canopy taxon present but occasional higher values are recorded for other canopy taxa, *Syzygium*, *Acmena*, *Flindersia*, *Ilex*, *Balanops*, *Longetia* and *Elaeocarpus*, especially in the middle and towards the top of the zone. Higher values for the secondary taxa, *Macaranga* and *Mallotus*, *Trema*, *Melicope*, *Euodia* and *Celtis* are recorded prior to the increase in rainforest canopy while *Glochidion* and *Homalanthus* follow the pattern of the rainforest canopy elements. *Petalostigma* still remains the most consistent understorey taxon with higher values aligned with the canopy taxa, a feature also seen in *Acalypha* and *Oraniopsis* while *Acronychia* has a notable presence from the base and top but is absent from the middle of the zone. Loranthaceae is the most consistent vine taxon in this zone although higher values are recorded in the middle for Mensipermaceae, *Cissus*, *Morinda* and *Maesa*.

Poaceae continues with the low values found in the previous zone until the top where values rise to 200% of the dryland sum. Chenopodiaceae records its highest values for the record in the middle of this zone but fluctuates throughout the rest of the zone unlike the Asteraceae (tubuliflorae and liguliflorae) where values are relatively consistent through the zone. Most pteridophytes values are erratic through this zone although Opliglossaceae spikes in the middle of the zone and both *Cyathea* and *Platycerium* are recorded through the whole zone.

Zone LC1-5 Depth 218–158 cm (samples 109–79) c. 18,630–13,470 yrs B.P.

Casuarinaceae remains the dominant dryland taxon (~60% to 70%) although values are reduced towards the top (~30% to 40%) where the sclerophyll Myrtaceae, especially *Eucalyptus* type (~30%) and *Melaleuca* (~20%), become the dominant elements. *Corymbia* and the other sclerophyll components have only minor values through this zone. The rainforest gymnosperms continue to have only minor representation with *Dacrydium*

intermittently present. The rainforest angiosperms fluctuate between 2–19% with the higher values recorded at the base and top of the zone. *O. paniculata* is the most consistent canopy taxon and records its highest values (12%) of the sequence at the base of this zone. *Elaeocarpus* and *Syzygium* are present throughout the zone while Sapindaceae spikes towards the top. The secondary component values continue to be spread across several taxa that, in this zone, are mainly *Macaranga* and *Mallotus*, *Celtis*, *Melicope* and Leguminosae while the understorey taxa, *Oraniopsis* and *Acronychia*, have a more consistent presence through this zone. The vine taxa, *Cissus*, Menispermaceae, *Maesa* and Loranthaceae are also present through this zone although values are variable.

Poaceae records high values (300%) through most of the zone except in the middle where values drop to 40%. Asteraceae (tubuliflorae) records its highest values (22%) of the diagram at the base of this zone but values fluctuate through the rest of the zone. Both Chenopodiaceae and Asteraceae (liguliflorae) have more consistent but low values through this zone. The pteridophytes only have minor values except for the sclerophyll fern, *Pteridium*, which records its highest values (11%) of the diagram at the top of this zone while monolete (psilate) ferns are consistently present and spike alongside *Pteridium* at the top of this zone.

Zone LC1-4 Depth 156–104 cm (samples 78–52) c. 13,370–8930 yrs B.P.

The sclerophyll component still dominates but the main elements, Casuarinaceae and *Eucalyptus* type, have similar values through this zone but, as in all previous zones, alternating trends. *Corymbia*, *Callitris* and *Dodonaea* have higher values especially through the middle of this zone. The rainforest gymnosperms have only minor values with *Dacrydium* only present at the base of this zone. The rainforest angiosperm values are variable but with values of 4% near the base increasing gradually to 31% at the top of the zone. *O. paniculata* is still the most consistent rainforest canopy taxa except towards the top of the zone. *Acmena* and *Syzygium* continue, with higher values from ~13 ka when *Rhizophora* makes its first appearance. *Elaeocarpus* percentages increase from ~11 ka, while *Ilex* has increased values from ~10.3 ka followed by Cunoniaceae (tricolpate), *Flindersia* and *Ficus* at ~9.7 ka. The secondary component also has higher values especially from ~13–12 ka with *Macaranga* and *Mallotus*, Leguminosae, *Trema* and *Celtis* the main contributors but, like the canopy taxa

from ~11 ka, less abundant taxa such as *Glochidion*, *Homolanthus*, *Alphitonia*, *Euodia* and *Melicope* make an appearance. Like the canopy taxa the understorey and vine taxa have higher values towards the top of the zone. *Rapanea* and *Oraniopsis* are the main contributors for the understorey with *Rapanea* having a relatively sporadic presence from ~13 ka but becoming more consistently present from ~11.6 ka along with the vine elements Menispermaceae, *Maesa* and *Freycinetia*.

Poaceae values are high at the base but lower values are recorded through the rest of the zone. Both Chenopodiaceae and Asteraceae (tubuliflorae) have lower values through this zone but the fast growing shrub *Melastoma* (Melastomaceae), previously only intermittently present, becomes more consistently present at ~13 ka with values up to 10% towards the top of the zone. All pteridophytes have higher values towards the top especially the epiphytic ferns, Davalliaceae, *Microsorium* and *Platynerium*, the ground ferns, *Lygodium* and *Gleichenia*, and the monolete (psilate) ferns.

Zone LC1-3 Depth 102–46 cm (samples 51–23) c. 8770–6430 yrs B.P.

Although this whole zone falls within the cut-off point of six total sum of squares, visually a great deal of variability is evident especially between the major dryland components, rainforest angiosperms, rainforest gymnosperms and sclerophyll taxa, suggesting that the zone should be divided into three subzones.

Subzone LC1-3c Depth 102–80 cm (samples 51–40) c. 8770–7820 yrs B.P.

The sclerophyll component still dominates with Casuarinaceae the main taxon having fluctuating values between 50-70% while the sclerophyll Myrtaceae have lower values and fluctuate between 13–30% with *Eucalyptus* type the main contributor. *Callitris* has higher values (9%) in the middle of the subzone while *Dodonaea* has lower values through this subzone. As in the previous zone, the rainforest gymnosperms record relatively low values but *Araucaria*, *Agathis* and *Podocarpus* all contribute. However, the rainforest angiosperms have a more consistent presence in this subzone with values fluctuating between 15–26% and, with the inclusion of *Syzygium*, rise to 40%. There is also a change in the main contributors of the canopy component with *Acmena*, *Syzygium*, *Elaeocarpus*, *Ficus*, *Ilex*,

Sapindaceae and *Rhizophora* replacing *O. paniculata*. *Trema* is the main contributor for the secondary component with *Macaranga* and *Mallotus* recording high values at the base with minor values recorded through the rest of the subzone; *Celtis*, Urticaceae and Moraceae, Leguminosae, *Glochidion* and *Alphitonia* are all represented. The understorey contribution is minor although *Rapanea* is present through most of the subzone as are Rubiaceae and *Oraniopsis* while *Freycinetia* is the most consistent vine element with *Cissus*, *Maesa* and Loranthaceae having minor values.

Poaceae has relatively high values (~150%) towards the middle of the subzone but records lower values (50%) through the rest of the subzone. Asteraceae (tubuliflorae) and *Melastoma* have slightly lower values through this subzone while Chenopodiaceae has slightly higher values in the middle of the subzone. *Cyathea*, *Davallia*, *Lygodium*, *Gleicheria*, *Pteridium* and *Pteris* have lower values through this subzone but *Microsorium* and *Platyserium* maintain the values of the previous zone as do the monolete (psilate) ferns except towards the top of the subzone where extremely high values (360%) are recorded.

Sub-zone LC1-3b Depth 78–68 cm (samples 39–34) c. 7800–7690 yrs B.P.

This short subzone sees a complete change in dryland taxon dominance. All sclerophyll components have significantly lower values with Casuarinaceae, although recording relatively high values of 50% at the base, these are reduced to 11% by the top of the subzone while the sclerophyll Myrtaceae record values of 30% at the base but are reduced to 7% by the top of the subzone. The rainforest gymnosperms have only minor representation while the rainforest angiosperms record values up to 80% by the top of the subzone. All rainforest components record higher values through this subzone but the canopy component is the main contributor with *Acmena*, *Syzygium* comp., Cunoniaceae (tricolpate and dicolpate), *Elaeocarpus*, *Sloanea*, *Ficus*, *Ilex*, Sapindaceae, and *Rhizophora* all recording high values with another 11 more identified taxa recorded. *Glochidion* is the main contributor to the secondary component while Rhamnaceae, *Homalanthus*, Leguminosae, *Melicope*, *Euodia*, *Schefflera* and Urticaceae and Moraceae are also consistently present and *Trema* and *Celtis* have lower representation. For the understorey, *Rapanea* records high values (16%) at the top of the subzone and consistently present are Rubiaceae, *Opisthiolepis* or *Apodytes* and

Symplocos with the vine taxa represented by Menispermaceae, *Calamus*, *Maesa*, *Freycinetia* and Loranthaceae.

Poaceae values are reduced from the previous zone while *Melastoma* records high values (10%) at the top of the subzone. Asteraceae (tubuliflorae) is absent through most of this subzone except near the base where relatively high values are recorded (10%) while Chenopodiaceae is only occasionally represented. Although monolete (psilate) ferns values are reduced they are still relatively high (100% of the dryland pollen sum) while the epiphytic and ground ferns from the previous subzone are still consistently present.

Sub-zone LC1-3a Depth 66–46 cm (samples 33–23) c. 7670–6640 yrs B.P.

This subzone has several abrupt changes across the dryland components. The main sclerophyll components, Casuaranceae and *Eucalyptus* type, have a similar trend; both rising sharply at the base to contribute to 75% of the dryland sum but dropping abruptly to 36% at 58 cm and then rising again to 52% at 52 cm. All other sclerophyll taxa show a similar pattern. It is the rainforest angiosperm canopy component which replaces the sclerophyll components at these key depths with a similar combination as seen in the *subzone 3b*. The secondary component has relatively low values through these key depths with *Macaranga* and *Mallotus* and *Trema* returning to be the main contributors. *Rapanea* (understorey) is still represented but values have dropped significantly and, although most of the vine taxa have lower values through this subzone, both Menispermaceae and *Freycinetia* are at least minor contributors. All rainforest gymnosperm values are low with *Dacrydium* making its last appearance of the diagram at the base of this subzone.

Poaceae values are still relatively low and have a similar patterning to the sclerophyll components while *Melastoma* records high values in accord with the rainforest angiosperm canopy component. Pteridophytes have higher values in this subzone especially towards the top except for the monolete (psilate) ferns which records its highest values (422%) of the diagram at the base of the subzone.

Zone LC1-2 Depth 44–28 cm (samples 22–14) c. 6430–4900 yrs B.P.

This zone sees a return of the rainforest angiosperms as the dominant taxa as in *subzone LC1-3b*, while the main sclerophyll components, Casuarinaceae and *Eucalyptus* type, record their lowest values of the diagram in this zone. *Agathis* and *Podocarpus* are the only rainforest gymnosperms present with minor values only. The rainforest angiosperms record values of over 90% of the dryland sum through this zone and although all components show an increase in diversity, the main contributor to these high values is the canopy component with both *Acmena* and Cunoniaceae (tricolpate) having high values and *Syzygium* comp. having its highest values through this zone. Some of the other canopy taxa present with high values are *Ficus*, Cunoniaceae (dicolpate), *Elaeocarpus*, *Ilex*, *Argyrodendron*, *Flindersia*, Sapindaceae, *Balanops*, *Rhizophora*, *Sloanea* and Proteaceae. The secondary taxon *Glochidion* returns with the similar high values seen previously in the subzone *LC1-3b* with *Homalanthus*, *Mallotus* and *Macaranga*, *Trema* and Leguminosae also present. *Rapanea* records its highest values (20%) of the diagram in this zone with the understorey elements *Opisthiolepis* or *Apodytes*, Rubiaceae and *Quintinia* also present. *Freycinetia* has the highest values for the vine taxa although Loranthaceae, *Maesa* and Menispermaceae are consistently present.

Poaceae values are further reduced in this zone while *Melastoma* has higher and more consistent representation. Most of the pteridophytes have higher values, especially *Cyathea*, and the epiphytic ferns, Davalliaceae and *Platyserium*; a notable exception is the sclerophyll fern, *Pteridium* which has significantly lower values through this zone.

Zone LC1-1 Depth 26–0cm (samples 13–1) c. 4760–~3000 yrs B.P.

The main sclerophyll components, Casuarinaceae and the sclerophyll Myrtaceae, have a similar patterning but with higher values (12%) for the sclerophyll Myrtaceae towards the top and higher values (28%) for Casuarinaceae at the very top of the zone. Minor values are recorded for the rainforest gymnosperms, *Podocarpus* and *Agathis*. The rainforest angiosperms continue their high values, (80–90% of the dryland sum) from the previous zone although at the top of the zone values decline to 64%. The canopy component as previously is the main contributor to these high values (45–70%) although values decline (31%) at the top of the zone.

Cunoniaceae (tricolpate) records its highest values of the diagram near the base of the zone while *Elaeocarpus*, *Ficus*, and Cunoniaceae (dicolpate) record their highest values of the diagram towards the top of the zone. Although there is still a great deal of diversity within the canopy taxa, for some like *Acmena*, *Ilex* and *Balanops* their occurrence is more erratic. The Proteaceae, especially *Cardwellia*, have a greater presence and, for the first time, the canopy palm, *Archontophoenix*, is well represented, at least towards the top of the zone. Initially values are high for *Glochidion* (secondary) but it has minor values only through the rest of the zone, mirroring the pattern for *Acmena* and leaving *Macaranga* and *Mallotus* as the main secondary component contributor. Both the understorey and vine taxa record high but erratic values through this zone with *Quintinia*, *Oraniopsis* and *Rapanea* the main contributors to the understorey, although *Rapanea* has a similar patterning to *Acmena* (canopy) and *Glochidion* (secondary) of intermittent presence towards the top of the zone. *Freycinetia* and Menispermaceae are the major contributors for the vines but also present are *Calamus*, *Cissus*, *Maesa*, and Loranthaceae.

Poaceae records low values through most of the zone except at the top where high values (131%) are recorded while *Melastoma* records its highest values (70%) of the sequence near the top of the zone. Asteraceae (tubuliflorae and liguliflorae) and Chenopodiaceae have relatively low values through this zone although the Asteraceae taxa do increase towards the top of the zone. The ferns *Cyathea*, *Dicksonia*, Davalliaceae, *Microsorium*, *Platynerium*, *Lygodium* and *Gleichenia* have their highest values of the diagram in this zone with *Gleichenia* recording values up to 345% of the dryland sum in the middle of this zone. The monolete (psilate) ferns have similar values to the previous zone while the sclerophyll fern, *Pteridium*, has relatively low values except at the top of the zone where values rise to 6% of the dryland sum.

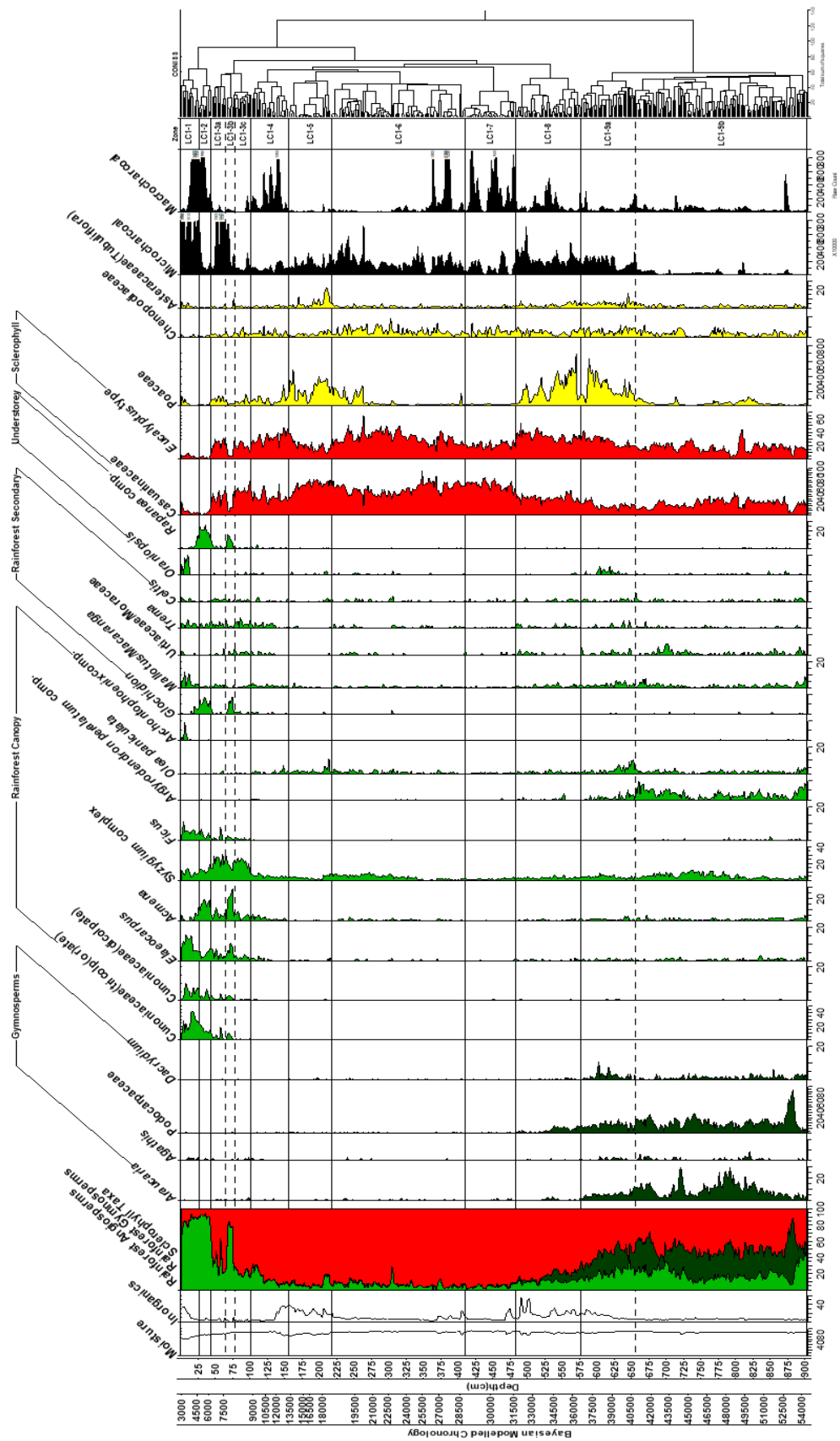


Figure 7.6. Dryland percentage summary diagram with charcoals, with Coniss (detrended correspondence analysis) used for zoning based on the percentage dryland pollen sum.

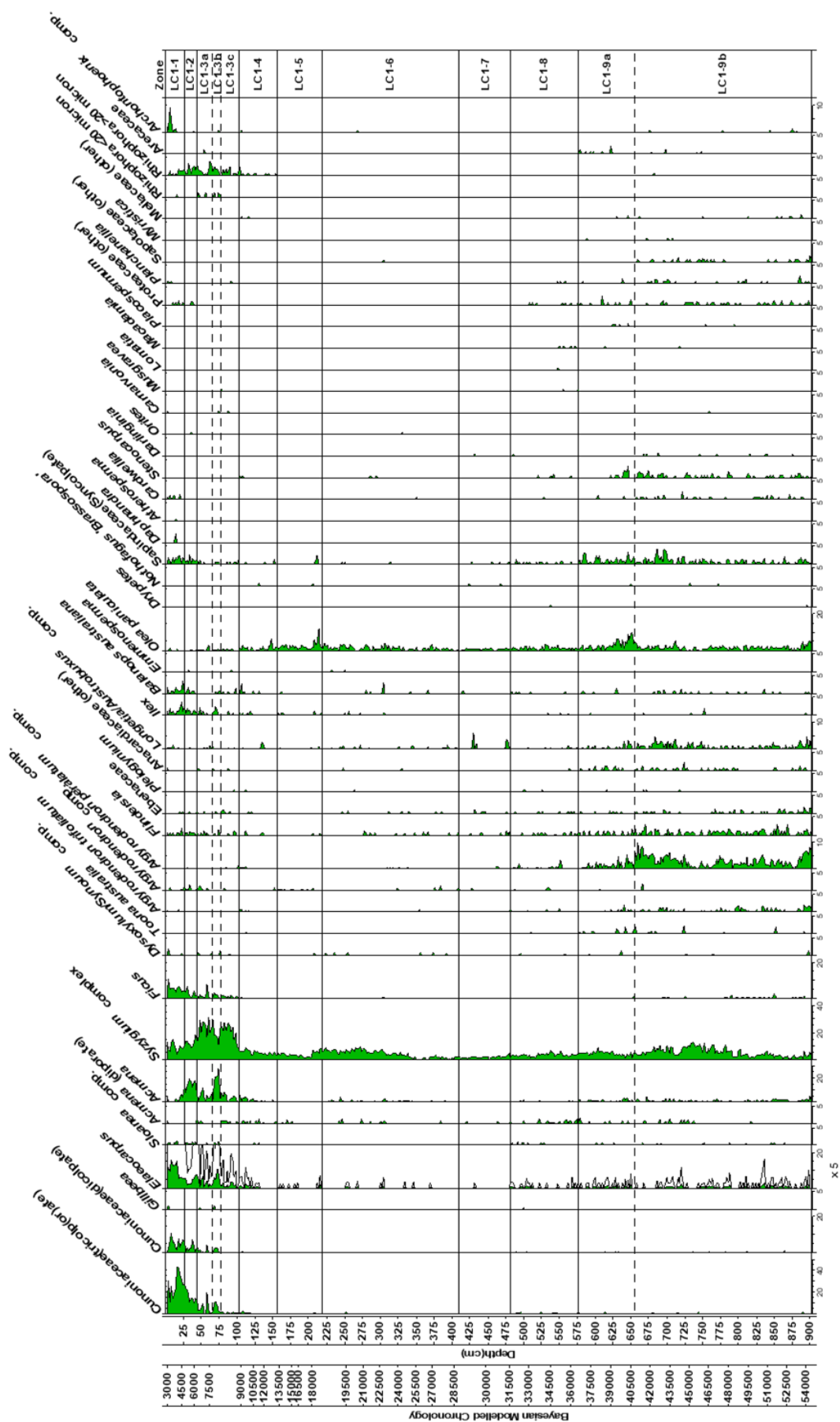


Figure 7.7. Dryland percentage rainforest canopy taxa diagram with percentage dryland pollen sum zoning.

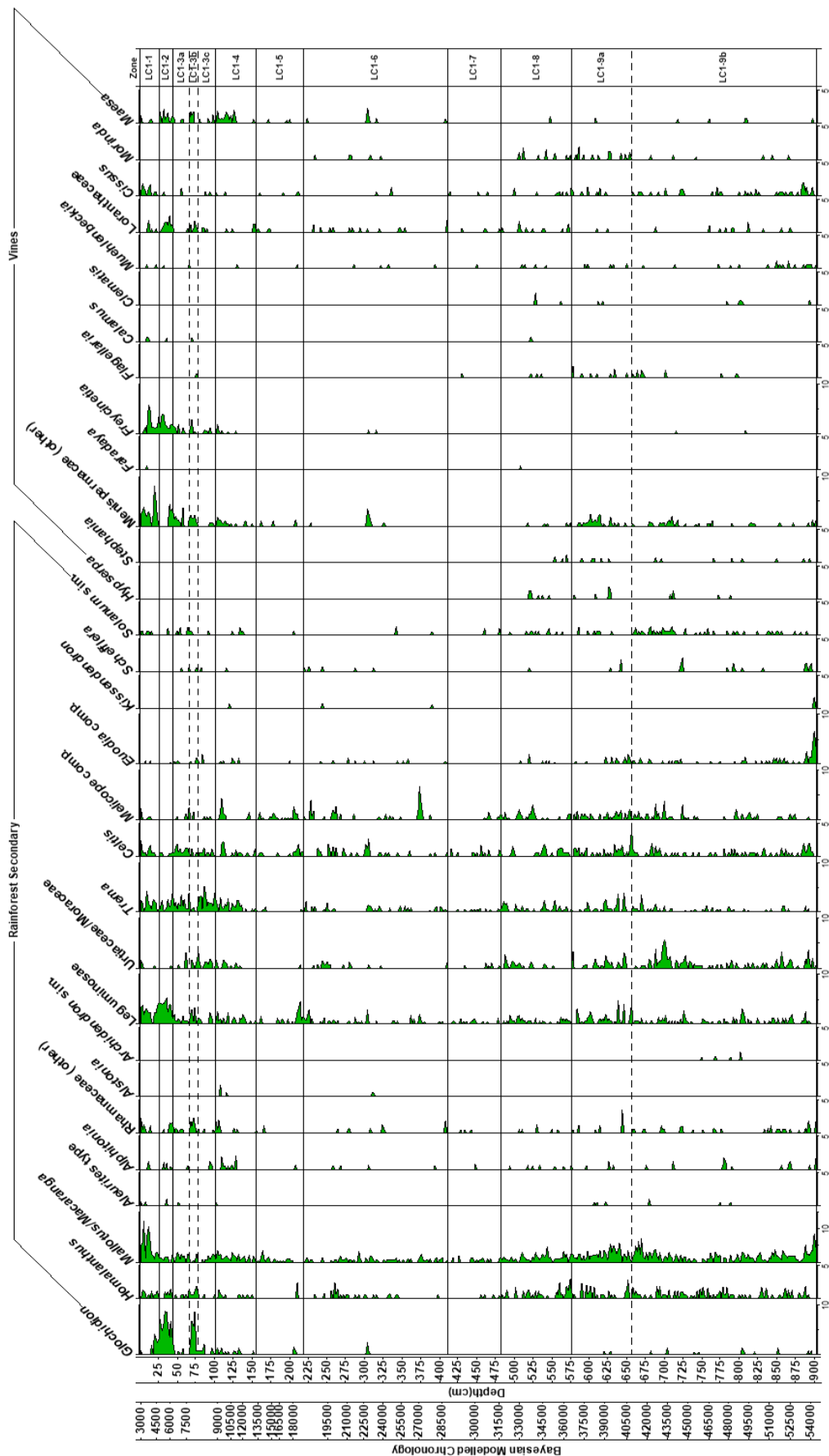


Figure 7.8. Dryland percentage rainforest secondary and vine taxa diagram with percentage dryland pollen sum zoning.

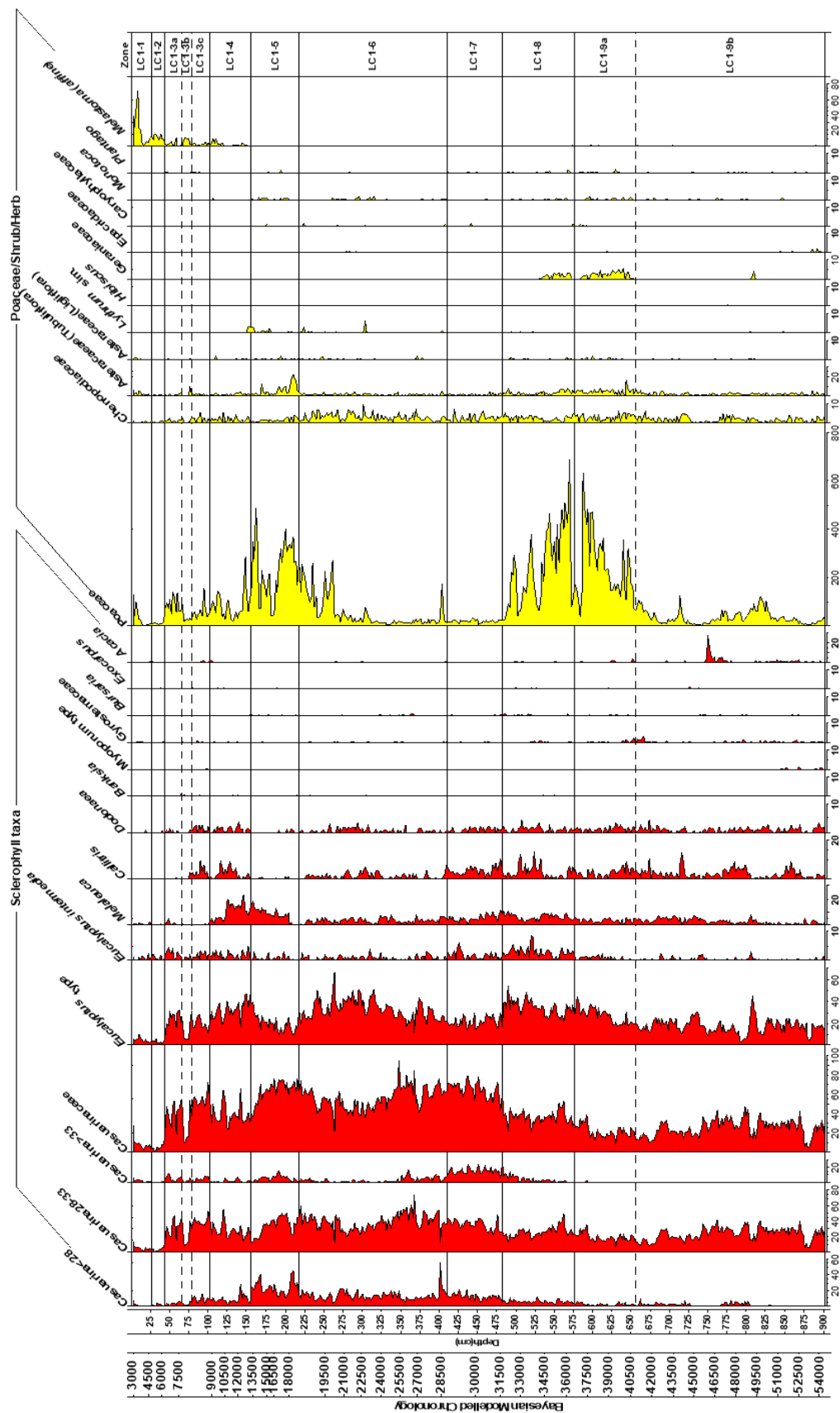


Figure 7.10. Dryland percentage sclerophyll taxa, Poaceae, shrub and herb taxa diagram with percentage dryland pollen sum zoning.

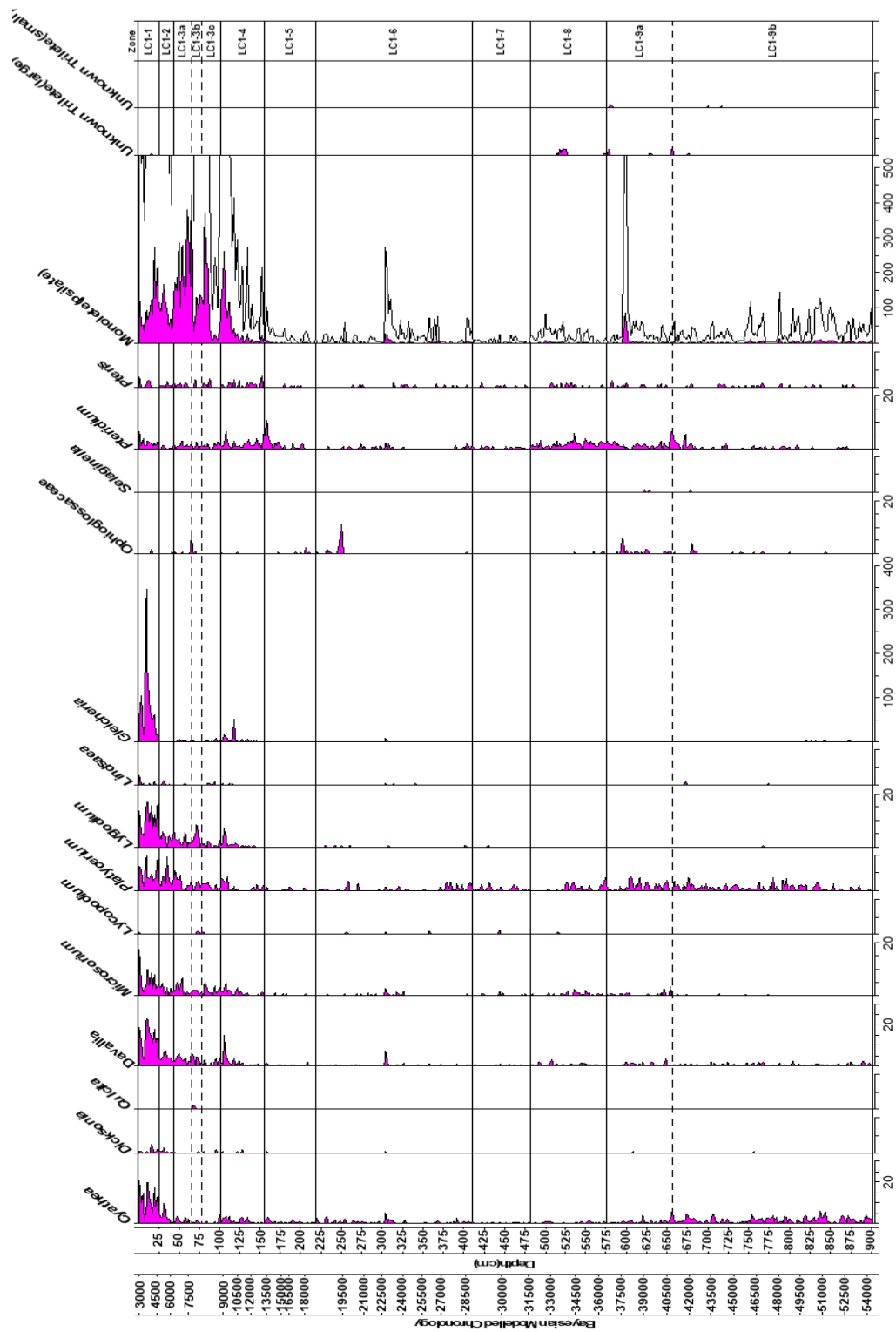


Figure 7.11. Dryland percentage pteridophyte taxa diagram with percentage dryland pollen sum zoning.

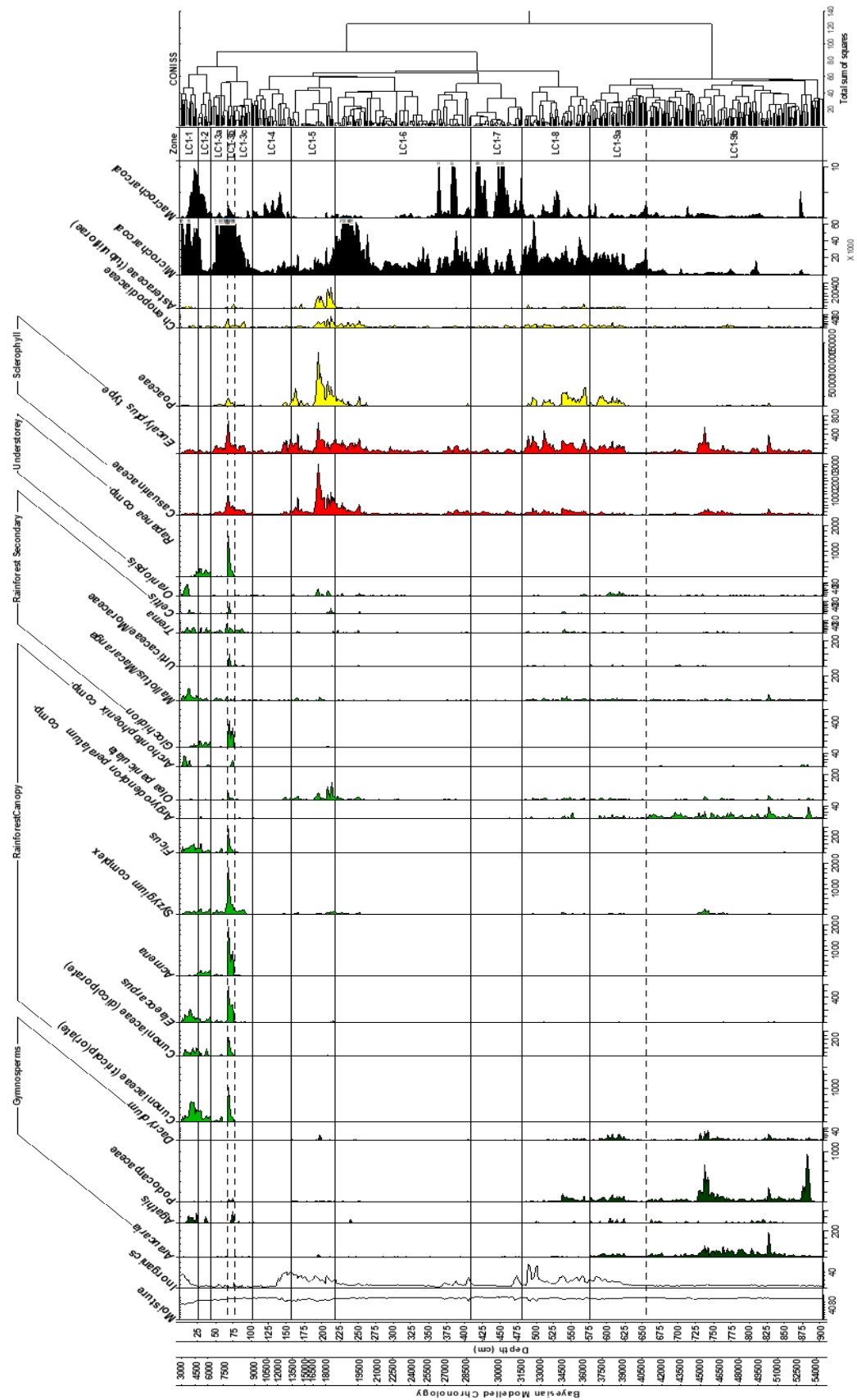
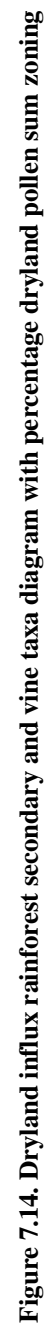


Figure 7.12. Dryland influx summary diagram including charcoal and pollen sum zoning.



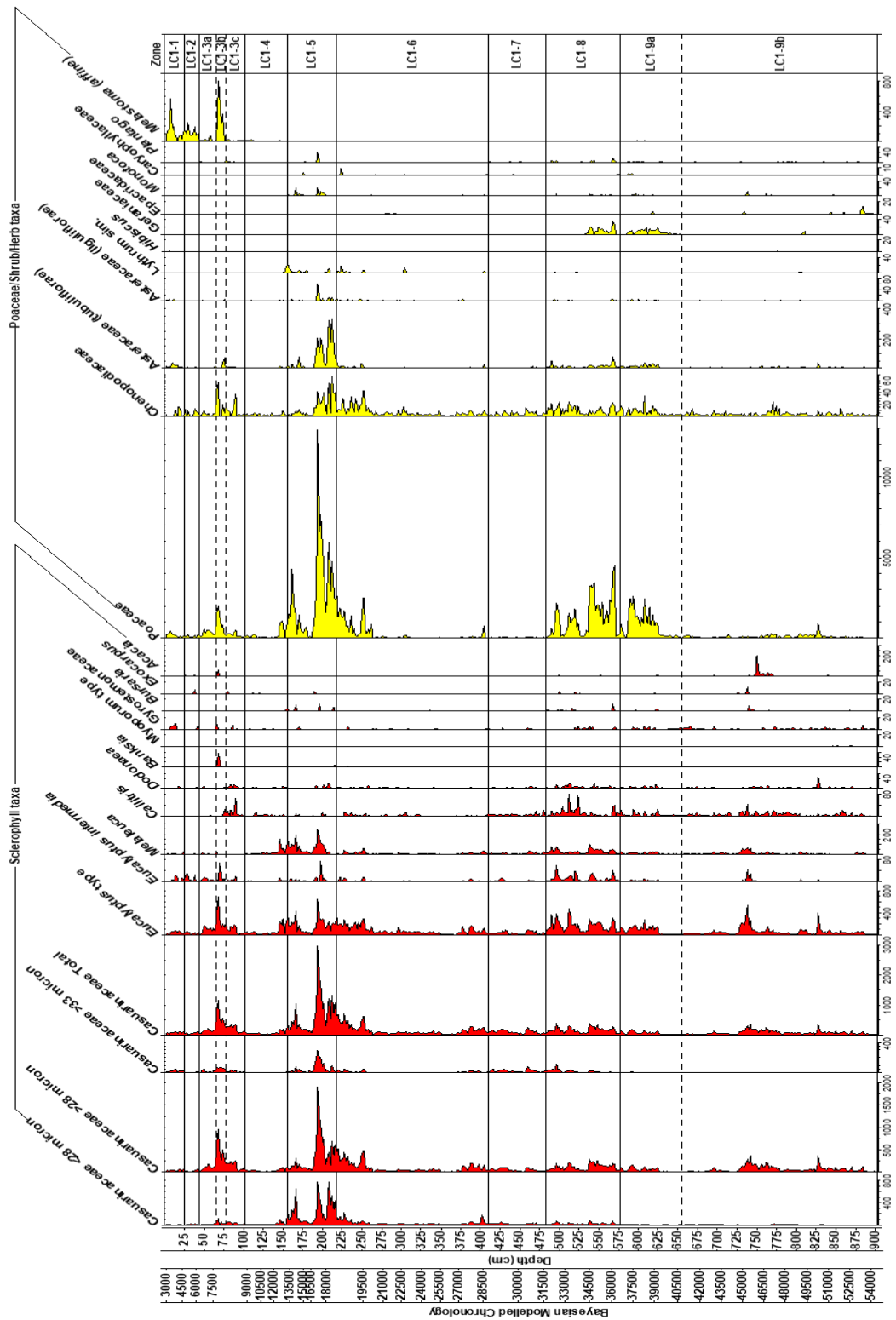


Figure 7.16. Dryland influx sclerophyll taxa, Poaceae, shrub and herb taxa diagram with percentage dryland pollen sum zoning.

7.2.3. Charcoal representation

The two categories of charcoal (macroscopic and microscopic) are generally considered separately as there are distinct differences in their representation and also because different elements (size, shape and observational data) are utilised in their analysis (Figure 7.18). However, where appropriate, they will be discussed together.

7.2.3.1. Macrocharcoal representation

Macrocharcoal values are low through zone LCA–F (dryland pollen *sub-zone* LC1–9b) although there are isolated spikes, especially at the base and towards the top of the zone. Of interest is that the spike near the base of the zone sees ‘blocky’ and ‘elongated’ charcoal values on par, which is an uncommon occurrence as ‘elongated’ charcoal is the dominant type through most of the record. Charred sedge nuts, likely to be from *Schoenoplectus mucronatus* (Plate 7.7 a), as well as woody fragments with some charreing are also present. Brown charcoal is evident in all but the middle of the zone. Through this zone macro- and microcharcoal have a similar patterning.

Zones LCA–F–E2/E1 (dryland pollen zones LC1–9a–LC1–7) record a significant rise in macrocharcoal values. The sub-zone E2, although dominated by ‘elongated’ charcoal, ‘lattice’ charcoal records similar values in places. From the middle to the top of this sub-zone charred seeds both whole and fragmented, are found and identified as *Liparophyllum exaltatum* (formerly *Villarsia exaltata*) and *Nymphoides indica* (Plate 7.7 b and c). Sub-zone E1 sees a further increase in charcoal across all components with charred sedge nuts and charred *Persicaria strigosa* seeds also present (Plate 7.7 d). Macrocharcoal records its highest values (5,110 particles per 4 cm³) near the base of zone LCA–D but significantly lower values are recorded in the middle to the top of the zone.

Brown charcoal is present through most of the zone LCA–F but relatively low except near the base and top of the zone. Through sub-zone E2 and E1 brown charcoal is relatively low except through to the top of sub-zone E2 (dryland pollen zone LC1–8).

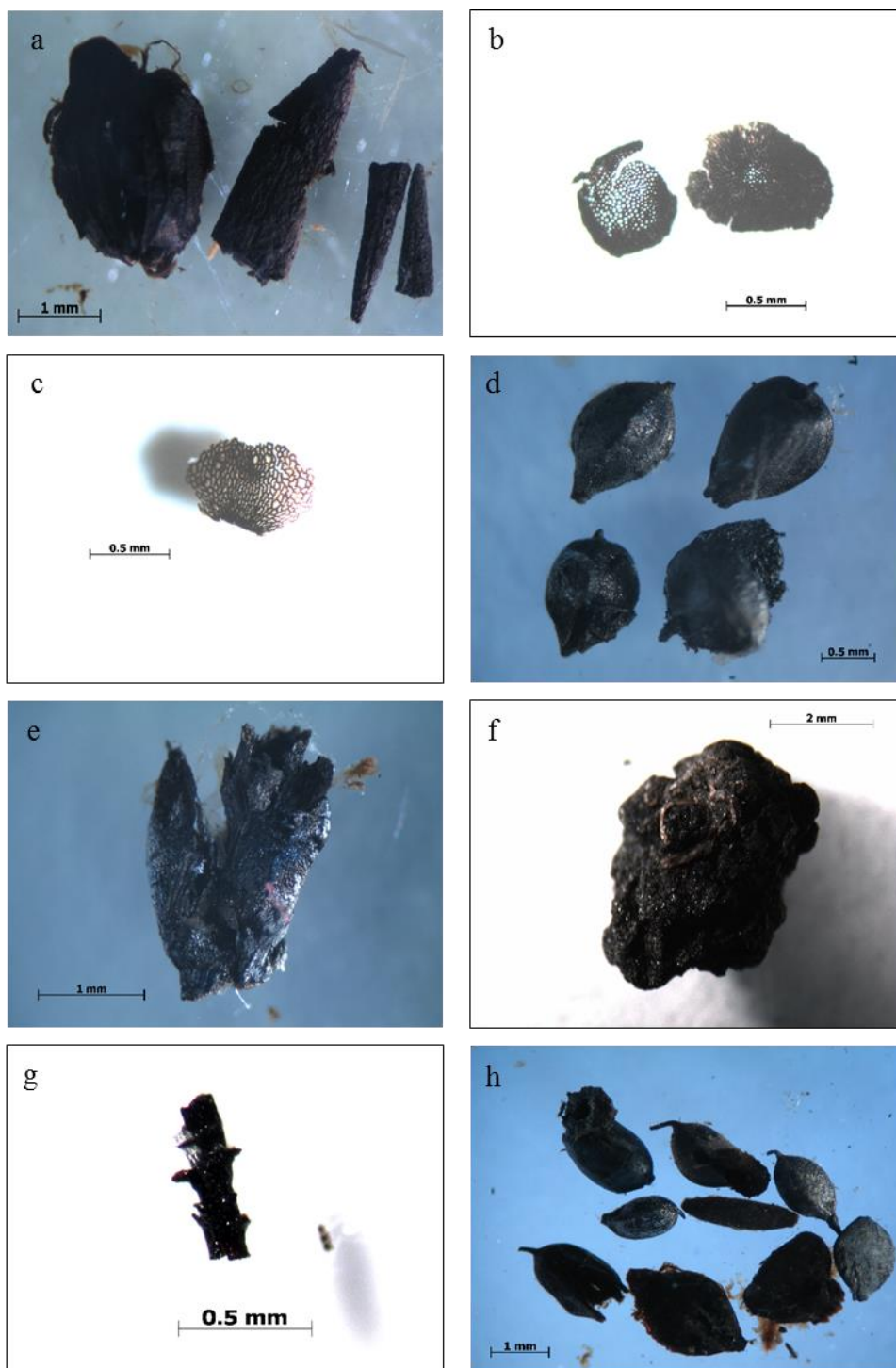


Plate 7.7. Charred remains recorded in zone LCA-F, sub-zone LCA-E1, sub-zone LCA-E2 and LCA-D. (a) - charred *Schoenoplectus* nut with other charred plant remains, (b) - *Nymphoides indica*, (c) - *Liparophyllum exaltatum*, (d) - ? *Carex* spp., nuts, (e) - sedge plant remains, (f) - peat, (g) - *A.pinnata* fragment, (h) - a number of different sedge species (*Schoenoplectus*, *Carex*, *Cyperus*), *Typha* and *Lipocarpa* (364 cm).

Charred seeds and nuts are rare through zone LCA-F but are consistently present through sub-zones *E2* and *E1* and at times are quite abundant especially at 364 cm, 464 cm and 466 cm where multiple species are found, *P. strigosa*, several different sedges (*Carex*, *Eleocharis*, *Lipocarpa microcephala*) and *Typha domingensis*.

At the top of the zone LCA-D the charred sedge nut is *Eleocharis* but also present is charred peat and of particular interest is the presence of charred *Azolla pinnata* fragments (Plate 7.7 e-h). High macrocharcoal values are present at the base of the zone LCA-D (dryland zone LC1-6) which sees relatively low brown charcoal values which increase once macrocharcoal values are reduced. Low macrocharcoal values are recorded through zone LCA-C (dryland pollen zones LC1-5 and part of LC1-4) except at the very top although 'other' charcoal values are relatively constant. Brown charcoal abundance is low except towards the top of the zone. Charred seeds and fragments identified as *N. indica* are present near the base, in the middle and at the top of the zone. High values are recorded across all the charcoal components in zone LCA-B (dryland pollen zones LC1-4 and LC1-3), especially for 'lattice' which records its highest values in this zone (Plate 7.8. a-b).

Brown charcoal is consistently present with higher values from the base to the middle of the zone LCA-B. Charred seeds and attached epidermis are present from the base to the middle while woody fragments and sedges are present from the middle and towards the top of the zone, where there is also extensive evidence of charred pollen grains. Through zone LCA-B the patterning of microcharcoal representation is the complete opposite to the macrocharcoal trend. It is also interesting to note that the charred woody fragments are present when microcharcoal rather than macrocharcoal increases. In zone LCA-A (dryland pollen zones LC1-2 and LC1-1) all macrocharcoal values, except 'lattice', have increased substantially from the previous zone although at the top low values are recorded. 'Elongated' charcoal has dominated all previous zones with counts usual double to triple those of the other components but 'blocky' charcoal counts through this whole zone are, on average, double those of 'elongated' charcoal (Figure 7.18). Brown charcoal has high values near the base of the zone but is low to absent through the rest of the zone. Charred seeds are present near the top of the zone with some identified as the sedge nut, *Cyperus polystachyos*, but others remain

unidentified. Unlike macrocharcoal, microcharcoal continues with high values to the top of the zone.

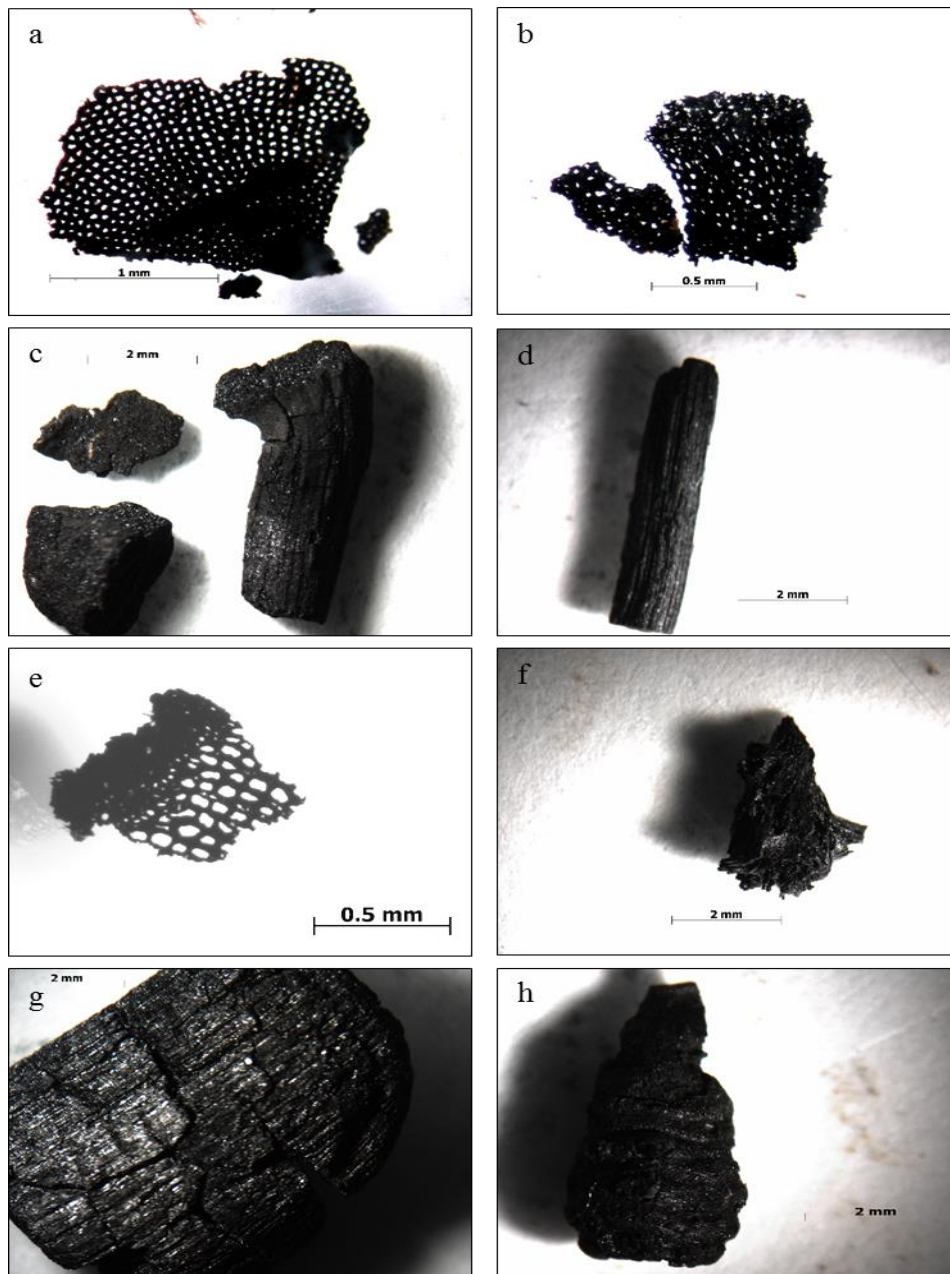


Plate 7.8. Lattice-type charcoal zone LCA-B, (a) – Lattice-type charcoal single epidermis layer, (b) – Lattice-type charcoal double epidermis layer, (c) - Woody/sedge fragments, (d) - Sedge stem, (e) - Epidermis ? *Typha* (see Figure 5.10 3b), (f) – Woody and sedge remains, (g) - Woody remains, (h) - Flowering or seed head of sedge.

7.2.3.2. Microcharcoal representation

Microcharcoal values (10,000–300,000 particles per cm³) are extremely low through the dryland pollen zone LC1–9 with isolated peaks corresponding to the macrocharcoal patterning, although by the top of the *sub-zone 9a* values have increased to 2,815,697 particles per cm³. This increase has been mainly generated by the smaller size fractions (8–52 µm and 53–104 µm). Microcharcoal values continue to increase through zone LC1–8 and, unlike the macrocharcoal trend, is not spiky although this changes in zone LC1–7 where microcharcoal values are lower and have a similar patterning to the macrocharcoal trends. Microcharcoal values (2,888,075–4,638,246 particles per cm³) are relatively more consistent through zone LC1–6 although extremely low values (< 200,000 particles per cm³) are recorded towards the middle. This marks the end of extremely high macrocharcoal values. Lower values are recorded through zone LC1–5 with some correspondence to the macrocharcoal patterning especially the larger size fractions (105–156 µm and 156–208 µm) but by zone LC1–4 all microcharcoal size fractions follow the macrocharcoal patterning (Figure 7.18).

This correlation to the macrocharcoal patterning continues through to sub-zone *LC1–3c* but through sub-zones *LC1–3b* and *LC1–3a* extremely high values (10,625,605 per cm³) are recorded, especially through sub-zone *LC1–3a*, unlike the macrocharcoals where counts are low. Microcharcoal values are slightly reduced through zone LC1–2 except for the larger size fractions (105–156 µm and 156–208 µm) which have a similar patterning to the macrocharcoal trends. The high microcharcoal values in zone LC1–1 are on par with those found in sub-zone *LC1–3a*. These high values persist through the whole zone unlike macrocharcoal where high values are only recorded from the base to the middle of this zone.

7.2.4. Influx patterning

As in previous result presentations the aquatic and swamp taxa and dryland taxa will be examined within their respective zones but where appropriate both will be discussed together. Although the concentration patterning for both macro- and microcharcoal did not vary significantly from the influx patterning, towards the top of the record more variability was present and reasons for this will provide a focus for discussion (Figures 7.12-18).

7.2.4.1. Aquatic and swamp taxa influx patterning

The greatest difference between the patterning of the percentage and influx through the aquatic and swamp diagram is mainly related to Cyperaceae (Figure 7.4). It is the dominant taxon on the swamp, but the influx patterning suggests there is a greater pronounced variability than that evident in the percentage curves. Influx values are generally low (200 grains per $\text{cm}^{-2} \text{ yr}^{-1}$) through zone LCA-F, except for *Leptospermum* and the two swamp Myrtaceae where influx values are $> 11\,200$ grains per $2 \text{ cm}^{-2} \text{ yr}^{-1}$ at times, although higher values are recorded intermittently for the majority of the taxa present. The high influx values for both *Leptospermum* and the two swamp Myrtaceae suggest that both are close to the coring site and likely influencing (blocking) the pollen signal of the other swamp taxa. Consistently higher influx values are recorded through the sub-zone LCA-E2 and partly into the sub-zone LCA-E1 with the influx patterning more aligned with the percentage curves. High inorganic values are also recorded at these times. Extremely low influx values are recorded for all taxa through most of the zone LCA-D with Cyperaceae and *Nymphoides* the main contributors to the high values at the top of the zone. As in zone LCA-E high influx values recorded in zone LCA-C at times up to $5,000$ grains per $2 \text{ cm}^{-2} \text{ yr}^{-1}$ corresponds with high inorganic values. In previous zones the influx patterning for Cyperaceae and Poaceae was similar but through LCA-C they have opposite trends. Relatively low influx values are recorded through LCA-B although higher values are recorded towards the top of the zone with Cyperaceae, *Haloragis*, *Hydrocotyle* and *Anthoceros* the main contributors.

7.2.4.2. Dryland taxa influx patterning

In most cases the percentage and influx patterning is similar although the influx curves are spiky, likely influenced by the changing sedimentation rates. However, the major sclerophyll components, Casuarinaceae, *Eucalyptus* type, *Corymbia* and *Melaleuca*, would seem to go against this trend with Casuarinaceae and the sclerophyll Myrtaceae types seeming to have opposite trends in their percentage curves, except from zone LC1–3 to LC1–1, whereas the influx curves for all sclerophyll components are similar. It is likely that the extremely high influx values mute any differences, especially for Casuarinaceae, as the Casuarinaceae and *Eucalyptus* ratios for percentage and influx were the same. In zone LC1–9 dryland influx values are extremely variable across all components but there is a similar influx patterning across all taxa, that is relatively low near the base and top of the zone and higher values in the middle of the zone. This patterning is especially obvious for the major sclerophyll components and the rainforest gymnosperms except for *Podocarpus* near the base where high influx values are recorded. The influx values for the rainforest angiosperms through LC–9 are not as erratic as for the sclerophylls with the rainforest canopy the highest contributor. The sclerophyll taxa influx values fluctuate through zone LC1–8 although the sclerophyll Myrtaceae types influx patterning is considerably spiky while the rainforest angiosperms influx values fluctuate at a lower level than those of the sclerophyll Myrtaceae types. This spiky pattern present for the sclerophyll Myrtaceae is also present for some of the vine taxa—*Hypserpa*, *Stephania* and *Morinda*.

Influx values are low through zone LC1–7 with Casuarinaceae the major contributor for the sclerophyll component, followed by *Eucalyptus* type. The influx values for the rainforest angiosperms are extremely low through this zone while influx values for the rainforest gymnosperms are even lower with *Podocarpus* the major contributor. These low influx values continue through to zone LC1–6 except near the top of the zone where higher influx values are present especially for *Eucalyptus* type, Casuarinaceae and Chenopodiaceae. Higher values are recorded for some rainforest canopy taxa especially *O. paniculata* and *Syzygium* comp. and the secondary rainforest taxa, *Celtis*, *Trema* and *Melicope*. Higher influx values continue through to the middle of the zone LC1–5 with Casuarinaceae having its highest values through this period as does Poaceae, Asteraceae (tubuliflorae), and *O. paniculata*. Isolated spikes are also present for other rainforest taxa, *Argyrodendron* comp.,

Sapindaceae (syncolpate), and *Dacrydium* and the sclerophyll fern, *Pteridium* as well as the monolete (psilate) ferns. Influx values are reduced by the top of the zone except for the sclerophyll components where influx values remain high.

All influx values are reduced in zone LC1–4 with influx values for Casuarianaceae and the sclerophyll Myrtaceae taxa on parity. Low influx values continue for the major sclerophyll components through sub-zone LC1–3c but slightly higher values are recorded for *Callitris* and *Dodonaea*. Slightly higher influx values are recorded for the rainforest angiosperms especially *Trema* through this sub-zone. Through sub-zone LC1–3b extremely high influx values are recorded for the rainforest angiosperms, especially for the canopy species, Cunoniaceae (tricolpate and dicolpate), *Elaeocarpus*, *Acmena*, *Syzygium*, *Ficus*, *Flindersia*, *Ilex* and *Rhizophora* while for the secondary and understorey species extremely high values are recorded for *Glochidion* and *Rapanea*. The major sclerophyll components influx values are also higher although not to the same degree as the rainforest angiosperms. All influx values are reduced through sub-zone LC1–3a but especially for the rainforest angiosperms which is on parity with the sclerophylls. These relatively low values continue through zones LC1–2 and LC1–1 for the sclerophylls whereas the rainforest angiosperms continue with higher values through these zones but for the canopy component not at the same degree as seen in sub-zone LC1–3b.

7.2.4.3. Charcoal influx patterning

Throughout most of the record there is a similar patterning across the concentration and influx records for both the macro- and microcharcoal except towards the top of the record. Between ~21,000 yrs BP–19,500 yrs BP the microcharcoal influx pattern shows high and consistent values in contrast to a spiky pattern for the concentration record. For the period ~9,000 yrs BP–~8,000 yrs BP the microcharcoal influx pattern is high in the dryland pollen sub-zone LC1–3c whereas the concentration pattern is high later, in dryland pollen sub-zone LC1–3b. The influx pattern for macrocharcoal between ~13,000 yrs BP and 12,000 yrs BP is relatively high while the concentration pattern is significantly higher. This pattern is also recorded at ~6,000 yrs BP where the concentration pattern is significantly higher than the influx pattern (Figure 7.18).

7.2.5. Non-quantified observational data and target counts

Although non-quantified data cannot be statistically quantified it may indicate where problems may be occurring such as where oxidation and drying conditions are prevalent may have resulted in degraded and corroded pollen grains. Similarly, aberrant grains in some taxa such as stephanoporate (4-pored) or diporate (2-pored) Myrtaceae and Casuarinaceae may be associated with specific species types or may indicate unusual flowering conditions (Thornhill 2010; Thornhill et al. 2012*a,b*). Pollen clumping (aggregation of pollen grains adhering or clumping together) is a relatively common phenomenon and, when consistently present, it may also indicate a more local presence for dryland taxa considered to have an extra-local to regional signal. Targeted pollen counts for the dryland sum were met 96% of the time. Where they were not met may indicate either the presence of dense local swamp and aquatic taxa or that conditions were not conducive for pollen preservation. Table 7.2 summaries the non-quantified observational data and target counts with full details given in Appendix B, section 1.

Table 7.2. Non-quantified observational data and target counts (TC), N/O-nil observed (for full details see Appendix B)

Zones/sub-zones	TC (%)	Corroded/Degraded	Clumping
LC1-9	92%	Casuarinaceae, <i>Araucaria</i> , <i>Dacrydium</i>	<i>Podocarpus</i> , <i>Araucaria</i> , <i>Dacrydium</i> , Casuarinaceae, <i>Eucalyptus</i> , <i>Melaleuca</i> , <i>Callitris</i> , <i>Dodonaea</i> , <i>Syzygium</i> , <i>O. paniculata</i> , <i>Ilex</i> , <i>Elaeodendron</i> , <i>Dissilaria</i> , Sapindaceae, Urticaceae
LC1-8	100%	<i>Dacrydium</i> , <i>Podocarpus</i> , Proteaceae, <i>Argyrodendron</i>	Myrtaceae, <i>Podocarpus</i>
LC1-7	95%	Myrtaceae and unspecified	Casuarinaceae, Myrtaceae
LC1-6	95%	Casuarinaceae, Myrtaceae, Cunoniaceae, <i>Araucaria</i> , <i>O. paniculata</i> , <i>Acmena</i>	Casuarinaceae, Myrtaceae, <i>Podocarpus</i> , <i>Syzygium</i> , <i>O. paniculata</i>
LC1-5	100%	<i>Argyrodendron</i> , <i>Podocarpus</i> , <i>Dacrydium</i>	Myrtaceae, esp. <i>Eucalyptus</i> , Casuarinaceae, Asteraceae (tubuliflora and liguliflora)
LC1-4	100%	Myrtaceae	Myrtaceae, Casuarinaceae, Ferns
LC1-3c	100%	Casuarinaceae, <i>Hibbertia</i> , <i>Dodonaea</i> , <i>Acmena</i> , Ferns	Myrtaceae, Casuarinaceae, Ferns
LC1-3b	100%	Casuarinaceae, Myrtaceae, <i>Melastoma</i>	Myrtaceae (unspecified), <i>Acmena</i> , Ferns
LC1-3a	100%	Myrtaceae, <i>Ficus</i> , Casuarinaceae, <i>Dacrydium</i> , <i>Rapanea</i> , <i>Dodonaea</i> , Ferns	Myrtaceae (unspecified), <i>Acmena</i> , Ferns
LC1-2	100%	N/O	<i>Acmena</i> , Cunoniaceae, <i>Syzygium</i> , Ferns
LC1-1	100%	N/O	<i>Archontophoenix</i> , <i>Macaranga</i> , Rubiaceae, <i>Melastoma</i> , Ferns

Chapter 8

Statistical Analysis

Introduction

This chapter presents the results of statistical analyses undertaken on various constructed data sets. Principle component analysis (PCA), an ordination technique, has been executed on the percentage and influx data across both the dryland pollen sum and aquatic and swamp pollen sum. In an attempt to reduce the influence that more abundant taxa may have had on the results, the data was compartmentalised into time-periods, Full record (3–54 ka), Pleistocene (11.8–54 ka) and Holocene (3–11.7 ka), within each pollen sum (dryland and aquatic and swamp). This was also intended to assist in the interpretation of data presented in the previous chapter. This compartmentalization was also implemented for Spectral Analysis although the requirement of a minimum sample number (100) for this analysis meant that it was not possible for the Holocene period and therefore this time-period was extended into the Pleistocene until 100 samples had been achieved. Preliminary discussion of the results is presented after each analysis.

8.1. Principle Component Analysis (PCA)

PCA is widely used in palaeoecology with the first factor providing the greatest variance. This is followed by the second factor and so on with each factor completely independent of or uncorrelated with the following factor. The eigenvalues, the proportion of variance accounted for by the correlation between the respective taxa, not only determine the factor coordinates of the taxa and samples, they inform about the variance that can be explained by the given number of factors. The eigenvalues also provide information on how far one can reduce the dimensions of the original space of taxa and samples without losing important information (Jambu 1991). There are a number of approaches to determine the number of eigenvalues that are interpretable. The broken-stick method takes eigenvalues from random data and if the total variances is randomly divided amongst the various components the expected distribution of the eigenvalues will follow a broken-stick distribution. Those observed eigenvalues that exceed the eigenvalues generated by the broken-stick model are considered interpretable (Jackson 1993; Legendre and Legendre 2012). The scree method sees the plotting of values of each successive eigenvalue against the rank order. The point where the eigenvalue departs from the straight line of the smaller eigenvalues is the point where interpretation is considered valid (Jackson 1993). The

broken-stick method is considered to correctly assess the dimensionality of the data (Jackson 1993) although it is suggested that there is the possibility that it underestimates the number of eigenvalues that are interpretable (Legendre and Legendre 2012) and this may become more pronounced the larger the dataset (Caron 2016). The scree plot method can overestimate the number of eigenvalues that are interpretable (Legendre and Legendre 2012) although if applying Cattell's (1966) original criterion - points to the left of the straight line segment – results are more conservative (Jackson 1993). A scree plot will be provided for each section with Cattell's (1966) original criterion in place.

The gradient and axis length can be assessed for linearity with detrended correspondence analysis (DCA) with recommendations that this should be < 4 Standard Deviation (SD) (ter Braak and Šmilauer 2002; Lepš and Šmilauer 2003). Although still interpretable, it has been advocated that the analysed data needs to be linear for PCA to be an effective and informative summary of the data (Hill and Gauch 1980; Birks 1985; Oksanen and Minchin 1997).

Grimm et al. (2011) utilized the correlation matrix on their multi-proxy study (pollen, minerals and charcoal) where reconstruction of the palaeoclimate and landscapes over both long and short-term was investigated. The vegetation dynamics and influences over varying time-periods was of particular interest in this study so the correlation matrix was utilized. When using the correlation matrix, the factor coordinates for the taxa indicate the greatest correlation between taxa with an axis limit of -1 and 1, so taxa closest to either -1 or 1 are the major contributor to that factor. The factor coordinates of the samples are not correlations rather it is the relative magnitude of the samples so those with the largest contribution are the main control of the construct of that factor which limits the merging of biplots for the taxa and samples as there is no axis limit for samples and therefore separate biplots are used for taxa and samples (Jambu 1991; Statsoft 2011).

PCA was also executed on the time-period (28,500 yrs B.P.–37,900 yrs B.P.), covering humification analysis on the aquatic and swamp taxa for the percentage data. Bennett and Hicks (2005) suggest that influx data tends to have only positive values and that it is primarily separating the high influx values from the low influx values and therefore PCA will not be undertaken on the influx data in this study. For PCA the aquatic and swamp

pollen sum was re-summed to 100% to include both Poaceae and *Botryococcus*. It is likely that Poaceae, at times, was a component of the swamp and the continuous presence of the aquatic alga *Botryococcus* suggests it may also have had an important role within the aquatic and swamp environment. The taxa to be included in the analysis was dependent on the time-period analysed with only those with a major representation and those that had a relatively constant representation being included. This would lessen the problem of magnification of noise in uncommon taxa which may present a problem when using the correlation matrix (Jambu 1991; Jolliffe and Cadima 2016).

To test whether the data was linear, DCA was performed on all time sequences to be analysed and all had gradient lengths < 4 SD. The statistical software, STATISTICA (StatSoft, Inc. 2011) used for PCA in this study allowed taxa to be omitted from the primary analysis but included as supplementary taxa. The supplementary taxa have reference to the same context as the active taxa so can then be placed within the ordination for the purpose of interpretation. A number of supplementary taxa were used in this analysis, especially the charcoals, and are noted in the relevant sections. They will be identified with red lines and pointers. STATISTICA also provided statistical tables and graphs, with the scree plot and biplots for the first two factors for the taxa provided in this chapter. Also in this chapter are the biplots for the samples which were executed in Microsoft Excel. The statistical results for the eigenvalues of the correlation matrix and the factor coordinates of the variables are found in Appendix B, Section 2 (Jambu 1991; Grimm et al. 2011).

8.1.1. PCA of the aquatic and swamp percentage data (Full record 54,000 yrs BP–3,000 yrs BP).

The scree plot suggests that the first four eigenvalues (Figure 8.1) are the main contributors (58.12%) for the interpretation of the data. The number of eigenvalues are dictated by how many active taxa are included in the dataset, so 12 active taxa = 12 factors. F1 (Figure 8.2) shows the major separation is the positive correlation of Poaceae and *Botryococcus* followed by *Persicaria*, *Typha*, *Liparophyllum* and *Nymphoides* from the negative *Haloragis* and *Hydrocotyle* followed by *Anthoceros* with Cyperaceae close to zero. The supplementary moisture, inorganics, sponge spicules and to a lesser degree macro'lattice' are aligned positively with Poaceae while microcharcoal, macro'blocky'.

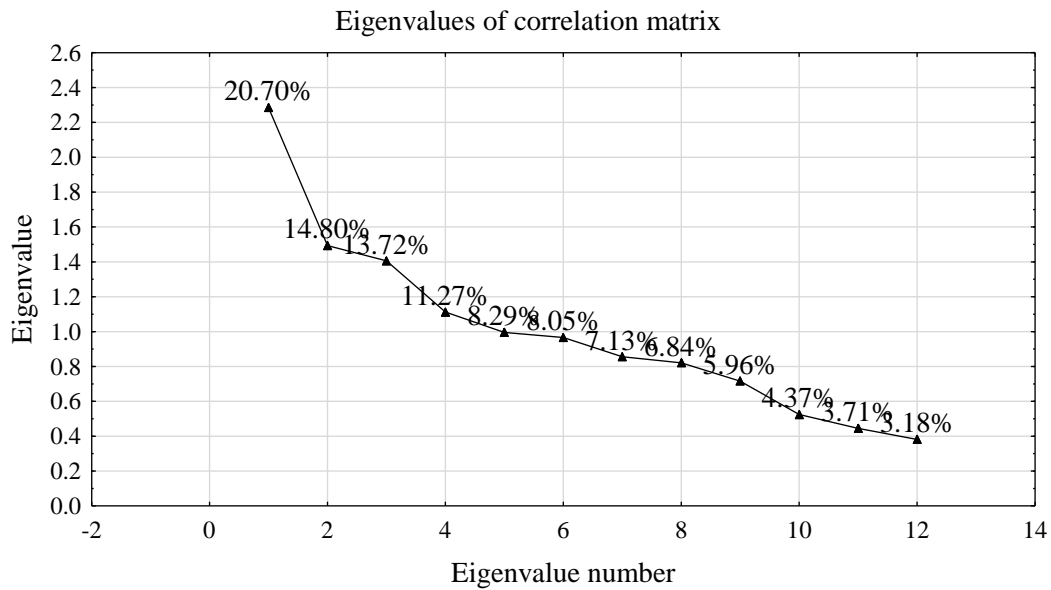


Figure 8.1. Scree plot of the eigenvalues of the correlation matrix of the active taxa for the aquatic and swamp percentage data (Full record 3 ka–54 ka).

and macro'other' are aligned negatively with *Haloragis* and *Hydrocotyle*. *Neurospora*, *Gelasinospora* and macro'elongated' are close to the centre. This would suggest a separation of stable swamp taxa, *Haloragis* and *Hydrocotyle*, from the more variable conditions indicated by Poaceae, and, although the aquatics *Liparophyllum* and *Nymphoides* are aligned with Poaceae they also indicate an element of change that would affect other aquatic and swamp taxa.

F2 still sees separation of Poaceae alongside *Liparophyllum*, *Anthoceros* and to a lesser degree *Nymphoides* from *Botryococcus*, *Typha* and *Persicaria* with *Haloragis*, *Hydrocotyle* and Cyperaceae having no influence in these correlations. Nearly all the taxa with high values, positive and negative, for F2 indicate some level of fluctuating conditions so could suggest a separation of local changing conditions, *Typha* and *Persicaria*, from a wider regional variability, Poaceae, *Liparophyllum* and *Nymphoides*. The charcoal types would support this scenario with macrocharcoal aligned with the local taxa (*Persicaria* and *Typha*) and microcharcoal aligned with the more regional taxon (Poaceae).

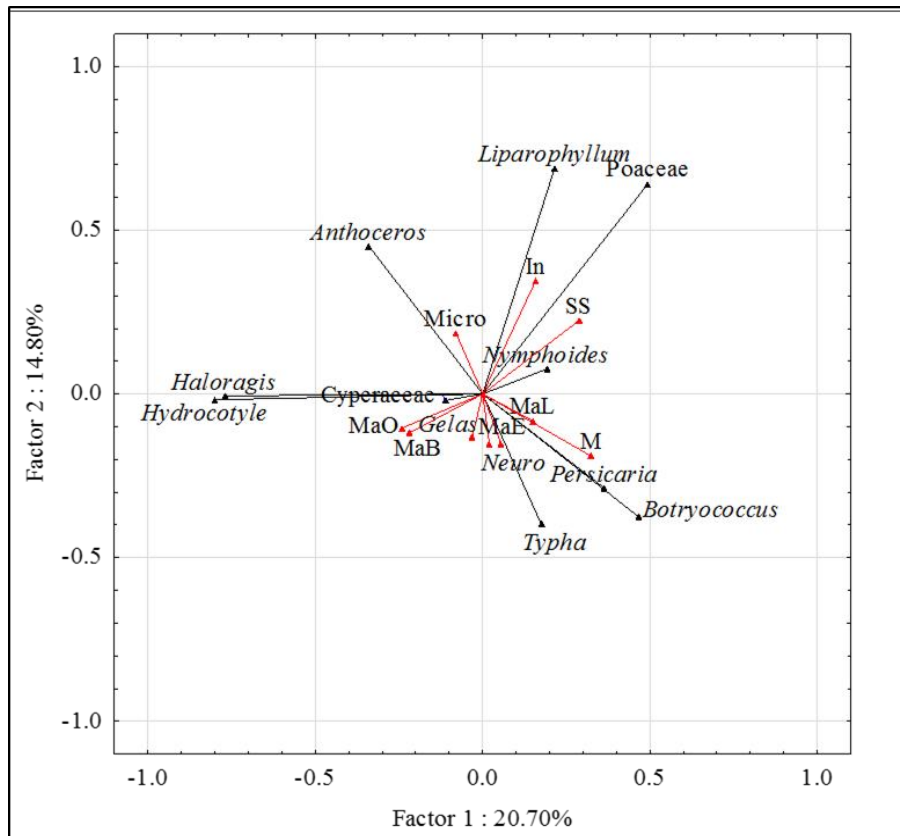


Figure 8.2. Projection of the taxa on F1 and F2 for the aquatic and swamp percentage data, full record. Abbreviations are given for supplementary variables:- MaE-macrocharcol ‘elongated’, MaB-macrocharcol ‘blocky’, MaL-macrocharcol ‘lattice’, MaO-macrocharcol ‘other’, Micro-microcharcol, In-inorganics, M-moisture, Gelas=*Gelasinospora*, Neuro=*Neurospora*, SS-Sponge spicules.

Projection of the samples (Figure 8.3) shows that primarily the separation is centred on zone F, where relatively stable conditions are present with *Haloragis* and *Hydrocotyle* prominent and on zones A and B, separated from zones E2 and C where changing water levels are indicated by the presence of the aquatics *Liparophyllum* and *Nymphoides* while zones E1 and D are characterized by dry conditions and the continual presence of both local and regional fire with *Persicaria* and *Poaceae* prominent.

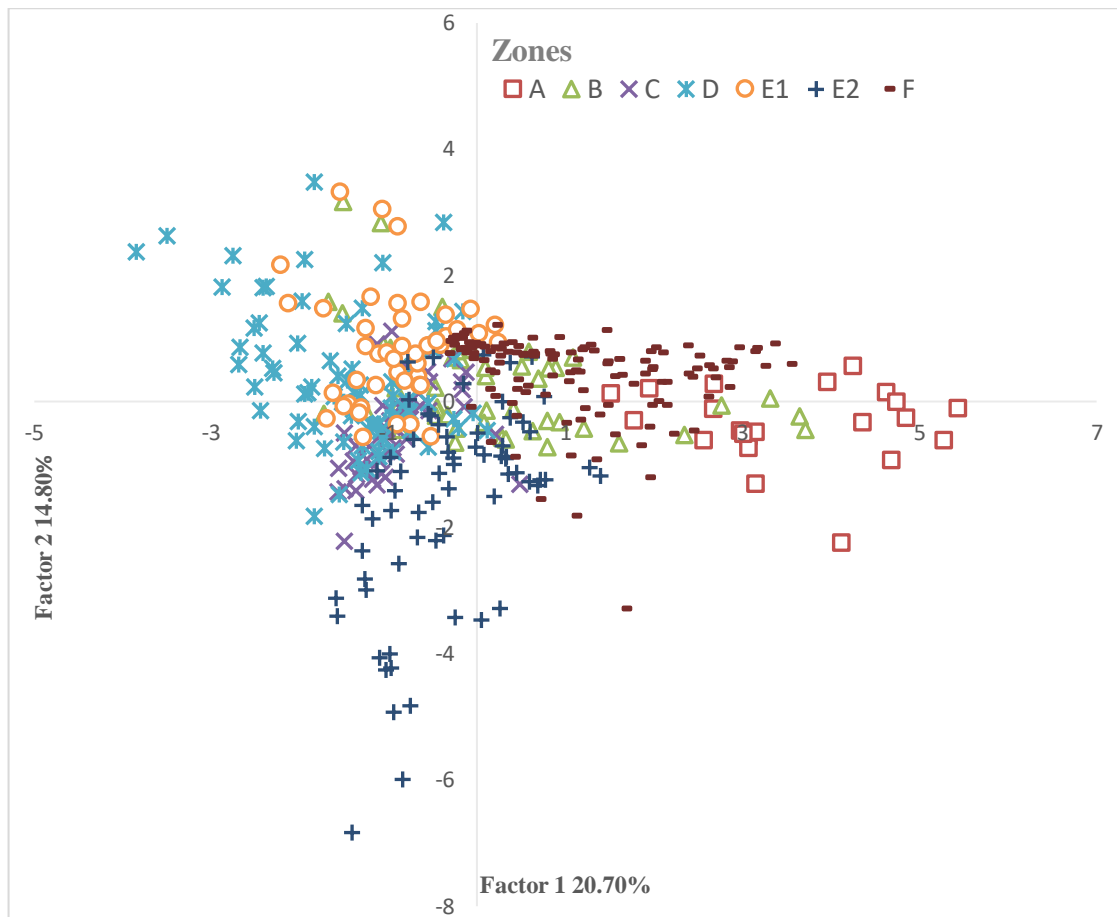


Figure 8.3. Projection of samples on F1 and F2 for the aquatic and swamp percentage data, full record.

8.1.2. PCA of the dryland percentage data (Full record 54,000 yrs BP–3,000 yrs BP).

The scree plot (Figure 8.4) suggests that the first four eigenvalues are the major contributors (58.03%) for the interpretation of the data. F1 (Figure 8.5) shows that the greatest variance is from the wetter rainforest taxa, Cunoniaceae-tricolpate and dicolpate, *Ficus*, *Elaeocarpus*, *Glochidion* and *Rapanea* which are primarily separated from the sclerophyll taxa, *Eucalyptus* and Casuarinaceae, so essentially a separation of wet from dry. The alignment of both charcoal fractions with the wetter rainforest taxa seems counter-intuitive but fire is a major factor when these wetter elements are present. F2 is primarily the separation of the drier rainforest taxa, *Araucaria*, Podocarpaceae and *A. peralatum* from the sclerophyll taxa.

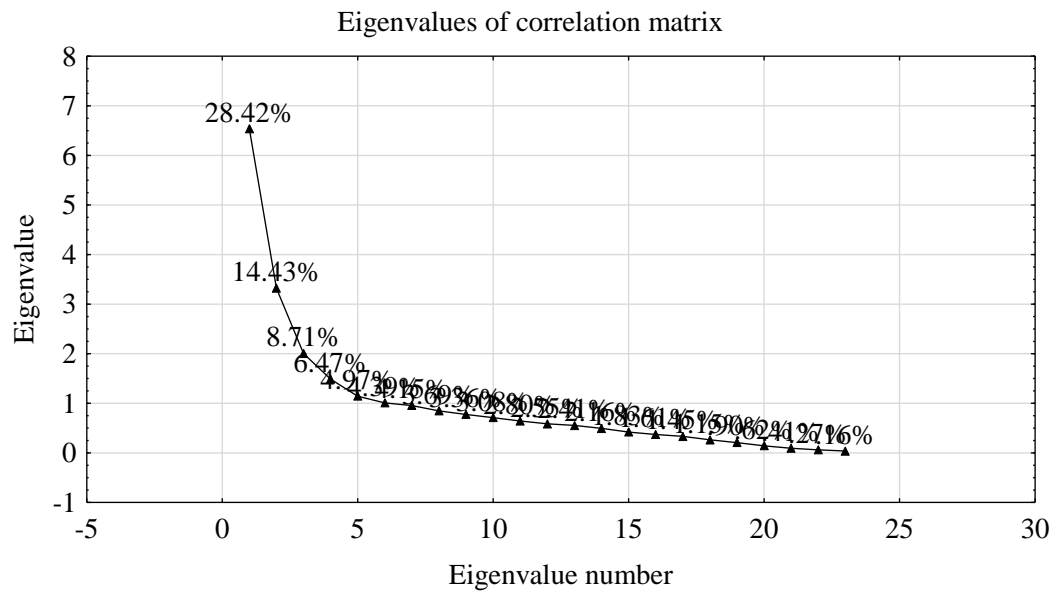


Figure 8.4. Scree plot of the eigenvalues of the correlation matrix of the active taxa for the dryland percentage data (Full record).

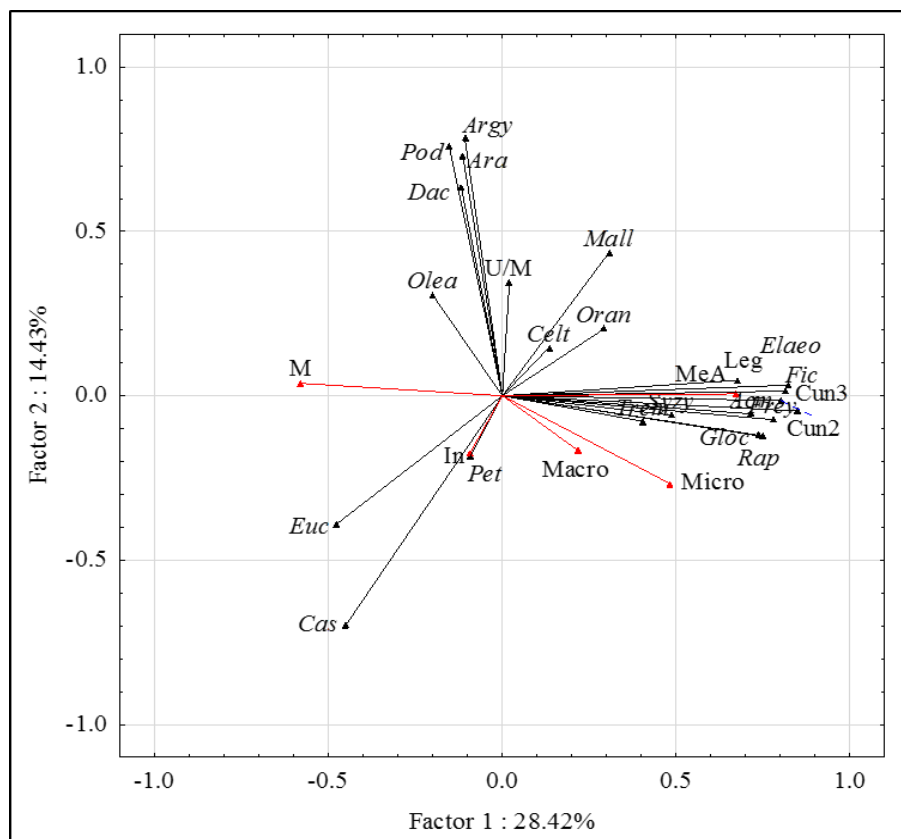


Figure 8.5. Projection of the taxa on F1 and F2 for the dryland percentage data, full record. *Cas*-Casuarinaceae, *Euc*-Eucalyptus, *Pet*-Petalostigma, *Aga*-Agathis, *Arau*-Araucaria, *Pod*-Podocarpus, *Dac*-Dacrydium, *Argv*-A. peralatum, *Syz*-Syzygium, *Elaeo*-Elaeocarpus, *CunT*-CunoniaceaeTricolpate, *CunD*-CunoniaceaeDicolpate, *Fic*-Ficus, *Mall*-Mallatus, *Celt*-Celtis, *Olea*-*O. paniculata*, *Trem*-Trema, *Leg*-Leguminosae, *U/M*-Urticaceae and Moraceae, *Gloc*-Glochidon and supplementaries *In*-inorganics, *Micro*-microacharcoal, *Macro*-macrocharcoal, *M*-moisture and *MeA*-Melastoma affine.

The projection of the samples (Figure 8.6) shows the major construct of F1 is the separation of zones 1, 2, 3*b* and to a lesser degree zones 3*a* and 3*c*, all situated within the Holocene, while F2 sees a separation of zones 9*a* and 9*b* with some overlap with zone 1 from all other zones. Clearly the projection of the samples is showing a separation of the Holocene (zones 1, 2, 3*a*, 3*b*, 3*c* and 4) from the late Pleistocene (zones 9*a* and 9*b*). That the majority of zone 1 is in the same vector space as zone 9*a* and 9*b* on F2 could indicate some similarity within these disparate time-periods.

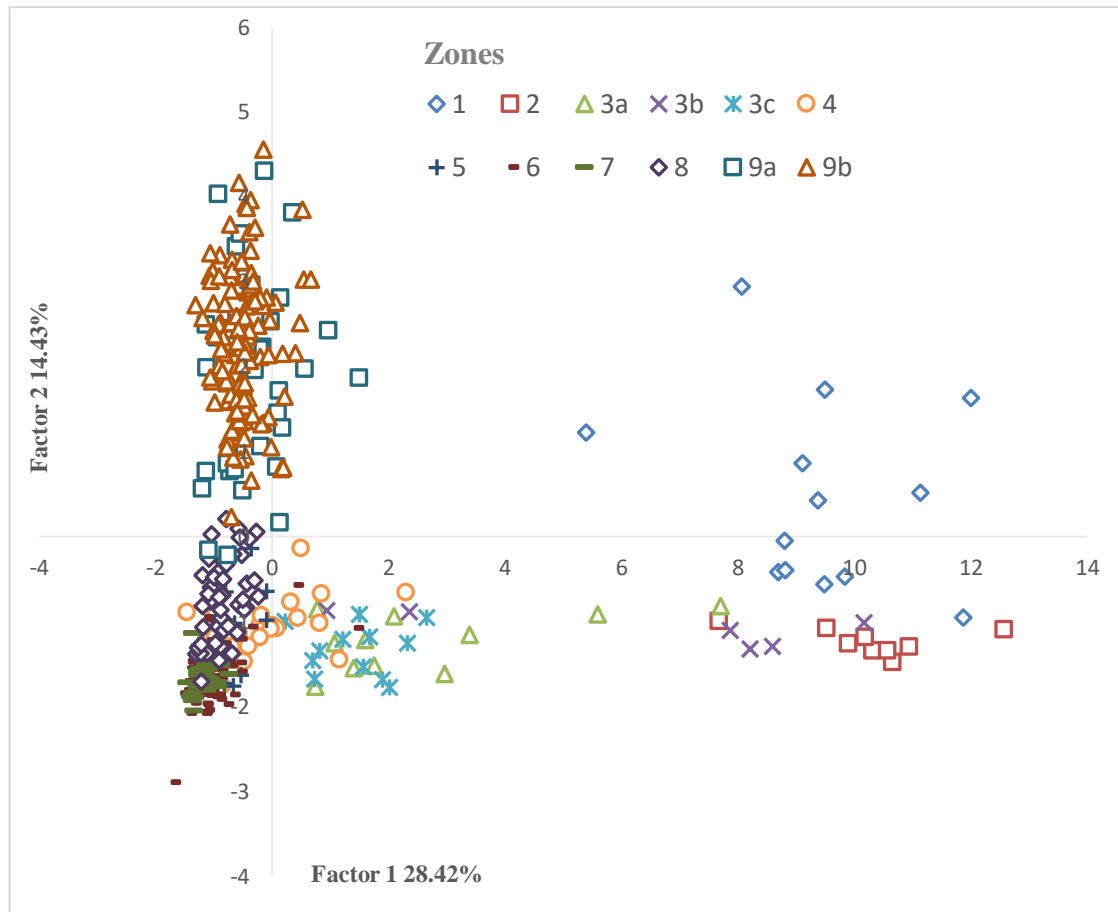


Figure 8.6. Projection of samples on F1 and F2 for the dryland percentage data, full record.

8.1.3. PCA of the aquatic and swamp percentage data (Pleistocene record 54,000 yrs BP–11,800 yrs BP)

The scree plot (Figure 8.7) show that the first four eigenvalues (49.60%) are the major factors for interpretation of the variance in the data. As previous, supplementary taxa have been utilized in this analysis. F1 (Figure 8.8) sees a separation of primarily *Poaceae* and *Botryococcus*, followed by the sedges *Baumea* and *Eleocharis*, *Persicaria*, and to a lesser extent *Nymphoides*, *Liparophyllum* and *Typha* (all positive) from *Hydrocotyle* and

Haloragis the major negative contributors followed by *Cyperus*, *Carex* and *Schoenoplectus* with *Anthoceros* only a minor contributor.

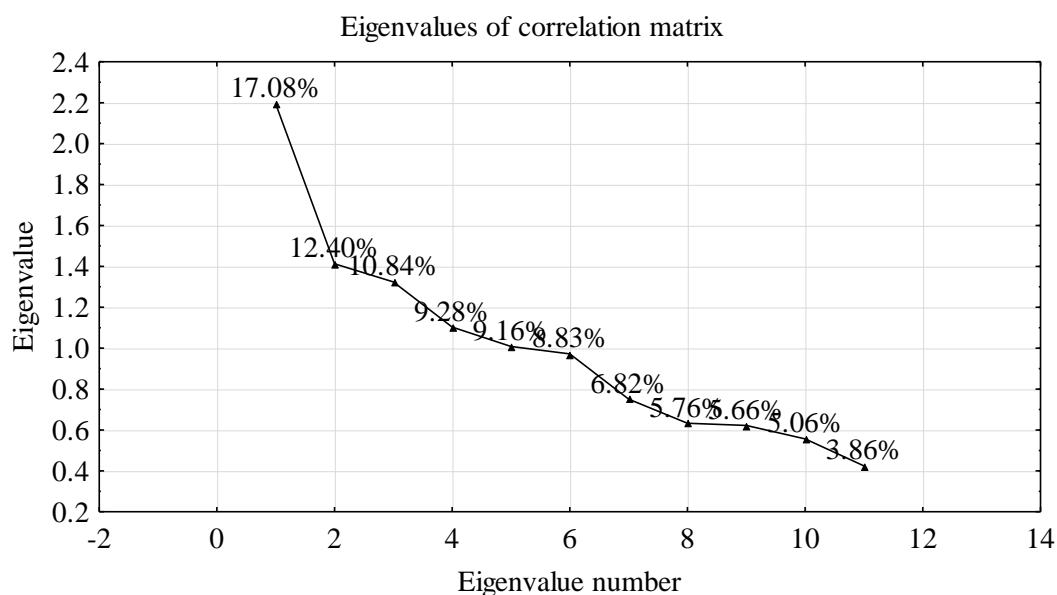


Figure 8.7. Scree plot of the eigenvalues of the correlation matrix of the active taxa for the aquatic and swamp percentage data (Pleistocene record 11.8 ka–54 ka).

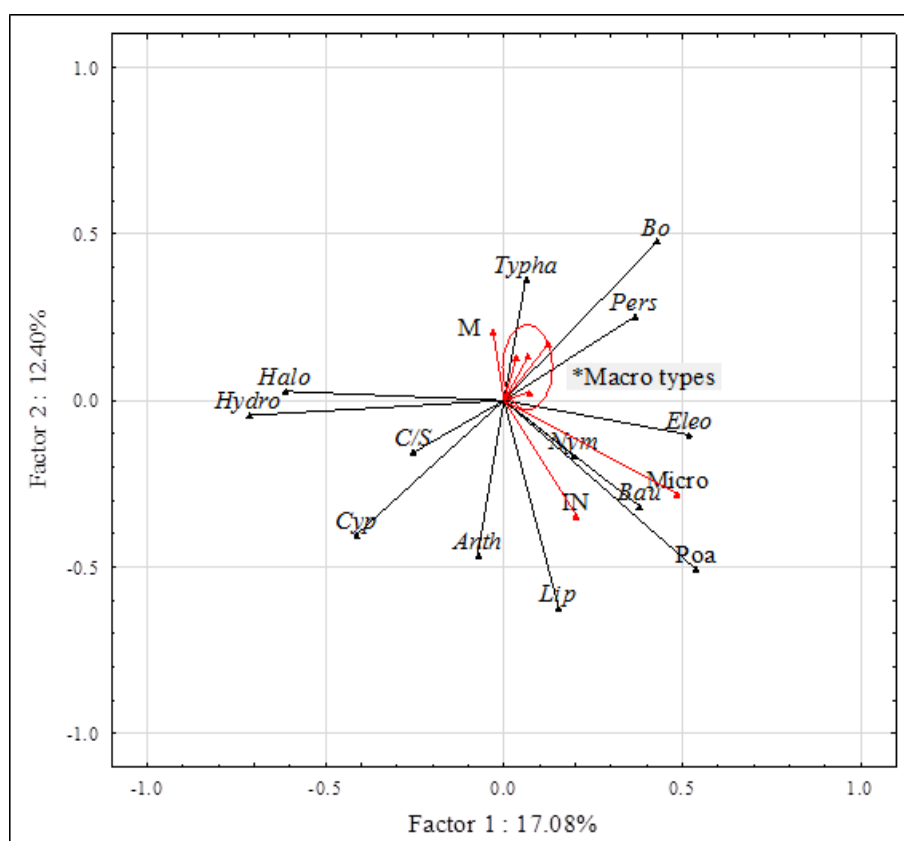


Figure 8.8. Projection of the taxa on F1 and F2 for the aquatic and swamp percentage data, Pleistocene record. The red circle encloses all the macrocharcoal components ('blocky', 'elongated', 'lattice-type' and 'other'), *Halo-Haloragis*, *Hydro-Hydrocotyle*, *Cyp-Cyperus*, *C/S-Carex/Schoenoplectus*, *Anth-Anthoceros* *IN-inorganics*, *M-moisture*, *Bo-Botryococcus*, *Pers-Persicaria*, *Eleo-Eleocharis*, *Nym-Nymphoides*, *Poa-Poaceae*, *Bau-Baumea*, *Lip-Liparophyllum*, *Poa-Poaceae* and *Micro-microcharcoal*.

The separation is likely to reflect stable swamp versus more variable conditions suggested by the presence of both Poaceae and *Liparophyllum*. This is further suggested with the alignment of the supplementary proxies, microcharcoal and inorganics with the Poaceae and *Botryococcus* correlation while the supplementary inorganic has a close alignment with *Liparophyllum* which is indicative of higher water levels. Although macrocharcoal is placed low (F1) it is aligned positively especially alongside *Persicaria* and *Typha*. F2 is essentially a separation of *Botryococcus* followed by *Persicaria* and *Typha* with the supplementaries moisture and macro types separated from *Liparophyllum* followed by Poaceae, the sedges and *Anthoceros* with the supplementaries inorganics and microcharcoal. This separation is likely to do with the local vegetation dynamics and fire with both *Persicaria* and *Typha* known to be advantaged by fire.

Projection of the samples (Figure 8.9) shows separation on F1 of zone LCA-F from nearly all other zones a separation of the more stable period of the late Pleistocene to the more variable conditions that followed, and this was also seen in the full sequence where *Haloragis* and *Hydrocotyle* were indicative of more stable conditions as indicated here. F2 separation is not so clear although zone E2, which is characterized by changing water levels and the prominence of *Liparophyllum*, is primarily separated from zone D where the drier elements *Persicaria* and Poaceae are prominent features of the swamp, and also to a lesser extent zone E1 where receding water levels sees *Typha* and local fire prominent.

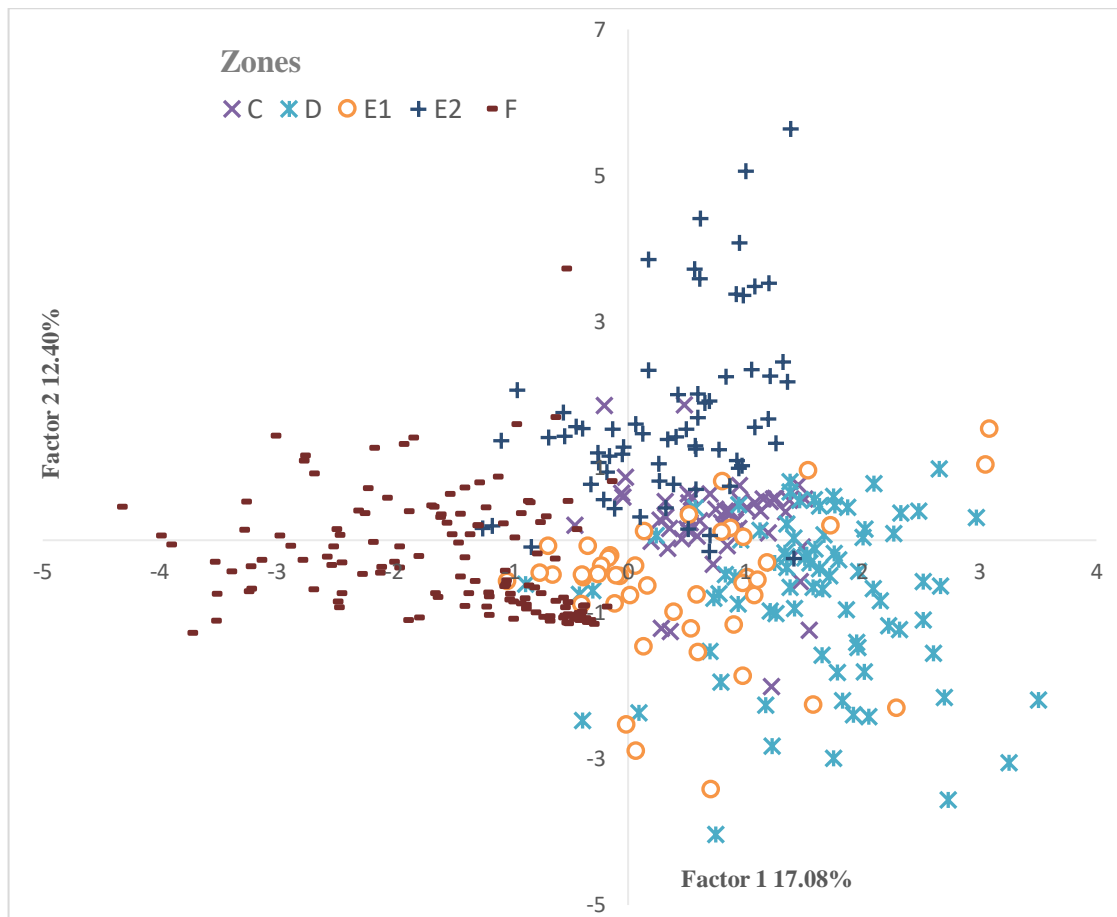


Figure 8.9. Projection of the samples on F1 and F2 for the aquatic and swamp percentage data, Pleistocene record.

8.1.4. PCA of the aquatic and swamp percentage data (Humification record 37,900 yrs BP–28,500 yrs BP).

The scree plot (Figure 8.10) suggests the first three eigenvalues (59.7%) are the major factors for interpretation. The supplementary proxies are humification (%), moisture, inorganics, microcharcoal and macrocharcoal (all sub-categories). F1 (Figure 8.11) sees the separation of Poaceae, *Liparophyllum*, *Anthoceros*, and *Haloragis* (positive) and, to a lesser extent, *Cyperus* alongside the supplementaries microcharcoal, humification and inorganics, from the negative *Carex* and *Schoenplectus*, *Persicaria* and *Typha*, alongside the supplementaries macro types and moisture with *Baumea* and *Eleocharis* close to the centre. The separation of Poaceae and *Anthoceros* from the major sedges could suggest a dry and wet divide but the alignment of *Liparophyllum* with Poaceae would suggest otherwise.

However, it is likely not so much the alignment of *Liparophyllum* and Poaceae but rather the separation of *Liparophyllum* from the major sedges and *Typha* likely due to the

distinct difference in the hydrological requirements of these taxa with the alignment of the supplementary inorganics with *Liparophyllum* a key indicator of changed hydrological conditions.

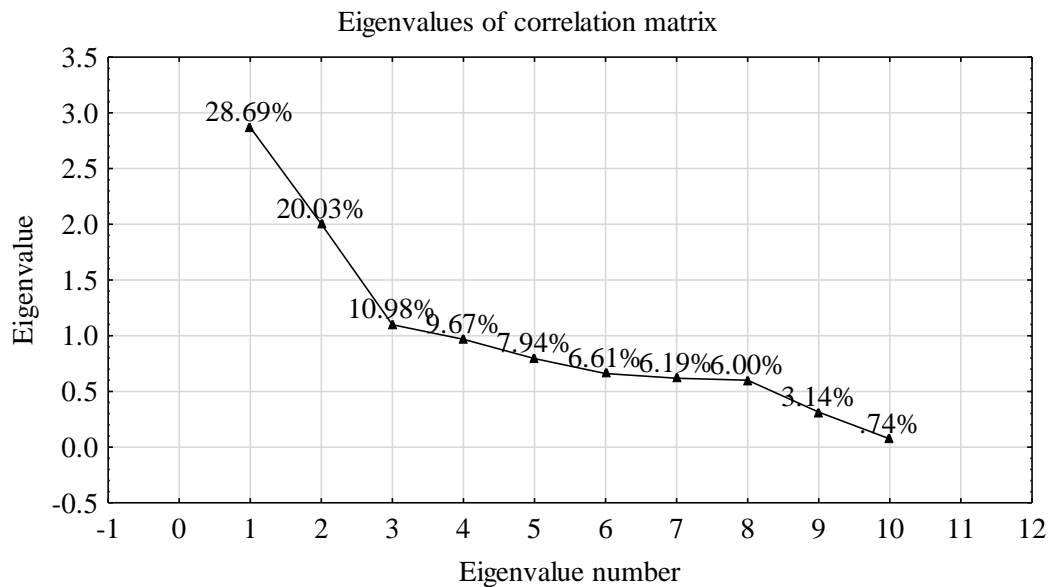


Figure 8.10. Scree plot of the eigenvalues of the correlation matrix of the active taxa for the aquatic and swamp percentage data (Humification record 37.9–28.5 ka).

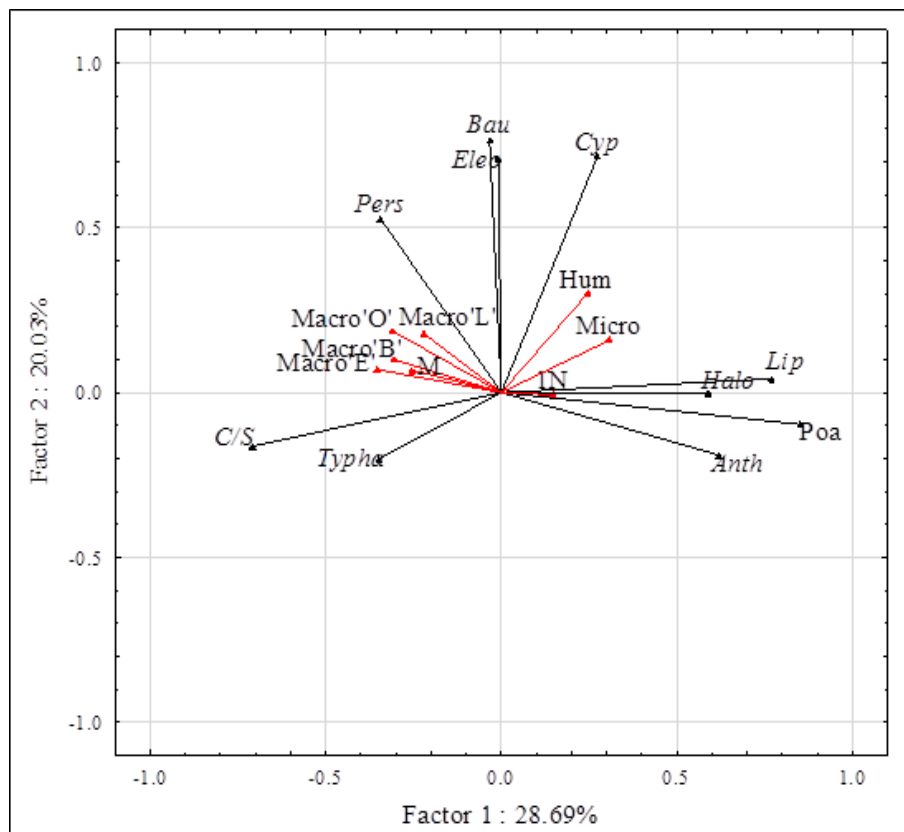


Figure 8.11. Projection of the taxa on F1 and F2, for the aquatic and swamp percentage data, humification record. C/S-Carex/Schoenplectus, Pers-Persicaria, Bau-Baumea, Eleo-Eleocharis, M-Moisture, Macro'O'-macroOther, Macro'L'-macroLattice, Macro'E'-macroElongated, Macro'B'-macroBlocky, Cyp-Cyperus, Hum-humification, IN-inorganics, Halo-Haloragis, Poa-Poaceae, Anth-Anthoceros, Lip-Liparophyllum, Micro-microcharcoal.

That the supplementaries moisture and macrocharcoal are aligned with *Carex* and *Schoenoplectus*, *Typha* and *Persicaria* likely confirms the important influence these factors have locally, while humification and microcharcoal aligned with Poaceae could suggest the presence of a drier and more regional influence. F2 sees *Baumea*, *Eleocharis*, *Cyperus* and *Persicaria* aligned positively alongside, but a lesser degree, the supplementaries macro types, humification, microcharcoal and moisture, separated from the negative *Typha*, *Anthoceros*, *Carex* and *Schoenoplectus* and Poaceae. *Haloragis*, *Liparophyllum* and supplementary inorganic are close to the centre and play a minor role in F2. The F2 separation is primarily reflecting the important role of the minor sedges alongside *Persicaria* and the secondary influence of fire.

F1 of the projection of the samples (Figure 8.12) sees primarily the separation of zone *E1* from *E2* although there is certainly some overlap, which would be expected as there is some commonality of taxa across the two zones. However, the major difference between the two zones is water levels with higher levels (*Liparophyllum*) through zone *E2* and receding levels through zone *E1* with *Persicaria*.

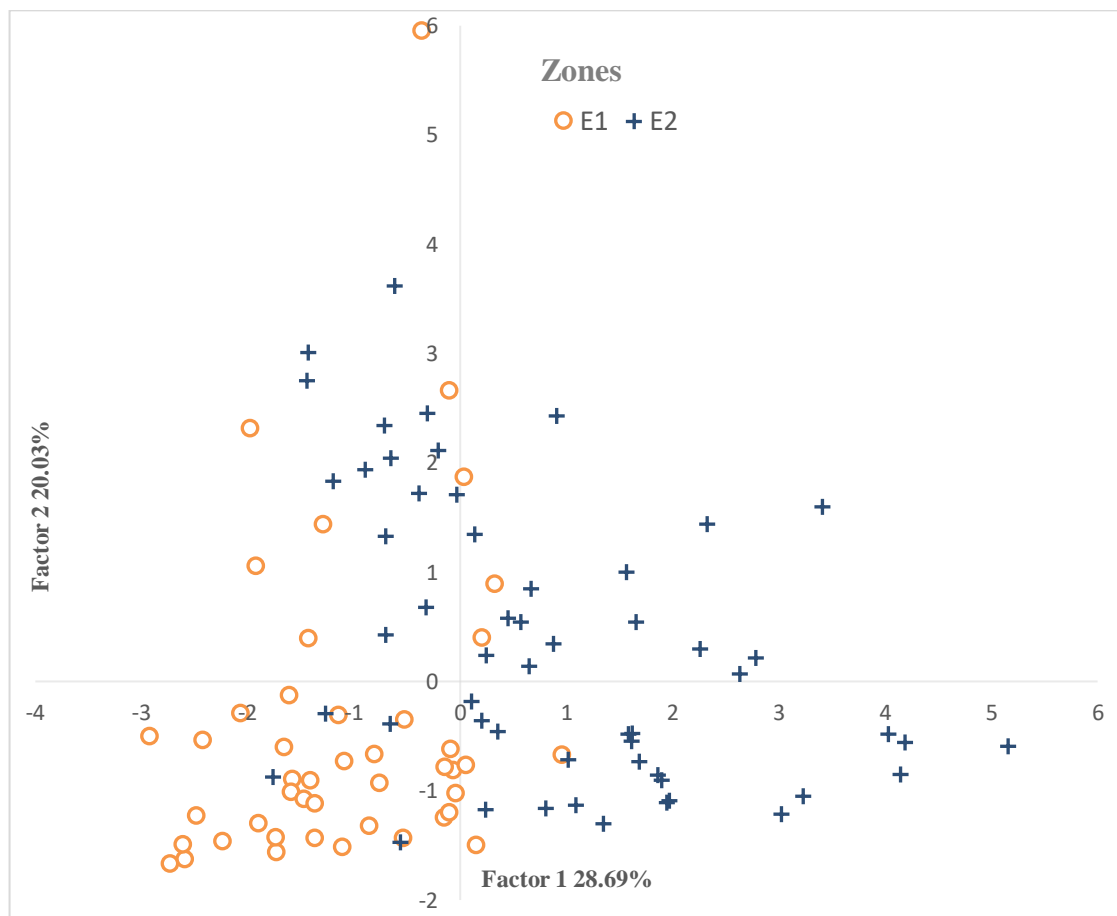


Figure 8.12. Projection of the cases on F1 and F2 for the aquatic and swamp percentage data, humification record.

8.1.5. PCA of the aquatic and swamp percentage data (Holocene record 11,700 yrs BP–3,000 yrs BP)

The scree plot (Figure 8.13) indicates that the first two or three eigenvalues (57.7%) are the major factors for interpretation. The supplementary proxies are moisture, inorganics, microcharcoal and macrocharcoal (all sub-categories). F1 (Figure 8.14) sees high negative loadings for Poaceae, *Typha* and *Carex* and *Schoenoplectus* and to a lesser extent for *Baumea* and *Nymphoides*. Moisture is also lying on this factor plane with high loadings, and to a lesser extent macro'lattice' which is separated from the rest of the macro types and aligned closely to *Typha*.

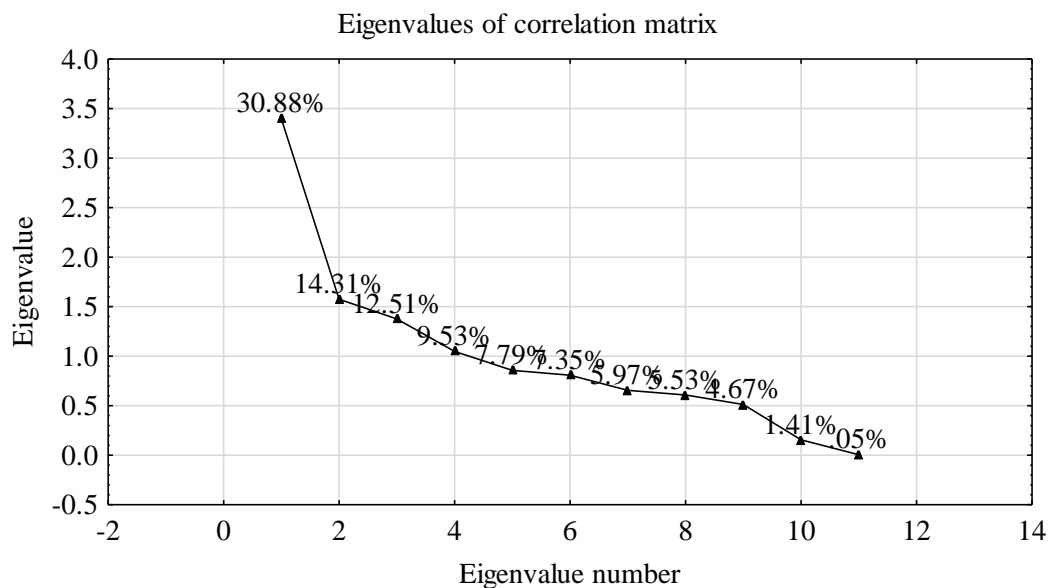


Figure 8.13. Scree plot of the eigenvalues of the correlation matrix of the active taxa for the aquatic and swamp percentage data (Holocene record).

While high positive loadings are present for *Haloragis* and *Hydrocotyle* followed by *Anthoceros*, *Eleocharis*, *Cyperus*, and *Eriocaulon* with inorganics, microcharcoal and macro types (blocky, elongated and other) are all within this vector sub-space. This separation with the alignment of Poaceae, *Typha* and *Schoenoplectus* with moisture would seem to be indicative of a relatively productive swamp but with a level of variability. With F2 the major separation is between *Carex* and *Schoenoplectus* (negative) and *Typha* (positive) and likely reflects the opposing dynamics between these taxa. Of interest is that for both F1 and F2 although loadings are relatively low for macro'lattice' despite having relatively low loadings is completely separated from the other sub-categories of macrocharcoal and lies in the same vector sub-space as *Typha*.

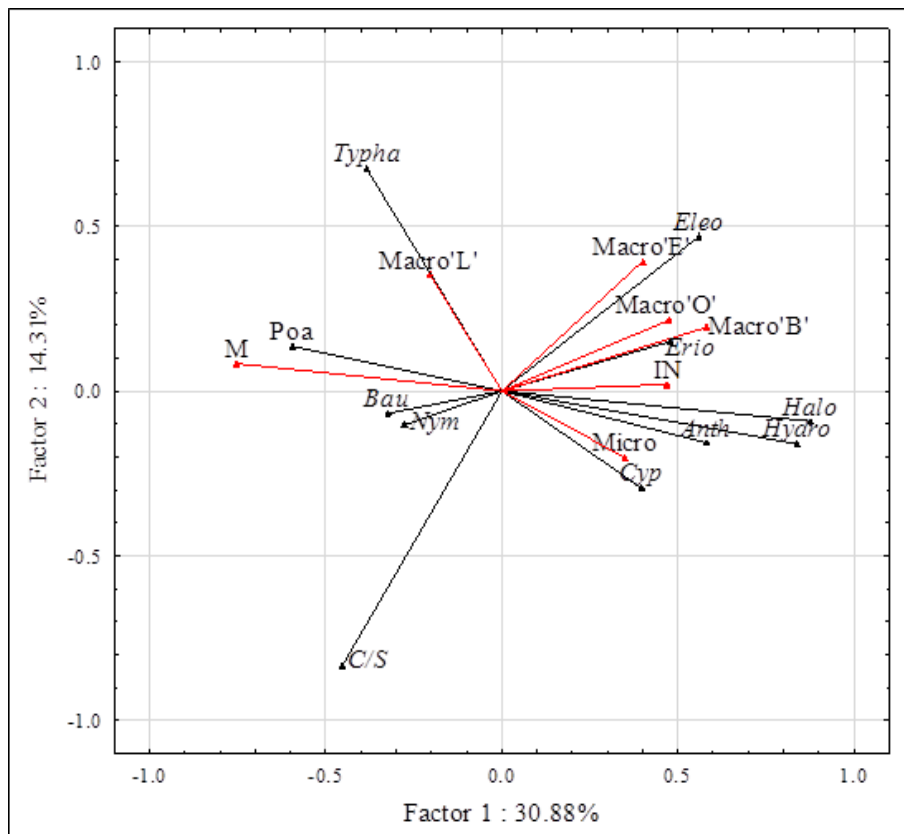


Figure 8.14. Projection of the taxa on F1 and F2 for the aquatic and swamp percentage data, Holocene period. Macro'L'-macroLattice, Poa-Poaceae, M-Moisture, Bau-Baumea, Nym-Nymphoides, C/S-Carex/Schoenplectus, Eleo-Eleocharis, erio-Eriocaulon, Halo-Haloragis, Hydro-Hydrocotyle, Anth-Anthoceros, Cyp-Cyperus, Macro'E'-macroElongated, Macro'O'-macroOther, Macro'B'-macroBlocky, IN-inorganics, Micro-microcharcoal.

The projection of the samples (Figure 8.15) sees the separation of zone B, the early Holocene, from Zone A, middle to late Holocene. The early Holocene period is characterized by the dominance of Poaceae, *Carex* and *Typha* on the swamp and, although macro'lattice' is aligned with *Typha* as indicated Figure 8.14, it is only on the secondary axis (F2) that all other macrocharcoal types are aligned with *Typha*. The middle to late Holocene is dominated by *Eleocharis* and the return of *Haloragis* and *Hydrocotyle* which previously suggested more stable conditions but the alignment of all charcoal types with this grouping, except macro'lattice' may suggest otherwise. It does suggest quite a different dynamic is happening on the swamp during the Holocene in comparison to the late Pleistocene especially in relation to fire both locally and regionally and this could also be related to changing climate conditions which sees a significant return of rainforest angiosperms onto the swamp and surrounding area. There is a short period, 7.7–7.75 ka shaded area, where zone B samples are more aligned with zone A samples and this was also found in the dryland Holocene results and will be discussed further in the dryland results.

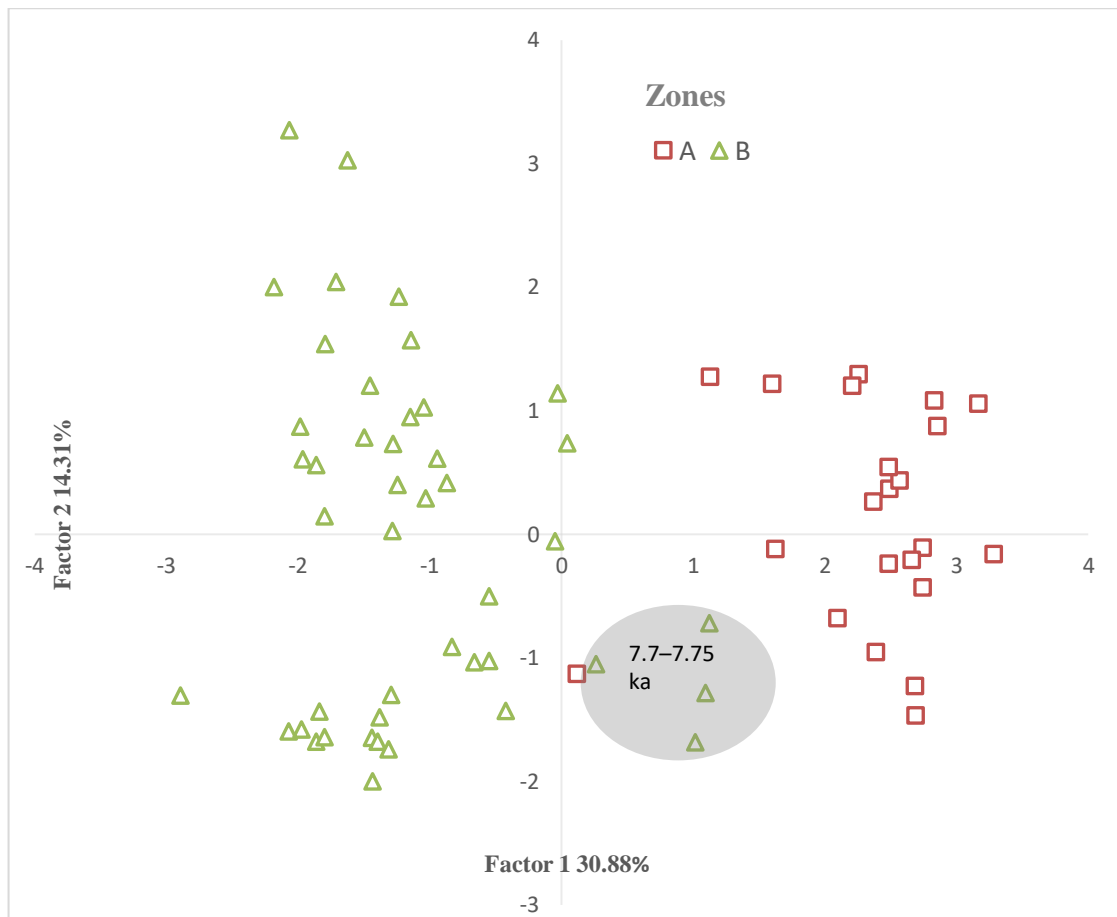


Figure 8.15. Projection of the samples on F1 and F2 for the aquatic and swamp percentage data, Holocene period, shaded area depicts zone B samples aligned with zone A samples.

8.1.6. PCA of the dryland percentage data (Pleistocene record 54,000 yrs BP–11,800 yrs BP)

The scree plot (Figure 8.16) suggests that it is primarily the first three eigenvalues (37.84%) that are the primary interpretable eigenvalues. The supplementary proxies are moisture, inorganics, microcharcoal and macrocharcoal. F1 (Figure 8.17) shows high negative loadings for Casuarinaceae followed by the sclerophyll Myrtaceae and to a lesser extent the secondary dry rainforest taxon *Petalostigma* in contrast to high positive loadings for *A. peralatum* and the rainforest gymnosperms and to a lesser extent the secondary rainforest taxa and sclerophyll taxa *Dodonaea* and *Callitris*.

This separation of dry-negative from humid-positive is also likely related to fire where the sclerophyll Myrtaceae are seen to be closely aligned with the supplementary microcharcoal and this close alignment is evident also on F2.

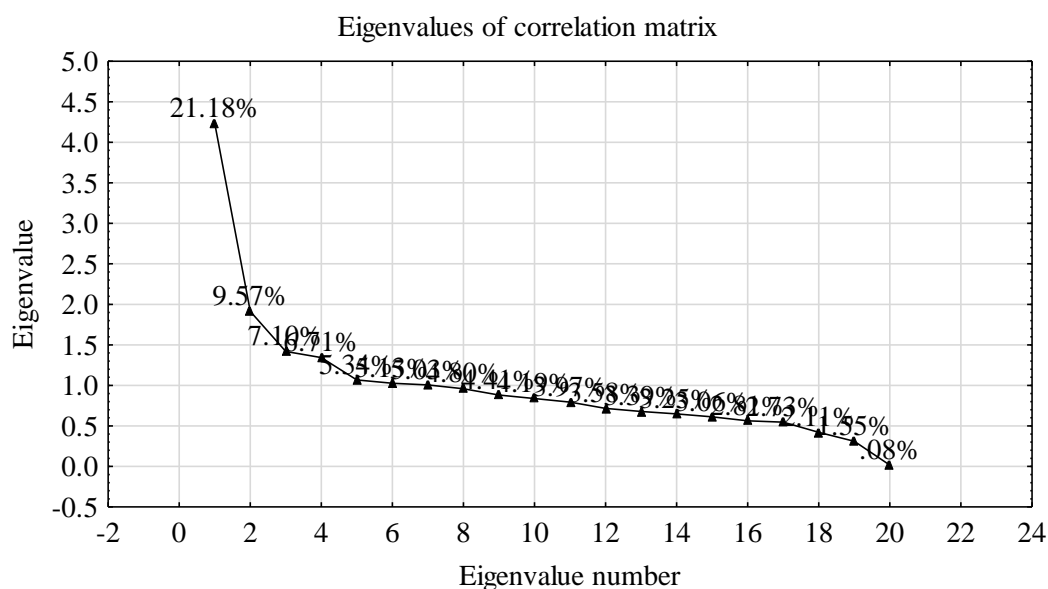


Figure 8.16. Scree plot of the eigenvalues of the correlation matrix of the active taxa for the dryland percentage data (Pleistocene record).

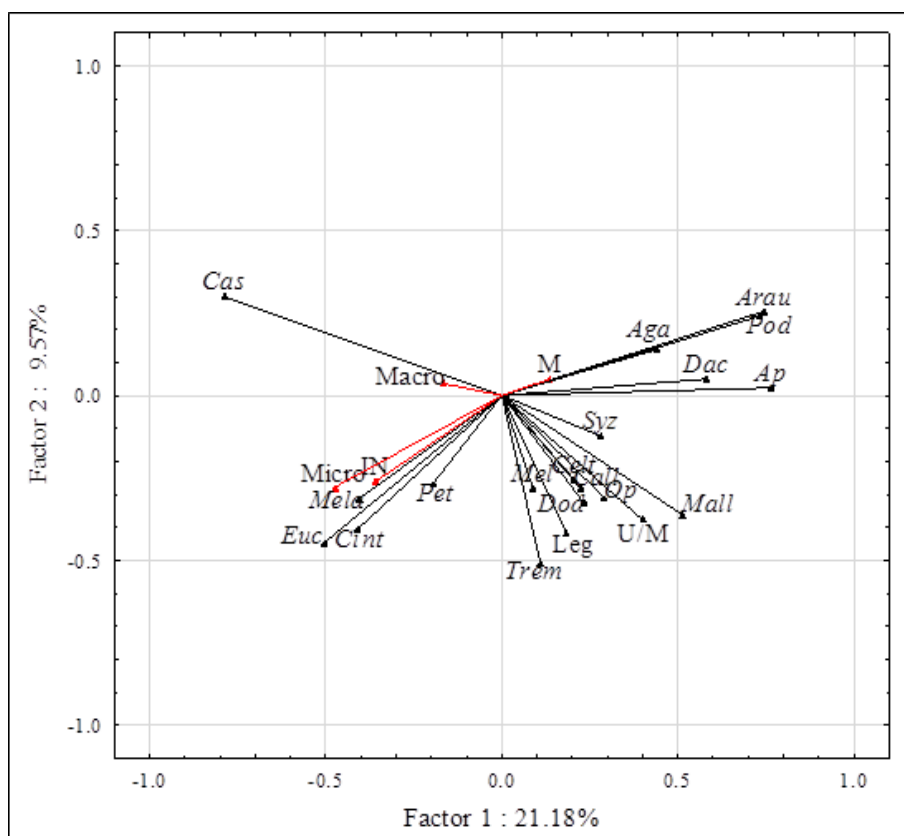


Figure 8.17. Projection of the taxa on F1 and F2 for the dryland percentage data, Pleistocene record. *Cas*-Casuarina, *Mela*-Melaleuca, *Euc*-Eucalyptus, *Cint*-Corymbia intermedia, *Pet*-Petalostigma, *IN*-inorganics, *Micro*-microacharcoal, *Macro*-macrocharcoal, *M*-moisture, *Aga*-Agathis, *Arau*-Araucaria, *Pod*-Podocarpus, *Dac*-Dacrydium, *Ap*-A.peralatum, *Syz*-Syzygium, *Mall*-Mallatus, *Celt*-Celtis, *Mel*-Melicope, *Dod*-Dodonaea, *Call*-Callitris, *Op*-O.paniculata, *Trem*-Trema, *Leg*-Leguminosae, *U/M*-Urticaceae/Moraceae.

That macrocharcoal is aligned with Casuarinaceae may seem counter-intuitive but macrocharcoal is relatively close to zero on the axis suggesting low correlation and it

could just be that there was no correlation at all with the other taxa and this is seen further on F2 where macrocharcoal has lower values. F2 shows high negative loadings for *Trema* followed by Leguminosae (dry rainforest), the sclerophyll Myrtaceae and other dry rainforest taxa, in contrast to moderate positive loadings for Casuarinaceae, *Araucaria* and Podocarpaceae, and suggests a separation of relatively stable conditions (positive) in contrast to the changing conditions indicated by the rainforest secondary taxa and the sclerophyll Myrtaceae. The close alignment of the sclerophyll Myrtaceae with the supplementary inorganics, would also suggest a more local origin for this taxon in comparison to the other major sclerophyll taxon, Casuarianaceae.

The projection of the samples (Figure 8.18) primarily sees a separation of zone 9b and 9a, 54–37 ka, from all other zones and is indicative of pre- and post-major fire activity culminating in the replacement of dry rainforest dominated by rainforest gymnosperms, especially *Araucaria*, by the flammable sclerophylls.

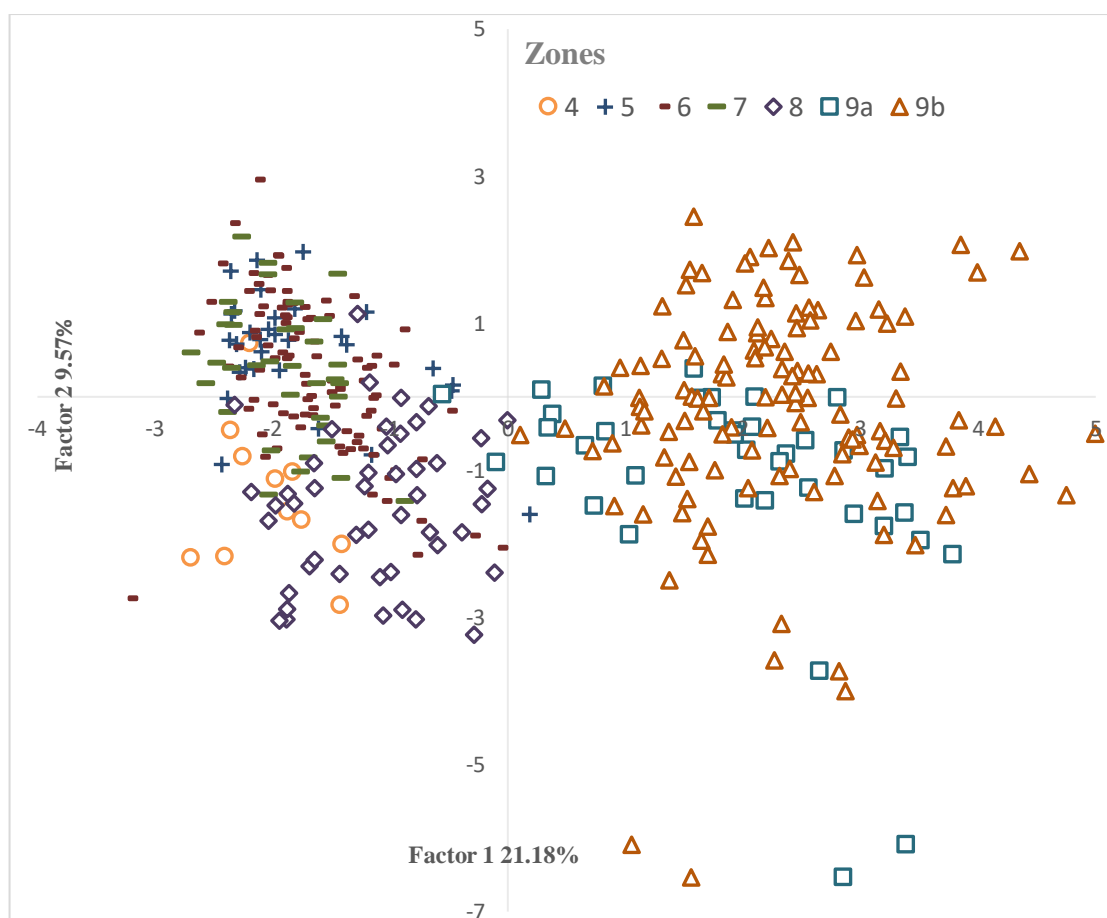


Figure 8.18. Projection of the samples on F1 and F2 for the dryland percentage data, Pleistocene record.

There is a minor separation of zone 4 and 8 from zone 7 and to a less degree zone 6 on F2 and this is related to a greater presence of *Eucalyptus* (zone 4 and 8) and fire, more so for zone 8, while zone 7 and 6 indicate a greater representation for Casuarinaceae and reduced fire.

8.1.7. PCA of the dryland percentage data (Holocene record 11,700 yrs BP–3,000 yrs BP)
The scree plot (Figure 8.19) indicates that the first two eigenvalues and possibly the third eigenvalue (56.8%) are the primary eigenvalues for interpretation. The supplementary proxies are, as previous, moisture, inorganics, microcharcoal and macrocharcoal with the addition of the secondary (small shrub) rainforest taxon *Melastoma* which is considered to have had a local origin (swamp) due to the presence of numerous seeds.

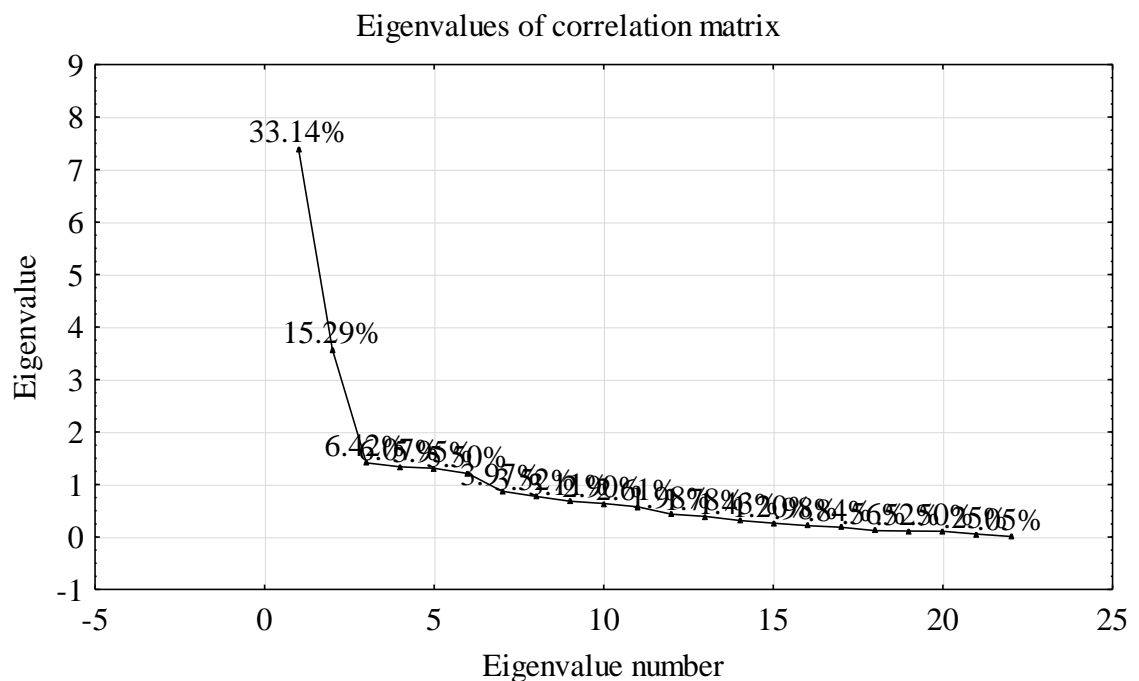


Figure 8.19. Scree plot of the eigenvalues of the correlation matrix of the active taxa for the dryland percentage data (Holocene record).

F1 (Figure 8.20) indicates high negative loadings for the two major sclerophyll taxa, *Eucalyptus* and Casuarinaceae, with moderate loadings for dry rainforest taxa including *Syzygium*, while high positive loadings are present for rainforest canopy taxa, Cunoniaceae-tricolpate and dicolpate, *Ficus* and *Elaeocarpus*, Leguminosae and *Freycinetta*, and the likely swamp forest taxa, *Acmena*, *Glochidion* and *Rapanea*. The alignment of the supplementary proxies, micro- and macrocharcoal and inorganics, alongside the more humid rainforest taxa is in contrast with the PCA results from the late Pleistocene and does suggest forcing factors are quite different through the Holocene.

While F2 sees high positive loadings for the swamp forest taxa, *Acmena*, *Glochidion* and *Rapanea* and to a lesser degree *Syzygium* with moisture in the same sub-vector space could suggest the local origin of these taxa, there are high negative loadings for *Mallotus* and *Macaranga*, palms, and the rainforest canopy which are aligned with the supplementary taxon *Melastoma* and microcharcoal, both indicators of disturbance.

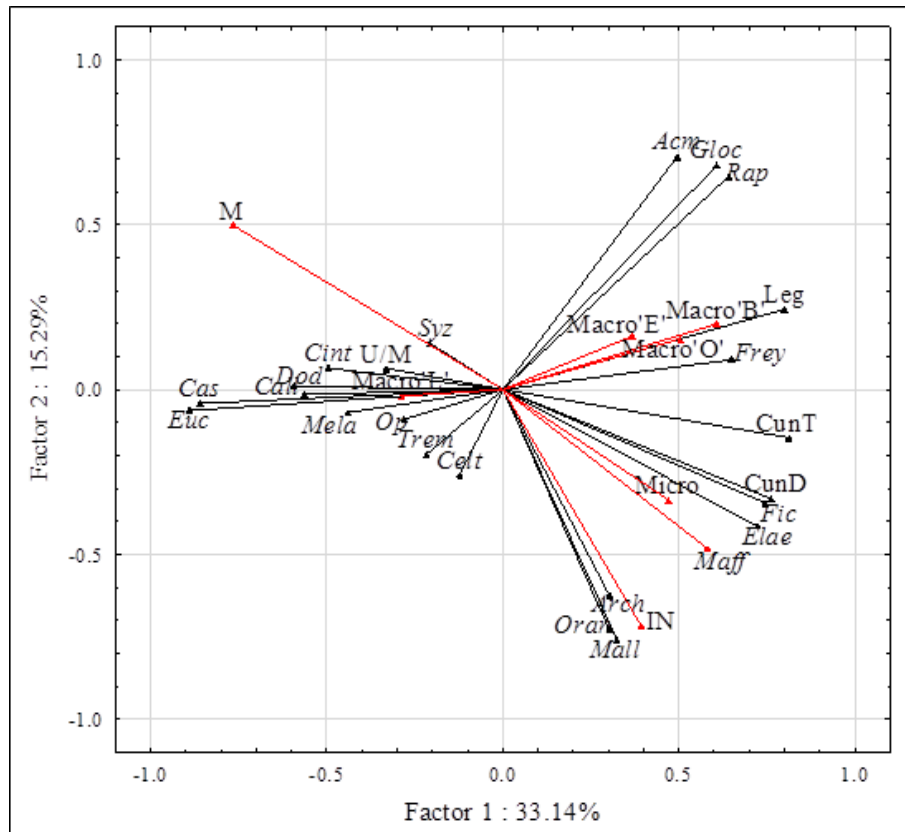


Figure 8.20. Projection of the taxa on F1 and F2 for the dryland percentage data, Holocene record. M-moisture, IN-inorganics, Macro'L'-macroLattice, Macro'E'-macroElongated, Macro'B'-macroBlocky, Macro'O'-macroOther, Micro-microcharcoal, U/M-Urticaceae/Moraceae, Syz-Syzygium, Cint-C.intermedia, Cas-Casuarina, Euc-Eucalyptus, Mela-Melaleuca, Dod-Dodonea, Call-Callitris, Celt-Celtis, Trem-Trema, Op-O.paniculata, Acm-Acmena, Gloc-Glochidion, Rap-Rapanea, Leg-Leguminosae, Frey-Freycinetta, CunT-Cunoniaceae(tricolpate), CunD-Cunoniaceae(dicolpate), Fic-Ficus, Elae-Elaeocarpus, Maff-M.affine, Oran-Oraniopsis, Arch-Archontophoenix, Mall-Mallotus.

F1 of the samples (Figure 8.21) separates zones 1, 2 and a part of zone 3b, late to mid-Holocene, from zones 3a, 3c and 4, mid to late Holocene. Zones 1 and 2 are characterized by rainforest angiosperm dominance with ever increasing fire activity while zones 4 and 3c indicate the initial establishment of rainforest under reduced fire activity but with a significant sclerophyll component still present. The shaded area in Figure 8.21 encloses a time-slice of zone 3b, 7.6–7.75 ka, which, like zones 1 and 2, is characterized by rainforest dominance but, on either side, zone 3a and 3c, quite different conditions are present, with both sclerophyll and fire activity prominent. F2 is primarily the separation

of zone 1 from zone 2 and 3b. Zone 1 is quite different to all other zones in the Holocene and sees changes especially on the swamp with the replacement of swamp rainforest taxa with the palms, *Oraniopsis* and *Archontophoenix*.

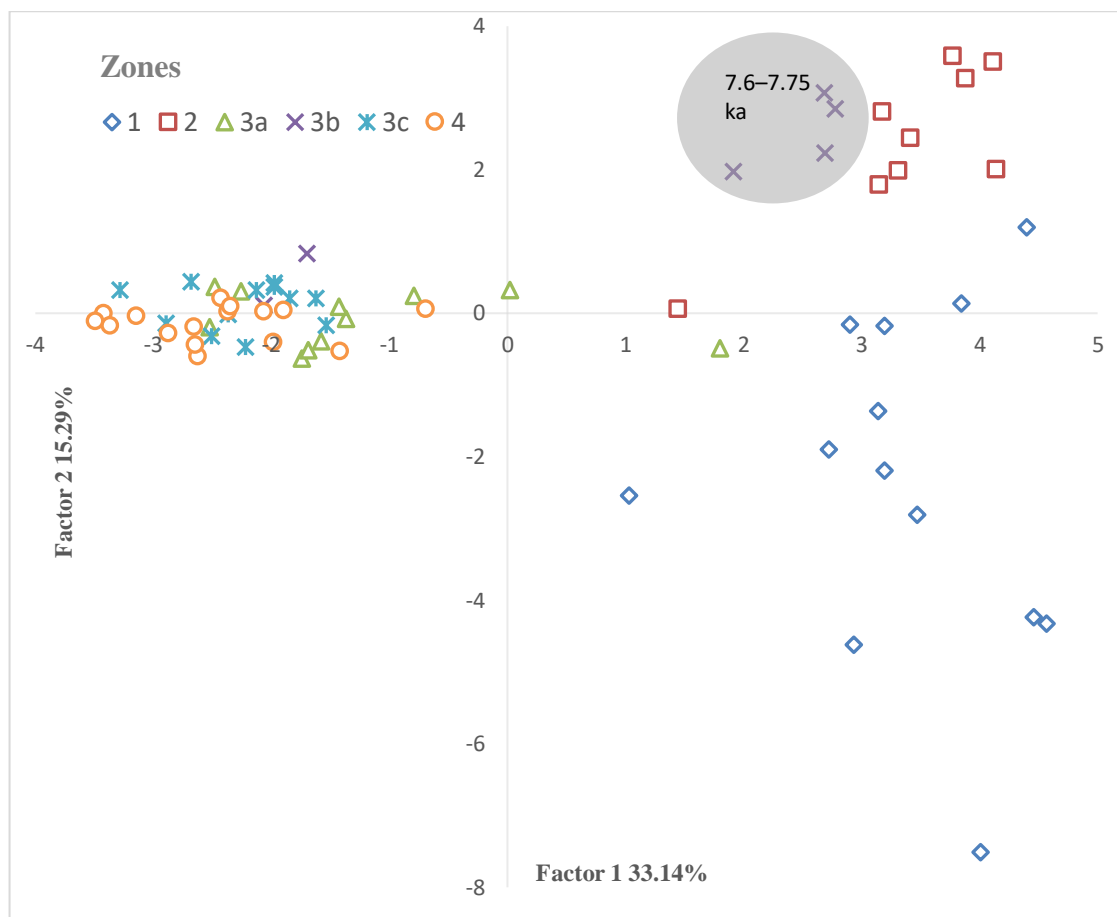


Figure 8.21. Projection of the samples on F1 and F2 for the dryland percentage data, Holocene record, shaded area depicts zone 3b cases aligned with zones 1 and 2 cases.

PCA clearly groups the different rainforest types in the Holocene percentage dryland data and of particular interest is the separation of the swamp forest group from the other rainforest elements (Figure 8.20) and its alignment with moisture suggesting its local origin on the swamp as does its alignment with macrocharcoal (local fire). The close association of inorganics with the two palms (*Archonotophoenix* and *Oraniopsis*), both which are capable of surviving in seasonally inundated areas for several months or longer, would suggest a high degree of variability is present on the swamp in the late Holocene. The inclusion of the secondary taxa, *Mallotus* and *Macaranga*, which has been implicated as a disturbance taxa, within this grouping substantiates an increase in variability. The close alliance of microcharcoal with *Melastoma*, which is known to proliferate after fire (Hopkins and Graham 1984; Williams 2000) is interesting as evidence from the macrofossils indicates a local origin for this taxon. That the rainforest canopy elements

are also associated with microcharcoal would suggest that fire is operating both locally and regionally. In Figure 8.21 the separation of the time-slice 7.6–7.75 ka, which was evident in the aquatic and swamp PCA (Figure 8.15), suggests a significant change in dynamics, a feature that will be examined in more detail in the discussion chapter.

8.2 Spectral Analysis

Spectral analysis has been used to assess the presence of both Milankovitch and non-Milankovitch cycles which are thought to be integral components of the climate system (Heinrich 1988; Bond et al. 1993; Hagelberg et al. 1994; Williams et al. 1998; Schulz et al. 2004). A detailed spectral and wavelet analyses has already been undertaken on the full Lynch's Crater record as well as the nearby off-shore site ODP-820 (Moss 1999; Bretherton 2006; Kershaw et al. 2007a) providing an insight into the dominant Milankovitch cycles across two different spatial scales, local and regional. Bretherton (2006) and Kershaw et al. (2007a) found that the 100,000-year eccentricity frequency dominates the Lynch's Crater record followed by the 41,000-year obliquity period. Although the precessional frequency is known to be highly influential over tropical climate change (Clemens et al. 1991; Hagelberg et al. 1994; Clement et al. 2001; Kershaw et al. 2003; Clement and Peterson 2008), no significant precessional forcing was found at Lynch's Crater but was found from proxies at ODP-820. The strength of the precessional forcing, 23,000 and 19,000-years, on the seasonality in the northeastern Queensland region is clearly shown in spectral analysis of the mid-January insolation record from 15°S, shown in Figure 8.22, and the absence from the Lynch's Crater record of this frequency was deemed to be unusual (Kershaw et al. 2007a).

Non-orbital forcing frequencies were also found and were likely related to long-term trends with some likely to be related to human occupation but also autogenic processes within the lake basin itself associated with aquatic successional trends (Bretherton 2006). The 30,000-year frequency that is thought to be related to non-linear responses within the climate system and/or ENSO variability, and is present in climate proxies from the Pacific and Indian Ocean and Sulu Sea records, was a dominant frequency for the ODP-820 record but was not a significant forcing at Lynch's Crater (Beaufort et al. 2001, 2003; Kershaw et al. 2003; Bretherton 2006).

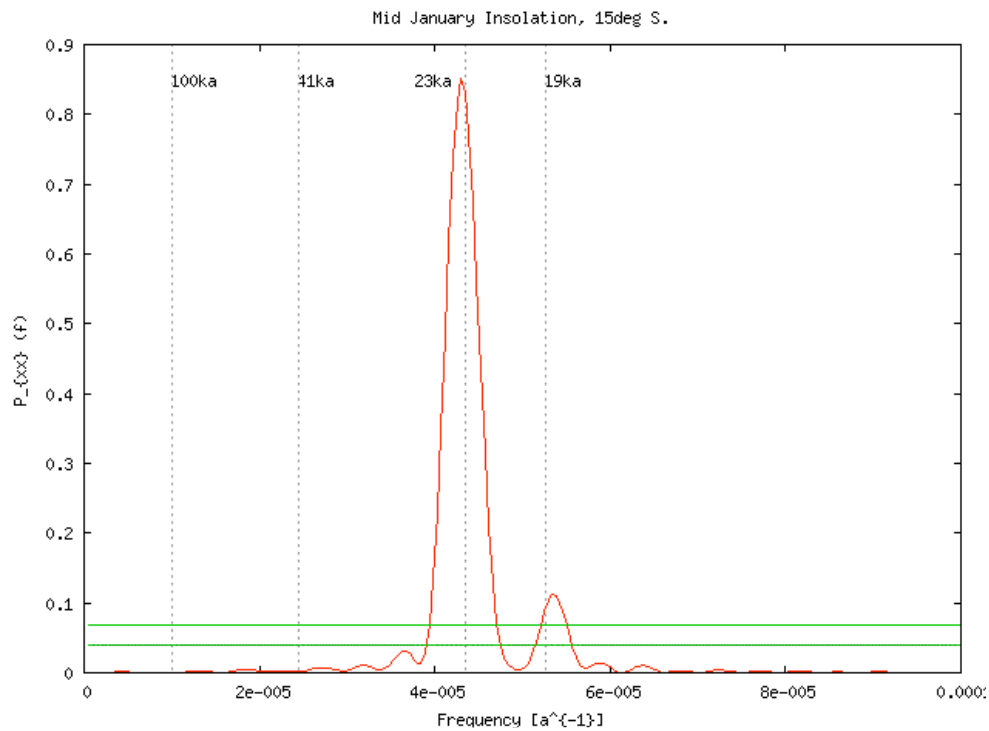


Figure 8.221. Spectral analysis of the mid-January insolation record (15°S) over the last 220,000 years using SPECTRUM (data from NCDC, 2006).

The discrepancy between the two records was initially considered to be an artifact of sampling methods but it was concluded that the complexities of vegetation response to climate change may not be fully represented in fossil assemblages, especially the initial community response to climate change, as well as other factors that may impinge on the structural integrity of vegetation communities that are not readily discernable in fossil assemblages, such as human impacts and/or the role of megafauna (Kershaw et al. 2007a; Rule et al. 2012).

Turney et al. (2004) found that both a semi-precessional (11.7 kyr) and millennial frequency (1490 year) were present at Lynch's Crater. However, there is still much debate on the origin of the 1470-year frequency (Bond et al. 1997; Schulz et al. 1999; Schulz 2002; Rahmstorf 2003; Dima and Lohmann 2009) and whether it is present during the Holocene (Schulz *et al.* 2004), there is even less certainty about other proposed sub-orbital frequencies. The millennial frequencies, 3,300–4,200 years, reported from planktonic foraminifera from southern and northern tropical Indian Ocean (Pestiaux et al. 1988), Arabian Sea (Sirocko et al. 1996) and an East-Asian Monsoon record from the Sulu Sea (de Garidel-Thoron et al. 2001), are thought to be combinations of orbital parameters on monsoon dynamics. This association with monsoon dynamics has also

been suggested for a 820 year and 1046 year frequency within the Asian region (Hong et al. 2000) while 779 year and 206 year frequencies have been linked to rainfall intensity within the African monsoon (Neff et al. 2001). It is thought that these periodicities along with ~2200 year and ~210 year frequencies are linked to the Suess solar cycles (Bond et al. 1997; Chambers et al. 1999; Jiménez-Moreno et al. 2008) which have also been related to century-scale drought frequency in the northern Great Plains of the USA (Yu and Ito 1999). Others (Baker et al. 2005; Roth and Reijmer 2005) suggest that centennial cycles linked to quasi-periodic signals of climate origin may be associated with long-term trends of sunspot cycles or harmonics and modulations of individual solar cycles. It could be that these higher frequencies are more visible in shorter and higher resolution records and so the objective is to see whether these frequencies are more visible in this relatively short sequence. However, caution is needed with such analyses, not only because of the length of the time-series that is to be analysed but also because of the situation within the time-period where anthropogenic impacts are likely, especially the impact of fire, which may distort spectral outcomes (Bretherton 2006).

8.2.1 Methods

As a detailed analysis has already been undertaken for Lynch's Crater, only spectral analysis with the accompanying REDFIT analysis will be performed on this much shorter record, 3,000 yrs B.P.–54,390 yrs B.P, see Chapter 5 section 5.8 for details of software, SPECTRUM, used for spectral analysis. However, as this record covers significant climate changes it was decided to compartmentalize the record to see whether there were any differences in the frequencies generated across these time periods. The time series aimed for spectral analysis investigation in this study are the full time sequence, 3,000–54,390 years (length of series to be analysed 51,390 years), the Pleistocene sequence, 11,800–54,390 (length of series to be analysed 42,590 years), and the Holocene and LGM sequence 3,000–18,000 years (length of series to be analysed 15,000 years). Unfortunately the Holocene sequence was not able to be analysed separately as there were under 100 samples available which is the minimum number needed for spectral analysis (Spectrum). Consequently, the analysed record was increased by inclusion of late Pleistocene samples to the required 100 samples. Of course this combination of Holocene and late Pleistocene samples will not be able to differentiate between frequencies that may have only been found in the Holocene period. Spectral analysis undertaken on peat humification by Turney et al. (2004) observed that the results for the period 28.5–37.9 ka

were highly variable. Humification results were available for this short sequence in this study and spectral analysis was also completed across this sequence.

It is also clear from the length of all the sequences to be analysed that there is a limit to the frequencies, especially Milankovitch, which can be generated. There is also disagreement on the length of the time-series that is needed to verify frequencies with Schulz and Mudelsee (1997) arguing that the presence of two full cycles is the minimum needed for validation of periodicities, while Muller and MacDonald (2000) argue that one cycle length in a time-series is adequate and Wunsch (2004) suggests that at least seven full cycles are needed. In all these examples it is the low frequency cycles, eccentricity and obliquity, that are being examined but this would also be applicable to high frequency cycles. This would suggest that the full sequence, in accordance with Schulz and Mudelsee (1997) would have valid precessional and semi-precessional cycles. The Pleistocene sequence would also have valid semi-precessional cycles and a valid precessional cycle for one of the periodicities 19,000 years, but as there is not two complete cycles for the 23,000 year periodicity caution would be needed when interpreting this cycle when present in the Pleistocene sequence. Studies have also found that frequencies close to known orbital cycles, such as obliquity and precessional/semi-precessional, are likely to be amplitude modulations or frequency modulations of these cycles (Mélise et al. 2001; Huybers and Aharonson 2010). The Holocene and LGM sequence is not long enough for valid Milankovitch and sub-Milankovitch cycles but, as for all of the time-series sequences analysed, millennial and centennial frequencies > 200 years, would be valid.

Spectral analysis was undertaken for the percentage on the major components of the dryland and aquatic and swamp taxa within the time sequences outlined above and unlike the PCA spectral analysis was also undertaken on the influx data. It is likely that local basin and catchment conditions maybe more influential on the influx data results than that seen for the percentage data results, see Chapter 1, sub-section 1.4.1.2. The humification data which covers the period, 28,500 yrs B.P.–37,900 yrs B.P., was also analysed across both the percentage and influx data and, as for PCA, only the major swamp components including Poaceae from the re-summed aquatic and swamp pollen sum were utilized for this analysis.

8.2.2 Spectral analysis dryland taxa results

Although there was a reduction in statistical significant frequencies following red-noise analysis, see the Appendix B (2), Section 3, and therefore indicating for these components that orbital forcing is not significant and/or present, both Milankovitch and sub-Milankovitch as well as millennial and centennial frequencies were recognised for a substantial number of taxa including key indicator taxa.

The full time-series, both percentage and influx, also had a significant frequency that was the length of the time-series (51.3 ka) or near to it and was more commonly found for the rainforest taxa, especially the canopy, understorey and vines, as well as for a number of pteridophytes. In most cases where this was the primary frequency the data was filtered, (Schulz and Muddelsee 1997; Schulz and Stattegger 1997) and a 41,200 or 34,000 year frequency remained. Although this was not a common occurrence, for the rainforest secondary taxa the 41,200 year frequency was present as a primary frequency for some secondary taxa. For the Pleistocene time-series, only the percentage pteridophytes had a primary frequency that covered the full sequence (42,590 years) while, for the Holocene and LGM time-series, a 15,000 year frequency (length of the time-series) was common across all analysed pollen taxa with a full list of these frequencies and the filter results given in Appendix B (2), Section 3. In all cases frequency was determined to be significant using both Fisher and Siegel's critical tests (Schulz and Stattegger 1997) while the confidence levels for all frequencies and in most instances the frequency generated for both spectral and red-noise have been noted on all graphs (plots).

All spectral frequencies of all analysed components are given in Appendix B (2), Section 3 which also includes the results determined from REDFIT analysis when required. The statistically significant peaks for precessional, semi-precessional, the 15–17 kyr frequency and millennial frequencies between 1–2 kyr for the full record, percentage and influx are given in Table 8.1 and, for the Pleistocene time-period are given in Table 8.2 for only those taxa that did not require filtering. It is important to note that although there were frequencies common across the percentage and influx data suggesting a common influence this was not always the result. It could be as suggested earlier that local conditions especially changing sedimentation rates greatly influence influx. This may see high influx due to changes in sedimentation rate rather than high pollen production.

Table 8.1. Critical spectral analysis frequencies, precessional, semi-precessional, 15–17 kyr and millennial, using Siegel’s significance test for the dryland percentage, concentration, and influx data for the full record (3 ka–54 ka). X – primary frequency (99% confidence level), X – secondary frequency (99% confidence level), X – frequency within Fisher 99% and Siegel’s 95% critical confidence levels.

Percentage, Influx and Concentration Components Full Record 3 ka – 54 ka	19–23 kyr %	15–17 kyr %	9.5–11.5kyr %	1–2 kyr %	19–23 kyr Influx	15–17 kyr Influx	9.5–11.5kyr Influx	1–2 kyr Influx
Pollen Conc./Influx			X				X	
Dryland Conc./Influx			X					
Aquatic Conc./Influx					X			
Tree Ferns	X		X		X			
<i>Pteridium</i>			X	X				
Podocarpaceae		X		X				
<i>Dacrydium</i>		X						
<i>A. peralatum</i>		X						X
<i>Olea paniculata</i>	X				X			
<i>Celtis</i>		X		X				X
<i>Mallotus/Macaranga</i>		X		X		X		X
Urticaceae/Moraceae			X					
<i>Elaeodendron</i>		X				X		X
<i>Oraniopsis</i>		X	X			X	X	
<i>Menispermaceae</i>		X		X				
<i>Loranthaceae</i>				X				
Myrtaceae (Sclerophyll)	X		X		X			X
Sclerophyll Total		X	X			X	X	
Casuarinaceae		X	X			X	X	
<i>Eucalyptus</i>						X	X	X
<i>Corymbia</i>	X							
<i>Melaleuca</i>	X	X	X	X	X		X	X
<i>Gyrostemon</i>								X
<i>Callitris</i>			X	X				
<i>Dodonaea</i>	X		X					
Chenopodiaceae						X	X	
Asteraceae(Tubiflorae)	X							
Poaceae	X		X		X		X	
<i>Leptospermum</i>	X		X		X		X	
Inorganics	X							
Moisture		X	X					

For the Holocene and LGM time-period, the sequence is not long enough for valid precessional and semi-precessional peaks to be generated and overall the analysis for this period generated few frequencies for the percentage data and even fewer frequencies for the influx data, with full details in the Appendix B (2), section 3. However there were a number of taxa and groupings, *Eucalyptus*, *Callitris*, Podocarpaceae, *Agathis*, *Pteridium*, monolete (psilate) ferns, microcharcoal/pollen ratio, Cyperaceae/Poaceae ratio, and Myrtaceae (sclerophyll), that had a millennial frequency between 1–2 kyr but fell within the Siegel and Fisher confidence level (95%–99%). A REDFIT comparison of the time-

series was undertaken for the majority of these taxa and groupings with the autoregressive (ARI) model of red-noise indicating that this peak, 1–2 kyr, was not distinguishable from red-noise (see Appendix B (2). Section 3). This would suggest that either the frequency is invalid through this time-series or that the sequence (Holocene and LGM) itself is problematic.

Table 8.2. Critical spectral analysis frequencies, precessional, semi-precessional, 15–17 kyr and millennial, using Siegel’s significance test for the dryland percentage, concentration and influx data for the time-period 11.8 ka–54 ka, **X – primary frequency (99% confidence level), **X** – secondary frequency (99% confidence level) and **X** – frequency within Fisher 99% and Siegel’s 95% critical confidence levels.**

Percentage, Influx and Concentration Components Pleistocene record 11.8 ka – 54 ka	19–23 kyr %	15–17 kyr %	9.5–11.5kyr %	1–2 kyr %	19–23 kyr Influx	15–17 kyr Influx	9.5–11.5kyr Influx	1–2 kyr Influx
Pollen Conc./Influx		X	X				X	X
Dryland Conc./Influx		X				X	X	X
Rainforest (angiosperms)	X		X					
Rainforest secondary	X				X			
Rainforest understorey	X							
Vines	X				X			
Tree Ferns				X				X
Davalliaceae				X		X		
<i>Pteridium</i>			X		X		X	
Podocarpaceae				X				X
<i>Dacrydium</i>	X						X	
<i>Acmena</i>		X						X
<i>Elaeocarpus</i>				X		X		X
<i>Olea paniculata</i>	X					X		
<i>Celtis</i>				X		X		X
<i>Mallotus/Macaranga</i>	X				X			X
Urticaceae/Moraceae			X					
<i>Elaeodendron</i>								X
<i>Oraniopsis</i>	X		X					
<i>Zanthoxylum</i>							X	
<i>Menispermaceae</i>	X			X				
Myrtaceae (Sclerophyll)			X			X		X
Sclerophyll Total						X	X	X
Casuarinaceae			X			X	X	
<i>Eucalyptus</i>						X		X
<i>Corymbia</i>			X			X		X
<i>Melaleuca</i>						X	X	X
<i>Callitris</i>			X	X				
<i>Dodonaea</i>			X			X		
Chenopodiaceae						X	X	
Asteraceae(Tubiliflorae)	X					X	X	
Poaceae	X		X					
<i>Leptospermum</i>			X				X	
Inorganics	X		X					
Moisture	X		X					

8.2.2.1. Red-noise analysis

All frequencies generated from Spectrum underwent REDFIT analysis to verify the presence of red-noise. A number of those shown in the above tables did have red-noise but the autoregressive (AR1) model of red-noise indicated these frequencies were distinguishable from red-noise. The spectral frequency plots for major dryland taxa and other components (percentage and influx) for the full sequence are given in Figures 8.23–8.27 and for the Pleistocene sequence Figures 8.28–8.33. The two green lines on the spectra plot indicate Fisher and Siegal’s critical confidence levels, with a frequency above both lines indicating a 99% confidence level while a frequency found within the two lines indicates a 95% confidence level. For those shown to have red-noise, the red-noise spectra plots are given instead. All spectral frequency plots from the results in Table 8.1 and 8.2 are presented in Appendix B (2), Section 3.

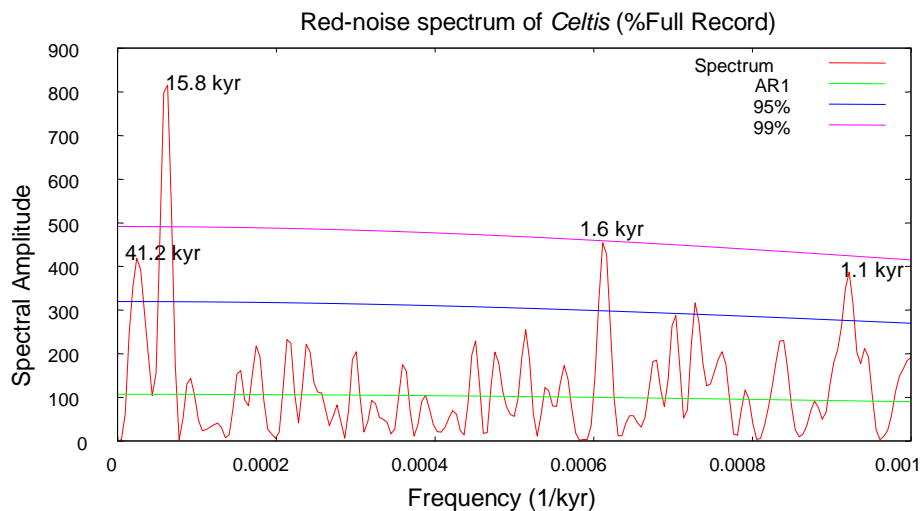


Figure 8.23. Red-noise spectra of *Celtis* (%Full), frequencies noted on plot

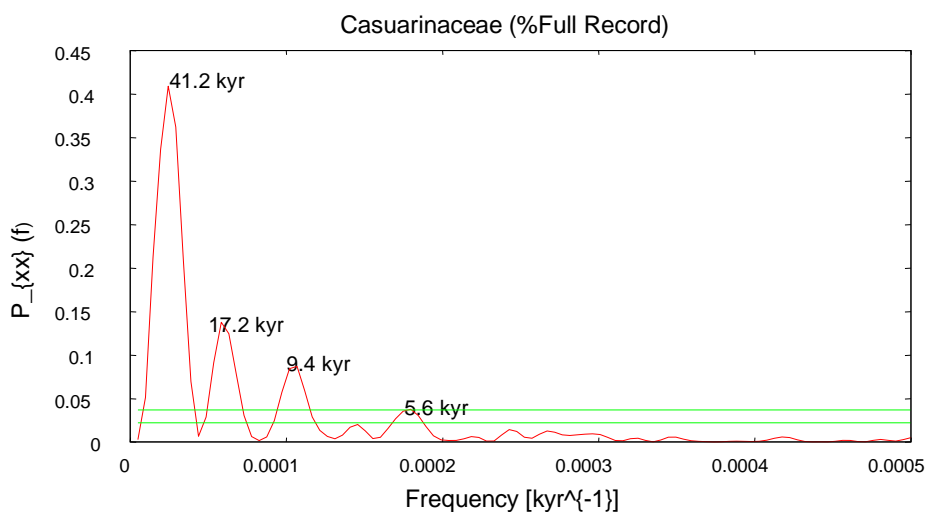


Figure 8.24. Spectra plot of Casuarinaceae (%Full), frequencies noted on plot

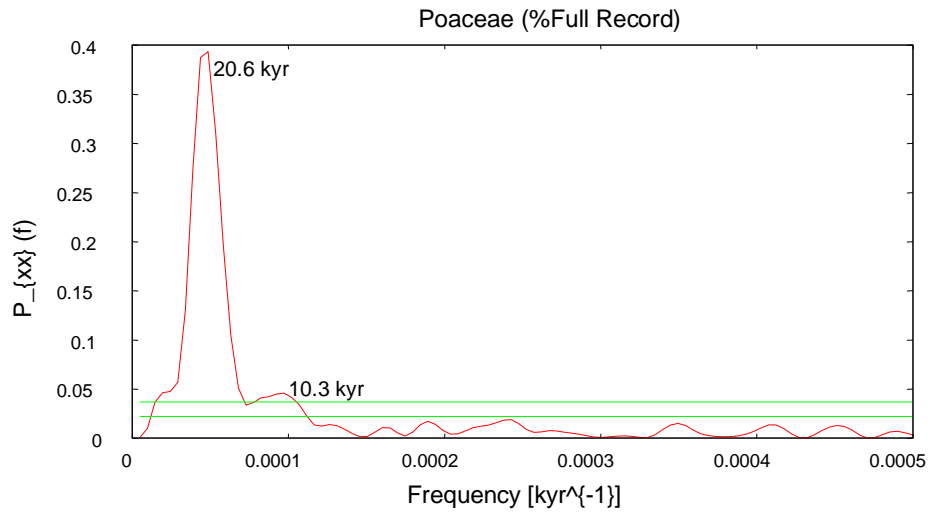


Figure 8.25. Spectra plot of Poaceae (%Full), frequencies noted on plot

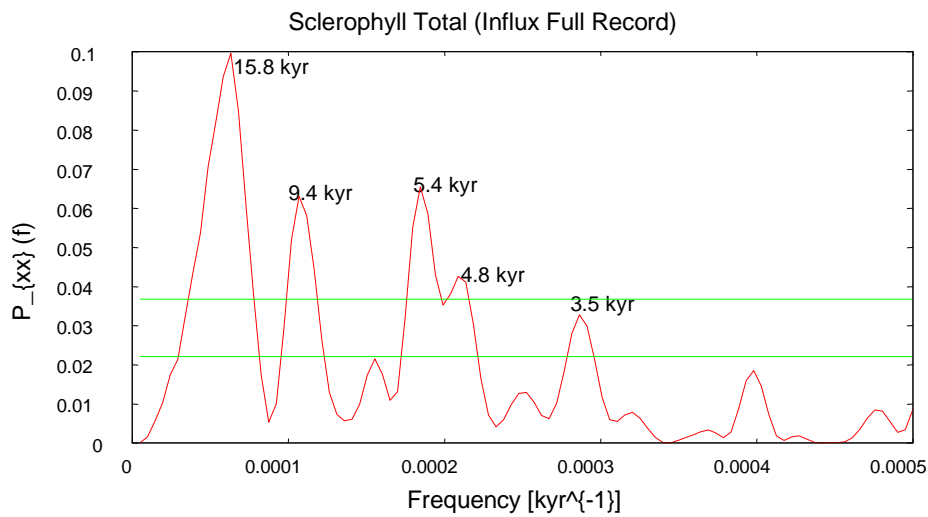


Figure 8.26. Spectra plot of Sclerophyll total (Influx Full), frequencies noted on plot

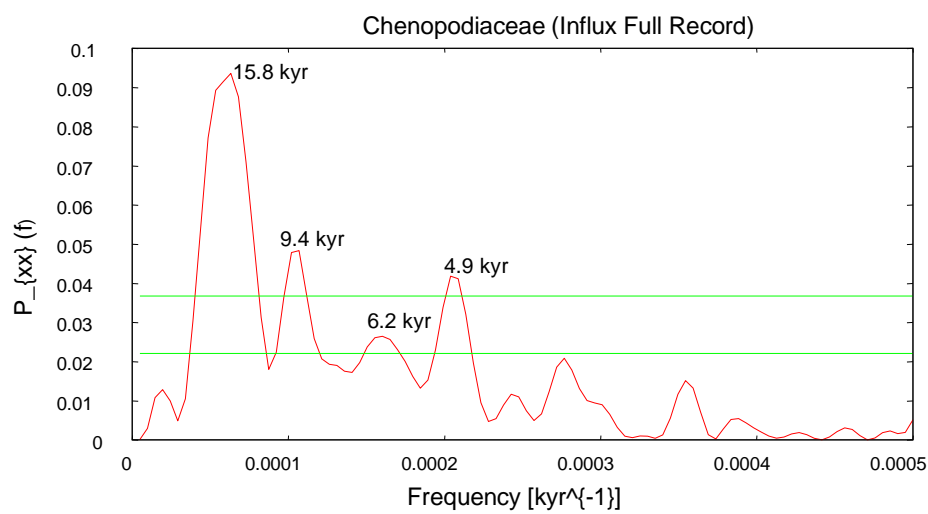


Figure 8.27. Spectra plot of Chenopodiaceae (Influx Full), frequencies noted on plot

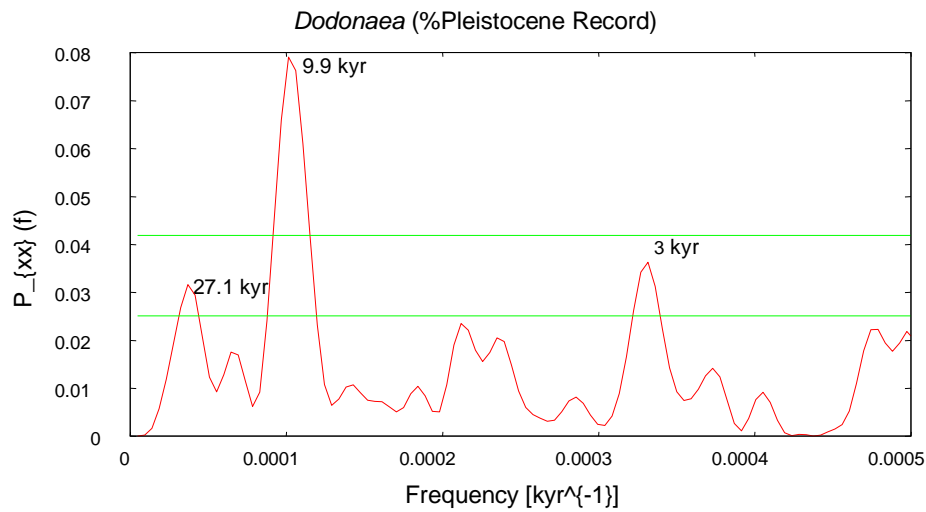


Figure 8.28. Spectra plot of *Dodonaea* (%Pleistocene), frequencies noted on plot

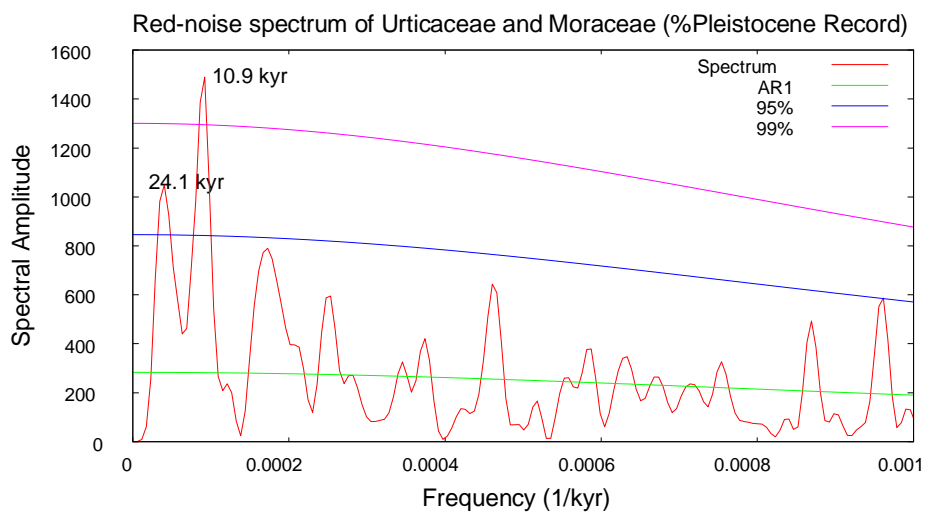


Figure 8.29. Red-noise spectra plot of Urticaceae and Moraceae (%Pleistocene), frequencies noted on plot

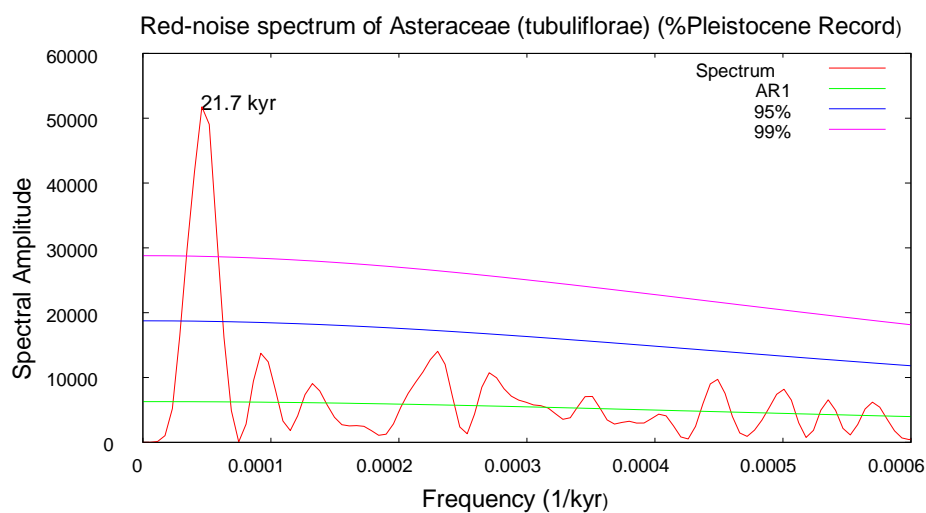


Figure 8.30. Red-noise spectra plot of Asteraceae (tubuliflorae), (%Pleistocene), frequencies noted on plot

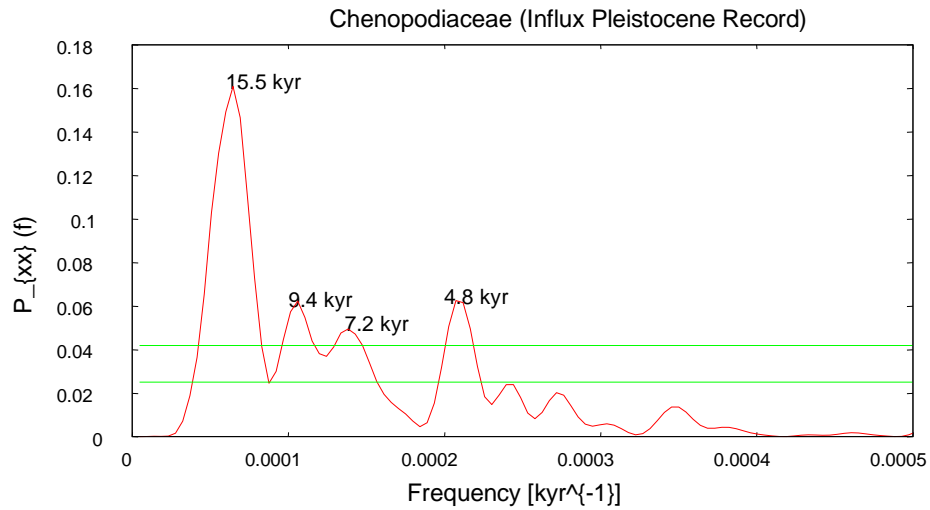


Figure 8.31. Spectra plot of Chenopodiaceae (Influx Pleistocene), frequencies noted on plot

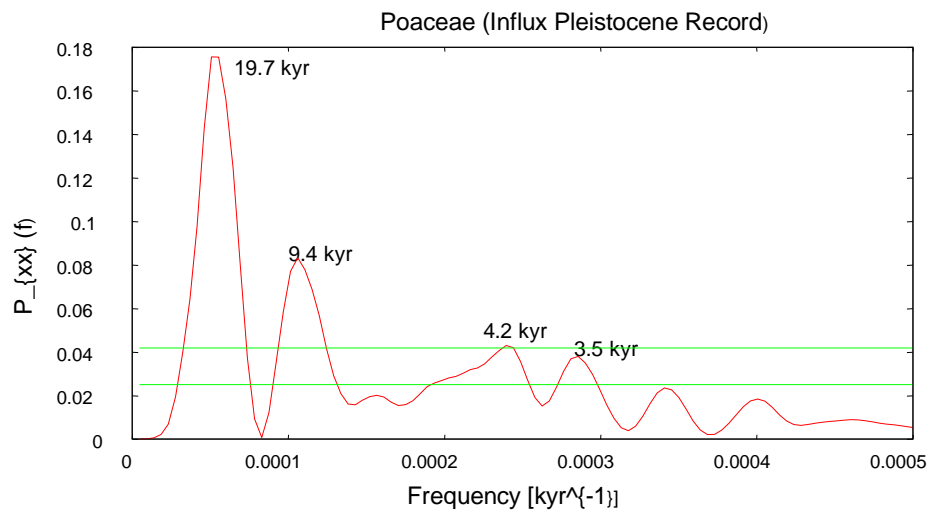


Figure 8.32. Spectra plot of Poaceae (Influx Pleistocene), frequencies noted on plot

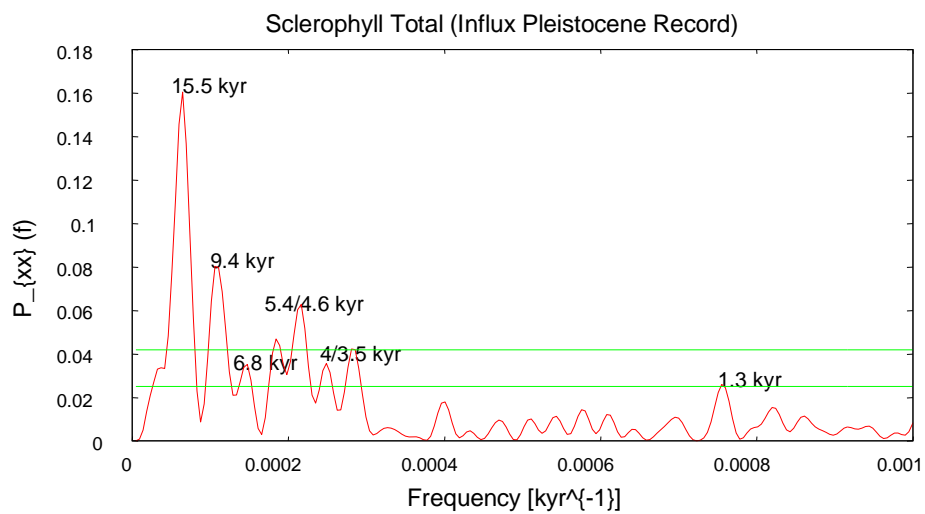


Figure 8.33. Spectra plot of Sclerophyll total (Influx Pleistocene), frequencies noted on plot

8.2.3. Spectral analysis aquatic and swamp results

Like PCA, a re-summed aquatic and swamp pollen sum has been used for the spectral analysis. The list of the frequencies for the full record including concentration, percentage and influx data is given in Table 8.3 and, for the Pleistocene record, in Table 8.4. These results also include both the microcharcoal and macrocharcoal and its sub-categories. The spectral frequency plots for selected major aquatic taxa and charcoal (concentration, percentage, and influx) for the full sequence and the Pleistocene sequence are given in Figures 8.34–8.39 with full details given in Appendix B (2), Section 3. The same confidence level found in the spectra plot for the dryland taxa also applies for the aquatic and swamp taxa with the two green lines on the spectra plot indicating Fisher and Siegel’s critical confidence levels, with a frequency above both lines indicating a 99% confidence level while a frequency found within the two lines indicating a 95% confidence level.

Table 8.3. Critical spectral analysis frequencies, precessional, semi-precessional, 15–17 kyr and millennial, using Siegel’s significance test for the aquatic and swamp inc. macrocharcoal and microcharcoal percentage, concentration and influx data for the full record (3 ka–54 ka), X – primary frequency (99% confidence level), X – secondary frequency (99% confidence level) and X – frequency within Fisher 99% and Siegel’s 95% critical confidence levels.

Percentage, Influx and Concentration Components Full record 3 ka–54 ka	19–23 kyr %	15–17 kyr %	9.5–11.5kyr %	1–2 kyr %	19–23 kyr Influx	15–17 kyr Influx	9.5–11.5kyr Influx	1–2 kyr Influx
Microcharcoal total		X		X				
Macro’Blocky’				X				X
Macro’Elongated’				X				X
Macro’Lattice’		X		X				X
Macrocharcoal total				X				X
<i>Botryococcus</i>		X						X
<i>Eleocharis</i>	X	X		X		X		
<i>Schoenoplectus/Carex</i>				X	X			
<i>Baumea</i>	X			X	X			
Cyperaceae total				X	X			
Poaceae	X		X	X	X		X	
<i>Persicaria</i>					X			
<i>Haloragis/Gonocarpus</i>		X		X				
<i>Hydrocotyle</i>	X		X					

Table 8.41. Critical spectral analysis frequencies, precessional, semi-precessional, 15–17 kyr and millennial, using Siegel’s significance test for the aquatic and swamp inc. macrocharcoal and microcharcoal percentage, concentration and influx data for the time-period (11.8 ka–54 ka), X – primary frequency (99% confidence level), X – secondary frequency (99% confidence level) and X – frequency within Fisher 99% and Siegel’s 95% critical confidence levels.

Percentage, Influx and Concentration Components Pleistocene record 11.8 ka–54 ka	19–23 kyr %	15–17 kyr %	9.5–11.5kyr %	1–2 kyr %	19–23 kyr Influx	15–17 kyr Influx	9.5–11.5kyr Influx	1–2 kyr Influx
Microcharcoal total						X	X	
Macro’Blocky’	X			X				X
Macro’Elongated’	X			X				X
Macro’Lattice’								X
Macro’Other’	X				X		X	X
Macrocharcoal total	X			X	X		X	X
<i>Botryococcus</i>	X					X		X
<i>Eleocharis</i>			X				X	
<i>Schoenoplectus/Carex</i>		X		X			X	
<i>Baumea</i>	X			X	X			
Cyperaceae total		X	X	X	X			X
Poaceae	X		X	X				
Cyperaceae/Poaceae ratio		X						
<i>Typha</i>	X			X				
<i>Persicaria</i>		X			X			X
<i>Haloragis/Gonocarpus</i>		X		X				
<i>Hydrocotyle</i>						X		

Microcharcoal results for the influx data full sequence did not fall within the frequencies shown in Tables 8.3 and 8.4 but the spectra plots indicate a dominant 4.1 kyr and a secondary 14.7 kyr frequency, both at 95% confidence level. A 14–18 kyr frequency was found across all microcharcoal (concentration) size classes for the Pleistocene sequence as were secondary millennial frequencies, all at 99% confidence level. The spectra plots for selected proxies are given in Figures 8.34–8.39. For those shown to have red-noise, the red-noise spectra plots are instead given. As for the dryland analysis, all spectra frequency plots from the results in Table 8.3 and Table 8.4 as well as other minor aquatic and swamp taxa including the results determined from REDFIT, are given in Appendix B (2), Section 3.

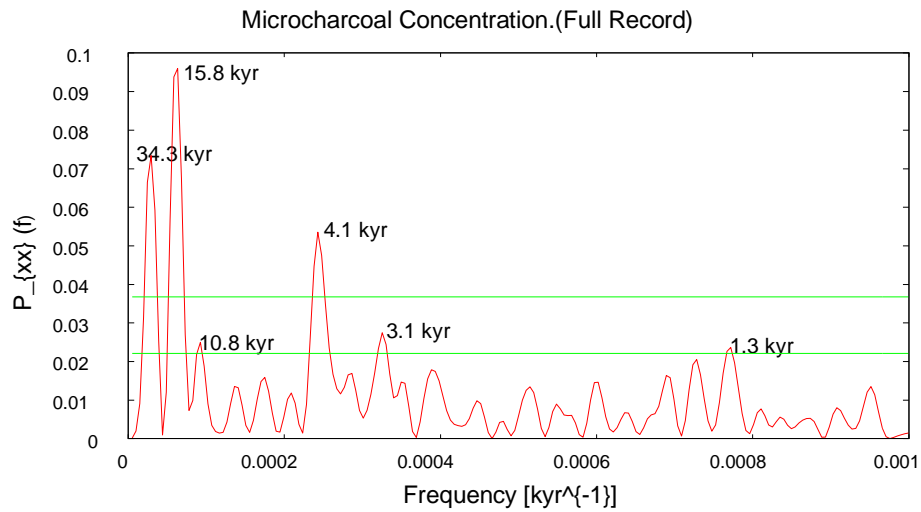


Figure 8.34. Spectra plot of microcharcoal (Conc. Full), frequencies noted on plot

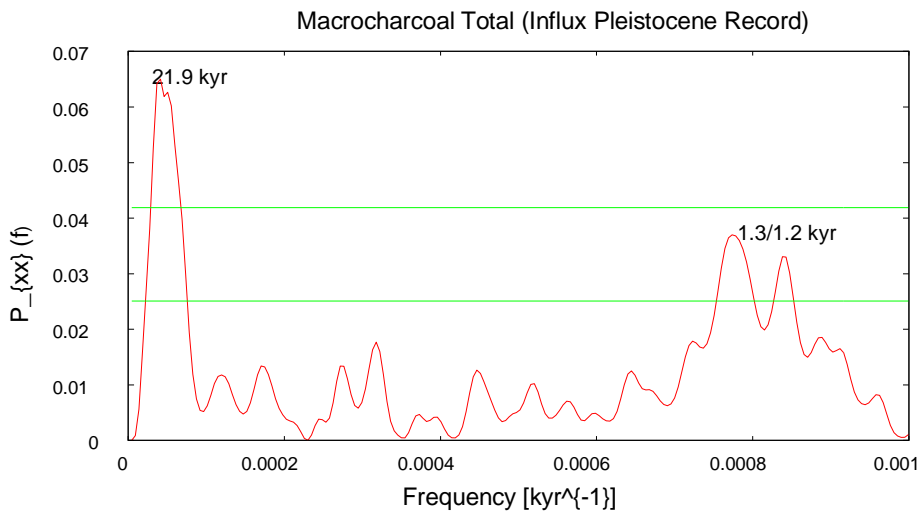


Figure 8.35. Spectra plot of macrocharcoal (Influx Pleistocene), frequencies noted on plot

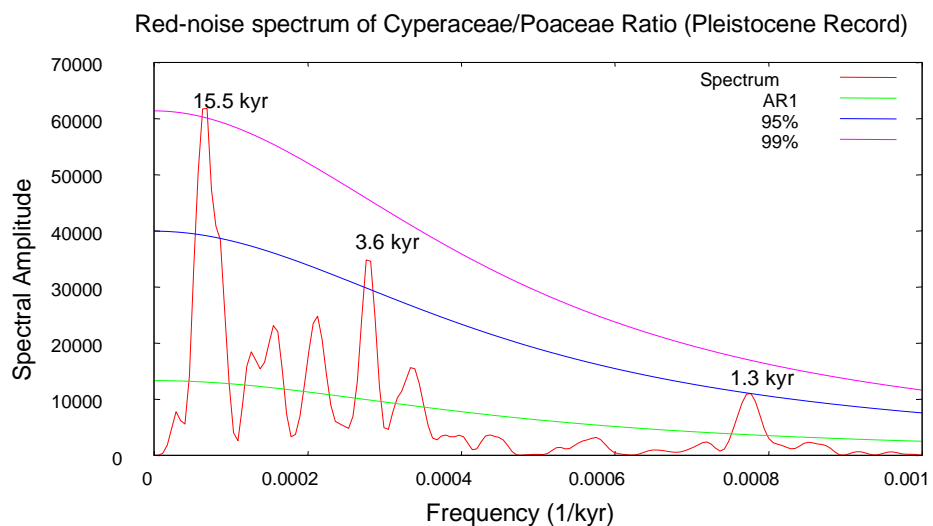


Figure 8.36. Red-noise spectra plot of Cyperaceae/Poaceae ratio (Pleistocene), frequencies noted on plot

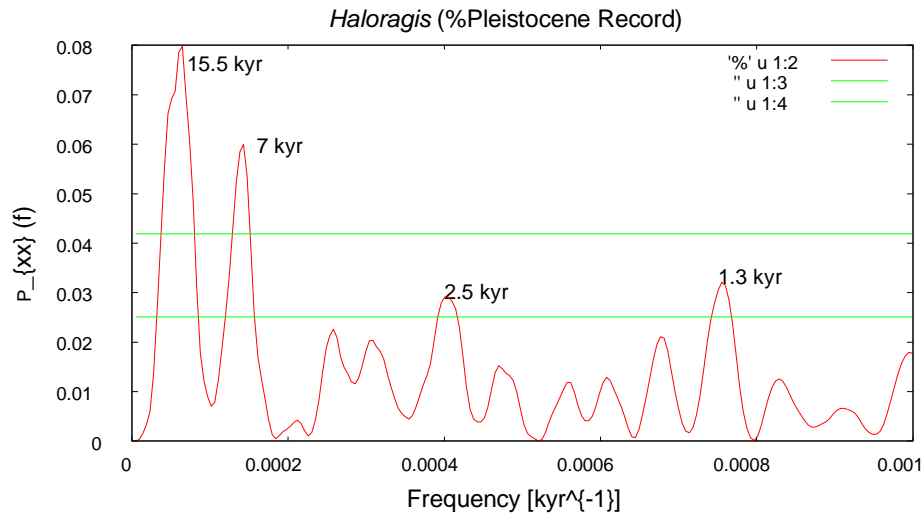


Figure 8.37. Spectra plot of *Haloragis* (% Pleistocene), frequencies noted on plot

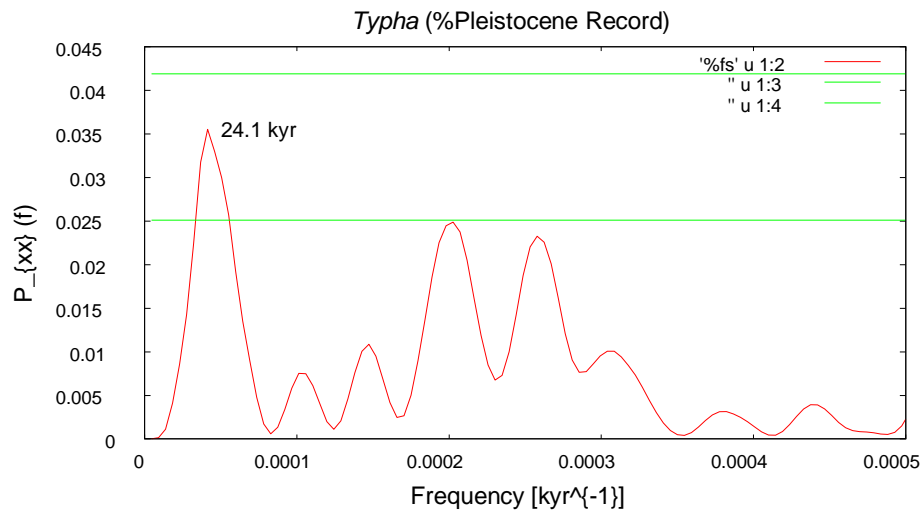


Figure 8.38. Spectra plot of *Typha* (% Pleistocene), frequencies noted on plot

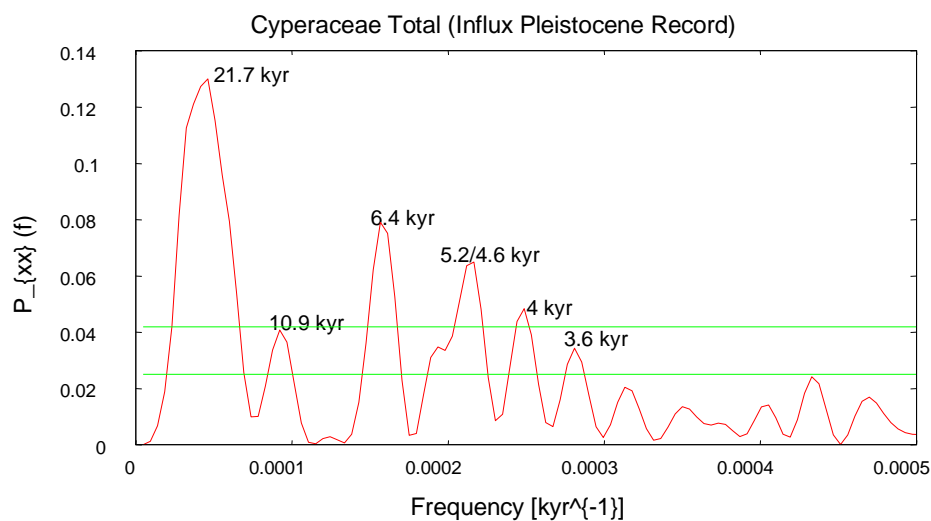


Figure 8.39. Spectra plot of Cyperaceae (Influx Pleistocene), frequencies noted on plot

8.2.4. Spectral analysis humification results

Spectral analysis already undertaken on the aquatic/swamp taxa, see sub-section 8.2.3, did indicate that, although not a primary frequency, the millennial frequency of 1–2 kyr was common across the analysed data and so spectral analysis was performed across the humification time sequence, 28.5 ka–37.9 ka, for both the percentage and influx data to test for the presence of this frequency herre. Besides the humification data, the Cyperaceae taxa, Poaceae, moisture, inorganics, microcharcoal, macrocharcoal (and sub-categories) and the Cyperaceae/Poaceae ratio from the re-summed aquatic/pollen sum were analysed.

Although the 1–2 kyr frequency was common across the data for the spectral analysis, the presence of red-noise was also common with REDFIT analysis further reducing the validity of this frequency. Full details of these results are given in Appendix B, section 3. However, humification, *Eleocharis* (%), the Cyperaceae/Poaceae ratio, macrocharcoal and especially Poaceae (% and influx) had a valid 1–2 kyr frequency. The spectra and red-noise spectra plots, when needed, are given in Figures 8.40–8.44.

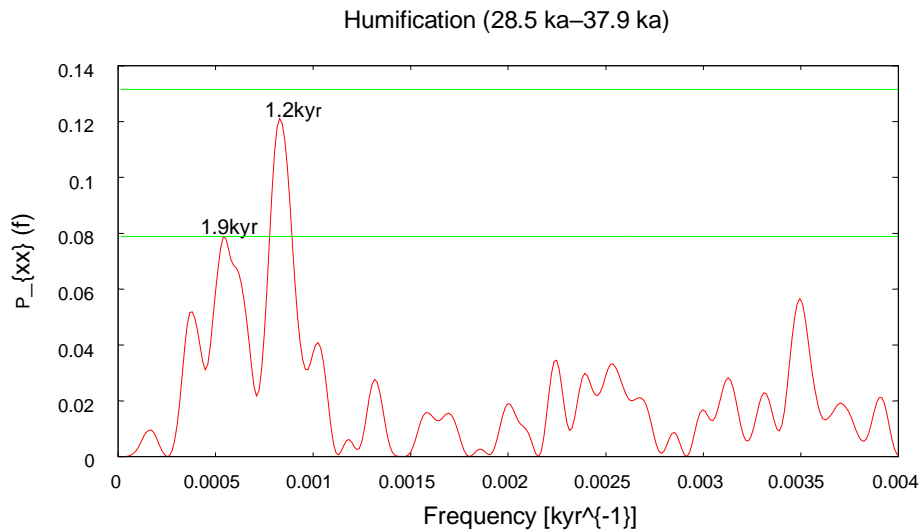


Figure 8.40. Spectra plot of humification (28.5 ka–37.9 ka sequence), frequencies noted on plot

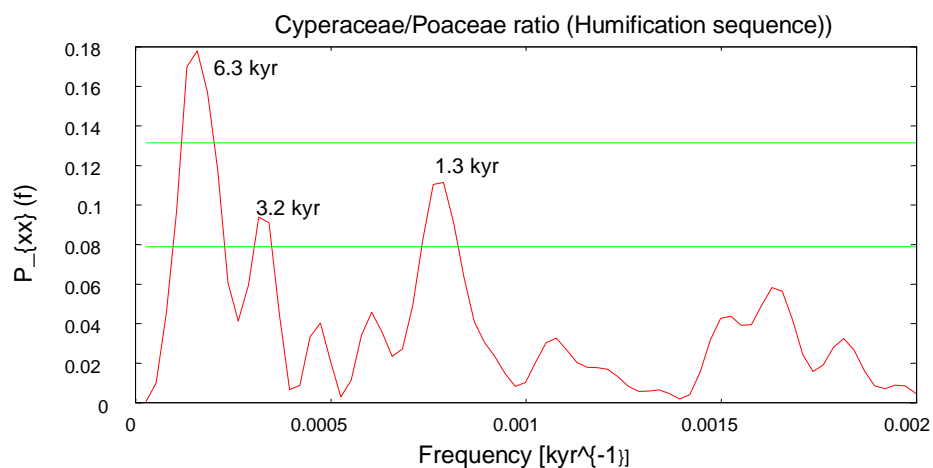


Figure 8.41. Spectra plot of Cyperaceae/Poaceae ratio (28.5 ka–37.9 ka sequence), frequencies noted on plot

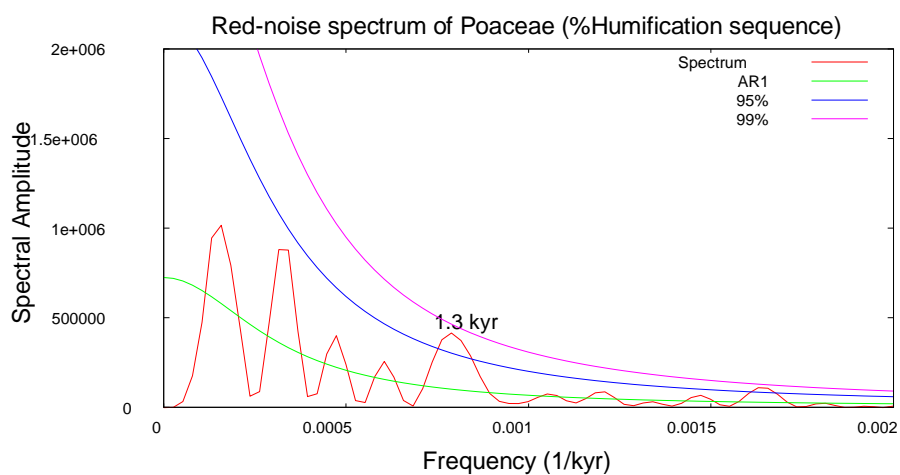


Figure 8.42. Red-noise spectra plot of Poaceae (%28.5 ka–37.9 ka sequence), frequencies noted on plot

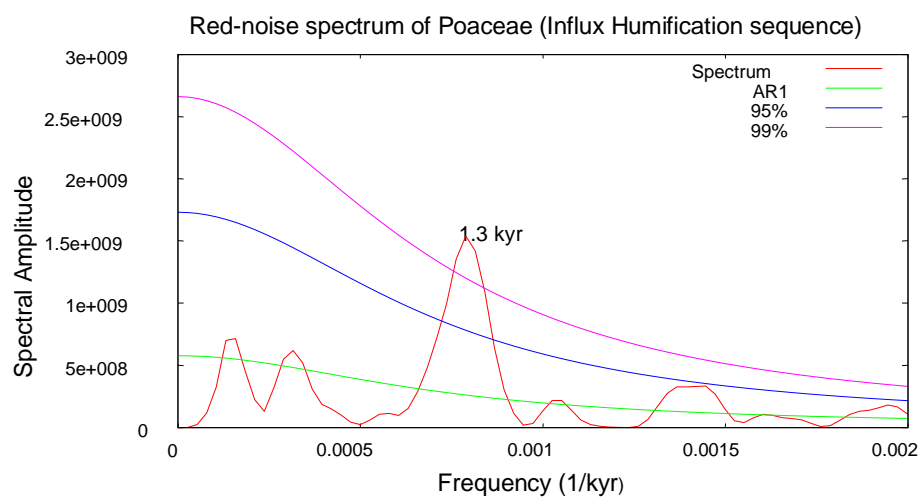


Figure 8.43. Red-noise spectra plot of Poaceae (Influx 28.5 ka–37.9 ka sequence), frequencies noted on plot

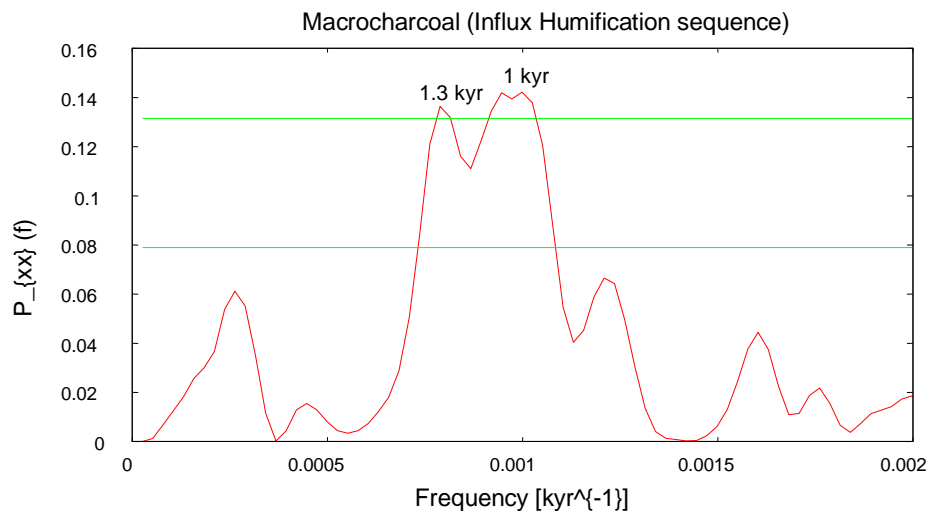


Figure 8.44. Spectra plot of macrocharcoal (Influx 28.5 ka–37.9 ka sequence), frequencies noted on plot

8.2.5. The precessional/semi-precessional frequency

As indicated in tables, Tables 8.1–8.4, both precessional and semi-precessional cycles are relatively common significant frequencies, above 99% confidence level, but was also common frequencies at the 95% confidence level for a great many taxa for both % and influx. However, although Schulz and Mudelsee (1997) argue that only two full cycles are needed to verify frequencies, it has also been suggested that even with two full cycles it is not possible to statistically infer these cycles (Garcin et al. 2006) and so caution is needed, in particular, for those taxa that presented with a precessional frequency especially during the Pleistocene sequence. However, it was relatively common for some taxa to have both a precessional cycle and a semi-precessional cycle. This would suggest that for the time-period analysed in this study, ~3 ka–~54 ka, low frequency variability for a good proportion of the taxa is associated with both the precessional and semi-precessional bands.

In a number of proxies that had the precessional or semi-precessional frequency a 15,000 yr–17,000 yr frequency was also present, *Dacrydium*, Casuarinaceae, Poaceae, Asteraceae (tubuliflorae) *Elaeodendron* and *Persicaria*, see Tables 8.1–8.4 for full details. This 15,000 yr–17,000 yr frequency was relatively common and was particularly prominent across the sclerophyll trees, dryland herbs and microscopic charcoal but also the secondary rainforest taxa and herbaceous aquatic taxa see Tables 8.1–8.4 for full

details. This frequency, 15–17 kyr, has also been found in several other sites, predominantly sub-tropical/tropical (Berger et al. 1991; Hooghiemstra et al. 1993). Whether this frequency is a modulated harmonic of the precessional or semi-precessional cycle (Berger et al. 1991) is not known but its dominant presence within these taxa, some which are advantaged by disturbance suggests that it is an important frequency for this record.

8.2.6. Millennial frequencies

Millennial frequencies were common across all time sequences though in most of the cases they were usually at the 95% confidence level (see Appendix B (2) section 3 for full details). However, there were some proxies that did have millennial frequencies at the 99% confidence level. This was the case for Chenopodiaceae and *Callitris* with a 3550 year and 3680 year frequency, respectively, as their primary frequency across the full and Pleistocene percentage time-series, while the primary frequency for Podocarpaceae was a 3680 year frequency across the full and Pleistocene influx time-series. This frequency, 3550 or 3680 year, was a common secondary frequency in both the full and Pleistocene time-series. A 6650 year frequency was the primary frequency for *Dacrydium* across the full and Pleistocene influx time-series and was also a common secondary frequency for the Cyperaceae taxa, rainforest canopy taxa, *Acmena* and *Elaeocarpus*, dryland herbs and *Eucalyptus*. (Appendix B(2) Section 3).

When comparing the present study with the results from Turney et al. (2004), there were few that specifically had a 1,490 or 1,470 yr frequency. Although the pacing interval of Dansgaard-Oeschger (D/O) events is known to vary, for example Rahmstorf (2003) suggests they may vary as little as $\pm 8\%$ while Schulz (2002) suggests a higher value of $\pm 20\%$, their duration (1470 yr) here seems to be more fixed. *Elaeocarpus* (1470 yr), *A. peralatum* (1510 yr), *Celtis* (1480 yr) and Menispermaceae (1500 yr), Figures 8.45–8.49, were the only pollen proxies that had or were near this frequency. *A. peralatum* only had this frequency across the full time-series while, for the other three, it was present across the Pleistocene time-series but for all proxies it was at the 95% confidence level. All had red-noise but this frequency was still present after ARI correction. This would suggest this frequency is relatively stable for these proxies and could still be regarded as significant.

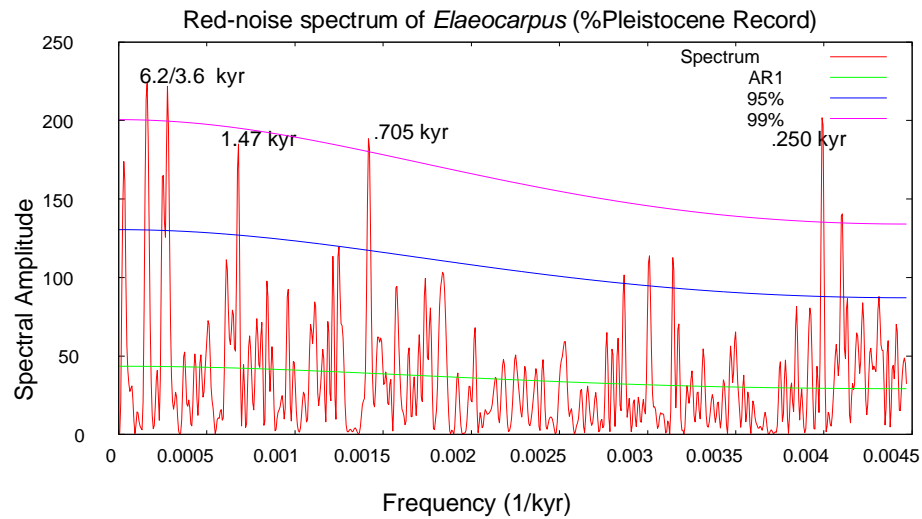


Figure 8.45. Red-noise spectra plot of *Elaeocarpus* (%Pleistocene), frequencies noted on plot

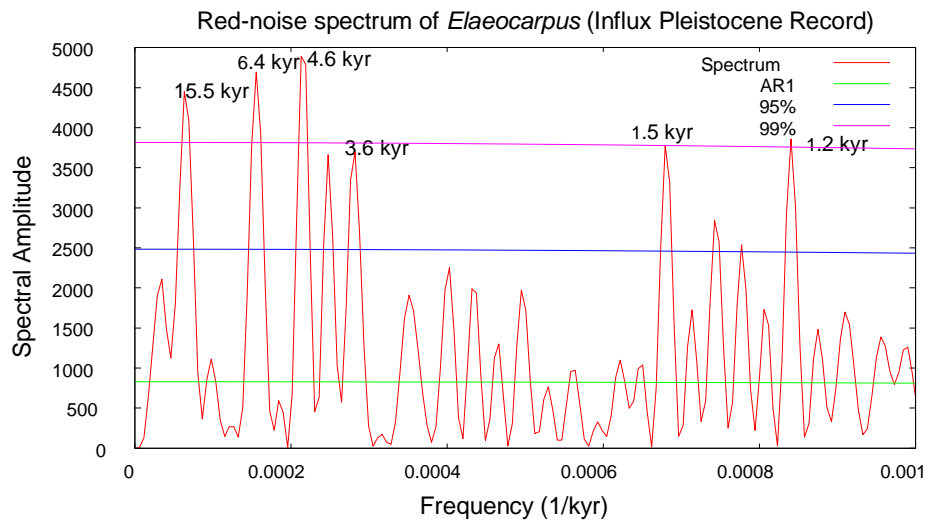


Figure 8.46. Red-noise spectra plot of *Elaeocarpus* (Influx Pleistocene), frequencies noted on plot

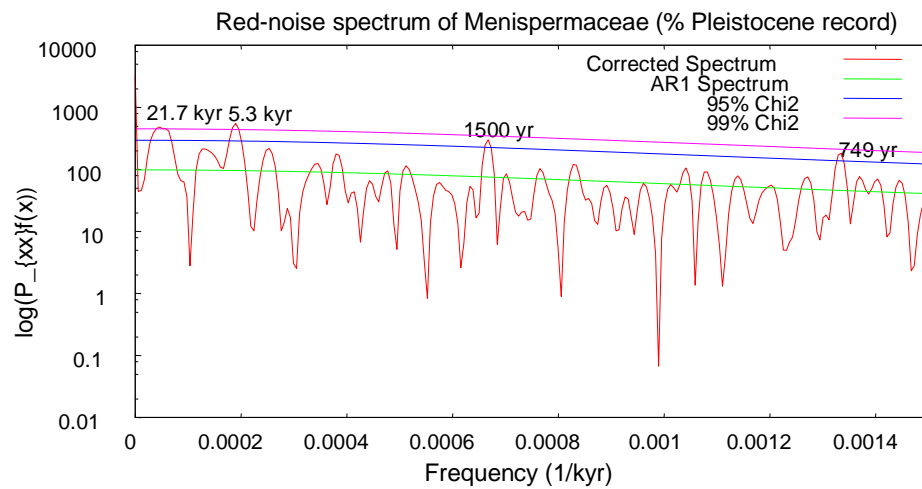


Figure 8.47. Red-noise log-linear spectra plot of Menispermaceae (%Pleistocene), frequencies noted on plot

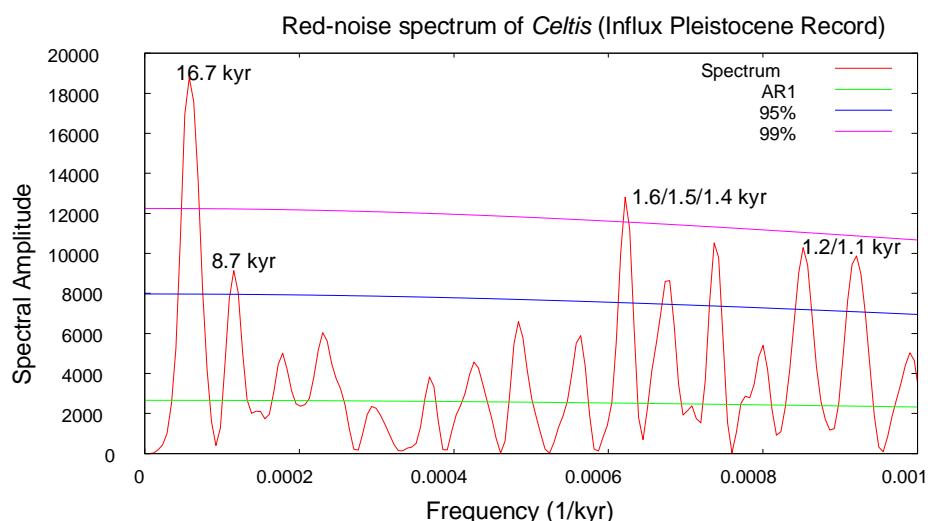


Figure 8.48. Red-noise spectra plot of *Celtis* (Influx Pleistocene), frequencies noted on plot

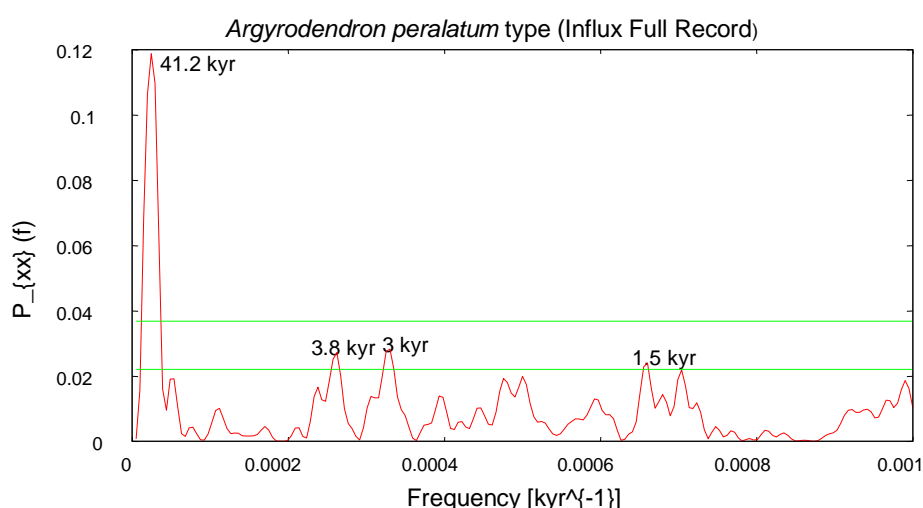


Figure 8.49. Spectra plot of *Argyrodendron peralatum* type (Influx Full), frequencies noted on plot

Elaeocarpus, *Celtis* and Menispermaceae had good representation throughout the Pleistocene sequence and, although *Elaeocarpus* has better representation during the Holocene, it was one of the few (wetter) canopy rainforest elements that had a relatively consistent, albeit minor, presence through the Pleistocene period, and was also the only one out of the four that had this frequency across both the percentage and influx data. However, what is also evident when looking at the results for *Elaeocarpus* and *Celtis*, Figures 8.45, 8.46 and 8.48, is the presence of a number of frequencies within the 1.2 kyr–1.7 kyr range. Frequencies between 1.2 kyr–1.7 kyr were fairly common for both the percentage and influx data, especially for the sclerophyll taxa, vines and secondary rainforest taxa and the major aquatic taxa including both Poaceae and macrocharcoal

although it was also present for some of the rainforest canopy taxa. *Acmena* and *A. peralatum* only displayed this frequency for the influx data. The pteridophytes, *Davallia* and *Cyathea*, had this frequency but only in the percentage Pleistocene time-series. These results are summarized in Table 8.5, with full details given in Appendix B (2), Section 3.

Table 8.5. Significant spectral frequency, 1.2–1.7 kyr, using Fisher and Siegel’s significance test for selected components across all time-series and percentage, concentration and influx data.

	Frequency (yr) %	Red-noise present	Red-noise > 99%	Frequency (yr) Influx	Red-noise present	Red-noise > 99%
Cyperaceae	1300 ²	Yes	Yes			
Poaceae	1350 ^{1,2}	No				
<i>Typha</i>	1720 ²	No				
<i>Botryococcus</i>				1580 ¹ /1600, 1270 ²	No	
<i>Haloragis/Gonocarpus</i>	1340 ¹ /1330 ²	No				
<i>Persicaria</i>				1320 ²	No	
<i>Davallia</i>	1160 ²	Yes	Yes			
<i>Cyathea</i>	1510,1350,1300 ²	No				
Chenopodiaceae	1250 ¹	No				
Macrocharcoal	1300 ¹ /1290 ²	No		1300 ^{1,2}	No	
Microcharcoal	1300 ¹	No				
Podocarpaceae	1570 ¹ /1600,1540 ²	No		1570,1310 ¹ / 1600,1550,1320 ²	No	
<i>A. peralatum</i>				1510 ¹	No	
<i>Elaeocarpus</i>	1470 ²	Yes	Yes	1470,1190 ²	Yes	Yes
<i>Acmena</i>				1630,1230 ²	Yes	Yes
<i>Austrobuxus</i>				1600 ²	No	
<i>Celtis</i>	1620,1360,1070 ²	Yes	Yes	1610,1480,1360, 1170 ²	Yes	Yes
<i>Mallotus/Macaranga</i> *				1720,1310,1210 ²	Yes	Yes
<i>Homalanthus</i>	1540 ¹ /1620 ²	No				
Loranthaceae	1340 ¹	Yes	Yes			
Menispermaceae	1510 ¹ /1500 ²	Yes	No			
<i>Callitris</i>	1290 ¹ /1280 ²	No				
<i>Melaleuca</i>				1320 ²	No	
<i>Corymbia</i>				1320,1160 ²	No	
<i>Eucalyptus</i>	1230 ³	Yes	Yes	1320 ²	Yes	Yes
<i>Gyrostemon</i>	1390 ³	Yes	Yes	1350 ¹ /1310 ³	No	

¹Full time-series, ²Pleistocene time-series, ³Holocene/LGM time-series, **Mallotus/Macaranga*

All proxies in Table 8.5 had these frequencies at the 95% confidence level (Fisher and Siegel 99% and 95% critical confidence levels) except for *Mallotus* and *Macaranga* where the 1310 yr frequency was at the 99% confidence level and although red-noise was present this frequency remained valid (see Figure 8.50). Frequencies near this cycle (1300–1350 yr) were the most common within the 1.2–1.7 kyr range, Table 8.5.

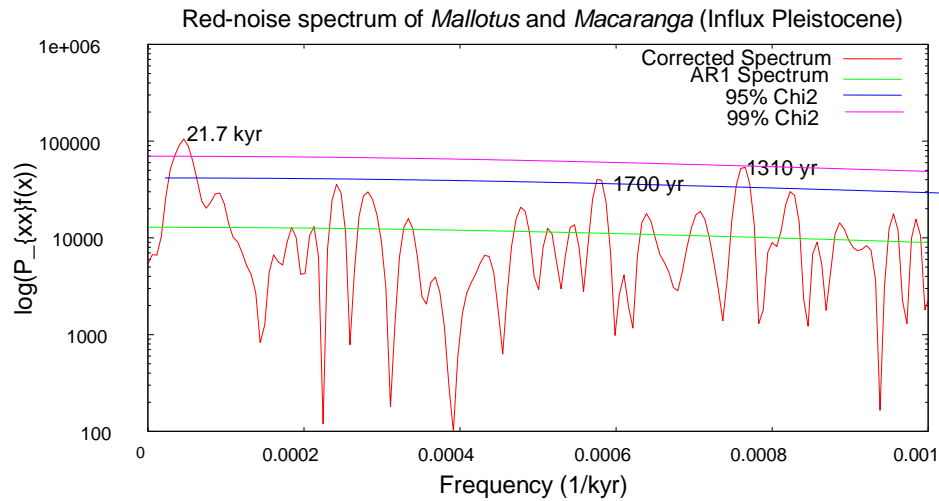


Figure 8.50. Red-noise log-linear spectra plot for *Mallotus* and *Macaranga* (influx Pleistocene record) with both the 21.7 kyr (precessional) and 1.31 kyr (millennial) frequency at 99% confidence level.

Frequencies near this cycle have also been found in proxies from temperate eastern Australia (Skilbeck et al. 2005; Black et al. 2007), and also from radiocarbon data exploring population densities within an archaeological context in the Australian drylands (Smith et al. 2008). However, these studies have been situated primarily within the Holocene time-period and the only taxon in this study with this frequency within the Holocene period is *Gyrostemon*, see Table 8.5.

Centennial frequencies were also common but, except for *Trema* (725 yr) (Figure 8.51) were at the 95% confidence level. A frequency between 640–750 years was present for some of the rainforest components, *Cissus*, *Elaeodendron*, *Menispermaceae*, *Flindersia* and *Zanthoxylum*, but also the larger size fraction > 156 μm for microcharcoal (see Appendix B (2), section 3 for full details).

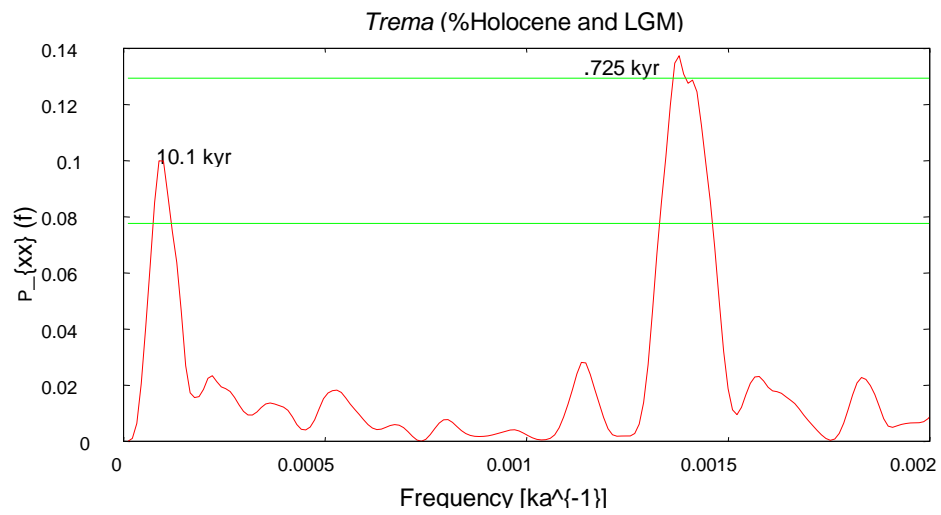


Figure 8.51. Spectra plot of *Trema* (%Holocene and LGM) indicating the centennial frequency, 725 yr, at 99% confidence level.

Chapter 9

Discussion

Introduction

Lynch's Crater on the Atherton Tableland, northeast Queensland, has provided one of the longest and most continuous records of vegetation and environmental change in the late Quaternary of Australia (Kershaw et al. 2007). However, the resolution of this record is coarse and therefore interpretation is limited to broad generalisations, of concern especially for the last 50,000 years, a critical time-period for which there is generally good radiocarbon dating control and which covers all or a large part of Aboriginal occupation of the continent, the period of suggested impact of Aboriginal people, and a demonstrated marked influence of climatic variability especially associated with Heinrich events (Turney et al. 2004; Muller et al. 2008b). This project has aimed to counter these limitations by providing a more refined palaeoenvironmental record through the last 50,000 years from the use of a multi-proxy high frequency sampling approach which provides a more comprehensive representation of changes both on local and regional scale changes. The availability of more refined and accurate chronology has allowed pollen influx to be calculated providing information on changes in vegetation density through time, and the investigation of cycles of orbital to sub-millennial frequency through the use of statistical analyses has provided insight into the influence of global and broad regional climate variation on vegetation dynamics. The nature and extent of fire, as determined from micro- and macrocharcoal analysis, has been assessed for its potential to determine human influences on the landscape, particularly in the demise of both moist and complex rainforest formations and changing rainforest-sclerophyll distributions. A general environmental description for the time-period covered in this project is given below followed by the discussion of the achievements of the project aims outlined above.

9.1. Climatic conditions during MIS 3 to 1 in the north-east Australian region

Climatic variation is very much influenced by sea level changes that, in turn, are largely a reflection of global ice volume. Estimates of sea-level within the northeastern Australasian region during MIS 3 (60/57 ka) have been calculated from coral reef structures on the Huon Peninsula, Papua New Guinea, suggesting that sea-level oscillated 45 – 65 m below present sea-level during the period 64 – 32 ka and was further reduced

at ~30 ka (Woodroffe and Webster 2014). During MIS 2 (29/24 ka) sea-level was at its lowest, ~125 m below present, and sea-surface temperatures around the Australian margin, were coldest at $20,500 \pm 1400$ cal yr. B.P. (Barrows and Juggins 2005; Lewis et al. 2013). Greatest cooling, ~4°C, within the tropics was found in the eastern Indian Ocean/northwest Australia with estimates elsewhere in the tropics, including the Coral Sea/northeast Australia region ranging from 1–2.5°C (Yokoyama et al. 2000; Reeves et al. 2013*b*). The lower sea levels during MIS 2, ~125 m, also resulted in larger landmasses and, with the exposure of the continental shelves, an increase in continentality. The study site region itself has a relatively narrow continental shelf which would have restricted the increase in landmass to a maximum ~70 km (Lewis et al. 2013; Hinestrosa et al. 2016) and the study site region to ~155 km from the coast. This would have resulted in either a reduction and/or change in the modes of large-scale climate systems. It has been proposed that there was a lack of an operating monsoon or one that was greatly reduced and this is suggested with the presence of extensive drying shelves in northern Australia with the Gulf of Carpentaria largely a confined shallow waterbody from 40 – 12 ka (Barrows and Juggins 2005; Reeves et al. 2013*a*). It has also been suggested that the ITCZ stayed close to the (thermal) equator due to perennial upwelling in the Java upwelling system under persistent southeast Trade Winds, and continental cooling on the northern Australian continent possibly reduced the heat lows which contribute to the movement of the ITCZ across northern Australia (Barrows and Juggins 2005). This would have greatly influenced the strength (reduction) of the Walker circulation, and therefore influenced (reduced) the extent of precipitation from the (weakened) south-east trade winds within the study region (Barrows and Juggins 2005; Reeves et al. 2013*a,b*). McGee et al. (2014) suggest that the relationship between SST gradients and atmospheric heat transport (AHT) is extremely sensitive to small changes in mean ITCZ position and that inferred large-scale precipitation changes should be viewed alongside different climate forcings rather than attributed to global ITCZ ‘shifts’.

Prior to and continuing into MIS 1 (14/11.6 ka), sea-level increase was likely to have been rapid around the northern Australian margin during meltwater pulse (MWP) 1A (14.6–14.3 ka) and through to MWP 1B (~11.5–11.3 ka) (Bard et al. 1996; Fleming et al. 1998; Milne et al. 2005; Deschamps et al. 2012; Lewis et al. 2013). The general consensus of when sea-level reached modern levels within the study site region is between ~8,000–6,200 cal. yr. B.P. (Lewis et al. 2008; Woodroffe 2009; Yu and Zhao 2010; Lewis

et al. 2013). There are differences in the estimates for the elevation of the mid-Holocene highstand and whether it was a global response or purely a response to glacial hydro-isostatic rebound (Lewis et al. 2013; Lambeck et al. 2014). However, around the northern Australian margin within the study site region an estimated highstand of + 1.0 m to 1.5 m between 6770–5750 cal. yr. B.P. is suggested (Chappell et al. 1983; Beaman et al. 1994; Hopley et al. 2007; Lewis et al. 2008, Lewis et al. 2013; Perry and Smithers 2011). After the Holocene highstand there are varying views on whether sea-levels fell smoothly or oscillated from the mid to late Holocene in response to a regional hydro-isostatic variation as well as the influence of the local geomorphological setting, and, therefore may only have had a very localised impact (Hopley et al. 2007; Lambeck et al. 2010; Lewis et al. 2013; Woodroffe and Webster 2014).

9.1.1. Araucarian dominant forest–54-41 ka

The main indicator of what type of rainforest was present, based on present-day distributions prior to ~54 ka is Araucariaceae, especially *Araucaria*. Kershaw (1973, 1976) suggested that Low Microphyll Vine forest (LMVF) + Araucariaceae or Complex Notophyll Vine forest (CNVF) + Araucariaceae was prominent from ~64 ka to 38 ka based on forests in south Queensland where *Araucaria* is still relatively abundant. LMVF + Araucariaceae is characterised palynologically by high *Araucaria* values, and drier elements of the rainforest angiosperms, *Olea paniculata*, *Acalypha*, *Longetia* (now *Austrobuxus*) and *Dodonaea* and low values for *Trema*, pteridophytes, *Macaranga* and Cunoniaceae. CNVF + Araucariaceae exists under higher rainfall and is indicated by reduced *Araucaria* values, an increase in the number of rainforest angiosperm such as *Argyrodendron*, *Elaeocarpus* and *Helicia*, and a decrease in sclerophyll taxa. Estimates for rainfall prior to ~38 ka was ~1000 mm lower than the present mean annual rainfall (~2500–2100 mm) and may have been more seasonal while the temperature may have been like that of today (Webb 1968; Webb et al. 1984; Kershaw and Nix 1988, 1989).

The presence of LMVF + *Araucaria* through 54–41 ka, Figure 9.1, a composite diagram of selected dryland taxa from Figure 7.6, (sub-zone *LCI-9b*) and the high values present for *Araucaria* would also suggest proximity to the crater as its large pollen grains are unlikely to be transported a great distance (Kershaw and McGlone 1995; Smith et al. 2007).

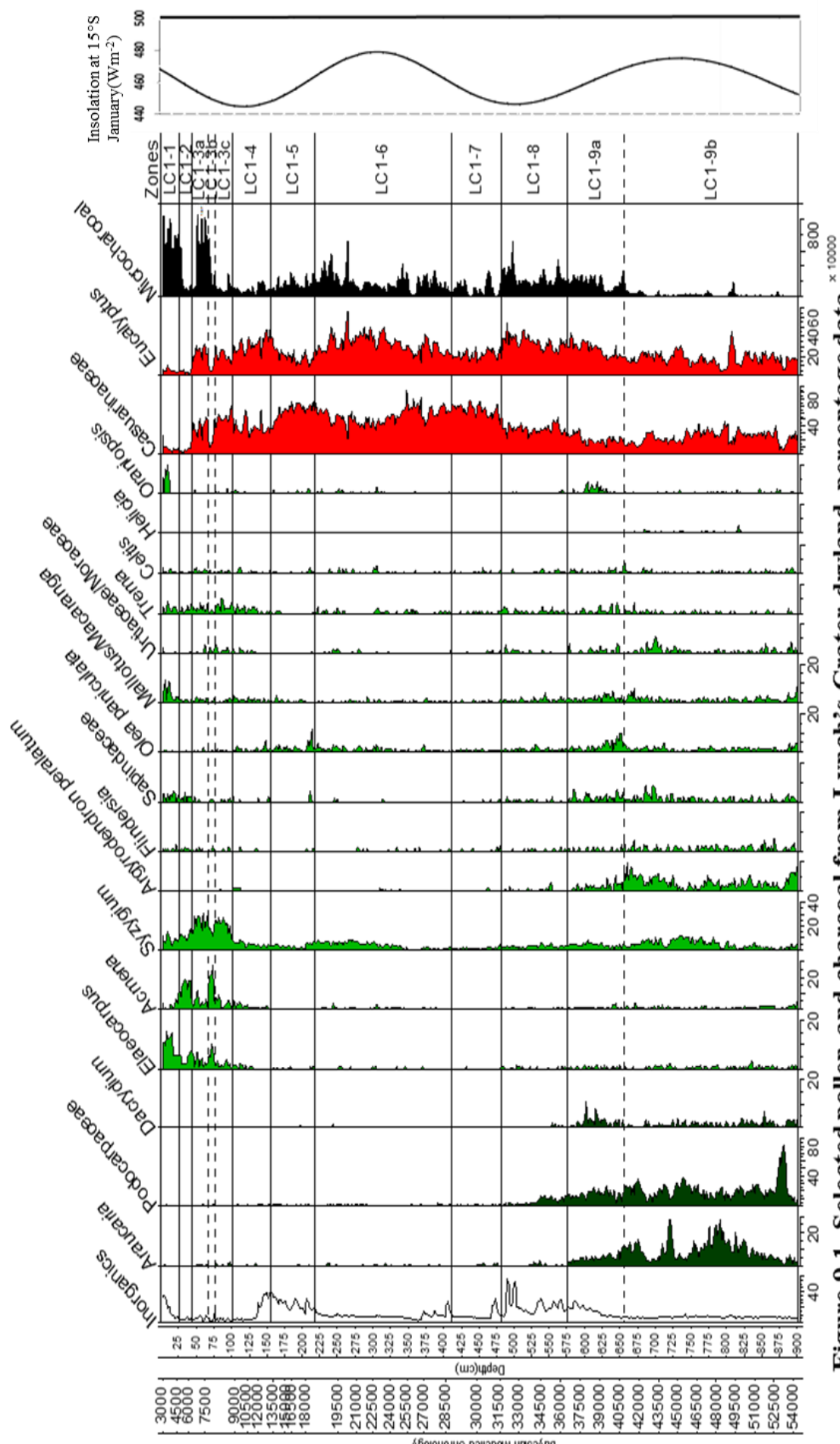


Figure 9.1. Selected pollen and charcoal from Lynch's Crater dryland percentage data

The consistent presence also of both, Casuarinaceae and *Eucalyptus*, would suggest at least a regional presence of sclerophyll vegetation. There is some variability across this period especially from 46 ka with more variable values recorded for *Araucaria* and higher fluctuating values for the rainforest canopy elements, *Argyrodendron peralatum* and Sapindaceae (syncolpate) and the likely swamp resident *Syzygium* which could suggest slightly higher rainfall levels. However, the increases in Urticaceae and Moraceae and *Macaranga* and *Mallotus* that follow from these increases may suggest warmer conditions, but more seasonal rainfall as suggested by Kershaw (1986). Insolation is at maximum at this time and therefore could be a factor for the more seasonal rainfall.

9.1.1.1. Local environment

From the evidence in Kershaw's record (1973, 1986, 1994; Kershaw et al. 2007a) the present record dates from the end of an interstadial marked by a shift from lake to swamp sediments. In this record the presence of *Cyclosorus* accompanied by the increase in Cyperaceae (Figure 9.2, a composite diagram of selected aquatic and swamp taxa taken from Figure 7.3) could suggest the development of a floating root-mat. Kershaw (1978, 1979) suggests that floating root-mats are not likely to develop over a water depth greater than about 2-3 m, with present-day Bromfield Swamp's floating root-mats containing *Cyclosorus*, *Leersia* (aquatic grass), *Persicaria*, *Cyperus*, *Baumea* and *Sparganium* providing a probable modern analogue (Kershaw 1975, 1978, 1979; Burrows et al. 2014b).

The presence of *Myriophyllum*, *Nymphoides* and *Potamogeton* pollen would also suggest the presence of free water although the macrofossils (Figure 9.7) are dominated by the sedges, *Carex appressa* and *Carex fascicularis*, *Gonocarpus chinensis* and *Hydrocotyle* spp. with only limited representation from the hydrophytic taxa, *Nymphoides indica* and *Potamogeton tricarinatus*. Pollen grains are more evenly and widely dispersed than macrofossils and therefore provide a better overview of the swamp and aquatic environment. Macrofossils represent very local-scale vegetation possibly metres to tens of metres around a core site (Birks and Birks 2000, Birks 2003, 2007; Zhao et al. 2006) so very limited areas of free water are suggested. The suggested significant presence of a dryland component on the swamp, composed of *Leptospermum* and Myrtaceae spp., would also suggest limited areas of free water.

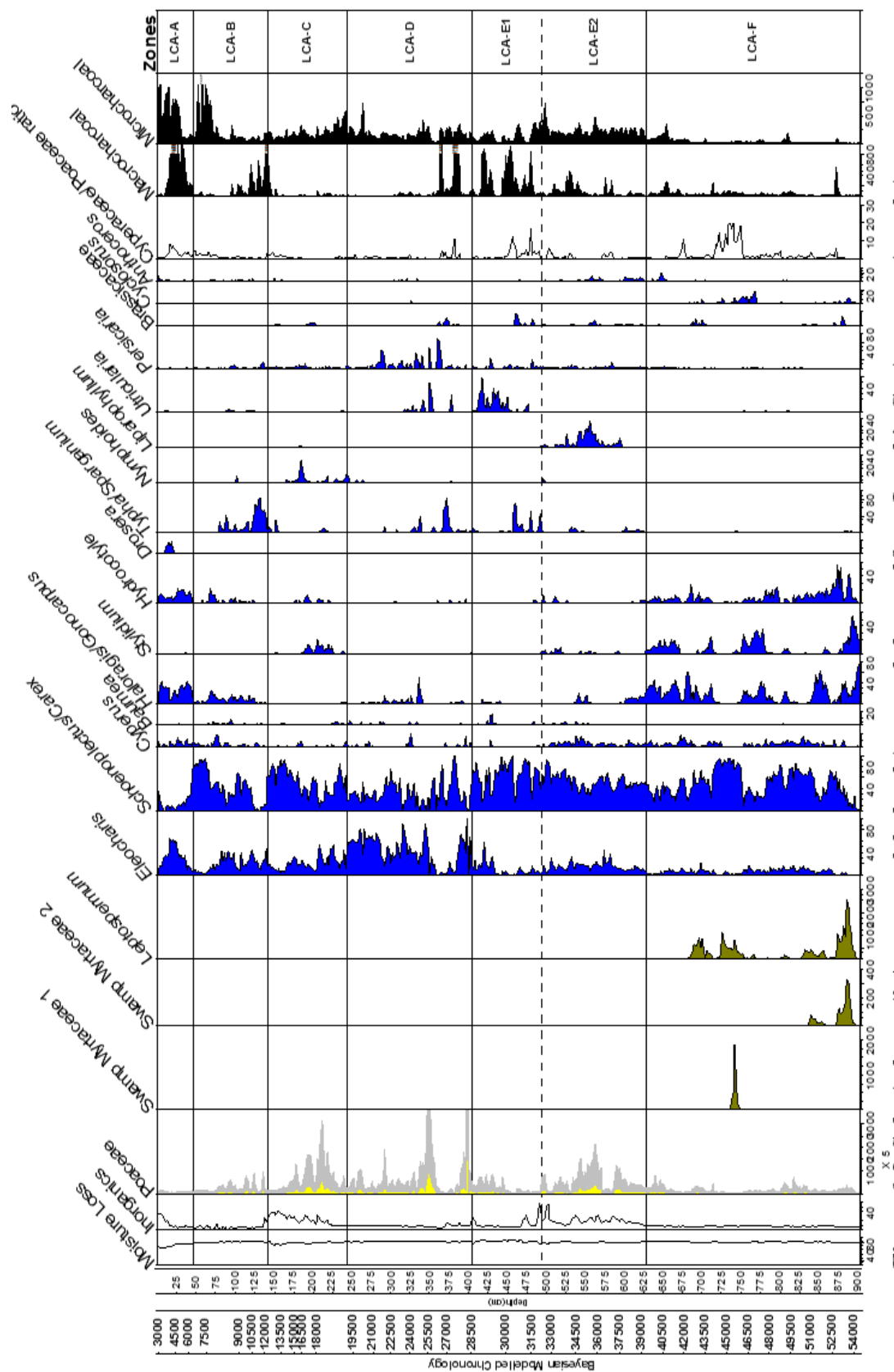


Figure 9.2. Selected aquatic/swamp and dryland taxa, and charcoal from Lynch's Crater percentage data

This ‘dryland’ component is also likely to have included *Syzygium*, *Dacrydium* and *Oraniopsis* and possibly the unknown Podocarpaceae (Bohte 1994; Bohte and Kershaw 1999). Minimal evidence of fire indicated by the low values for both micro- and macrocharcoal suggest that fire was not a major environmental factor during the period 54 to 41 ka.

9.1.2. The rainforest to sclerophyll transition 41–32ka

At ~41 ka the more seasonal drier rainforest element *O. paniculata* becomes the primary rainforest canopy taxon at the expense of *A. peralatum* which, from BIOCLIM estimates, indicate drier conditions (Moss and Kershaw 2000). This increase in *O. paniculata* is also accompanied by an increase in fire and a reduction of *Araucaria* to 2% of the dryland sum. *Araucaria* never recovers from these low values suggesting the end of a significant presence of araucarian forest within the landscape (Kershaw 1976; Kershaw et al. 2007a). The continuation of representation of the other major gymnosperm, *Podocarpus*, at relatively moderate levels through to 34.5 ka is likely to represent a more delayed regional response to fire than *Araucaria*. However, the climate significance of *Podocarpus* is unknown as there is no rainforest vegetation type containing both abundant *Araucaria* and *Podocarpus* in Australia today and, the suggested extinction of at least a component of the genus just adds to the uncertainty.

From ~39 ka–32 ka the sclerophyll taxa, especially *Eucalyptus*, alongside Poaceae, dominate the landscape. In the present-day in north-east Australia the predominant understorey taxa of eucalypt woodland and savannas are grasses (Tracey 1982; Webb and Tracey 1984). This association of sclerophyll and fire in opposition to rainforest (angiosperm and gymnosperm) was clearly indicated in Factor 1 Figure 8.17, Chapter 8, which also indicated that the drier rainforest elements had a close association with Myrtaceae and fire in contrast to the grouping of Casuarianaceae and the rainforest gymnosperms. Clearly providing a good analogy of those taxa able to adapt to changing conditions brought on by the presence of fire in contrast to those that require a more stable environment.

There is no older record of a landscape dominated by sclerophyll vegetation, especially with *Eucalyptus*, within the study region and therefore, in combination with the demise

of fire sensitive rainforest taxa, the arrival of humans and their use of fire was long since proposed as, if not the primary cause of this change, at least the necessary catalyst (Kershaw 1986, Kershaw et al. 1997, 2002; Flannery 1994) with more recent research showing a positive association between human use of fire at this time and the demise of the megafauna (Rule et al. 2012; Johnson et al. 2015). This aspect will be discussed further in section 9.3. *Eucalyptus* and Casuarinaceae continue to dominate through to 32 ka with a reduction in rainforest elements under the continual presence of fire which also sees higher values for Poaceae, the dryland herbs, Asteraceae (tubuliflorae and liguliflorae) and, *Plantago*, the shrub *Monotoca* and the sclerophyll ferns, *Pteridium* and *Pteris*—the ‘so-called’ fire weeds (Jackson 1968, 1977) and suggesting an open woodland or savanna landscape.

9.1.2.1. Local changes and fluctuating water levels 41–32 ka

Locally through 41–32 ka, evidence of standing water on the crater is indicated by high inorganics which are primarily made up of broken diatoms, sponge spicules and phytoliths that may indicate conditions too humid for extensive local fire activity. There is a diverse suite of aquatic and swamp vegetation present indicated by the pollen record with the macrofossil record providing more precise evidence of a floristic diverse sedge community and confirming the presence of taxa not recorded in the pollen record. Nevertheless, many Cyperaceae species including those identified in this record are relatively widespread and cosmopolitan and so gauging a temperature range from these species is limited (Roberts et al. 2017). The aquatics, *Nymphoides (indica)* and *Liparophyllum (exaltatum)* are also relatively widespread although *Liparophyllum (exaltatum)* is not recorded in north-east Queensland in the present-day, this will be discussed further in *sub-section 9.1.3.1*. Although it may not sound very promising the aquatic fern, *Azolla pinnata*, at least provides an optimum temperature for growth between 18° and 28°C with *A. pinnata* at the higher range suggesting conditions were still relatively warm (Wagner 1997). While the low insolation may also be providing a more conducive environment for water retention on the swamp with a reduced evaporation to precipitation ratio present.

However, it is also likely that *Syzygium*, to varying degrees continued to occupy the crater surface. It was initially suggested by Kershaw (1986) that swamp forest was likely only to be on the crater during the early to middle Holocene but this was later revised when

evidence based on pollen and macrofossils extended the presence of swamp forest to the early part of the last glacial period (Bohte 1994). Plant cuticle fragments, for *Syzygium* sp., *Xanthomyrtus* sp., (extinct in Australia), and *Rapanea* sp., and pollen evidence for both *Oraniopsis* and *Dacrydium* suggest all were components of this forest type (Bohte 1994, Bohte and Kershaw 1999).

9.1.2.2. *The impact of drier conditions regionally and locally 32 ka–27 ka*

From ~32 ka, although *Eucalyptus* continues to provide a major contribution, Casuarinaceae is the dominant sclerophyll and is accompanied by a reduction in fire. Declines are also recorded for *Corymbia* and *Melaleuca* but not so clearly for other sclerophyll components, such as *Callitris* and *Dodonaea*. The primary factor for declines in *Eucalyptus* spp. is prolonged drought and significant changes to rainfall availability (Williams et al. 1999; Fensham and Fairfax 2007, Fensham et al. 2009). However, these changes would also be detrimental to Casuarinaceae with the more likely scenario being the reduction in fire. While the more prominent presence of *Petalostigma*, a taxon generally found in both open eucalypt woodlands and vine thickets as a shrub or small tree (Hyland et al. 2003) which although it does have some tolerance to fire via resprouting (Russell-Smith et al. 2003; Vigilante and Bowman 2004) its greater visibility maybe more a direct response to the reduction of the *Eucalyptus* canopy.

The reduction in fire is likely the consequence of a reduced fuel load primarily the reduction of the more flammable sclerophyll elements, such as *Eucalyptus*. The reduction in fire is not seen locally with episodic high macrocharcoal levels evident from 32 to 27 ka. There is also high and consistent representation of swamp and aquatic taxa and is more clearly seen in the influx and macrofossil records where *Eleocharis sphacelata*, *Lipocarpa microcephala*, *Typha domingensis* and *Rorippa* sp. intermittently provide nuts and seeds. Although there is high representation of the aquatic and swamp taxa there is indication that shifting dynamics are present which could just be natural succession or natural succession being interrupted by fire. Another factor which complicates the interpretation is the presence of Poaceae which may indicate increase aridity although Poaceae may not be strictly a dryland taxa (Bush 2002).

9.1.2.3. Local and regional representation of Poaceae through the sequence

Another indicator of increased regional aridity, as suggested above, is higher values for Poaceae. Turney et al. (2004) found that a high Cyperaceae/Poaceae ratio was indicative of wetter conditions with low values and the presence of charcoal indicative of drier conditions. The Cyperaceae/Poaceae ratio (Figure 9.2 and 9.3) does indicate some agreement with low ratio values corresponding to elevated charcoal but this is not always the case. There have been suggestions that looking purely at the Poaceae percentage as an indicator of regional vegetation change may exaggerate dry episodes and the degree of change from wet to dryland environments and suggests that contribution from wetland grasses need to be acknowledged (Bush 2002).

To see whether it's possible to differentiate a regional Poaceae signal from the more local wetland signal, the correlation coefficient r^2 were calculated for Cyperaceae and Poaceae for both the percentage and influx data. All data was log transformed to base 2 prior to analysis. Both Cyperaceae and Poaceae are known to be high pollen producers (Bush 2002; Sjögren et al. 2015) and therefore at least their influx values should be on parity. The result for the influx data (Figure 9.4) shows a positive trendline with $r^2 = 0.66$ indicating a high degree of correlation between the two taxa suggesting a more local Poaceae signal overall while the percentage data (Figure 9.5) suggests little to no correlation.

Figure 9.3 indicates there are major changes across the data usually associated with elevated inorganics to which both Cyperaceae and Poaceae respond and that this synchronicity could suggest a much closer relationship between the two taxa.

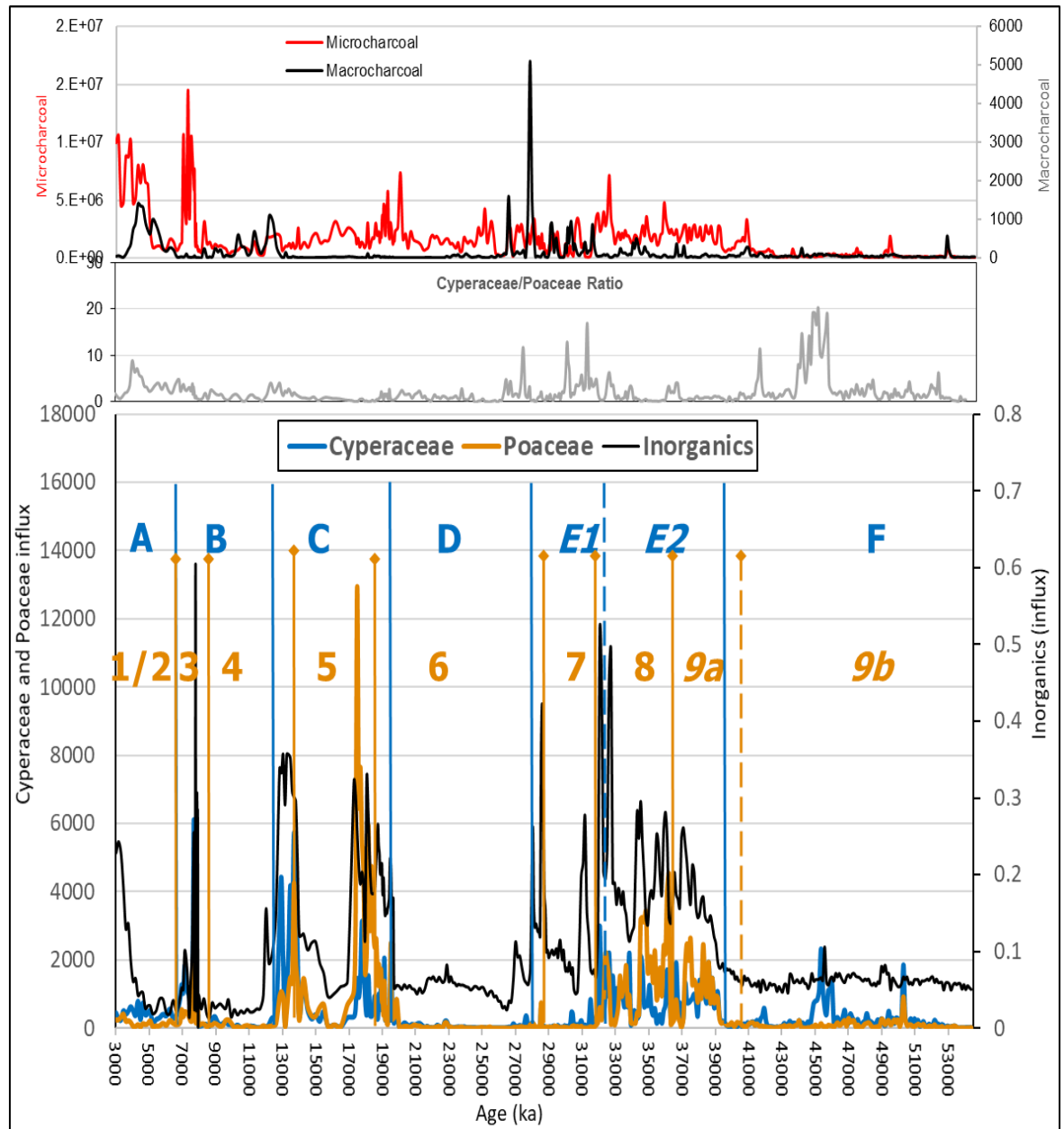


Figure 9.3. Microcharcoal and macrocharcoal top graph; Cyperceae/Poaceae ratio middle graph; Cyperaceae and Poaceae (y-axis) and Inorganics (y2-axis) full influx record with blues lines (inc. dashed) and letters denoting the aquatic/swamp pollen zones and the orange lines with diamond arrow (inc. dashed) and numbers denoting the dryland pollen zones.

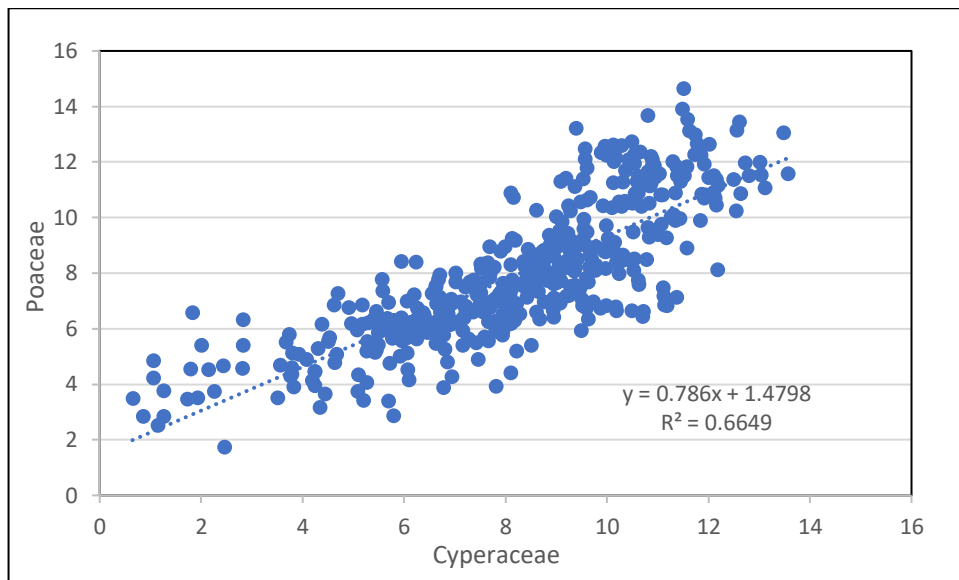


Figure 9.4. Cyperaceae versus Poaceae influx on the full record biplot.

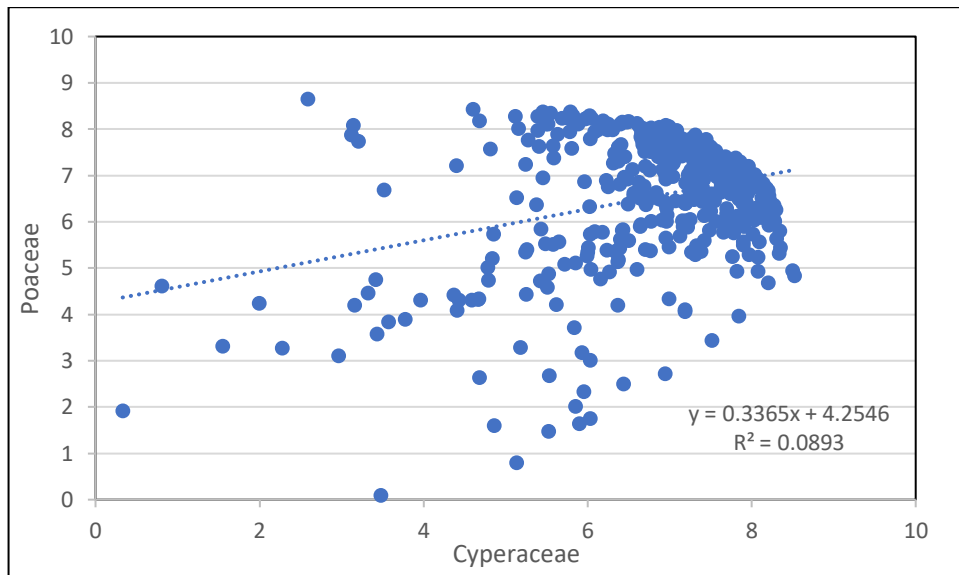


Figure 9.5. Cyperaceae versus Poaceae percentage on the full record biplot.

It is likely from 54-41 ka that Poaceae has a local origin with Cyperaceae the dominant taxon on the swamp. It could be that Poaceae occupied the floating root-mat alongside *Cyclosorus* as in the present-day at nearby Bromfield Swamp, the aquatic grass, *Leersia*, and other herbaceous taxa alongside the fern, *Blechnum*, reside on floating root-mats, see sub-section 9.1.1.1. Through sub-zone E2 and E1 both Cyperaceae and Poaceae have high influx values corresponding to elevated inorganics and also increased fire activity. It is likely that the high influx values for Poaceae indicate a dryland Poaceae signal or a Poaceae occupying the drier margins of the swamp. However, the Cyperaceae/Poaceae ratio is still relatively high suggesting wet conditions, it could be that fire initially

accelerated the Poaceae signal until zone D where reduced Cyperaceae/Poaceae ratio values and inorganics suggest the presence of dry conditions. Through zone C there is a return to high influx values for both Cyperaceae and Poaceae alongside elevated inorganic values. The Cyperaceae/Poaceae ratio is relatively low although the presence of the aquatic, *Nymphoides*, could suggest that Cyperaceae was constricted to more shallower areas of the swamp and so a more regional Poaceae signal is recorded suggested by the low Cyperaceae/Poaceae ratio values. Through zones B and A the Cyperaceae/Poaceae ratio is moderate to low with influx values low for both taxa. However, the reduction in influx is not likely due to drier conditions but the advance of rainforest both locally and regionally while the elevated inorganics through the top of zone A alongside the low Cyperaceae/Poaceae ratio values and elevated fire activity (Figure 9.3) suggests increased variability which corresponds to the suggested start of present-day ENSO conditions (McGlone et al. 1992).

Overall, there was correspondence with the findings of Turney et al. (2004) that low values of the Cyperaceae/Poaceae ratio correspond to increased fire activity and therefore provide support for the suggested presence of variability due to ENSO conditions. However, the high resolution of this record suggested that there was also a local influence embedded within the signal likely indicated by the positive correlation recorded for the Cyperaceae and Poaceae influx suggesting that a wetland Poaceae was a major contributor at times to the aquatic and swamp environment. The increase in fire and Poaceae at 40 ka is more likely influenced by initial human activity and their role in the demise of the megafauna rather than variability due to ENSO conditions. This suggests that an understanding of both the local and regional environment is necessary.

9.1.3. An extended Last Glacial Maximum

Globally the Last Glacial Maximum (LGM) is defined as the time of maximum global ice volume and minimum sea-levels (c. 23–19 ka) (Hughes et al. 2013). However, there is regional variation with some areas reaching glacial maximum before the defined LGM (Hughes et al. 2013). In the Southern Hemisphere full glacial temperatures were achieved by 27 ka in Antarctica and in the Southern Ocean by ~26 ka (Bostock et al. 2013). On mainland Australia only a small part of the Snowy Mountains were glaciated, while Tasmania had more extensive glaciation with moraines deposited by cirque and valley glaciers dated in the range of 17–20 ka (Barrows et al. 2002) with a more extensive

maximum glacial advance in the Snowy Mountains centred on 19.1 ± 1.6 ka although cooling began around 32 ka. In Tasmania, maximum glacial advance was at 23 ± 2 ka (Turney et al. 2006b). Reeves et al. (2013b) suggest that in the northern Australasian region the late MIS3 was relatively wet but with increasing variability from ~28–24 ka. This variability is seen at Lake Carpentaria where episodic flooding events became more variable after 30 ka, and a short lived rainforest expansion is seen from ~26–24 ka in NE Queensland followed by much drier conditions (Moss and Kershaw 2007; Reeves et al 2013b) This suggestion of cooling or LGM starting prior to (c. 23–9ka) and interspersed with periods of more favourable conditions occurred in a number of sites from the Southern Hemisphere encompassing temperate, sub-tropical and tropical sites (van der Kaars et al. 2000; Vandergoes et al. 2005; Williams et al. 2009; Reeves et al. 2013a,b; Woltering et al. 2014; Petherick et al. 2011, 2016).

The time of maximum aridity at Lynch's Crater has been suggested to be between ~20–10 ka based on high humification and low Cyperaceae values (Turney et al. 2006a), with Kylander et al. (2007) also suggesting increased aridity through this interval with low Eu/Eu* anomaly profiles and the decreased variation in the $^{206}\text{Pb}/^{207}\text{Pb}$ ratios, indicators of atmospheric mineral dust source. The period, ~20–10 ka, certainly covers a period of fluctuating influx values for those taxa in and surrounding Lynch's Crater but influx values begin to decline at ~30 ka for the aquatic/swamp taxa. Although, for a short period, 28.7 ka through to 26.8 ka, aquatic/swamp counts are high in line with slightly higher inorganic values, which could suggest the presence of variable conditions, although the diversity of macrofossils does suggest a short period of ponding and the absence of *Gelasinospora* through this period would also suggest a return to wetter conditions on the swamp.

There are also lower absolute values for both *Eucalyptus* and Poaceae at ~30 ka and rainforest elements are greatly reduced. However, like the swamp taxa there is a small resurgence in the sclerophyll Myrtaceae and to a lesser extent rainforest from 28.7 ka through to 26.8 ka, (Figure 9.6). For the sclerophyll Myrtaceae, it is *Eucalyptus* which shows the largest increase with representation increasing from 20 to 40 % of the dryland sum. For the rainforest, increases are primarily due to the secondary taxa although *O. paniculata* and Podocarpaceae at times register up to 4% of the dryland sum. The previously more intermittent occurrence of *Macaranga* and *Mallotus* becomes more

consistent but it is *Melicope* that registers up to 6% of the dryland sum at 27 ka with the rainforest angiosperms at times registering up to 12% of the dryland sum.

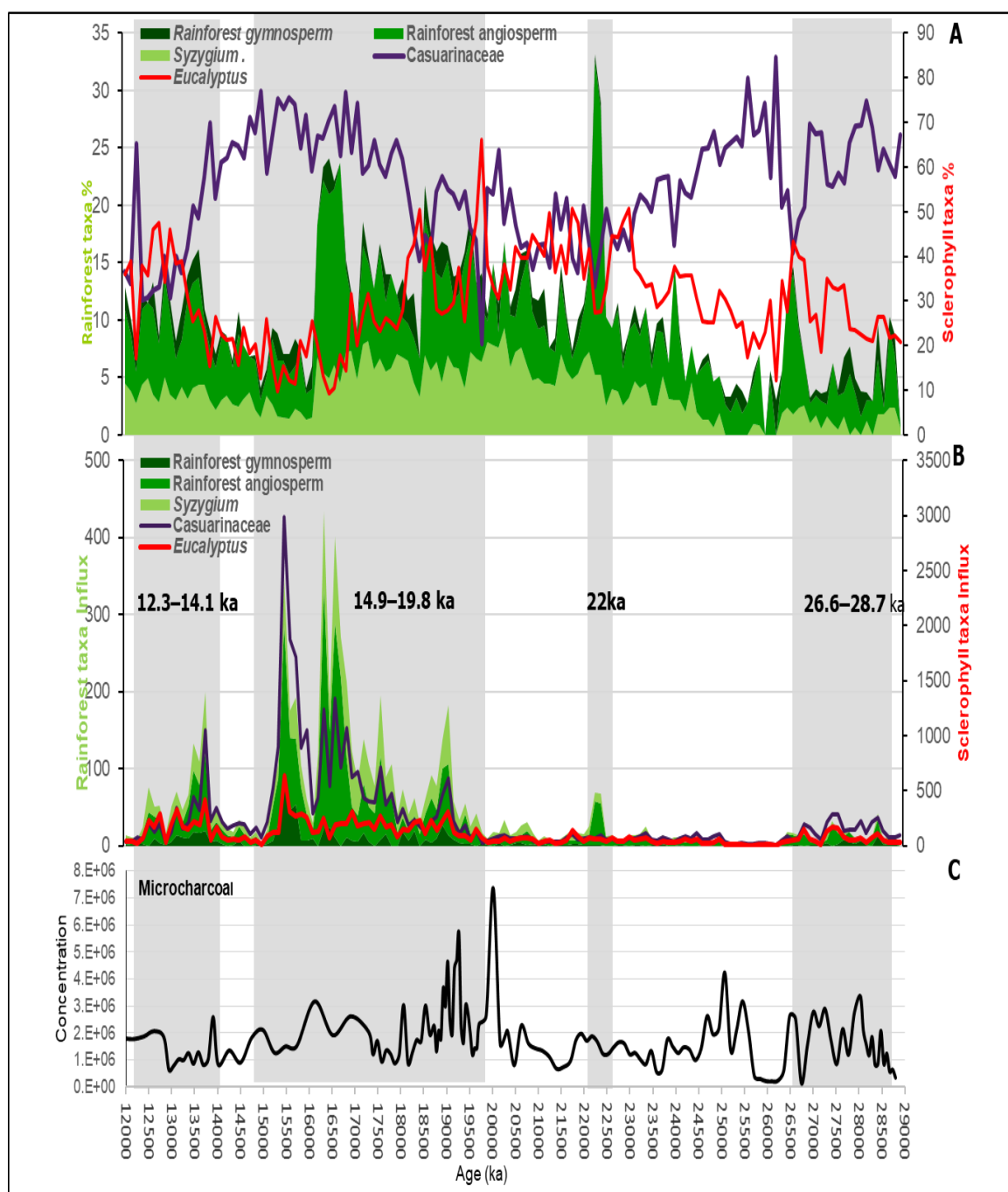


Figure 9.6. Major vegetation types and groups for the period 12 ka through to 28.9 ka for (A) Percentage data for major sclerophyll taxa, *Casuarinaceae* and *Eucalyptus*, (y2-axis), rainforest gymnosperms, rainforest angiosperms and *Syzygium* (y-axis), (B) Influx data for major sclerophyll taxa, *Casuarinaceae* and *Eucalyptus*, (y2-axis), rainforest gymnosperms, rainforest angiosperms and *Syzygium* (y-axis), (C) Microcharcoal. Shaded areas indicate periods of high influx for pollen.

Trema continues with low percentage values with only a slight increase in influx values suggesting that changes are limited or at least only visible at a local to extra-local level and this may be further suggested with the occasional presence of the rainforest understorey taxon *Rapanea* previously only seen prior to 33 ka.

There is no significant increase in regional fire at 28 ka that may have facilitated a thickening up of the savanna vegetation through this period which may have restricted the more understorey taxa such as Poaceae, Chenopodiaceae and Asteraceae, although local fire has an occasional peak. Low influx values are recorded from ~26.8 ka for both dryland and aquatic/swamp taxa with the lowest values for the whole sequence found between ~26.7–24 ka and so the proposed return to more favourable conditions at this time (Moss and Kershaw 2007; Reeves et al. 2013b) is not supported. Turney et al. (2006a) suggest from the geochemical signature and high humification values found at Lynch's Crater that there was an increase in 'warm' ENSO events close to this time of suggested maximum aridity, ~26.7–24 ka while nearby Bromfield Swamp displays drier conditions prior to 30 ka (between 32,690–30,080 cal.yr BP) but wetter conditions following and extending through to 28,790 cal.yr BP followed by a period through to 24,660 cal.yr BP where, like the suggestion by Turney et al. (2006a), variable rainfall with the suggestion of warm 'ENSO' events was likely at this time (Burrows et al. 2016).

Although lower influx values may suggest a decline in the sclerophyll density there are fluctuating shifts between *Eucalyptus* and its other co-dominant sclerophyll Casuarinaceae. This is suggested for the period ~25 ka through to 21 ka where percentage data suggests a significant increase in *Eucalyptus* which is not seen in its influx values. Although there is a short-lived resurgence of rainforest angiosperms (percentage and influx) at ~22, ka this is followed by lower influx values and a return to sclerophyll dominance (Figure 9.6 A and B). Fire activity increases just prior to 20 ka followed by higher *Eucalyptus* and lower Casuarinaceae which is repeated until Casuarinaceae becomes the dominant sclerophyll at ~18.5 ka, a position maintained until 13.2 ka. Throughout this time of ebb and flow between the sclerophyll taxa, rainforest angiosperms increase, initially *Melicope*, *Celtis*, Leguminosae, *Trema* and *O. paniculate*, followed by canopy taxa such as *Flindersia*, *Diospyros*, *Austrobuxus*, *Ilex*, Sapindaceae, *Agyrodendron* and *Elaeocarpus* that are intermittently present from 20 ka. These taxa are augmented by the secondary taxon *Homalanthus* and the understorey taxa *Acronychia*

and *Rapanea* while locally both *Oraniopsis* and especially *Syzygium* (Figure 9.6 A and B) have a greater representation. These changes are occurring at a time of insolation maximum (Figure 9.1) that indicates a period of more effective precipitation.

The influx for Chenopodiaceae (see Figure 7.16, Chapter 7) suggests a greater representation from ~20 ka might seem to be counter-intuitive to the evidence for more effective moisture but it is highly likely that, prior to this increase, precipitation further inland was greatly reduced and therefore the two dominant regional taxa, Casuarinaceae and Chenopodiaceae, were the first to respond and become more visible in the record. Another influence could be the increase in fire intensity (~20.5 ka–18.5 ka) which may have periodically opened up this grassy savanna landscape which would then have allowed a more distant pollen signal to be recorded.

Insolation may not be the only driver for this period of more effective precipitation after ~20 ka. Although the lowest sea-surface temperatures around the Australian margin are recorded at 20,500±1400 cal BP, there is evidence from plunge pools in northern Australia which suggest severe and continual flooding from at least ~20–18 ka (Nott and Price 1999; May et al. 2015). However, these plunge pool flooding events may only have been short-lived and therefore not a likely long-term driver. More compelling evidence of sustained humid conditions is provided by evidence of a sea-surface temperature rise in the Coral Sea as early as 20 ka (Barrows and Juggins 2005; Tachikawa et al. 2009; Reeves et al. 2013b) Although present, there is no real increase in wetter rainforest canopy elements, so any structural change would have been limited to sclerophyll vegetation, especially *Eucalyptus*, changing from a relatively sparsely treed savanna grassland to a more densely treed savanna initially impacted by fire. Studies of present-day savannas in Australia suggest this so-called woody thickening is due to both increased rainfall and changes to fire patterns (Williams et al. 1999; Sharp and Bowman 2004; Liedloff and Cook 2007; Murphy and Russell-Smith 2010; Murphy et al. 2014).

The sclerophyll elements, particularly Casuarinaceae, remain at relatively high levels after the reduction in fire activity at 18.5 ka, while Chenopodiaceae is reduced. However, there is a greater representation of Asteraceae (tubuliflorae and liguliflorae) with evidence (of continual clumping) suggesting a local origin for both these taxa while rainforest representation remains relatively high until ~16 ka according to the percentage data but

the influx data (Figure 9.6 A and B) remains relatively high until ~15 ka. The reduction in fire (both local and regional) after 18.5 ka could either be that conditions were too humid for large scale fires or could be related to the consumption of a lower biomass such as Poaceae which was evident prior to 20 ka. The increases in the sclerophyll and especially rainforest taxa from 20 ka are not recorded in Kershaw's record (1973, 1976) which may be due to the coarser resolution of that record. Although the changes seen in the rainforest elements are ultimately not sustained at this time, they do suggest that rainforest may not have been very far away and therefore not confined to refuge type environments as might be anticipated from the sharp decrease of rainforest pollen on the sclerophyll side of rainforest-sclerophyll boundaries today (Walker and Sun 2000).

Within the greater Australian tropical region there are mixed responses to forcing influences around ~20 ka. Although there are intrinsic factor reasons for reef development along the Great Barrier Reef (GBR), the IODP 325 record suggests that coral reef assemblages are primarily the product of changing hydrodynamic conditions controlled by sea-level change. Along the GBR, inner terrace reef growth terminated at ca. 22 ka when sea-level dropped to its lowest LGM level. However, evidence of deglaciation, indicated by a change in coral assemblage, occurred as early as ~20 ka in some mid to outer reef terraces with the re-flooding of most inner terraces by 17 ka (Webster et al. 2018; Humblet et al. 2019).

Along the Arafura shelf (MD-2175) maximum aridity is found from 27 ka to 19.1 ka when grassland is dominant but after 19.1 ka through to 13.8 ka wetter conditions prevailed with the development of swamp across the Arafura shelf indicative of sea level rise (Kershaw et al. 2006a,b; Williams et al. 2009). Initially a very similar response is found north of the Kimberley (MD98-2167) where dry conditions are indicated from 35 ka to 20.7 ka followed by wetter conditions from 20.7 ka to 18.1 ka as indicated by increases in the pteridophytes but this is followed by a time of maximum aridity which continues to 13.8 ka (Kershaw et al. 2006a,b). The inland site of Wolfe Creek Crater (eastern Kimberley) suggests a dry LGM with a rise in the water table at ~14 ka coinciding with the onset of the monsoon found elsewhere in northern Australia (Wyrwoll and Miller 2001; Miller et al. 2018). The differences between these sites and Lynch's Crater could be related to their geographical position with any influence from the Coral Sea blocked by the land bridge between Australia and Papua New Guinea (PNG), and in both marine

sites, MD-2175 and MD98-2167) and the more inland Kimberley site, there is a greater influence than at Lynch's Crater of the Australian monsoon which was not activated or at least not reinvigorated until ~14 ka (Wyrwoll and Miller 2001, Wyrwoll et al. 2007; Kershaw et al. 2006a; Williams et al. 2009; Mohtadi et al. 2011; Reeves et al. 2013a,b).

Variability from ~30 ka at Lynch's Crater suggests the beginning of glacial conditions but was interrupted by a short period of rainforest expansion from 28.7 ka through to 26.8 ka, while, from 26.7 ka through to 24 ka, the lowest influx values in the record could suggest periods where drought conditions became more prevalent with the dominance of ENSO warm events, as suggested by Turney et al. (2006a) and Burrows et al. (2016). These results suggest that conditions were deteriorating from ~26.7 ka and that full LGM conditions were present soon after. The interruption of a short-lived resurgence in rainforest angiosperms at 28.7 ka and ~22 ka may have just been a rare cooler ENSO event as influx values are relatively low. This would suggest the timing of maximum aridity started before 20 ka and may have started as early as ~26.7 ka and rather than a continuous period of aridity was interrupted by much shorter cooler ENSO events. However, the increases seen in both the sclerophyll and rainforest taxa at ~20 ka indicating the presence of more effective precipitation and which continues at least to ~15 ka was influenced by both the insolation maximum and the warming of the Coral Sea at ~20 ka and its early re-flooding of the GBR from 20 ka through to 17 ka (Tachikawa et al. 2009; Webster et al. 2018; Humblet et al. 2019).

9.1.3.1. Regional influences at a local level from 20–12 ka

Locally changes are also evident from 20 ka and are characterised by pollen of the floating leaved aquatic *N. indica* which, although present intermittently throughout the record, shows greatest consistency ~19.6 ka through to 12 ka in association with elevated inorganics. Its pollen record is supported by macrofossils, except for the period between 18.6 ka through to 17.3 ka where macrofossils are absent (Figure 9.2 and 9.7 composite diagram of selected taxa taken from Figure 7.5). Kershaw's (1978, 1979) study on modern pollen distribution within local swamp environments on Atherton Tableland found that *Nymphoides* pollen was a reliable indicator of a free-water habitat. This would suggest that free water was present from at least 19.6 ka through to 12 ka as had been suggested for the earlier period, 38 ka through to ~31 ka, where elevated inorganics are associated with another floating-leaved aquatic *Liparophyllum exaltatum*. The presence of a free-

water habitat has also been suggested by Muller et al. (2008a,b) and Kaal et al. (2014) based on inorganics and the use of pyrolysis-GC-MS to clarify ecological and hydrological conditions at Lynch's Crater.

There is some ecological similarity between *N. indica* and *L. exaltatum* with both species usually found at a water depth of < 2 m and both can survive for some time on drying mud (Aston 1973; Sainty and Jacobs 1981; Stephens and Dowling 2002). However, there are some differences between these two periods of elevated inorganics, (38 ka through to ~31 ka and ~19.6 ka through to 12 ka). Although *N. indica* (pollen and macrofossil) was present during the earlier period, *Liparophyllum* pollen type is rare through the latter period and macrofossils of *L. exaltatum* are only found to 33 ka (Figure 9.17). The present-day distribution of these two species shows that there is an overlap with the southern limit of *N.indica* north of Sydney and *L. exaltatum*'s northern limit within the Noosa region north of Brisbane (see Appendix C, Figure 1). *N. indica* is generally regarded as pantropical in distribution while *L. exaltatum* is restricted to Australia and is more abundant in the more southern temperate region of its distribution (Sainty and Jacobs 1981; Stephens and Dowling 2002; Shibayama and Kadono 2007; Middleton et al. 2015; Australia's Virtual Herbarium 2015) which could suggest a temperature regime change to warmer conditions with the replacement of *L. exaltatum* by *N. indica*.

Cyperaceae values are high through both these inorganic phases and there is a diversity of other aquatic and swamp taxa present (Figure 9.2) but macrofossil representation (Figure 9.7—composite diagram of selected taxa from Figure 7.5) is limited in the latter period except for *N. indica* and the occasional rare sedge nut (*Cyperus polystachyos*). However, *A. pinnata* which is generally found free-floating in still shallow water is well-represented through both inorganics phases and supports the evidence from the floating-leaved aquatics of the presence of generally shallow open water. However, only the lighter microsporangia are present in the later inorganic period (Stephens and Dowling 2002; Small and Darbyshire 2011). It could be that the lighter weight and size of the microsporangia compared to megasporocarps (see Plate 7.2, Chapter 7) allowed it to float to some distance (Zhao et al. 2006). The other more notable difference is the near absence of fire in the latter period.

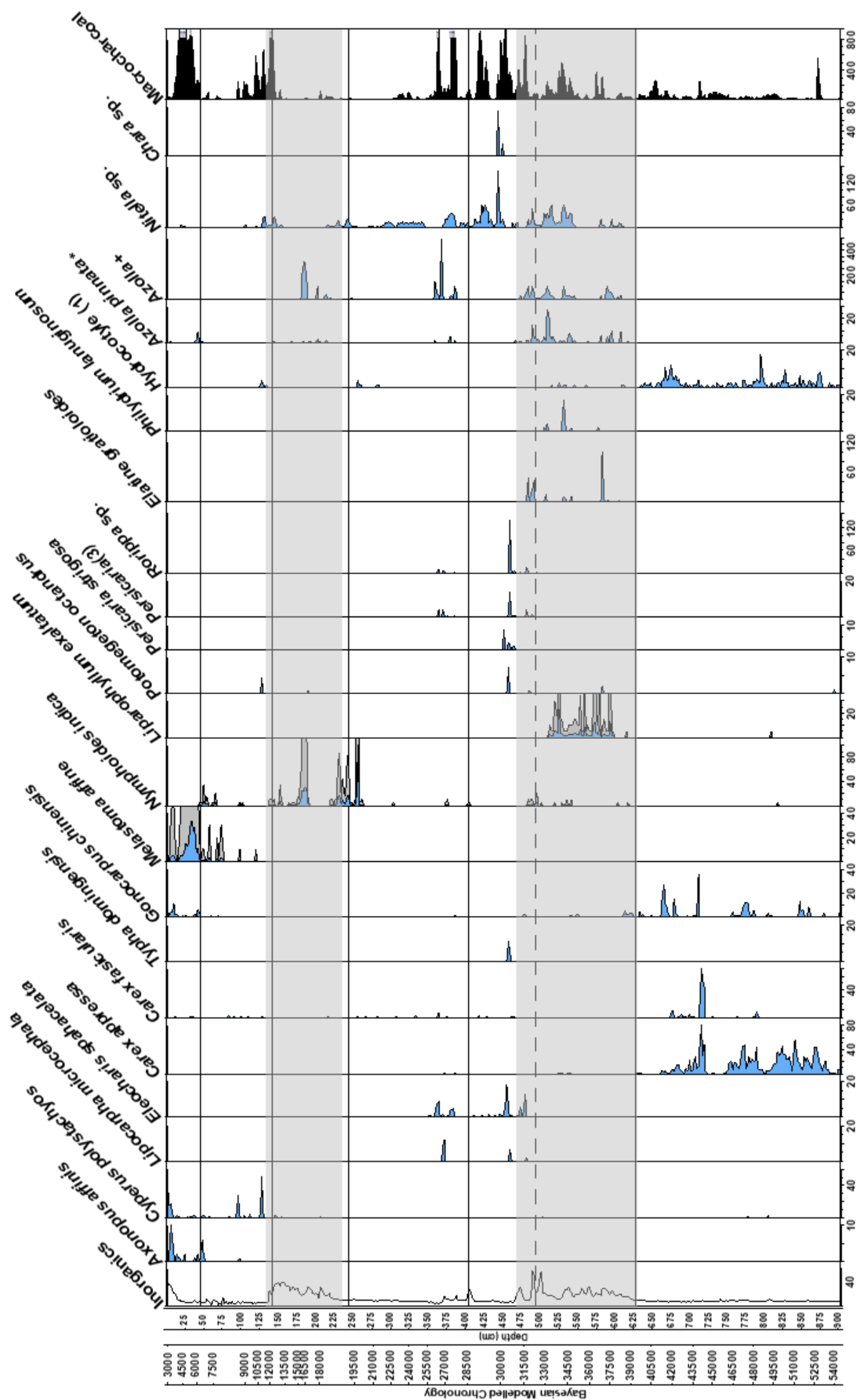


Figure 9.7. Selected macrofossil taxa from Lynch's Crater. *M.affine*, *N.indica* and *L.exaltatum* have been exaggerated x10 and *Azolla**=megasporecarpan*Azolla*+microsporangia/microspores. Shaded area show major inorganic phases where aquatic hydrophytes are present.

Although fire is relatively moderate when *L. exaltatum* is present, the continuous presence of both *Anthoceros* and charred seeds through this earlier period suggests a mixed community with shallow ponding areas interspersed with swamp and bog areas and marginally drier areas as suggested previously (*sub-section 9.1.2.1*) while the later period is likely to have had more extensive shallow ponding and, at least near the coring site, it could be that water depth was too deep for other taxa to survive (Dieffenbacher-Krall and Halterman 2000; Väiliranta 2006; Koff and Vandel 2008). However, caution is suggested in interpretation of the period ~16 ka–12 ka as there are likely to be constraints on water depth as sediment accumulation is likely to be close to the breached level although there is also likely to be some variability across the crater surface.

9.1.4. Sclerophyll to rainforest dominance

Timing of rainforest advancement on the Atherton Tableland prior to and during the Holocene is based on pollen and chronological data from several maar lakes and swamps. The early radiocarbon dates for Lake Barrine, Bromfield Swamp, Lake Euramoo and Quincan Crater (Kershaw 1970, 1971, 1973, 1975, 1983a, 1994; Chen 1986, 1988; Walker and Chen 1987) have been calibrated (cal. BP.) (OxCal 4.3) to allow a better comparison with more recent studies. They indicate that rainforest advancement was not uniform and was most likely dependant on rainfall thresholds as well as the availability of or distance from a likely rainforest source, the underlying substrate, topography and fire activity alongside local factors (Chen 1986, 1988; Haberle 2005; Kershaw 1970, 1971, 1973, 1975, 1983a). Ash (1988) suggests that rainforest on basalt or scoria substrates could be found under drier conditions than on other substrates—as is the case today.

Around Lake Barrine rainforest expansion began about 10,480 cal. BP. likely due to an increase in rainfall and, although a lower fire frequency which followed the calculated 230 year fire interval meant that full rainforest potential was not possible until 7,630 cal. BP. when burning was no longer evident (Chen 1986). Walker (2007) re-analysed the original Lake Barrine pollen and microcharcoal data (Chen 1986; Allison 1990) and suggested that, although maximum pioneer rainforest was attained about 7,600 cal. BP, it was followed by a hiatus with a decline in both the percentage and influx of rainforest pollen accompanied by a rise in sclerophyll forest pollen, particularly *Allocasurina*. Rainforest recovery began again about 7,080 cal. BP, initially with increasing numbers

of the secondary rainforest taxa, such as *Macaranga* and *Mallotus* with a minor downturn at ~ 6,200 cal. BP but rainforest secondary taxa quickly recovered. Bromfield swamp also saw a similar transition beginning about 10730 cal. BP. but extensive rainforest advancement is seen much earlier (9,420 cal. BP.) than at Lake Barrine. Rainforest advancement around Lake Euramoo was initially timed at about 8,305 cal. BP. and, around Quincan Crater, rainforest became dominant between 7,825 cal. BP and 6,820 cal. BP. (Kershaw 1970, 1971, 1975) with recent analyses suggesting that, like Lake Barrine although slightly later, there was a shift back to sclerophyll taxa especially Casuarinaceae from ~7,000 cal. BP through to 6,600 cal. BP (Rule *unpubl*). Haberle (2005) suggests that at Lake Euramoo there was a shift from drier sclerophyll to wet sclerophyll from 16,800 cal. BP. likely providing a more conducive environment for rainforest elements and, although there were shifts to drier sclerophyll, especially *Casuarina*, after 16,800 cal. BP., by 8,700 cal. BP. rainforest dominated.

Kershaw (1983a) suggests at Lynch's Crater that by 12,320 cal. BP. rainfall had increased but that fire activity delayed the replacement of sclerophyll by rainforest until 9,500 cal. BP. In this present study of Lynch's Crater regional conditions become more favourable at ~12 ka with local conditions more favourable from ~13 ka. The swamp shows the initial influx of rainforest elements with the consistent presence of *Melastoma*, *Syzygium* and *Acmena* by ~13 ka, although it is not until ~11 ka that a more substantial increase is recorded (Figure 9.8). This is also noted regionally where initially it is the secondary rainforest component which has a greater representation from ~13–12 ka with *Macaranga* and *Mallotus*, Leguminosae, *Trema* and *Celtis* the main contributors and this is followed by a more consistent representation from the canopy taxon *Elaeocarpus* by ~11 ka.

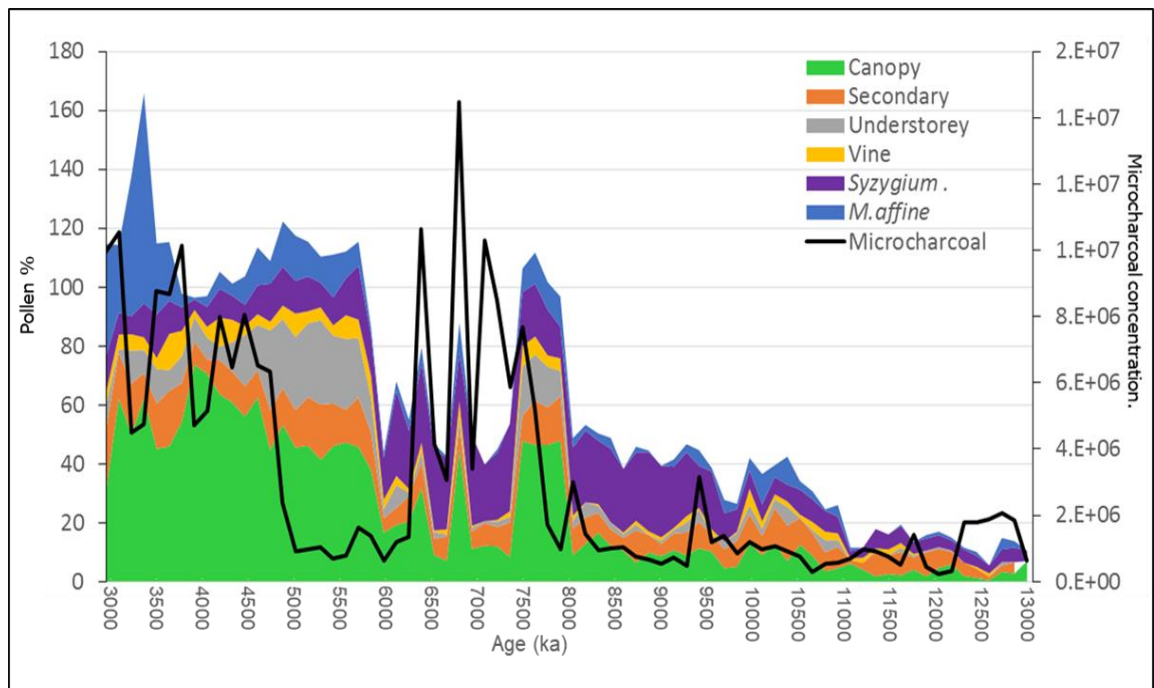


Figure 9.8. Percentages of major rainforest elements and microcharcoal (concentration) for the period 3–13 ka, *Syzygium* and *M. affine* were not included in the dryland pollen sum.

The increased values for *Trema*, indicative of low-altitude mesophyll rainforest would also indicate higher temperatures from bioclimatic estimates (Moss and Kershaw 2000; Kershaw et al. 2007a). From ~11–9 ka there is a continual increase in the contribution of rainforest elements, canopy (*Cunoniaceae*, *Ficus*, *Flindersia* and *Ilex*), secondary (*Glochidion*, *Homolanthus* and *Alphitonia*), understorey (*Apodytes* and *Rapanea*) and vines (*Freyinetia*, *Maesa* and *Cissus*) at a time of low fire activity regionally. This broadly corresponds to the transition periods found at Bromfield Swamp and Lake Barrine although there is a slight drop at 9.8 ka in secondary rainforest which could suggest that the canopy rainforest component, although not increasing substantially, may have become more established (Kershaw 1975; Chen 1986), while the increase overall in rainforest taxa shown in Figure 9.8 at ~11 ka could also indicate that the rainforest signal is becoming more local.

These increases are not limited to the rainforest elements but also the pteridophytes (Figure 9.9) although the high influx values for the pteridophytes, especially the monolete (psilate) ferns, obscure the initial increase at ~13 ka, which also corresponds to increased local fire activity.

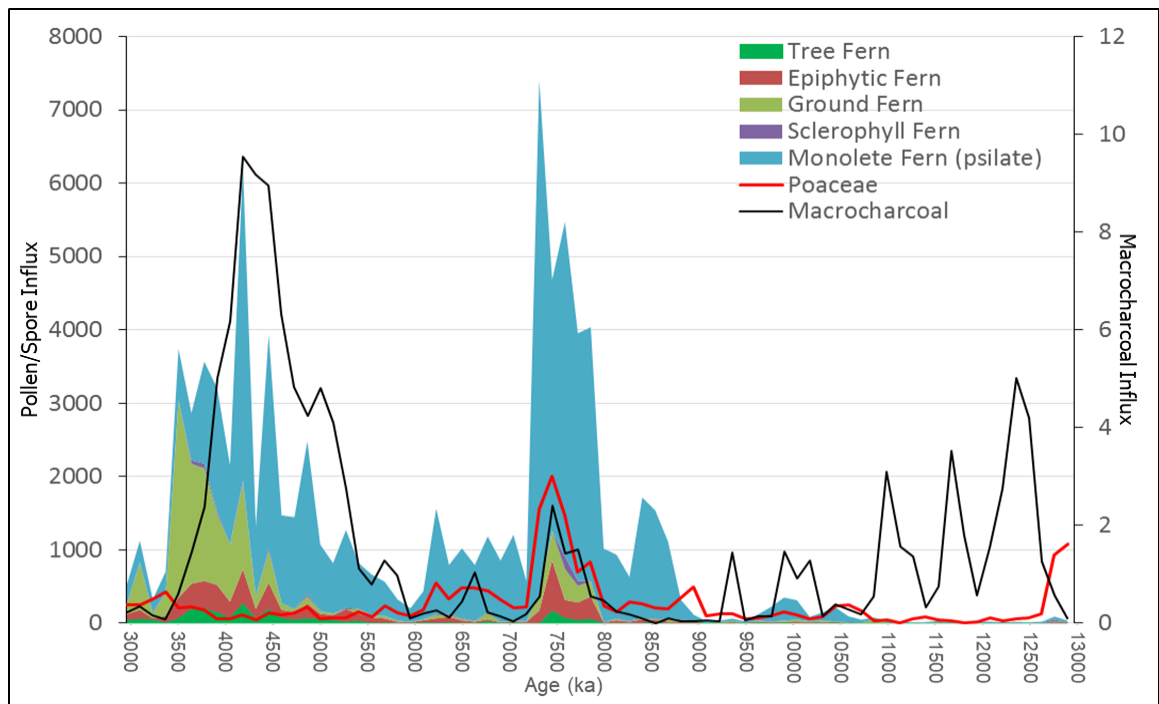


Figure 9.9. Influx data for the pteridophytes, Poaceae and macrocharcoal for the period 3–13 ka.

It is likely that the majority of the monolete (psilate) ferns spores are derived from either *Blechnum* sp. or *Cyclosorus* sp. which have lost their exosporia. In the present-day *B. indicum* is found at Lynch’s Crater, Bromfield swamp and Quincan Crater on a variety of swamp substrates while *Cyclosorus* is largely restricted to floating root mats on Bromfield swamp. The increases in both rainforest taxa and pteridophytes certainly would confirm higher precipitation levels but also suggest a close proximity of the two components. *B. indicum* tends to grow in large colonies on the edges of swamps or lakes and can quickly colonise burnt areas so is likely to be the most common monolete (psilate) fern found in this record (Kershaw 1971, 1983, Haberle 2005; Kahler 2005; Burrows et al. 2014a, b, 2016). Burrows et al. (2014a) looked at the *Blechnum* (wet) to Poaceae (dry) pollen ratio to identify wet and dry shifts at Bromfield Swamp for the last 4000 years and suggested it was a reliable indicator of centennial-scale shifts from wet (dry) to dry (wet) identified in the humification record.

Neither humification, nor a reliable *Blechnum* to Poaceae ratio was available for Holocene samples from this record. However, fire is important for the representation of both taxa especially from 9 ka through to 7.2 ka (Figure 9.9) followed by lower values for pteridophytes, Poaceae and local fire, until 6 ka when only pteridophytes (*Blechnum*) continues with high values in the presence of continuing local fire. The initial increase of

local fire from 13 ka through to 10.8 ka is also found at approximately the same time at Bromfield swamp (13.7 ka–11.3 ka) and, like Lynch's Crater, it is the local swamp taxa, Cyperaceae, Poaceae and *Typha*, that provide the likely fuel source (Burrows et al. 2016; Kershaw *unpublish.*).

The evidence certainly suggests the encroachment of rainforest elements, *Acmena*, *Syzygium* and *M. affine* onto the swamp in the early Holocene and that the presence of relatively intense local fires was primarily associated with the local sedges and *Typha*. However, the presence of charred Myrtaceae pollen grains (see Chapter 7, section 7.2.5) likely *Eucalyptus*, through the early Holocene suggests locally it was still present. Locally the prominence of *Syzygium* from 9.6 ka through to 8.2 ka is likely due to the reduction of local fire which subsequently sees a reduction in the local disturbance taxon, *Melastoma*, but it is not until 8 ka that rainforest dominates, primarily the canopy component (Figure 9.8) although the understorey also makes a greater contribution. This is later than Kershaw's (1976, 1983a) suggested time of rainforest encroachment, ~9.5 ka. This earlier time of rainforest advance may be influenced by quite significant age reversals especially the second core taken which targeted the sclerophyll/rainforest boundary, see Appendix C, Table 1 (Kershaw 1983a), while dates from the initial core suggest a younger age, 7649±46 cal. BP (ANU 958) and 7867±100 cal. BP (ANU 959) for rainforest dominance (Kershaw 1976). However, the same suite of rainforest taxa, *Acmena*, *Glochidion*, Rhamnaceae, *Rapanea* and *Freycinetia* likely dominated on the swamp surface. The suggestion by Kershaw that dilution by these swamp occupants lowered representation of the more extra-local rainforest taxa is also found in this record although Cunoniaceae contributes up to 10% of the dryland sum with *Elaeocarpus*, *Ficus*, *Ilex*, *Balanops*, *Trema* and *Celtis* all present alongside another 30 or more known rainforest taxa. It is also likely that the rainforest swamp residents were not exclusively confined to this environment and it could be that once conditions became more favourable, essentially a decrease in wetland taxa and lower water levels, there was the opportunity to occupy the drier areas of the swamp.

Although obscured by the swamp forest taxa, the prominence of Cunoniaceae, especially the tricolpate pollen type, from bioclimatic estimates would indicate higher precipitation but also maybe cooler conditions. That rainfall was higher is confirmed by the higher values of *Elaeocarpus* although, on the whole, the range of *Elaeocarpus* species suggest

generally warmer conditions than those of Cunoniaceae (tricolpate) but more in line with temperature ranges of Cunoniaceae (dicolpate) species (Tracey 1982; Moss and Kershaw 2000).

Although PCA (Figure 8.20, Chapter 8) indicated that the major separation during the Holocene is the sclerophyll from the primary rainforest, it clearly identified distinct groupings within the rainforest taxa. The swamp forest elements, *Acmena*, *Glochidion* and *Rapanea* were grouped together (Bohte 1994, Bohte and Kershaw 1999) while Cunoniaceae, *Elaeocarpus* and *Ficus* are likely members of rainforest adjacent to the swamp, with the secondary rainforest taxa aligned with the sclerophyll perhaps because they are more common alongside disturbed rainforest margins and therefore their contribution is reduced in the Holocene period.

There are interruptions and/or transitional shifts between ~7.3 and 6.3 ka from rainforest dominance back to sclerophyll dominance likely related to the close proximity of sclerophyll taxa and associated fire which is discussed further in sub-section 9.3.4. The last transitional shift to rainforest dominance sees the primary canopy elements, Cunoniaceae (tricolpate) and *Elaeocarpus*, the swamp canopy occupants, *Acmena* and *Syzygium*, and the secondary taxa, *Trema* and *Glochidion*, showing the greatest increase and is seen in both the percentage and influx data at a time of low fire activity. However at ~5 ka fire activity increases, an event proposed by McGlone et al. (2002) to most likely signal the onset of more variable ENSO conditions, and one which has subsequently been supported by records elsewhere (e.g. Liu et al. 2000; Gagan et al. 2004; Haberle 2005; Moros et al. 2009) although some suggest a slightly later date, ~4 ka for its onset (Lynch et al. 2007) or an onset at ~5 ka but intensifying at ~3 ka (Donders et al. 2007, 2008).

Local fire is more evident earlier, 6 ka, with rainforest swamp taxa greatly reduced by 4.2 ka (see *sub-section 9.3.4*). The decreases seen in the swamp forest correspond with higher values for Cunoniaceae (tricolpate) but also for Cunoniaceae (dicolpate), *Elaeocarpus*, *Ficus*, *Ilex* and Sapindaceae suggesting warmer temperatures (Tracey 1982; Moss and Kershaw 2000). It is also likely that, with the reduction of extensive swamp vegetation and ultimately the disappearance of a densely canopied forest on the swamp, effectively two pollen filtering mechanisms have been removed. This would have allowed an increased extra-local to regional pollen signal to be recorded (Walker and Sun 2000;

Walker 2007). The more open and lower structural environment would also have been beneficial for fern growth (Figure 9.9).

The reduction of rainforest elements on the swamp not only allows a greater signal from the extra-local taxa, especially the canopy taxa, Cunoniaceae (tricolpate and dicolpate) (Figure 9.8), but may also be one of the factors responsible for the increase seen in *Quintinia*, a rainforest taxon usually associated with wetter but also cooler conditions (Kershaw et al. 2007a). That both Cunoniaceae (tricolpate) and *Quintinia* together with *Balanops australiana* peak at similar times, 4.8–4 ka, and then all decline could suggest a short period of cooler conditions and one with variable and sometimes lower burning activity. That there is no real decrease in the warmer rainforest taxa, Cunoniaceae (dicolpate), *Elaeocarpus* and *Ficus*, could suggest that *Quintinia* (most likely *Q. quatrefagesii*) and *B. australiana* are being regionally sourced as both are more commonly found at higher altitudes (>1000 m). Another suggestion put forward by Kershaw (1975) but in relation to Bromfield Swamp where a similar trend is found is the possibility of higher precipitation due to a longer wet season which would then maintain lower temperatures.

Although the warmer rainforest canopy taxa, Cunoniaceae (dicolpate), and *Elaeocarpus* continue with slightly higher values after the decline in the ‘cooler’ rainforest taxa, the contribution of the rainforest canopy is reduced from ~70% to ~50% of the dryland sum and it is the secondary rainforest taxa, primarily *Macaranga* and *Mallotus* but also vine taxa, especially Mensipermaceae and *Freycinetia*, which increase after this decline in line with an increase in regional fire. That *Celtis* also shows a slight increase at this time would also suggest warmer and drier conditions, or a longer dry season due to an increase in seasonality (Moss and Kershaw 2000), either explanation being compatible with increased burning. There are general similarities but also minor differences between Lynch’s and other pollen records within this period, 4.8–3.8 ka, probably mainly due to the rainfall gradient across the Atherton Tableland (Hiscock and Kershaw 1992).

The age (3000 ka) at the top of the record is only an estimate as a ^{14}C date at 15 cm is 1520 ± 60 BP and at 48 cm a ^{14}C date of 6060 ± 70 BP. It is likely that because of extensive drainage, burning for pasture and peat striping across the crater surface over several decades that there has been significant reworking especially in the top 20 cm and possible

further down. However, the reduction in rainforest canopy taxa and rise in secondary taxa, *Macaranga* and *Mallotus*, alongside moderate increases in sclerophyll taxa including Poaceae which is present through to the top at Lynch's Crater is also found in some form across the other Atherton Tableland sites. This suggests that Lynch's Crater does capture some information on the last 2000 years with a change to warmer drier conditions indicated by the presence of *Macaranga* and *Mallotus* and could suggest heightened seasonality due to ENSO conditions.

9.2. Orbital and sub-orbital frequencies in the Lynch's Crater record

The present study was limited to the late Pleistocene/Holocene and therefore not long enough to test obliquity frequencies and the more prominent eccentricity frequency found in the longer Lynch's Crater record (Kershaw et al. 2007a). Nonetheless it was noted (Chapter 8, sub-section 8.2.2) that a number of taxa (mainly rainforest canopy) had a frequency the length of the time-series (51.3 ka and 43.4 ka) and when filtered a similarly long frequency of 41,200 or 34,000 remained. Whether these frequencies are amplitude or frequency modulations of eccentricity or the obliquity (Berger et al. 1991; Mélice et al. 2001; Huybers and Aharonson 2010) cannot be verified in this study because of the restricted sequence length but as both eccentricity and obliquity are prominent in the longer Lynch's Crater record it is perhaps expected that these frequencies would also be evident in this record.

9.2.1. Precessional and semi-precessional influence

Unlike the longer Lynch's Crater record (Bretherton 2006; Kershaw et al. 2007a) precessional and semi-precessional frequencies were dominant and common across both the full and Late Pleistocene sequence and across numerous taxa (Tables 8.1 to 8.4) Turney et al. (2004) found in their record, covering a similar period of time as the present study, that the semi-precessional frequency was dominant. Turney et al. (2004) suggested the semi-precessional frequency is associated with changes in ENSO while the precessional frequency is associated with precipitation. Changes in the ENSO mode is likely to affect the seasonal migration of the ITCZ and its influence on the strength of the south-east trade winds and therefore the timing and levels of precipitation within the study site region at the present-day and likely to have been in the past because of the relatively

narrow continental shelf off the study site region of northeastern Australia (Turney et al. 2004; Leduc et al. 2009; Lewis et al. 2013; Hinestrosa et al. 2016).

Another common frequency was the 15–17 kyr frequency which, for some including microcharcoal (Tables 8.1 to 8.4) was the dominant frequency. It was also not unusual that taxa advantaged by disturbance or able to respond quickly had either a semi-precessional and/or precessional frequency alongside the 15–17 kyr frequency. This could suggest that the 15–17 kyr frequency is a modulated harmonic of the semi-precessional or precessional frequencies (Berger et al. 1991; Hooghiemstra et al. 1993). Another possibility is an association with the 30 kyr frequency which was found across a number of taxa and other proxies in both the full and Pleistocene sequences, see Appendix B section 3, and was found to be a dominant frequency at ODP Site 820 associated with charcoal (Kershaw et al. 2007a).

9.2.2. Millennial frequencies

Millennial-scale frequencies were common across all time sequences. In the majority they were only at the 95% confidence level, although several, including *Chenopodiaceae* and *Callitris* (3.5 kyr and 3.6 kyr), had millennial frequencies at the 99% confidence level (see Appendix B for full details). Similar frequencies to *Chenopodiaceae* and *Callitris* have been found in marine proxies from the southern and northern Indian Ocean and also from the Sulu Sea and are thought to be combinations of orbital parameters on monsoon dynamics (Pestiaux et al. 1988; Sirocko et al. 1996; de Garidel-Thoron et al. 2001). However, of particular interest is the 1470 yr frequency which is associated with Dansgaard-Oeschger (D/O) and Heinrich (H) events (Dansgaard et al. 1984, 1993; Bond et al. 1997, 1999). Turney et al. (2004) recorded a 1490 yr frequency in the humification record alongside the semi-precessional frequency. For this study humification analysis was limited to the period 37.9 ka to 28.5 ka as this period showed the greatest variability in the Turney et al. (2004) record. Spectral analysis was undertaken on this short sequence and, as was found in longer sequences analysed (Table 8.5) frequencies between 1–2 kyr were relatively common and although none of the elements analysed across this short sequence where humification was analysed (see sub-section 8.2.4) returned a 1470/1490 yr frequency. A 1.3 kyr was particularly evident, for the *Cyperaceae*/*Poaceae* ratio (1.3 kyr), macrocharcoal (1/1.3 kyr influx), but especially for *Poaceae* (1.3 kyr % and influx) (sub-section 8.2.4, Figures 8.40–8.44, Chapter 8).

However, there were a number of dryland taxa that had frequencies ranging from 1–2 kyr but particularly 1.2 to 1.5 kyr (see Table 8 and Table 8.15) but only *Elaeocarpus* (1470 yr) and *Celtis* (1480 yr), both rainforest taxa, had a 1470 yr frequency (Figure 9.10 and Figure 9.11). The frequencies were not recorded in the full record but were present in the Pleistocene sequence analysed (Table 8.11 and Table 8.15).

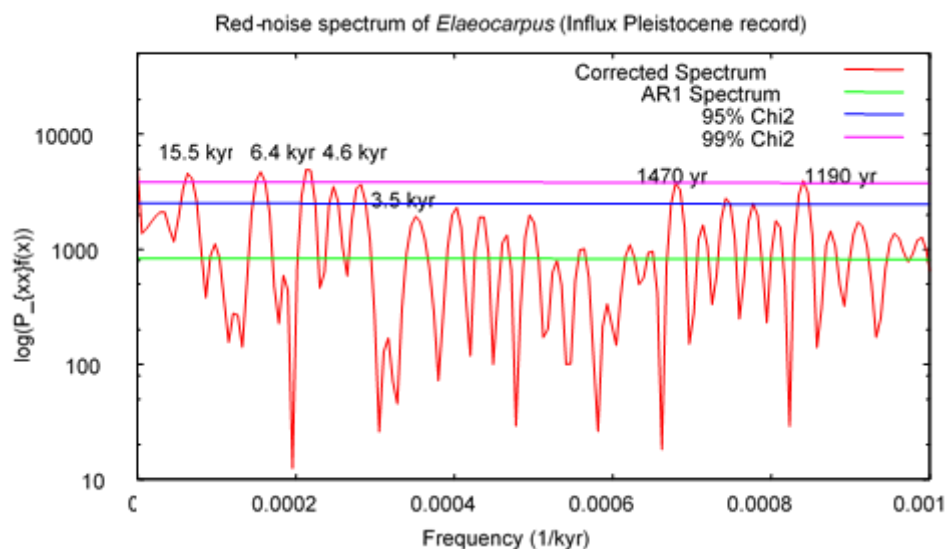


Figure 9.10. Red-noise log-linear spectra plot for *Elaeocarpus*. Frequencies noted on plot.

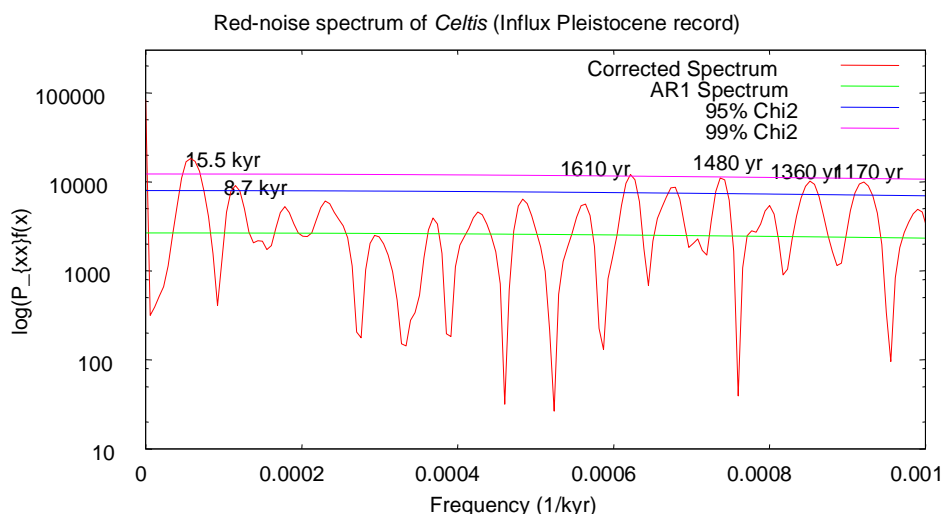


Figure 9.11. Red-noise log-linear spectra plot for *Celtis*. Frequencies noted on plot.

Elaeocarpus (rainforest canopy) and *Celtis* (rainforest secondary) had consistent representation through the whole record and therefore they should be a reliable indicator of long-term changes in precipitation availability. Turney et al. (2004) suggest the 1490 yr period is related to changes in precipitation associated with long-term changes in

ENSO in the tropical Pacific Ocean region, through a disruption of the trade winds. This would certainly suggest that long-term changes in ENSO are a major influence at Lynch's Crater although neither taxon have recorded a precessional or semi-precessional frequency during the Pleistocene sequence analysed. However, both have a 15.5 kyr frequency which was also present in a number of other taxa and the charcoals and has been discussed in the previous sub-section 9.2.1, it could be that the changed environmental dynamics due to increased fire activity and the subsequent vegetation response played a role in this suggested modulated frequency.

9.2.3. 'Heinrich Events'

It is important to note that, prior to discussing Heinrich events (H), there is no suggestion in this thesis that actual Heinrich events are recorded within the sediment record itself and the term 'Heinrich event' is only used as a chronological comparison time-frame as has been suggested from other sites well removed from known sites where there is a clear geochemical signature from iceberg discharge events linked to the Hudson Strait/Hudson Bay region, H-1, H-2, H-4 and H-5 or H-3 and H-6 linked to the European ice sheets (Grousset et al. 2000; Voelker 2002; Andrews and Voelker 2018).

Muller et al. (2008 *a, b*) compared the Si/Al ratio and the high inorganic phases from their study with the Cyperaceae/Poaceae ratio from the Turney et al. (2004) study and suggested that high Cyperaceae/Poaceae ratio values corresponded to high inorganic phases, which they suggested are wet Heinrich events (H-events). They also suggested that the off-set between the high inorganic phases and high Cyperaceae/Poaceae ratio values seen in the Turney et al. (2004) record is due to a lag effect (1 ka) from the vegetation. Turney et al. (2004) looked at the carbon (%) rather than LOI so inorganic levels were not as pronounced but it was suggested that H-events corresponded instead to ENSO dry periods recorded in the humification record (see sub-section 3.2.8, Figure 3.10).

The high inorganic phases present in Muller's record (2008 *a, b*) were also found in the present record and there was also a relatively good match between the two records with regard the age of the onset of these inorganic phases (see Chapter 6, sub-section 6.3.2 and Figure 6.5). This makes it possible to compare the Cyperaceae/Poaceae ratio with the

inorganics within the same sequence to observe the nature of these H-events alongside other key elements, micro- and macrocharcoal which are major influences throughout this record. Turney et al. (2004) suggested that H-1 (15 kyr ago), H-2 (25 kyr ago) and H-4 (40 kyr ago) coincided with ‘warm’ (dry) ENSO activity on the semi-precessional timescale while ‘cold’ (wet) events are recorded for H-3 (30 kyr ago) and also for the period 21 kyr. Figure 9.2 and 9.3 show that, prior to 43 ka, high Cyperaceae/Poaceae ratio values do not correspond to high inorganics, but evidence from the dryland components does indicate that conditions were relatively humid, likely the influence of high insolation and increased seasonality (see sub-section 9.1.1 and Figure 9.1). The low values for both charcoal types would also suggest that fire activity was at a minimum. From ~41 ka, (Figure 9.12(b)), there is a continuation of low inorganics but low Cyperaceae/Poaceae ratio values and a decrease in the influx of Cyperaceae with a minor increase in both Poaceae (see Figure 9.3) and microcharcoal suggests H-4 is dry as suggested by Turney et al. (2004).

From 39–32 ka there is a steady increase in inorganics during austral autumn (Figure 9.1) and, although insolation values are lower, it has been suggested from ocean-atmosphere modelling studies that extreme strengths of the seasonal cycle on the semiprecessional cycle experience frequent El Niño events during boreal spring or autumn (austral autumn or austral spring) while ENSO shutdown is predicted when the perihelion is in either the austral summer or winter (Clement et al. 2001; Turney et al. 2004) which may suggest that these inorganic phases are related to frequent El Niño events. The Cyperaceae/Poaceae ratio through this period is low with an isolated peak suggesting relatively dry conditions although, when looking at the influx values for both these taxa it shows both have high values (see *sub-section 9.1.2.3*). It is very likely that the big increases seen for Poaceae are related to fire as there is a step-wise increase in microcharcoal which is also seen for *Eucalyptus*.

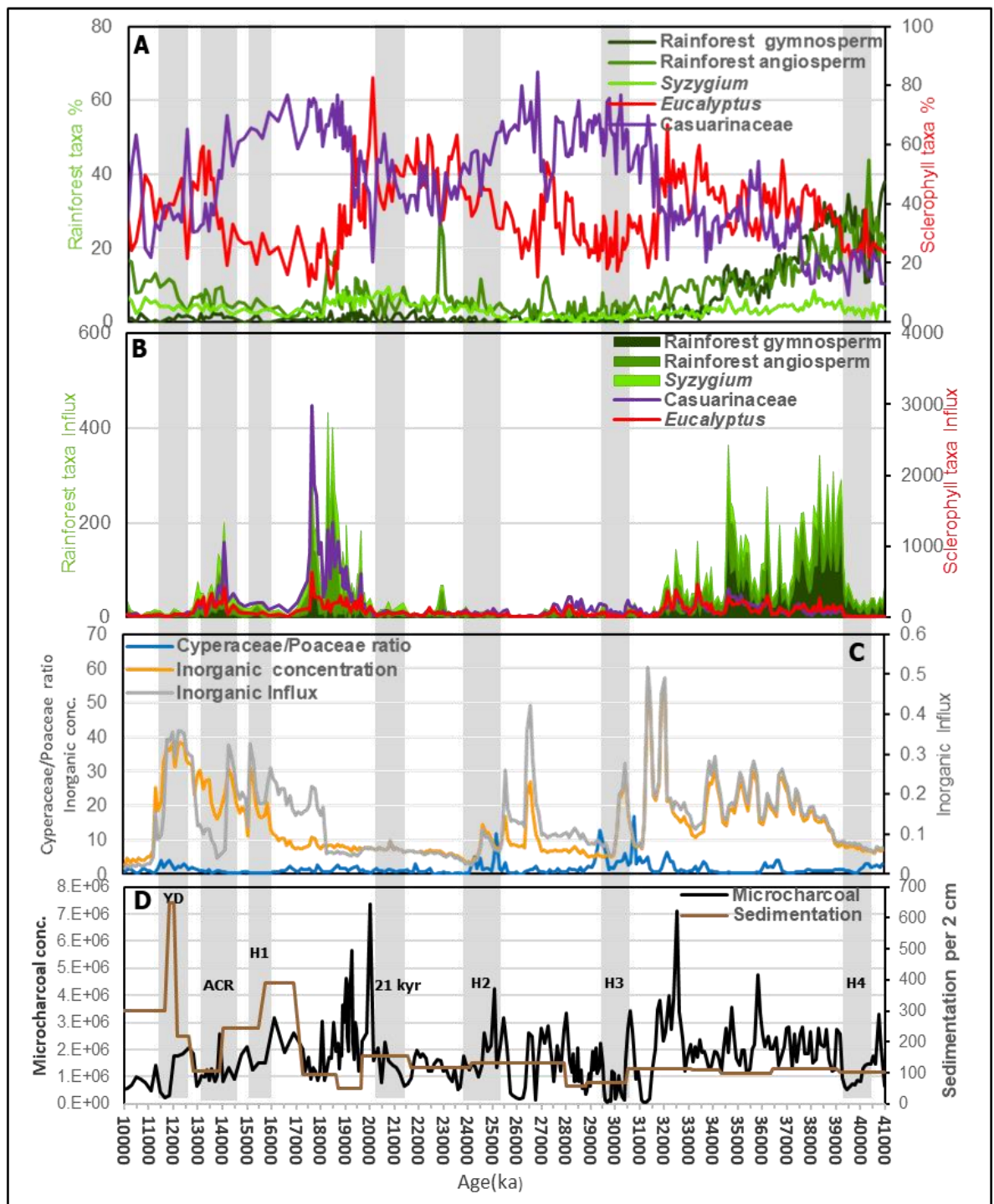


Figure 9.12. Major dryland summary types for period ~10–40 ka - A-Percentage, B-Influx, C-Inorganics (concentration and Influx) and Cyperaceae/Poaceae ratio, D-Charcoal (micro). Grey shaded areas indicate H-events (1-4) and ACR and YD.

Both Muller et al. (2008b) and Turney et al. (2004) suggest that it was wet at 30 ka with Muller et al. (2008b) suggesting a wet Heinrich event (H-3) with its origin related to the southward migration of the ITCZ due to cooling in the Northern Hemisphere. The period 32–29 ka is highly variable at Lynch’s Crater. The period 32–31 ka and possibly 30.9–

30.8 ka is wet locally and regionally and this coincides with higher inorganic values (Figure 9.12) and, although the sclerophyll component especially *Eucalyptus* has greater representation, there is also a greater diversity of rainforest angiosperms especially canopy taxa with 21 recorded for the period 32–30.8 ka in contrast to 8 for the period 30.7–29.6 ka. At 30.4–30.2 ka the Cyperaceae/Poaceae ratio is high but inorganics are reduced as are the influx values for both taxa although for Poaceae more significantly. It has already been suggested that cooler and drier conditions existed from 30 ka, (see subsection 9.3.1) with deteriorating conditions noticeable from ~30.3 ka and becoming more persistently dry from 30.2–29.6 ka based on influx and percentage data and inorganics. More recent dating and contiguous carbon analysis of the Lynch’s Crater sediments suggests a ~420-year downturn that commences at 30,920 ±340 BP, with low sediment accumulation rates and low sedges to grass ratios suggesting drier conditions (Turney et al. 2017). This would be in agreement with the present record although there is not an exact match with the more precisely dated record (44 ¹⁴C ages) of Turney et al. (2017) which was focused on a 2000-year period with an onset of 31,540 ±660 BP.

This proposed dry period is in contrast to the findings of Muller et al. (2008b) where H-3 is inferred as wet. However, as these changes are quite abrupt, the chronology could also be a factor for these differences as the standard deviation ranges from 300 to 370 years which suggests that a degree of flexibility maybe warranted across this period. There is also a difference of resolution undertaken for the inorganics between Muller et al. (2008b), 10 cm interval, and the present study, contiguous, which may have also been influential as the inorganics were the primary source for Muller’s et al. (2008b) suggestion.

Studies on spethothems from Flores, Indonesia (Lewis et al. 2011) and Hulu Cave, China (Wang et al. 2001, 2006; Zhao et al. 2010) suggest dry conditions due to the southward migration of the ITCZ resulting in both a weak Australian/Indonesian Summer monsoon (Flores) and East Asian monsoon (China) during H3, ~30.8 to 29.6 ka (Figure 9.13). By contrast, in sub-tropical, Botuvera, southern Brazil, spethothems indicate an antiphasing relationship with China and Flores with an intensification of the South American Monsoon and therefore increased precipitation at H-3, Figure 9.13 (Wang et al. 2006; Lewis et al. 2011). Turney et al. (2017) suggests that the local hydroclimatic response at

Lynch's Crater was likely due to weakened moisture-laden equatorial Pacific trade winds which were synchronous with southward migration of the ITCZ.

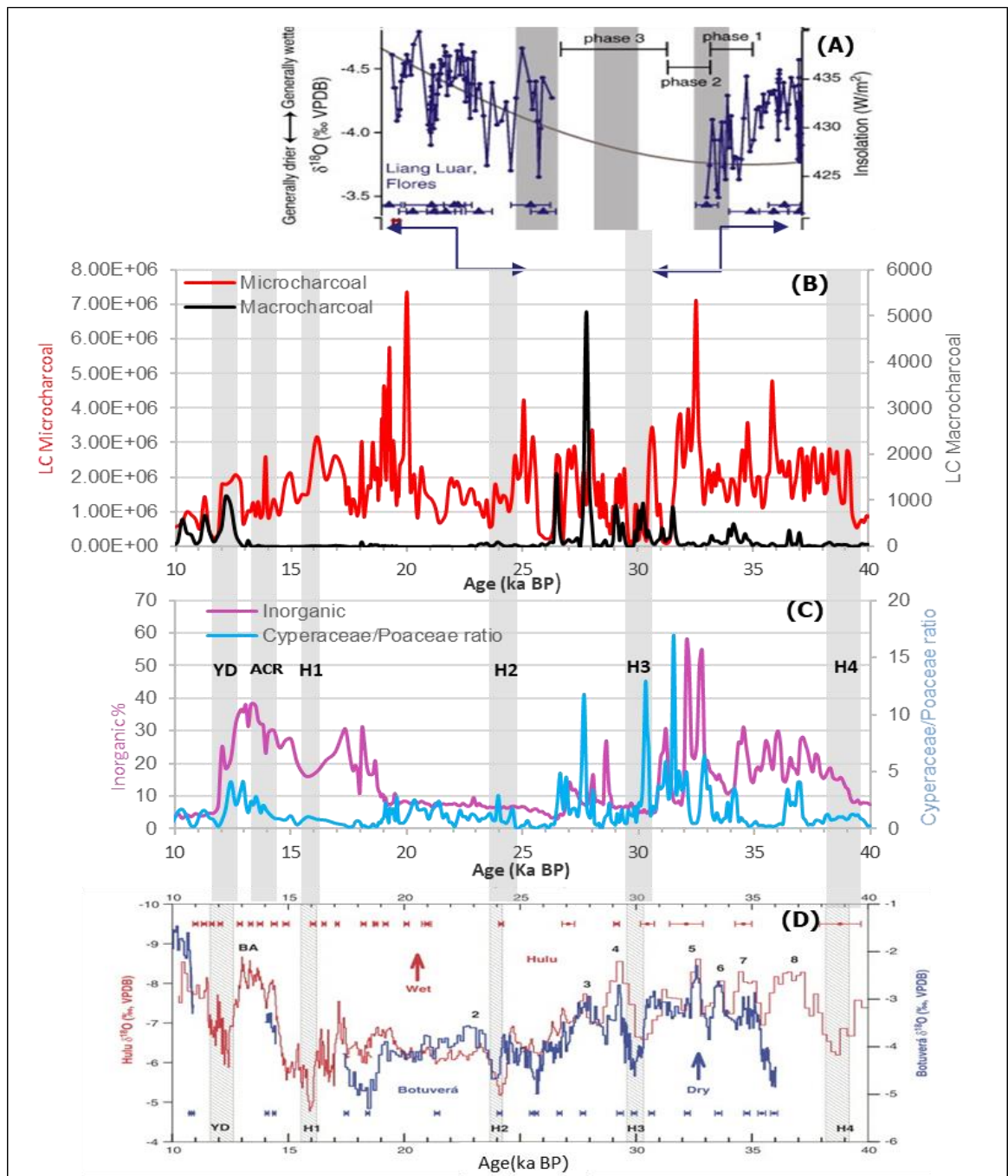


Figure 9.13. Comparison of LC macrocharcoal and microcharcoal (B), LC Cyperaceae/Poaceae ratio and inorganics (C), with Flores, Indonesia (Lewis et al. 2011) (A), and Hula Cave, China, and Botuverá, Brazil (Wang et al. 2001, 2006; Zhao et al 2010). Shaded areas indicate time of climate anomalies, H – Heinrich, YD – Younger Dryas and ACR – Antarctica Cold Reversal for time sequence 40–10 ka.

The extent of the southward migration of the ITCZ may have been limited due to Australia and New Guinea being one landmass which would have impacted the circulation of ocean

surface currents such as the Indonesian Throughflow (ITF) and the extent of the Indo-Pacific Warm Pool (IPWP) (Lewis et al. 2013; Reeves et al. 2013b; McGee et al. 2014; Schneider et al. 2014). A further lowering of the sea-level at ~30 ka (Chappell et al. 1996; Woodroffe and Webster 2014) certainly indicates that climate variation is impacting a wider region (Lewis et al. 2013).

Relatively dry conditions continue after 29.6 ka although interspersed with the occasional more humid phase (see sub-section 9.1.3) but from 26.7–24.5 ka the lowest influxes of the record are recorded and certainly suggest that H-2 is dry (Figure 9.12). From ~22 ka influx values are higher and more so after 20 ka where there is also an increase in the diversity of rainforest angiosperms and, as suggested earlier, both a warmer Coral Sea and insolation maximum would indicate relatively warm and wet conditions at this time (Tachikawa et al. 2009). Locally from ~19.6 ka to 12 ka inorganic levels are higher possibly indicating that H-1 (15 ka) was wet as suggested by Muller et al. (2008b).

Lake Carpentaria has fluctuating lake levels after 18 ka and the highest lake levels and lowest salinity are found between 14–12 ka suggesting an increase in precipitation with the arrival of the monsoon in northeast Queensland (Reeves et al. 2008, 2013a). There is also evidence of regional aggradation with the formation of fans and terraces between 30 and 13 ka across north-east Queensland with widespread catchment erosion at 13 ka. This period also sees the highest rates of terrigenous sedimentation in the Great Barrier Reef all suggesting wetter conditions (Hughes and Croke 2017). Wet conditions are suggested for parts of south-east Asia as indicated by increased detrital and biogenic fluxes in the Flores Sea due to enhanced precipitation runoff likely because of the southward migration of the ITCZ (Muller et al. 2012). On the Sunda shelf sea-level rise was gradual from 19–14.6 ka but became more rapid after 14.6 ka with increased precipitation seen initially in Indonesia then in northern Australia especially to the north-west coinciding with the reactivation of the monsoon (Hanebuth et al. 2000; Wyrwoll and Miller 2001; Reeves et al. 2008, 2013a,b).

The continuation of high inorganics in Lynch's Crater suggests that wet conditions prevailed during the Antarctica Cold Reversal (ACR) (14–12.5 ka) with *Nymphoides* still present (pollen and seeds) and some of the highest recorded pollen counts for Cyperaceae. There are higher values for both *Eucalyptus* and Poaceae but low values for both

Chenopodiaceae and Asteraceae with only a slight increase in microcharcoal. *Tasmannia* makes a rare appearance as does Acanthaceae while both *Anthoceros* and *Pteridium* return to higher values but macrocharcoal levels are extremely low. This could suggest that conditions may have been too humid for large scale fires. However, as suggested in *sub-section 9.1.3.1*, the presence of variable sedimentation rates (Figure 9.12(D)) suggests caution is needed in interpretation of conditions through this period (ACR) and the following YD. The ACR in the temperate areas of Australia is suggested to be relatively dry in south-east Queensland (Moss et al. 2013), increased relative moisture is suggested for western Tasmania between 14–11.7 ka (Fletcher and Moreno 2011, 2012) and reversals and stabilisation are indicated from marine cores off southern Australia between 15–12.5 ka (Calvo et al. 2007; Sikes et al. 2009; Lopes dos Santos et al. 2012; Tibby 2012). Lake Carpentaria expanded with increased precipitation resulting in the establishment of a freshwater lake from 14 ka (Reeves et al. 2008) while further north marine records show little variation during the ACR although there is some cooling and drying in some areas of the IPWP with a short hiatus present in Borneo around the ACR (Reeves et al. 2013b).

At Lynch's Crater all influx values are reduced except for *Typha* at 12.8–11.5 ka with fire activity likely to be restricted to the local environment with lower microcharcoal, high macrocharcoal but lower *Anthoceros* and *Pteridium*. There is also a change in the composition of rainforest taxa. Prior to 12.5 ka cooler rainforest elements, *Balanops*, Podocarpaceae and *Tasmannia*, are conspicuous but these are reduced or absent after 12.5 ka relative to warmer rainforest elements, such as *Trema* and *Macaranga* and *Mallotus* as well as those taxa that are components of the swamp forest, *Acmena*, *Glochidion*, *Rapanea*, *Melastoma* and *Flindersia*. The reduction in inorganic content is considered to represent drier conditions while the increase in taxa indicative of warmer conditions would suggest that effective rainfall was at least maintained through the period 12.8–11.5 ka.

Marine records from the low latitudes of the Northern Hemisphere show cooling during the YD (Linsley and Thunell 1990) but there is little indication of cooling from marine cores in the low latitudes of the Southern Hemisphere with reactivation of the monsoon as early as 15 ka (Reeves et al. 2013a,b) while warming of the IPWP ensured increased precipitation and ice retreat, evident during the YD. Ice disappeared from the highest

altitudes around 11.5 ka in Mt Giluwe, PNG (Barrows et al. 2011) and, although the tree-line on Mt Wilhelm PNG was below 2700 m and glaciers were still present at 10 200 yrs B.P., ice retreat had begun about 15000 years ago but vegetation migration was limited by severe storms and drier conditions (Hope 1976). Dry conditions and sea-level stabilisation are suggested from marine cores off the Gulf of Papua, northern Coral Sea from 12.5 to 11.5 ka and, though an increase in fungal spores and decrease in the abundance of pollen and spores could indicate cooler conditions, the decrease was primarily from the cooler rainforest elements (Howell et al. 2014; Thomas et al. 2018).

It could be that the suggested cooling for the ACR is related to an increase in precipitation due to the influence of the monsoon as proposed at Lake Carpentaria. However, although Lake Carpentaria expanded from 14 ka and was marine from 12 ka with the flooding of the Arafura Sill, the eastward Pacific Ocean side (Coral Sea) remained connected to PNG until ~ 8 ka (Reeves et al. 2008, 2013*a, b*). This may have affected or constrained the influence of the monsoon in areas to the east of the Torres Strait Sill where the south-east Trades may have been a greater influence (Connor and Bonell 1998; Reeves et al. 2008; Klingaman 2012). That the Torres Strait Sill remained connected to PNG until 8 ka could have also limited the influence of the monsoon during the YD where no cooling is evident but rather warmer conditions prevailed (Reeves et al. 2008, 2013*a, b*). A review of the presence of the YD in southern and eastern Australia concluded there is no evidence of significant climate variability during the YD chronozone (Tibby 2012).

9.3. Fire patterns: the role of climate variability and potential human influence

Fire has been perceived as a major biological shaper within the study area with climate change and/or human activities put forward as the main protagonists (Kershaw 1986; Flannery 1994; Roberts et al. 2001). Initially several possible reasons were put forward for the replacement of dry rainforest by sclerophyll vegetation at Lynch's Crater at ~38,000 radiocarbon years BP with a decrease in both precipitation and temperature suggested. However, although charcoal was not recorded in this record, it was proposed that fire was most likely agent of the landscape transformation because there was no evidence of major climate change and the transition was from a fire sensitive to a fire tolerant vegetation (Kershaw 1973, 1974). Burning by Indigenous people was considered to be the cause as recent research had demonstrated that people practised 'Firestick

Farming' (Jones 1969, 1974) and had been in Australia for at least the last 32,000 years ago (Barbetti and Allen 1972). This hypothesis was reinforced first by an extension of the Lynch's Crater record from c. 60,000 years BP to c. 120,000 years BP that demonstrated the lack of a similar change towards the end of the penultimate glacial that, with change taking place over a period much longer than those related to major glacial-interglacial switches, effectively eliminated a natural cause (Kershaw 1978). The subsequent addition of a charcoal curve cemented the hypothesis (Figure 3.4) (Singh et al 1981; Kershaw 1983b). However, the detailed analytical synthesis of all charcoal records in Australia by Mooney et al. (2011) concluded that fire regimes were overwhelmingly controlled by changing climate conditions although it was suggested that the broad overview of the study might make it hard to distinguish small-scale or low intensity fires more characteristic of Aboriginal burning. Rule et al. (2012) found that, though fire was an integral component of both vegetation transformation and human arrival, it was megafauna and its role within the environment that was considered to be highly influential on fire activity. Fire has been a relatively continual feature throughout this sequence and therefore, it was hoped that high resolution charcoal analyses undertaken alongside the pollen and macrofossil records would allow refined assessment of the patterns and causes of fire activity through this whole period.

9.3.1. From low to high intensity fire

The presence of a swamp/aquatic community, albeit varying through time, on the crater surface from the start of this sequence, ~54 ka, through to ~3ka provides the means of assessing fire activity both prior to and since the suggested time of human arrival within the region (O'Connell et al 2018). Changes in the depositional environment from lake muds to peat sediment from ~70–64 ka, was likely to have provided a ready source of swamp vegetation for fire to consume, but prior to 42 ka fire was minimal (Figure 9.14) (Black et al. 2007; Kershaw et al. 2007a). There were certainly changes on the swamp and within the surrounding dryland vegetation, but no apparent significant changes in fire magnitude.

The small changes seen for fire locally, primarily 'elongated' type macrocharcoal at ~52.5 ka, correspond to the presence of charred plant remains as well as a charred sedge nut, likely *Schoenoplectus mucronatus* (Chapter 7, Plate 7.7), confirming the local origin of fire and as suggested in *sub-section 9.1.2.3.*, a wetland Poaceae is likely to have been

dominant. There is no match between the charcoal values and the large spike recorded for Swamp Myrtaceae 1, *Eucalyptus* sp., suggesting that fire activity was small scale and localised. That fire remains low prior to 42 ka at a time of increasing insolation may suggest a so called ‘natural fire regime’ prior to human arrival. It could be that the presence of large herbivores (megafauna), which were likely to be mixed feeders or grazers and browsers, were influential in maintaining both tree and grass distribution and density and effectively reduced available fuel biomass (Janzen and Martin 1982; Feer 1995; Dudley 2000; Couvreur et al. 2004; Johnson 2006, 2009; Guimarães et al. 2008; D’hondt et al. 2012; Rule et al. 2012).

From 42 ka the increase in microcharcoal is accompanied by reduced *Sporormiella* values (Figure 9.14). Large values of *Sporormiella* have been linked to the presence of large herbivores (Davis and Shafer 2006; Graf and Chmura 2006; Raper and Bush 2009) and Rule et al. (2012) surmised that hunting by humans caused the demise of the megafauna at this site. It was also found that, although the decline in *Sporormiella* and the rise in charcoal at Lynch’s Crater were negatively correlated ($r = -0.54$; 95% CI -0.72 to -0.30), neither were correlated with vegetation change. This could suggest that fire was only used to hunt/kill megafauna and therefore any impact on the vegetation was incidental at this time.

However, although there may not have been any statistical evidence for an immediate correlation between fire and vegetation change especially for the sclerophylls, there are discrete changes happening locally and regionally. The initial increase in fire locally and regionally at ~41 ka sees slightly higher values for the secondary rainforest components, *Mallotus*, *Homalanthus*, *Trema* and *Celtis*, alongside vine taxa, Menispermaceae and *Morinda*, at the expense of the rainforest canopy taxa (Figure 9.1). It is known that rainforest trees, especially secondary trees, are able to withstand infrequent fire and low intensity fires and the disturbance provides the opportunity for shade intolerant species to propagate (Williams 2000; Williams et al. 2006, 2012; Williamson and Mesquita 2001).

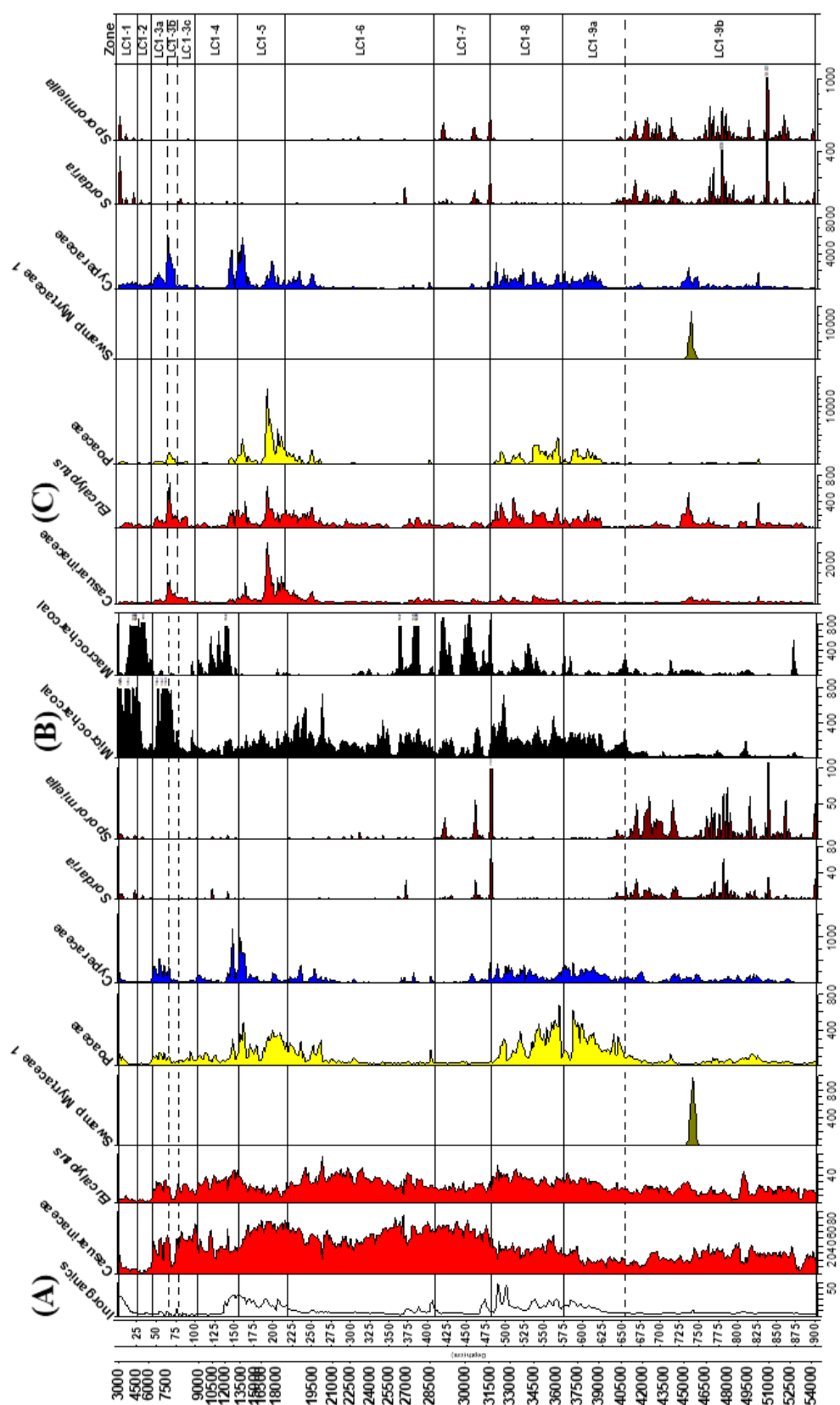


Figure 9.14. Percentage (A) and influx (C) values of *Eucalyptus*, *Casuarinaceae*, *Swamp Myrtaceae 1*, *Poaceae*, *Cyperaceae*, *Sordaria* and *Sporormiella* and (B) micro- and macro-charcoal concentrations shown in relation to the zonation based on the dryland pollen sum. Both micro- and macro-charcoal truncated with actual values indicated at the end of each relevant sample. Composite diagram of selected taxa from Figures 7.3, 7.4, 7.6 and 7.12 and Rule et al. (2012) and Johnson et al. (2015).

This early beneficial response to fire that was present in the secondary rainforest taxa was not found in the gymnosperm *Araucaria* and the rainforest canopy species *Argyrodendron peralatum* as the declines of both started from that initial increase in fire (~41 ka) and for *Araucaria* it never recovered. It has been suggested that *Araucaria* was in a long-term decline over the last 1.2 million years due to the Australian plate drifting to lower latitudes and therefore outside its optimum growth conditions (Moss and Kershaw 2000; Kershaw and Wagstaff 2001) but also, although entirely speculative, the removal of megafauna may have meant that long distance dispersal of *Araucaria* seeds was no longer available (Guimarães et al. 2008; Pires et al. 2018). Locally there were no major changes initially except the return of the fungal spore, *Gelasinospora*, which has been found to be a good indicator of relatively dry conditions and the presence of local fire (Krug et al. 1994; Stivrins et al. 2019); this spore was absent from 48–42 ka. The presence of the hornwort, *Anthoceros* could also suggest at least some areas of the swamp were affected by fire enabling *Anthoceros* to colonise the bare areas (Esposito et al. 1999; Morgan 2004).

However, the more sustained increase in fire at 39 ka, correlating to a more substantial increase in *Eucalyptus*, is only found in the microcharcoal and initially is more evident in the smaller size categories, 8–52 µm and 53–102 µm (Figure 9.15—see Figure 7.18 for full details) indicating a distinct change in fire type and intensity. Studies suggest that an increase in the smaller size fraction of microcharcoal indicates both a more regional fire signal and an increase in fire intensity (Clark et al. 1998; Pitkanen and Huttunen 1999; Duffin et al. 2008; Conedera et al. 2009). Rule et al. (2012) suggested that, with the relaxation of herbivory, fuel increased and a more fire prone environment evolved.

Archaeologically, although it has been suggested that human occupation in Australia could go back to 65,000 years BP (Clarkson et al. 2015, 2017), others suggest that the critical site of Madjedbebe (Northern Territory) has problems with dating and that there is little evidence of human presence within the Australian region beyond > 50 ka (O’Connell et al. 2018).

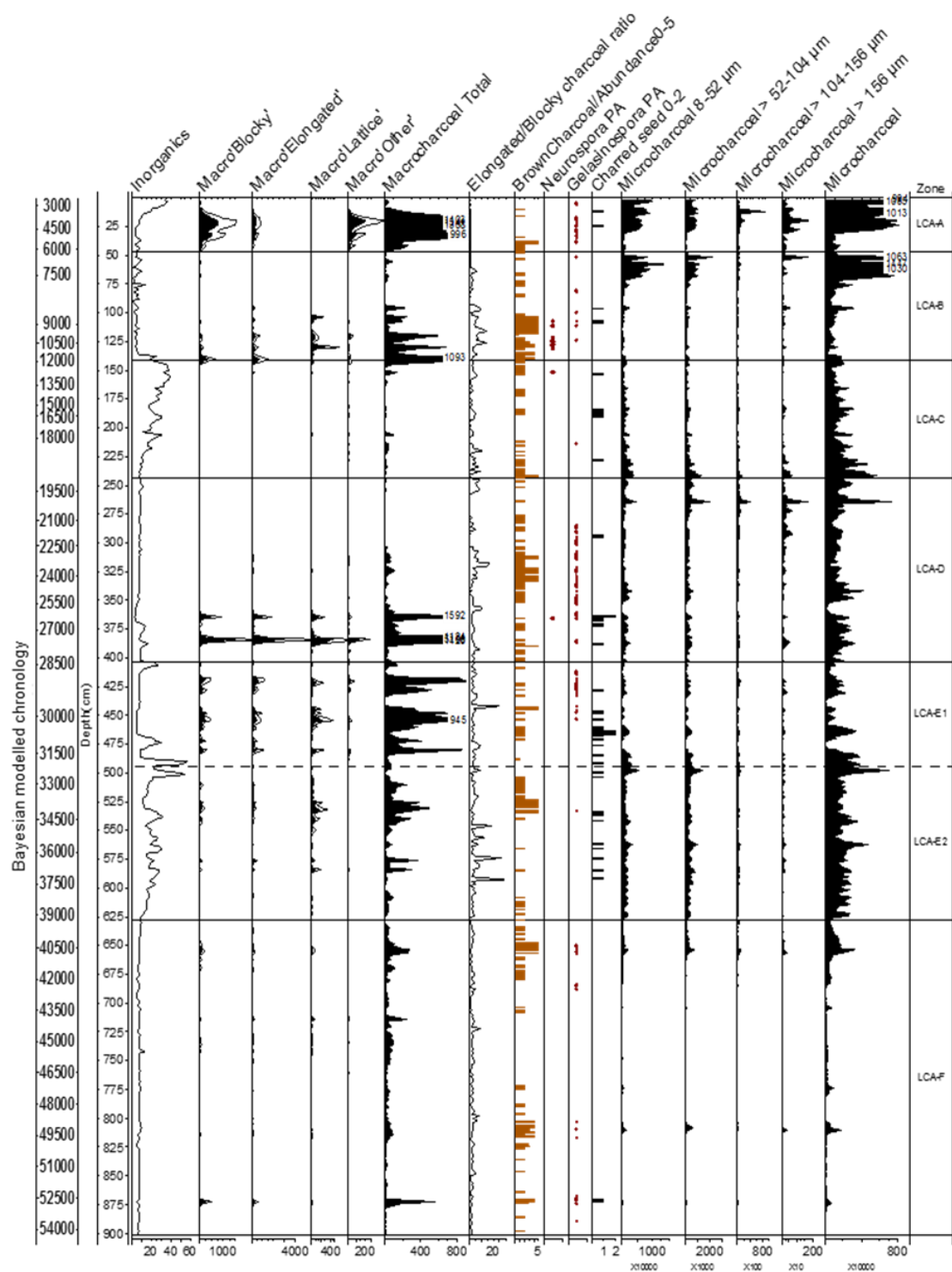


Figure 9.15. Macrocharcoal types and total alongside inorganics and microcharcoal as well as the Elongated/Blocky macrocharcoal ratio, brown charcoal abundance on a 0-5 scale, *Neurospora* and *Gelasinspora* (present/absent) and charred seeds on a 0-2 scale). Both microcharcoal and macrocharcoal are expressed as concentrations with highest values truncated and macrocharcoal types have been exaggerated x2. Zonation is based on the aquatic and swamp pollen sum.

The earliest dates for known human occupation in northern Queensland are mainly west of the Great Dividing Range with the oldest at Ngarrabullgan Cave dated to $40,540 \pm 650$ yr cal BP, a site 80 km northwest of Atherton Tableland area, but it has been suggested that, even with limited occupation and few people their use of fire could have had a catalytic impact on the vegetation (David et al. 1998).

The increase in the sclerophylls is primarily in *Eucalyptus* and Poaceae and, although Casuarinaceae is well represented, it does not increase its percentage or influx across this period, ~42–39 ka (Figure 9.14). That the two major sclerophylls, Casuarinaceae and *Eucalyptus*, are likely occupying different environments is suggested in Figure 8.24 where, although the PCA clearly separates the sclerophyll taxa and microcharcoal from the rainforest taxa on Factor 1, Casuarinaceae is at a distance from the sclerophyll Myrtaceae and microcharcoal. While on the secondary axis (Factor 2) the sclerophyll Myrtaceae are aligned with the secondary rainforest taxa while Casuarinaceae is correlated with the Gymnosperms. This distance between the sclerophyll Myrtaceae and Casuarinaceae may not only indicate the occupation of different environments but also that they have a distinctly different relationship with fire.

Marine records to the north and west of the study site show that prior to 42 ka fire activity was variable but usually associated with drier conditions that led to the expansion of drier woodland and grassland taxa (van der Kaars and De Deckker 2002; van der Kaars et al. 2000; Wang et al. 1999). There is consensus within some marine records that there was an increase in fire activity from 50 ka through to 30 ka likely related to the burning activities of people (Wang et al. 1999; van der Kaars et al. 2000; Beaufort et al. 2003). Closer to the study site, the marine record ODP Site 820 shows episodic increases in charcoal prior to 50 ka likely due to drier conditions. However, a substantial increase at ~130,000 ka is associated with much higher sclerophyll values although Poaceae is the only sclerophyll taxon that continues with these high values up to and beyond 45 ka (Moss and Kershaw 2007). The longer Lynch's Crater record does show slightly higher charcoal values when sclerophyll taxa, especially *Eucalyptus* and Poaceae, are more prominent in association with drier conditions even in the earlier part of the record, ~220,000 ka, but also associated with secondary rainforest taxa. However, there is no comparison to the extremely high charcoal levels found after ~42 ka which are present in both the longer Lynch's Crater record (Kershaw et al. 2007a) and the present record.

Currently, there are no other long terrestrial records in north Queensland for comparison with but sites in southeast Queensland show mixed charcoal representation around this time. Fraser Island shows a similar decline in Araucariaceae at a slightly earlier time, ~50 ka, than found at Lynch's Crater but no real associated increase in charcoal, while on North Stradbroke Island charcoal increases are found at ~44 ka where there is a higher sclerophyll presence than on Fraser Island. Human activity is given as its likely origin although it is suggested that the fire was more likely to be sourced regionally rather than locally (Donders et al. 2006; Petherick et al. 2008, 2011; Moss et al. 2013). A contrasting scenario from Fraser Island is found in New Caledonia where both Araucariaceae and fire were present at ~50 ka but the decline in Araucariaceae after 50 ka is considered to have been climate driven as people were not present. However, there are significant age problems (severe reversals) for the New Caledonia site, Lake Xere Wapo, and likely distinct ecological differences in Araucariaceae between New Caledonia and Australia (Stevenson and Hope 2005).

9.3.2. Changing trends in regional and local fire

The continuation of high fire activity through to 33 ka when insolation is at its minimum is likely influenced by the presence of both a densely treed savanna of primarily *Eucalyptus* with a Poaceae understorey encroaching on the crater rim and human activity. It is also likely that, with the dominance of a sclerophyll landscape, fire was being maintained by positive feedback loops which would allow the sclerophylls to maintain a degree of stability (Jackson 1968, 1977; Ash 1988; Turton and Sexton 1996; Warman and Moles 2009). Locally fire and vegetation were variable with elevated inorganics suggesting shallow lake or ponding conditions maybe limiting the presence of extensive fires. However the more consistent representation of charred seeds and brown charcoal suggests the presence of low intensity fires (Figure 9.15) which is also indicated by an increase in elongated type macrocharcoal compared to blocky type macrocharcoal suggesting locally that sedges and grasses are the primary fuel source (Clark 1988; MacDonald 1991; Umbanhowar and McGrath 1998; Jensen et al. 2007).

This contrast between regional and local fire (Figure 9.15) was indicated in PCA (Figure 8.4) where Poaceae is aligned with microcharcoal in contrast to *Carex* and *Schoenoplectus*, and *Typha* aligned with macrocharcoal. It could be that, with the

reduction of ponding, the crater became more accessible and therefore more conducive for human activity. Bickford and Gell (2005) and Kenyon (1989) suggest that human activity may be inferred in swamp environments especially where humid conditions prevail but where there is fire activity. In both studies *Typha* was the main indicator of human activity. Although these studies are from a temperate location, there is evidence further north that the young shoots, roots and pollen of *Typha* were a food source while the sap was used for leech protection and cordage was made from the plant fibre in Queensland coastal wetlands (Nagadjonji Antiquity 2007; Jaensch and Joyce 2006).

Rule et al. (2012) suggest that the return of *Sporormiella* in the presence of fire from ~32 ka through to 28.5 ka could indicate more discernable evidence of human activity (Figure 9.14). It could be that fire was used to manipulate the vegetation dynamics for the purpose of attracting large herbivores (extant kangaroos) and, unlike earlier where *Sporormiella* declined with increased fire, the opposite occurred here. Another possible indicator of increased human activity, although, 'equally' speculative, is a change in the species representation of the dung fungal spore *Sordaria*. It has been suggested that an increase in variability and extended presence of this fungal spore, which is usually assigned to *Sordaria fimicola*, could also belong to *Sordaria humana*, which, although found on herbivore dung, has its preferred substrate as carnivore and human dung (Lundqvist 1972; Doveri 2004; Johnson et al. 2015).

Sporormiella is reduced from 28 ka but *Sordaria* continues through to 26 ka suggesting either the absence or reduction in the fire-human-herbivore scenario. Fires continue even when inorganic values are slightly higher (see sub-section 9.1.3) with the presence of charred peat, low brown charcoal levels, an abundance of charred seeds and the presence of the fire indicator fungal spore, *Neurospora*, as well as the charred stem remains of *A. pinnata* suggesting local fires of relatively high intensity now extending across previous ponding areas (Holyoak 1984; Clark 1988; Tiffney 1990; Wright 2003). This would suggest that there is still an ample fuel-load although influx values are reduced especially for Cyperaceae and Poaceae from 31 ka and could indicate a degree of fire management or control. It also likely that Poaceae is on the rim of the crater or on more marginal areas of the swamp. *Typha* continues with slightly elevated influx values from 31 ka and the percentage data suggest that *Typha* trends with both 'elongated' and 'lattice' macrocharcoal suggesting that it at least is one of the main fuel sources. The closest

Aboriginal occupation site is Fern Cave in the Chillagoe area, about 120 km northwest of the study site, from 29,000 ^{14}C yrs BP (David 1991; Morword and Hobbs 1995; David et al. 1998).

9.3.3. Fires of the Last Glacial Maximum

Like local fire there is an increase in regional fire from ~28 ka except for a very short period, 26.1–25.7 ka, where values for both charcoal types are extremely low. This period is followed by a return to more consistent values for regional fire while local fire is reduced, although the low but consistent occurrence of brown charcoal could indicate the presence of low intensity fires locally and the absence of charred seeds could also indicate that the nearby grassland was a major biomass contributor which may have encroached onto the swamp at this time (Clark 1988; MacDonald 1991; Pitkänen et al. 1999). *Eucalyptus* becomes more prominent from ~25 ka although the influx data indicates this is not apparent until ~21 ka which is also the case for Poaceae and, once this combination is established, high fire activity follows. That *Eucalyptus* was a fuel source in now present-day rainforested sites is also indicated by soil charcoal analysis by Hopkins et al. (1990, 1993) who found that positively identified dated *Eucalyptus* charcoal from ~c. 27,000 BP at Mt Windsor and from ~c. 24,000 BP at Mt Nomico (Figure 3.7).

One of the causes for the increase in fire activity especially from 20.5 ka is likely to have been a direct response to the increase in flammable vegetation and the likely presence of positive feedback loops as suggested earlier (sub-section 9.3.2) (Jackson 1968, 1977; Ash 1988; Turton and Sexton 1996; Warman and Moles 2009). However, these increases in the flammable sclerophylls and fire may have been effective in reducing the extent and expansion of rainforest elements which were also benefitting from warmer and wetter conditions from ~20 ka. The increasing representation of these more abundant pollen producing taxa, sclerophylls including Poaceae, may have overwhelmed the primarily entomophily pollen signal from rainforest taxa (Kershaw and Strickland 1990, Kershaw and Bulman 1994; Bush 1995, Bush & Rivera 1998; Walker and Sun 2000). Although positive feedback loops may have been influential regarding the increase in sclerophylls, heightened seasonality at a time of insolation maximum may also have been important.

From 17 ka both *Eucalyptus* and Poaceae continue to have high values but fire is greatly reduced and this may have been influenced by decreasing insolation. This scenario is supported locally with the continuing high inorganic sediment content indicating the presence of more consistent ponding, a feature discussed in detail in sub-section 9.3.1, although the occurrence of the sclerophyll fern, *Pteridium* through this period (Figures 7.11 and 7.17) may suggest that fire was a continuing element within the environment. *Pteridium* is able to survive repeated fires and can accumulate large amounts of inflammable dead fronds and deep litter thereby providing an environment that is persistently fire-prone. In New Zealand Maori relied on the bracken rhizome starch as a food source and used fire to create open landscapes for access and ease of travel enabling bracken to proliferate (McGlone et al. 2005). In southern Australia bracken roots were processed by Indigenous people to obtain the sticky starch (Gott 2008). However, the presence of *Pteridium* itself may not be completely detrimental as it may provide facilitative effects for shade tolerant species (Tolhurst and Turvey 1992; Gallegos et al. 2015), although it has also been found that usually a lower diversity forest is present when *Pteridium* persists (Senyazobe et al. 2020). The archaeological record also indicates a period of increased usage at Fern Cave, Chillogee, ~17 ka (Morwood and Hobbs 1995) and may suggest that either there was a more concerted or more continuous use of landscape resources. Further north, Haeapugua core from the Tari Basin in Papua New Guinea also shows an increase in fire at ~21 ka although it is suggested this represents the initial human arrival in the area (Haberle 1998).

9.3.4. Fire in an ever increasing humid environment

Regional fire remains relatively moderate through to ~8.5 ka while local fire becomes prominent from ~12.5 ka. This increase in local fire is associated with macro'elongated' and macro'lattice' type charcoals and a greater abundance of *Typha*. There is a close resemblance to some of the macro'lattice' type charcoal to the epidermis of *Typha* (Figure 5.10 3b and Figure 7.21c) and, as suggested earlier, this association of fire and *Typha* may have been influenced by human activity. There is an increase in regional fire from ~8.5 ka (Figure 9.15) and this is within the period, 13–8 ka, Hopkins et al. (1990, 1993) found the more abundant charcoal fragments identified as *Eucalyptus* within now present-day rainforested areas, (see Chapter 3 sub-section 3.2.6 and Figure 3.8). However extremely high values for microcharcoal, the highest in the entire sequence up to 14,470,045 per cm³ (349,300 per cm⁻² yr⁻¹) continue after this period. This increase is not

found in the later more detailed Holocene record of Kershaw (1983a) where a higher sampling regime was undertaken, every 5cm as opposed to the ~10 cm sampling regime of the earlier record (Kershaw 1976; Kershaw 1983a). Although influx was not calculated for the later record, it may have had a slightly higher sedimentation rate than the present record, if core retrieval was similar to the earlier Kershaw (1976) record (see Figure 6.4, Chapter 6) and therefore it could be suggested that there is parity between the later Kershaw record and the present record through the Holocene period (Kershaw 1983a). This could suggest that this increase in charcoal in the present record which is also accompanied by equally significant shifts from rainforest to sclerophyll vegetation (see sub-section 9.1.4 sub-zone *LCI-3a*) is not real but an artefact of sediment redeposition, (see Chapter 6 sub-sections 6.2.1 and 6.3.1). Another complication is the presence of a tree stump on the crater surface belonging to the rainforest genus, *Flindersia* which was radiocarbon dated to 7270 ± 70 , suggesting that conditions may have been too wet to carry fire (Kershaw 1983a).

However, although the Holocene record of Kershaw (1983a) may have a higher resolution than the Holocene component of the longer Pleistocene record of Kershaw (1976), it is not contiguous and therefore these changes may not have been recorded as the shifts are abrupt (within ~200 years) and, although in both records reversals were present through the Holocene period (see Chapter 6, Table 6.2) these were minor. It could be that, though fire was restricted on the swamp surface due to humid conditions, this may not have applied to the wider region. Both of the major sclerophyll components, Casuarinaceae and *Eucalyptus* and especially the former, have higher values through these transitory shifts back to sclerophyll dominance. It was noted in Chapter 7 sub-section 7.2.5 that it was more common for Casuarinaceae pollen grains to be degraded but not significantly until 7.9 ka through to 6.6 ka, and it is also at this time that degraded *Eucalyptus* pollen grains became more frequent. This could suggest the occurrence of reworking though degradation to other dryland and aquatic pollen is minimal (Havinga 1984). Bunting and Tipping (2000) suggest that degradation values > 35% are considered to be evidence of post-depositional biasing which certainly would apply to Casuarinaceae and to a lesser degree *Eucalyptus*, but as pollen degradation is limited to these taxa it would suggest that local post-depositional reworking through sediment drying is not likely to be the cause of erosional episodes as inorganics are low at this time. However, re-deposition of earlier

sclerophyll phase material could be a possibility (Wilmschurst and McGlone 2005b; Tweddle and Edwards 2010).

Although these abrupt shifts were not present at Lake Barrine, Casuarinaceae continues to have a significant presence until 6.5 ka and *Eucalyptus* until 6.2 ka but, unlike Lynch's Crater, fire is not seen as an influence. However, Chen (1986) does suggest that fire intervals of 230 years were still likely to be operating. At Quincan Crater sclerophyll vegetation, especially *Casuarina*, is dominant until ~7 ka but continues to have a considerable representation for another 1000 years with the recent study on a longer core with a refined chronology showing similar abrupt shifts from rainforest to sclerophyll from ~7 ka through to 6.6 ka (Kershaw 1971; Rule *unpubl.*). This would suggest that these abrupt shifts from rainforest to sclerophyll are real but at Lynch's Crater influenced by re-deposition caused by increased regional fire activity. The presence of *M. affine* (both pollen and macrofossils), a secondary rainforest species advantaged by disturbance especially fire (Williams 2000), and the presence of charred woody fragments through this period (see Chapter 7 *sub-section* 7.2.3.1 and Figure 7.21) could also suggest a degree of variability. This period (7.5–6.6 ka) is prior to any evidence of abrupt climate events or ENSO, with most sources suggesting the initiation of present-day ENSO conditions dated from ~5 kyrs ago or slightly later (McGlone et al. 1992; Gagan et al. 2000, 2004; Liu et al. 2000; Donders et al. 2007; Lynch et al. 2007; Moros et al. 2009). However there is evidence that sea-level was fluctuating from ~7 ka along the north-eastern coastal margin suggesting that regional and more local influences unique (dominant) within this latitude are having a greater impact than insolation which is low at this time (Lewis et al. 2013). It is likely that fire was restricted to areas that had a ready source of flammable vegetation such as the sclerophylls. That positively identified *Eucalyptus* charcoal persisted until c. 6000 years BP in the Macalister Range (north-east of Lynch's Crater) and Mt Formartine and Mt Nomico (Bartle Frere region) (see Figure 3.7) although not a direct indication of fire activity, does suggest that rainforest had not yet expanded to its present extent (Hopkins et al. 1993).

The reduction of microcharcoal from 6.5 ka is followed by high macrocharcoal values and local fires became a central component of the swamp at this time. It is also the first time that 'blocky' type charcoal values achieve at least the same level as 'elongated' type charcoal suggesting a reduced local cyperaceous swamp and that woody taxa were now

an important fuel source on the swamp (Umbanhowar and McGrath 1998; Doubleday 1999, Doubleday and Smol 2005; Enache and Cumming 2006). Numerous charred woody fragments were found at this time although there is no suggestion from pollen data that there was any reduction in swamp forest taxa at least until ~4.5 ka when *Acmena*, *Glochidion* and *Rapanea* are greatly reduced. Macrocharcoal was not counted in the original Lynch's Crater records (Kershaw 1973, 1976, 1983a) so a comparison is not possible although the disappearance of the swamp forest is present in all three records. This could suggest that from 6.5 ka to 4.5 ka conditions were too humid for extensive fires as indicated by reduced regional fire (microcharcoal) but evidence of charred woody fragments does suggest fire of relatively high intensity. It could be that there was some form of resource management on the swamp as the relatively high productivity of a swamp environment would be more favourable for human usage in comparison to a closed canopy forested environment but humid conditions may have limited fire extent. However, from ~5 ka ENSO conditions are likely present (McGlone et al. 1992; Gagan et al. 2000, 2004; Liu et al. 2000; Donders et al. 2007; Lynch et al. 2007; Moros et al. 2009) with increased regional fire activity and by ~4.2 ka the swamp rainforest taxa are significantly reduced as is local fire. The reduction in the rainforest canopy taxa after 4 ka and rise in secondary taxa alongside sclerophyll taxa suggests a continuation of regional fire activity enhanced by heightened seasonality due to ENSO conditions.

Archaeological evidence is limited prior to the Holocene but that people are recorded in the greater area, from limited occupation at Ngarrabullgan Cave (40,540±650 yr cal BP) to occupation at Fern Cave (29,000 ¹⁴C yrs BP), and at times at increased levels as at Fern Cave at 17 ka, suggests that people were moving across the landscape and therefore likely to be actively engaged in food requisition with the help of fire. This idea of movement across the landscape was recorded during the early European contact period and was done to avoid adverse climatic conditions but more importantly to benefit from abundant food sources (Lumholtz 1889; Morwood and Hobb 1995; David et al. 1998). Although there is no archaeological evidence from Lynch's Crater during the early to middle Holocene, nearby Jiye Cave, (Figure 3.16 Chapter 3) ~20 km north-west, has initial human occupation dated at 5,000 years BP, a time of increased variability regionally. Cosgrove et al. (2007) suggest that within the rainforest and its western margin there are three phases of rainforest occupation, with the first two phases (8200 to 8000 cal. BP and 6000 to 5000 cal. BP) showing low discard rates suggesting low occupation but from 3300 and

2100 cal BP more intense settlement is shown with extremely high levels of activity after 2000 cal. BP indicating permanent occupation of the north-east Queensland rainforest.

Chapter 10

Conclusion

The aim of this thesis was to build on existing studies of the vegetation and environmental history of Lynch's Crater through the construction of a high-resolution multi-proxy record of environmental change in tropical northeast Queensland. Although the Lynch's Crater record spans some 230,000 years, this study focusses on the last ~ 50,000 years, a period for which there is the potential for tight chronological control through the application of radiocarbon dating, whilst also spanning the known presence of people on the continent. The availability of more exact dating allowed the calculation and comparison of pollen influx rates; the latter enabling the determination of absolute, in addition to conventional relative, changes in vegetation and individual taxa through time. Spectral analysis was employed to examine frequency variation within the record and it has identified millennial and especially semi-precessional cycles, the later providing an assessment of conditions possibly associated with Heinrich events (H-events). The nature and extent of fire, as determined from micro- and macrocharcoal analysis, allowed for identification to a certain degree of changes in fire type, local and regional, while macrocharcoal provided evidence of changing fuel type.

10.1. Vegetation and Environment Overview

The results of examination of vegetation and associated environments can be framed within a general classification used in previous studies that divided the record into an older and drier rainforest phase, sclerophyll phase and a younger, humid rainforest phase with transitions between them, and separate treatments of dryland and aquatic evidence. The older rainforest phase was co-dominated by rainforest pollen, the majority of which was derived from gymnosperms with the emergent *Araucaria* being the definitive taxon, and pollen of open sclerophyll vegetation of whose canopy would have been composed almost entirely of Casuarinaceae and *Eucalyptus*. The phase extends from the base of the sequence to about 41.5 ka, a date almost identical to that derived from the original Lynch's Crater study (Kershaw 1976) but younger than the subsequent study of Turney et al. (2004). The actual age may be resolved by further dating using a range of pretreatment methods, as well as utilising macrofossils (seeds) which were relatively abundant across the sequence, but could prove challenging due to the sensitivity of samples to contamination close to the limit of radiocarbon dating. Regardless, this period is one of relative stability with the drier rainforest taxa indicating a rainfall of about half

the 2500 mm MAR of today, an estimate consistent with the dominance of swamp vegetation on the site, and very low charcoal suggesting that fires, both local and regional, were occasional and of low intensity. Research undertaken in association with this thesis on the representation of dung fungi, especially *Sporormiella* within this record, demonstrates that large herbivores were likely an intricate component of the landscape.

10.2. Sclerophyll Phase

The transition to almost total sclerophyll vegetation, after a sharp initial decline in rainforest taxa, then took place relatively slowly over about 10,000 years, culminating about 32 ka. The vegetation transition was associated with an increase in burning, here marked by increases in both micro- and macrocharcoal, indicating rises in both local and regional fires, and long considered to be the result of burning by Aboriginal people. However, this high resolution record combined with the addition of dung fungi has resulted in a new and robust explanation (Rule et al. 2012). The order of change in proxies from the decline in *Sporormiella*, through the increase in sclerophyll vegetation to the increase in charcoal is interpreted to mean that people most likely hunted out the large animals in their colonisation of the continent as a contribution to the major phase of megafaunal extinction in Australia, resulting in a surplus of biomass that then became consumed by fire *in lieu* of the relative lack of herbivores. After this event, it appears as though burning locally, but not regionally, declined, while the rainforest gymnosperms virtually disappeared, except for *Podocarpus* that maintained notable values for several thousand more years. *Araucaria* and *Dacrydium* appear to have never recovered, with the former today only occurring in a few small, scattered populations in NE Queensland and the latter becoming extinct Australia-wide probably at latest in the early Holocene as indicated in this record.

Sclerophyll vegetation dominated the landscape from about 32 (or even 38 ka) to about 13 ka with this dominance alternating between Casuarinaceae and *Eucalyptus* type. It is likely that a number of different species and, in the case of *Eucalyptus* type, genera, were associated with this variability but, in the absence of taxonomic detail, it was not possible to refine community composition and environment conditions. Rainforest did not totally disappear and there are sufficient recordings, particularly of relatively high pollen-producing canopy and secondary taxa through the sclerophyll phase, to indicate the survival of drier rainforest patches, most likely within fire-protected rocky outcrops, in wet depressions and along streams. The degree of similarity of rainforest taxa between

this phase and the preceding dry rainforest phase suggest that climatic conditions may have changed little going into the height of the last glacial period. This relatively homogeneous dryland landscape is in contrast to that provided by the local aquatic diagram. Regardless of inter-sample taxon variability that is high because of the dominance of local pollen dispersal, selected features have been identified as responding to broad regional to global climatic variability (Turney et al. 2004).

10.3. Regional to Global Variability

The intensive spectral analysis of Lynch's Crater data undertaken here, that incorporated many dryland taxa as well as local basin attributes, demonstrated the situation to be more complicated than indicated by Turney et al. (2004) but certainly many taxa showed significant frequencies around the D-O and semi-precessional frequencies, specifically c. 1.5 kyr and c.11.5 kyr length cycles respectively. Perhaps surprisingly, though only two proxies displaying almost the exact millennial frequency detected by Turney et al. (2004) were rainforest taxa, the canopy *Elaeocarpus* and the secondary genus *Celtis*. However, these taxa do provide important information of forest type and consequently precipitation levels suggesting that the ENSO signal does extend to most likely pollen production at least in dryland vegetation.

With respect to the inferred Heinrich events of Muller et al. (2008a), these could be interpreted as related to, rather than be indicative of semi-precessional length variation. In the current record, there are two extended inorganic phases, from c. 39 to 31 ka BP almost spanning the ages between H4 and H3, and the youngest, c. 19 to 12 ka BP, almost spanning the ages between H1 and H0 (YD). These two phases are supported by distinctively high values for Poaceae and also in the youngest phase (c. 19 to 12 ka BP) the only notable values for Asteraceae generally indicative of drier conditions, but there is also high representation of floating leaved aquatics, considered to indicate wet conditions, within the two end members. One explanation for this apparent contradiction could be that drier conditions facilitated dryland herb invasion of a relatively dry and a little vegetated swamp surface that also facilitated inwash of inorganic sediment onto the swamp and water ponding rather than swamp incorporation during infrequent high rainfall events. This explanation is certainly plausible for the younger phase, c. 19 to 12 ka BP where both Asteraceae sub-families (tubuliflorae and liguliflorae), are likely on the swamp and the highly variable sedimentation rate certainly suggests the high inorganics are most likely indicative of infrequent high rainfall events. The scenario is different for

the older phase, c. 39 to 31 ka BP, where the uniform high sedimentation rate suggests overall a relatively well vegetated swamp surrounding the ponded areas. Either explanation is limited by the resolution of the sampling in this study, 120 years per sample, and although speculative it could be that heightened Indigenous activity within the region may have also played a role.

Overall, the difference between the middle and end members of the sclerophyll period could simply be that the end members experienced more extreme or at least different ENSO climatic conditions. This is likely the case at ~20 ka where dryland taxa suggest warm and wet conditions and a muted ENSO signal. It does not appear that fire was a major influence on the pattern of variation with microcharcoal values being relatively consistent and moderate through the sclerophyll period and macrocharcoal showing a phase of high peaks that span the lower and middle periods likely influenced by human activity. It is likely though that, with the dominance of the sclerophyll landscape, fire was being maintained by positive feedback loops allowing the system to maintain a degree of stability.

10.4. Transitioning into Tropical Rainforest

The period between 13 ka and about 7.8 ka represents the transition from sclerophyll vegetation to humid mesophyll vine forest or tropical rainforest with a gradual increase in representation of generalist, largely secondary, taxa to about 9 ka. Here there is also an almost total loss of *Olea*, the major taxon faithful to dry rainforest, but a major increase in the generalist *Syzygium* complex, while there is a sharp decline in dominant macrocharcoal, a position it had held since the beginning of the transition. Major humid rainforest forest taxa, including forest epiphytes as well as aquatic ferns, become increasingly important and sclerophyll dominants sharply decline towards 8 ka. This transition is similar to that in other Tableland records although the timing varies, suggested to depend on a number of factors, rainfall thresholds, the availability of or distance from a rainforest source, the underlying substrate, topography and fire activity, although the flooding of the Torres Strait Sill at 8ka, opening up the Arafura Sea at 8ka, could have triggered the major rainforest expansion.

The record from around 8 ka to about 3 ka, the top of the sequence, is complicated and uncertain, deviating from previous Lynch's reconstructions in displaying different times of major change and, unique to the Tableland records, additional shifts from sclerophyll and back to rainforest about 1000 years after a sharp reversal. These repeated events could

be real in that the initial rainforest phase lasted only a few hundred years, or a 2-3 contiguous samples, so could have been missed in previous coarser sampling. However, determining a cause is difficult and most likely results from unreliable dating of sediment mixed by falling trees from within what was an on-site swamp forest. Sequences come back into phase about 6 ka with continued dominance of swamp forest taxa, especially *Rapania*. About 4.5 ka, dryland forest pollen dominated by Cunoniaceae largely replaced swamp forest pollen and the swamp forest assemblage itself was replaced largely by ferns spores, notably *Gleichenia* and *Lygodium*. The destruction of swamp forest was no doubt caused by fire, indicated by high microcharcoal values in the record of Kershaw (1983) and confirmed as locally derived by high macrocharcoal values in this record. The most likely explanation for the destruction is that it was the result of burning by Indigenous people, for some as yet undetermined reason but possibly for horticultural purposes, at a time when they are known to have inhabited the rainforest of the region, and when impact could have been facilitated by the onset of the latest period of enhanced ENSO activity.

10.5. General overview, contributions and limitations

The execution of this high-resolution record where all proxies were sampled at the same resolution was highly informative but complex. In some cases (especially with the rainforest canopy) it allowed for turnover rates to be visible in the record and therefore confirming their persistence in the environment. The combining of all proxies into a coherent record is complex as the different proxies are not likely to response uniformly to the same environmental changes especially when viewed across multiple scales (local-regional-global). However, this should not deter further high-resolution multi-proxy studies as the benefits and insights far outweigh any additional resources or time needed to achieve these outcomes.

The benefits of a multi-proxy study are particular evident with the addition of macrofossils. This is one of the first substantial systematic studies of macrofossils undertaken in association with pollen in the late Quaternary of Australia and it is suggested that, where possible but especially for swamp environments, it should be included as a routine component of palaeoecological studies. The benefits of being able to identify plants to species level and confirm the presence of taxa not recorded in the pollen record allows a better understanding of the real dynamics that are present in these swamp communities. The same claim can be made for the identification and routine counting of fungal spores from species of dung fungi, especially *Sporormiella*. Although

not originally or formerly a component of this thesis project, it has proved important in adding information on megafauna, especially in relation to the late Pleistocene landscape transformation evident from the site.

A significant contribution to this thesis is from the study of charcoal preserved within the sediments as a measure of past fire. The separation of size categories in the microcharcoal analysis provided a clearer idea of changes in likely fire intensity while the macrocharcoal analyses have taken macrocharcoal studies to a new level for Australia with both routine counting and separation of morphological types representative of broad structural or taxonomic units. The separation of morphological types is most probably most beneficial when there is likely to be a close association with nearby boundary conditions, such as tree lines and swamp-dryland margins. Many of the macrocharcoal remains are also classified as macrofossils through the survival and recognition of intricate structural features. The deciphering of the relative influence of climate and people on fire is difficult to resolve and ideally signs of human activity should be corroborated with archaeological evidence of occupation and resource exploitation but this is not always possible. The combination of both macrocharcoal and macrofossils alongside the more common proxies used in palaeoecological studies were used in this thesis as an independent tool with the results indicating the potential for the separation of natural and human fire activity on local and regional scales.

In relation to variations through time, spectral analysis was employed on selected sequences primarily to detect or test for known frequencies of climate-forcing significance and provide insight into the likely activity of ENSO-like conditions within the region, but also help explain the high degree of variability which presented itself with modulated harmonic frequencies related to changing fire conditions with the presence of the flammable sclerophylls and human activity. Another influence on the results generated from spectral analyses is that the influx data outcome did vary from the percentage data outcome and this is likely due to the greater influence of the sedimentation rate and local catchment changes on the influx data. Overall, the results of this work are extremely encouraging for the widespread development of high-resolution, multi-proxy records to generate a detailed understanding of environmental-human interactions across tropical northeast Queensland and Australia more generally.

REFERENCES

- Abram, NJ, Gagan MK, Liu Z, Hantoro, WS, McCulloch, MT & Suwargadi, B (2007). Seasonal characteristics of the Indian Ocean Dipole during the Holocene epoch. *Nature*, vol. 445, pp.299-302.
- Abram, NJ, McGregor, HV, Gagan, MK, Hantoro, WS & Suwargadi, BW (2009). Oscillations in the southern extent of the Indo-Pacific Warm Pool during the mid-Holocene. *Quaternary Science Reviews*, vol. 28, pp.2794-2803.
- Alexander, J, Fielding, CR & Jenkins, G (1999). Plant-material deposition in the tropical Burdekin River, Australia: implications for ancient fluvial sediments. *Palaeogeography, Palaeoclimatology, Palaeoecology*, vol. 153, pp. 105-125.
- Allan, RJ & D'Árrigo, RD (1999). Persistent ENSO sequences: how unusual was the 1990-1995 El Niño? *The Holocene*, vol. 9, pp. 101-118.
- Alley, RB & Clark, PU (1999). The deglaciation of the northern hemisphere: a global perspective. *Annual Reviews of Earth and Planetary Sciences*, vol. 27, pp. 149-182.
- Allison, J (1990). A pollen and sedimentological study of two cores from Lake Barrine, northeast Queensland, BS (thesis), Monash University, Clayton, Australia.
- Andreae, MO (1991). Biomass burning: Its History, Use and Distribution and Its Impact on Environmental Quality and Global Climate. in JS, Levine (ed.). *Global biomass burning: atmospheric, climatic and biospheric implications*, Massachusetts Institute of Technology Press, Massachusetts USA, pp. 3-21.
- Andrews, JT & Voelker, AHL (2018). "Heinrich events" (& sediments): A history of terminology and recommendations for future usage. *Quaternary Science Reviews*, vol. 187, pp. 31-40.
- Ash, J (1988). The location and stability of rainforest boundaries in North-Eastern Queensland, Australia. *Journal of Biogeography*, vol. 15, pp. 619-630.
- Ashok, K, Guan, Z, Saji, NH & Yamagata, T (2004). Individual and combined influences of ENSO and the Indian Ocean Dipole on the Indian summer monsoon. *Journal of Climate*, vol. 17, pp. 3141-3155.
- Aston, HI (1973). *Aquatic plants of Australia*. Melbourne University Press, Melbourne, pp. 368.
- Auer, G, De Vleeschouwer, D, Smith, RA, Bogus, K, Groeneveld, J, Grunnert, P, Castañeda, IS, Petrick, B, Christensen, B, Fulthorpe, C, Gallagher, SJ & Henderiks, J (2019). Timing and pacing of Indonesian Throughflow restriction and its connection to Late Pliocene climate shifts. *Paleoceanography and Paleoclimatology*, vol. 34, pp. 635-657.
- Australian Bureau of Meteorology & CSIRO (2011). Climate Change in the Pacific: Scientific assessment and new research. 2 vols. Available online at <http://www.pacificclimatechangescience.org/publications/reports/report-climate-change-in-the-pacific-scientific-assessment-and-new-research/>.
- Australia's Virtual Herbarium (2015). Map output for *Liparophyllum exaltatum* and *Nymphoides indica*. Council of Heads of Australasian Herbaria, <http://avh.ala.org.au/> viewed 3rd February 2015.
- Bääh, E & Arnebrant, K (1994). Growth rate and response of bacterial communities to pH in limed and ash treated forest soils. *Soil Biology and Biochemistry*, vol. 26, pp. 995-1001.

- Baker, PA, Fritz, SC, Garland, J & Ekdahl, E (2005). Holocene hydrologic variation at Lake Titicaca, Bolivia/Peru and its relationship to North Atlantic climate variation. *Journal of Quaternary Science*, vol. 20, pp. 655-662.
- Baker, AG, Cornelissen, P, Bhagwat, SA, Vera, FWM & Willis, KJ (2016). Quantification of population sizes of large herbivores and their long-term functional role in ecosystems using dung fungal spores. *Methods in Ecology and Evolution*, vol. 7, pp. 1273-1281.
- Balco, G (2011). Contributions and unrealized potential contributions of cosmogenic-nuclide exposure dating to glacier chronology, 1990-2010. *Quaternary Science Reviews*, vol. 30, pp. 3-27.
- Balston, J & Turton, SM (2005). *A study of the climate of the FNQ water strategy area and consideration of the impacts of climate change*, Technical Document 2, Queensland Government, pp. 35.
- Bard, E, Hamelin, B, Arnold, M, Montaggioni, L, Cabiocch, G, Faure, G & Rougerie, F (1996). Deglacial sea-level record from Tahiti corals and the timing of global meltwater discharge. *Nature*, vol. 382, pp. 241-244.
- Barbetti, M & Allen, H (1972). Prehistoric man at Lake Mungo, Australia, by 32,000 years BP. *Nature*, vol. 240, pp.46-48.
- Barr, C, Tibby, J, Moss, PT, Halverson, GP, Marshall, JC, McGregor, GB & Stirling, E (2017). A 25,000-year record of environmental change from Welsby Lagoon, North Stradbroke Island, in the Australian subtropics. *Quaternary International*, vol. 449, pp.106-118.
- Barr, C, Tibby, J, Leng, MJ, Tyler, JJ, Henderson, ACG, Overpeck, JT, Simpson, GL, Cole, JE, Phipps, SJ, Marshall, JC, McGregor, GBM, Hua, Q & McRobie, FH (2019). Holocene El Niño-Southern Oscillation variability reflected in subtropical Australian precipitation. *Scientific Reports*, vol. 9, 1627, <https://doi-org.virtual.anu.edu.au/10.1038/s41598-019-38626-3>.
- Barrows, TT, Stone, JO, Fifield, LK & Cresswell, RG (2002). The timing of the Last Glacial Maximum in Australia. *Quaternary Science Reviews*, vol. 21, pp. 159-173.
- Barrows, TT & Juggins, S (2005). Sea-surface temperatures around the Australian margin and Indian Ocean during the Last Glacial maximum. *Quaternary Science Reviews*, vol. 24, pp. 1017-1047.
- Barrows, TT, Hope, GS, Prentice, ML, Fifield, L & Tims, SG (2011). Late Pleistocene glaciation of the Mt Giluwe volcano, Papua New Guinea. *Quaternary Science Reviews*, vol. 30, pp. 2676-2689.
- Beaman, R, Larcombe, P & Carter, RM (1994). New evidence for the Holocene sea-level high from inner shelf central Great Barrier Reef, Australia. *Journal of Sedimentary Research*, A64, pp. 881-885.
- Beaudoin, AB (2007). On the laboratory procedure for processing unconsolidated sediment samples to concentrate subfossil seed and other plant macroremains. *Journal of Paleolimnology*, vol. 37, pp. 301-308.
- Beaufort, L, de Garidel-Thoron, T, Mix, AC & Pisias, NG (2001). ENSO-like Forcing on Oceanic Primary Production during the Late Pleistocene. *Science*, vol. 293, pp. 2440-2444.
- Beaufort, L, Garidel-Thoron, T, Linsley, B, Oppo, D & Buchet, N (2003). Biomass burning and oceanic primary production estimates In the Sulu Sea area over the last 380 kyr and the East Asian monsoon dynamics. *Marine Geology* vol. 201, pp. 53-65.

- Beck, KK, Fletcher, M-S, Gadd, PS & Heijnis, H (2017). An early onset of ENSO influence in the extra-tropics of the southwest Pacific inferred from a 14,600 year high resolution multi-proxy record from Paddy's Lake, northwest Tasmania. *Quaternary Science Reviews*, vol. 157, pp. 164-175.
- Belcher, CM (ed) (2013). *Fire Phenomena and the Earth System: An Interdisciplinary Guide to Fire Science*, Wiley-Blackwell, pp. 350.
- Bennett, KD (1994). Confidence intervals for age estimates and deposition times in late-Quaternary sediment sequences. *The Holocene*, vol. 4, pp. 337-348.
- Bennett, KD (2007). *Documentation for Psimpoll 4.25 and Pscomb 1.0.3.C Programs for plotting diagrams and analysing pollen data, software manual*, <http://www.kv.geo.uu.se>, accessed July 15th 2016.
- Bennett, KD & Hicks, S (2005). Numerical analysis of surface and fossil pollen spectra from northern Fennoscandia. *Journal of Biogeography*, vol. 32, pp. 407-423.
- Bennion, H, Sayer, CD, Clarke, SJ, Davidson, TA, Rose, NL, Goldsmith, B, Rawcliffe, R, Burgess, A, Clarke, g, Turner, S & Wiik, E (2018). *Journal of Paleolimnology*, vol. 60, pp. 329-348.
- Berger, A (1978). Long-term variations of daily insolation and Quaternary climatic changes. *Journal of Atmospheric Sciences*, vol. 35, pp. 2362-2367.
- Berger, A (1989). Pleistocene climatic variability at astronomical frequencies. *Quaternary International*, vol. 2, pp. 1-14.
- Berger, A, Melice, JL & Hinnov, L (1991). A strategy for frequency spectra of Quaternary climate records. *Climate Dynamics*, vol. 5, pp. 227-240.
- Berry, GJ & Reeder, MJ (2016). The Dynamics of Australian Monsoon bursts. *Journal of Atmospheric Science*, vol. 73(1), pp. 55-69.
- Best, JG (1960/78). Some Cainozoic Basaltic Volcanoes in North Queensland. *Bureau of Mineral Resources*, Australia Records, vol. 1-18 (unpublished).
- Best, JG, Stevens, NC & Tweedale, GW (1960). Igneous Rocks, in D, Hill and AK, Denmead, Geology of Queensland, *Journal of the Geological Society of Australia*, vol. 7, pp. 419-423.
- Bickford, S & Gell, P (2005). Holocene vegetation change, Aboriginal wetland use and the impact of European settlement on the Fleurieu Peninsula, South Australia. *The Holocene*, vol. 15, pp. 200-215.
- Bintanja, R, Van de Wal, RSW & Oerlemans, J (2005). Modelled atmospheric temperatures and global sea levels over the past million years. *Nature*, vol. 437, pp. 125-128.
- Bintanja, R & van de Wal, RSW (2008). North American ice-sheet dynamics and the onset of 100,000-year glacial cycles. *Nature*, vol. 454, pp. 869-872.
- Bird, MI, Ayliffe, LK, Fifield, LK, Turney, CSM, Cresswell, RG, Barrows, TT & David, B (1999). Radiocarbon dating of "old" charcoal using a wet oxidation, stepped-combustion procedure. *Radiocarbon*, vol. 41, pp. 127-140.

- Bird, MI, Brand, M, Diefendorf, AF, Haig, JL, Hutley, LB, Levchenko, V, Ridd, PV, Rowe, C, Whinney, J, Wurster, CM & Zwart, C (2019). Identifying the 'savanna' signature in lacustrine sediments in northern Australia. *Quaternary Science Reviews*, vol. 203, pp. 233-247.
- Birks, HH (1973). Modern macrofossil assemblages in lake sediments in Minnesota, in HJB, Birks & RG, West (eds.). *Quaternary Plant Ecology* Blackwell Scientific Publications, Oxford, pp 326.
- Birks, HH (2003). The importance of plant macrofossils in the reconstruction of Lateglacial vegetation and climate: examples from Scotland, western Norway, and Minnesota USA. *Quaternary Science Review*, vol. 22, pp. 453-473.
- Birks, HH (2007). Plant Macrofossil Introduction, in E, Scott (editor-in-chief) *Encyclopedia of Quaternary Science Vol 3* Elsevier, Amsterdam, pp. 2266-2288.
- Birks, HH (2017). Plant Macrofossil Introduction. *Reference Module in Earth Systems and Environmental Sciences*, Elsevier, doi: 10.1016/B978-0-12-409548-9.10499-3.
- Birks, HH & Birks, HJB (2000). Future uses of pollen analysis must include plant macrofossils. *Journal of Biogeography*, vol. 27, pp. 31-35.
- Birks, HH & Birks, HJB (2006). Multi-proxy studies in palaeolimnology. *Vegetation history and Archaeobotany*, vol. 15, pp. 235-251.
- Birks, HJB (1985). Recent and possible future mathematical developments in qualitative palaeoecology. *Palaeogeography, Palaeoclimatology, Palaeoecology*, vol. 50, pp. 107-147.
- Birtles, TG (1982). Trees to burn: settlement in the Atherton-Evelyn rainforest, 1880-1900. *North Australia Research Bulletin*, vol. 8, pp. 31-36.
- Birtles, TG (1997). First contact: colonial European preconceptions of tropical Queensland rainforest and its people. *Journal of Historical Geography*, vol. 23, pp. 393-417.
- Blaauw, M & Christen, A (2005). Radiocarbon peat chronologies and environmental change. *Journal of the Royal Statistical Society Series C Applied Statistics*, vol. 54, pp. 805-816.
- Blaauw, M, Heuvelink, GBM, Mauquoy, D, van der Plicht, J & van Geel, B (2003). A numerical approach to ¹⁴C wiggle-match dating of organic deposits: best fits and confidence intervals. *Quaternary Science Reviews* vol. 22, pp. 1485-1500.
- Black, MP, Mooney, SD & Martin, HA (2006). A >43,000-year vegetation and fire history from Lake Baraba, New South Wales, Australia. *Quaternary Science Reviews*, vol. 25, pp. 3003-3016.
- Black, MP, Mooney, SD & Haberle, SG (2007). The fire, human and climate nexus in the Sydney Basin, eastern Australia. *The Holocene*, vol. 17, pp. 469-480.
- Blackford, JJ (2000). Charcoal fragments in surface samples following a fire and the implications for interpretation of subfossil charcoal data. *Palaeogeography Palaeoclimatology Palaeoecology*, vol. 164, pp. 33-42.
- Blong, RJ (1982). *The time of darkness: local legends and volcanic reality in Papua New Guinea*, University of Washington Press, Seattle, pp. 257.
- Blunier, T & Brook, EJ (2001). Timing of millennial-scale climate change in Antarctica and Greenland during the last glacial period. *Science*, vol. 291, pp. 109-112.

- Bohte, A (1994). Local vegetation and environments of the last glacial cycle at Lynch's Crater, northeast Queensland, BSc (Hons) Thesis, Monash University, Melbourne, pp. 92.
- Bohte, A & Kershaw, AP (1999). Taphonomic influences on the interpretation of the palaeoecological record from Lynch's Crater, northeastern Australia. *Quaternary International* vol. 57/58, pp. 49-59.
- Bond, G, Broecker, W, Johnsen, S, McManus, J, Labeyrie, L, Jouzel, J & Bonani, G (1993). Correlations between climate records from North Atlantic sediments and Greenland ice. *Nature*, vol. 365, pp. 143-147.
- Bond, G, Showers, W, Cheseby, M, Lotti, R, Almasi, P, deMenocal, P, Priore, P, Cullen H, Hajdas, I & Bonani, G (1997). A pervasive millennial-scale cycle in North Atlantic Holocene and Glacial climates. *Science*, vol. 278, pp. 1257-1266.
- Bond, G, Showers, W, Elliot, M, Evans, M, Lotti, R, Hajdas, I, Bonani, G & Johnson, S (1999). The North Atlantic's 1-2 ka climate rhythm: relation to Heinrich events, Dansgaard/Oeschger cycles and the Little Ice Age, in PU, Clark, RS, Webb. and LD, Keigwin, (eds.). *Mechanism of Global Change at millennial time scales*, AGU, Washington, DC, pp. 35-58.
- Bond, G, Kromer, B, Beer, J, Muscheler, R, Evans, MN, Showers, W, Hoffmann, S, Lotti-Bond, R, Hajdas, I & Bonani, G (2001). Persistent solar influence on North Atlantic climate during the Holocene. *Science*, vol. 294, pp. 2130-2136.
- Bonell, M (1991). Progress and future research needs in water catchment conservation within the wet tropical coast of NE Queensland. in N, Goudberg, M, Bonell & D, Benzken (eds.). *Tropical Rainforest Research in Australia: Present Status and Future Directions for the Institute of Tropical Rainforest Studies*, Proceedings of a workshop held in Townsville, Australia, 4-6 May, 1990, Institute of Tropical Rainforest Studies, Townsville, pp. 59-86.
- Bonell, M & Gilmour, DA (1980). Variations in short-term rainfall intensity in relation to synoptic climatological aspects of the humid tropical north Queensland coast. *Singapore Journal of Tropical Geography*, vol. 1, pp. 16-30.
- Bostock, HC, Barrows, TT, Carter, L, Chase, Z, Cortese, G, Dunbar, GB, Ellwood, M, Hayward, B, Howard, W, Neil, HL, Noble, TL, Mackintosh, A, Moss, PT, Moy, AD, White, D, Williams, MJM & Armand, LK (2013). A review of the Australian-New Zealand sector of the Southern Ocean over the last 30 ka (Aus-INTIMATE project). *Quaternary Science Reviews*, vol. 74, pp. 35-57.
- Boulter, SL, Kitching, RL, Howlett, BG & Goodall, K (2005). Any which way will do – the pollination biology of a northern Australian rainforest canopy tree (*Syzygium sayeri*, Myrtaceae). *Botanical Journal of the Linnean Society*, vol. 149, pp. 69-84.
- Boulter, SL, Kitching, RL, Gross, CL, Goodall, KI & Howlett, BG (2008). Floral morphology, phenology and pollination in the wet tropics, in N, Stork & SM, Turton (eds.). *Living in a Dynamic Tropical Forest Landscape*, Blackwell Publishing Australia, pp. 224-239.
- Bowman, DMJS (1998). The impact of Aboriginal landscape burning on the Australian biota. Tansley review No.101. *New Phytologist*, vol. 140, pp. 385-410.
- Bowman, DMJS, Wilson, BA & Hooper, RJ (1988). Response of *Eucalyptus* forest and woodland to four fire regimes at Munmarlany, Northern Territory, Australia. *Journal of Ecology*, vol. 76, pp. 215-232.
- Bowman, S (1990). *Radiocarbon Dating*, University of California Press, pp. 64.

- Boyd, WE (1992). *A pollen flora of the native plants of South Australia and southern Northern Territory, Australia*, Royal Geographical Society of Australasia, South Australia Branch, pp. 212.
- Bradbury, JP (1996). Charcoal deposition and redeposition in Elk Lake, Minnesota, USA. *The Holocene*, vol. 6, pp. 339-344.
- Bradley, RS (1999). *Paleoclimatology: Reconstructing Climates of the Quaternary* (2nd ed), Academic Press Limited, London, pp. 613.
- Bradley, RS (2000). Past global changes and their significance for the future. *Quaternary Science Reviews*, vol. 19, pp. 391-402.
- Bradstock, RA, Gill, MA & Williams, RJ (2012). *Flammable Australia*, CSIRO Publishing.
- Bretherton, SC (2006). The completion and time-series analysis of the Lynch's Crater palaeoenvironmental record, northeastern Queensland, BSc (Hons) Thesis, Monash University, Melbourne, pp. 97 and appendices.
- Briles, CE, Whitlock, C, Bartlein, PJ & Higuera, P (2008). Regional and local controls on postglacial vegetation and fire in the Siskiyou Mountains, northern California, USA. *Palaeogeography, Palaeoclimatology, Palaeoecology*, vol. 265, pp. 159-169.
- Brock, MA & Casanova, MT. (1997). Plant life at the edges of wetlands; ecological responses to wetting and drying patterns. in N, Klomp and I, Lunt I (eds.). *Frontiers in ecology; Building the links*, Elsevier Science, Oxford, pp.181-192.
- Broecker, WS (1998). Paleoocean circulation during the last deglaciation: a bipolar seesaw?. *Paleoceanography*, vol. 13, pp. 119-121.
- Broecker, WS (2003). Does the trigger for abrupt climate change reside in the ocean or in the atmosphere?. *Science*, vol. 300, pp. 1519-1522.
- Bronk Ramsey, C (2003). Deposition models for chronological records. *Quaternary Science Reviews*, vol. 27, pp. 42-62.
- Bronk Ramsey, C (2008). Radiocarbon dating: revolutions in understanding. *Archaeometry*, vol. 50, pp. 249-275.
- Bronk Ramsey, C (2009). Bayesian analysis of radiocarbon dates. *Radiocarbon*, vol. 51, pp. 337-360.
- Bronk Ramsey, C & Lee, S (2013). Recent and planned developments of the program oxcal. *Radiocarbon*, vol. 55(2.3), pp. 720-730.
- Bronk Ramsey, C, Staff, RA, Bryant, CL, Brock, F, Hiroyuki, K, van der Plicht, J, Schlolaut, G, Marshall, MH, Brauer, A, Lamb, HF, Payne, RL, Tarasov, PE, Haraguchi, T, Gotanda, K, Yonenobu, H, Yokoyama, Y, Tada, R & Nakagawa, T (2012). A complete terrestrial radiocarbon record for 11.2 to 52.8 kyr B.P. *Science*, vol. 338, pp. 370-374.
- Brown, JR, Lengaigne, M, Lintner, BR, Widlansky, MJ, van der Wiel, K, Dutheil, C, Linsley, BK, Matthews, AJ & Renwick, J (2020). South Pacific Convergence Zone dynamics, variability and impacts in a changing climate. *Nature Reviews Earth and Environment*, vol.1, pp. 530-543.
- Brown, M, Korte, M, Holme, R, Wardinski, I & Gunnarson (2018). Earth's magnetic field is probably not reversing. *Proceedings of the National Academy of Science*, vol. 115 (20), pp. 5111-5116.

- Brunelle, A & Anderson, RS (2003). Sedimentary charcoal as an indicator of late-Holocene drought in the Sierra Nevada, California, and its relevance to the future. *The Holocene*, vol. 13, pp. 21-28.
- Bruun, S, Jensen, ES & Jensen, LS (2008). Microbial mineralisation assimilation of black carbon: dependency on degree of thermal alteration. *Organic Geochemistry*, vol. 39, pp. 839-845.
- Bryden, KM & Hagge, MJ (2003). Modeling the combined impact of moisture and char shrinkage on the pyrolysis of a biomass particle. *Fuel*, vol. 82, pp. 1633-1644.
- Bultitude, RJ, Garrad, PD, Donchak, PJT, Domagala, J, Champion, DC, Rees, ID, Mackenzie, DE, Wellman, P, Knutson, J, Fanning, CM, Fordham, BG, Grimes, KG, Oversby, BS, Rienks, IP, Stephenson, PJ, Chappell, BW, Pain, CF, Wilford Rigby, JF & Woodbury, MJ. (1997). Cairns Region (Chapter 7). in JHC, Bain & JJ, Draper (eds.). *North Queensland Geology*, Australian Geological Survey Organisation Bulletin, vol. 240, pp. 600.
- Bunting, MJ & Tipping, R (2000) Sorting the dross from data: possible indicators of post depositional assemblage biasing in archaeological palynology. in G, Bailey, N, Winder. and R, Charles R, (eds.). *Human Ecodynamics*, Oxbow Books, Oxford, UK, pp. 63-69.
- Bureau of Meteorology (2019). The three phases of the El Niño-Southern Oscillation (ENSO). <http://www.bom.gov.au/climate/enso/history/ln-2010-12/three-phases-of-ENSO.shtml> viewed 27th July 2020.
- Burney, DA, Robinson, GS & Burney, LP (2003). *Sporormiella* and the late Holocene extinctions in Madagascar. *PNAS*, vol. 100, pp. 10800-10805.
- Burrows, MA, Fenner, J & Haberle, SG (2014a). Testing peat humification analysis in an Australian context: identifying wet shifts in regional climate over the past 4000 years. *Mires and Peats*, vol. 14, pp. 1-19.
- Burrows, MA, Fenner, J & Haberle, SG (2014b). Humification in northeast Australia: Dating millennial and centennial scale climate variability in the late Holocene. *The Holocene*, vol. 24, pp. 1707-1718.
- Burrows, MA, Heijnis, H, Gadd, P & Haberle, SG (2016). A new late Quaternary palaeohydrological record from the humid tropics of northeastern Australia. *Palaeogeography, Palaeoclimatology, Palaeoecology*, vol. 451, pp. 164-182.
- Busby, JR (1991). BIOCLIM – A bioclimatic analysis and predictive system. in CR, Margules. and MP, Austin. (eds.). *Nature Conservation: Cost effective biological surveys and data analysis*, CSIRO, Canberra, pp. 64-68.
- Bush, MB (1995). Neotropical plant reproductive strategies and fossil pollen representation. *The American Naturalist*, vol. 145, pp. 594-609.
- Bush, MB (2002). On the interpretation of fossil Poaceae pollen in the lowland humid neotropics. *Palaeogeography, Palaeoclimatology, Palaeoecology*, vol. 177, pp. 5-17.
- Bush, MB & Rivera, R (1998). Pollen dispersal and representation in a neotropical rainforest. *Global Ecology and Biogeography Letters*, vol. 7, pp. 379-392.
- Byrne, R, Michaelsen, J & Soutar, A (1977). Fossil charcoals as a measure of wildfire frequency in southern California: A preliminary analysis. in HA, Mooney and CE, Conrad (eds.). *Proceedings of the symposium on the environment consequences of fire and fuel management in Mediterranean ecosystems*, USADA. Forest Service, General Technical report WO-3, Washington, DC, pp. 361-367.

- Cadd, H, Tibby, J, Barr, C, Tyler, J, Unger, L, Leng, MJ, Marshall, JC, McGregor, GB, Lewis, R, Arnold, LJ, Lewis, T & Baldock, J (2018). Development of a southern hemisphere subtropical wetland (Welsby Lagoon, south-east Queensland, Australia) through the last glacial cycle. *Quaternary Science Reviews*, vol. 202, pp. 53-65.
- Calvo, E, Pelejero C, De Deckker P & Logan, G (2007). Antarctic deglacial patterns in a 30 kyr record of sea surface temperature offshore South Australia. *Geophysical Research Letters*, vol. 34, L130707.
- Caron, PO (2016). A Monte Carlo examination of the broken-stick distribution to identify components to retain in principal component analysis. *Journal of Statistical Computation and Simulation*, vol. 86 (12), pp. 2405-2410.
- Campbell, ID & Campbell C (1994). Pollen preservation: experimental wet-dry cycles in saline and desalinated sediments. *Palynology*, vol. 18, pp. 5-10.
- Cappers, RTJ (1993). Seed dispersal by water; a contribution to the interpretation of seed assemblages. *Vegetation history and Archaeobotany*, vol. 2, pp. 173-186.
- Carcaillet, C, Bouvier, M, Fréchette, B, Larouche, AC & Richard, PJH (2001). Comparison of pollen-slide and sieving methods in lacustrine charcoal analyses for local and regional fire history. *The Holocene*, vol. 11, pp. 467-476.
- Cattell, RB (1966). The scree test for the number of factors. *Journal of Multivariate Behavioral Research*, vol. 1, pp. 245-276.
- Certini, G (2005). Effects of fire on properties of forest soils: a review. *Oecologia*, vol. 143, pp. 1-10.
- Chambers, DP & Attiwill, PM (1994). The ash-bed effect in *Eucalyptus regnans* forest: chemical, physical and microbiological changes in soil after heating or partial sterilisation. *Australian Journal of Botany*, vol. 42, pp. 739-749.
- Chambers, FM, Ogle, MI & Blackford, JJ (1999). Palaeoenvironmental evidence for solar forcing of Holocene climate: linkages to solar science. *Progress in Physical Geography*, vol. 23, pp. 181-204.
- Chandler, C, Cheney, P, Thomas, P, Trabaud, L & Williams, D (1983). *Forest Fire Behavior and Effects (Fire in Forestry Vol 1)* John Wiley & Sons Ltd, New York, pp. 1-450.
- Chappell, J, Chivas, A, Wallensky, E, Polach, HA & Aharon, P (1983). Holocene palaeoenvironmental changes, central to north Barrier Reef inner zone. *BMR Journal of Australian Geology and Geophysics*, vol. 8, pp. 223-235.
- Chappell, J, Ota, Y & Berryman, K (1996). Late Quaternary coseismic uplift history of Huon Peninsula, Papua New Guinea. *Quaternary Science Reviews*, vol. 15, pp. 7-22.
- Chatfield, C (1989). *The analysis of time series: an introduction*. Chapman and Hall, London.
- Chen, G, Han, W, Li, Y & Wang, D (2016). Interannual variability of equatorial eastern Indian Ocean upwelling: Local versus remote forcing. *Journal of Physical Oceanography*, vol. 46 (3), pp. 789-807.
- Chen, Y (1986). *Early Holocene vegetation dynamics of Lake Barrine basin northeast Queensland, Australia*, Unpublished PhD Thesis, Australian National University, Canberra, pp. 246.

- Chen, Y (1987). Pollen and sediment distribution in a small crater lake in northeast Queensland, Australia. *Pollen et Spores*, vol. 29, pp. 8
- Chen, Y (1988). Early Holocene population expansion of some rainforest trees at Lake Barrine basin, Queensland. *Australian Journal of Ecology*, vol. 13, pp. 225-233.
- Chen, H, Edwards, RL, Southon, J, Matsumoto, K, Feinberg, JM, Sinha, A, Zhou, W, Li, H, Li, X, Xu, Y, Chen, S, Tan, M, Wang, Q, Wang, Y & Ning, Y (2018). Atmospheric $^{14}\text{C}/^{12}\text{C}$ changes during the last glacial period from Hulu Cave. *Science*, vol. 362, pp. 1293-1297.
- Chung, CTY, Power, SB, Sullivan, A & Delage, F (2019). The role of the South Pacific in modulating Tropical Pacific variability. *Scientific Reports*, vol. 9, 18311, <https://doi-org.virtual.anu.edu.au/10.1038/s41598-019-52805-2>.
- Clark, JS (1988). Particle motion and the theory of charcoal analysis: source area, transport, deposition and sampling. *Quaternary Research* vol. 30, pp. 67-80.
- Clark, JS & Hussey, TC (1996). Estimating the mass flux of charcoal from sedimentary records: effects of particle size morphology and orientation. *The Holocene* vol. 6, pp. 129-144.
- Clark, JS, Lynch, J, Stocks, BJ & Goldammer, JG (1998). Relationship between charcoal particles in air and sediments in west-central Siberia. *The Holocene* vol. 8, pp. 19-29.
- Clark, PU, Pisias, NG, Stocker, TF & Weaver, AJ (2002). The role of the thermohaline circulation in abrupt climate change. *Nature*, vol. 415, pp. 863-869.
- Clark, RL (1982). Point count estimation of charcoal in pollen preparations and thin sections of sediments. *Pollen et Spores*, vol. 24, pp. 523-535.
- Clark, RL (1983). Fire history from fossil charcoal in lake and swamp sediments, PhD Thesis, Australian National University, Canberra, pp. 197.
- Clark, RL (1984). Effects on charcoal of pollen preparation procedures. *Pollen et Spores*, vol. 26, pp. 559-576.
- Clark, RL (1986). Pollen as a chronometer and sediment tracer, Burrinjuck Reservoir, Australia. *Hydrobiologia*, vol. 143, pp. 63-69.
- Clarke, P (2019). A study of the deposition of, and taphonomic processes affecting, plant macrofossils records for an island in Palaeolake Flixton, North Yorkshire, Masters Thesis, University of Chester, UK.
- Clarkson, C, Smith, M, Marwick, B, Fullagar R, Wallis, WA, Faulkner, P, Manne, T, Hayes, E, Roberts, RG, Jacobs, Z, Carah, X, Lowe, KM, Matthews, J & Florin, A (2015). The archaeology, chronology and stratigraphy of Madjedbebe (Malakunanja II): a site in northern Australia with early occupation. *Journal of Human Evolution*, vol. 83, pp. 46-64.
- Clarkson, C, Jacobs, Z, Marwick, B, Fullagar, R, Wallis, L, Smith, M, Roberts, RG, Hayes, E, Lowe, K, Carah, X, Florin SA, McNeil, J, Cox, D, Arnold, LJ, Hua, Q, Huntley, J, Brand, HEA, Manne, T, Fairbairn, A, Shulmeister, J, Lyle, L, Salinas, M, Page, M, Connell, K, Park, G, Norman, K, Murphy, T & Pardoe, C (2017). Human occupation of northern Australia by 65,000 years ago. *Nature*, vol. 547, pp. 306-310.
- Clemens, S, Prell, W, Murray, D, Shimmield, G & Weedon, G (1991). Forcing mechanisms of the Indian Ocean monsoon. *Nature*, vol. 353, pp. 720-758.

- Clement, AC, Seager, R & Cane, MA. (1999). Orbital controls on the El Niño/Southern Oscillation and the tropical climate. *Paleoceanography*, vol. 14, pp. 441-456.
- Clement, AC, Cane, MA & Seager, R (2001). An orbitally driven tropical source for abrupt climate change. *Journal of Climate*, vol. 14, pp. 2369-2375.
- Clement, AC & Peterson, LC (2008). Mechanisms of abrupt climate change of the last Glacial period. *Review of Geophysics*, vol. 46, RG4002, 8755-1209.08/2006RG000204.
- Clymo, RS & Mackay, D (1987). Upwash and downwash of pollen and spores in the unsaturated surface layer of Sphagnum-dominated peat. *New Phytologist*, vol. 105, pp. 175-183.
- Cobb, KM, Charles, CD, Cheng, H & Edwards, RL (2003). El-Niño/Southern Oscillation and tropical Pacific climate during the last millennium. *Nature*, vol. 424, pp. 271-276.
- Cochrane, MA (2003). Fire science for rainforests. *Nature* vol. 421, pp. 913-919.
- Coffey, EED, Froyd, CA & Willis, KJ (2012). Lake or bog? Reconstructing baseline ecological conditions for the protected Galápagos Sphagnum peatbogs. *Quaternary Science Reviews*, vol. 52, pp. 60-74.
- Cole, N & Watchman, A (2005). AMS dating of rock art in the Laura Region, Cape York Peninsula, Australia: Protocols and results of recent research. *Antiquity*, vol. 79, pp. 661-668.
- Colhoun, EA, Pola, JS, Barton, CE & Heijnis, H (1999). Late-Pleistocene vegetation and climate history of Lake Selina, western Tasmania. *Quaternary International*, vol. 57, pp. 5-23.
- Collinson, ME (1983). Accumulations of fruit and seeds in three small sedimentary environments in southern England and their palaeoecological implications. *Annals of Botany*, vol. 52, pp. 583-592.
- Conedera, M, Tinner, W, Neff, C, Meurer, M & Dickens, AF (2009). Reconstructing past fire regimes: methods, applications and relevance to fire. *Quaternary Science Reviews*, vol. 28, pp. 435-456.
- Conley, DJ & Schelske, CL (1993). Potential role of sponge spicules in influencing the silicon biogeochemistry of Florida lakes. *Canadian Journal of Fisheries and Aquatic Sciences*, vol. 50, pp. 296-302.
- Connor, GJ & Bonell, M (1998). Air mass and dynamic parameters affecting trade wind precipitation on the northeast Queensland tropical coast. *International Journal of Climatology* vol. 18, pp. 1357-1372.
- Cosgrove, R (1996). Past human use of rainforests: an Australasian perspective. *Antiquity*, vol. 70, pp. 900-912.
- Cosgrove, R & Raymont, E (2002). Jiye Cave revisited: preliminary results from northeast Queensland rainforest. *Australian Archaeology*, vol. 54, pp. 29-36.
- Cosgrove, R, Field, J & Ferrier, Á (2007). The archaeology of Australia's tropical rainforests. *Palaeogeography, Palaeoclimatology, Palaeoecology*, vol. 251, pp. 150-173.
- Coulter, SE (2007). The geochemical characterization and chronological significance of Quaternary tephra deposits in Greater Australia, PhD Thesis, Queen's University, Belfast, UK.

Couvreux, M, Christiaen B, Verheyen, K & Hermy, M (2004). Large herbivores as mobile links between isolated nature reserves through adhesive seed dispersal. *Applied Vegetation Science*, vol. 7, pp. 229-236.

Crawford, AJ (2015). Understanding fire histories: the importance of charcoal morphology, PhD, University of Exeter, pp. 207.

Cronin, TM (2012). Rapid sea level rise. *Quaternary Science Reviews*, vol. 56, pp. 11-30.

Crowley, GM & Garnett, ST (2000). Changing fire management in the pastoral lands of Cape York Peninsula of northeast Australia, 1623 to 1996. *Australian Geographical Studies*, vol. 38, pp. 10-26.

Cruz, MG, Gould, JS, Hollis, JJ & McCaw, WL (2018). A hierarchical classification of wildland fire fuels for Australian vegetation types. *Fire*, vol. 1(13), doi: 10.3390/fire1010013.

Currie, LA, Benner, BA, Kessler, JD, Klinedinst, DB, Klouda, GA, Marulf, JV, Slater, JF, Wise, SA, Cachier, H, Cary, R, Chow, JC, Watson, J, Druffel, ERM, Masiello, CA, Eglinton, TI, Pearson, A, Reddy, CM, Gustafsson, Ö, Quinn, JG, Hartman, PC, Hedges, JI, Prentice, KM, Kirchsteller, TW, Novakov, T, Pukbaum, H & Schmidt, H (2002). A critical evaluation of interlaboratory data on total, elemental and isotopic carbon in carbonaceous particle reference material NIST SRM 1649a. *Journal of Research of the National Institute of Standards and Technology*, vol. 107, pp. 279-298.

Dai, A, Fung, IY & Del Genio, AD (1997). Surface observed global land precipitation variations during 1900-1988. *Journal of Climate*, vol. 10, pp. 2943-2962.

Dai, A & Wigley, TML (2000). Global patterns of ENSO-induced precipitation. *Geophysical Research Letters*, vol. 27, pp. 1283-1286.

Dansgaard, W, Johnsen, SJ, Clausen, HB, Dahl-Jensen, D, Gundestrup, N, Hammer, CU & Oeschger, H (1984). North Atlantic climate oscillations revealed by deep Greenland ice cores. *Climate Processes and Climate Sensitivity, Geophysical Monograph, Am. Geophys. Union*, vol. 29, pp. 288-298.

Dansgaard, W, Johnsen, SJ, Clausen, HB, Dahl-Jensen, D, Gundestrup, NS, Hammer, CU, Hvidberg, CS, Steffensen, JP, Sveinbjörns-dottir, AE, Jouzel, J & Bond, G (1993). Evidence for general instability of past climate from a 250-kyr ice-core record. *Nature*, vol. 364, pp. 218-220.

David, B (1991). Fern Cave, rock art and social formations: rock art regionalisation and demographic changes in southeastern Cape York Peninsula. *Archaeology in Oceania*, vol. 26, pp. 41-57.

David, B (1993). Nurrabullgin Cave: preliminary results from a pre-37,000 year rockshelter, North Queensland. *Archaeology in Oceania*, vol. 28, pp. 50-54.

David, B (1998). *Ngarrabullgan: Geographical investigations in Djungan country, Cape York Peninsula*, Department of Geography and Environmental Science, Monash University, pp.

David, B & Lourandos, H (1997). 37,000 years and more in tropical Australia: investigating long-term archaeological trends in Cape York Peninsula. *Proceedings of the Prehistoric Society*, vol. 63, pp. 1-23.

David, B, McNiven, I, Bekessy, L, Bultitude, B, Clarkson, C, Lawson, E, Murray, C & Tuniz, C (1998). More than 37,000 years of Aboriginal occupation. in B, David (ed.). *Ngarrabullgan: Geographical investigations in Djungan country, Cape York Peninsula*, Department of Geography and Environmental Science, Monash University, Clayton, pp.

David, M (1990). Beyond the Calamus: an archaeological survey of the Mount Carbine Tableland and Baker's Blue Mountain region, Conducted as part of the ANZSES 'Daintree Falls' expedition, 1989-1990, unpublished report, Archaeological Branch, Brisbane.

Davidson, TA, Sayer, CD, Bennion, H, David, C, Rose, N & Wade, MP (2005). A 250 year comparison of historical, macrofossil and pollen records of aquatic plants in a shallow lake. *Freshwater Biology*, vol.50, Issue 10, <https://doi.org/10.1111/j.1365-2427.2005.01414.x>.

Davis, MB (1969). Palynology and environmental history during the Quaternary period. *American Scientist*, vol. 57, pp. 317-332.

Davis, OK (1987). Spores of dung fungus *Sporormiella*: increased abundance in historic sediments and before Pleistocene megafaunal extinction. *Quaternary Research*, vol. 28, pp. 290-294.

Davis, OK & Shafer, DS (2006). *Sporormiella* fungal spores, a palynological means of detecting herbivore density. *Palaeogeography, Palaeoclimatology, Palaeoecology*, vol. 237, pp. 40-50.

Dawson, JW (1866). The evidence of fossil plants as to the climate of the Post-Pliocene period in Canada. *The Canadian Naturalist*, vol. 3, pp. 69-76.

Dean, WE (1974). Determination of carbonate and organic matter in calcareous sediments and sedimentary rocks by loss on ignition; comparison with other methods. *Journal of Sedimentary Research*, vol. 44, pp. 242-248.

De Garidel-Thoron, T, Beaufort, L, Braddock, KL & Dannenmann, S (2001). Millennial-scale dynamics of the East Asian winter monsoon during the last 200,000 years. *Paleoceanography*, vol. 16, pp. 491-502.

Dennell, RW, Martín-Torres, M & Castro, JMB (2011). Hominin variability, climatic instability and population demography in Middle Pleistocene Europe. *Quaternary Science Reviews*, vol. 30, pp. 1511-1524.

Department of Natural Resources and Mines (2006). Aerial scan of Lynch's Crater, <https://www.dnrm.qld.gov.au/>, viewed June 2010.

Department of Sustainability, Australian Government (2008). *Wet Tropics of Queensland World Heritage values*, <http://www.environment.gov.au/heritage/places/world/wet-tropics/values.html>, accessed 25th May 2009.

Deschamps, P, Durand, N, Bard, E, Hamelin, B, Camoin, G, Thomas, AL, Henderson, GM, Okuno, J & Yokoyama Y (2012). Ice-sheet collapse and sea-level rise at the Bølling warming 14,600 years ago. *Nature*, vol. 483, pp. 559-564.

Desprat, S, Sánchez Goñi, MF & Loutre, MF (2003). Revealing climatic variability of the last three millennia in northwestern Iberia using pollen influx data. *Earth and Planetary Science Letters*, vol. 213, pp. 63-78.

de Vernal, A & Hilliard-Marcel, C (2008). Natural variability of Greenland climate, vegetation and ice volume during the past million years. *Science*, vol. 320, pp. 1622-1625.

D'hondt, B, D'hondt, S, Bonte, D, Brys, R & Hoffmann, M (2012). A data-driven simulation of endozoochory by ungulates illustrates directed dispersal. *Ecological Modelling*, vol. 230, pp. 114-122.

- Dieffenbacher-Krall, AC & Halteman, WA (2000). The relationship of modern plant remains to water depth in alkaline lakes in New England, USA. *Journal of Paleolimnology*, vol. 24, pp. 213-219.
- Dijkstra, HA & Neelin, JD (1995). Ocean-atmosphere interaction and the tropical climatology. Part II: Why the Pacific cold tongue is in the east. *Journal of Climate*, vol. 8, pp. 1343-1359.
- Dima, M & Lohmann, G (2009). Conceptual model for millennial climate variability: a possible combined solar-thermohaline circulation origin for the ~ 1,500-year cycle. *Climate Dynamics*, vol. 32, pp. 301-311.
- Dixon, RMW (1972). *The Dyirbal language of north Queensland*. Cambridge Studies in Linguistics, 9, Cambridge University Press, London, pp. 452.
- Dixon, RMW (1991). *Words of our Country: Stories, place names and vocabulary in Yidiny, the Aboriginal language of the Cairns-Yarrabah region*. University of Queensland Press, St Lucia, pp. 312.
- Doerr, SH & Santin, C (2016). Global trends in wildfire and its impacts: perceptions versus realities in a changing world. *Philosophical Transactions of the Royal Society London B Biological Sciences*, vol. 371(1696), doi: 10.1098/rstb.2015.0345.
- Donders, TH, Wagner, F & Visscher, H (2006). Late Pleistocene and Holocene subtropical vegetation dynamics recorded in perched lake deposits on Fraser Island, Queensland, Australia. *Palaeogeography, Palaeoclimatology, Palaeoecology*, vol. 241, pp. 417-439.
- Donders, T, Haberle, S, Hope, G, Wagner, F & Visscher, H (2007). Pollen evidence for the transition of the eastern Australian climate system from the post-glacial to the present-day ENSO mode. *Quaternary Science Reviews*, vol. 26, pp. 1621-1637.
- Donders, TH, Wagner-Cremer, F & Visscher, H (2008). Integration of proxy data and model scenarios for the mid-Holocene onset of modern ENSO variability. *Quaternary Science Reviews*, vol. 27, pp. 571-579.
- Doubleday, NC (1999). *A paleolimnological survey of combustion particles from lakes and ponds in the eastern Arctic, Nunavut, Canada: an exploratory classification, inventory and interpretation at selected sites*. PhD. Thesis, Biology, Queen's University, Kingston, Canada, pp.343.
- Doubleday, NC & Smol, JP (2005). Atlas and classification scheme of arctic combustion particles suitable for paleoenvironmental work. *Journal of Paleolimnology*, vol. 33, pp. 393-431.
- Doveri, F (2004). *Fungi Fimicoli Italici*. AMB-Fondazione Centro Studi Micologici, Vicenza, pp. 1104.
- Dudley, JP (2000). Seed dispersal by elephants in semiarid woodland habitats of Hwange National Park, Zimbabwe 1. *Biotropica*, vol. 32, pp. 556-561.
- Duffin, KI, Gillson, L & Willis, KJ (2008). Testing the sensitivity of charcoal as an indicator of fire events in savanna environments: quantitative predictions of fire proximity, area and intensity. *The Holocene*, vol. 18, pp. 279-291.
- Edwards, W & Krockenberger, A (2006). Seedling mortality due to drought and fire associated with the 2002 El Niño event in a tropical rain forest in north-east Queensland, Australia. *Biotropica*, vol. 38, pp. 16-26.

- Elliot, M, Labeyrie, L & Duplessy, JC (2002). Changes in North Atlantic deep-water formation associated with the Dansgaard-Oeschger temperature oscillations (60-10 ka). *Quaternary Science Reviews*, vol. 21, pp. 1153-1165.
- Enache, MD & Cumming, BF (2006). Tracking recorded fires using charcoal morphology from the sedimentary sequence of Prosser Lake, British Columbia (Canada), *Quaternary Research*, vol. 65, pp. 282-292.
- Enache, MD & Cumming, BF (2009). Extreme fire under warmer and drier conditions inferred from sedimentary charcoal morphotypes from Opatcho Lake, central British Columbia, Canada. *The Holocene*, vol. 19, pp. 835-846.
- Esposito, A, Mazzoleni, S & Strumia, S (1999). Post-fire bryophyte dynamics in Mediterranean vegetation. *Journal of Vegetation Science*, vol. 10, pp. 261-268.
- Etienne, D, Wilhelm, B, Sabatier, P, Reyss, JL & Arnaud, F (2013). Influence of sample location and livestock numbers on *Sporormiella* concentrations and accumulation rates in surface sediments of Lake Allos, French Alps. *Journal of Paleolimnology*, vol. 49, pp. 117-127.
- Faegri, K & Iversen, J (1975). *Textbook of Pollen Analysis (3rd ed)*. Hafner Press, New York, pp. 295.
- Feer, F (1995). Seed dispersal in African forest ruminants. *Journal of Tropical Ecology*, vol. 11, pp. 683-689.
- Fensham, RJ & Fairfax, RJ (2007). Drought-related tree death of savanna eucalypts: species susceptibility, soil conditions and root architecture. *Journal of Vegetation Science*, vol. 18, pp. 71-80
- Fensham, RJ, Fairfax, RJ & Ward, DP (2009). Drought-induced tree death in savanna. *Global Change Biology*, vol. 15, pp. 380-387.
- Ferguson, DK (2005). Plant Taphonomy: Ruminations on the past, the present, and the future. *Palaos*, vol. 20, pp. 418-428.
- Finlayson, CM, Roberts, J, Chick, AJ & Sale, PJM (1983). The biology of Australian weeds. *Typha domingensis* Pers. and *Typha orientalis* Presl. *The Journal of Australian Institute of Agricultural Science*, vol. 49, pp. 3-10.
- Flannery, TF (1994). *The Future Eaters: an ecological history of the Australasian lands and people*, Reed Books, Sydney, pp. 423.
- Fleming, K, Johnston, P, Zwartz, D, Yokoyama, Y, Lambeck, K & Chappell, J (1998). Refining the eustatic sea-level curve since the Last Glacial Maximum using far- and intermediate-field sites. *Earth and Planetary Science Letters*, vol. 163, pp. 327-342.
- Fletcher, M-S & Moreno, PI (2011) Zonally symmetric changes in the strength and position of the Southern Westerlies drove atmospheric CO₂ variations over the past 14 ky. *Geology*, vol. 39, pp. 419-422.
- Fletcher, M-S & Moreno, PI (2012). Have the Southern Westerlies changed in a zonally symmetric manner over the last 14,000 years? A hemispheric-wide take on a controversial problem. *Quaternary International*, vol. 253, pp. 32-46.
- Fransden, WH (1997). Ignition probability of organic soils. *Canadian Journal of Forest Research*, vol. 27, pp. 1471-1477.

- Freitas, ACV, Aímoda, L, Ambrizzi, T & de Oliveira, CP (2017). Extreme Intertropical Convergence Zone shifts over the Southern Maritime Continent. *Atmospheric Science Letters*, vol. 18, pp. 2-10.
- Gadek, PA & Martin, HA (1981). Pollen morphology in the subtribe *Metrosiderinae* of the *Leptospermoideae* (Myrtaceae) and its taxonomic significance. *Australian Journal of Botany*, vol. 29, pp. 159-184.
- Gadek, PA & Martin, HA (1982). Exine Ultrastructure of Myrtaceous pollen. *Australian Journal of Botany*, vol. 30, pp. 75-86.
- Gagan, MK, Ayliffe, LK, Beck, JW, Cole, JE, Druffel, ERM, Dunbar, RB & Schrag, DP (2000). New views of tropical paleoclimates from corals. *Quaternary Science Reviews*, vol. 19, pp. 45-64.
- Gagan, MK, Hendy, EJ, Haberle, SG & Hantoro, WS (2004). Post-glacial evolution of the Indo-Pacific Warm Pool and El Niño-Southern Oscillation. *Quaternary International*, vol. 118-119, pp. 127-143.
- Gallegos, SC, Hensen, I, Saavedra, F & Schleuning, M (2015). Bracken fern facilitates tree seedling recruitment in tropical fire-degraded habitats. *Forest Ecology and Management*, vol. 337, pp. 135-143.
- García, D, Stchigel, AM, Cano, J, Guarro, J & Hawksworth, DL (2004) A synopsis and re-circumscription of *Neurospora* (syn. *Gelasinospora*) based on ultrastructural and 28S rDNA sequence data. *Mycology Research*, vol. 108, pp. 1119-1142.
- Garcin, Y, Williamson, D, Taieb, M, Vincens, A, Mathé, PE & Majule, A (2006). Centennial to millennial changes in maar-lake deposition during the last 45,000 years in tropical southern Africa (lake Masoko, Tanzania). *Palaeogeography, Palaeoclimatology, Palaeoecology*, vol. 239, pp. 334-354.
- Garstang, M, Tyson, PD, Cachier, H & Radke, L (1997). Atmospheric Transports of Particulate and Gaseous Products by Fires. in JS, Clark, H, Cachier, JS, Goldammer & B, Stocks (eds.). *Sediment Records of Biomass Burning and Global Change*, Springer-Verlag, Germany, pp. 207-249.
- Gelorini, V, Verbeken, A, van Geel, B, Cocquyt, C & Verschuren, D (2011). Modern non-pollen palynomorphs from East African lake sediments. *Review of Palaeobotany and Palynology*, vol. 164, pp. 143-173.
- Genever, M, Grindrod, J & Barker, B (2003). Holocene palynology of Whitehaven Swamp, Whitsunday Island, Queensland and implications for the regional archaeological record. *Palaeogeography, Palaeoclimatology, Palaeoecology*, vol. 201, pp. 141-156.
- Gill, AM, Moore, PHR & William, RJ (1996). Fire weather in the wet-dry tropics of the World Heritage Kakadu National Park, Australia. *Australian Journal of Ecology*, vol. 21, pp. 302-308.
- Gill, JL, Williams, JW, Jackson, ST, Lininger, KB & Robinson, GS (2009). Pleistocene megafaunal collapse, novel plant communities and enhanced fire regimes in North America. *Science*, vol. 326, pp. 1100-1103.
- Gill, JL, McLauchlan, KK, Skibbe, AM, Goring, S, Zirbel, CR & Williams, JW (2013). Linking abundances of the dung fungus *Sporormiella* to the density of bison: implications for assessing grazing by megaherbivores in palaeorecords. *Journal of Ecology*, vol. 101, pp. 1125-1136.

Giovannini, G, Lucchesi, S & Giachetti, M (1990). Beneficial and detrimental effects of heating on soil quality. in JC, Goldammer & MJ, Jenkins (eds.). *Fire in Ecosystem Dynamics*, SPB Academic Publishing, The Hague, pp. 95-102.

Glasspool, IJ (2000) A major fire event recorded in the mesofossils and petrology of the late Permian, lower Whybrow coal seam, Sydney basin, Australia. *Palaeogeography, Palaeoclimatology, Palaeoecology*, vol. 164, pp. 373-396.

Glasspool, IJ (2003). Hypautochthonous-allochthonous coal deposition in the Permian, South African, Witbank Basin No. 2 seam; a combined approach using sedimentology, coal petrology and palaeontology. *International Journal of Geology*, vol. 53, pp. 81-135.

Godwin, H (1962). Half life of radiocarbon. *Nature*, vol. 195, pp. 984.

Godwin, H & Willis, E (1959). Cambridge University natural radiocarbon measurements 1. *Radiocarbon*, vol. 1, pp. 63-75.

Goldammer, JG (1991). Tropical Wild-land Fires and Global Changes: Prehistoric Evidence, Present Fire Regimes, and Future Trends. in JS, Levine (ed.). *Global biomass burning: atmospheric, climatic and biospheric implications*, Massachusetts Institute of Technology Press, Massachusetts USA, pp. 83-91.

Goldammer, JG (1993). Historical biogeography of Fire: Tropical and Subtropical. in PJ, Crutzen & JG, Goldammer (eds.). *Fire in the environment: The Ecological, Atmospheric and Climatic Importance of Vegetation Fires*, John Wiley & Sons Ltd, London, pp. 297-314.

Golledge, NR, Menviel, L, Carter, L, Fogwill, C, England, MH, Cortese, G & Levy, R (2014). Antarctic contribution to meltwater pulse 1A from reduced Southern Ocean overturning. *Nature Communications*, vol. 5, pp.1-10.

Goren-Inbar, N, Alperson, N, Kislev, ME, Simchoni, O, Melamed, Y, Ben-Nun, A & Werker, E (2004). Evidence of Hominin control of fire at Gesher Benot Ya`aqov, Israel. *Science*, vol. 304, pp. 725-727.

Gott, B (1999). Cumbungi, *Typha* species: a staple Aboriginal food in southern Australia. *Australian Aboriginal Studies*, vol. 1, pp. 33-50.

Gott, B (2005). Aboriginal fire management in southeastern Australia: aims and frequency. *Journal of Biogeography*, vol. 32, pp. 1203-1208.

Gott, B (2008). Indigenous use of plants in south-eastern Australia. *Telopea*, vol. 12(2), pp. 215-226.

Gowlett, JAJ (2016). The discovery of fire by humans: a long and convoluted process. *Philosophical transactions of the Royal Society of London, Series B, Biological sciences*, vol. 371, (1696), 20150164. <https://doi.org/10.1098/rstb.2015.0164>

Graf, MT & Chmura, GL (2006). Development of modern analogues for natural, mowed and grazed grasslands using pollen assemblages and coprophilous fungi. *Review of Palaeobotany and Palynology*, vol. 141, pp. 139-149.

Graves, BP, Ralph, TJ, Hesse, PP, Westaway, KE, Kobayashi, T, Gadd, PS & Mazumder, D (2019). Macro-charcoal accumulation in floodplain wetlands: problems and prospects for reconstruction of fire regimes and environmental conditions. *Plos ONE*, 14(10):e0224011.<https://doi.org/10.1371/journal.pone.0224011>.

- Green, DG (1983). The ecological interpretation of fine resolution pollen records. *New Phytologist*, vol. 94, pp. 459-477.
- Green, D & Dolman, GS (1988). Fine resolution pollen analysis. *Journal of Biogeography*, vol. 15, pp. 685-701.
- Green, D, Singh, G, Polach, H, Moss, D, Banks, J & Geissler, EA (1988). A fine-resolution palaeoecology and palaeoclimatology from south-eastern Australia. *Journal of Ecology*, vol. 76, pp. 790-806.
- Grimm, EC (2004). *TILIA and TILIA GRAPH computer programs version 2.0.2*. Illinois State Museum Research and Collections Center.
- Grimm, EC, Donovan, JJ & Brown, KJ (2011). A high-resolution record of climate variability and landscape response from Kettle Lake, northern Great Plains, North America. *Quaternary Science Reviews*, vol. 30, pp. 2626-2650.
- Grindean, R, Tantău, I & Feurdean, A (2019). Linking vegetation dynamics and stability in the old-growth forests of Eastern Europe: Implications for forest conservation and management. *Biological Conservation*, vol. 229, pp. 160-169.
- Grishin, AM, Golovanov, AN, Sukov, YV & Preis, YI (2006). Experimental study of peat ignition and combustion. *Journal of Engineering Physics and Thermophysics*, vol. 79, pp. 563-568.
- Grousset, FE, Pujol, C, Labeyrie, L, Auffret, G & Boelaert, A (2000). Were the North Atlantic Heinrich events triggered by the behaviour of the European ice sheets?. *Geology*, vol. 28, pp. 123-126.
- Grüger, E (1972). Late Quaternary vegetation development in south-central Illinois. *Quaternary Research*, vol. 2, pp. 217-231.
- Guimarães Jr, PR, Galetti, M & Jordano, P (2008). Seed dispersal anachronisms: rethinking the fruits extinct megafauna ate. *PLoS ONE*, vol. 3, e1745.
- Guy-Ohlson, D (1992). *Botryococcus* as an aid in the interpretation of palaeoenvironment and depositional processes. *Review of palaeobotany and Palynology*, vol. 71, pp. 1-15.
- Haberle, SG (1998). Late Quaternary vegetation change in the Tari Basin, Papua New Guinea. *Palaeogeography, Palaeoclimatology, Palaeoecology*, vol. 137, pp. 1-24.
- Haberle, SG (2005). A 23,000-yr pollen record from Lake Euramoo, wet tropics of NE Queensland, Australia. *Quaternary Research*, vol. 64, pp. 343-356.
- Haberle, S & David, B (2004). Climates of change: human dimensions of Holocene environmental change in low latitudes of the PEPII transect. *Quaternary International*, vol. 118-119, pp. 165-179.
- Haberle, SG, Rule, S, Roberts, P, Heijnis, H, Jacobsen, G, Turney, C, Cosgrove, R, Ferrier, A, Moss, P, Mooney, S & Kershaw, P (2010). Paleofire in the wet tropics of northeast Queensland, Australia. *Pages news*, vol. 18(2), pp. 78-80.
- Haberstroh, PR, Brandes, JA, Gelinas, Y, Dickens, AF, Wirick, S & Cody, G (2006). Chemical composition of the graphic black carbon fraction in riverine and marine sediments at sub-micron scales using carbon x-ray spectromicroscopy. *Geochim. Cosmochim. Acta*, vol. 70, pp. 1483-1494.

- Hagelberg, TK, Bond, G & deMenocal, P (1994). Milankovitch band forcing of sub-Milankovitch climate variability during the Pleistocene. *Paleoceanography*, vol. 9, pp. 545-558.
- Haig, JD (1996). The impact of solar variability on climate. *Science*, vol. 272, pp. 981-984.
- Hallett, DJ & Walker, RC (2000). Paleoecology and its application to fire and vegetation management in Kootenay National Park, British Columbia. *Journal of Paleolimnology*, vol. 24, pp. 401-414.
- Hammes, K, Smernik, RJ, Skjemstad, JO, Herzog, A, Vogt, UF & Schmidt, MWI (2006). Synthesis and characterisation of laboratory-charred grass straw (*Oryza sativa*) and chestnut wood (*Castanea sativa*) as reference materials for black carbon quantification. *Organic Geochemistry*, vol. 37, pp. 1629-1633.
- Hanebuth, T, Stattegger K and Grootes PM 'Rapid flooding of the Sunda shelf: A late-glacial sea-level record' *Science* 288 (2000) 1033-1035.
- Harle KJ, Heijnis, H, Chisari, R, Kershaw, AP, Zoppi, U & Jacobsen, G (2002). A chronology for the long pollen record from Lake Wangoom, western Victoria (Australia) as derived from uranium/thorium disequilibrium dating. *Journal of Quaternary Science*, vol. 17, pp. 707-720.
- Harrington, GN, Thomas, MR, Bradford, MG, Sanderson, KD & Irvine, AK (2000). Structure and plant species dominance in north Queensland and wet sclerophyll forests. *Proceedings of the Royal Society of Queensland*, vol. 109, pp. 59-74.
- Harrington, GN, Bradford, MG & Sanderson, KD (2005). *The wet sclerophyll and adjacent forests of North Queensland: A directory to vegetation and physical survey data* Cooperative Research Centre for Tropical Rainforest Ecology and Management, Rainforest CRC, Cairns, pp. 78.
- Harrison, SP & Sanchez Goñi, MF (2010) Global patterns of vegetation response to millennial-scale variability and rapid climate change during the last glacial period. *Quaternary Science Reviews*, vol. 29, pp. 2957-2980.
- Hartley, J (2004). *The Ngadjonji, the original inhabitants of the rainforest country around Malanda in Far North Queensland*, <http://www.ngadjonji.bigpondhosting.com/default.html>, viewed February 2008.
- Hausfather, Z, Drake, HF, Abbott, T & Schmidt, GA (2019). Evaluating the Performance of Past Climate Model Projections. *Geophysical Research Letters*, vol. 47, Issue 1, <https://doi.org/10.1029/2019GL085378>.
- Havinga, AJ (1984). A 20-year experimental investigation into the differential corrosion susceptibility of pollen and spores in various soil types. *Pollen et spores*, vol. 26, pp. 514-558.
- Hawthorne, D, Mustaphi, CJC, Aleman, JC, Blarquez, O, Colombaroli, D, Daniau, AL, Marlon, JR, Power, M, Vannière, B, Han, Y, Hantson, S, Kehrwald, N, Magi, B, Yue, X, Carcaillet, C, Marchant, R, Ogunkoya, A, Githumbi, EN & Muriuki, RM (2018). Global Modern Charcoal Dataset (GMCD): A tool for exploring proxy-fire linkages and spatial patterns of biomass burning. *Quaternary International*, vol. 488, pp. 3-17.
- Head, LM & Stuart, IMF (1980). *Change in the Aire: palaeoecology and prehistory in the Aire Basin, south western Victoria*, Monash Publications in Geography, Melbourne, No. 24, pp. 102.
- Heer, O (1862). On the fossil flora of Bovey Tracey. *Philosophical Transactions of the Royal Society*, vol. 152, pp. 1039-86.

- Heinrich, H (1988). Origin and consequence of cyclic ice rafting in the northeast Atlantic Ocean during the past 130,000 years. *Quaternary Research*, vol. 29, pp. 142-152.
- Heiri, O, Lotter, AF & Lemcke, G (2001). Loss on ignition as a method for estimating organic and carbonate content in sediments: reproducibility and comparability of results. *Journal of Paleolimnology*, vol. 25, pp. 101-110.
- Heusser, CJ (1971). *Pollen and spores of Chile*, University of Arizona Press, Tucson, pp. 167.
- Higham, T (2011). European Middle and Upper Palaeolithic radiocarbon dates are often older than they look: problems with previous dates and some remedies. *Antiquity*, vol. 85(327), pp. 235-249.
- Higuera, PE, Sprugel, DG & Brubaker, LB (2005). Reconstructing fire regimes with charcoal from small-hollow sediments: a calibration with tree-ring records of fire. *The Holocene*, vol. 15, pp. 238-251.
- Hill, MO & Gauch, HG (1980). Detrended correspondence analysis: an improved ordination technique. *Vegetatio*, vol. 42, pp. 47-58.
- Hill R, Baird, A & Buchanan, D (1999). Aborigines and fire in the wet tropics of Queensland, Australia: Ecosystem management across cultures. *Society and Natural Resources*, vol. 12, pp. 205-223.
- Hill, R & Baird, A (2003). Kuku-Yalanji rainforest Aboriginal people and carbohydrate resource management in the wet tropics of Queensland, Australia. *Human Ecology*, vol. 31, pp. 27-52.
- Hinestrosa, G, Webster, JM & Beaman, RJ (2016). Postglacial sediment deposition along a mixed carbonate-siliciclastic margin: new constraints from the drowned shelf-edge reefs of the Great Barrier Reef, Australia. *Palaeogeography, Palaeoclimatology, Palaeoecology*, vol. 446, pp. 168-185.
- Hiscock, P (1999). Holocene coastal occupation of western Arnhem Land. In J, Hall & IJ McNiven (eds.). *Australian Coastal Archaeology*, ANH Publications, Department of Archaeology and Natural History, RSPAS, Canberra, pp. 91-104.
- Hiscock, P & Kershaw, AP (1992). Palaeoenvironments and prehistory of Australia's top end. in JR, Dodson (ed.). *The Naive Lands: Prehistory and Environmental Change in Australia and the Southwest Pacific*, Longman Cheshire, Melbourne, pp. 43-75.
- Hodgson, DA, Verleyen, E, Squier, AH, Sabbe, K, Keely, BJ, Saunders, KM, & Vyverman, W (2006). Interglacial environments of coastal east Antarctica: comparison of MIS 1 (Holocene) and MIS 5e (Last Interglacial) lake-sediment records. *Quaternary Science Reviews*, vol. 25, pp. 179-197.
- Hogg, AG, Hua, Q, Blackwell, PG, Niu, M, Buck, CE, Guilderson, TP, Heaton, TJ, Palmer, JG, Reimer, PJ, Reimer, RW, Turney, CSM & Zimmerman, SRH (2013). SHCal13 Southern Hemisphere calibration, 0-50,000 years cal BP. *Radiocarbon*, vol. 55(4), pp. 1889-1903.
- Holdaway, S, Fanning, P & Rhodes, E (2008). Challenging intensifications: human-environment interactions in the Holocene geoarchaeological record from western New South Wales, Australia. *The Holocene*, vol. 18, pp. 403-412.
- Holyoak, DT (1984). Taphonomy of prospective plant macrofossils in a river catchment on Spitsbergen. *New Phytologist*, vol. 98, pp. 405-423.

- Holz, A, Haberle, S, Veblen, TT, De Pol-Holz, R & Southon, J (2012). Fire History in western Patagonia from paired tree-ring fire-scar and charcoal records. *Climate of the Past*, vol. 8, pp. 451-466.
- Hong, YT, Jiang, HB, Liu, TS, Zhou, LP, Beer, J, Li, HD, Leng, XT, Hong, B & Qin, XG (2000). Response of climate to solar forcing recorded in a 6000-year $\delta^{18}\text{O}$ time-series of Chinese peat cellulose. *The Holocene*, vol. 10, pp. 1-7.
- Hooghiemstra, H, Melice, JL, Berger, A & Shackleton, NJ (1993). Frequency spectra and paleoclimatic variability of the high-resolution 30-1450 ka Funza 1 pollen record (eastern Cordillera, Colombia). *Quaternary Science Reviews*, vol. 12, pp. 141-156.
- Hope, GS (1976). The vegetational history of Mt Wilhelm, Papua New Guinea. *Journal of Ecology*, vol. 64, pp. 627-663.
- Hope, G, Chokkalingam, U & Anwar, S (2005). The Stratigraphy and fire history of the Kutai Peatlands, Kalimantan, Indonesia. *Quaternary Research*, vol. 64, pp. 407-417.
- Hopkins, MS, Graham, AW & Hewett, R (1990). Evidence of late Pleistocene fires and eucalypt forest from a North Queensland humid tropical rainforest site. *Australian Journal of Ecology*, vol. 15, pp. 345-347.
- Hopkins, MS, Ash, J, Graham, AW, Head, J & Hewett, RK (1993) Charcoal evidence of the spatial extent of the Eucalyptus woodland expansions and rainforest contractions in North Queensland during the late Pleistocene. *Journal of Biogeography*, vol. 20, pp. 357-372.
- Hopley, D, Smithers, SG & Parnell, K (2007). *Geomorphology of the Great Barrier Reef: Development, Diversity and Change*, Cambridge University Press, pp. 546.
- Horsfall, N (1987). Living in the rainforest: the prehistoric occupation of North Queensland's humid tropics, PhD thesis. James Cook University, Townsville, pp. 501 (2 vols.).
- Howell, AL, Bentley, SJ, Kehui, X, Ferrell, RE, Muhammad, Z & Septama, E (2014). Fine sediment mineralogy as a tracer of latest Quaternary sediment delivery to a dynamic continental margin: Pandora Trough, Gulf of Papua, Papua New Guinea. *Marine Geology*, vol. 357, pp. 108-122.
- Hua, Q (2009). Radiocarbon: A chronological tool for the recent past. *Quaternary Geochronology*, vol. 4, pp. 378-390.
- Huang, TC (1972). *Pollen Flora of Taiwan*, National Taiwan University, Botany Department Press, Taiwan, pp. 297 and plates 177.
- Hughen, K, Southon, J, Lehman, S, Bertrand, C & Turnbull, J (2006). Marine-derived ^{14}C calibration and activity record for the past 50,000 years updated from the Cariaco Basin. *Quaternary Science Reviews*, vol. 25, pp. 3216-3227.
- Hughes, K & Croke, J (2017). How did rivers in the wet tropics (NE Queensland, Australia) respond to climate changes over the past 30 000 years. *Journal of Quaternary Science*, vol. 32, pp. 744-759.
- Hughes, PD, Gibbard, PL & Ehlers, J (2013). Timing of glaciation during the last glacial cycle: evaluating the meaning and significance of the 'Last Glacial Maximum' (LGM). *Earth Science Reviews*, vol. 125, pp. 171-198.
- Humblet, M, Potts, DC, Webster, JM, Braga, JC, Iryu, Y, Yokoyama, Y, Séard, C, Droxler, A, Fugjita, K, Gischler, E & Kan, H (2019). Late glacial to deglacial variation of coralgal

- assemblages in the Great Barrier Reef, Australia. *Global and Planetary Change*, vol. 174, pp. 70-91.
- Humphreys, FR & Craig, FG (1981). Effects of fire on soil chemical, structural and hydrological properties. in AM, Gill, RH, Groves & IR, Noble (eds.). *Fire and the Australian Biota*, Australian Academy of Science, Canberra, pp. 177-200.
- Huybers, P & Aharonson, O (2010). Orbital tuning, eccentricity and the frequency modulation of climatic precession. *Paleoceanography and Paleoclimatology*, vol. 25, doi:10.1029/2010PA001952.
- Hyland, BPM, Whiffin, Zic,h FA, Duffy, S, Venter, F, Christophel, DC, Gray, B & Elick, RW (2003/2010). *Australian Tropical Rain Forest Plants, Trees, Shrubs and Vines*, CSIRO Publishing, Cairns, CD-Rom.
- Imbrie, J, Berger, A, Boyle, EA, Clemens, SC, Duffy, A, Howard, WR, Kukla, G, Kutzbach, J, Martinson, DG, McIntyre, A, Mix, AC, Molfino, B, Morley, JJ, Peterson, LC, Pisias, NG, Prell, WL, Raymo, ME, Shackleton, NJ & Toggweiler, JR (1993). On the structure and origin of major glaciation cycles. 2. the 100,000-year cycle. *Paleoceanography*, vol. 8, pp. 699-735.
- Innes, JB & Blackford, JJ (2003). The ecology of Late Mesolithic woodland disturbances: model testing with fungal spore assemblage data. *Journal of Archaeological Science*, vol. 30, pp. 185-194.
- Isbell, RF, Stephenson, PG, Murtha, GG & Gillman, GP (1976). *Red basaltic soils in North Queensland*, CSIRO, Division of Soils Technical Paper, No.28, pp. 49.
- Ivanov, KE (1981). *Water movement in mirelands*, Academic Press.
- Iversen, J (1941). Land occupation in Denmark's Stone Age. *Danmarks Geologiske Undersogelse II*, vol. 66, pp. 1-68.
- Jackson, DA (1993). Stopping rules in principal components analysis: a comparison of heuristical and statistical approaches. *Ecology*, vol. 74, pp. 2204 – 2214.
- Jackson, WD (1968). Fire, air, water and earth – an elemental ecology of Tasmania. *Proceedings of the Ecological Society of Australia*, vol. 3, pp. 9-16.
- Jackson, WD (1977). Nutrient cycling in Tasmanian oligotrophic environments. *Proceedings symposium nutrient cycling in indigenous forest ecosystems*, CSIRO Division of Land Resources Management, Perth, pp. 122-123.
- Jacobson, DJ, Dettman, JR, Adams, RI, Boesl, C, Sultana, S, Roenneberg, T, Merrow, M, Duarte, M, Marques, I, Ushakova, A, Carneiro, P, Videira, A, Navarro-Sampedro, L, Olmedo, M, Corrochano, LM & Taylor, JW (2006). New findings of *Neurospora* in Europe and comparisons of diversity in temperate climates on continental scales. *Mycologia*, vol. 98, pp. 550-559.
- Jaensch, R & Joyce, K (2006). *Coastal grass-sedge wetlands*, Queensland Wetland Programme, Queensland Government EPA, pp. 34.
- Jambu, M (1991). *Exploratory and multivariate data analysis*, Academic Press, Orlando,FL.
- Jankovská, V & Komárek, J (2000). Indicative value of *Pediastrum* and other coccal green algae in palaeoecology. *Folia Geobotanica*, vol. 35, pp. 59-82.
- Janzen, DH & Martin, PS (1982). Neotropical Anachronisms: The fruits the Gomphotheres ate. *Science*, vol. 215, pp. 19-27.

- Jensen, K, Lynch, EA, Calcote, R & Hotchkiss, SC (2007). Interpretation of charcoal morphotypes in sediments from Ferry Lake, Wisconsin, USA: do different plant fuel sources produce distinctive charcoal morphotypes?. *The Holocene*, vol. 17, pp. 907-915.
- Jiménez-Moreno, G, Fawcett, PJ & Anderson, RS (2008). Millennial- and centennial-scale vegetation and climate changes during the late Pleistocene and Holocene from northern New Mexico (USA). *Quaternary Science Reviews*, vol. 27, pp. 1442-1452.
- Johnson, CN (2006). *Australia's mammal extinctions: a 50,000 year history*, Cambridge University Press, Cambridge, pp. 310.
- Johnson, CN (2009). Ecological consequences of Late Quaternary extinctions of megafauna. *Proceedings of the Royal Society B*, vol. 276, pp. 2509-2519.
- Johnson, CN & Brook, BW (2011). Reconstructing the dynamics of ancient human populations from radiocarbon dates: 10 000 years of population growth in Australia. *Proceedings of the Royal Society B*, vol. 278, pp. 3748-3754.
- Johnson, CN, Rule, S, Haberle, SG, Turney, CSM, Kershaw, AP & Brook, BW (2015). Using dung fungi to interpret decline and extinction of megaherbivores: problems and solutions. *Quaternary Science Reviews*, vol. 110, pp. 107-113.
- Johnson, CN, Rule, S, Haberle, S, Kershaw, AP, McKenzie, GM & Brook, BW (2016). Geographic variation in the ecological effects of extinction of Australia's Pleistocene megafauna. *Ecography*, vol. 39, pp. 109-116.
- Jolliffe, IT & Cadima, J (2016). Principal component analysis: a review and recent developments. *Philosophical Transactions of the Royal Society A*, vol. 374, 20150202.
- Jones, R (1969). Fire-stick Farming. *Australian Natural History*, vol. 16, pp. 224-228.
- Jones, R (1974). *Department of Prehistory, Research School of Pacific Studies*, Australian National University. Annual report.
- Jones, TP & Chaloner, WG (1991). Fossil charcoal, its recognition and palaeoatmospheric significance. *Palaeogeography, Palaeoclimatology, Palaeoecology*, vol. 97, pp. 39-50.
- Joosten, H & de Klerk, P (2007). In search of finiteness: the limits of fine-resolution palynology of *Sphagnum* peat. *The Holocene*, vol. 17, pp. 1023-1031.
- Jouzel, J, Vaikmae, R, Petit, JR, Martin, M, Duclos, Y, Stievenard, M, Lorius, C, Toots, M, Melieres, MA, Burckle, LH, Barkov, NI & Kotlyakov, VM (1995). The two-step shape and timing of the last deglaciation in Antarctica. *Climate Dynamics*, vol. 11, pp. 151-161.
- Kaal, J, Schellekens J, Nierop, KGJ, Cortizas, AM & Muller, J (2014). Contribution of organic matter molecular proxies to interpretation of the last 55 ka of the Lynch's Crater record (NE Australia). *Palaeogeography, Palaeoclimatology, Palaeoecology*, vol. 414, pp. 20-31.
- Kahler, C (2005). Report on the vegetation of Lynch's Crater, Atherton Tableland, North Queensland, Queensland Herbarium, Brisbane, pp. 6.
- Kaniewski, D, Paulissen, E, de Laet, V & Waelkens, M (2008). Late Holocene fire impact and post-fire regeneration from the Bereket basin, Taurus Mountains, southwest Turkey. *Quaternary Research*, vol. 70, pp. 228-239.

- Kemp, CW, Tibby, J, Arnold, LJ and Barr, C (2019). Australian hydroclimate during Marine Isotope Stage 3: A synthesis and review. *Quaternary Science Reviews*, vol. 204, pp. 94-104.
- Kenyon, CE (1989). A late Pleistocene and Holocene palaeoecological record from Boulder Flat, east Gippsland, BSc (Hons) thesis, Department of Botany and Zoology, Monash University, Melbourne, pp. 104.
- Kershaw, AP (1970). A pollen diagram from Lake Euramoo, north-east Queensland, Australia. *New Phytologist*, vol. 69, pp. 785-805.
- Kershaw, AP (1971). A pollen diagram from Quincan Crater, north-east Queensland, Australia. *New Phytologist*, vol. 70, pp. 669-681.
- Kershaw, AP (1973). Late Quaternary vegetation of the Atherton Tableland, north-east Queensland, Australia, PhD Thesis, Australian National University, Canberra, pp. 439.
- Kershaw, AP (1975). Stratigraphy and pollen analysis of Bromfield Swamp, north eastern Queensland, Australia. *New Phytologist* vol. 75, pp. 173-191.
- Kershaw, AP (1976). A late Pleistocene and Holocene pollen diagram from Lynch's Crater, North-eastern Queensland, Australia. *New Phytologist*, vol. 77, pp. 469-498.
- Kershaw, AP (1978). The analysis of aquatic vegetation on the Atherton Tableland, north-east Queensland, Australia. *Australian Journal of Ecology*, vol. 3, pp. 23-42.
- Kershaw, AP (1979) Local pollen deposition in aquatic sediments on the Atherton Tableland, north-eastern Australia. *Australian Journal of Ecology*, vol. 4, pp. 253-263.
- Kershaw, AP (1980a). Evidence for vegetation and climatic change in the Quaternary. in RA, Henderson & PJ, Stephenson (eds.). *The Geology and Geophysics of Northeastern Australia*, Geological Society of Australia, Queensland Division, Brisbane, pp. 398-402.
- Kershaw, AP (1983a). A Holocene pollen diagram from Lynch's Crater, Northeastern, Queensland, Australia. *New Phytologist*, vol. 94, pp. 669-682.
- Kershaw, AP (1983b). The vegetation record of northeastern Australia 15-10 ka. in JMA, Chappell & A, Grindrod (eds.). *Climanz 1: Proceedings of the first Climanz – a symposium of results and discussions concerned with Late Quaternary Climatic History of Australia, New Zealand and surrounding seas*, Australian National University, Canberra, pp. 149.
- Kershaw, AP (1984). Late Cenozoic plant extinctions in Australia. in PS, Martin & RG, Klein (eds.). *Quaternary Extinctions: a prehistoric revolution*, University of Arizona Press, Tucson, pp. 691-707.
- Kershaw, AP (1985). An extended late Quaternary vegetation record from north-eastern Queensland and its implications for the seasonal tropics of Australia. *Proceedings, Ecological Society of Australia*, vol. 13, pp. 17-39.
- Kershaw, AP (1986). Climatic change and Aboriginal burning in north-east Australia during the last two glacial/interglacial cycles. *Nature*, vol. 322, pp. 47-49.
- Kershaw, AP (1994). Pleistocene vegetation of the humid tropics of northeastern Queensland, Australia. *Palaeogeography, Palaeoclimatology, Palaeoecology*, vol. 109, pp. 399-412.
- Kershaw, AP & Hyland, BPM (1975). Pollen transfer and periodicity in a rain-forest situation. *Review of Palaeobotany and Palynology*, vol. 19, pp. 129-138.

- Kershaw, AP & Nix, HA (1988). Quantitative palaeoclimatic estimates from pollen data using bioclimatic profiles of extant taxa. *Journal of Biogeography*, vol. 15, pp. 589-602.
- Kershaw, AP & Nix, HA (1989). The use of bioclimatic envelopes for estimation of quantitative palaeoclimatic values. in TH, Donnelly & RJ, Wasson (eds.). *Climanz3: Proceedings of the third symposium on the Late Quaternary Climatic History of Australia*, CSIRO, Canberra, pp. 158.
- Kershaw, AP & Strickland, KM (1990). A 10 year pollen trapping record from rainforest in northeastern Queensland, Australia. *Review of Palaeobotany and Palynology*, vol. 64, pp. 281-288.
- Kershaw, AP, Baird, JG, D'Costa, DM, Edney, PA, Peterson, JA & Strickland, KM (1991). A comparison of long Quaternary pollen records from the Atherton and Western Plains volcanic provinces, Australia. in MAJ, Williams, P, De Deckker & AP, Kershaw (eds.). *The Cainozoic in Australia: A re-appraisal of the evidence*, Special Publication – Geological Society of Australia, vol. 18, pp. 288-301.
- Kershaw, AP & Bulman, D (1994). The relationship between modern pollen samples and environment in the humid tropics region of northeastern Australia. *Review of Palaeobotany and Palynology*, vol. 83, pp. 83-96.
- Kershaw, AP & McGlone, MS (1995). The Quaternary history of the southern conifers. in NJ, Enright & RS, Hill (eds.). *Ecology of the Southern Conifers*, Melbourne University Press, Carlton, p. 30-63.
- Kershaw, AP, Moss, PT & van der Kaars, S (1997). Environmental change and the human occupation of Australia. *Anthropologie*, vol. 35, pp. 35-43.
- Kershaw, P & Wagstaff, B (2001). The southern conifer family Araucariaceae: history, status and value for palaeoenvironmental reconstruction. *Annual Review of Ecology and Systematics*, vol. 32, pp. 397-414.
- Kershaw, AP, Clark, JS, Gill, MA & D'Costa, DM (2002) A history of fire in Australia. in RA, Bradstock, JE, Williams & AM, Gill (eds.). *Flammable Australia: the fire regimes and biodiversity of a continent*, Cambridge University Press, Melbourne, pp. 3-25.
- Kershaw, AP, van der Kaars, S & Moss, PT (2003). Late Quaternary Milankovitch-scale climatic change and variability and its impact on monsoonal Australasia. *Marine Geology*, vol. 201, pp. 81-95.
- Kershaw, AP, van der Kaars, S & Flenley, J (2006a). The Quaternary history of the far eastern rainforests. in M, Bush M & J, Flenley (eds.). *Tropical Rainforest Responses to Climate Change*, Springer-Praxis, Berlin, pp. 77-115.
- Kershaw, AP, van der Kaars, S, Moss, P, Opdyke, B, Guichard, F, Rule, S & Turney, C (2006b). Environmental change and the arrival of people in the Australian region. *Before Farming*, vol. 1(2), pp.1-24.
- Kershaw, AP, Bretherton, SC & van der Kaars, S (2007a). A complete record of the last 230 ka from Lynch's Crater, north-eastern Australia. *Palaeogeography, Palaeoclimatology, Palaeoecology*, vol. 251, pp. 23-45.
- Kidwell, SM (2001). Major biases in the fossil record (chapter 3.3.1). in DEG, Briggs & PR, Crowther (eds.). *Palaeobiology 2*, Osney Mead, Oxford ; Malden, MA, Blackwell Science.
- Kitzberger, T, Swetnam, TW & Veblen, TT (2001). Inter-hemispheric synchrony of forest fires and the El Niño-Southern Oscillation. *Global Ecology & Biogeography*, vol. 10, pp. 315-326.

- Klingaman, N (2012). Queensland rainfall – past, present and future. Department of Environment and resource management, www.climatechange.qld.gov.au
- Knicker, H (2007). How does fire affect the nature and stability of soil organic nitrogen and carbon? A review. *Biogeochemistry*, vol. 85, pp. 91-118.
- Koff, T & Vandel, E (2008). Spatial distribution of macrofossil assemblages in surface sediment of two small lakes in Estonia. *Estonian Journal of Ecology*, vol. 57, pp. 5-20.
- Koutavas, A, deMenocal PB & Lynch-Stieglitz, J (2006a). Holocene trends in tropical Pacific sea surface temperatures and the El Niño-Southern Oscillation. *Pages*, vol. 14, No.3.
- Koutavas, A, deMenocal, PB, Olive, GC & Lynch-Stieglitz, J (2006b). Mid-Holocene El Niño-Southern Oscillation (ENSO) attenuation revealed by individual foraminifera in eastern tropical Pacific sediments. *Geology*, vol. 34, pp. 993-996.
- Krebs, U, Park, W and Schneider, B (2011). Pliocene aridification of Australia caused by tectonically induced weakening of the Indonesian Throughflow. *Palaeogeography, Palaeoclimatology, Palaeoecology*, vol. 309, pp. 111-117.
- Krug, JC, Khan, RS & Jeng, RS (1994). A new species of *Gelasinospora* with multiple germ pores. *Mycologia*, vol. 86, pp. 250–253.
- Kumar, KK, Rajagopalan, B, Hoerling, M, Bates, G & Cane, M (2006). Unravelling the mystery of Indian monsoon failure during El Niño events. *Science*, vol. 314, pp. 115-119.
- Kutiel, P & Inbar, M (1993). Fire impacts on soil nutrients and soil erosion in a Mediterranean pine forest plantation. *Catena*, vol. 20, pp. 129-139.
- Kylander, ME, Muller, J, Wüst, RAJ, Gallagher, K, Garcia-Sanchez, Coles, BJ & Weiss, DJ (2007). Rare earth element and Pb isotope variations in a 52 kyr peat core from Lynch's Crater (NE Queensland, Australia): proxy development and application to paleoclimate in the Southern Hemisphere. *Geochimica et Cosmochimica Acta*, vol. 71, pp. 942-960.
- Laepfle, T, Werner, M & Lohmann, G (2011). Synchronicity of Antarctic temperatures and local solar insolation on orbital scales. *Nature*, vol. 471, pp. 91-94.
- Laffan, MD (1988). *Soils and land use on the Atherton Tableland, North Queensland*, CSIRO, Australian Division of Soils, Soils and Land use Series No.61, pp. 72.
- Lambeck, K, Woodroffe, CD, Antonioli, F, Anzidei, M, Gehrels, WR, Laborel, J & Wright, AJ (2010). Paleoenvironmental records, geophysical modelling and reconstruction of sea-level trends and variability on centennial and longer timescales. in J, Church, PI, Woodworth, T, Aarup & WS, Wilson (eds.). *Understanding sea-level rise and variability*, Wiley-Blackwell, Chichester, pp. 61-121.
- Lambeck, K, Rouby, H, Purcell, A, Sun, Y & Sambridge, M (2014). Sea level and global ice volumes from the Last Glacial Maximum to the Holocene. *Proceedings of the National Academy of Science*, vol. 111, pp. 15296-15303.
- LaMoreaux, HK, Brook, GA & Knox, JA (2009). Late Pleistocene and Holocene environments of the southeastern United States from the stratigraphy and pollen content of a peat deposit on the Georgia Coastal Plain. *Palaeogeography, Palaeoclimatology, Palaeoecology*, vol. 280, pp. 300-312.

- Lang, N & Wolff, EW (2011). Interglacial and glacial variability from the last 800 ka in marine ice and terrestrial archives. *Climate of the Past*, vol. 7, pp. 361-380.
- Large, MF & Braggins, JE (1991). Spore atlas of New Zealand ferns and fern allies. *New Zealand Journal of Botany Supplement*, pp. 168.
- LaRowe, DE, Arndt, S, Bradley, JA, Estes, ER, Hoarfrost, A, Lang, SQ, Lloyd, KG, Mahmoudi, N, Orsi, WD, Shah Walter, SR, Steen, AD & Zhao, R (2020). The fate of organic carbon in marine sediments – New insights from recent data and analysis. *Earth-Science Reviews*, vol. 204, 103146.
- Leck, MA & Schütz, W (2005). Regeneration of Cyperaceae with particular reference to seed ecology and seed banks. *Perspectives in Plant Ecology, Evolution and Systematics*, vol. 7, pp. 95-133.
- Leduc, G, Vidal, L, Tachikawa, K & Bard, E (2009). ITCZ rather than ENSO signature for abrupt climate changes across the tropical Pacific? *Quaternary Research*, vol. 72, pp. 123-131.
- Legendre, P & Legendre, L (2012). *Numerical Ecology*, 3rd English Ed, Elsevier, pp.1006.
- Leng, LY, Ahmed, OH & Jalloh, MB (2019). Brief review on climate change and tropical peatlands. *Geoscience Frontiers*, vol. 10, pp. 373-380.
- Lepš, J & Šmilauer, P (2003). *Multivariate analysis of ecological data using CANOCO*, Cambridge University Press, Cambridge, pp. 269.
- Levine, JS (1991). *Global biomass burning: atmospheric, climatic and biospheric implications*, Massachusetts Institute of Technology Press, Massachusetts USA, pp. 1-600.
- Lewis, SC, Gagan, MK, Ayliffe, LK, Zhao, J-X, Hantoro, WS, Treble, PC, Hellstrom, JC, LeGrande, AN, Kelley, M, Schmidt, GA & Suwargadi, BW (2011). High resolution stalagmite reconstructions of Australian-Indonesian monsoon rainfall variability during Heinrich stadial 3 and Greenland interstadial 4. *Earth and Planetary Science Letters*, vol. 303, pp. 133-142.
- Lewis, SE, Wüst, RAJ, Webster, JM & Shields, GA (2008). Mid-late Holocene sea-level variability in eastern Australia. *Terra Nova*, vol. 20, pp. 74-81.
- Lewis, SE, Sloss, CR, Murray-Wallace, CV, Woodroffe, CD & Smithers, SG (2013). Post-glacial sea-level changes around the Australian margin: a review. *Quaternary Science Reviews*, vol. 74, pp. 115-138.
- Leys, B, Brewer, SC, McConaghy, S, Mueller, J & McLauchlan, KK (2015). Fire history reconstruction in grassland ecosystems: amount of charcoal reflects local area burned. *Environmental Research Letters*, vol. 10, 114009.
- Liedloff, AC & Cook, GD (2007). Modelling the effects of rainfall variability and fire on tree population in an Australian tropical savanna with the FLAMES simulation model. *Ecological Modelling*, vol. 201, pp. 269-282.
- Limaye, RB, Kumaran, KPN, Nair, KM & Padmalal, D (2007). Non-pollen palynomorphs as potential palaeoenvironmental indicators in the Lake Quaternary sediments of the west coast of India. *Current Science*, vol. 92, pp. 1370-1382.
- Linsley, BK & Thunell, RC (1990). The record of deglaciation in the Sulu Sea: evidence for the younger dryas event in the tropical western Pacific. *Paleoceanography*, vol. 5, pp. 1025-1039.
- Lisiecki, LE & Raymo, ME (2005). A Pliocene-Pleistocene stack of 57 globally distributed benthic $\delta^{18}\text{O}$ records. *Paleoceanography*, vol. 20, PA 1003, doi:10.1029/2004PA001071.

- Liu, Z, Kutzbach, J & Wu, L (2000). Modeling climate shift of El Niño variability in the Holocene. *Geophysical Research Letters*, vol. 27, pp. 2265-2268.
- Liu, Z, Brady, E & Lynch-Stieglitz, J (2003). Global ocean response to orbital forcing in the Holocene. *Paleoceanography*, vol. 18, pp. 1041-1061.
- Lobert, JM & Warnatz, J (1993). Emissions from the Combustion Process in vegetation. in PJ, Crutzen & JG, Goldammer (eds.). *Fire in the environment: The Ecological, Atmospheric and Climatic Importance of Vegetation Fires*, John Wiley & Sons Ltd, London, pp. 15-37.
- Long, CJ, Whitlock, C, Bartlein, PJ & Millspaugh, SH (1998). A 9000-year fire history from the Oregon Coast Range, based on a high-resolution charcoal study. *Canadian Journal of Forest Research*, vol. 28, pp. 774-787.
- Longmore, ME (1997). Quaternary palynological records from perched lake sediments, Fraser Island, Queensland, Australia: rainforest, forest history and climatic control. *Australian Journal of Botany*, vol. 45, pp. 507-526.
- Longmore, ME & Heijnis, H (1999). Aridity in Australia: Pleistocene records of palaeohydrological and palaeoecological change from the perched lake sediments of Fraser Island, Queensland, Australia. *Quaternary International*, vol. 57/58, pp. 35-47.
- Lopes dos Santos, RA, Wilkins, D, De Deckker, P & Schouten, S (2012). Late Quaternary productivity changes from offshore Southeastern Australia: a biomarker approach. *Palaeogeography Palaeoclimatology Palaeoecology*, vol. 363-364, pp. 48-56.
- Lorenz, V (1986). On the growth of maars and diatremes and its relevance to the formation of tuff rings. *Bulletin of Volcanology*, vol. 48, pp. 265-274.
- Lough, JM, Llewelyn, LE, Lewis, SE, Turney, CSM, Palmer, JG, Cook, CG & Hogg, AG (2014). Evidence for suppressed mid-Holocene northeastern Australian monsoon variability from coral luminescence. *Paleoceanography*, vol. 29, pp. 581-594.
- Lourandos, H (1980). Change or stability? Hydraulics, hunter gatherers and population in temperate Australia. *World Archaeology*, vol. 11, pp. 245-266.
- Lourandos, H (1983). Intensification: a late Pleistocene-Holocene archaeological sequence from southwestern Victoria. *Archaeology in Oceania*, vol. 18, pp. 81-94.
- Lourandos, H (1985). Intensification and Australian prehistory. in TD, Price & JA, Brown (eds.). *Prehistoric Hunter-Gatherers: The Emergence of Cultural Complexity*, Academic Press, Orlando, FL, pp. 385-423.
- Lourandos, H & Ross, A (1994). The great 'Intensification Debate': Its history and place in Australian archaeology. *Australian Archaeology*, vol. 39, pp. 54-63.
- Lourandos, H & David, B (2002). Long-term archaeological and environmental trends: a comparison from late Pleistocene-Holocene Australia. in AP, Kershaw, B, David, N, Tapper, D, Penny & J, Brown (eds.). *Bridging Wallace's Line: The Environmental and Cultural History and Dynamics of the SE-Asian-Australian Region*, Catena Verlag, Reiskirchen, pp. 97-118.
- Luly, JG, Grindrod, JF & Penny, D (2006). Holocene palaeoenvironments and change at Three-Quarter Mile Lake, Silver Plains Station, Cape York Peninsula, Australia. *The Holocene*, vol. 16, pp. 1085-1094.
- Lumholtz, CS (1889). *Among Cannibals*, John Murray, London, pp. 383.

- Lundqvist, N (1972). Nordic Sordariaceae s. lat. – *Symb. Bot. Upsal*, vol. 20, pp. 1-374.
- Lynch, AH, Beringer, J, Kershaw, P, Marshall, A, Mooney, S, Tapper, N, Turney, C & van der Kaars, S (2007). Using the palaeorecord to evaluate climate and fire interactions in Australia. *Annual Review of Earth Planetary Science*, vol. 35, pp. 215-239.
- Lynch, EA, Calcote, R & Hotchkiss, S (2006). Late-Holocene vegetation and fire history from Ferry Lake, northwestern Wisconsin. *The Holocene*, vol. 16, pp. 495-504.
- Lynch, EA, Hotchkiss, SC & Calcote, R (2011). Charcoal signatures defined by multivariate analysis of charcoal records from 10 lakes in northwest Wisconsin (USA). *Quaternary Research*, vol. 75, pp. 125-137.
- Lynch, JA, Clark, JS & Stocks, BJ (2004). Charcoal production, dispersal and deposition from the Fort Providence experimental fire: interpreting fire regimes from charcoal records in boreal forests. *Canadian Journal of Forest Research*, vol. 34, pp. 1642-1656.
- MacDonald, GM, Larsen, CPS, Szeicz, JM & Moser, KA (1991). The reconstruction of boreal forest fire history from lake sediments: a comparison of charcoal, pollen, sedimentological and geochemical indices. *Quaternary Science Reviews*, vol. 10, pp. 53-71.
- McBrearty, S & Brooks, AS (2000). The revolution that wasn't: a new interpretation of the origin of modern human behavior. *Journal of Human Evolution*, vol. 39, pp. 453-563.
- McCarthy, TS, McIver JR, Caincross, B, Ellery, WN & Ellery, K (1989). The inorganic chemistry of peat from the Maunachira channel swamp system, Okavango Delta, Botswana. *Geochim. Cosmochim. Acta*, vol. 53, pp. 1077-1089.
- McCormac, FG, Hogg, AG, Blackwell, PG, Buck, CE, Higham, TFG & Reimer, PJ (2004). SHCal04 Southern Hemisphere calibration, 0-11.0 cal kyr BP. *Radiocarbon*, vol. 46(3), pp. 1087-1092.
- McCormick, MP, Thomason, LW & Trepte, CR (1995). Atmospheric effects of the Mt Pinatubo eruption, *Nature*, vol. 373, pp. 399-404.
- McGee, D, Donohoe, A, Marshall, J & Ferreira, D (2014). Changes in ITCZ location and cross-equatorial heat transport at the Last Glacial Maximum, Heinrich Stadial 1 and the mid-Holocene. *Earth and Planetary Science Letters*, vol. 390, pp. 69-79.
- McGinnes, EA, Kandeel Jr, SA & Szopa, PS (1971). Some structural changes observed in the transformation of wood into charcoal. *Wood and Fiber*, vol. 3, pp. 77-83.
- McGlone, MS, Kershaw, AP & Markgraf, V (1992). El Niño/Southern Oscillation climatic variability in Australasian and South American paleoenvironmental records. in HF, Diaz & V, Markgraf (eds.). *EL NIÑO Historical and Paleoclimatic Aspects of the Southern Oscillation*, Cambridge University Press, Cambridge, pp. 435-462.
- McGlone, MS, Wilmschurst, JM & Leach, HM (2005). An ecological and historical review of bracken (*Pteridium esculentum*) in New Zealand, and its cultural significance. *New Zealand Journal of Ecology*, vol. 29(2), pp.165-184.
- McGowan, HA, Petherick, LM & Kamber, BS (2008). Aeolian sedimentation and climate variability during the late Quaternary in southeast Queensland, Australia, *Palaeogeography, Palaeoclimatology, Palaeoecology*, vol. 265, pp. 171-181.

- McGowan, H, Marx, SK, Moss, P & Hammond, AM (2012). Evidence of ENSO mega-drought triggered collapse of prehistory Aboriginal society in northwest Australia. *Geophysical Research Letters*, vol. 39, Issue 22: L22702.
- McGree, S, Schreider, S & Kuleshov, Y (2016). Trends and Variability in Droughts in the Pacific Islands and Northeast Australia. *Journal of Climate*, vol. 29 (23), pp. 8377-8397.
- McJannet, DL, Wallace, JS & Reddell, P (2007a). Precipitation interception in Australian tropical rainforests: 1. Measurement of stemflow, throughfall and cloud interception. *Hydrological Processes*, vol. 21, pp. 1692-1702.
- McJannet, DL, Wallace, JS & Reddell, P (2007b). Precipitation interception in Australian tropical rainforests: II. Altitudinal gradient of cloud interception, stemflow, throughfall and interception. *Hydrological Processes*, vol. 21, pp. 1703-1718.
- McKenzie, GM (1989). Late Quaternary vegetation and climate in the Central Highlands of Victoria: with special reference to *Nothofagus cunninghamii* (Hook.) Oerst. Rainforest, PhD Thesis, Monash University, Melbourne.
- McKenzie, N, Jacquier, D, Isbell, R & Brown, K (2004). *Australian Soils and Landscapes: An Illustrated Compendium*, CSIRO Publishing, doi: 10.1071/9780643100732.
- McMullan-Fisher, SJ, May, TW, Robinson, RM, Bell, TL, Lebel, T, Catcheside, P & York, A (2011). Fungi and fire in Australian ecosystems: a review of current knowledge, management implications and future directions. *Australian Journal of Botany*, vol. 59, pp. 70-90.
- Malmström, C (1923). A botanical hydrological and developing historical investigation of a North Swedish mire. *Communications from the State Forest Research Institute*, vol. 20, pp.
- Mantua, NJ & Hare, SR (2002). The Pacific Decadal Oscillation. *Journal of Oceanography*, vol. 58(1), pp. 35-44.
- Markgraf, V, Whitlock, C, Anderson, RS & García, A (2009). Late Quaternary vegetation and fire history in the northernmost Nothofagus forest region: Mallín Vaca Lauquen, Neuquén Province, Argentina. *Journal of Quaternary Science*, vol. 24, pp. 248-258.
- Markgraf, V, Iglesias, V & Whitlock, C (2013). Late and postglacial vegetation and fire history from Cordón Serrucho Norte, northern Patagonia. *Palaeogeography, Palaeoclimatology, Palaeoecology*, vol. 371, pp. 109-118.
- Martinson, DG, Pisias, NG, Hays, JD, Imbrie, J, Moore Jr, TC & Shackleton, NJ (1987). Age dating and the orbital theory of the ice ages: Development of a high-resolution 0 to 300,000-year chronostratigraphy. *Quaternary Research*, vol. 27, pp. 1-29.
- Masiello, C (2004). New directions in black carbon organic geochemistry. *Marine Chemistry*, vol. 92, pp. 201-213.
- May, JH, Preusser, F & Gliganic, LA (2015). Refining late Quaternary plunge pool chronologies in Australia's monsoonal Top End. *Quaternary Geochronology*, vol. 30, pp. 328-333.
- Medeanic, S (2006). Freshwater algal palynomorph records from Holocene deposits in the coastal plain of Rio Grande do Sul, Brazil. *Review of Palaeobotany and Palynology*, vol. 141, pp. 83-101.
- Medeanic, S & Silva, MB (2010). Indicative value of non-pollen palynomorphs (NPPs) and palynofacies for palaeoreconstructions: Holocene peat, Brazil. *International journal of coal geology*, vol. 84, pp. 248-257.

- Medeanic, S, Hirata, F & Dillenburg, S (2010). Algal palynomorphs response to environmental changes in the Tramandaí Lagoon, southern Brazil and climatic oscillations during the 20th century. *Journal of Coastal Research*, vol. 26, pp. 736-742.
- Mélice, JL, Coron, A & Berger, A (2001). Amplitude and frequency modulations of the earth's obliquity for the last million years. *Journal of Climate*, vol. 14, pp. 1043-1054.
- Mensing, SA, Michaelsen, J & Byrne, R (1999). A 560-year record of Santa Ana fires reconstructed from charcoal deposited in the Santa Barbara basin, California. *Quaternary Research*, vol. 51, pp. 295-305.
- Merrill, RT & McElhinny, MW (1983). *The Earth's magnetic field, its history, origin and planetary perspective*, Academic Press, London, pp. 401.
- Middleton, BA, van der Valk, AG & Davis, CB (2015). Responses to water depth and clipping of twenty-three plant species in an Indian monsoonal wetland. *Aquatic Botany*, vol. 126, pp. 38-47.
- Millard, AR (2014). Conventions for reporting radiocarbon determinations. *Radiocarbon*, vol. 56(2), pp. 555-559.
- Miller, GH, Magee, JW, Fogel, ML, Wooller, MJ, Hesse, PP, Spooner, NA, Johnson, BJ & Wallis, L (2018). Wolfe Creek Crater: A continuous sediment fill in the Australian Arid Zone records changes in monsoon strength through the Late Quaternary. *Quaternary Science Review*, vol. 199, pp. 108-125.
- Milne, GA, Long, AJ & Bassett, SE (2005). Modelling Holocene relative sea-level observations from the Caribbean and South America. *Quaternary Science Reviews*, vol. 24, pp. 1183-1202.
- Mitchell, DS & Rogers, KH (1985). Seasonality/aseasonality of aquatic macrophytes in Southern Hemisphere inland waters. *Hydrobiologia*, vol. 125, pp. 137-150.
- Mohtadi, M, Oppo, DW, Steinke, S, Stuut, J.-BW, De Pol-Holz, R, Hebbeln, D & Lückge, A (2011). Glacial to Holocene swings of the Australian-Indonesian monsoon. *Nature Geoscience*, vol. 4, pp. 540-544.
- Montoya, E, Rull, V & van Geel, B (2010). Non-pollen palynomorphs from surface sediments along an altitudinal transect of the Venezuelan Andes. *Palaeogeography, Palaeoclimatology, Palaeoecology*, vol. 297, pp. 169-183.
- Mooney, SD, Radford, KL & Hancock, G (2001). Clues to the 'burning question': Pre-European fire in the Sydney coastal region from sedimentary charcoal and palynology. *Ecological Management and Restoration*, vol. 2, pp. 203-212.
- Mooney, SD & Maltby, EL (2006). Two proxy records revealing the late Holocene fire history at a site on the central coast of New South Wales, Australia. *Austral Ecology*, vol. 31, pp. 682-695.
- Mooney, SD, Webb, M & Attenbrow, V (2007). A comparison of charcoal and archaeological information to address the influences on Holocene fire activity in the Sydney basin. *Australian Geographer*, vol. 38, pp. 177-194.
- Mooney, SD, Harrison, SP, Bartlein, PJ, Daniau, A -L, Stevenson, J, Brownlie, KC, Buckman, S, Cupper, M, Luly, J, Black, M, Colhoun, E, D'Costa, D, Dodson, J, Haberle, S, Hope, GS, Kershaw, P, Kenyon, C, McKenzie, M & Williams, N (2011). Late Quaternary fire regimes of Australia. *Quaternary Science Review*, vol. 30, pp. 28-46.
- Moore, PD, Webb, JA & Collinson, ME (1991). *Pollen Analysis (2nd Ed)*, Blackwell Scientific Publications, London, pp. 216.

Moreno, PI, Jacobson, GLJ, Lowell, TV & Denton, GH (2001). Interhemispheric climate links revealed by a late-glacial cooling episode in southern Chile. *Nature*, vol. 409, pp. 804-808.

Morgan, JW (2004). Bryophyte composition in a native grassland community subjected to different long-term fire regimes. *Cunninghamia*, vol. 8, pp. 485-489.

Morgan, WR (1968). The petrology of some Cainozoic basalt rocks from the Atherton Tableland and Einasleigh-Mount Garnet areas, North Queensland, *Proceedings of the Royal Society of Queensland*, vol. 80, pp. 1-12.

Moros, M, De Deckker, P, Jansen, E, Perner, K & Telford, RJ (2009). Holocene climate variability in the Southern Ocean recorded in a deep-sea sediment core off South Australia. *Quaternary Science Reviews*, vol. 28, pp. 1932-1940.

Morrison, KD (1994). Monitoring regional fire history through size-specific analysis of microscopic charcoal: the last 600 years in South India. *Journal of Archaeological Science*, vol. 21, pp. 675-685.

Morwood, MJ & Hobbs, D (eds.). (1995). Quinkan Prehistory: the Archaeology of Aboriginal Art in SE Cape York Peninsula, Australia. *Tempus*, vol. 3, University of Queensland, Brisbane, pp. 208.

Moss, PT (1999). Late Quaternary environments of the humid tropics of northeastern Australia, PhD Thesis, Monash University, Clayton, pp

Moss, PT & Kershaw, AP (2000). The last glacial cycle from the humid tropics of northeastern Australia: a comparison of a terrestrial and a marine record. *Palaeogeography, Palaeoclimatology, Palaeoecology*, vol. 155, pp. 155-176.

Moss, PT & Kershaw, AP (2007). A late Quaternary marine palynological record (oxygen isotope stages 1 to 7) for the humid tropics of northeastern Australia based on ODP Site 820. *Palaeogeography, Palaeoclimatology, Palaeoecology*, vol. 251, pp. 4-22.

Moss, PT, Tibby, J, Petherick, L, McGowan, H & Barr, C (2013). Late Quaternary vegetation history of North Stradbroke Island, Queensland, eastern Australia. *Quaternary Science Reviews*, vol. 74, pp. 257-272.

Moy, CM, Seltzer, GO, Rodbell, DT & Anderson, DM (2002). Variability of El Nino/Southern Oscillation activity at millennial timescales during the Holocene epoch. *Nature*, vol. 420, pp. 162-165.

Mudie, PJ, Marret, F, Rochon, A & Aksu, AE (2010). Non-pollen palynomorphs in the Black Sea corridor. *Vegetation History and Archaeobotany*, vol. 19, pp. 531-544.

Muller, J, Wüst, RAJ, Weiss, D & Hu, Y (2006). Geochemical and stratigraphic evidence of environmental change at Lynch's Crater, Queensland, Australia. *Global and Planetary Change*, vol. 53, pp. 269-277.

Muller, J, Kylander, M, Martinez-Cortizas, A, Wüst, RAJ, Weiss, D, Blake, K, Coles, B & Garica-Sanchez, R (2008a). The use of principle component analyses in characterising trace and major elemental distribution in 55 kyr peat deposit in tropical Australia: implications to paleoclimate. *Geochimica et Cosmochimica Acta*, vol. 72, pp. 449-463.

Muller, J, Kylander, M, Wust, RAJ, Weiss, D, Martinez-Cortizas, A, LeGrande, AN, Jennerjahn, T, Behling, H, Anderson, WT & Jacobson, G (2008b). Possible evidence for wet Heinrich phases

- in tropical NE Australia: the Lynch's Crater deposit. *Quaternary Science Reviews*, vol. 27, pp. 468-475.
- Muller, J, McManus, JF, Oppo, DW & Francois, R (2012). Strengthening of the northwest monsoon over the Flores Sea, Indonesia, at the time of Heinrich event 1. *Geology*, vol. 40, pp. 635-638.
- Muller, RA & MacDonald, GJ (2000). *Ice ages and astronomical causes: data, spectral analysis and mechanisms*, Springer-Verlag, New York, pp. 318.
- Mumbi, CT, Marchant, R, Hooghiemstra, H & Wooller, MJ (2008). Late Quaternary vegetation reconstruction from the Eastern Arc Mountains, Tanzania. *Quaternary Research*, vol. 69, pp. 326-341.
- Murphy, BP & Russell-Smith, J (2010). Fire severity in a northern Australian savanna landscape: the importance of time since previous fire. *International Journal of Wildland Fire*, vol. 19, pp. 46-51.
- Murphy, BP, Bradstock, RA, Boer, MM, Carter, J, Cary, GJ, Cochrane, MA, Fensham, RJ, Russell-Smith, J, Williamson, GJ & Bowman, DMJS (2013). Fire regimes of Australia: a pyrogeographic model system. *Journal of Biogeography*, vol. 40, pp. 1048-1058.
- Murphy, BP, Lehmann, CER, Russell-Smith, J & Lawes, MJ (2014). Fire regimes and woody biomass dynamics in Australian savannas. *Journal of Biogeography*, vol. 41, pp. 133-144.
- Mustaphi, CJC & Pisaric, MFJ (2014). A classification for macroscopic charcoal morphologies found in Holocene lacustrine sediments. *Progress in Physical Geography*, vol. 38(6), pp. 734-754.
- Mworia-Maitima, J (1997). Prehistoric fires and land-cover change in western Kenya: evidences from pollen, charcoal, grass cuticles and grass phytoliths. *The Holocene*, vol. 7, pp. 409-417.
- Ngadjonji Antiquity, (2004). Traditional knowledge of the Ngadjonji and Yidinji rainforest people. <http://earthsci.org/aboriginal/index.html>, viewed 2007.
- NCDC (National Climate Data Centre), (2006). <http://www.ncdc.noaa.gov/data-access/paleoclimatology-data/2006>
- Neff, U, Burns, SJ, Mangini, A, Mudelsee, M, Fleitmann, D & Matter, A (2001). Strong coherence between solar variability and the monsoon in Oman between 9 and 6 ka ago. *Nature*, vol. 411, pp. 290-293.
- Neldner, VJ, Kirkwood, AB & Collyer, BS (2004). Optimum time for sampling floristic diversity in tropical eucalypt woodlands of northern Queensland. *The Rangeland Journal*, vol. 26, pp. 190-203.
- Nix, HA & Switzer, MA (1991). *Rainforest animals, atlas of vertebrates endemic to Australia's wet tropics* Kowari 1, Australian Parks and Wildlife Service Publication, Canberra, pp. 112.
- Njankouo, JM, Dotreppe, J –C & Franssen, J –M (2005). Fire resistance of timbers from tropical countries and comparison of experimental charring rates with various models. *Construction and Building Materials*, vol. 19, pp. 376-386.
- Nott, JF (2003). The urban geology of Cairns, Australia. *Quaternary International*, vol. 103, pp. 75-82.

- Nott, JF & Price, DM (1999). Waterfalls, floods and climate change: evidence from tropical Australia. *Earth and Planetary Science Letters*, vol. 171, pp. 267-276.
- Nott, J, Thomas, MF & Price, DM (2001). Alluvial fans, landslides and Late Quaternary climatic change in the wet tropics of northeast Queensland. *Australian Journal of Earth Sciences*, vol. 48, pp. 875-882.
- Novakov, T, Cachier, H, Clark, JS, Gaudichet, A, Macko, S & Masclet, P (1997). Characterisation of particulate products of Biomass Combustion. in JS, Clark, H, Cachier, JS, Goldammer & B, Stocks (eds.). *Sediment Records of Biomass Burning and Global Change*, Springer-Verlag, Germany, pp. 117-143.
- O'Connell, JF, Allen, J, Williams, MAJ, Williams, AN, Turney, CSM, Spooner, NA, Kamminga J, Brown, G & Cooper, A (2018). When did *Homo sapiens* first reach Southeast Asia and Sahul? *PNAS*, vol. 115, pp. 8482-8490.
- Ohlson, M & Tryterud, E (2000). Interpretation of the charcoal record in forest soils: fires and their production and deposition of macroscopic charcoal. *The Holocene*, vol. 10, pp. 519-525.
- Oksanen, J & Minchin, PR (1997). Instability of ordination results under changes in input data order: explanations and remedies. *Journal of Vegetation Science*, vol. 8, pp. 447-454.
- Ollier, CD (1967). Maars, their characteristics, varieties and definition. *Bulletin of Volcanology*, vol. 31, pp. 45-73.
- Olsson, I (1986). Radiocarbon dating. in BE, Berglund (ed.). *Handbook of Holocene Palaeoecology and Palaeohydrography*, John Wiley & Sons, Chichester, pp. 273.
- Orvis, KH, Lane, CS & Horn, SP (2005). Laboratory production of vouchered reference charcoal from small wood samples and non-woody plant tissues. *Palynology*, vol. 29(1), pp. 1-11.
- Page, MC, Dickens, GR & Dunbar, GB (2003). Tropical view of Quaternary sequence stratigraphy: Siliciclastic accumulation on slopes east of the Great Barrier Reef since the Last Glacial Maximum. *Geology*, vol. 31, pp. 1013-1016.
- Pannell, S (2005). *Yamani Country: A spatial history of the Atherton Tableland, north Queensland*, Cooperative Research Centre for Tropical Rainforest Ecology and Management, Rainforest CRC, Cairns, pp. 112.
- Parsons, WT & Cuthbertson, EG (2001). *Noxious Weeds of Australia*, CSIRO Publishing, Victoria.
- Patterson, WA, Edwards, KJ & Maguire, KJ (1987). Microscopic charcoal as a fossil indicator of fire. *Quaternary Science Review*, vol. 6, pp. 3-23.
- Pausas, JG & Keeley, JE (2009). A burning story: the role of fire in the history of life. *Bioscience*, vol. 59, pp. 593-601.
- Pearce, C, Andrews, JT, Bouloubassi, I, Hillaire-Marcel, C, Jennings, AE, Olsen, J, Kuijpers, A & Seidenkrantz, MS (2015). Heinrich 0 on the east Canadian margin: Source, distribution and timing. *Paleoceanography and Paleoclimatology*, vol. 30, pp. 1613-1624.
- Pedro, J, Bostock, HC, Bitz, C, He, F, Vandergoes, MJ, Steig, EJ, Chase, BM, Krause, CE, Rasmussen, SO, Markle, B & Cortese, G (2016). The spatial extent and dynamics of the Antarctic Cold Reversal. *Nature Geoscience*, vol. 9, pp. 51-55.

- Peeters, PJ & Butler, DW (2014). *Eucalypt open-forests: regrowth benefits management guideline*. Department of Science, Information Technology, Innovation and the Arts, Brisbane, pp.1-49.
- Perry, CT & Smithers, SG (2011). Cycles of coral reef ‘turn-on’, rapid growth and ‘turn-off’ over the past 8500 years; a context for understanding modern ecological states and trajectories. *Global Change Biology*, vol. 17, pp. 76-86.
- Pestiaux, P, van der Mersch, I, Berger, A & Duplessy, JC (1988). Paleoclimatic variability at frequencies ranging from 1 cycle per 10 000 years to 1 cycle per 1000 years: evidence for nonlinear behaviour of the climate system. *Climate Change*, vol. 12, pp. 9-37.
- Petherick, L, McGowan, H & Moss, P (2008). Climate variability during the Last Glacial Maximum in eastern Australia: evidence of two stadials? *Journal of Quaternary Science*, vol. 23, pp. 787-802.
- Petherick, L, Moss, PT & McGowan, HA (2011). Climatic and environmental variability during the termination of the Last Glacial Stage in coastal Australia: a review. *Australian Journal of Earth Sciences*, vol. 58, pp. 563-577.
- Petherick, LM, Moss, PT & McGowan, HA (2016). An extended Last Glacial Maximum in subtropical Australia. *Quaternary International*, vol. 432, pp. 1-12.
- Petit, J, Jouzel, J, Reynard, D, Barkov, NI, Barnola, JM, Basile, I, Bender, M, Chappellaz, J, Davis, M, Delaygue, G, Delmotte, M, Kotlyakov, VM, Legrand, M, Lipenkov, VY, Lorius, C, Pepin, L, Ritz, C, Saltzman, E & Stievenard, M (1999). Climate and atmospheric history of the past 420,000 years from the Vostok ice core, Antarctica. *Nature*, vol. 399, pp. 429-436.
- Pike, KM (1956). Pollen morphology of Myrtaceae from the south-west Pacific area. *Australian Journal of Botany*, vol. 4, pp. 13-53.
- Pillans, B (1997). Soil development at snails’s pace: evidence from a 6 Ma soil chronosequence on basalt in north Queensland, Australia. *Geoderma*, vol. 80, pp. 117-128.
- Piotrowska, N, Blaauw, M, Mauquoy, D & Chambers, FM (2011). Constructing deposition chronologies for peat deposits using radiocarbon dating. *Mires and Peats*, vol. 7(10), pp.1-14.
- Pires, MM, Guimarães Jr, PR, Galetti, M and Jordano, P (2018). Pleistocene megafaunal extinctions and the functional loss of long-distance seed-dispersal services. *Ecography*, vol. 41, pp. 153-163.
- Pisaric, MFJ (2002). Long-distance transport of terrestrial plant material by convection resulting from forest fires. *Journal of Paleolimnology*, vol. 28, pp. 349-354.
- Pitkänen, A, Lehtonen, H & Huttunen, P (1999). Comparison of sedimentary microscopic charcoal particle records in a small lake with dendrochronological data: evidence for the local origin of microscopic charcoal produced by forest fires of low intensity in eastern Finland. *The Holocene*, vol. 9, pp. 559-567.
- Pittock, AB (2009). *Climate Change: The science, impacts and solutions* (2nd edition), CSIRO Publishing, Melbourne, pp. 350.
- Polach, H & Singh, G (1980). Contemporary ¹⁴C levels and their significance to sedimentary history of Bega Swamp, New South Wales. *Radiocarbon* vol. 22, pp. 398-409.
- Post, WM, Tsung-Hung, P, Emanuel, WR, King, AW, Dale, VH & DeAngelis, DL (1990). The Global Carbon Cycle. *American Scientist*, vol. 78, pp. 310-326.

- Power, MJ, Whitlock, C, Bartlein, P & Stevens, LR (2006). Fire and vegetation history during the last 3800 years in northwestern Montana. *Geomorphology*, vol. 75, pp. 420-436.
- Power, MJ, Marlon, JR, Bartlein, PJ & Harrison, SP (2010). Fire history and the global charcoal database: a new tool for hypothesis testing and data exploration. *Palaeogeography, Palaeoclimatology, Palaeoecology*, vol. 291, pp. 52-59.
- Prager, A, Barthelmes, A, Theuerkauf, M & Joosten, H (2006). Non-pollen palynomorphs from modern Alder carrs and their potential for interpreting microfossil data from peat. *Review of Palaeobotany and Palynology*, vol. 141, pp. 7-31.
- Pyne, SJ (2001). *Fire : a brief history*, University of Washington Press, Seattle, pp. 204.
- Quigley, MC, Horton, T, Hellstrom, JC, Cupper, ML & Sandiford, M (2010). Holocene climate change in arid Australia from speleothem and alluvial records. *The Holocene*, vol. 20, pp. 1093-1104.
- Quinn, G & Keough, M (2002). *Experimental design and data analysis for biologists*, Cambridge University Press, Cambridge, pp. 537.
- Radiocarbon Laboratory, ANU (2020). Radiocarbon dating: background. ANU Radiocarbon Laboratory, Canberra, viewed 22nd June, 2020, <http://rsl.anu.edu.au/research/facilities/anu-radiocarbon-laboratory/radiocarbon-dating-background>
- Rahmstorf, S (2003). Timing of abrupt climate change: A precise clock. *Geophysical Research Letters*, vol. 30, NO. 10, 1510, doi:10.1029/2003GL017115.
- Rahmstorf, S & Schellnhuber, (2006).
<http://www.global-greenhouse-warming.com/Milankovitch-cycles.html>).
- Randall, DA, Wood, S, Bony, R, Colman, T, Fichet, J, Fyfe, V, Kattsov, A, Pitman, J, Shukla, J, Srinivasan, RJ, Stouffer, A, Sumi & Taylor, KE (2007) Climate Models and Their Evaluation. In *Climate Change 2007: The Physical Science Basis. Contribution of Working Group I to the Fourth Assessment Report of the Intergovernmental Panel on Climate Change*, Solomon, SD, Qin, M, Manning, Z, Chen, M, Marquis, KB, Averyt, M, Tignor and Miller, HL (eds.). Cambridge University Press, Cambridge, United Kingdom and New York, NY, USA.
- Raper, D & Bush, M (2009). A test of *Sporormiella* representation as a predictor of megaherbivore presence and abundance. *Quaternary Research*, vol. 71, pp. 490-496.
- Rasmusson, EM & Wallace, JM (1983). Meteorological aspects of the El Niño/Southern Oscillation. *Nature*, vol. 222, pp. 1195-1202.
- Rees, ABH, Cwynar, LC & Fletcher, MS (2015). Southern Westerly Winds submit to the ENSO regime: A multiproxy paleohydrology record from Lake Dobson, Tasmania. *Quaternary Science Reviews*, vol. 126, pp. 254-263.
- Reeves, JM, Chivas, AR, Garcia, A, Holt, S, Couapel, MJJ, Jones, BG, Cendón, DI & Fink, D (2008). The sedimentary record of palaeoenvironments and sea-level change in the Gulf of Carpentaria, Australia, through the last glacial cycle. *Quaternary International*, vol. 183, pp. 3-22.
- Reeves, JM, Barrows, TT, Cohen, TJ, Kiem, AS, Bostock, HC, Fitzsimmons, KE, Jansen, JD, Kemp, J, Krauss, C, Petherick, L, Phipps, SJ & OZ-INTIMATE Members (2013a). Climate variability over the last 35,000 years recorded in marine and terrestrial archives in the Australian region: an OZ-INTIMATE compilation. *Quaternary Science Reviews*, vol. 74, pp. 21-34.

Reeves, JM, Bostock, HC, Ayliffe, LK, Barrows, TT, De Deckker, P, Devriendt, LS, Dunbar, GB, Drysdale, RN, Fitzsimons, KE & Gagan, MK (2013b). Palaeoenvironmental change in tropical Australasia over the last 30,000 years – a synthesis by the OZ-INTIMATE group. *Quaternary Science Reviews*, vol. 74, pp. 97-114.

Reimer, PJ, Baillie, MGL, Bard, E, Bayliss, A, Beck, W, Bertrand, CJH, Blackwell, PG, Buck, CE, Burr, GS, Cutler, KB, Damon, PE, Edwards, RL, Fairbanks, RG, Friedrich, M, Guilderson, TP, Hogg, AG, Hughen, KA, Kromer, B, McCormac, G, Manning, S, Bronk Ramsey, C, Reimer, RW, Remmele, S, Southon, JS, Stuiver, M, Talamo, S, Taylor, FW, van der Plicht & Weyhenmeyer, CE (2004). Intcal04 Terrestrial radiocarbon age calibration, 0-26 kyr BP. *Radiocarbon*, vol. 46, pp. 1029-1058.

Reimer, PJ, Bard, E, Bayliss, A, Beck, JW, Blackwell, PG, Bronk Ramsey, C, Grootes, PM, Guilderson, TP, Hafflidason, H, Hajdas, I, Hatt, C, Heaton, TJ, Hoffmann, DL, Hogg, AG, Hughen, KA, Kaiser, KF, Kromer, B, Manning, SW, Niu, M, Reimer, RW, Richards, DA, Scott, EM, Southon, JR, Staff, RA, Turney, CSM & van der Plicht, J (2013). IntCal13 and Marine 13 Radiocarbon age calibration curves 0-50,000 years cal BP. *Radiocarbon*, vol. 55(4), pp. 1869-1887.

Renbušs, M, Chilvers, GA & Pryor, LD (1973). Microbiology of an ashbed. *Proceedings of the Linnean Society of New South Wales*, vol. 97, pp. 302-311.

Rhodes, AN (1998). A method for the preparation and quantification of microscopic charcoal from terrestrial and lacustrine sediment cores. *The Holocene*, vol. 8, pp. 113-117.

Rial, JA & Anaclerio, CA (2000). Understanding nonlinear responses of the climate system to orbital forcing. *Quaternary Science Review*, vol. 19, pp. 1709-1722.

Richardson, MJ (2001). Diversity and occurrence of coprophilous fungi. *Mycological Research*, vol. 105, pp. 387-402.

Roberts, J, Casanova, MT, Morris, K & Papas, P (2017). *Vegetation recovery in inland wetlands: an Australian perspective*. Arthur Rylah Institute for Environmental Research, Technical Report Series No. 270. Department of Environment, Land, Water and Planning, Heidelberg, Victoria.

Roth, S & Reijmer, JJG (2005). Holocene millennial to centennial carbonate cyclicity recorded in slope sediments of the Great Bahama Bank and its climatic implications. *Sedimentology*, vol. 52, pp. 161-181.

Roubik, DW & Moreno, JEP (1991). *Pollen and Spores of Barro Colorado Island*, Monographs in Systematic Botany, No.36. Missouri Botanical Garden, St Louis, Missouri, pp. 274.

Rowe, C (2007a). A palynological investigation of Holocene vegetation change in Torres Strait, seasonal tropics of northern Australia. *Palaeogeography, Palaeoclimatology, Palaeoecology*, vol. 25, pp. 83-103.

Rowe, C (2007b). Vegetation change following mid-Holocene marine transgression of the Torres Strait shelf: a record from the island of Mua, northern Australia. *The Holocene*, vol. 17, pp. 927-937.

Rowe, C, Brand, M, Hutley, LB, Wurster, C, Zwart, C, Levchenko, V & Bird, M (2019). Holocene savanna dynamics in the seasonal tropics of northern Australia. *Review of Palaeobotany and Palynology*, vol. 267, pp. 17-31.

Rowley, JR & Rowley, J (1956). Vertical migration of spherical and aspherical pollen in a Sphagnum bog. *Proceedings Minnesota Academy of Science*, vol. 24, pp. 2-30.

- Rucina, SM, Muiruri, M, Kinyanjui, RN, McGuiness, K & Marchant, R (2009). Late Quaternary vegetation and fire dynamics on Mount Kenya. *Palaeogeography, Palaeoclimatology, Palaeoecology*, vol. 283, pp. 1-14.
- Rule, S (2001). A high resolution palaeoecological study within the late Quaternary: The demise of the Araucarian forest around Lynch's Crater, Northeast Queensland, BA (Hons), Monash University, Melbourne, pp. 90.
- Rule, S, Brook, BW, Haberle, SG, Turney, CSM, Kershaw, AP & Johnson, CN (2012). The aftermath of megafaunal extinction: ecosystem transformation in Pleistocene Australia. *Science*, vol. 335, pp. 1483-1486.
- Rull, V, Lopéz-Sáez, JA & Vegas-Vilarrúbia, T (2008). Contribution of non-pollen palynomorphs to the paleolimnological study of a high-altitude Andean lake (Laguna Verde Alta, Venezuela). *Journal of Paleolimnology*, vol. 40, pp. 399-411.
- Rumes, B, Eggermont, H & Verschuren, D (2005). Representation of aquatic invertebrate communities in subfossil death assemblages sampled along a salinity gradient of western Uganda crater lakes. *Hydrobiologia*, vol. 542, pp. 297-314.
- Russell-Smith, J, Lucas, D, Gapindi, M, Gunbunuka, B, Kipirigi, N, Namingum, G, Lucas, K, Giuliani, P & Chaloupka, G (1997). Aboriginal resource utilization and fire management practice in western Arnhem Land, monsoonal northern Australia: notes for prehistory, lessons for the future. *Human Ecology*, vol. 25, pp. 159-195.
- Russell-Smith, J, Whitehead, PJ, Cook, GD & Hoare, JL (2003). Response of *Eucalyptus*-dominated savannah to frequent fires: lessons from Munmarlary, 1973-1996. *Ecological Monographs*, vol. 73, pp. 349-375.
- Sainty, GR & Jacobs, SWL (1981). *Waterplants of New South Wales*, Water Resources Commission, New South Wales, Sydney, pp. 550.
- Salinger, MJ, Renwick, JA & Mullan, AB (2001). Interdecadal Pacific Oscillation and South Pacific Climate. *International Journal of Climatology*, vol. 21, pp. 1705-1721.
- Salinger, MJ, McGree, S, Beucher, F, Power, SB & Delage, F (2014). A new index for variations in the position of the South Pacific convergence zone 1910/11-2011/2012. *Climate Dynamics*, vol. 43, pp. 881-892.
- Santoso, A, & Coauthors (2019). Dynamics and Predictability of El Niño-Southern Oscillation: An Australian perspective on progress and challenges. *Bulletin of American Meteorological Society*, vol. 100, pp. 403-420.
- Savage, P (1992). *Christie Palmerston, Explorer*, James Cook University, Townsville, pp. 289.
- Schenk, F, Välranta, M, Muschitiello, F, Tarasov, L, Heikkilä, M, Björck, S, Brandefelt, J, Johansson, AV, Näslund, J & Wohlfarth, B (2018). Warm summers during the Younger Dryas cold reversal. *Nature Communications*, vol. 9, 1634, <https://doi-org.virtual.anu.edu.au/10.1038/s41467-018-04071-5>.
- Schlachter, KJ & Horn, SP (2010). Sample preparation methods and replicability in macroscopic charcoal analysis. *Journal of Paleolimnology*, vol. 44, pp. 701-708.
- Schmidt, MWL & Noack, AG (2000). Black carbon in soils and sediments: analysis, distribution, implications, and current challenges. *Global biogeochemical cycles*, vol. 14, pp. 777-793.

- Schmidt, MW, Masiello, CA & Skjemstad, JO (2003). Final recommendations for reference materials in black carbon analysis. *Eos*, vol. 84, pp. 582-583.
- Schneider, T, Bischoff, T & Haug, GH (2014). Migrations and dynamics of the intertropical convergence zone. *Nature*, vol. 513, pp. 45-53.
- Schreuder, LT, Donders, TH, Mets, A, Hopmans, EC, Sinninghe Damsté, JS & Schouten, S (2019). Comparison of organic and palynological proxies for biomass burning and vegetation in a lacustrine sediment record (Lake Allom, Fraser Island, Australia). *Organic Geochemistry*, vol. 133, pp. 10-19.
- Schulz, M (2002). On the 1470-year pacing of Dansgaard-Oeschger warm events. *Paleoceanography and Paleoclimatology*, vol. 17(2), pp. 4-14-9.
- Schulz, M & Mudelsee, M (1997). Simultaneous presence of orbital inclination and eccentricity in proxy climate records from Ocean Drilling Program Site 806: Comment and Reply. *Geology*, vol. 25, pp. 860-862.
- Schulz, M & Statteger, K (1997). SPECTRUM: Spectral analysis of unevenly spaced palaeoclimatic time series. *Computers and Geoscience*, vol. 23, pp. 929-945.
- Schulz, M & Mudelsee, M (2002). REDFIT: estimating red-noise spectra directly from unevenly spaced palaeoclimatic time series. *Computers and Geoscience*, vol. 28, pp. 421-426.
- Schulz, M, Berger WH, Sarnthein, M & Grootes, PM (1999). Amplitude variations of 1470-year climate oscillations during the last 100,000 years linked to fluctuations of continental ice mass. *Geophysical Research Letters*, vol. 26, pp. 3385-3388.
- Schulz, M, Paul, A & Timmermann, A (2004). Glacial-interglacial contrast in climate variability at centennial-to-millennial timescales: observations and conceptual model. *Quaternary Science Reviews*, vol. 23, pp. 2219-2230.
- Schwandes, IP & Collins, ME (1994). Distribution and significance of freshwater sponge spicules in selected Florida soils. *Transactions of the American Microscopy Society*, vol. 113, pp. 242-257.
- Scott, AC (2000). The Pre-Quaternary history of Fire. *Palaeogeography, Palaeoclimatology, Palaeoecology*, vol. 164, pp. 297-345.
- Scott, AC (2010). Charcoal recognition, taphonomy and uses in palaeoenvironmental analysis. *Palaeogeography, Palaeoclimatology, Palaeoecology*, vol. 291, pp. 11-39.
- Scott, AC & Glasspool, IJ (2007). Observations and experiments on the origin and formation of inertinite group macerals. *International Journal of Coal Geology*, vol. 70, pp. 53-66.
- Scott, AC, Lomax, BH, Collinson, ME, Upchurch, GR & Beerling, DJ (2000). Fire across the K-T boundary: initial results from the Sugarite Coal, New Mexico, USA. *Palaeogeography, Palaeoclimatology, Palaeoecology*, vol. 167, pp. 381-395.
- Scott, L (1992). Environmental implications and origin of microscopic *Pseudoschizaea* Thiergart and Frantz ex R. Potonié emend. in sediments. *Journal of Biogeography*, vol. 19, pp. 349-354.
- Scotter, DR (1970). Soil temperature under grass fires. *Australian Journal of Soil Research*, vol. 8, pp. 273-279.

- Semeniuk, V & Semeniuk, CA (2004). Sedimentary fill of basin wetlands, central Swan Coastal Plain, southwestern Australia, Part 1: sediment particles, typical sediments and classification of depositional systems. *Journal of the Royal Society of Western Australia*, vol. 87, pp. 139-186.
- Senyanzobe, JMV, Mulei, JM, Bizuru, E & Nsengimuremyi, C (2020). Impact of *Pteridium aquilinum* on vegetation in Nyungwe Forest, Rwanda. *Heliyon*, vol. 6(9), e04806.
- Shakesby, RA & Doerr, SH (2006). Wildfire as a hydrological and geomorphological agent. *Earth Science Reviews*, vol. 74, pp. 269-307.
- Sharp, BR & Bowman, DMJS (2004). Net woody vegetation increase confined to seasonally inundated lowlands in an Australian tropical savanna, Victoria River District, Northern Territory. *Austral Ecology*, vol. 29, pp. 667-683.
- Shibayama, Y & Kadono, Y (2007). Reproductive success and genetic structure of populations of the heterostylous aquatic plant *Nymphoides indica* (L.) Kuntze (Menyanthaceae). *Aquatic Botany*, vol. 86, pp. 1-8.
- Shore, JS, Bartley, DD & Harkness, DD (1995). Problems encountered with the ^{14}C dating of peat. *Quaternary Science Reviews*, vol. 14, pp. 373-383.
- Shulmeister, J (1992). A Holocene pollen record from lowland tropical Australia. *The Holocene*, vol. 2, pp. 107-116.
- Shulmeister, J & Lees, BG (1995). Pollen evidence from tropical Australia for the onset of an ENSO-dominated climate at c. 4000 BP. *The Holocene*, vol. 5, pp. 10-18.
- Sikes, EL, Howard, WR, Samson, CR, Mahan, TS, Robertson, LG & Volkman, JK (2009). Southern ocean seasonal temperature and subtropical front movement on the South Tasman Rise in the late Quaternary. *Paleoceanography and Paleoclimatology*, vol. 24, doi:10.1029/2008PA001659.
- Simmons, IG & Innes, JB (1981). Tree remains in a North York Moors peat profile. *Nature*, vol. 294, pp. 76-78.
- Singer, DK, Jackson, ST, Madsen, BJ & Wilcox, DA (1996). Differentiating climatic and successional influences on long-term development of a marsh. *Ecology*, vol. 77, pp. 1765- 1778.
- Singh, G, Kershaw, AP & Clark, R (1981). Quaternary vegetation and fire history in Australia. in AM, Gill, RH, Groves & IR, Noble (eds.). *Fire and the Australian Biota*, Australian Academy of Science, Canberra, pp. 582.
- Singh, D & Geissler, EA (1985). Late Cainozoic history of vegetation, fire, lake levels and climate at Lake George, New South Wales, Australia. *Philosophical Transactions of the Royal Society of London B*, vol. 311, pp. 379-447.
- Sirocko, F, Garbe-Schönberg, D, McIntyre, A & Molino, B (1996). Teleconnections between the subtropical monsoons and high-latitude climates during the last deglaciation. *Science*, vol. 272, pp. 526-529.
- Sjöström, JK, Cortizas, AM, Hansson, SV, Sánchez, NS, Bindler, R, Rydberg, J, Mörtz, CM, Ryberg, EE & Kylander, ME (2020). Paleodust deposition and peat accumulation rates – Bog size matters. *Chemical Geology*, vol. 554, 119795.
- Skilbeck, GC, Rolph, TC, Hill, N, Woods, J & Wilkens, RH (2005). Holocene millennial/centennial-scale multiproxy cyclicity in temperate eastern Australian estuary sediments. *Journal of Quaternary Science*, vol. 20, pp. 327-347.

Skinner, LC, Primeau, F, Freeman, E, de la Fuente, M, Goodwin, PA, Gottschalk, J, Huang, E, McCave, IN, Noble, TL & Scrivner, AE (2017). Radiocarbon constraints on the glacial ocean circulation and its impact on atmospheric CO₂. *Nature Communications*, vol. 8 (16010), doi: 10.1038/ncomms16010.

Skinner, L, Menviel, L, Broadfield, L, Gottschalk, J & Greaves, M (2020). Southern Ocean convection amplified past Antarctic warming and atmospheric CO₂ rise during Heinrich Stadial 4. *Communications Earth and Environment*, vol.1, 23, <https://doi.org/10.1038/s43247-020-00024-3>.

Small, E & Darbyshire, SJ (2011). Blossoming treasures of biodiversity. *Biodiversity*, vol. 12, pp. 119-128.

Smith, IR, Withers, K & Billingsley, J (2007). Maintaining the ancient bunya tree (*Araucaria bidwillii* Hook) – dispersal and mast years. In presentation given at the 5th Southern Connection Conference, South Australia, Adelaide.

Smith, MA, Williams, AN, Turney, CSM & Cupper, ML (2008). Human-environment interactions in Australian drylands: exploratory time-series analysis of archaeological records. *The Holocene*, vol. 18, pp. 389-401.

Sonneman, JA, Sincock, A, Fluin, J, Reid, M, Newall, P, Tibby, J & Gell, P (1999). *An illustrated guide to common stream diatom species from temperate Australia*, Cooperative Research Centre for Freshwater Ecology, Identification Guide No. 33, Albury NSW, pp. 166.

Spessa, A, McBeth, B & Prentice, C (2005). Relationships among fire frequency, rainfall and vegetation patterns in the wet-dry tropics of northern Australia: an analysis based on NOAA-AVHRR data. *Global Ecology and Biogeography*, vol. 14, pp. 439-454.

Spicer, RA (1989). The formation and interpretation of plant fossil assemblages. *Advances in Botanical Research*, vol. 16, pp. 95-191.

Stahle, LN, Chin, H, Haberle, S & Whitlock, C (2017). Late-glacial and Holocene records of fire and vegetation from Cradle Mountain National Park, Tasmania, Australia. *Quaternary Science Reviews*, vol. 177, pp. 57-77.

Stanton, P (1995). A tropical Queensland perspective' in DB, Bird (ed) *Country in Flames* Proceedings of the 1994 symposium on biodiversity and fire in North Australia, Department of the Environment, Sport and Territories and the North Australian Research Unit, Canberra and Darwin.

StatSoft, Inc (2011). *STATISTICA*, (data analysis software system), version 10. www.statsoft.com.

Stephens, KM & Dowling, RM (2002). *Wetland plants of Queensland, a field guide*, CSIRO Publishing, Collingwood, pp. 145.

Stephenson, PJ, Griffin, TJ & Sutherland, FL (1980). Cainozoic volcanism in northeastern Australia. in RA, Henderson & PJ, Stephenson (eds.). *The Geology and Geophysics of Northeastern Australia*, Geological Society of Australia Inc., Queensland Division, Brisbane, pp. 349-372.

Stevenson, J & Hope, G (2005). A comparison of late Quaternary forest changes in New Caledonia and northeastern Australia. *Quaternary Research*, vol. 64(3), pp. 372-383.

Stevenson, J, Brockwell, S, Rowe, C, Proske, U & Shiner, J (2015). The palaeo-environmental history of Big Willum Swamp, Weipa: an environmental context for the archaeological record. *Australian Archaeology*, vol. 80, pp. 17-31.

Stivrins, N, Aakala, T, Livonen, L, Pasanen, L, Kuuluvainen, T, Vasander, H, Galka, M, Disbrey, HR, Liepins, J, Holmström, L & Seppä, H (2019). Integrating fire-scar, charcoal and fungal spore data to study fire events in the boreal forest of northern Europe. *The Holocene*, vol. 29, pp. 1480-1490.

Stocker, GC & Irvine, AK (1983). Seed dispersal by Cassowaries (*Casuarius casuarius*) in north Queensland's rainforests. *Biotropica*, vol. 15, pp. 170-176.

Stocker, GC, Thompson, WA, Irvine, AK, Fitzsimon, JD & Thomas, PR (1995). Annual patterns of litterfall in a lowland and tableland rainforest in tropical Australia. *Biotropica*, vol. 27, pp. 412-420.

Stott, L, Poulsen, C, Lund, S & Thunell, R (2002). Super ENSO and Global Climate Oscillations at Millennial Time Scales. *Science*, vol. 297, pp. 222-226.

Street-Perrott, FA & Barker, PA (2008). Biogenic silica: a neglected component of the coupled global continental biogeochemical cycles of carbon and silicon. *Earth Surface Processes and Landforms*, vol. 33, pp. 1436-1457.

Sturman, A & Tapper, N (1996). *The Weather and Climate of Australia and New Zealand*, Oxford University Press, Australia, pp. 476.

Sturman, A & Tapper, N (2006). *The Weather and Climate of Australia and New Zealand* Oxford University Press, Australia, pp. 476.

Subbotin, AN (2003). Special features of propagation of peat fire. *Journal of Engineering Physics and Thermophysics*, vol. 76, pp. 1145-1153.

Sumner, G & Bonell, M (1986). Circulation and daily rainfall in the north Queensland wet seasons 1979-1982. *Journal of Climatology*, vol. 6, pp. 531-549.

Suppiah, R (1992). The Australian summer monsoon: a review. *Progress in Physical Geography*, vol. 16(3), pp. 283-318.

Tachikawa, K, Vidal, L, Sonzogni, C & Bard, E (2009). Glacial/interglacial sea surface temperature changes in the southwest Pacific Ocean over the past 360 ka. *Quaternary Science Reviews*, vol. 28, pp. 1160-1170.

Taffs, KH, Logan, B, Parr, JF & Jacobsen, GE (2012). The evolution of a coastal peatland at Byron Bay, Australia: multi-proxy evidence from the microfossil record. in SG, Haberle & B, David (eds.). *Terra Australis 34: peopled landscapes: archaeological and biogeographic approaches to landscapes*, ANU E-press, Canberra, Australia, pp. 429-442.

Tauber, H (1965). Differential pollen deposition and the interpretation of pollen diagrams. *Dan. Geol. Unders. Ser.III*, vol. 89, pp. 66.

Tauber, H (1967). Investigations of the mode of pollen transfer in forested areas. *Review of Palaeobotany and Palynology*, vol. 3, pp. 277-286.

ter Braak, CJF & Šmilauer, P (2002). *CANOCO reference manual and CanoDraw for Windows user's guide: software for Canonical community ordination (version 4.5)*, Microcomputer power, Ithaca, New York, pp. 500.

- Thevenon, F, Williamson, D, Bard, E, Anselmetti, FS, Beaufort, L & Cachier, H (2010). Combining charcoal and elemental black carbon analysis in sedimentary archives: implications for past fire regimes, the pyrogenic carbon cycle and the human-climate interactions. *Global and Planetary Change*, vol. 72, pp. 381-389.
- Thomas, MF, Nott, J & Price, DM (2001). Late Quaternary stream sedimentation in the humid tropics: a review with new data from NE Queensland, Australia. *Geomorphology*, vol. 39, pp. 53-68.
- Thomas, MF, Nott, J, Murray, AS & Price, DM (2007). Fluvial response to late Quaternary climate change in NE Queensland, Australia. *Palaeogeography, Palaeoclimatology, Palaeoecology*, vol. 251, pp. 119-136.
- Thomas, ML, Warny, S, Jarzen, Bentley, SJ, Droxler, AW, Harper, BB, Nittrouer, CA & Xu, K (2018). Palynomorph evidence for tropical climate stability in the Gulf of Papua, Papua New Guinea, over the latest marine transgression and highstand (14,500 years BP to today). *Quaternary International*, vol. 467, pp. 277-291.
- Thornhill, AH (2010). Can Myrtaceae pollen of the Holocene from Bega Swamp be compared with extant taxa? *Terra Australia*, vol. 32, pp. 405-427.
- Thornhill, AH, Hope, GS, Craven, LA & Crisp, MD (2012a). Pollen morphology of the Myrtaceae. Part 1: tribes Eucalypteae, Lophostemoneae, Syncarpieae, Xanthostemoneae and subfamily Psiloxylloideae. *Australian Journal of Botany*, vol. 60, pp. 165-199.
- Thornhill, AH, Hope, GS, Craven, LA & Crisp, MD (2012b). Pollen morphology of the Myrtaceae. Part 2: tribes Backhousieae, Melaleuceae, Metrosidereae, Osbornieae and Syzygieae. *Australian Journal of Botany*, vol. 60, pp. 200-224.
- Thornhill, AH, Hope, GS, Craven, LA & Crisp, MD (2012c). Pollen morphology of the Myrtaceae. Part 3: tribes Chamelaucieae, Leptospermeae and Lindsayomyrteae. *Australian Journal of Botany*, vol. 60, pp. 225-259.
- Thornhill, AH, Hope, GS, Craven, LA & Crisp, MD (2012d). Pollen morphology of the Myrtaceae. Part 4: tribes Kanieae, Myrteae and Tristanieae. *Australian Journal of Botany*, vol. 60, pp. 260-289.
- Thunell, R, Anderson, D, Gellar, D & Miao, Q (1994). Sea-surface temperature estimates for the tropical western Pacific during the last glaciation and their implications for the Pacific Warm Pool. *Quaternary Research*, vol. 41, pp. 255-264.
- Tibby, J (2012). The younger dryas: relevant in the Australian region? *Quaternary International*, vol. 253, pp. 47-54.
- Tibby, J & Haberle, SG (2007). A late glacial to present diatom record from Lake Euramoo, wet tropics of Queensland, Australia. *Palaeogeography, Palaeoclimatology, Palaeoecology*, vol. 251, pp. 46-56.
- Tibby, J, Barr, C, Marshall, JC, McGregor, GB, Moss, PT, Arnold, LJ, Page, TJ, Questiaux, J, Olley, J, Kemp, J, Spooner, N, Petherick, L, Penny, D, Mooney, S & Moss, E (2017). Persistence of wetlands on North Stradbroke Island (south-east Queensland, Australia) during the last glacial cycle: implications for Quaternary science and biogeography. *Journal of Quaternary Science*, vol. 32, pp. 770-781.
- Tiffney, BH (1990) The collection and study of dispersed angiosperm fruit and seeds. *Palaios*, vol. 5, pp. 499-519.

- Tng, DYP, Williamson, GJ, Jordan, GJ & Bowman, DMJS (2012). Giant eucalypts – globally unique fire-adapted rain-forest trees? *New Phytologist*, vol. 196, pp. 1001-1014.
- Tolhurst, KG & Turvey, ND (1992). Effects of bracken (*Pteridium esculentum* (forst. f.) cockayne) on eucalypt regeneration in west-central Victoria. *Forest Ecology and Management*, vol. 54, pp. 45-67.
- Toohey, E (2001). *From bullock team to puffing billy: the settling of the Atherton Tableland and its hinterland*, Central Queensland University Press, Rockhampton, pp. 100.
- Tracey, JG (1982). *The Vegetation of the Humid Tropical Region of North Queensland*, CSIRO, Melbourne, pp. 124.
- Tracey, JG & Webb, LJ (1975a). *Vegetation of the humid tropical region of north Queensland*, Rainforest Ecology Unit, CSIRO Division of Plant Industry, Indooroopilly, Queensland.
- Tracey, JG & Webb, LJ (1975b). *Key to the vegetation of the humid tropical region of North Queensland, with 15 maps at 1:100,000 scale*, CSIRO, Long Pocket laboratories, Indooroopilly, Queensland.
- Trenberth, KE (1991). General characteristics of El Niño-Southern Oscillation. in MH, Glantz MH, RW, Katz & N, Nicholls (eds.). *Teleconnections Linking Worldwide Climate Anomalies*, Cambridge University Press, Cambridge, pp. 535.
- Tudhope, AW, Chilcott, CP, McCulloch, MT, Cook, ER, Chappell, J, Ellam, RM, Lea, DW, Lough, JM & Shimmield, GB (2001). Variability in the El Niño-Southern Oscillation through a Glacial-Interglacial Cycle. *Science*, vol. 291, pp. 1511-1516.
- Turner, BC (2001). Geographic distribution of *Neurospora* spore killer strains and strains resistant to killing. *Fungal Genetic Biology*, vol. 32, pp. 93-104.
- Turner, BC, Perkins, DD & Fairfield, A (2001). *Neurospora* from natural populations: a global study. *Fungal Genetic Biology*, vol. 32, pp. 67-92.
- Turney, CSM & Hobbs, D (2006). ENSO influence on Holocene Aboriginal populations in Queensland, Australia. *Journal of Archaeological Science*, vol. 33, pp. 1744-1748.
- Turney, CSM, Bird, ML, Fifield, LK, Roberts, RG, Smith, M, Dortch, CE, Grün, R, Lawson, E, Ayliffe, LK, Miller, GH, Dortch, J & Cresswell, RG (2001a). Early human occupation at Devil's Lair southwestern Australia 50,000 years ago. *Quaternary Research*, vol. 55, pp. 3-13.
- Turney, CSM, Kershaw, AP, Moss, P, Bird, MI, Fifield, LK, Cresswell, RG, Santos, GM, Di Tada, ML, Hausladen, PA & Zhou, Y (2001b). Redating the onset of burning at Lynch's Crater (North Queensland): implications for human settlement in Australia. *Journal of Quaternary Science*, vol. 16, pp. 767-771.
- Turney, CSM Bird, MI, Fifield, LK Kershaw, AP, Cresswell, RG, Santos, GM, Di Tada, ML, Hausladen, PA & Youping, Z (2001c). Development of a robust ^{14}C chronology for Lynch's Crater (North Queensland, Australia) using different pre-treatment strategies. *Radiocarbon*, vol. 43, pp. 45-54.
- Turney, CSM, Kershaw, AP, Clemens, SC, Branch, N, Moss, PT & Fifield, LK (2004). Millennial and orbital variations of El Niño/Southern Oscillation and high-latitude climate in the last glacial period. *Nature*, vol. 428, pp. 306-310.

Turney, CSM, Kershaw, AP, James, S, Branch, N, Cowley, J, Fifield, LK, Jacobsen, G & Moss, P (2006a). Geochemical changes recorded in Lynch's Crater, northeastern Australia, over the past 50 ka. *Palaeogeography, Palaeoclimatology, Palaeoecology*, vol. 23, pp. 187-203.

Turney, CSM, Haberle, S, Fink, D, Kershaw, AP, Barbetti, M, Barrows, TT, Black, M, Cohen, TJ, Corrège, T, Hesse, PP, Hua, Q, Johnston, R, Morgan, V, Moss, P, Nanson, G, van Ommen, T, Rule, S, Williams, NJ, Zhao, JX, D'Costa, D, Feng, YX, Gagan, M, Mooney, S & Xia, Q (2006b). Integration of ice-core, marine and terrestrial records for the Australian Last Glacial Maximum and Termination: a contribution from the OZ INTIMATE group. *Journal of Quaternary Science*, vol. 21, pp. 751-761.

Turney, CSM, Jones, RT, Phipps, SJ, Thomas, Z, Hogg, A, Kershaw, AP, Fogwill, CJ, Palmer, J, Bronk Ramsey, C, Adolphi, F, Muscheler, R, Hughen, KA, Staff, RA, Grosvenor, M, Golledge, NR, Rasmussen, SO, Hutchinson, DK, Haberle, S, Lorrey, A, Boswijk, G & Cooper, A (2017). Rapid global ocean-atmosphere response to Southern Ocean freshening during the last glacial. *Nature Communications*, vol. 8(520) DOI <https://doi.org/10.1038/s41467-017-00577-6>.

Turton, SM & Sexton, GJ (1996). Environmental gradients across four rainforest-open forest boundaries in northeastern Queensland. *Austral Ecology*, vol. 21, pp. 245-254.

Tweddle, JC & Edwards, KJ (2010). Pollen preservation zones as an interpretative tool in Holocene palynology. *Review of Palaeobotany and Palynology*, vol. 161, pp. 59-76.

Umbanhowar, CE & McGrath, MJ (1998). Experimental production and analysis of microscopic charcoal from wood, leaves and grasses. *The Holocene*, vol. 8, pp. 341-346.

Väliiranta, MM (2006). Long term changes in aquatic plant species composition in north-eastern European Russia and Finnish Lapland, as evidenced by plant macrofossil analysis. *Aquatic Botany*, vol. 85, pp. 224-232.

Väliiranta, M, Salonen, JS, Heikkilä, M, Amon, L, Helmens, K, Klimaschewski, A, Kuhry, P, Kultti, S, Poska, S, Veski, S & Birks, HH (2015). Plant macrofossil evidence for an early onset of the Holocene summer thermal maximum in northernmost Europe. *Nature Communications*, 6:6809 doi: 10.1038/ncomms7809.

van Bergen, PF, Goñi, M, Collinson, ME, Barrie, PJ, Sinninghe-Damsté, JS & de Leeuw, JW (1994). Chemical and microscopic characterization of outer seed coats of fossil and extant water plants. *Geochimica et Cosmochimica Acta*, vol. 58, pp. 3823-3844.

van den Broek, T, van Diggelen, R & Bobbink, R (2005). Variation in seed buoyancy of species in wetland ecosystems with different flooding dynamics. *Journal of Vegetation Science*, vol. 16, pp. 579-586.

Vandergoes, MJ, Newnham, RM, Preusser, F, Hendy, CH, Lowell, TV, Fitzsimons, SJ, Hogg, AG, Kasper, HW & Schlüchter, C (2005). Regional insolation forcing of late Quaternary climate change in the Southern Hemisphere. *Nature*, vol. 436, pp. 242-245.

van der Kaars, S & De Deckker, P (2002). A late Quaternary pollen record from deep sea core Fr10/95, GC17 offshore Cape Range Peninsula, northwestern Western Australia. *Review of Palaeobotany and Palynology*, vol. 120, pp. 17-39.

van der Kaars, S, Wang, X, Kershaw, AP, Guichard, F & Setiabudi, DA (2000). A late Quaternary palaeoecological record from the Banda Sea, Indonesia: patterns of vegetation, climate and biomass burning in Indonesia and northern Australia. *Palaeogeography, Palaeoclimatology, Palaeoecology*, vol. 155, pp. 135-153.

- van der Plicht, J & Hogg, A (2006). A note on reporting radiocarbon. *Quaternary Geochronology*, vol. 1, pp. 237-240.
- van Geel, B (1978). A palaeoecological study of holocene peat bog sections in Germany and The Netherlands, based on the analysis of pollen, spores and macro- and microscopic remains of fungi, algae, cormophytes and animals. *Review of Palaeobotany and Palynology*, vol. 25, pp. 1-120.
- van Geel, B (1986). Application of fungal and algal remains and other microfossils in palynological analyses. in BE, Berglund (ed.). *Handbook of Holocene Palaeoecology and Palaeohydrology*, Wiley, Chichester, pp. 497–505.
- van Geel, B (2001). Non-pollen palynomorphs. in JP, Smol, HJB, Birks & WM, Last (eds.). *Tracking environmental change using lake sediments; Vol 3: Terrestrial, algal and siliceous indicators*, Kluwer, Dordrecht, pp. 99-119.
- van Geel, B (2006). Fossil ascomycetes in Quaternary deposits. *Nova Hedwigia*, vol. 82, (2-3), pp. 313-329.
- van Geel, B & van der Hammen, T (1978). Zygnemataceae in quaternary Columbian sediments. *Review of Palaeobotany and Palynology*, vol. 25, pp. 377-391.
- van Geel, B, Bohncke, SJP & Dee, H (1981). A palaeoecological study of an upper Late Glacial and Holocene sequence from “De Borchert, The Netherlands. *Review of Palaeobotany and Palynology*, vol. 31, pp. 367-448.
- van Geel, B, Coope, GR & van der Hammen, T (1989). Palaeoecology and stratigraphy of the lateglacial type section at Usselo (the Netherlands). *Review of Palaeobotany and Palynology*, vol. 60, pp. 25-129.
- van Geel, B, Pals, JP, van Reenen, GBA & van Huissteden, J (1995). The indicator value of fossil fungal remains, illustrated by a palaeoecological record of a late Eemian/Weichselian deposit in the Netherlands. in GFW, Herngreen, & AG, van der Valk (eds.). *Neogene and Quaternary geology of north-west Europe Meded Rijks Geol. Dienst*, vol. 52, pp. 297-315.
- van Geel, B, Gelorini, V, Lyaruu, A, Aptroot, A, Rucina, S, Marchant, R, Sinnighe-Damsté, JS & Verschuren, D (2011). ‘Diversity and ecology of tropical African fungal spores from a 25,000-year palaeoenvironmental record in southeastern Kenya. *Review of Palaeobotany and Palynology*, vol. 164, pp. 174-190.
- van Meerbeeck, CJ, Renssen, H & Roche, DM (2009). How did Marine Isotope Stage 3 and Last Glacial Maximum climates differ? – Perspectives from equilibrium simulations. *Climates of the Past*, vol. 5, pp. 33-51.
- van Zant, K (1979). Late glacial and postglacial pollen and macrofossils from Lake West Okoboji, northwestern Iowa. *Quaternary Research*, vol. 12, pp. 358-380.
- Vanni re, B, Colombaroli, D, Chapron, E, Leroux, A, Tinner, W & Magny, M (2008). Climate versus human-driven fire regimes in Mediterranean landscapes: the Holocene record of Lago dell’Accesa (Tuscany, Italy). *Quaternary Science Reviews*, vol. 27, pp. 1181-1196.
- Vigilante, T & Bowman, DMJS (2004). Effects of fire history on the structure and floristic composition of woody vegetation around Kalumburu, North Kimberley, Australia: a landscape-scale natural experiment. *Australian Journal of Botany*, vol. 52, pp. 381-404.
- Voelker, AHL (2002). Global distribution of centennial-scale records for Marine Isotope Stage (MIS) 3: a database. *Quaternary Science Reviews*, vol. 21, pp. 1185-1212.

- Vogt, K, Rasran, L & Jensen, K (2004). Water-borne seed transport and seed deposition during flooding in a small river-valley in Northern Germany. *Flora*, vol. 199, pp. 377-388.
- Von Post, L (1916). About the snow tree pollen in southern turf moss storage sequences. *Bulletin of the Geological Institute*, University of Uppsala, vol. 15, pp. 219-278.
- Wagner, GM (1997). *Azolla*: A review of its biology and utilisation. *The Botanical Review*, vol. 63, pp. 1-26.
- Walker, D (2000). Pollen input to, and incorporation in, two crater lakes in tropical northeast Australia. *Review of Palaeobotany and Palynology*, vol. 111, pp. 253-283.
- Walker, D (2007). Holocene sediments of Lake Barrine, north-east Australia, and their implications for the history of lake and catchment environments. *Palaeogeography, Palaeoclimatology, Palaeoecology*, vol. 251, pp. 57-82.
- Walker, D & Chen, Y (1987). Palynological light on tropical rainforest dynamics. *Quaternary Science Reviews*, vol. 6, pp. 77-92.
- Walker, D & Owen, JAK (1999). The characteristics and source of laminated mud at Lake Barrine, Northeast Australia. *Quaternary Science Reviews*, vol. 18, pp. 1597-1624.
- Walker, D & Sun, X (2000). Pollen fall-out from a tropical vegetation mosaic. *Review of Palaeobotany and Palynology*, vol. 110, pp. 229-246.
- Walker, D, Head, MJ, Hancock, GJ & Murray, AS (2000). Establishing a chronology for the last 1000 years of laminated sediment accumulation at Lake Barrine, a tropical upland maar lake, northeastern Australia. *The Holocene*, vol. 10, pp. 415-427.
- Walsh, MK, Whitlock, C & Bartlein, PJ (2008). A 14,300 year-long record of fire-vegetation-climate linkages at Battle Ground Lake, southwestern Washington. *Quaternary Research*, vol. 70, pp. 251-264.
- Wang, X, van der Kaars, S, Kershaw, AP, Bird, M & Jansen, F (1999). A record of fire, vegetation and climate through the last three glacial cycles from Lombok Ridge core G6-4, eastern Indian Ocean, Indonesia. *Palaeogeography, Palaeoclimatology, Palaeoecology*, vol. 147, pp. 241-256.
- Wang, X, Auler, AS, Edwards, RL, Cheng, H, Ito, E & Solheid, M (2006). Interhemispheric anti-phasing of rainfall during the last glacial period. *Quaternary Science Reviews*, vol. 25, pp. 3391-3403.
- Wang, YJ, Cheng, H, Edwards, RL, An, ZS, Wu, JY, Shen, CC & Dorale, JA (2001). A high-resolution absolute-dated late Pleistocene monsoon record from Hulu Cave, China. *Science*, vol. 294, pp. 2345-2348.
- Warman, L (2011). Two systems or one? Vegetation dynamics in Australia's Wet Tropics, PhD, University of New South Wales, Sydney, pp. 184.
- Warman, L, Bradford, MG & Moles, AT (2013). A broad approach to abrupt boundaries: looking beyond the boundary at soil attributes within and across tropical vegetation type. *Plos One*, vol. 8, e60789. 10 Apr. 2013, doi:10.1371/journal.pone.0060789.
- Warman, L & Moles, AT (2009). Alternative stable states in Australia's Wet Tropics: a theoretical framework for the field data and a field-case for the theory. *Landscape Ecology*, vol. 24, pp. 1-13.
- Warner, BG (1988). Methods in Quaternary Ecology. *Geoscience Canada*, vol. 15, pp. 121-129.

- Webb, LJ (1959). A physiognomic classification of Australian rainforests. *Journal of Ecology*, vol. 47, pp. 551-570.
- Webb, LJ (1963). The influence of soil parent materials on the nature and distribution of rain forests in south Queensland. *Proceedings of Symposium in Ecological Research in Humid Tropics Vegetation*, Koching, Sarawak, p. 3-14.
- Webb, LJ (1968). Environmental relationships of the structural types of Australian rainforest vegetation. *Ecology*, vol. 49, pp. 296-311.
- Webb, LJ (1978). A general classification of Australian rainforests. *Australian Plants*, vol. 9, pp. 349-363.
- Webb, L (2007). *Ecological images from the Len Webb collection: Australia*, Griffith University, Queensland, archived 15 Feb, 2007, http://webb.archive.org/web/20091001045832if_/http://www.grith.edu.au/ins/collections/webb
- Webb, LJ, Tracey, JG, Williams, WT & Lance, GN (1967). Studies in the numerical analysis of complex rainforest communities. II. The problems of species sampling. *Journal of Ecology*, vol. 55, pp. 525-538.
- Webb, LJ, Tracey, JG & Williams, WT (1976). The values of structural features in tropical forests typology. *Australian Journal of Ecology*, vol. 1, pp. 3-28.
- Webb, LJ & Tracey, JG (1981). Australian rainforests: patterns and change. in A, Keast (ed.). *Ecological biogeography in Australia*, Dr W, Junk, The Hague, pp. 605-694.
- Webb, LJ, Tracey, JG & Williams, WT (1984). A floristic framework of Australian rainforests. *Australian Journal of Ecology*, vol. 9, pp. 169-198.
- Webster, PJ, Magana, VO, Palmer, TN, Shukla, J, Tomas, RA, Yanai, M & Yasunari, T (1998). Monsoons: processes, predictability, and the prospects for prediction. *Journal of Geophysical Research*, vol. 103, pp. 14451-14510.
- Webster, JM, Braga, JC, Humblet, M, Potts, DC, Iryu, Y, Yokoyama, Y, Fujita, K, Bourillot, R, Esat, TM, Fallon, SJ, Thompson, WG, Thomas, AL, Kan, H, McGregor, H, Hinestrosa, G, Obrochta, SP & Loughheed, B (2018). Response of the Great Barrier Reef to sea-level and environmental changes over the past 30,000 years. *Nature Geoscience*, vol. 11, pp. 426-432.
- Wen, X, Li, B, Zheng, Y, Yang, Q, Niu, D & Shu, P (2016). Early Holocene multi-centennial moisture change reconstructed from lithology, grain-size and chemical composition data in the eastern Mu Us desert and potential driving forces. *Palaeogeography, Palaeoclimatology, Palaeoecology*, vol. 459, pp. 440-452.
- Whitau, R, Balme, J, O'Connor, S & Wood, R (2017). Wood charcoal analysis at Riwi cave, Gooniyandi country, Western Australia. *Quaternary International*, vol. 457, pp. 140-154.
- Whitehead, PW (2008). Volcanoes of the Atherton Tableland. in W, Willmott & BG, Lottermoser (eds.). *Rocks, Landscapes and Resources of the Wet Tropics*, Geological Society of Australia, Brisbane, pp. 13-20.
- Whitehead, PW, Stephenson, PJ, McDougall, I, Hopkins, MS, Graham, AW, Collerson, KD & Johnson, DP (2007). Temporal development of the Atherton Basalt Province, north Queensland. *Australian Journal of Earth Sciences*, vol. 54, pp. 691-709.

Whitehead, PW & Nelson, PN (2014). Displacement of the Great Divide in north Queensland associated with Neogene lava flows. *Australian Journal of Earth Sciences*, vol. 61(6), pp. 803-809.

Whitlock, C & Millspaugh, SH (1996). Testing the assumptions of fire-history studies: an examination of modern charcoal accumulation in Yellowstone National Park, USA. *The Holocene*, vol. 6, pp. 7-15.

Whitlock, C, Skinner, CN, Bartlein, PJ, Minckley, T & Mohr, JA (2004). Comparison of charcoal and tree-ring records of recent fires in the eastern Klamath Mountains, California, USA. *Canadian Journal of Forest Research*, vol. 34, pp. 2110-2121.

Wieder, WR, Allison, SD, Davidson, EA, Georgiou, K, Hararuk, O, He, Y, Hopkins, F, Luo, Y, Smith, MJ, Sulman, B, Todd-Brown, K, Wang, Y, Xia, J & Xu, X (2015). Explicitly representing soil microbial processes in Earth system models. *Global Biogeochemical Cycles*, vol. 29, Issue 10, <https://doi.org/10.1002/2015GB005188>. Haus.

Willeit, M, Ganopolski, A, Dalmonch, D, Foley, AM & Feulner, G (2014). Time-scale and state dependence of the carbon-cycle feedback to climate. *Climate Dynamics*, vol. 42, pp. 1699-1713.

Williams, M, Dunkerley, D, De Deckker, P, Kershaw, AP & Chappell, J (1998). *Quaternary Environments* (2nd Edition), Arnold Publishers, London, pp. 329.

Williams, M, Cook, E, van der Kaars, S, Barrows, T, Shulmeister, J & Kershaw, P (2009). Glacial and deglacial climatic patterns in Australia and surrounding regions from 35 000 to 10 000 years ago reconstructed from terrestrial and near-shore proxy data. *Quaternary Science Reviews*, vol. 28, pp. 2398-2419.

Williams, PR (2000). Fire-stimulated rainforest seedling recruitment and vegetative regeneration in a densely grassed wet sclerophyll forest of north-eastern Australia. *Australian Journal of Botany*, vol. 48, pp. 651-658.

Williams, P, Parsons, M & Devlin, T (2006). Rainforest recruitment and mortality in eucalypt forests of the wet tropics – refining the model for better management. *Bushfire Conference Life in a Fire-prone Environment: translating Science into Practice*, Brisbane, 6-9 June 2006.

Williams, PR, Parsons, M, Jensen, R & Tran, C (2012). Mechanisms of rainforest persistence and recruitment in frequently burnt wet tropical eucalypt forests. *Austral Ecology*, vol. 37, pp. 268-275.

Williams, RJ, Cook, GD, Gill, AM & Moore, PH (1999). Fire regime, fire intensity and tree survival in a tropical savanna in northern Australia. *Australian Journal of Ecology*, vol. 24, pp. 50-59.

Williams, T & Kelley, C (2004/2006). *Gnuplot 4*, <http://sourceforge.net/projects/gnuplot>.

Williamson, GB & Mesquita, RCG (2001). Effects of fire on rainforest regeneration in the Amazon Basin. in R Jr, Bierregard, C, Gascon, TE, Lovejoy & RCG, Mesquita (eds.). *Lessons from Amazonia: the ecology and conservation of a fragmented forest*, Yale University Press, New Haven, pp. 325-334.

Wilmshurst JM & McGlone (2005a). Origin of pollen and spores in surface lake sediments: comparison of modern palynomorph assemblages in moss cushions, surface soils and surface lake sediments. *Review of Palaeobotany and Palynology*, vol. 136, pp. 1-15.

- Wilmshurst, JM & McGlone, MS (2005b). Corroded pollen and spores as indicators of changing lake sediment sources and catchment disturbance. *Journal of Paleolimnology*, vol. 34, pp. 503-517.
- Winkler, MJ (1985). Charcoal analysis for palaeoenvironmental interpretation: a chemical assay. *Quaternary Research*, vol. 23, pp. 313-326.
- Wolf, M, Lehndorff, E, Wiesenberg, GLB, Stockhausen, M, Schwark, L & Amelung, W (2013). Towards reconstruction of past fire regimes from geochemical analysis of charcoal. *Organic Geochemistry*, vol. 55, pp. 11-21.
- Woltering, M, Atahan, P, Grice, K, Heijnis, H, Taffs, K & Dodson, J (2014). Glacial and Holocene terrestrial temperature variability in subtropical east Australia as inferred from branched GDGT distributions in a sediment core from Lake McKenzie. *Quaternary Research*, vol. 82, pp. 132-145.
- Wood, JR, Wilmshurst, JM, Worthy, TH & Cooper, A (2011). *Sporormiella* as a proxy for non-mammalian herbivores in island ecosystems. *Quaternary Science Reviews*, vol. 30, pp. 915-920.
- Woodroffe, CD (2009). Testing models of mid to late Holocene sea-level change, north Queensland, Australia. *Quaternary Science Reviews*, vol. 28, pp. 2474-2488.
- Woodroffe, CD, Thom, BG & Chappell, J (1985). Development of widespread mangrove swamps in mid-Holocene times in northern Australia. *Nature*, vol. 317, pp. 711-713.
- Woodroffe, CD, Chappell, JMA, Thom, BG & Wallensky, E (1986). Geomorphological dynamics and evolution and the South Alligator Tidal River and Plains, Northern Territory. *Mangrove Monograph*, vol. 3, Northern Australian Research Unit, The Australian National University, pp. 206.
- Woodroffe, CD & Webster, JM (2014). Coral reefs and sea-level change. *Marine Geology*, vol. 352, pp. 248-267.
- Wooller, MJ, Street-Perrott, FA & Agnew, ADQ (2000). Late Quaternary fires and grassland palaeoecology of Mount Kenya, East Africa: evidence from charred grass cuticles on lake sediments. *Palaeogeography, Palaeoclimatology, Palaeoecology*, vol. 164, pp. 207-230.
- Wooller, MJ, Swain, DL, Ficken, KJ, Agnew, ADQ, Street-Perrott, FA & Eglinton, G (2003). Late Quaternary vegetation changes around Lake Rutundu, Mount Kenya, East Africa: evidence from grass cuticles, pollen, and stable carbon isotopes. *Journal of Quaternary Science*, vol. 18, pp. 3-15.
- Wright, P (2003). Preservation or destruction of plant remains by carbonization? *Journal of Archaeological Science*, vol. 30, pp. 577-583.
- Wunsch, C (2004). Quantitative estimate of the Milankovitch-forced contribution to observed Quaternary climate change. *Quaternary Science Reviews*, vol. 23, pp. 1001-1012.
- Wust, RA, Jacobsen, GE, von der Gaast, H & Smith, AM (2008). Comparison of Radiocarbon Ages from different organic fractions in tropical peat cores: insights from Kalimantan, Indonesia. (2008). *Radiocarbon*, vol. 50(3), pp. 359-372.
- Wyrwoll, KH & Miller, GH (2001). Initiation of the Australian summer monsoon 14,000 years ago. *Quaternary International*, vol. 83-85, pp. 119-128.

- Wyrwoll, KH, Liu, Z, Chen, G, Kutzbach, JE & Liu, X (2007). 'Sensitivity of the Australian summer monsoon to tilt and precession forcing. *Quaternary Science Reviews*, vol. 26, pp. 3043-3057.
- Xu, H, Hong, Y, Lin, Q, Zhu, Y, Hong, B & Jiang, H (2006). Temperature responses to quasi-100-yr solar variability during the past 6000 years based on $\delta^{18}\text{O}$ of peat cellulose in Hongyuan, eastern Qinghai-Tibet plateau, China. *Palaeogeography, Palaeoclimatology, Palaeoecology*, vol. 230, pp. 155-164.
- Yang, S, Li, Z, Yu, JY, Hu, X, Dong, W & He, S (2018). El Niño-Southern Oscillation and its impact in the changing climate. *National Science Review*, vol. 5 (6), pp. 840-857.
- Yen, DE (1995). The development of Sahul Agriculture with Australia as Bystander. *Antiquity*, vol. 69, pp. 831-847.
- Yokoyama, Y, Lambeck, K, De Deckker, P, Johnston, P & Fifield, LK (2000). Timing of the Last Glacial Maximum from observed sea-level minima. *Nature*, vol. 406, pp. 713-716.
- Yu, KF & Zhao, JX (2010). U-series dates of Great Barrier Reef corals suggest at least +0.7 m sea-level ~ 7000 years ago. *The Holocene*, vol. 20, pp. 161-168.
- Yu, Z & Ito, E (1999). Possible solar forcing of century-scale drought frequency in the northern Great Plains. *Geology*, vol. 27, pp. 263-266.
- Zhang, W, Li, J & Jin, F-F (2009). Spatial and temporal features of ENSO meridional scales. *Geophysical Research Letters*, vol. 36, L15605 1-5.
- Zhang, Y, Wallace, JM & Battisti, DS (1997). ENSO-like interdecadal variability: 1900-93. *Journal of Climate*, vol. 10, pp. 1004-1020.
- Zhao, Y, Wang, Y, Edwards, L, Cheng, H & Liu, D (2010). High-resolution stalagmite $\delta^{18}\text{O}$ records of Asian monsoon changes in central and southern China spanning the MIS 3/2 transition. *Earth and Planetary Science Letters*, vol. 298, pp. 191-198.
- Zhao, Y, Sayer, CD, Birks, HH, Hughes, M & Peglar, SM (2006). Spatial representation of aquatic vegetation by macrofossils and pollen in a small and shallow lake. *Journal of Paleolimnology*, vol. 35, pp. 335-350.

Appendices

Appendix A-Map, reference pollen and charcoal material



Figure 1. Map of the WTWHA region (after Prideaux and Falco-Mammone 2007).

Section 1. Pollen Reference Material Myrtaceae

Details for pollen reference material (Australian National University pollen reference collection)

See sub-section 5.3.2. Myrtaceae Identification Figure 5.5

Acmena smithii (now *Syzygium smithii*)

Reference Number 225-43-7

Acmena graveolens (now *Syzygium graveolens*)

Reference Number 225-43-3b

Syzygium leuhmannii (formerly *Eugenia leuhmannii*)

Reference Number 225-13-22

Syzygium kuranda (formerly *Eugenia kuranda*)

Reference Number 225-13-54

Syzygium cormiflorum (formerly *Eugenia cormiflora*)

Reference Number 225-13-10c

Austromyrtus dallachiana (now *Gossia dallachiana*)

Reference Number 225-31-3a

Rhodomyrtus trineura

Reference Number 225-14-6a

Syncarpia glomulifera

Reference Number 225-24-1a

Melaleuca dealbata

Reference Number 225-9-38a

Melaleuca leucadendra

Reference Number 225-9-19

Tristaniopsis exiliflora (formerly *Tristania exiliflora*)

Reference Number 225-27-6

Leptospermum wooroonooran

Reference Number 225-12-16

Corymbia intermedia (formerly *Eucalyptus intermedia*)

Reference Number 225-3-35a

Eucalyptus tereticormis

Reference Number 225-3-30b

Eucalyptus macta (formerly *E.resinifera*)

Reference Number 225-3-101c

Section 2. Pollen Reference Material Urticaceae/Moraceae

Details for pollen reference material (Monash University pollen reference collection)

See sub-section 5.3.3. Moraceae/Urticaceae Identification Figure 5.6

Ficus rubiginosa (Moraceae)

Reference Number 61 (Melb RBG 2003/K.Sniderman)

Ficus virens

Reference Number 61 (Melb RBG 2003/K.Sniderman)

Ficus coronata

Reference Number 61 (Melb RBG 2003/K.Sniderman)

Ficus macrophylla

Reference Number 61 (Melb RBG 2003/K.Sniderman)

Streblus glaber (Moraceae)

Reference Number 61-4-2 and 61-MG91

Laportea photinophylla (Urticaceae)

Reference Number 62-B269

Pipturus argenteus (Urticaceae)

Reference Number 62-4-3b and 62-MG914

Urtica incise (Urticaceae)

Reference Number 62-248 and 62-MG351

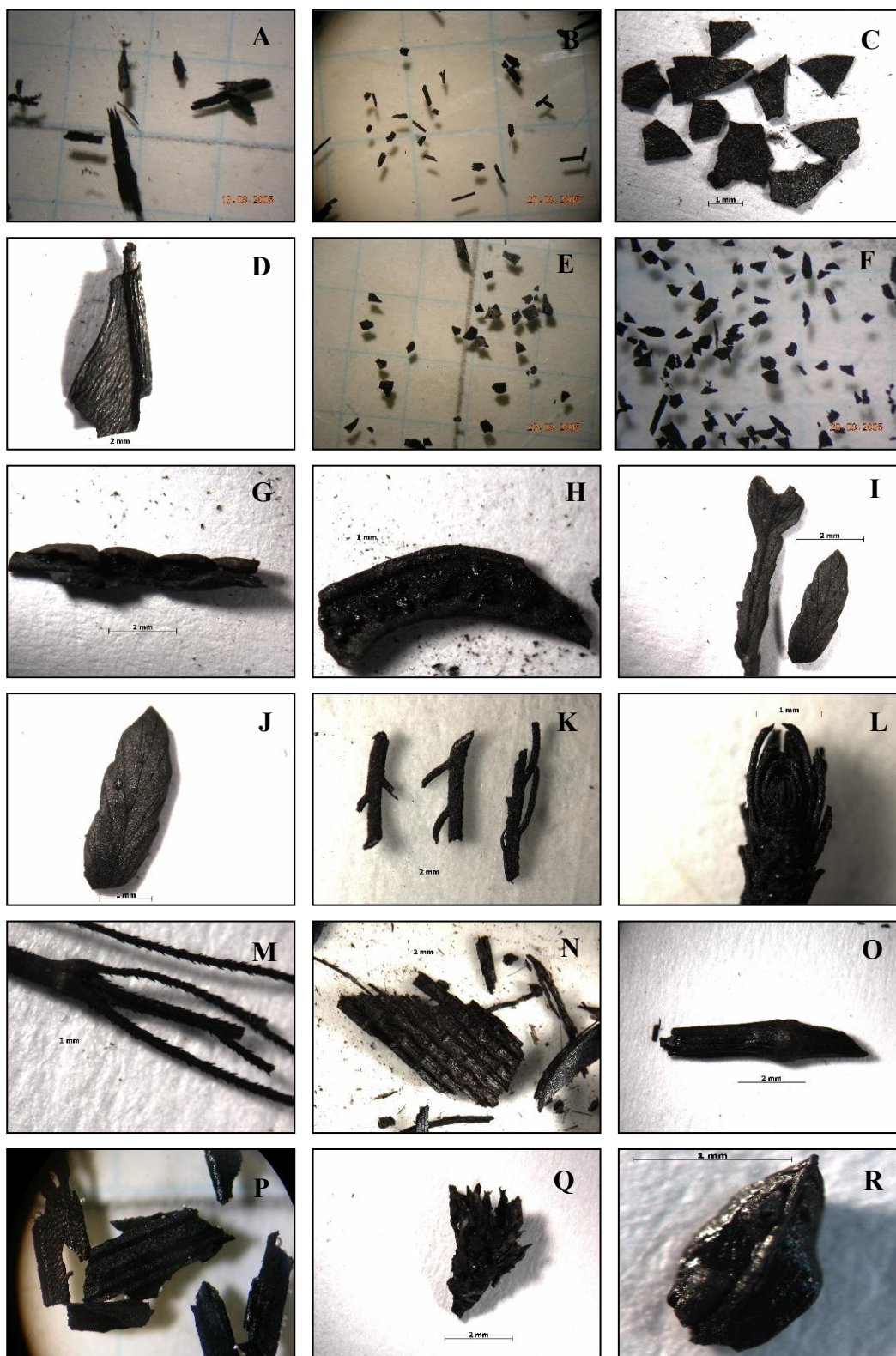


Plate 1. Reference burn photos – A – *Melaleuca* bark >500 μ m, B – *Casuarina* leaf >250 μ m, C – *Acmena* leaf >500 μ m, D – *Acmena* leaf with attached stem, E – *Eucalyptus regnans* leaf >500 μ m, F – *Pteridium* >500 μ m, G – *Pteridium* frond, H – *Pteridium* underside, I – *Cyathea* part of frond, J – *Cyathea* part of frond (closeup), K – *Myriophyllum* stem, L – *Myriophyllum* stem (closeup), M – Poaceae flower stem, N – *Typha* epidermis, O – *Eleocharis* mid-ridge of stem, P – *Carex appressa* distinct venations, Q – *Carex appressa* flower head, R – *Carex appressa* bract sepal.

Table 1. Reference Burn Counts (1-3) – 2:1 Length:Width (L:W) ratio was used to denote herbaceous/woody origin												
	Count 1			Count 2			Count 3					
	>2:1	<2:1	% >2:1	>2:1	<2:1	% >2:1	>2:1	<2:1	% >2:1	<2:1	% >2:1	% Average (1-3) >2:1
Poaceae												
>500	92		9	92.92	113	24	82.5	185	80	69.8	81.8	
>250	102		14	87.93	159	47	77.2	158	72	68.7	78	
>125	107		31	77.5	198	53	78.9	236	82	74.2	77	
Carex appressa												
>500	46		5	90.2	135	36	78.9	145	57	71.8	80.3	
>250	140		15	90.3	193	44	81.4	141	52	73.1	81.6	
>125	90		10	90	231	38	85.9	368	134	73.2	83.1	
Carex fascicularis												
>500	52		16	76.5	143	42	77.3	146	62	70.2	75.2	
>250	86		17	83.5	201	56	78.2	204	70	74.5	78.7	
>125	57		10	85.1	113	26	81.3	164	71	69.8	78.8	
Typha												
>500	33		4	89.2	107	32	77	125	45	73.5	80	
>250	204		39	83.9	286	80	78.1	256	85	75.1	79	
>125	54		8	87.1	149	44	77.2	223	75	74.8	79.7	
Eucalyptus pauciflora												
>500	38		270	12.3	26	176	12.8	57	243	19	14.7	
>250	25		140	15.1	19	135	12.3	32	120	21.1	16.2	
>125	37		117	24	27	190	12.4	89	358	19.9	18.8	
Eucalyptus regnans												
>500	15		108	12.2	55	228	19.5	40	184	17.9	16.5	
>250	21		213	8.9	70	300	18.9	81	330	19.7	15.8	
>125	46		200	18.6	80	300	21.1	80	319	20.1	19.9	
Acmena												
>500	70		300	18.9	65	317	17	60	300	16.7	17.5	
>250	93		310	22.5	84	301	21.8	90	330	21.4	21.9	
>125	77		300	20.4	92	340	21.3	90	325	21.7	21.1	

Table 1.Reference Burn Count.

Appendix B (1) Table 1 Ecological Information on taxa represented in the pollen fossil spectra of this study (Kershaw 1976, 1983a; Stephens and Dowling 2002; Hyland et al. 2010)

Aquatics/Swamp taxa (macrofossils*)	Family	Plant Habit	Distribution NE Qld.
<i>Baumea/Machaerina</i>	Cyperaceae	Aquatic herb	Swamps
<i>Carex appressa</i> *	Cyperaceae	Aquatic herb	Widespread in damp areas
<i>Carex fascicularis</i> *			
<i>Carex</i> * sp.			
<i>Cyperus polystachyos</i> *	Cyperaceae	Aquatic herb	Swamps-often in disturbed areas
<i>Cyperus</i>			
<i>Eleocharis spahacelata</i> *	Cyperaceae	Aquatic herb	Still water up to 5 m deep
<i>Eleocharis</i> sp.			
<i>Lipocarpha</i> *	Cyperaceae	Aquatic herb	Swamps
<i>microcerphala</i>			
<i>Schoenoplectus</i> *	Cyperaceae	Aquatic herb	Open swamps
<i>Haloragis</i>	Haloragaceae	Herb	Drier marginal areas
<i>Gonocarpus chinensis</i> *	Haloragaceae	Herb	Open wet or swamp habitat
<i>Hydrocotyle</i> *	Araliaceae	Herb	Mainly swamps (drier), vines sp. intertwined with taller sedges
<i>Oenanthe</i>	Apiaceae	Herb	Shallow water but also grassland at forest margins
<i>Stylidium</i>	Stylidiaceae	Herb	Margins of water bodies, but also grows in dry sclerophyll forest
<i>Myriophyllum</i> *	Haloragaceae	Aquatic herb	Still water > 30 cm
<i>Potamogeton octandrus</i> *	Potamogetonaceae	Aquatic herb	Still shallow water
<i>Liparophyllum exaltatum</i> *	Menyanthaceae	Aquatic herb	Stationary or slow-flowing water usually up to 1 m
<i>Nymphoides indica</i> *	Menyanthaceae	Aquatic herb	Still and flowing water to 2 m
<i>Typha domingensis</i> *	Typhaceae	Aquatic herb	Found rooting in inorganic sediments or organic sediments with a large inorganic fraction beneath shallow open water and thin floating root mat vegetation.
<i>Rorippa</i> * sp.	Brassicaceae	Herb	Swampy environments/drier marginal areas
<i>Ludwigia</i>	Onagraceae	Herb	Margins of swamps/seasonally wet places
<i>Eriocaulon</i>	Eriocaulaceae	Aquatic herb	Swamp environment-stable floating mat and fixed root mat swamps
<i>Lemna</i> *	Araceae	Aquatic/free floating	Slow moving streams

<i>Utricularia</i>	Lentibulariaceae	Aquatic/Carnivorous (submerged) herb	A variety of open water situations.
Geraniaceae	Geraniaceae	Herbs/shrubs	Variety of environments from open woodlands to swamp margins
<i>Elatine gratioloides</i> *	Elatinaceae	Aquatic annual	Margins of stationary or slow-flowing water
<i>Philydrum lanuginosum</i> *	Philydraceae	Emergent aquatic	Swamps, along margins of streams
<i>Persicaria strigosa</i> *	Polygonaceae	Herb	Open swamps, advantaged by disturbance
<i>Persicaria</i> * sp.			
<i>Ranunculus</i>	Ranunculaceae	Herb	Swamps bordering woodland
Liliaceae	Liliaceae	Herb	A variety of environments
<i>Azolla pinnata</i> *	Salvinaceae	Aquatic fern	Grows in slow-moving shallow water bodies up to 50 cm
<i>Nitella</i> * sp.	Characeae	Charophyte/Algal	Submerged in wetlands generally shallow water
<i>Chara</i> * sp.	Characeae	Charophyte/Algal	Submerged/attached to muddy bottom
<i>Cyclosorus</i>	Thelypteridaceae	Fern (swamp)	Present-day established on floating root mats/Bromfield Swamp
<i>Anthoceros</i>	Anthocerotaceae	Bryophyte	Moist and shady places, some can establish quickly after fire
<i>Botryococcus</i>	Botryococcaceae	Green algae	Found in both deep and shallow water and is tolerant to desiccation
Rainforest Gymnosperm	Family	Plant Habit	Distribution NE Qld
<i>Araucaria</i>	Araucariaceae	Emergent	Drier vine forests and thickets in southern Queensland. <i>A.bidwilli</i> restricted to Mt Lewis and Cannabullen Falls, while <i>A.cunninghamii</i> has scattered distribution and like <i>A.bidwilli</i> occurs in situations where other rainforest types are excluded by unfavourable soil or substrate conditions
<i>Agathis</i>	Araucariaceae	Emergent	Occurs in moister rainforest than <i>Araucaria</i>
Podocarpaceae	Podocarpaceae	Canopy/Understory	Grows in well-developed rainforest and more common in upland and mountain rainforest
<i>Dacrydium</i>	Podocarpaceae	Canopy/Shrub	In rainforests of New Guinea, New Zealand, Borneo, Tasmania and New Caledonia but not on the Australian mainland. Pollen in study has closest affinity to <i>D.guillauminii</i> (New Caledonia) a slow growing shrub found on the banks of rivers and lakes
Rainforest Angiosperm	Family	Plant Habit	Distribution NE Qld
Cunoniaceae (tricolpate)	Cunoniaceae	canopy	Cool upland rainforest types present in forest succession, <i>Spiraeanthemum davidsonii</i> , <i>Ackama australiensis</i> and <i>Davidsonia pruriens</i>
Cunoniaceae (dicolpate)	Cunoniaceae	canopy	Warm upland MVF types can come in early in succession <i>Ceratopetalum succirubrum</i> , <i>Pseudoweinmannia lachnocarpa</i> and <i>Schizomeria whitei</i>
<i>Gilbeea</i>	Cunoniaceae	canopy	Grows in well-developed rainforest
<i>Elaeocarpus</i>	Elaeocarpaceae	canopy	Many species common in complex rain forests although a few species are restricted to drier vine forests.
<i>Sloanea</i>	Elaeocarpaceae	canopy	Grows in well-developed rainforest on a variety of sites
<i>Acmena</i>	Myrtaceae	canopy	Now under <i>Syzygium</i>

<i>Syzygium</i>	Myrtaceae	canopy	Many species common across a variety of sites from well-developed rainforest to drier rainforests to the margins of wet sclerophyll forest
<i>Ficus</i>	Moraceae	canopy	Grows in rainforest on a variety of sites
<i>Dysoxylum</i>	Meliaceae	canopy	Widespread in rainforest
<i>Toona ciliata</i>	Meliaceae	canopy	Well-developed rainforest especially in upland rainforest on soils derived from basalt
<i>Argyrodendron trifoliatum</i>	Malvaceae	canopy	Grows in a variety of rainforest especially on upland sites on deep red soils derived from basalt
<i>Argyrodendron peralatum</i>	Malvaceae	canopy	Grows in a variety of rainforest especially on upland sites on deep red soils derived from basalt
<i>Flindersia</i>	Rutaceae	canopy	Grows in well-developed rainforest on a variety of sites
<i>Diospyros</i>	Ebenaceae	canopy	Widespread in rainforest
<i>Pleiogynium</i>	Anacardiaceae	canopy	Grows in drier rainforest
<i>Anacardiaceae</i>	Anacardiaceae	canopy	Widespread in rainforest on a variety of sites but most common in drier rainforest
<i>Austrobuxus</i>	Picrodendraceae	canopy	Grow in upland and mountain rainforest
<i>Ilex</i>	Aquifoliaceae	canopy	Grows in well-developed rainforest
<i>Balanops australiana</i>	Balanopaceae	canopy	Mainly in high cool cloudy rain forests on acid soils in northern Queensland
<i>Emmenosperma</i>	Rhamnaceae	canopy	Grows in dry rainforest and well-developed rainforest on a variety of sites
<i>Olea paniculata</i>	Oleaceae	canopy	Grows in well-developed rainforest but more common in drier, more seasonal rainforest
<i>Drypetes</i>	Putranjivaceae	canopy	Grows in upland rainforest but more common in drier rainforest
<i>Nothofagus 'Brassospora'</i>	Nothofagaceae	canopy	Frequent dominant of cool temperate rain forest or Nanophyll Mossy forest in N.S.W. and southern tip of Queensland but not represented in northern Queensland.
<i>Sapindaceae(syncolpate)</i>	Sapindaceae	canopy	Widespread in rain forests (syncolpate) second canopy trees
<i>Daphnandra</i>	Atherospermataceae	canopy	Grows in rainforest on a variety of sites
<i>Doryphora</i>	Atherospermataceae	canopy	Mountain rainforest reaches its best development on soils derived from basalt
<i>Cardwellia</i>	Proteaceae	canopy	Grows in well-developed rainforest on a variety of sites
<i>Stenocarpus</i>	Proteaceae	canopy	Grows in well-developed rainforest but also found in drier rainforest associated with <i>Agathis robusta</i>
<i>Darlinginia</i>	Proteaceae	canopy	Grows in well-developed rainforest but <i>D.darlingiana</i> is favoured by disturbance and is a characteristic component of rainforest regrowth
<i>Orites</i>	Proteaceae	canopy	Grows in mountain rainforest often found in stunted forest on windswept ridges
<i>Carnarvon</i>	Proteaceae	canopy	Grows in well-developed rainforest and reaches its best development on soils derived from basalt
<i>Musgravea</i>	Proteaceae	canopy	Upland and mountain rainforest, often in stunted windswept forest
<i>Lomatia</i>	Proteaceae	canopy	Upland and mountain rainforest
<i>Placospermum</i>	Proteaceae	canopy	Grows in well-developed rainforest and is favoured by disturbance
<i>Proteaceae</i>	Proteaceae	canopy	Widespread within and outside rainforests
<i>Planchonella</i>	Sapotaceae	canopy	Widespread in rainforest on a variety of sites

Sapotaceae	Sapotaceae	canopy	Widespread in rainforest on a variety of sites
<i>Myristica</i>	Myristicaceae	canopy	Found in mesophyll and notophyll vine forest but also found in drier more seasonal rainforest
Meliaceae	Meliaceae	canopy	Widespread in rainforest on a variety of sites
<i>Rhizophora</i>	Rhizophoraceae	canopy	Mangrove trees primarily coastal
Arecaceae	Arecaceae	canopy	Common in palm forests and understorey tropical lowland swamps and in lowland vine forests. Also occur in high altitude forests, if wet.
<i>Archontophoenix</i>	Arecaceae	canopy	Grows in rainforest, vine forest, swampy areas and wet sclerophyll forest
Rainforest Angiosperm	Family	Plant Habit	Distribution NE Qld
<i>Glochidion</i>	Phyllanthaceae	secondary	Grows in well-developed rainforest but also found in drier rainforest and favoured by disturbance
<i>Homalanthus</i>	Euphorbiaceae	secondary	Grows in disturbed areas in rainforest but also wet sclerophyll and swamp forest
<i>Mallotus</i>	Euphorbiaceae	secondary	Largely found in drier subtropical rainforests of northern and southern Queensland
<i>Macaranga</i>	Euphorbiaceae	secondary	Largely found in drier subtropical rainforests of northern and southern Queensland
<i>Aleurites</i>	Euphorbiaceae	secondary	Grows in disturbed rainforest but also found in well-developed rainforest
<i>Alphitonia</i>	Rhamnaceae	secondary	Grows in open forest and both dry and wetter rainforest but favoured by disturbance
Rhamnaceae	Rhamnaceae	secondary	Grows in a variety of rainforest types
<i>Alstonia</i>	Apocynaceae	secondary	Grows in rainforest, but also more open forest and is characteristic of regrowth areas and can cope with fire
<i>Archidendron</i>	Fabaceae	secondary	Grows in rainforest but more common in drier and more seasonal rainforest
Leguminosae	Number of families	secondary/vines	Caesalpiniaceae, Papilionaceae, Fabaceae-widespread through all major vegetation formations
Urticaceae/Moraceae	Urticaceae/Moraceae	Secondary/vines	Widely distributed in rainforests <i>Pipturus</i> and <i>Dendrocnide</i> best represented in drier vine forests throughout Queensland
<i>Trema</i>	Cannabaceae	secondary	Best represented in drier vine forests and is a characteristic feature of rainforest regrowth
<i>Celtis</i>	Cannabaceae	secondary	Drier rainforest
<i>Melicope</i>	Rutaceae	secondary	Grows in a variety of rainforest types, with a number of species favoured by disturbance
<i>Euodia/Melicope</i>	Rutaceae	secondary	Grows in a variety of rainforest types, with a number of species favoured by disturbance
<i>Schefflera</i>	Araliaceae	secondary	Grows in rainforest and open forest down to south-east Queensland
<i>Solanum</i>	Solanaceae	secondary	Widespread and common in disturbed rainforest
Rainforest Angiosperm	Family	Plant Habit	Distribution NE Qld
<i>Hypserpa</i>	Menispermaceae	vine	Widespread in rainforest
<i>Stephania</i>	Menispermaceae	vine	Found in primarily drier rainforest and vine thickets
Menispermaceae	Menispermaceae	vine	Widespread in rainforests but commonest in drier subtropical vines forests of northern and southern Queensland
<i>Faradaya</i>	Lamiaceae	vine	A variety of rainforest types
<i>Freycinetia</i>	Pandanaceae	vine	Montane or high latitude rainforests or lowland swamps

<i>Calamus</i>	Arecaceae	vine	Abundant in wet lowland rainforests
<i>Clematis</i>	Ranunculaceae	vine	Grows in lowland, upland rainforest and vine thickets
<i>Muehlenbeckia</i>	Polygonaceae	vine	Usually grows in open forest or wet sclerophyll forest but also found on rainforest margins
Loranthaceae	Loranthaceae	mistletoes	Grows in a variety of forest types from open forest, woodlands, wet sclerophyll and rainforest,
<i>Cissus</i>	Vitaceae	vine	Grows in rainforest but also open forest and woodlands
<i>Morinda</i>	Rubiaceae	vine	Grows in a variety of forest types from open forest, woodlands, wet sclerophyll and rainforest,
<i>Maesa</i>	Primulaceae	vine	Usually grows in drier rainforest and disturbed areas in upland and mountain rainforests
Rainforest Angiosperm	Family	Plant Habit	Distribution NE Qld
Rubiaceae	Rubiaceae	understorey	Widespread in rainforests
<i>Quintinia</i>	Paracryphiaceae	understorey	Most common in cooler, wetter parts of 'warm temperate' rainforests
<i>Helicia</i>	Proteaceae	understorey	Mainly found in well-developed upland and mountain rainforest
<i>Austromuellera</i>	Proteaceae	understorey	Grows in well-developed lowland and upland rainforest
<i>Opisthiolepis</i>	Proteaceae	understorey	Well developed rainforest especially upland and mountain rainforests best development on basalt
<i>Apodytes</i>	Icacinaeae	understorey	Well developed rainforest more common in upland and mountain situations
<i>Hibbertia</i>	Dilleniaceae	understorey	Open forest, wet sclerophyll forest and on the margins of rainforest
<i>Oraniopsis</i>	Arecaceae	understorey	Grows in high rainfall areas in rainforest, occasionally in wet sclerophyll forest
<i>Wrightia</i>	Apocynaceae	understorey	Open forest, vine thickets and drier rainforest
<i>Acalypha</i>	Euphorbiaceae	understorey	Common in drier vine forests and thickets of southern Queensland, but found in both rainforest and wet sclerophyll forests on the Atherton Tableland
<i>Claoxylum</i>	Euphorbiaceae	understorey	Grows on the margins of rainforest, wet sclerophyll and dry rainforest types
<i>Elaeodendron</i>	Celastraceae	understorey	Widespread in drier vine forests and thickets
<i>Breynia</i>	Phyllanthaceae	understorey	Grows in open forest, vine thickets and drier rainforest types
<i>Antidesma</i>	Phyllanthaceae	understorey	Grows in rainforest but also vine thickets and drier rainforest types
<i>Bischofia</i>	Phyllanthaceae	understorey	Grows in lowland and upland rainforest
<i>Dissilaria</i>	Picrodendraceae	understorey	Found in notophyll vine forests
<i>Choriceras</i>	Picrodendraceae	understorey	Grows in well-developed rainforest but also found in dry rainforests
<i>Petalostigma</i>	Picrodendraceae	understorey	Usually grows in open forest but also found in vine thickets
Goodeniaceae	Goodeniaceae	understorey	Grows in lowland and upland rainforest
<i>Acronychia</i>	Rutaceae	understorey	Grows in a variety of rainforest and is favoured by disturbance
<i>Zanthoxylum</i>	Rutaceae	understorey	Grows in well-developed rainforest but also found in drier more seasonal rainforest
<i>Irvingbaileya</i>	Icacinaeae	understorey	Grows in well-developed rainforest
<i>Sphenostemon</i>	Sphenostemonaceae	understorey	Common in moist gullies of high altitude rainforests
<i>Clerodendron</i>	Lamiaceae	understorey	Grows in open forest, but on the Atherton Tableland grows in disturbed upland rainforest and wet sclerophyll forest
Lamiaceae	Lamiaceae	understorey	Widespread in a variety of rainforest, open forest and woodland types

<i>Securingia cf Flueggea</i>	Euphorbiaceae	understorey	Vine thickets and open forest extends to southern NSW
<i>Abrophyllum</i>	Rousseaceae	understorey	Upland and mountain rainforest frequently as a regrowth species in disturbed areas
<i>Rapanea</i> now <i>Myrsine</i>	Primulaceae	understorey	Common in rainforests under high rainfall in northern and southern Queensland
Myrsinaceae/Primulaceae	Primulaceae	understorey	Common in rainforests under high rainfall in northern and southern Queensland
<i>Aglaiia</i>	Meliaceae	understorey	Grows in well-developed rainforest on a variety of sites
<i>Alectryon</i>	Sapindaceae	understorey	Vine thickets and drier rainforest types
<i>Symplocos</i>	Symplocaceae	understorey	Grows in upland and mountain rainforest
<i>Micrantheum</i>	Euphorbiaceae	understorey	Restricted distribution in open eucalypt woodlands
<i>Wikstroemia</i>	Thymelaeaceae	understorey	Grows in open forest or wet sclerophyll forest
<i>Tasmannia</i>	Winteraceae	understorey	Cool temperate forests and heaths
Rosaceae	Rosaceae	understorey	Grows in well-developed rainforest on a variety of sites
Sclerophyll taxa	Family	Plant Habit	Distribution NE Qld
Casuarinaceae	Casuarinaceae	canopy	Common in wet sclerophyll forests and some open woodlands of coastal swamp and drier country
<i>Eucalyptus</i>	Myrtaceae	canopy	Dominates much of Australia's forest and woodland communities but doesn't enter undisturbed rainforest
<i>Corymbia</i>	Myrtaceae	canopy	Grows in open forest and woodlands but also found in wet sclerophyll forest and on the margins of rainforest
<i>Melaleuca</i>	Myrtaceae	canopy	Woodland species that tolerates impeded drainage as on swamp surfaces
<i>Leptospermum</i>	Myrtaceae	Tree/shrub	Mainly in high altitude and coastal shrub heaths on acid soils, <i>L.wooroonooran</i> endemic to NEQ at altitudes from 1100-1550
<i>Callitris</i>	Cupressaceae	canopy	Widespread in drier country. <i>C.macleayana</i> is found in wet sclerophyll forests of Nth NSW and NE Qld
<i>Dodonaea</i>	Sapindaceae	shrubs	Widespread in open forests and woodlands and also in drier vine forests and thickets of Sth Qld
<i>Banksia</i>	Proteaceae	shrub	Grows in wet sclerophyll forest on rainforest margins <i>B.aquilonia</i> endemic to NEQ
<i>Myoporum</i>	Myoporaceae	shrubs	Dry country shrubs reaching vine forest fringes in southern Queensland
Gyrostemonaceae	Gyrostemonaceae	shrub/tree	Dry scrub and open forest and grows in disturbed areas particularly burnt areas of vine thickets
<i>Bursaria</i>	Pittosporaceae	sub-canopy trees	Widespread in drier rainforests
<i>Exocarpos</i>	Santalaceae	Parasitic trees	Common in open woodlands and vine thickets of southern Queensland
<i>Acacia</i>	Mimosaceae	trees	Mainly in open woodlands and sclerophyll forests but <i>A.aulacocarpa</i> is a secondary rainforest tree
Poaceae/Dryland Herbs	Family	Plant Habit	Distribution NE Qld
Poaceae	Poaceae	dryland/wetland	Common throughout swamp environments and widespread except in rainforest
Chenopodiaceae	Chenopodiaceae	herbs/shrubs	Common in very dry country
Asteraceae (tubuliflora)	Asteraceae	herbs/shrubs	Dry country and weeds of disturbance
Asteraceae (liguliflora)	Asteraceae	herbs/shrubs	Dry country and weeds of disturbance
<i>Lythrum</i>	Lythrum	herb	Grows in damp areas

<i>Hibiscus</i>	Malvaceae	shrub	Grows in various forest types; eucalypt woodland, vine thicket, grassland and rainforest margins
Ericaceae	Ericaceae	shrub	Grows in wet sclerophyll and eucalypt forest and in stunted windswept rainforest on mountain tops
Caryophyllaceae	Caryophyllaceae	herbs/shrubs	Mainly dry country herb but <i>Drymaria cordata</i> is found in disturbed areas in rainforest and other forest types
<i>Monotoca</i>	Ericaceae	shrub	Widespread in Australia in dry sclerophyll forest, woodland and heath; <i>Actrotriche baileyana</i> (previously <i>Monotoca</i>) grows in rainforest-heathland and wet sclerophyll (900-1600 m)
<i>Plantago</i>	Plantaginaceae	Herb	Widespread outside rainforest
<i>Melastoma affine</i>	Melastomataceae	Shrubs	Vine forests and also on drier swamps, advantaged by disturbance
Pteridophytes	Family	Plant Habit	Distribution NE Qld
<i>Cyathea</i>	Cyatheaceae	Tree ferns	High altitude rainforests and along streams in wet sclerophyll forests, especially where cool
<i>Dicksonia</i>	Dicksoniaceae	Tree ferns	Wet cool rainforests generally, but surviving in moist gullies in some warmer rainforests
<i>Davallia</i>	Davalliaceae	Epiphytic fern	Rainforest and also in more open enviroments
<i>Microsorium</i>	Polypodiaceae	Creeping fern	Often forming mats on boulders and tree trunks widespread in rainforest and fern gullies
<i>Lycopodium</i>	Lycopodiaceae	Clubmoss/Epiphytic	Found on trees and rocks in rainforest
<i>Platycerium</i>	Polypodiaceae	Epiphytic fern	Rainforest
<i>Lygodium</i>	Lygodiaceae	Climbing fern	Rainforest, swamp forest or open forest
<i>Lindsaea</i>	Lindsaeaceae	Ground ferns	Found in open forests, swamps or soaks
<i>Gleichenia</i>	Gleicheniaceae	Ground ferns	Cover large areas of cool wet simple rainforests on poor acidic soils
Ophioglossaceae	Ophioglossaceae	Ground ferns	Widespread outside rainforests
<i>Selaginella</i>	Selaginellaceae	Spikemosses	Terrestrial with most growing in damp shady areas of tropical forests
<i>Pteridium</i>	Dennstaedtiaceae	Sclerophyll fern	Highly adaptable fern which readily colonises disturbed areas
<i>Pteris</i>	Pteridaceae	Sclerophyll fern	Widespread fern occupying a variety of ecological niches from aquatic, terrestrial and disturbed areas
Monolete (psilate) ferns	Blechnaceae	Ground fern	Probably <i>Blechnum</i> which quickly colonises disturbed areas

Appendix B (2) -Observations and Statistical Analyses

Section 1. Non-quantified observational data and target counts dryland sum

Zone LC1-9 Depth 902-578 cm (samples 451-288) c. 54,391 – 36,656 yrs B.P.

Through LC1-9 there is a high degree of clumping for both the rainforest gymnosperms (*Podocarpus*, *Araucaria* and *Dacrydium*) and for the sclerophyll taxa (Casuarinaceae, *Eucalyptus* type, *Melaleuca*, *Callitris* and *Dodonaea*) and to a lesser degree for some of the rainforest angiosperms, *Syzygium* comp., *O.paniculata*, *Ilex*, *Elaeodendron*, *Dissilaria*, Sapindaceae (syncolpate) and Urticaceae. This zone had the most problem of achieving the targeted dryland pollen count (150-200 grains) with 13 samples out of 162 samples not reaching the targeted dryland pollen count. However, all dryland counts were between 100-150 grains except at 900 cm, 656 cm, 654 cm and 644 cm where counts were below 100 grains but total pollen counts were above 400 grains. Degraded pollen grains were present through the middle of the zone and towards the top of the zone especially for Casuarinaceae which also had evidence of charring and to a lesser degree *Araucaria* and *Dacrydium*.

Zone LC1-8 Depth 576-484 cm (samples 288-242) c. 36,548 – 31,735 yrs B.P.

Clumping is present across the main sclerophyll components especially the Myrtaceae group and for the rainforest gymnosperm *Podocarpus* near the base of the zone. All samples were above the targeted count for the dryland pollen sum. There is mild oxidation throughout the zone with degraded *Dacrydium*, *Podocarpus* and Proteaceae grains near the base through to the middle of the zone and aberrant *Podocarpus* and squashed *Argyrodendron* comp grains towards the top of the zone. Abundant 4-pored Casuarinaceae pollen grains were recorded at 562 cm.

Zone LC1-7 Depth 482-412 cm (samples 241-206) c. 31,623 – 28,799 yrs B.P.

Clumping was recorded for the main sclerophyll components, Casuarinaceae and the Myrtaceae group, sporadically through the zone. Targeted dryland counts were not achieved at 448 cm and 454 cm. However, counts were > 100 dryland grains and total pollen counts were > 200 grains and therefore these samples were included in the results.

Unidentified degraded pollen grains with some charred were present through the zone and at 446 cm identified as Myrtaceae.

Zone LC1-6 Depth 410-220 cm (samples 205-110) c. 28,735 – 18,728 yrs B.P.

Clumping is recorded across the main sclerophyll components, with Casuarinaceae mainly from the base to the middle while *Eucalyptus* type and *Melaleuca* have a wider range through the zone. Clumping is occasionally recorded for *Podocarpus*, *Syzygium* comp and *O.paniculata*. For the 95 samples counted for this zone the targeted dryland count was not achieved for 5 samples, 358 cm, 360 cm, 362 cm, 366 cm, and 368 cm, however all dryland counts were > 100 grains except at 368 cm where dryland counts were < 100 grains. This depth recorded the lowest dryland concentration (1274 dryland grains per cm³) as well as the lowest total pollen concentration (2841 grains per cm³) of the diagram. However, it is included in the results for continuity purposes. At 372 cm and 338 cm a significant amount of degraded, torn and charred Casuarinaceae grains were found and at 314 cm at a lesser extent and included Myrtaceae grains. At 220 cm and 222 cm a significant amount of Myrtaceae grains were 4-pored. Towards the top degraded grains of Cunoniaceae (tricolpate), *Araucaria*, *O.paniculata* and *Acmena* were occasionally recorded.

Zone LC1-5 Depth 218-158 cm (samples 109-79) c. 18,633 – 13,473 yrs B.P.

As in the previous zone clumping was recorded across the main sclerophyll components, Casuarinaceae and the Myrtaceae group, except for *Corymbia*, sporadically throughout the zone. Clumping was also recorded for the herb/shrub components Asteraceae (tubuliflora) and Asteraceae (liguliflora). All samples were above the targeted count for the dryland pollen sum. A significant amount of 4-pored Myrtaceae grains were recorded from 210 cm – 218 cm while aberrant 4-pored Casuarinaceae grains were recorded at 210 cm and 212 cm. Degraded *Argyrodendron* comp. and *Podocarpus* grains were recorded at 176 cm and 170 cm respectively. Towards the top of the zone aberrant *Podocarpus* and *Dacrydium* grains were present.

Zone LC1-4 Depth 156-104 cm (samples 78-52) c. 13,365 – 8,931 yrs B.P.

Clumping was recorded for the Myrtaceae group through the zone and for Casuarinaceae at the base of the zone, while clumping was recorded for monolete (psilate) ferns from the middle to the top of the zone. All samples were above the targeted count for the dryland pollen sum. A significant amount of Myrtaceae grains were degraded at 148 cm while at the same depth Casuarinaceae grains were considerably smaller than previous. At 138 cm and 140 cm a higher amount of grains were degraded and charred with Myrtaceae grains accounting for a sizable portion. Charred grains were also recorded at 130 cm while at 110 cm degraded and aberrant *Melastoma* grains were recorded.

Sub-Zone LC1-3c Depth 102-80 cm (samples 51-40) c. 8768 – 7820 yrs B.P.

Clumping was recorded for Myrtaceae through the zone and for Casuarinaceae at the base of the zone. Clumping was recorded through the zone for monolete (psilate) ferns while occasionally recorded for the ground fern, *Lygodium*, and sclerophyll fern, *Pteridium*. All samples were above the targeted count for the dryland pollen sum. A significant amount of degraded Casuarinaceae grains were recorded near the base while at 86 cm and 88 cm degraded grains of *Hibbertia*, *Lygodium* and *Ilex* were recorded. Degraded *Dodonaea* and *Acmena* grains were recorded at 82 cm and 84 cm.

Sub-Zone LC1-3b Depth 78-68 cm (samples 39-34) c. 7799 – 7690 yrs B.P.

Clumping was recorded for *Acmena* and Myrtaceae (unspecified) through the zone as well as for the pteridophytes, monolete (psilate) ferns, Davalliaceae, *Microsorium* and *Lygodium*. All samples were above the targeted count for the dryland pollen sum. Degraded Casuarinaceae grains were recorded at 78 cm, 76 cm and 74 cm where Myrtaceae and *Melastoma* degraded grains were also recorded. At 68 cm nearly all Casuarinaceae grains were degraded.

Sub-Zone LC1-3a Depth 66-46 cm (samples 33-23) c. 7668 – 6640 yrs B.P.

Clumping was recorded for Myrtaceae (unspecified) at the top and base of the zone and for *Acmena* at the base of the zone. Clumping was also recorded for the ground fern, *Gleichenia*, at the top of the zone while for monolete (psilate) ferns throughout the zone. All samples were above the targeted counts for the dryland pollen sum. Degraded *Ficus*

grains were recorded at 66 cm, while at 62 cm a significant amount of Myrtaceae grains were degraded and at 60cm Casuarinaceae and *Dacrydium* grains were degraded. At 52 cm all Myrtaceae grains, except for *Acmena* and *Syzygium*, were degraded while from 46 cm to 50 cm degraded grains of *Rapanea* and *Dodonaea* were present.

Zone LC1-2 Depth 44-28 cm (samples 22-14) c. 6433 – 4901 yrs B.P.

Clumping was recorded through the zone for *Acmena*, Cunoniaceae (tricolpate), *Syzygium* comp, monolete (psilate) ferns and the ground fern, *Lygodium*. All samples were above the targeted count for the dryland pollen sum.

Zone LC1-1 Depth 26-0cm (samples 13-1) c. 4755 – 3000 yrs B.P.

Clumping was occasionally recorded for *Archontophoenix*, *Macaranga/Mallotus* comp, Rubiaceae and *Melastoma* and for the pteridophytes, *Gleichenia*, *Lygodium*, *Cyathea*, Davalliaceae, *Platycerium* and monolete (psilate) ferns. All samples were above the targeted count for the dryland pollen sum.

Table 2.1. Aquatic and Swamp percentage data (Full record 3 ka–54 ka)

Variable	Factor coordinates of the variables, based on correlations (AqSw%FullResum) Active and Supplementary variables *Supplementary variable			
	Factor 1	Factor 2	Factor 3	Factor 4
Poaceae	-0.463139	-0.698510	0.108120	-0.009206
<i>Eleocharis</i>	0.036172	-0.124425	0.579557	0.463483
<i>Schoen/Carex</i>	0.123905	0.170527	-0.776345	0.224321
<i>Cyperus</i>	0.583663	-0.118275	-0.055230	0.318563
<i>Hydrocotyle</i>	0.801266	0.031402	0.198940	0.030443
<i>Botryococcus</i>	-0.467630	0.273841	0.410355	-0.105864
<i>Anthoceros</i>	0.343981	-0.439544	0.096334	-0.272393
<i>Haloragis/Gonocarpus</i>	0.735632	0.011271	0.339779	-0.188169
<i>Nymphoides</i>	-0.147322	-0.117050	0.011482	0.730336
<i>Liparophyllum</i>	-0.133916	-0.696095	-0.165838	-0.165103
<i>Persicaria</i>	-0.348557	0.201187	0.300137	0.092611
<i>Typha</i>	-0.176393	0.372139	0.050803	-0.233741
*Moisture	-0.308641	0.173097	-0.037675	-0.069466
*Inorganics	-0.150853	-0.314086	-0.233240	0.012302
*Macro'Other'	0.238087	0.054065	0.317580	0.165213
*Macro'Lattice'	-0.138052	0.086292	-0.102600	-0.044910
*Macro'Elongated'	-0.029366	0.145282	0.031860	0.007975
*Macro'Blocky'	0.217934	0.086192	0.225714	0.098635
*Microcharcoal	0.088339	-0.216231	0.159610	0.136710
Sponge Spicles	-0.274758	-0.211104	-0.186022	-0.038478
* <i>Gelasinospora</i> Presence/Absence	0.028846	0.076315	0.319711	0.037885
* <i>Neurospora</i> Presence/Absence	-0.057498	0.129376	0.093719	-0.074979

Table 2.2. Eigenvalues of the correlation matrix for the aquatic and swamp percentage (full).

Value Number	Eigenvalue	% Total Variance	Cumulative Eigenvalue	Cumulative %
1	2.069943	20.69943	2.06994	20.6994
2	1.479711	14.79711	3.54965	35.4965
3	1.229231	12.29231	4.77889	47.7889
4	1.033608	10.33608	5.81249	58.1249

**Table 2.3. Factor coordinates of the variables, based on correlations – Aquatic and Swamp percentage data
(Pleistocene record 11.8 ka – 54 ka)**

Active and Supplementary variables *Supplementary variable

Variable	Factor 1	Factor 2	Factor 3	Factor 4
Poaceae	0.464961	0.136912	0.701592	0.026332
<i>Eleocharis</i>	0.513594	0.320402	0.047399	-0.475504
<i>Schoenoplectus/Carex</i>	-0.268954	0.595838	-0.334814	0.385478
<i>Cyperus</i>	-0.452198	0.479893	-0.093838	-0.400036
<i>Baumea</i>	0.370444	0.620231	-0.162566	-0.212007
<i>Haloragis/Gonocarpus</i>	-0.606656	-0.284707	0.168396	-0.394253
<i>Hydrocotyle</i>	-0.720777	-0.015650	-0.013210	-0.298451
<i>Typha</i>	0.140035	-0.140217	-0.533074	0.251593
<i>Persicaria</i>	0.394991	-0.067576	-0.274554	-0.332276
<i>Anthoceros</i>	-0.110925	0.216505	0.507629	0.250441
<i>Botryococcus</i>	0.473664	-0.410362	-0.191649	-0.205225
*ML	0.010981	-0.129812	-0.128844	-0.310773
*Inorganics	0.147635	0.317593	0.147968	0.322627
*Macro'Other'	0.145014	-0.039397	-0.187159	0.031413
*Macro'Lattice'	0.084311	0.055222	-0.228542	0.106718
*Macro'Elongated'	0.090525	0.002856	-0.214906	0.101529
*Macro'Blocky'	0.054076	-0.015998	-0.182636	0.076582
*Microcharcoal Total	0.434599	0.231179	0.215662	0.022372

Table 2.4. Eigenvalues of the correlation matrix for the aquatic and swamp percentage (Pleistocene).

Value Number	Eigenvalue	% Total Variance	Cumulative Eigenvalue	Cumulative %
1	2.220387	17.07990	2.22039	17.0799
2	1.612160	12.40123	3.83255	29.4811
3	1.409521	10.84217	5.24207	40.3236
4	1.206148	9.27806	6.44822	49.6017

Table 2.5. Factor coordinates of the variables, based on correlations – Aquatic and Swamp percentage data (humification record)

Active and Supplementary variables *Supplementary variable

Variable	Factor 1	Factor 2	Factor 3	Factor 4
Poaceae	0.850005	-0.096169	0.174018	-0.416773
<i>Eleocharis</i>	-0.009140	0.711386	0.178433	0.004891
<i>Schoenoplectus/Carex</i>	-0.708980	-0.162958	0.318649	0.541255
<i>Cyperus</i>	0.273809	0.717226	0.070581	0.415473
<i>Baumea</i>	-0.033559	0.767767	-0.147298	-0.177782
<i>Typha</i>	-0.351171	-0.203000	-0.805103	0.015674
<i>Haloragis</i>	0.588709	-0.002967	-0.305792	0.339986
<i>Liparophyllum</i>	0.770932	0.041227	-0.082561	0.223885
<i>Persicaria</i>	-0.343997	0.527305	-0.359509	-0.106907
<i>Anthoceros</i>	0.620826	-0.189810	-0.172940	0.345173
*Humification	0.246019	0.301013	0.085532	0.032418
*Inorganics	0.148236	-0.006439	0.059763	0.118231
*Moisture	-0.254168	0.068196	-0.052561	-0.111644
*Microcharcoal	0.308079	0.159050	-0.117322	-0.121892
*Macro'Blocky'	-0.306538	0.100189	-0.170714	-0.017617
*Macro'Elongated'	-0.353559	0.069813	-0.150105	-0.024498
*Macro'Lattice'	-0.222236	0.179408	-0.156280	0.136502
*Macro'Other'	-0.308984	0.186734	-0.157370	-0.139282

Table 2.6. Eigenvalues of the correlation matrix for the aquatic and swamp percentage (Humification)

Value Number	Eigenvalue	% Total Variance	Cumulative Eigenvalue	Cumulative %
1	2.869336	28.69336	2.86934	28.6934
2	2.002749	20.02749	4.87208	48.7208
3	1.098007	10.98007	5.97009	59.7009
4	0.967439	9.67439	6.93753	69.3753

Table 2.7. Factor coordinates of the variables, based on correlations – Aquatic and Swamp percentage data (Holocene record)

Active and Supplementary variables *Supplementary variable				
Variable	Factor 1	Factor 2	Factor 3	Factor 4
Poaceae	-0.596083	0.136813	-0.349347	0.478156
<i>Eleocharis</i>	0.560070	0.469836	0.266229	-0.102475
<i>Schoenoplectus/Carex</i>	-0.452876	-0.833731	-0.060006	-0.077047
<i>Cyperus</i>	0.394599	-0.293687	0.590141	0.174726
<i>Baumea</i>	-0.325692	-0.068015	0.524487	0.107046
<i>Haloragis/Gonocarpus</i>	0.877202	-0.091445	-0.072803	-0.065727
<i>Hydrocotyle</i>	0.839938	-0.160773	0.193100	0.005056
<i>Typha</i>	-0.384045	0.676020	0.182599	-0.135819
<i>Eriocaulon</i>	0.477312	0.150727	-0.569295	-0.044757
<i>Nymphoides</i>	-0.274877	-0.102373	-0.076785	-0.851679
<i>Anthoceros</i>	0.579162	-0.156494	-0.387021	0.106952
*Moisture	-0.752194	0.083195	0.254489	0.122893
*Inorganics	0.471698	0.020288	-0.540941	-0.031893
*Microcharcoal	0.350923	-0.202198	-0.156050	-0.075905
*Macro'Blocky'	0.582552	0.194191	0.428630	-0.153045
*Macro'Elongated'	0.400086	0.394588	0.370052	-0.177042
*Macro'Other'	0.473305	0.215304	0.402345	-0.163435
*Macro'Lattice'	-0.204767	0.354059	0.018526	-0.125950

Table 2.8. Eigenvalues of the correlation matrix for the aquatic and swamp percentage (Holocene).

Value Number	Eigenvalue	% Total Variance	Cumulative Eigenvalue	Cumulative %
1	3.397159	30.88327	3.39716	30.8833
2	1.574350	14.31227	4.97151	45.1955
3	1.375583	12.50530	6.34709	57.7008
4	1.048650	9.53318	7.39574	67.2340

Variable	Table 2.9. Factor coordinates of the variables, based on correlations (Percentage Full record) Active and Supplementary variables *Supplementary variable			
	Factor 1	Factor 2	Factor 3	Factor 4
<i>Araucaria</i>	-0.066367	-0.760365	-0.177975	-0.219034
<i>Agathis</i>	0.136935	-0.445403	-0.222891	-0.040994
Podocarpaceae	-0.109548	-0.772634	-0.139865	-0.165878
<i>Dacrydium</i>	-0.097777	-0.624769	-0.019311	0.015985
<i>Elaeocarpus</i>	0.869820	0.052094	-0.028711	0.094709
Cunoniaceae(tricolpate)	0.884070	0.106971	-0.216265	0.108774
Cunoniaceae(dicolpate)	0.836485	0.087900	-0.198545	0.155256
<i>Syzygium</i>	0.474671	0.100031	0.495233	-0.437688
<i>Ficus</i>	0.870961	0.068588	-0.114198	0.135061
<i>Olea paniculata</i>	-0.185626	-0.309931	0.216428	0.511791
<i>Mallotus/Macaranga</i>	0.389061	-0.369525	0.184152	0.529205
Legume Grouping	0.647014	-0.003327	0.071834	0.004053
Urticaceae/Moraceae	0.048849	-0.317882	0.588516	-0.188360
<i>Glochidion</i>	0.621361	0.105545	-0.115862	-0.365360
<i>Trema</i>	0.450245	0.129745	0.526087	-0.126062
<i>Celtis</i>	0.164242	-0.120581	0.462668	0.201555
<i>Argyrodendron peralatum</i>	-0.063929	-0.796685	0.086687	0.003896
Casuarinaceae	-0.481118	0.678176	-0.103621	0.017137
<i>Eucalyptus</i>	-0.492342	0.367130	0.291951	0.180692
*Inorganics	-0.071438	0.200400	-0.020798	0.313987
*Moisture Loss	-0.615129	-0.116111	0.046485	-0.164608
*Macrocharcoal	0.204882	0.159194	-0.222503	0.009893
*Microcharcoal	0.511246	0.327597	0.083870	0.211854
* <i>Melastoma affine</i>	0.696155	0.085896	-0.052597	0.154456

Table 2.10. Eigenvalues of the correlation matrix for the dryland percentage (full).

Value Number	Eigenvalue	% Total Variance	Cumulative Eigenvalue	Cumulative %
1	6.537235	28.42276	6.53723	28.4228
2	3.319744	14.43367	9.85698	42.8564
3	2.004229	8.71404	11.86121	51.5705
4	1.487598	6.46782	13.34881	58.0383

Table 2.11. Factor coordinates of the variables, based on correlations**Dryland percentage data (Pleistocene record)****Active and Supplementary variables *Supplementary variable**

Variable	Factor 1	Factor 2	Factor 3	Factor 4
<i>Araucaria</i>	0.745065	0.255612	0.076317	0.119725
<i>Agathis</i>	0.441673	0.140773	0.206318	0.255432
Podocarpaceae	0.730161	0.240682	-0.133117	0.167753
<i>Dacrydium</i>	0.581387	0.050571	-0.102477	0.084163
<i>Syzygium</i>	0.280767	-0.122921	-0.677959	0.064535
<i>Argyrodendronperalatum</i>	0.764442	0.023783	-0.044734	0.041283
<i>Olea paniculata</i>	0.291007	-0.310836	0.153808	-0.454938
<i>Mallotus/Macaranga</i>	0.513477	-0.361898	0.103653	0.043432
Legume Grouping	0.182841	-0.417251	-0.015992	-0.526845
Urticaceae/Moraceae	0.399090	-0.376364	-0.270018	-0.071553
<i>Trema</i>	0.109814	-0.508827	0.007569	-0.194241
<i>Celtis</i>	0.203789	-0.253441	0.015606	-0.371245
<i>Melicope</i>	0.088599	-0.281329	-0.103001	0.072208
<i>Petalostigma</i>	-0.194707	-0.265599	0.144601	0.259668
<i>Dodonaea</i>	0.231727	-0.324042	0.540790	0.240834
<i>Callitris</i>	0.223041	-0.282638	0.516626	0.142543
Casuarinaceae	-0.788852	0.300765	0.200422	-0.340207
<i>Eucalyptus</i>	-0.504172	-0.446167	-0.314229	0.282906
<i>Corymbia</i>	-0.408641	-0.404449	0.091515	0.366643
<i>Melaleuca</i>	-0.406338	-0.313167	-0.186634	0.271964
*Moisture	0.136997	0.050741	0.329040	-0.003588
*Inorganics	-0.359404	-0.261060	-0.137552	0.100155
*Microcharcoal	-0.475217	-0.278517	-0.138860	0.005430
*Macrocharcoal	-0.163610	0.035428	0.187999	0.051684

Table 2.12. Eigenvalues of the correlation matrix for the dryland percentage (Pleistocene).

Value Number	Eigenvalue	% Total Variance	Cumulative Eigenvalue	Cumulative %
1	4.236960	21.18480	4.23696	21.1848
2	1.913544	9.56772	6.15050	30.7525
3	1.419101	7.09550	7.56960	37.8480
4	1.342895	6.71447	8.91250	44.5625

Table 2.13. Factor coordinates of the variables, based on correlations - Dryland percentage data (Holocene record)
Active and Supplementary variables *Supplementary variable

Variable	Factor 1	Factor 2	Factor 3	Factor 4
Cunoniaceae(tricolpate)	0.803280	-0.153655	-0.278249	0.256904
Cunoniaceae(dicolpate)	0.749755	-0.339651	-0.040635	0.200437
<i>Elaeocarpus</i>	0.705132	-0.437475	-0.093838	-0.092825
<i>Acmena</i>	0.476426	0.714721	0.172082	-0.260717
<i>Ficus</i>	0.730061	-0.359967	-0.282267	0.210280
<i>Olea paniculata</i>	-0.287829	-0.078390	0.251628	-0.192806
<i>Archontophoenix</i>	0.290442	-0.617100	0.454847	-0.241120
<i>Glochidion</i>	0.607584	0.688907	0.139808	-0.072344
<i>Mallotus/Macaranga</i>	0.310634	-0.758593	0.259622	-0.005602
Legume Grouping	0.790216	0.248366	0.198173	0.006519
Urticaceae/Moraceae	-0.330686	0.058292	-0.116418	-0.403567
<i>Trema</i>	-0.214005	-0.213431	-0.592729	0.119750
<i>Celtis</i>	-0.126363	-0.274902	-0.103610	-0.555179
<i>Oraniopsis</i>	0.285175	-0.731725	0.256766	-0.146434
<i>Rapanea</i>	0.636583	0.651406	0.127804	0.009907
<i>Freycinetia</i>	0.643920	0.085670	0.015724	0.047893
<i>Dodonaea</i>	-0.571122	-0.008725	-0.089241	0.230499
<i>Callitris</i>	-0.568490	0.030202	0.176625	0.374605
Casuarinaceae	-0.874102	-0.045039	-0.176175	-0.156136
<i>Eucalyptus</i>	-0.884945	-0.057975	0.168126	0.033368
<i>Corymbia</i>	-0.512784	0.065455	0.089129	0.001507
<i>Melaleuca</i>	-0.378572	-0.050455	0.504131	0.529248
*Moisture	-0.752373	0.529388	0.123624	0.043767
*Inorganics	0.379985	-0.723884	0.091356	-0.171507
* <i>Syzygium</i> .	-0.285198	0.102458	-0.360166	-0.354770
* <i>Melastoma affine</i>	0.562789	-0.487692	0.253484	-0.184155
*Microcharcoal	0.450775	-0.360317	-0.236072	-0.143172
*Macrocharcoal	0.537762	0.199669	-0.089976	0.347436
*Macro'Blocky'	0.609531	0.203664	-0.141711	0.310985
*Macro'Elongated'	0.429470	0.186990	-0.018851	0.350999
*Macro'Lattice'	-0.273983	0.007691	0.342538	0.206012
*Macro'Other'	0.501676	0.158593	-0.198538	0.304768

Table 2.14. Eigenvalues of the correlation matrix for the dryland percentage (Holocene).

Value Number	Eigenvalue	% Total Variance	Cumulative Eigenvalue	Cumulative %
1	7.621263	33.13592	7.62126	33.1359
2	3.517072	15.29162	11.13833	48.4275
3	1.914663	8.32332	13.05270	56.7509
4	1.363261	5.92722	14.41596	62.6781

Section 3. Tables for Spectral Analysis

3.1. Tables 3.1-3.6 Spectral analysis peaks for Full, Pleistocene and Holocene sequences

Table 3.1. Full Record 3 ka – 54 ka

Percentage, **Concentration**, **Influx** and **Other** results for Major Pollen Groupings, Ratios and Non-Pollen categories.

**Dominant frequency when several other frequencies are present

* Secondary frequency when several other frequencies are present

(B) Borderline significant frequency

(F) Dominant frequency length of time-series analysed and data filtered.

These above categories (**, *, (B) and (F)) apply to all the tables below

Group	Peaks
Pollen Concentration & Influx	38600, 14700, 10300*, 6720, 4610, 4010, 3510 ; 34300 (B), 13700*, 9810*, 6440(B), 5420(B), 4680(B), 3430(B), 2510(B)
Dryland Concentration & Influx	14700*, 10300, 6720, 5720, 4540, 4070
Aquatic Concentration & Influx	22100*, 10700, 6580, 4680, 4070, 3550; 22900**, 6440(B), 5280(B), 4790(B)
Inorganics	20600**, 10800*, 4790, 3750
Aquatic/Dryland Ratio	23800*, 6180, 3430; 25800**, 8580(B), 6240*, 4790(B), 3430*
Microcharcoal/Pollen Ratio	38600*, 15500
Microcharcoal 8-52 µm	34300*, 15800**, 10800(B), 4120*, 3490(B), 3070(B), 1300(B); 4120(B)
Microcharcoal 53-104 µm	34300*, 17200**, 4120*, 2580(B); 14700(B), 4120(B), 2990(B)
Microcharcoal 105-156 µm	34300(B), 17200**; 4120(B), 2610(B); 34300(B), 15800**, 4120*, 3030(B)
Microcharcoal 157-208 µm	25800/22900(B), 17200**, 7920(B), 654(B); 15800**, 4120(B), 2990(B), 2480(B)
Microcharcoal >208 µm	25800/22900(B), 17200**, 7920(B), 654(B); 15800**, 4120(B), 2990(B), 2480(B)
Microcharcoal	34300*, 15800**, 10800(B), 4120*, 3070(B), 1300(B); 14700(B), 4120(B)
Macrocharcoal	28100*, 5940; 29400**, 12900, 7920, 5890*, 3680(B), 1300(B)
Cyperaceae/Poaceae Ratio	38600, 19300/13400*, 7920, 6580, 4680, 3640
Sclerophyll (%F)	41200**, 18700*, 10800(B), 8580*, 5720; 15800**, 9360*, 6440(B), 5420*, 4790, 3490(B)

Myrtaceae (Sclerophyll component) (%F)	20600*, 10800**, 6240(B), 5280(B), 2120(B); 20600**, 9360(B), 6440*, 5280*, 4680, 3490(B), 1980(B), 1430/1300(B)
Casuarinaceae (% and Influx F)	41200**, 17200*, 9360* 5570(B); 29400, 15800**, 9360*, 5420*, 4790, 3490(B)
Rainforest gymnosperm (% and Influx F)	29400**, 3680(B), 2990(B), 2860(B), 2290*, 1870(B); 9360**, 7360(B), 6650(B), 3680**, 2540(B), 1980(B), 1620/1570(B), 1330/1310(B)
Podocarpaceae (%F)	41200**, 15800*, 6440(B), 3750, 3490, 2860(B), 2370, 2260, 1890/1820(B), 1570(B); 8960**, 3680*, 2540(B), 1980(B), 1570(B), 1310(B)
<i>Araucaria</i>	34300**, 20600*, 13700(B), 10800, 8580, 3680(B), 3380; 34300**, 20600*, 13700, 10300*, 8580(B), 4790(B)
Rainforest angiosperm (%F)	41200**, 18700*, 12900, 8960, 7360(B), 6440(B), 5570; No Frequency
Rainforest (angiosperm) canopy (%F)	41200**, 18700*, 12900, 8960, 7360(B), 6440(B), 5720(B); No Frequency
Rainforest (angiosperm) secondary (%F)	41200**, 17200*, 12100(B), 9360(B), 2220(B); No Frequency
Rainforest (angiosperm)understorey (%F)	41200**, 18700, 12900*, 10300, 8580(B), 6440, 5570, 4910(B), 4120(B), 3750(B); No Frequency
Vines (%F)	41200**, 15800*, 9810, 5570(B); No Frequency
Pteridophytes (% and Influx F)	34300**, 1800*, 10300, 4290(B); 34300
Epiphytic ferns (% and Influx F)	41200**, 18700*, 13700(B), 10800, 8960(B), 6440, 5890; 41200/34300
Ground ferns (% and Influx F)	41200**, 20600(B), 13700(B), 10800(B), 8960, 7630(B), 6650*; 5890, 2860(B), 2710(B); 41200/34300**, 20600(B), 13700*, 10800, 8960(B), 7630(B), 6440, 5890(B)
Tree ferns (% and Influx F)	41200**, 20600*, 13700, 11400*, 8960**, 7540, 6440 5280(B), 4680(B); 41200**, 20600*, 13700*, 10800*, 8960(B), 7630(B), 6650(B), 5890(B), 5150(B), 4680(B), 4200
Sclerophyll ferns	29400**, 11400*, 6440(B), 4680(B), 3430(B); 41200**, 10300(B)
Aquatic (Dryland%)	25800*, 6180, 3430
Cyperaceae (Dryland%)	23800*, 6180, 3470; 23800*, 6310
Herb/Shrub	41200*, 17200**, 114*00, 7360, 4580(B), 3750(B), 2940(B), 2420(B), 2190(B), 1860(B); 15800(B)
Poaceae	20600**, 10300*; 20600**, 9360*, 6240(B), 5280(B), 4120(B), 3550(B)
Unknown Pollen Grains (Influx F)	34300*, 18700**, 10800, 8580; 41200

Table 3.2. Full Record 3 ka – 54 ka

Percentage and **Influx** results for Minor Pollen Groupings and Individual Pollen taxa types

Group/Taxa type	Peaks
<i>Eucalyptus</i> (%F)	41200*, 20600, 12900**, 6240*, 4290(B), 2120(B), 1160(B); 15800**, 9360, 6240*, 5280*, 4680(B), 1980(B), 1430(B)
<i>Corymbia</i>	22900**, 12100* 5420(B); 29400, 14700**, 9810(B), 3120(B), 990(B)
<i>Melaleuca</i>	51500, 22900/15800**, 10800*, 3610, 2120(B); 20600**, 17200**, 10800, 4480, 3960(B), 3550*, 2120, 1860(B), 1320(B)
<i>Callitris</i>	34300*, 17200(B), 11400/9810*, 7920, 3680**, 3120(B), 2100(B), 1290(B); 29400(B), 12100**, 3680(B), 3120(B), 463(B)
<i>Dodonaea</i>	22900(B), 10300**, 2100(B), 2000(B); 13700(B), 848(B)
<i>Agathis</i> (% and Influx F)	41200**, 10800(B), 8960(B), 7920(B), 5720, 2860/2710(B); 41200**, 15800(B), 11400*, 8960(B), 5720, 958(B)
<i>Dacrydium</i>	34300*, 15800**, 11400*, 6440; 29400*, 10300*, 6650**, 4120(B), 3490(B), 2340(B)
<i>Acmena</i> (%F)	34300**, 17200(B); No Frequency
<i>Argyrodendron peralatum</i> (%F)	17200**, 10800(on main), 7920*, 6650, 3220, 2150(B); 41200**, 3820(B), 3030(B), 1510(B)
<i>Celtis</i>	41200(B), 15800**, 1640(B), 1080(B); 15800(B), 1780(B)
Cunoniaceae (tricolpate) (% and Influx F)	41200**, 20600, 13700*, 10800*, 8960, 7360(B), 6440(B), 5720(B); 34300
<i>Elaeocarpus</i> (%F)	41200**, 18700*, 13700, 10800, 8960(B), 6650(B), 5890(B), 4380(B), 3960(B), 3680(B); No Frequency
<i>Elaeodendron</i> (Influx F)	29400**, 17200*, 3270(B); 36800**, 17200(B), 6780(B), 1890(B), 425/420(B)
Leguminosae (%F)	41200**, 17200*, 11400, 6870, 2190(B); No Frequency
<i>Longetia</i> (%F)	41200*, 17200(B), 12900**, 2780(B); 20400(B), 13700(B), 8240**, 1980(B), 1580(B)
<i>Mallotus/Macaranga</i> (% and Influx F)	41200**, 17200*, 12100, 9810, 7360(B), 6240, 2540(B), 2400, 1810(B); 41200**, 15800*, 10800*, 5890(B), 4290(B), 3490(B), 1730(B)
Menispermaceae	41200**, 17200*, 5720(B), 2820(B), 2640(B), 1510(B); No Frequency
<i>Olea paniculata</i>	22900**, 9810(B), 7360*, 5150(B), 4290, 3490(B); 20600**, 9360(B), 6650(B), 5280(B), 4680(B), 4120(B)
<i>Homalanthus</i>	24100**, 12800(B), 2330(B), 1620(B); 41200(B)
<i>Oraniopsis</i>	41200, 17200**, 11400, 8960, 7100*, 5890, 5020, 3490(B), 3220(B), 2940(B), 2710(B), 2510(B); 17200*, 11400, 8580(B), 7100**, 5020(B), 3490(B), 2940, 2710(B), 2340(B)
<i>Petalostigma</i> (% and Influx F)	34300**, 10800(B), 315(B); 34300**, 315(B)
Sapindaceae(syncolpate) (%and Influx F)	41200**, 18700*, 12900(B), 5570(B), 2780(B); 41200**, 18700*, 13700(B), 10300(B), 6440(B), 381(B)

<i>Syzygium</i> comp. (%F)	41200**, 18700*, 12900, 9360, 7630, 6240, 4910(B), 4290(B), 3890(B); No Frequency
<i>Trema</i> (%F)	41200**, 15800*, 7920(B), 3960(B), 723(B), 708(B), 691(B); 34300**, 13700(B), 691(B)
Urticaceae/Moraceae	34300*, 17200(B), 11400**, 8960(B), 5890, 5020(B), 3960(B), 2220(B), 958(B); 6060(B)
<i>Zanthoxylum</i>	29400**, 2750(B); 34300(B), 11400/10300(B), 634(B)
<i>Anthoceros</i>	25800**, 12100*, 8960, 6060(B), 2710(B), 2480, 2080(B); 25800**, 11400(B), 2540(B)
Asteraceae(tubiliflorae)	20600**, 10800(B), 7630(B), 4380(B), 3680(B); 18700**, 9360(B), 6870(B), 4680(B), 4200(B), 3550(B), 2490(B)
<i>Botryococcus</i>	41200**, 17200/15800*; 18700**, 1580(B)
Chenopodiaceae	15800*, 10300, 4200(B), 3550**, 1250(B); 15800**, 9360*, 6240(B), 4910
<i>Haloragis</i>	41200*, 17200**, 12100, 7360, 6440(B), 2540(B), 2420(B), 1340(B); 34300(B)
<i>Hydrocotyle</i>	41200**, 15800, 11400, 8960*, 7630, 6240(B), 4910(B), 3750(B), 2120(B), 1500(B); No Frequency
Monolete ferns (% and Influx F)	34300**, 17200*, 12900(B), 9810, 8240, 7100(B), 2540(B); 34300(B)
<i>Persicaria</i>	41200**, 22900*, 2540(B); 51500*, 20600**, 6440(B), 2150(B)
<i>Platyserium</i>	41200**, 18700*, 10800, 8580(B), 958(B); 41200/34300**, 18700(B), 13700(B), 10800*
<i>Pteridium</i>	25800**, 11200*, 6440(B), 4680(B), 3480(B), 1050(B); 34300**, 17200(B), 10300*, 4580(B), 3490(B), 3120(B)
<i>Leptospermum</i>	44100, 19300, *9660; 34300, 20600, 12100, 9810**, 7920, 7100, 6240, 5280(B), 4680, 4120(B), 3820(B), 3490(B), 2860(B), 2680(B), 2540(B), 2000(B)

Table 3.3. Pleistocene Record 11.8 ka – 54 ka

Percentage, **Concentration**, **Influx** and **Other** results for Major Pollen Groupings, Ratios and Non-Pollen categories

Group	Peaks
Pollen Concentration & Influx	27600, 15200, 9810*, 6760, 4610, 4000, 3490, 2510; 27600, 14500, 9500*, 6760, 5430, 4610, 4000, 3490, 2510
Dryland Concentration & Influx	30400/16000*, 9500, 4610, 4000, 3530; 31000, 15500**, 9440*, 6790, 5430, 4620, 4020, 3500, 2500(B), 1320(B)
Aquatic Concentration & Influx	23400/21700*, 10500, 6330, 4680, 4110, 3530; 21700**, 10300(B), 6390, 4720*, 4110, 3560
Inorganics	21700**, 10300, 4830*, 3740
Aquatic/Dryland Ratio	25300*, 6200, 3450; 24100**, 8690(B), 6200*, 4720(B), 3450*, 2590(B)
Microcharcoal/Pollen Ratio	31400**, 22000, 5000(B)
Microcharcoal 8-52 µm	43400*, 18100**, 9870(B), 7490(B), 4340(B), 2710(B); 43400(B), 16700**, 9440*, 7490(B), 4430*, 3100(B), 2750(B), 2170(B)
Microcharcoal 53-104 µm	43400*, 16700**, 5870(B), 4260; 43400, 15500**, 9440, 7490(B), 4340*, 3340(B), 3020(B), 2710(B) < 2150(B)
Microcharcoal 105-156 µm	43400*, 15500**, 4180; 43400, 15500**, 9870*, 4340*, 3020(B)
Microcharcoal 157-208 µm	31000(B), 14500**, 4180*; 15500/14500**, 10300(B), 4260(B), 2710(B)
Microcharcoal >208 µm	31000(B), 14500**, 4180*; 3100(B), 14500(B), 10300**, 4260(B)
Microcharcoal	18100**, 6760, 4260*, 3740; 43400, 16700**, 9440*, 7490(B), 4430*, 3100(B), 2750(B), 2170(B)
Macrocharcoal	24100**, 19700**, 1290(B), 1190(B); 19700**, 9440*, 1300(B)
Cyperaceae/Poaceae Ratio	15500**, 7760, 6390, 4720, 3560*, 2970, 1290; *15200, 6330, 4750, 3580
Sclerophyll	27100**, 7000*, 2333; 15500**, 9440*, 6790(B), 5430, 4620*, 4020(B), 3500, 1320(B)
Myrtaceae (sclerophyll component)	27100*, 11400**, 5870, 3620(B), 2130(B); 15500**, 9440, 6390, 5300, 4620*, 3560(B), 1320
Casuarinaceae (%F)	27100**, 10900*, 6580, 5300(B), 3620(B); 31000, 15500**, 9440*, 7000(B), 5570, 4620, 4020(B), 3560
Rainforest gymnosperm	31000**, 3680(B), 2820(B), 2310*, 1890(B); 36200(B), 8350*, 6790*, 3680**, 2590(B), 1990(B), 1610/1550(B), 1320(B)
Podocarpaceae (%F)	31000**, 8040(B), 6580, 3680, 2820(B), 2310*, 1970(B), 1890, 1600(B), 1540(B); 8350**, 6790*, 3680**, 2590(B), 1990(B), 1890(B), 1600(B), 1550(B), 1320(B)
<i>Araucaria</i>	27100**, 10900, 9050*, 7490, 3560; 27100**, 15500, 10900*, 4720(B)
Rainforest angiosperm	21700**, 10300*; 7240(B), 5170(B), 3950(B), 3560(B), 2240(B); 27100**, 14500*, 9440*, 6580*, 5430, 4620, 4020, 3450(B), 2070(B)

Rainforest (angiosperm) canopy	27100**, 10300*, 7240(B), 3500(B); 27100**, 13600*, 9050, 6580, 5430, 4620, 3950, 3450(B), 2680(B), 2470(B), 2070(B)
Rainforest (angiosperm) secondary	21700**, 10300(B), 7240*, 2240(B); 19700**, 9050, 6580*, 4720, 4100(B), 717(B)
Rainforest (angiosperm) understorey	21700**, 6200(B), 5170*, 4020(B); 24100*, 15500(B), 9440*, 6790**, 5430(B), 4100(B), 3450(B)
Vine	21700**, 5300*, 2590(B), 330(B); 19700**, 9870(B), 4940*, 4100(B), 749(B)
Pteridophytes	31000*, 12800**, 4940(B), 2970(B), 2190(B), 1160(B), 650(B); 24100**, 11400*, 6390(B), 4830(B), 4180, 3620, 3100(B), 2500(B)
Epiphytic ferns (%F)	27100**, 5430(B), 795(B); 27100**, 12800(B), 5430, 3680, 2520(B)
Ground ferns	3810(B), 1630(B); No Frequency
Tree ferns/ <i>Cyathea</i> (%F)	4620(B), 3060(B), 1500(B), 1350(B), 1290(B), 454(B); 36200**, 15500, 5570(B), 4720*, 4100, 3620(B), 1870(B)
Sclerophyll ferns	27100**, 11400*, 7000, 3950(B), 3500(B); *23400, 10900, 3620
Aquatic (Dryland%)	25300*
Cyperaceae (Dryland%)	27100**, 11400, 6200*, 4720(B), 3500(B); 21700**, 10900, 6390*, 4620, 4020, 3560(B)
Herb/Shrub	19700**, 10300(B), 7490(B), 4340*, 3680; 18100**, 9440*, 6790(B), 4830(B), 4260(B), 3500(B), 2930(B)
Poaceae	21700**, 10300*; 19700**, 9440*, 4180, 3500(B)
Unknown Pollen Grains	24100**, 9050*, 27100**, 10300/9050*, 6200(B), 4180*

Table 3.4. Pleistocene Record 11.8 ka – 54 ka

Percentage and **Influx** results for Minor Pollen Groupings and Individual Pollen taxa types

Group/Taxa type	Peaks
<i>Eucalyptus</i>	36200, 13600**, 5870*, 2150(B); 15500**, 9440, 6390*, 5300, 4620*, 1320(B)
<i>Corymbia</i>	27100**, 11400*, 5430(B); 24100, 15500**, 9440(B), 1320(B), 1160(B)
<i>Melaleuca</i>	27100**, 16700*, 10300*, 4620, 3620, 2110(B); 31000, 21700, 16700**, 9870*, 4520*, 4020(B), 3560*, 2130, 1860(B), 1320(B)
<i>Callitris</i>	36200*, 9050, 4520(B), 3680**, 2070(B), 1280(B); 31000, 12800**, 4620(B), 3680(B)
<i>Dodonaea</i>	27100(B), 9870**, 3020(B); 15500**, 848(B)
<i>Agathis</i>	27100*, 9440**, 7490(B), 5870(B), 2750(B); 27100(B), 9440**, 5870**, 2780
<i>Dacrydium</i>	21000**, 14500*, 8690(B), 6580*; 27100*, 10300*, 6790**, 5570(B), 4100(B), 3500(B), 2330(B)
<i>Acmena</i>	43400(B), 15500**, 3500(B), 2050(B); 27100(B), 6580**, 4720*, 1630(B), 1230(B)
<i>Argyrodendron peralatum</i>	27100**, 14500*, 10300, 7240, 6030, 3240, 2130(B); 31000**, 3950(B), 3060(B)
<i>Celtis</i>	18100**, 1620(B), 1360(B), 1070(B); 16700**, 8690(B), 1610(B), 1480(B), 1360(B), 1170(B), 1090(B)
Cunoniaceae (tricolpate)	No Frequency; 1190(B)
<i>Elaeocarpus</i>	6200(B), 3620(B), 1470(B), 705(B), 250(B); 15500(B), 6390(B), 4620(B), 3560(B), 1470(B), 1190(B)
<i>Elaeodendron</i>	24100**, 3100(B), 746(B); 24100**, 1890(B)
Leguminosae	21700(B), 3680(B), 2170(B), 489(B); 16700**, 8690(B), 1610(B), 1480(B), 1360(B), 1170(B), 1090(B)
<i>Longetia</i>	13600**, 10900*, 2820(B); 27100(B), 13600(B), 8350**, 2650(B), 1990(B), 1600(B)
<i>Macaranga/Mallotus</i>	21700/19700**, 15500*, 6790(B), 2440, 324(B); 21700**, 4100(B), 3560(B), 1720(B), 1310*, 1210(B)
Menispermaceae	21700/16700*, 7760(B), 5300**, 3950(B), 1500(B), 749(B); 24100**, 5050(B), 4020(B)
<i>Olea paniculata</i>	21700**, 11400(B), 7240*, 5170(B), 4340, 3560(B); 27100*, 16700**, 8690(B), 6790(B), 4620(B), 4100(B)
<i>Homalanthus</i>	24100**, 12800*(B), 2330(B), 1620(B); 24100(B), 12800(B), 396(B)
<i>Oraniopsis</i>	19700**, 10300*, 6790, 5050(B); 19700**, 10300*, 7000*
<i>Petalostigma</i> (Influx F)	31000**, 9440(B), 314(B); 27100**, 12100(B), 314(B)
Sapindaceae(syncolpate)	27100**, 6030(B), 550(B); 24100(B), 1030(B)
<i>Syzygium</i>	24100**, 12100*, 8690, 6200(B), 3880(B); 27100*, 13600**, 9440*, 6580, 5300, 4520, 3950, 3390(B), 2680(B)
<i>Trema</i>	31000**, 7240(B), 4020(B), 1460(B); 24100(B), 696(B)

Urticaceae/Moraceae	24100*, 10900**, 5870(B); 27100(B), 12100, 6200**, 2170*
<i>Zanthoxylum</i>	27100**, 2710(B); 31000(B), 11400**, 635/608(B)
<i>Anthoceros</i>	29000**, 12400*, 8690, 6430(B), 2760(B), 2480(B), 2260(B); 24100**, 12100*, 4260(B), 3620(B), 3150(B), 2780(B), 2520(B)
Asteraceae(tubuliflorae)	21700**, 10900*, 7490(B), 4340*, 3680, 2240(B), 2000(B); 18100/16700**, 9440*, 6790, 4720(B), 4340(B), 3500, 2930(B)
<i>Botryococcus</i>	29000**, 1590(B), 882(B); 21700(B), 1600(B), 1270(B)
Chenopodiaceae	17900, *3580; 15500**, 9440*, 7240, 4830*
<i>Haloragis</i>	15500**, 7000*, 2500(B), 1320(B); 24100*, 7000, 4100**, 3290, 2680(B), 2130(B)
<i>Hydrocotyle</i>	31000*, 8000**, 4830, 3740, 2150(B); 31000(B), 15500**, 7490, 5570(B), 4830*, 4180(B), 3740(B), 3020(B)
Monolete (psilate) ferns	12800**, 6580(B), 5050(B), 2190(B), 1160(B); 21700(B), 12100(B), 6390(B), 4830**, 4100(B), 2190(B)
<i>Persicaria</i>	31000**, 5050(B), 2470(B), 1320(B); 21700**, 7000(B), 2150(B), 1320(B)
<i>Platyserium (%F)</i>	31000**, 11400(B), 9440(B), 961(B), 795(B); 31000**, 9440, 3680*, 965(B)
<i>Pteridium</i>	27100**, 11400, 7000*, 4620(B), 944(B); 21700**, 10900*, 4180(B), 3620
<i>Leptospermum</i>	33800/30400, 13800/10900*/8220, 6610; 27100, 14500*, 11400**, 8350, 6580*, 5430, 4620(B), 3880(B), 2650(B), 1990(B)

Table 3.5. Holocene and Last Glacial Maximum(LGM) Record 3 ka – 18 ka
Percentage, **Concentration**, **Influx** and **Other** results for Major Pollen Groupings, Ratios and Non-Pollen categories

Group	Peaks
Pollen Concentration & Influx (Conc.F)	Under ; Under
Dryland Concentration & Influx (Conc.F)	13400* ; Under
Aquatic Concentration & Influx	10100* ; Under
Inorganics	11000** , 5040 , 3360*
Aquatic/Dryland Ratio	6040* ; *6720
Microcharcoal/Pollen Ratio	11300(B) , 4320** , 1510(B)
Microcharcoal 8-52 µm	3020(B) ; Under
Microcharcoal 53-104 µm	No Frequency ; Under
Microcharcoal 105-156 µm	No Frequency ; Under
Microcharcoal 157-208 µm	6040(B) , 643(B) ; Under
Microcharcoal >208 µm	6040(B) , 643(B) ; Under
Microcharcoal (Conc.F)	3020(B) ; Under
Macrocharcoal	6970** , 3780(B) , 1970(B)
Cyperaceae/Poaceae Ratio	7560** , 2830(B) , 2270(B) , 1510 ; 7560*
Sclerophyll	No Frequency ; Under
Myrtaceae (sclerophyll component) (% F)	9070** , 3130(B) , 1970(B) , 1240(B) ; Under
Casuarinaceae	7560** ; Under
Rainforest gymnosperm	5040(B) , 357(B) ; Under
Podocarpaceae	1490(B) ; Under
<i>Araucaria</i>	1010(B) , 652(B) ; Under
Rainforest angiosperm	No Frequency ; Under
Rainforest (angiosperm) canopy (% F)	No Frequency ; Under
Rainforest (angiosperm) secondary	2920(B) , 643(B) ; Under
Rainforest (angiosperm)understorey (% F)	11300** , 6040* , 4120 , 3130 ; Under
Vine total	No Frequency ; Under
Pteridophytes	2670(B) , 1710(B) ; Under
Epiphytic ferns	No Frequency ; Under
Ground ferns (% and Influx F)	1010(B) , 5500(B) ; 13400
Tree ferns (% F)	10100** , 5330(B) ; *13400
Sclerophyll ferns	10100** , 3360(B) ; Under
Aquatic (Dryland%)	6040*
Cyperaceae (Dryland%)	6480** , 3240 ; Under
Herb/Shrub (% F)	10100(B) , 3130(B) , 2830(B) ; Under
Poaceae	5040(B) , 3630** , 2110(B) , 802(B) ; Under
Unknown Pollen Grains	No Frequency ; Under

Table 3.6. Holocene and Last Glacial Maximum (LGM) 3 ka- 18 ka
Percentage and **Influx** results for Minor Pollen Groupings and Individual Pollen taxa types

Group/Taxa type	Peaks
<i>Eucalyptus</i> (%F)	9070(B), 3130(B), 1230(B); Under
<i>Corymbia</i> (%F)	2110(B); Under
<i>Melaleuca</i> (%F)	10100**; Under
<i>Callitris</i> (%F)	8240**, 1590(B); Under
<i>Dodonaea</i>	No Frequency; Under
<i>Agathis</i>	2210(B), 1540(B); Under
<i>Dacrydium</i>	No Frequency; Under
<i>Acmena</i>	9070(B); Under
<i>Argyrodendron peralatum</i>	No Frequency; No Frequency
<i>Celtis</i>	No Frequency; Under
Cunoniaceae (tricolpate) (%F)	8240**, 4770(B), 2390(B); Under
<i>Elaeocarpus</i> (%F)	3240(B); Under
<i>Elaeodendron</i>	No Frequency; Under
Leguminosae	13000(B), 6040**, 3780(B); Under
<i>Longetia</i>	2110(B), 889(B); Under
<i>Macaranga/Mallotus</i>	13000(B), 8240(B), 2750(B); Under
Menispermaceae	2750(B); Under
<i>Olea paniculata</i>	1110(B), 370(B); Under
<i>Omalthus</i>	No Frequency; Under
<i>Oraniopsis</i> (%F)	10100(B), 6040(B), 3240(B), 2590(B); Under
<i>Petalostigma</i>	No Frequency; Under
Sapindaceae(syncolpate)	13000, 6070(B), 372**; Under
<i>Syzygium</i>	8250**; Under
<i>Trema</i>	10100(B), 725**; Under
Urticaceae/Moraceae	7560**; Under
<i>Zanthoxylum</i>	No Frequency; Not done
<i>Anthoceros</i>	11300(B), 3490**; Under
Asteraceae(tubuliflorae)	353/342(B); Under
<i>Botryococcus</i>	11300**, 2010(B); Under
Chenopodiaceae (%F)	9070(B), 470(B); Under
<i>Haloragis</i>	15100(B), 3500(B), 2920**; Under
<i>Hydrocotyle</i>	No Frequency; Under
Monolete (psilate) ferns	9070**, 2520*, 1680(B); Under
<i>Persicaria</i>	3780**, 1710(B), 817(B); Under
<i>Platynerium</i>	No Frequency; Under
<i>Pteridium</i>	10100(B), 5040(B), 1040(B); Under
<i>Leptospermum</i>	No Frequency; Not done

Spectral analysis peaks after filter from Red noise (Tables 3.7 – 3.12)

3.2. Tables 3.7-3.12 Spectral analysis peaks after filter from Red noise (ARI) for Full, Pleistocene and Holocene sequences

Table 3.7. Full Record 3 ka – 54 ka

Percentage, Concentration, Influx and Other results Data for Major Pollen Groupings, Ratios and Non-Pollen categories

All categories (**, * and (B)) as above apply to the tables below and details of data that was filtered is given in Tables 3.1– 3.6 above.

Group	Peaks
Pollen Concentration & Influx	38600, 14700, 10300*, 6720, 4610, 4010, 3510 ; 14000, 9660*,
Dryland Concentration & Influx	14700, 10300, 6720, 5720, 4540, 4070
Aquatic Concentration & Influx	22100*, 10700, 6580, 4680, 4070, 3550; 23800*
Inorganics	19300*
Aquatic/Dryland Ratio	23800*, 6180, 3430; 23800*, 6180, 3430
Microcharcoal/Pollen Ratio	38600*, 15500
Microcharcoal 8-52 µm	38600, 16300*, 4120
Microcharcoal 53-104 µm	38600, 17200*, 4120
Microcharcoal 105-156 µm	17200; 16300*, 4120
Microcharcoal 157-208 µm	17200*; 15500*
Microcharcoal >208 µm	17200*
Microcharcoal	34300, 16300*, 4120
Macrocharcoal	28100*, 5940
Cyperaceae/Poaceae Ratio	38600, 19300/13400*, 7920, 6580, 4680, 3640
Sclerophyll	44100*, 17200, 11900, 9360; 16300*, 9360, 4750
Myrtaceae (sclerophyll component)	20600*, 11000; 20600*, 5330
Casuarinaceae	38600*; 16300*, 9360, 5520
Rainforest gymnosperm	38600*, 18200, 2270; 9660*, 3680
Podocarpaceae	38600*, 16300, 3770, 2380; 8830*, 3720
<i>Araucaria</i>	34300*, 20600, 10700, 8350, 3400; 34300*, 20600, 13400, 10700
Rainforest angiosperm	38600*, 18200, 12900, 8830 Under
Rainforest (angiosperm) canopy	38600*, 19300, 12900, 9090 Under
Rainforest (angiosperm) secondary	44100*, 16300 Under
Rainforest (angiosperm)understorey	38600*, 18200, 10300, 6310, 5520
Vine	44100*, 16300 Under
Pteridophytes	38600*, 18200; 38600*
Epiphytic ferns	44100*, 22100, 16300, 11400, 6060; 38000*
Ground ferns	38600*, 8830, 6580; 38600*, 14000, 6580
Tree ferns	38600*, 20600, 13400, 11400, 9090, 7540, 6440; 38600*, 20600, 14000, 11000
Sclerophyll ferns	28100*, 11400; 38600*
Aquatic (Dryland%)	25800*, 6180, 3430
Cyperaceae (Dryland%)	23800*, 6180, 3470; 23800*, 6310
Herb/Shrub	44100, 17200*, 11900, 7360 Under
Poaceae	22100*, 10700*; 19300*, 9360
Unknown Pollen Grains	34300/18200, 11400, 8580; 38600*

Table 3.8. Full Record 3 ka – 54 ka

Percentage and **Influx** results data for Minor Pollen Groupings and Individual Pollen taxa types

Group/Taxa type	Peaks
<i>Eucalyptus</i>	38600, 13400*; 20600*/16300, 6310, 5330
<i>Corymbia</i>	23800*, 11900; 28100, 14000*
<i>Melaleuca</i>	20600*/18700, 10700, 3640; 20600*/17200, 10700, 3590, 2130
<i>Callitris</i>	34300, 11400/9970, 7920, 3640*; 12400
<i>Dodonaea</i>	10300* Under
<i>Agathis</i>	38600*; 44100*/38600, 11400
<i>Dacrydium</i>	34300, 15550*, 11000, 6440; 30900, 10300, 6720*
<i>Acmena</i>	34300*; Under
<i>Argyrodendron peralatum</i>	38600*, 17200, 11900, 9090, 3320; 38600*
<i>Celtis</i>	16300*; Under
Cunoniaceae (tricolpate)	38600*, 19300, 13400, 10700, 8830, 7540, 6440, 5720; 38600*
<i>Elaeocarpus</i>	38600*, 19300, 13400, 10700; Under
<i>Elaeodendron</i>	28100*/18200; 34300*
Legume	44100*, 16300, 11400 Under
<i>Longetia</i>	44100/38600, 12900*/12400; 44100*
<i>Macaranga/Mallotus</i>	38600*, 17200, 12400, 9660, 6310, 2400; 38600*, 15500, 11000
Menispermaceae	44100*, 17200 Under
<i>Olea paniculata</i>	22100*, 7360, 4350; 20600*/19300
<i>Homalanthus</i>	38600*/34300 Under
<i>Oraniopsis</i>	44100, 17200*, 11900, 8830, 7020, 5830, 4980; Under
<i>Petalostigma</i>	34300*; 34300*
Sapindaceae(syncolpate)	38600*, 18200; 38600*, 19300
<i>Syzygium</i>	38600*, 19300, 12900, 9360, 7730, 6310; Under
<i>Trema</i>	38600*, 16300; 38600*
Urticaceae/Moraceae	34300, 11400*, 5830; Under
<i>Zanthoxylum</i>	30900*; Under
<i>Anthoceros</i>	25800*; 28100*/25800
Asteraceae(tubuliflorae)	20600*; 19300*
<i>Botryococcus</i>	38600*, 16300; 44100*, 17200
Chenopodiaceae	16300, 10300, 3550*; 16300*, 9660, 4830
<i>Haloragis</i>	44100, 17200*, 12400, 7360; 44100*
<i>Hydrocotyle</i>	44100*, 11400, 8830, 7730; Under
Monolete (psilate) ferns	34300*, 17200, 9970, 8130; Under
<i>Persicaria</i>	44100*, 22100; 20600*/19300
<i>Platycerium</i>	44100*, 19300, 11000; 44100*, 22100
<i>Pteridium</i>	25800*, 11400; 34300*, 10300
<i>Leptospermum</i>	44100, 19300, 9660; 34300, 19300, 12400, 9660*, 7920, 7190, 6580, 6180

Table 3.9. Pleistocene Record 11.8 ka – 54 ka Percentage, Concentration, Influx and Other results Data for Major Pollen Groupings, Ratios and Non-Pollen categories

Group	Peaks
Pollen Concentration & Influx	27600, 15200, *9810, 6760, 4610, 4000, 3490, 2510; 9500*
Dryland Concentration & Influx	30400/16000*, 9500, 4610, 4000, 3530; 16000*, 9210, 6910, 5430, 4610, 4000, 3530
Aquatic Concentration & Influx	22100*, 4680; 21700*, 4680
Inorganics	21700*, 10500, 4830, 3750
Aquatic/Dryland Ratio	25300*, 6200, 3450; 25300*, 6200, 3450
Microcharcoal/Pollen Ratio	30800*/22000/20500
Microcharcoal 8-52 µm	38600, 17900*; 16900*, 9500, 4470
Microcharcoal 53-104 µm	16900*, 4220; 16900*, 4340
Microcharcoal 105-156 µm	16000*, 4160; 16000*, 10500, 4280
Microcharcoal 157-208 µm	15200*, 4160; 15200*/14500
Microcharcoal >208 µm	15200*, 4160; 10500*
Microcharcoal	17900*, 6760, 4280; 16900*, 9500, 4470
Macrocharcoal	25300*/19000
Cyperaceae/Poaceae Ratio	15200*, 3580
Sclerophyll	30400*/27600; 16000*, 9210, 5430, 4680
Myrtaceae (sclerophyll component)	27600, 11300*, 5850; 16000*, 4610
Casuarinaceae	27600*, 10500; 16000*/15200. 9210, 4680
Rainforest gymnosperm	30400*, 2300; 8440, 6760, 3660*
Podocarpaceae	30400*, 6610, 3660, 2320; 9210*, 3660*
<i>Araucaria</i>	27600*, 10900, 8940*, 7410, 3530; 30400*/27600, 15200, 10900
Rainforest angiosperm	23400*/21700, 10500; 27600*, 14500, 9210, 6610, 5330, 4610, 4000
Rainforest (angiosperm) canopy	25300*, 10500; 30400*, 6610, 4680
Rainforest (angiosperm) secondary	21700*, 7240; 20300*
Rainforest (angiosperm) understorey	21700*, 5150; 25300, 9500, 6760*
Vine	20300*, 5150; 20300*, 4980
Pteridophytes	13200*, 23400*
Epiphytic ferns	30400*; 27600*, 12500, 10100, 5430, 3660
Ground ferns	Under, Under
Tree ferns	38000*; 32600*, 15300, 4740, 4070
Sclerophyll ferns	27600*, 11300, 7070; 23400*, 10900
Aquatic (Dryland%)	25300*
Cyperaceae (Dryland%)	25300*, 6200; 21700*, 6330, 4680, 4050
Herb/Shrub	20300*, 4340, 3710; 17900*, 9500
Poaceae	21700*, 10500; 19000*, 9500
Unknown Pollen Grains	23400*, 8940; 27600*, 9500

Table 3.10. Pleistocene Record 11.8 ka – 54 ka

Percentage and **Influx** results data for Minor Pollen Groupings and Individual Pollen taxa types

Group/Taxa type	Peaks
<i>Eucalyptus</i>	38000, 13200*, 5960; 16000* , 6470
<i>Corymbia</i>	27600*, 11700; 23400*/15200*
<i>Melaleuca</i>	30400*/27600, 17900, 10500, 4610, 3660; 30400/21700/16900* , 10100, 4540, 3580*, 2110
<i>Callitris</i>	33800, 9210, 3660*; 30400, 12700*
<i>Dodonaea</i>	9810*; 15200* , 4170
<i>Agathis</i>	27600, 9500*; 9500* , 5960
<i>Dacrydium</i>	20300*, 6470; 27600, 10100, 6760*
<i>Acmena</i>	16000*, 3500; 30400, 6470* , 4680
<i>Argyrodendron peralatum</i>	27600*, 13800, 10500, 7240, 5960, 3230; 30400*
<i>Celtis</i>	17900*; 17900* , 8670
Cunoniaceae (tricolpate)	Under; Under
<i>Elaeocarpus</i>	Under; Under
<i>Elaeodendron</i>	23700*; 25300*
Legume	Under; No significant frequencies
<i>Longetia</i>	13800*, 10900; 8220*
<i>Macaranga/Mallotus</i>	23400*/21700, 2430; 21700* , 1730, 1310
Menispermaceae	21700/16900, 5240*; 23400* , 4980, 4050
<i>Olea paniculata</i>	21700*, 7240, 4340; 30400/27600, 16900*
<i>Homalanthus</i>	25300*/23400; 23400, 13200*
<i>Oraniopsis</i>	19000*, 10500, 6910; 20300* , 10100, 6910
<i>Petalostigma</i>	30400*; 27600*
Sapindaceae(syncolpate)	26100*; Under
<i>Syzygium</i>	25300*, 12200, 8690; 27600, 13800* , 9210, 6610, 5330, 4540, 3950
<i>Trema</i>	30400*; Under
Urticaceae/Moraceae	25300, 11300*/10900; 12200, 6200* , 2170
<i>Zanthoxylum</i>	29000*; 11700*
<i>Anthoceros</i>	27600*, 12700, 8690; 25300* , 12200
Asteraceae(tubuliflorae)	20300*; 17900* , 9500, 3530
<i>Botryococcus</i>	27600* Under
Chenopodiaceae	17900, 3580* 15200* 9500, 7240, 4750
<i>Haloragis</i>	16000* 7070; 4110*
<i>Hydrocotyle</i>	30400, 8000* 3750; 16000* 7410, 3750
Monolete (psilate) ferns	13200*; No significant frequencies
<i>Persicaria</i>	30400*; 21700*
<i>Platycerium</i>	33800*/30400; 30400* , 9810, 3660
<i>Pteridium</i>	25300*; 23400* , 10900
<i>Leptospermum</i>	33800/30400*, 13800/10900*/8220, 6610; 25300*, 14500, 11700* , 10100, 8220, 6470, 5430

Table 3.11. Holocene and Last Glacial Maximum(LGM) Record 3 ka – 54 ka Percentage, Concentration, Influx and Other results Data for Major Pollen Groupings, Ratios and Non-Pollen categories

Group	Peaks
Pollen Concentration & Influx	Under; Under
Dryland Concentration & Influx	Under; Under
Aquatic Concentration & Influx	No significant frequencies; Under
Residue after Ignition	11000*
Aquatic/Dryland Ratio	Conc&Influx no significant frequencies
Microcharcoal/Pollen Ratio	4440*
Microcharcoal 8-52 µm	Under; Under
Microcharcoal 53-104 µm	Under; Under
Microcharcoal 105-156 µm	Under; Under
Microcharcoal 157-208 µm	Under; Under
Microcharcoal >208 µm	Under; Under
Microcharcoal	Under; Under
MacroCharcoal	6720*
Cyperaceae/Poaceae Ratio	Conc&Influx no significant frequencies
Sclerophyll	13400*; Under
Myrtaceae (sclerophyll component)	No significant frequencies; Under
Casuarinaceae	7110*; Under
Rainforest gymnosperm	Under; Under
Podocarpaceae	Under; Under
<i>Araucaria</i>	Under; Under
Rainforest ngiosperm	13400*; Under
Rainforest (angiosperm) canopy	13400*; Under
Rainforest (angiosperm) secondary	Under; Under
Rainforest (angiosperm) understorey	4170*; Under
Vine	Under; Under
Pteridophytes	Under; Under
Epiphytic ferns	Under; Under
Ground ferns	Under; Under
Tree ferns	10100*; 13400*
Sclerophyll ferns	10100*; Under
Aquatic (Dryland%)	No significant frequencies
Cyperaceae (Dryland%)	6720*; Under
Herb/Shrub	Under; Under
Poaceae	No significant frequencies; Under
Unknown Pollen Grains	12100*; Under

Table 3.12. Holocene and Last Glacial Maximum (LGM) 3 ka – 18 ka

Percentage and **Influx** results data for Minor Pollen Groupings and Individual Pollen taxa types

Group/Taxa type	Peaks
<i>Eucalyptus</i>	Under; Under
<i>Corymbia</i>	Under; Under
<i>Melaleuca</i>	No significant frequencies; 4480*, 3560
<i>Callitris</i>	11000*; Under
<i>Dodonaea</i>	12100*; Under
<i>Agathis</i>	Under; Under
<i>Dacrydium</i>	Under; Under
<i>Acmena</i>	Under; Under
<i>Argyrodendron peralatum</i>	Under; Under
<i>Celtis</i>	Under; Under
Cunoniaceae (tricolpate)	No significant frequencies; Under
<i>Elaeocarpus</i>	Under; Under
<i>Elaeodendron</i>	Under; Under
Legume	6040*; Under
<i>Longetia</i>	Under; Under
<i>Macaranga/Mallotus</i>	Under; Under
Menispermaceae	Under; Under
<i>Olea paniculate</i>	Under; Under
<i>Omalanthus</i>	Under; Under
<i>Oraniopsis</i>	Under; Under
<i>Petalostigma</i>	Under; Under
Sapindaceae(syncolpate)	Under; Under
<i>Syzygium</i>	8060*/6040; Under
<i>Trema</i>	727*; Under
Urticaceae/Moraceae	Under; Under
<i>Zanthoxylum</i>	Not done
<i>Anthoceros</i>	3420*; Under
Asteraceae(tubuliflorae)	Under; Under
<i>Botryococcus</i>	11000*; Under
Chenopodiaceae	11000*; Under
<i>Haloragis</i>	No significant frequencies; Under
<i>Hydrocotyle</i>	Under; Under
Monolete (psilate) ferns	9300*, 2520; Under
<i>Persicaria</i>	3780*; Under
<i>Platynerium</i>	Under; Under
<i>Pteridium</i>	Under; Under
<i>Leptospermum</i>	Not done

Section 4. Plates for Spectrum and red-noise spectrum plots

Plates 4.1-4.5. Dryland percentage data full sequence (3-54 ka)

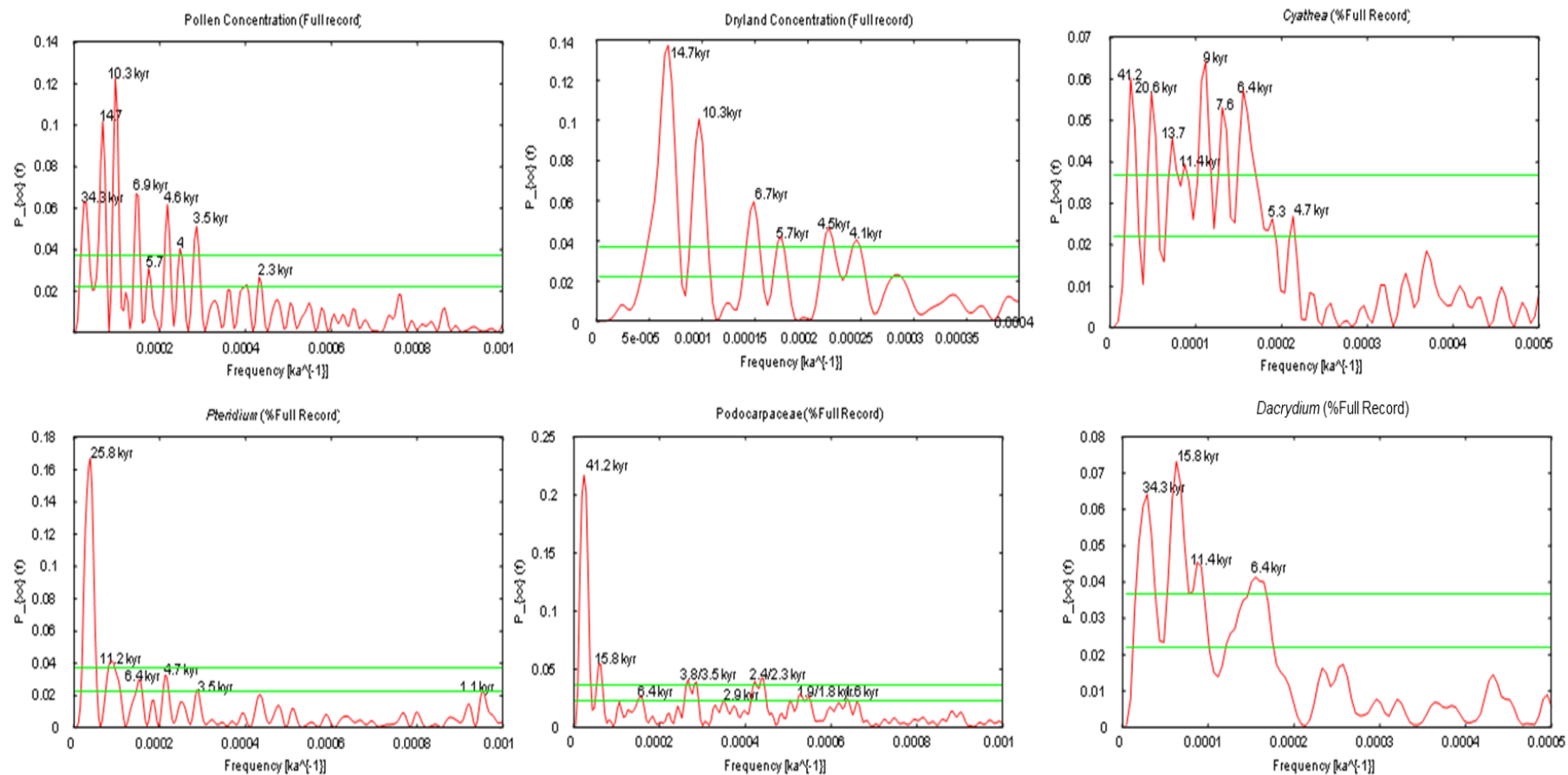


Plate 4.1. Taxon and frequencies noted on graph

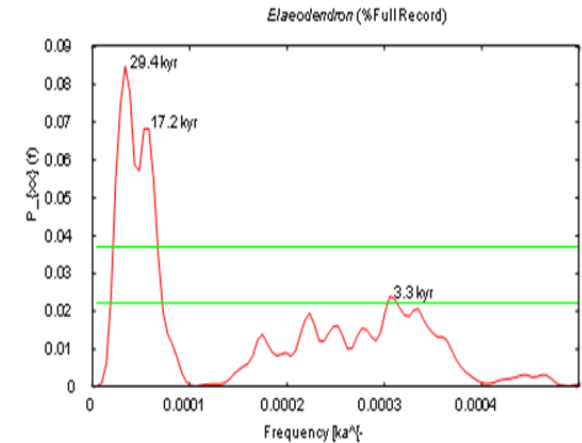
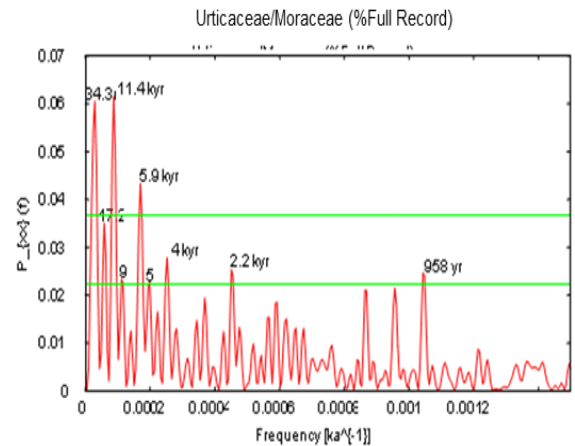
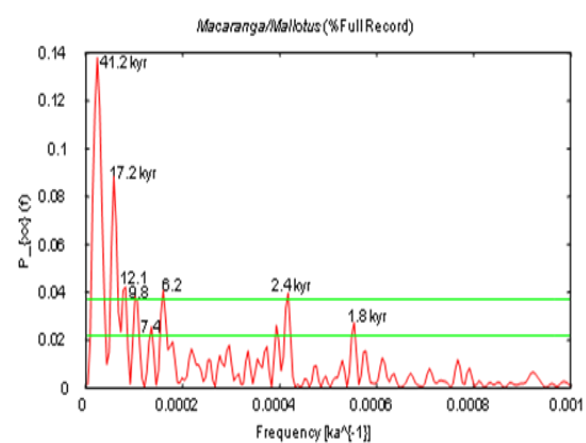
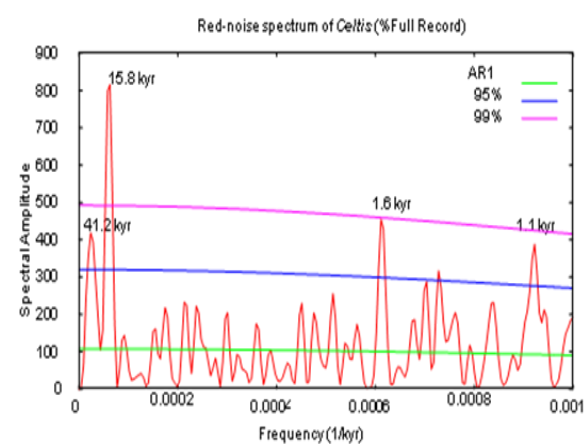
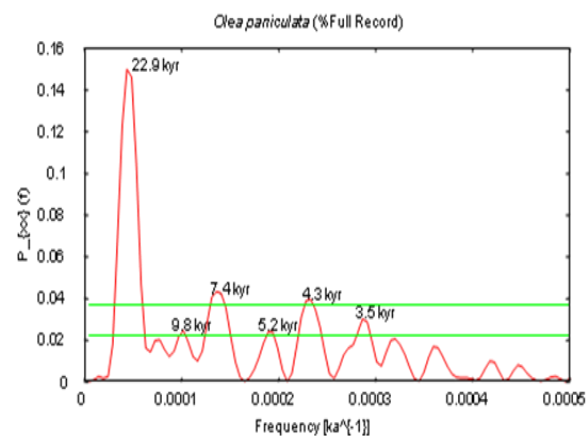
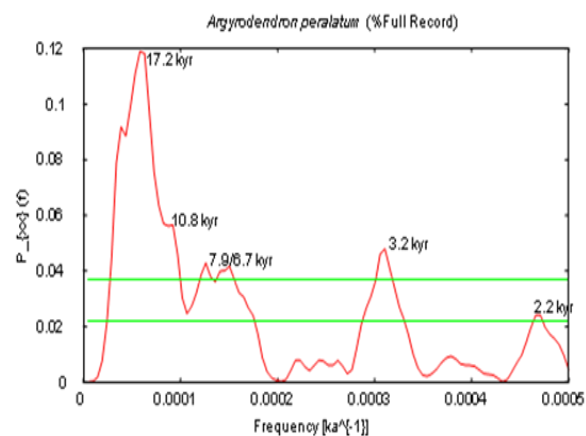


Plate 4.2. Taxon and frequencies noted on graph

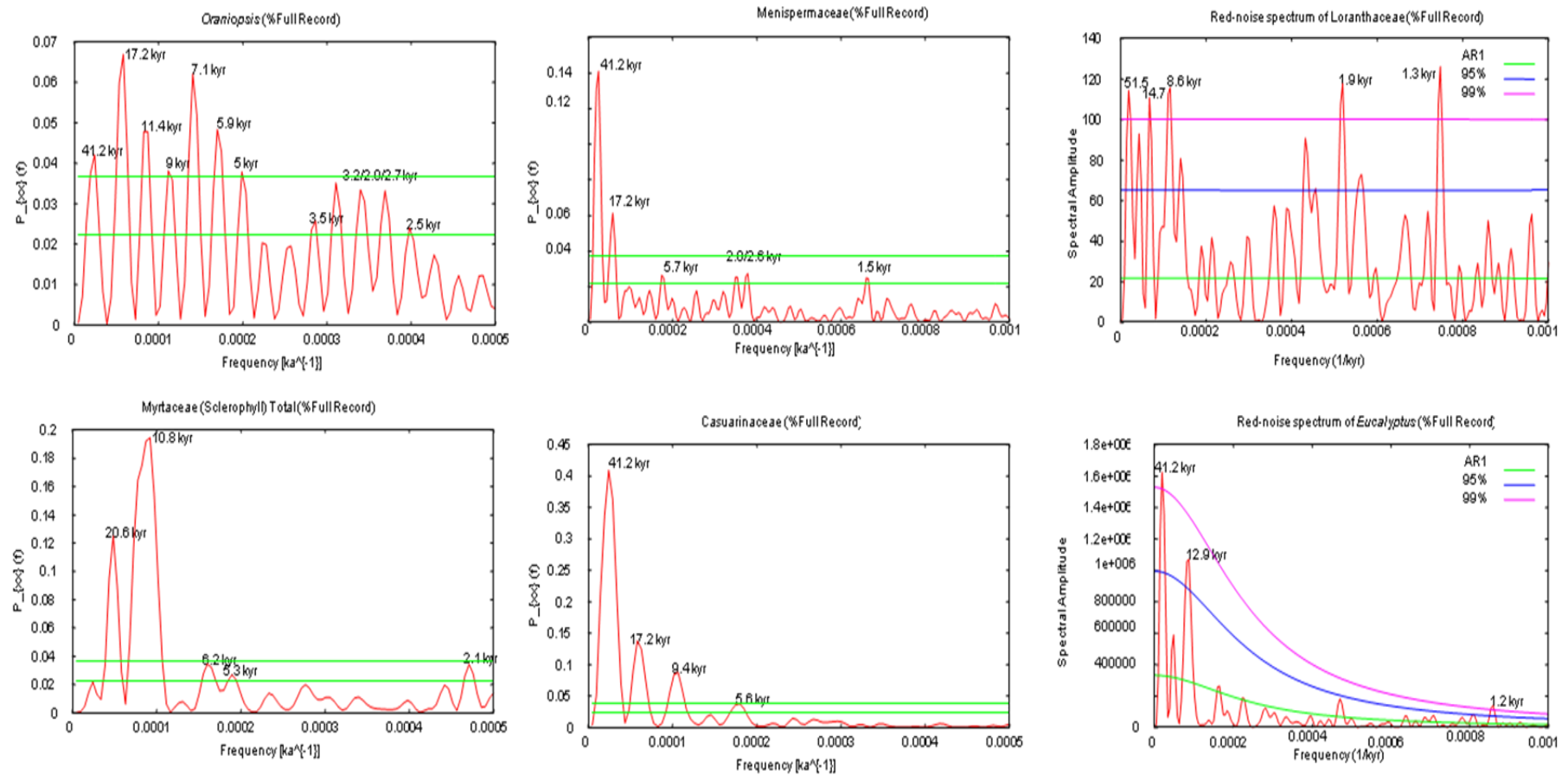


Plate 4.3. Taxon and frequencies noted on graph

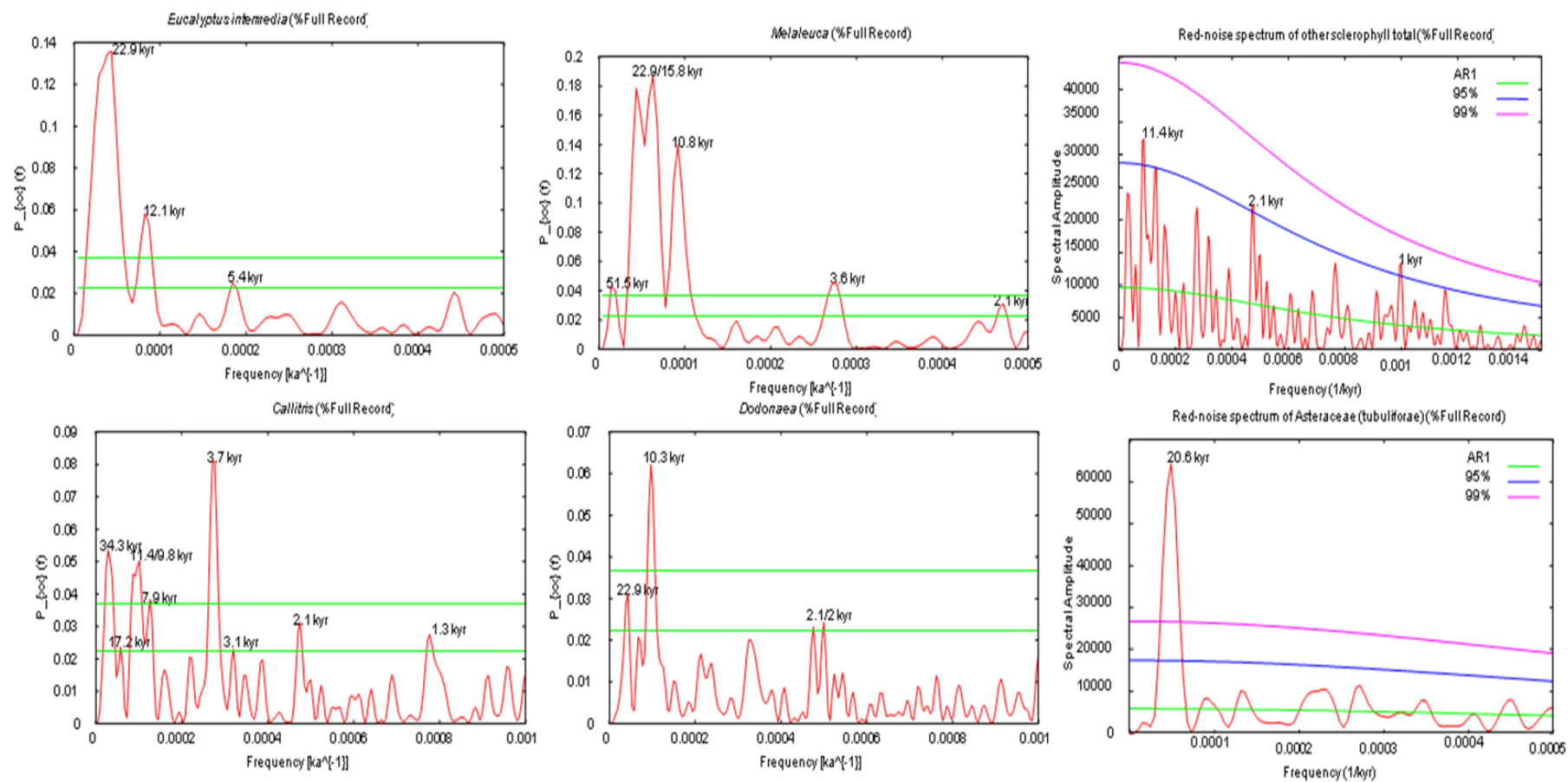


Plate 4.4. Taxon and frequencies noted on graph

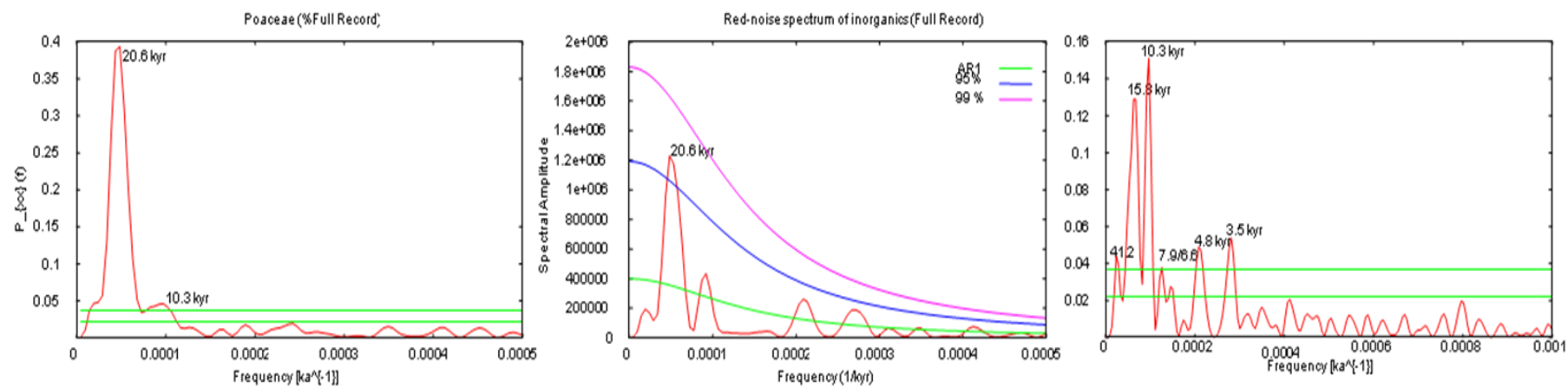


Plate 4.5. Taxon and frequencies noted on graph

Plates 4.6-4.8. Dryland influx data full sequence (3-54 ka)

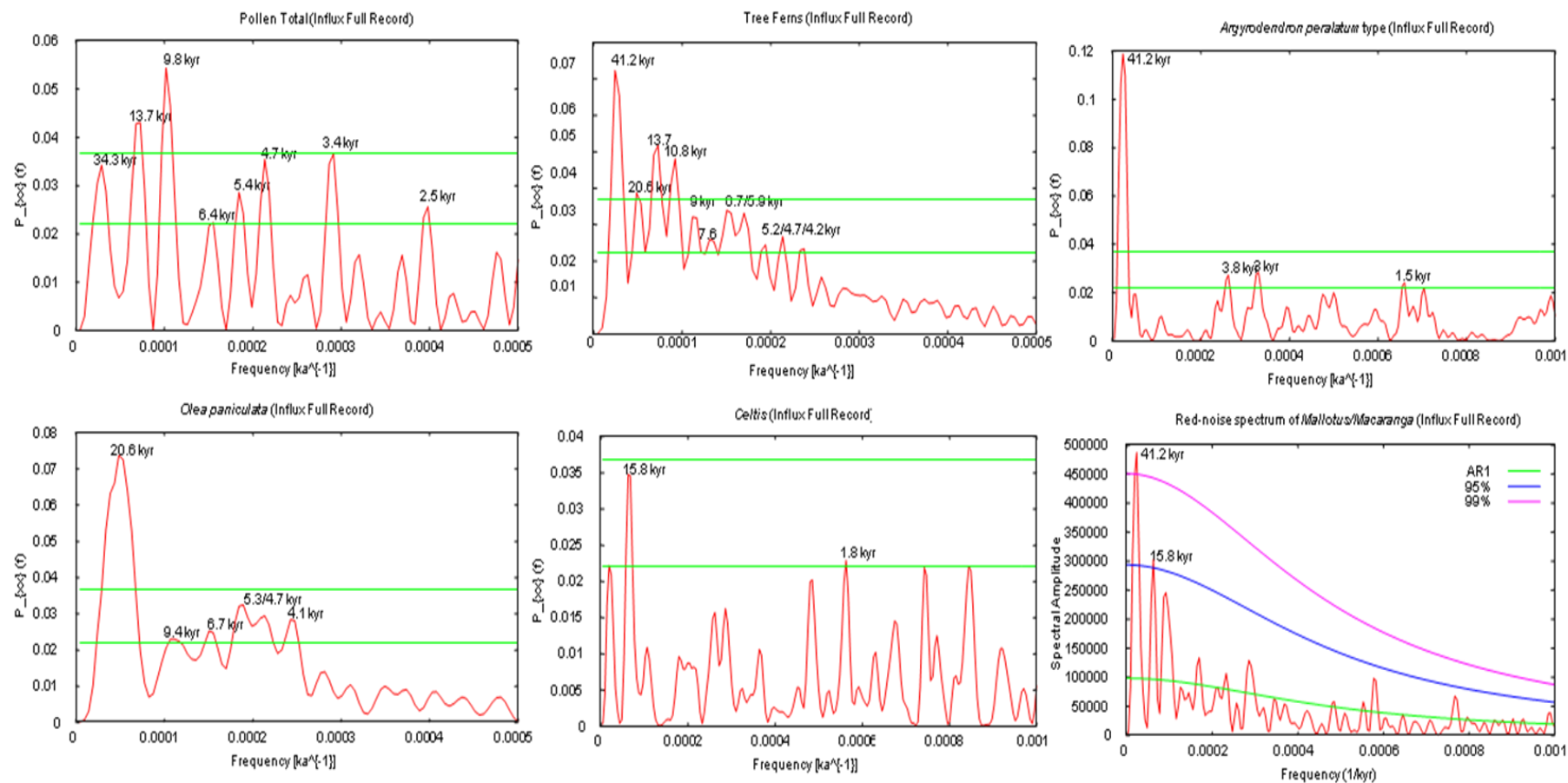


Plate 4.6. Taxon and frequencies noted on graph

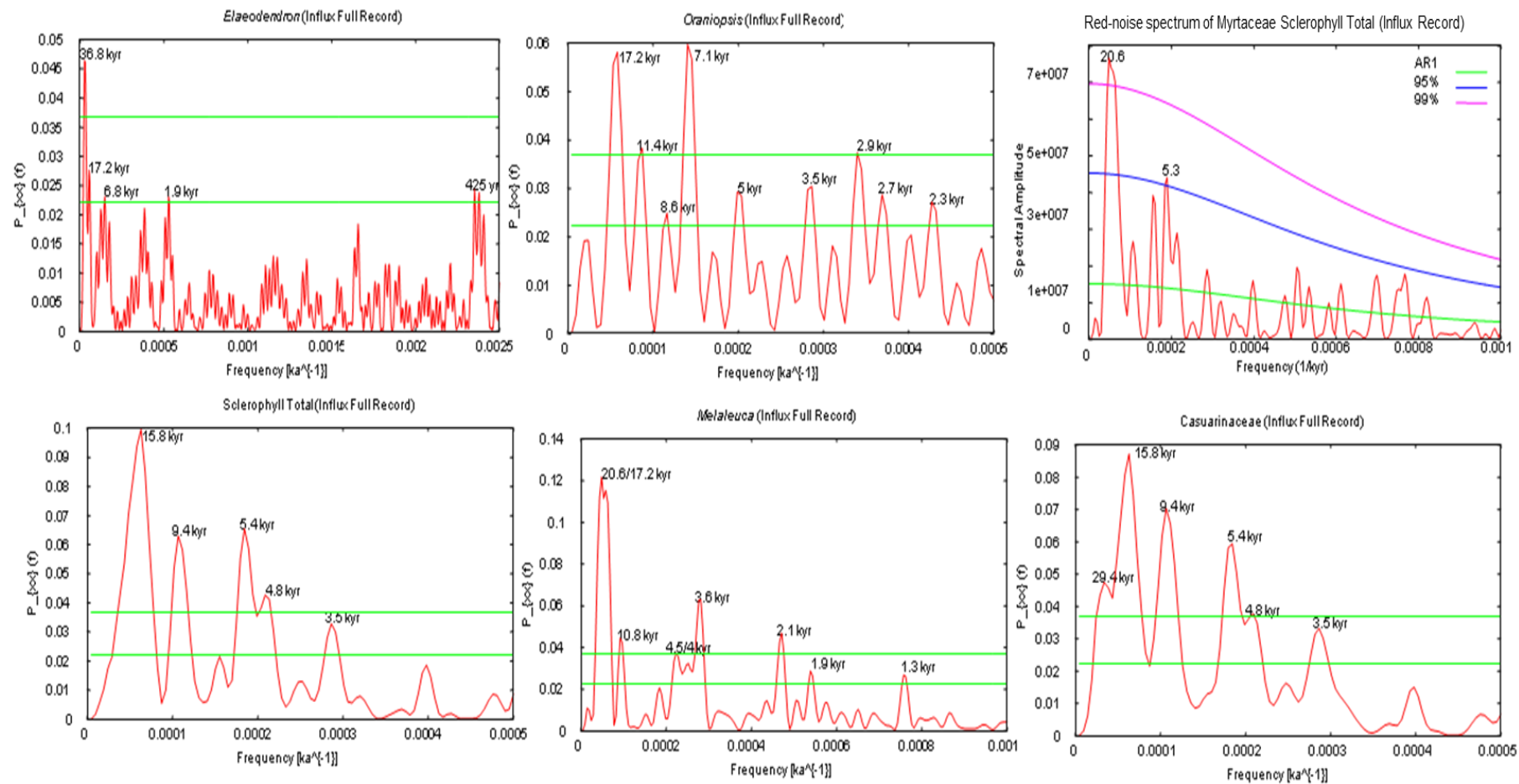


Plate 4.7. Taxon and frequencies noted on graph

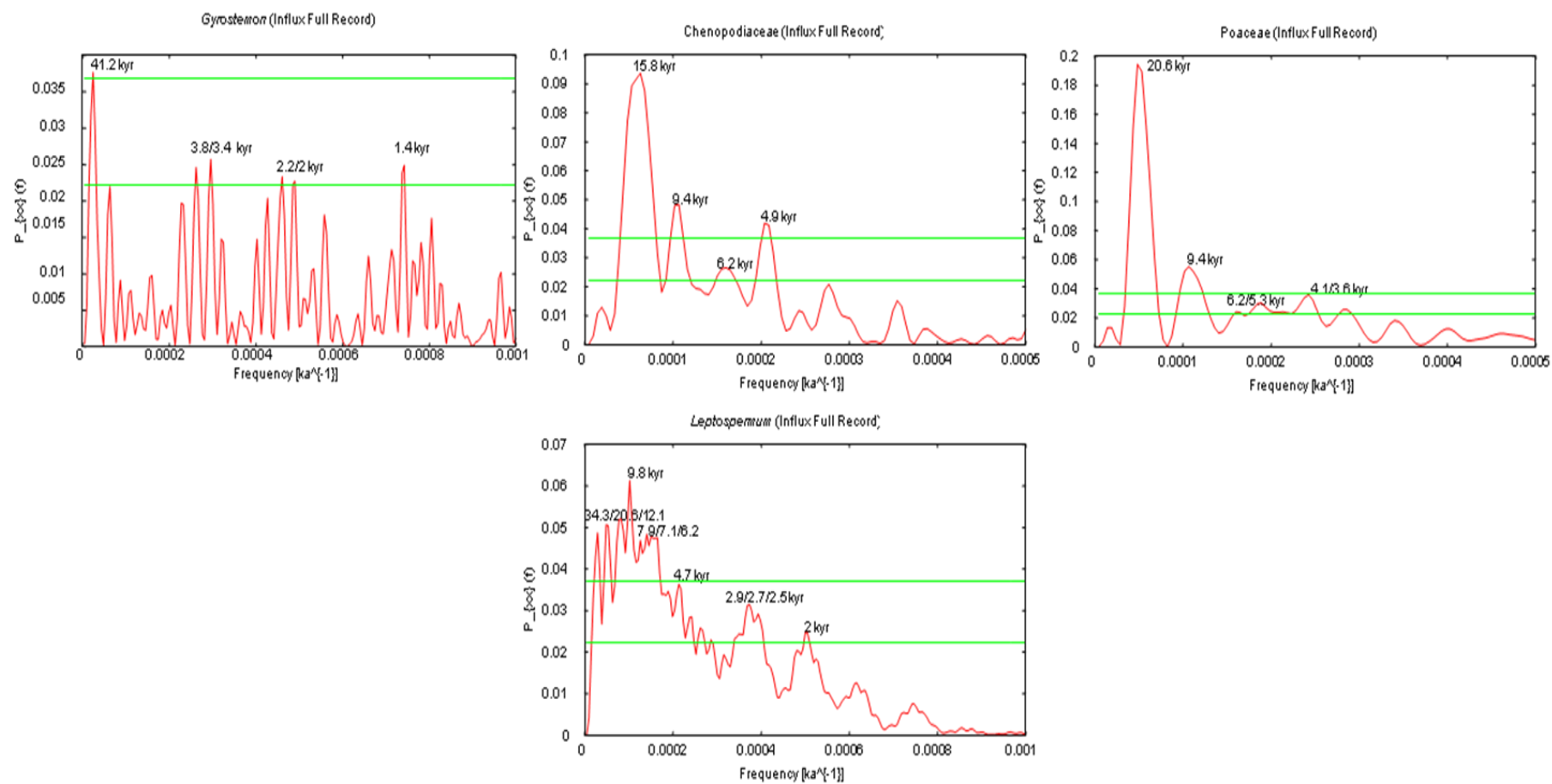


Plate 4.8. Taxon and frequencies noted on graph

Plates 4.9-4.13. Dryland percentage data Pleistocene sequence (11.8-54 ka)

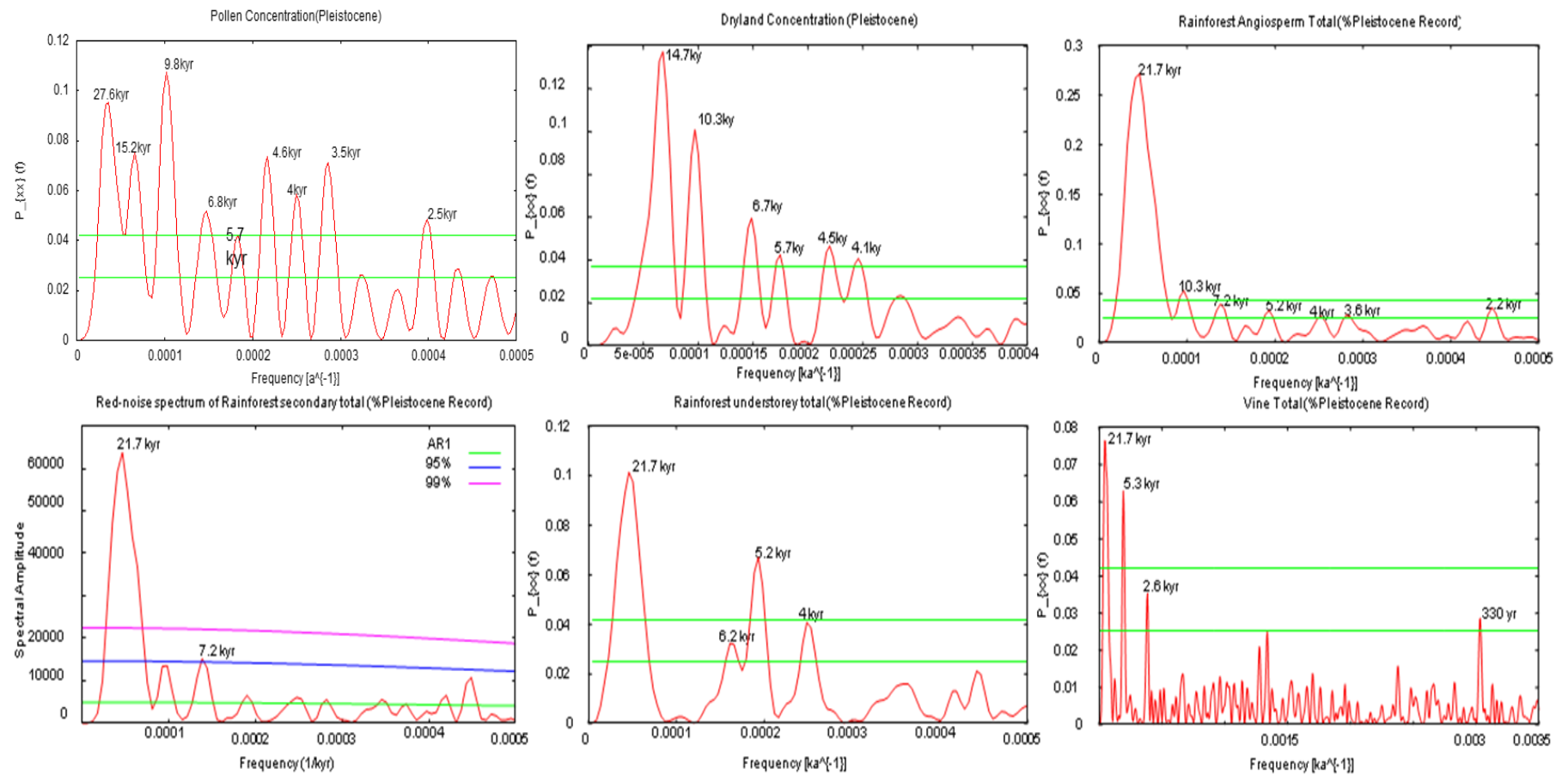


Plate 4.9. Taxon and frequencies noted on graph

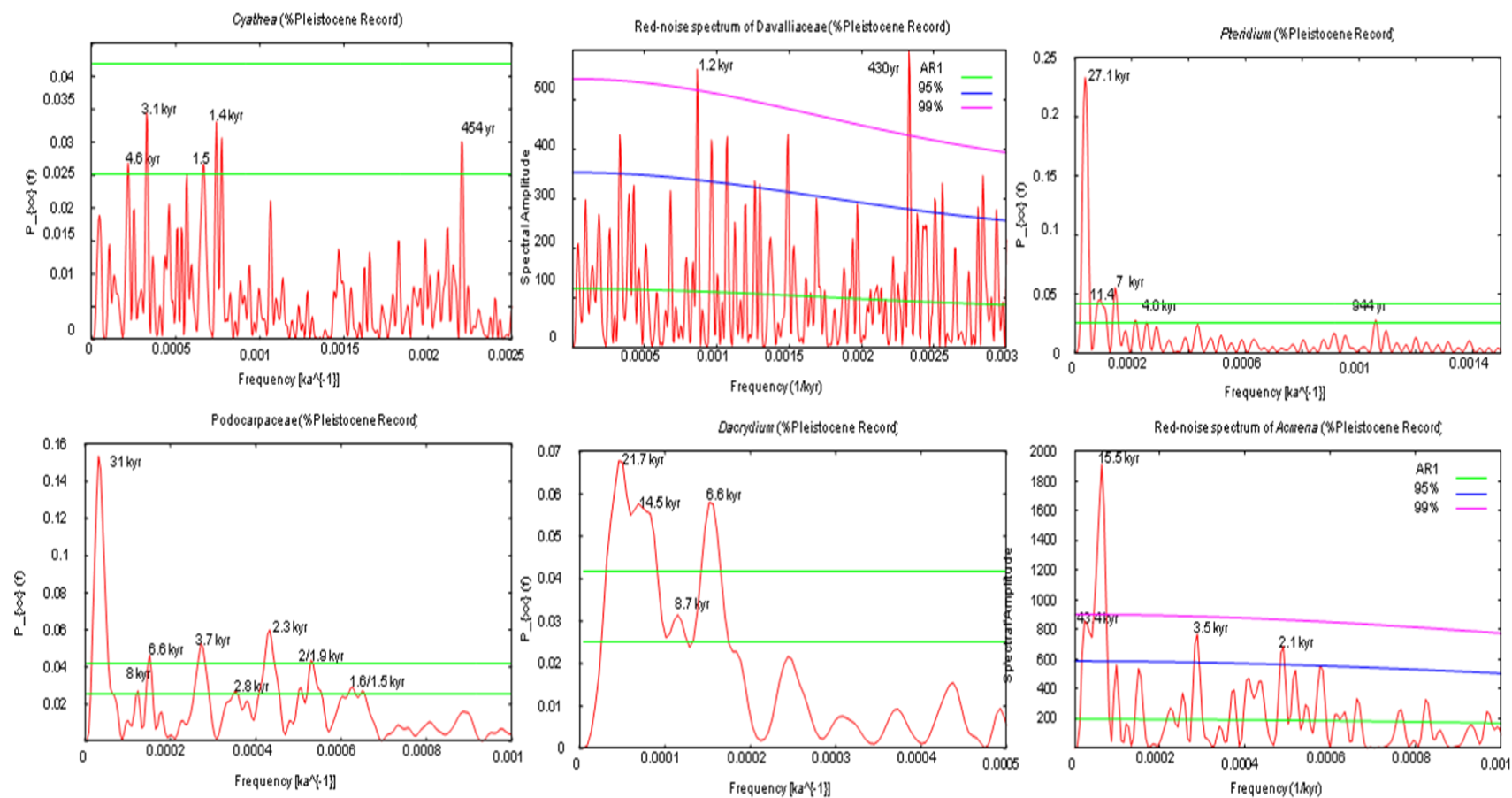


Plate 4.10. Taxon and frequencies noted on graph

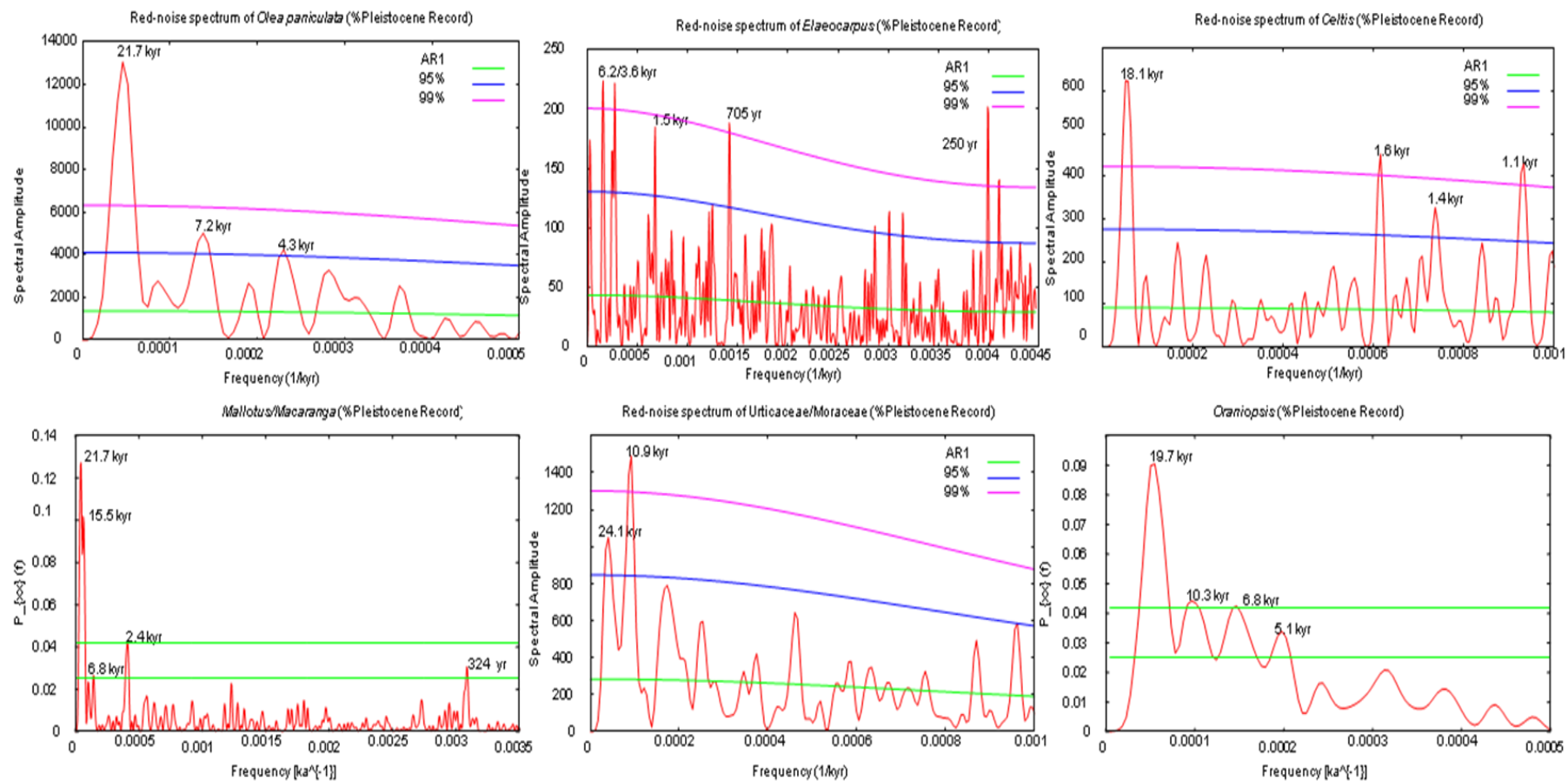


Plate 4.11. Taxon and frequencies noted on graph

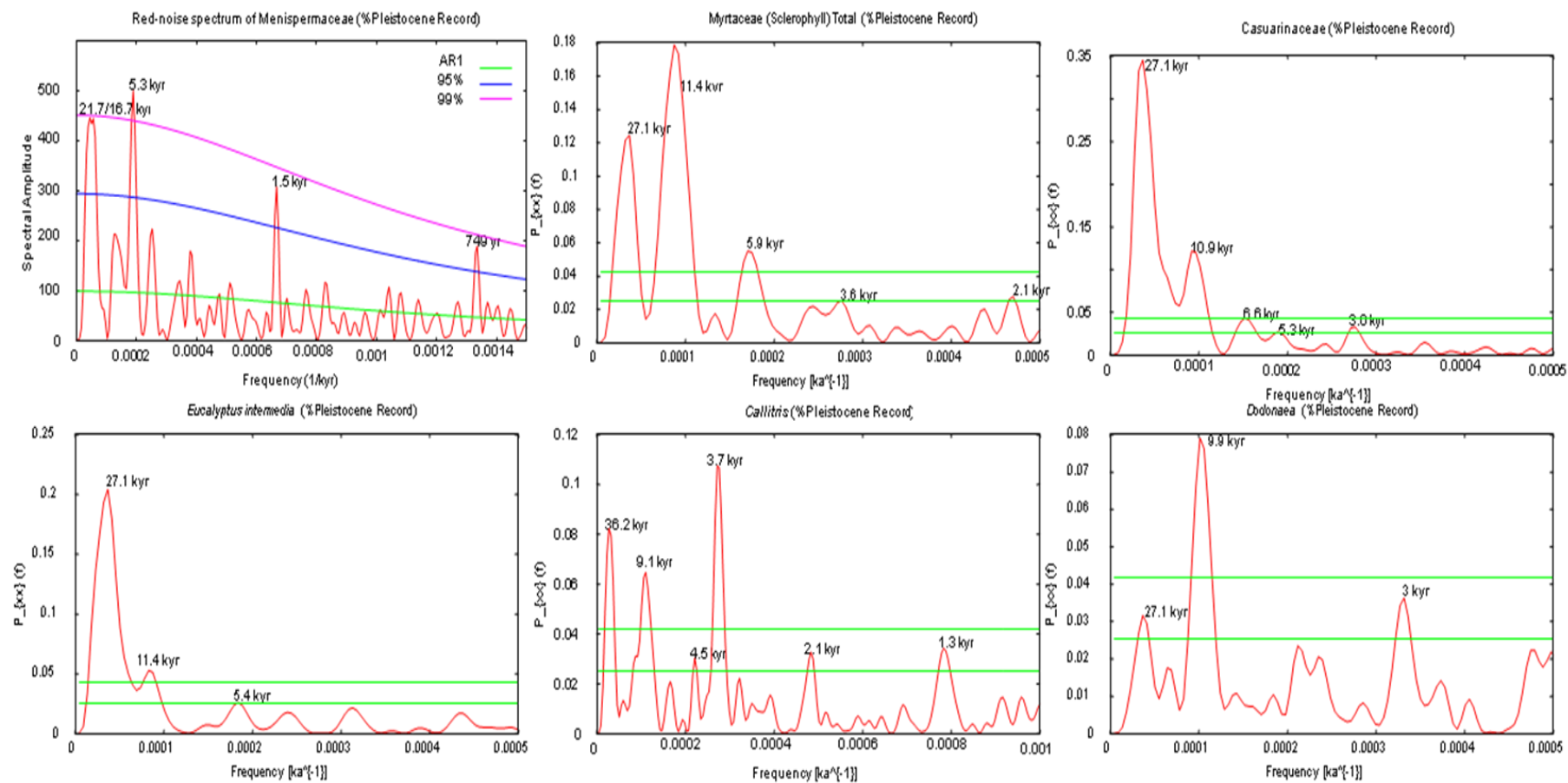


Plate 4.12. Taxon and frequencies noted on graph

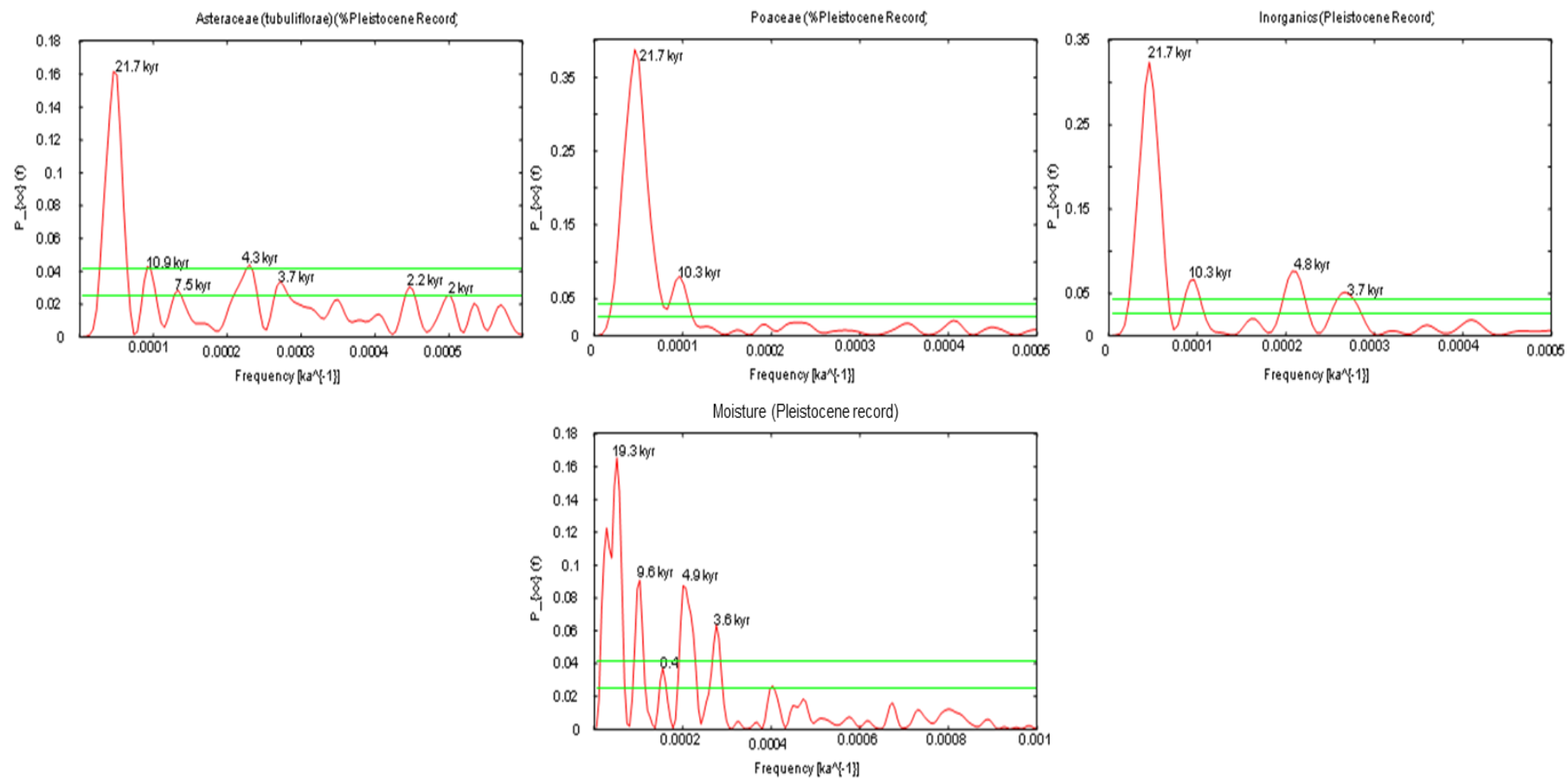


Plate 4.13. Taxon and frequencies noted on graph

Plates 4.14-4.19. Dryland influx data Pleistocene sequence (11.8-54 ka)

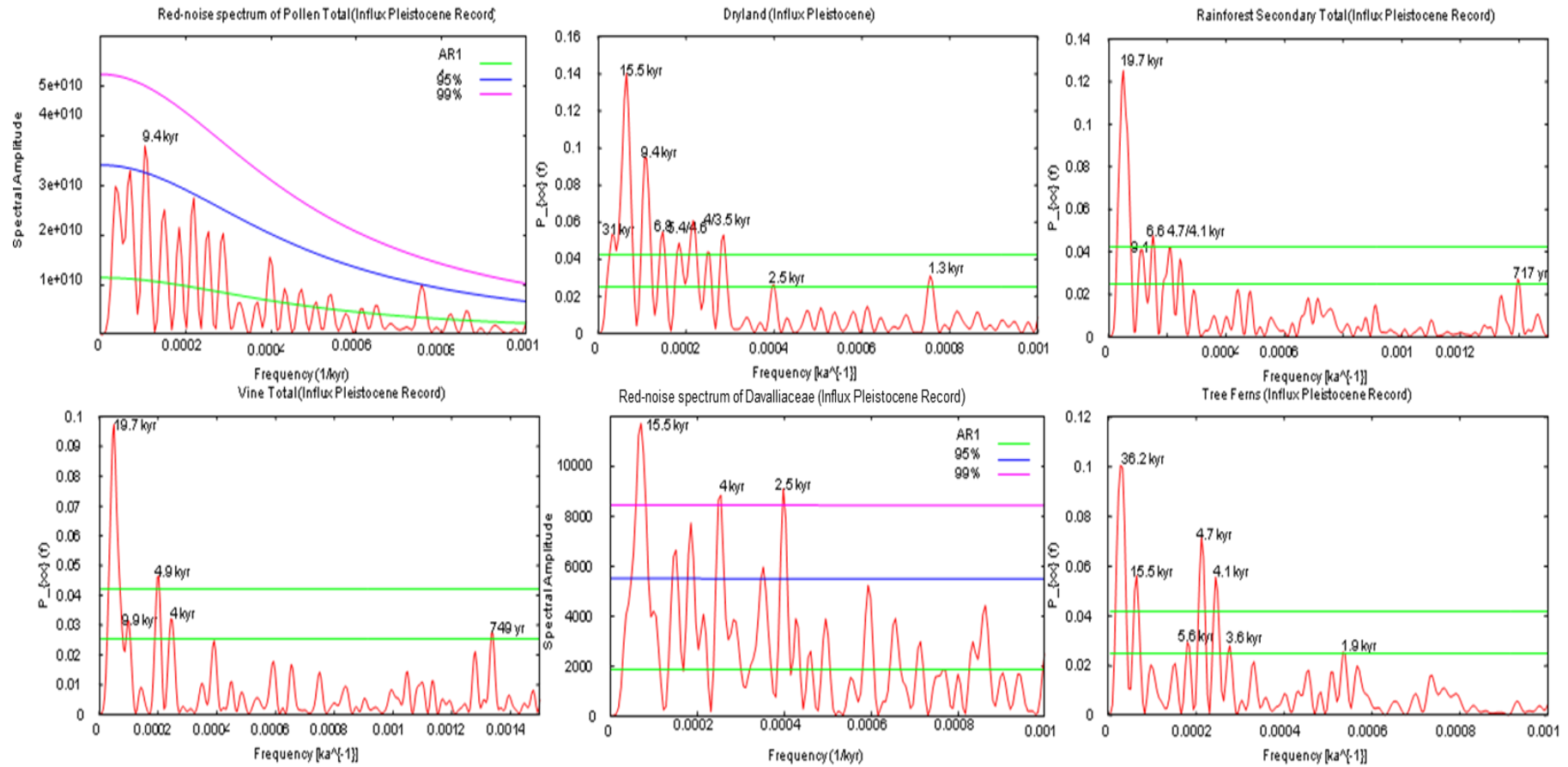


Plate 4.14. Taxon and frequencies noted on graph

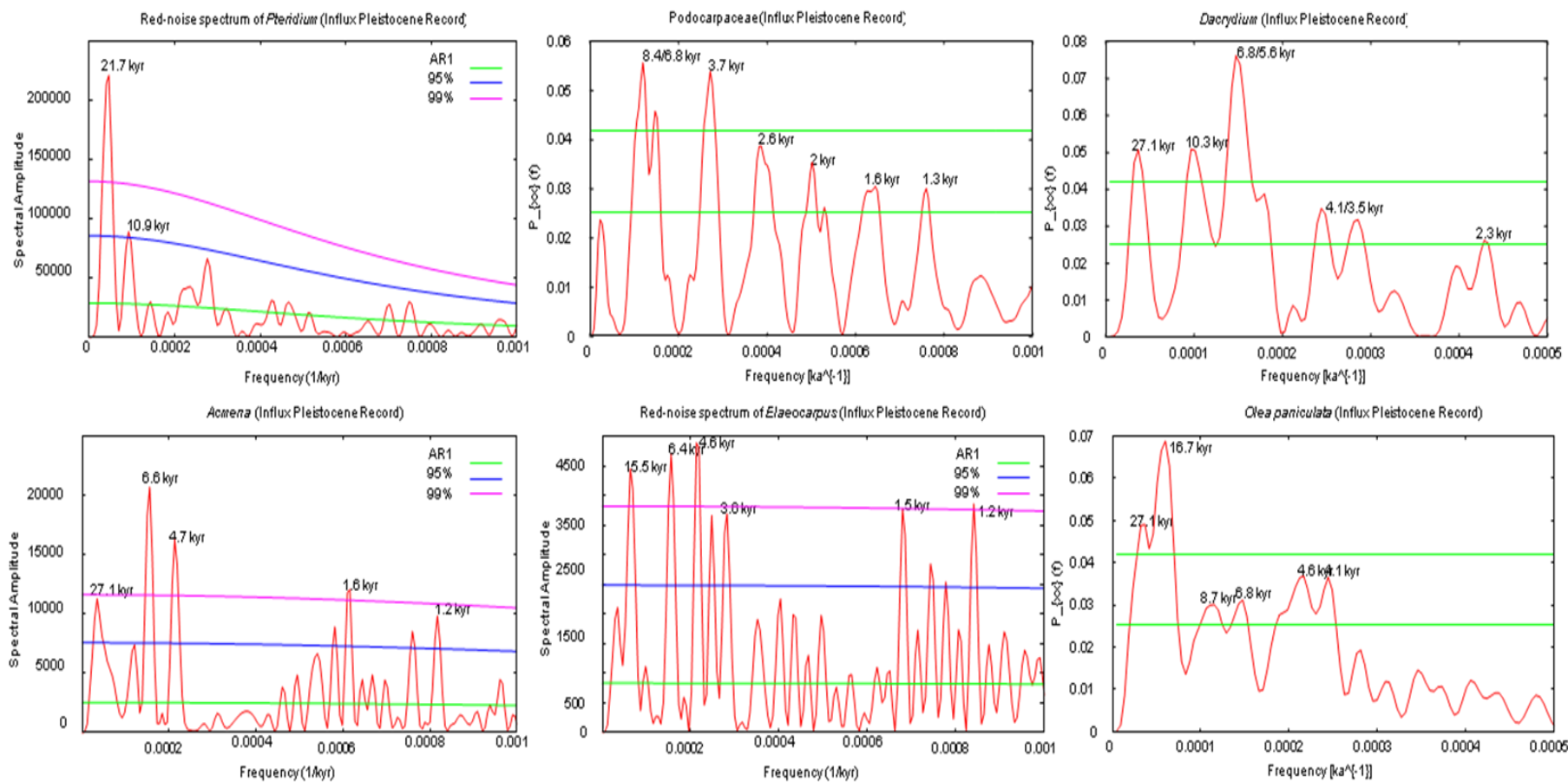


Plate 4.15. Taxon and frequencies noted on graph

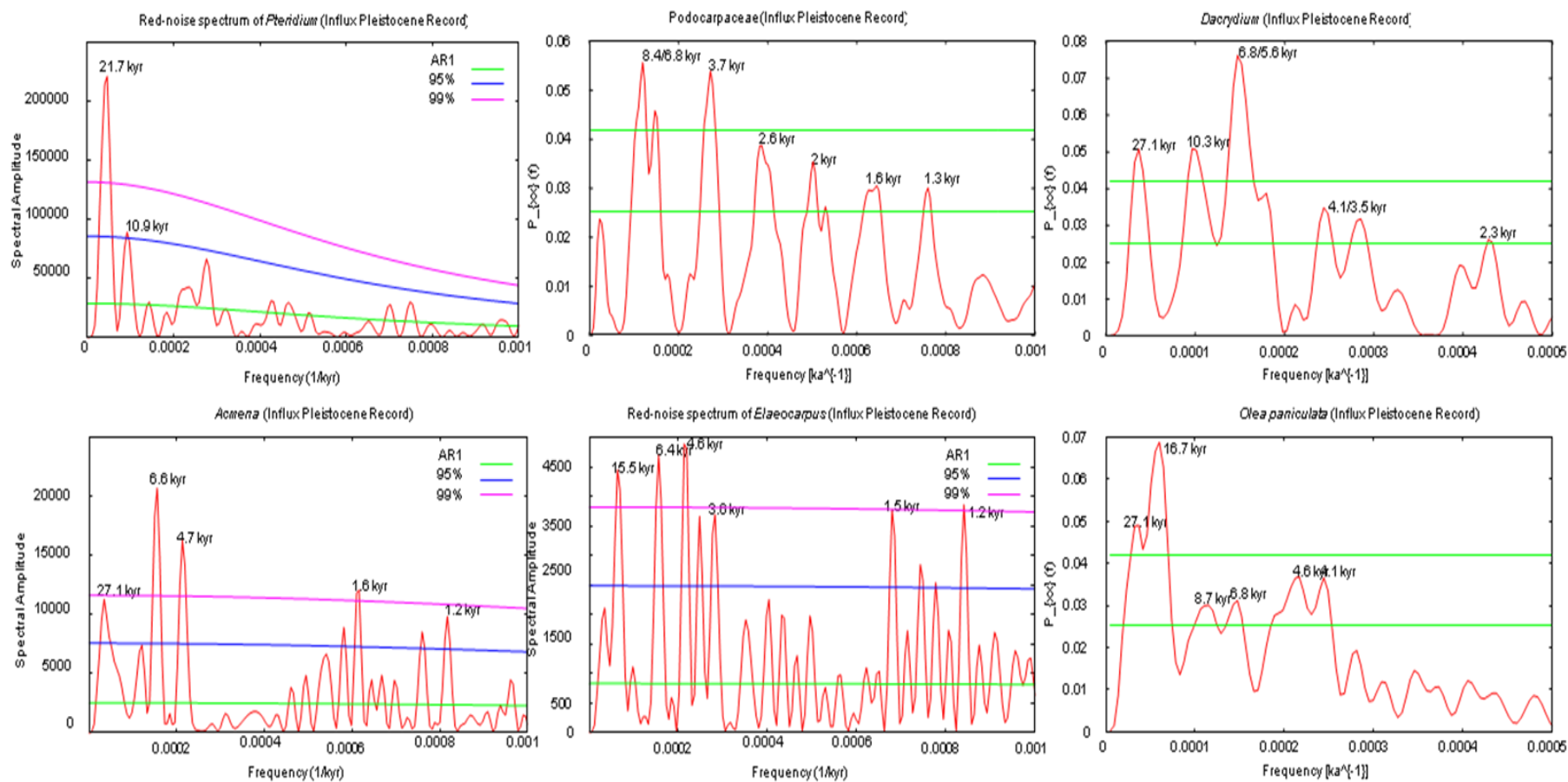


Plate 4.16. Taxon and frequencies noted on graph

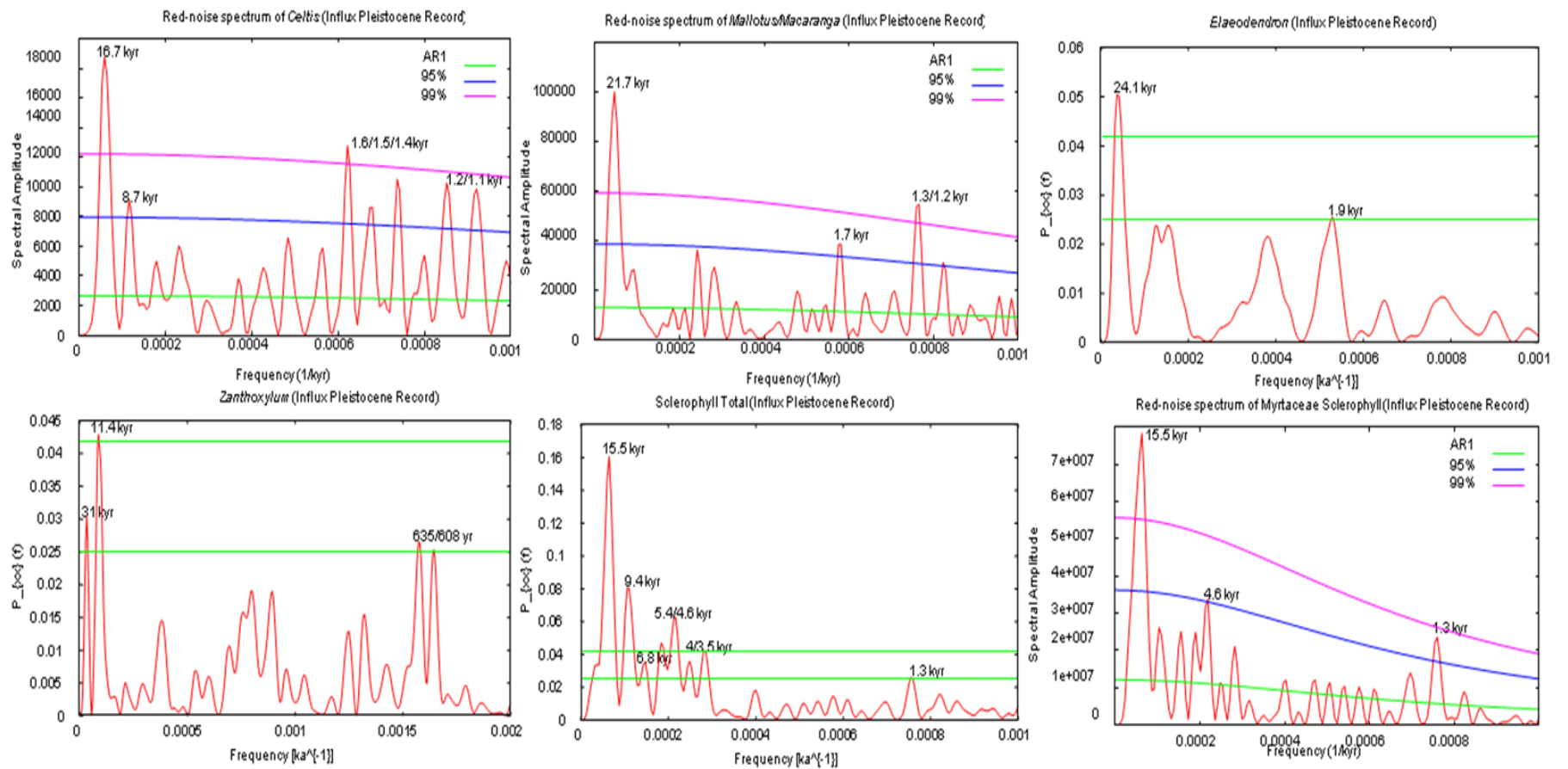


Plate 4.17. Taxon and frequencies noted on graph

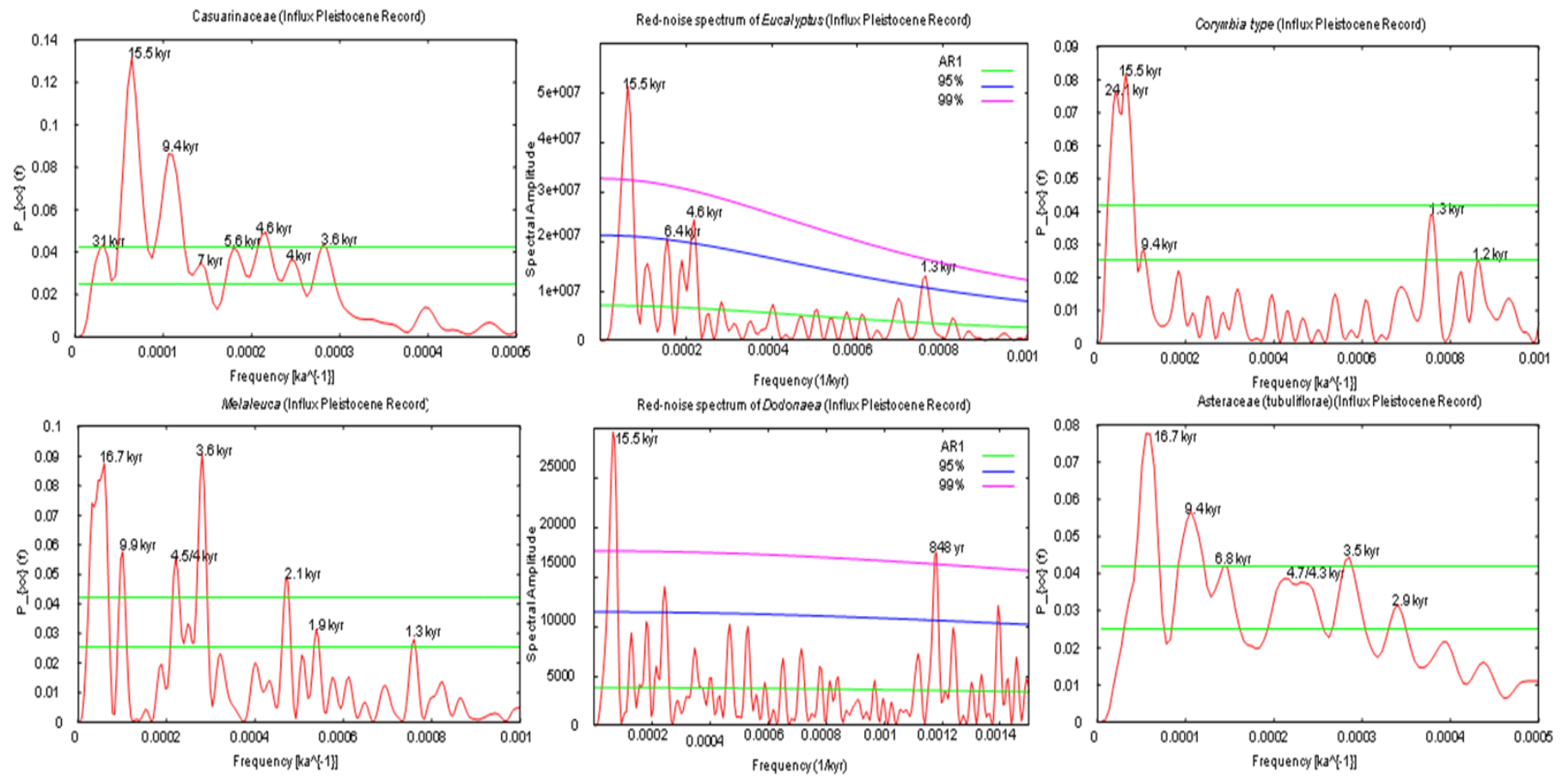


Plate 4.18. Taxon and frequencies noted on graph

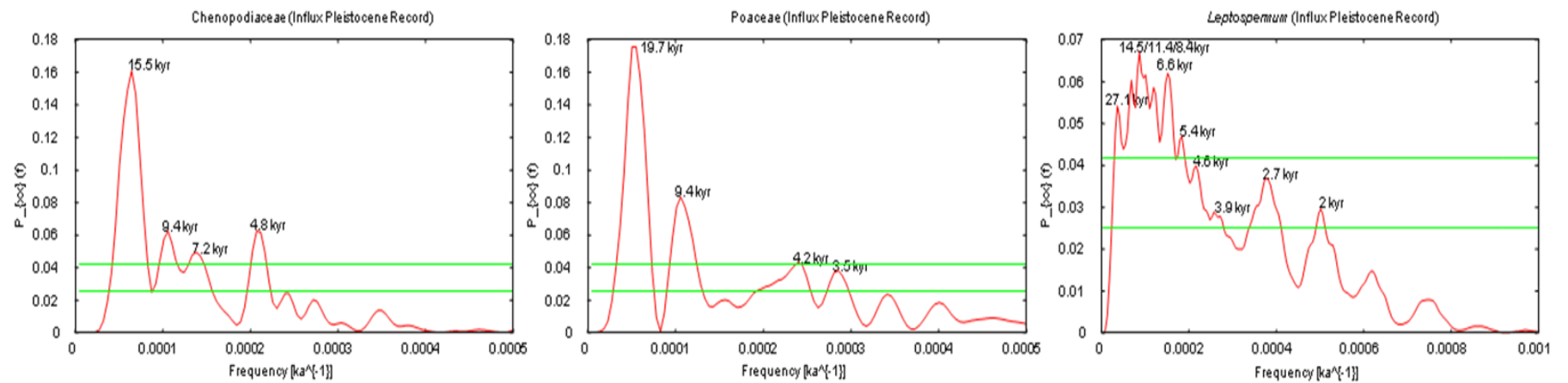


Plate 4.19. Taxon and frequencies noted on graph

Plates 4.20-4.22. Aquatic/swamp (inc, charcoal) percentage data Full sequence (3-54 ka)

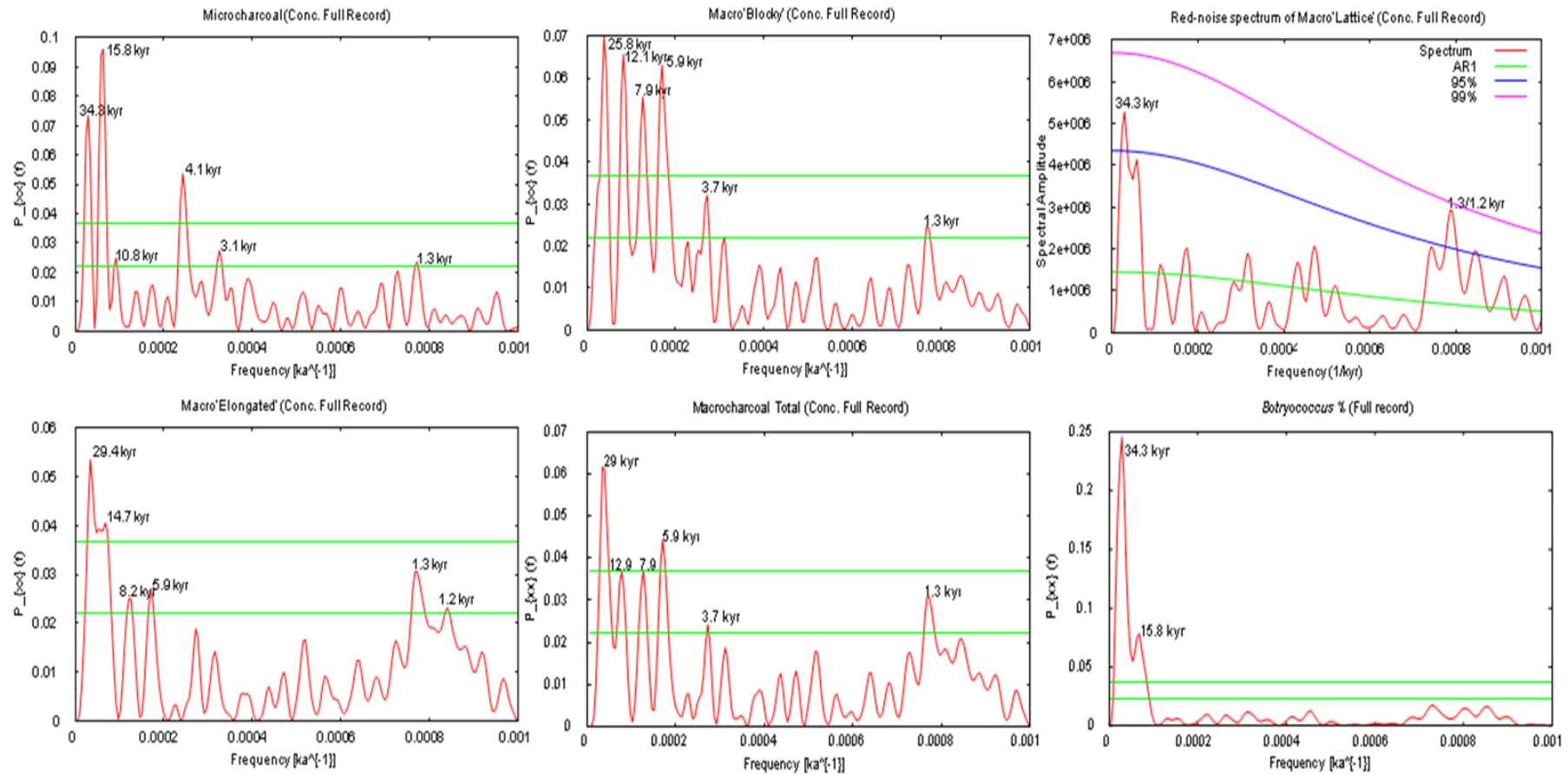


Plate 4.20. Taxon and frequencies noted on graph

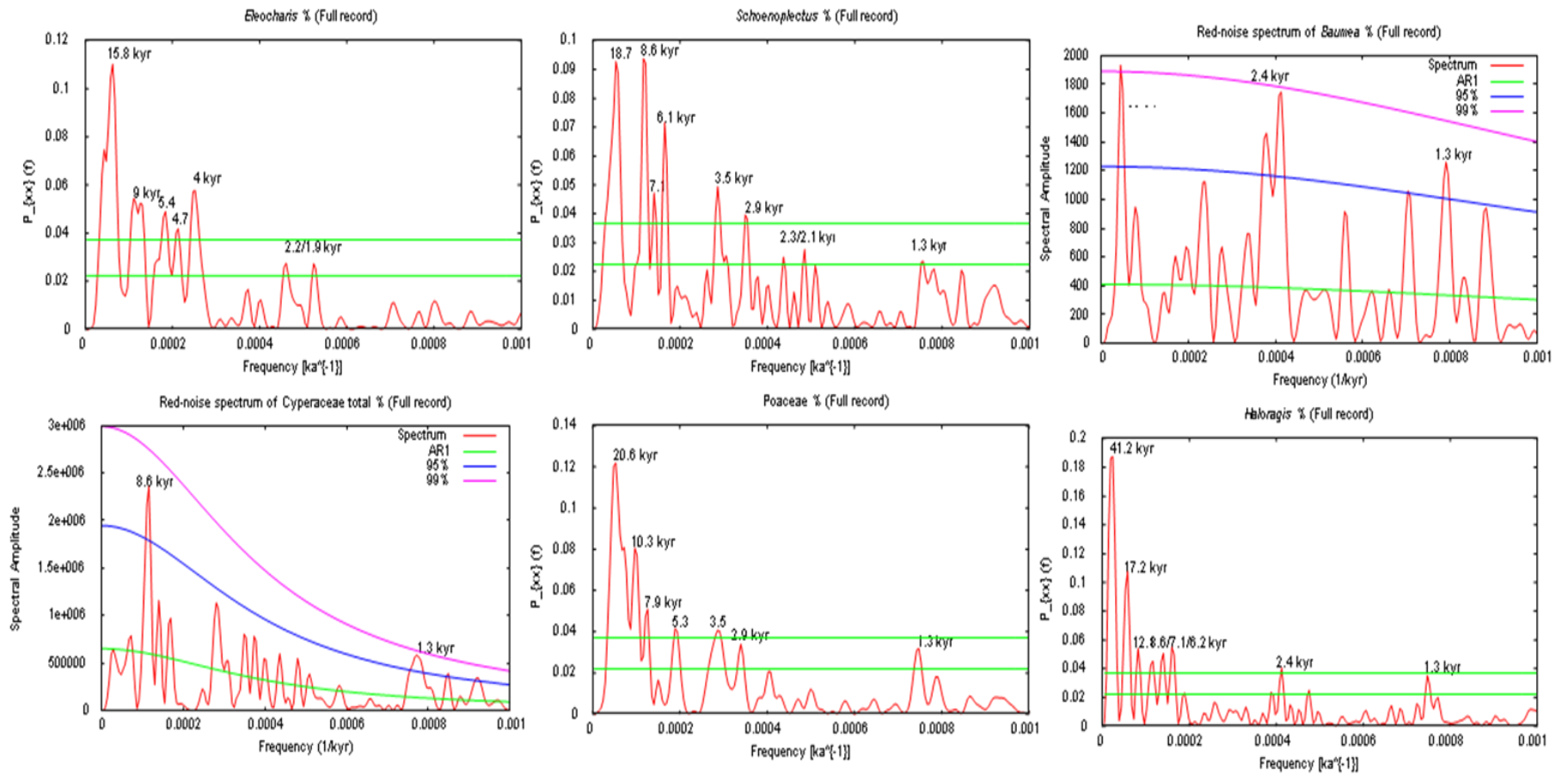


Plate 4.21. Taxon and frequencies noted on graph

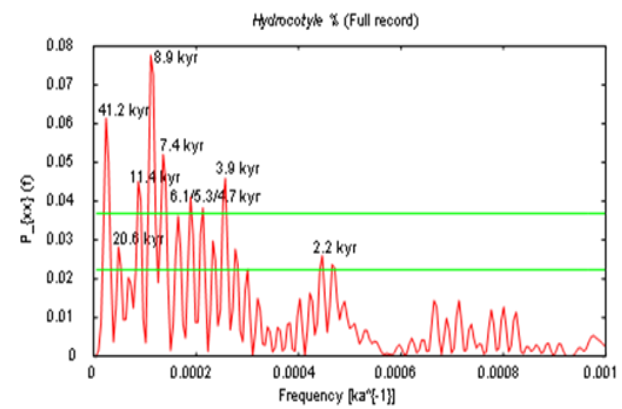


Plate 4.22. Taxon and Frequencies noted on graph

Plates 4.23-4.24. Aquatic/swamp (inc. charcoal) influx data Full sequence (3-54 ka)

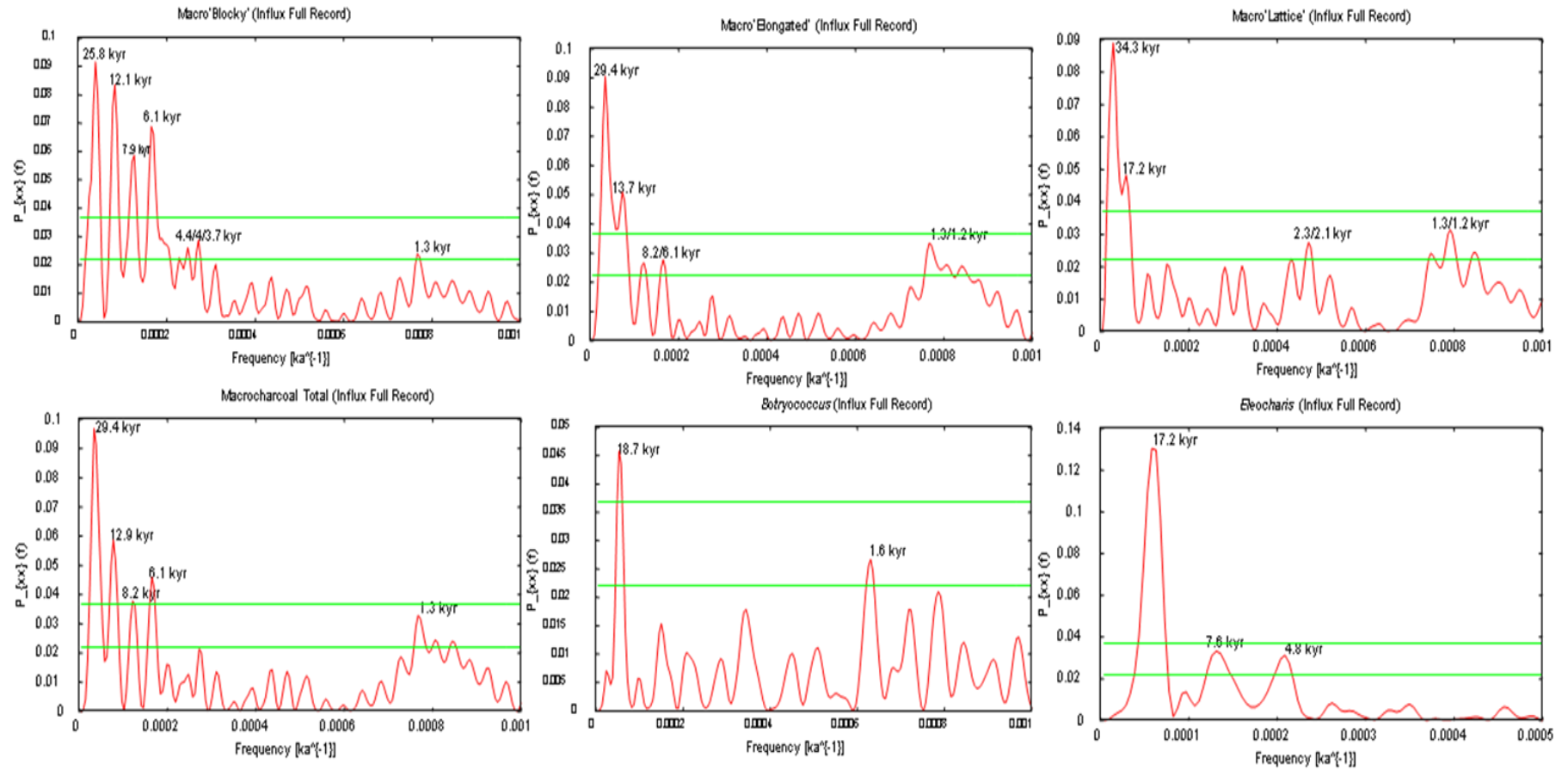


Plate 4.23. Taxon and frequencies noted on graph

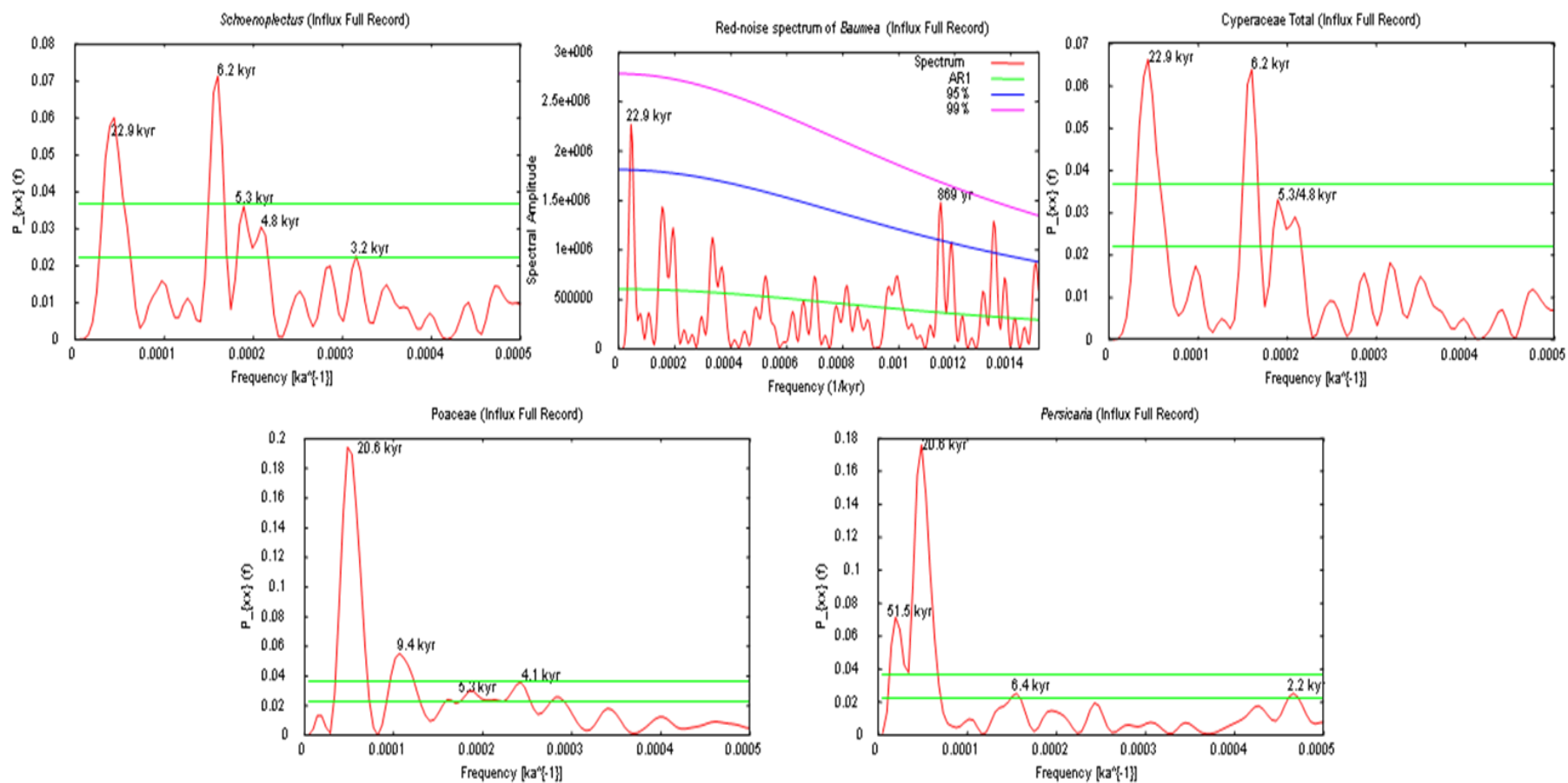


Plate 4.24. Taxon and frequencies noted on graph

Plates 4.25-4.27. Aquatic/swamp (inc. charcoal) percentage data Pleistocene sequence (11.8-54 ka)

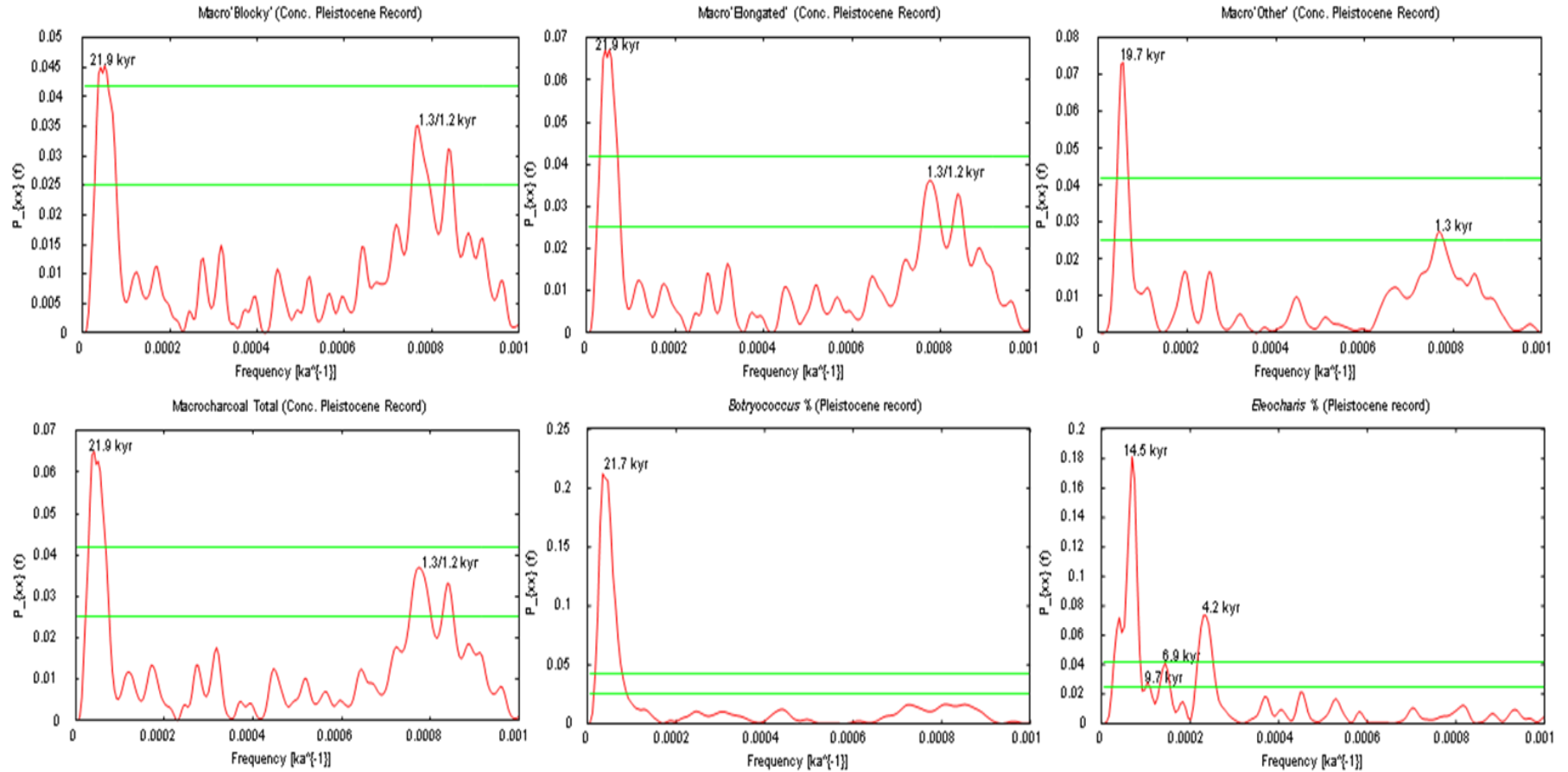


Plate 4.25. Taxon and frequencies noted on graph

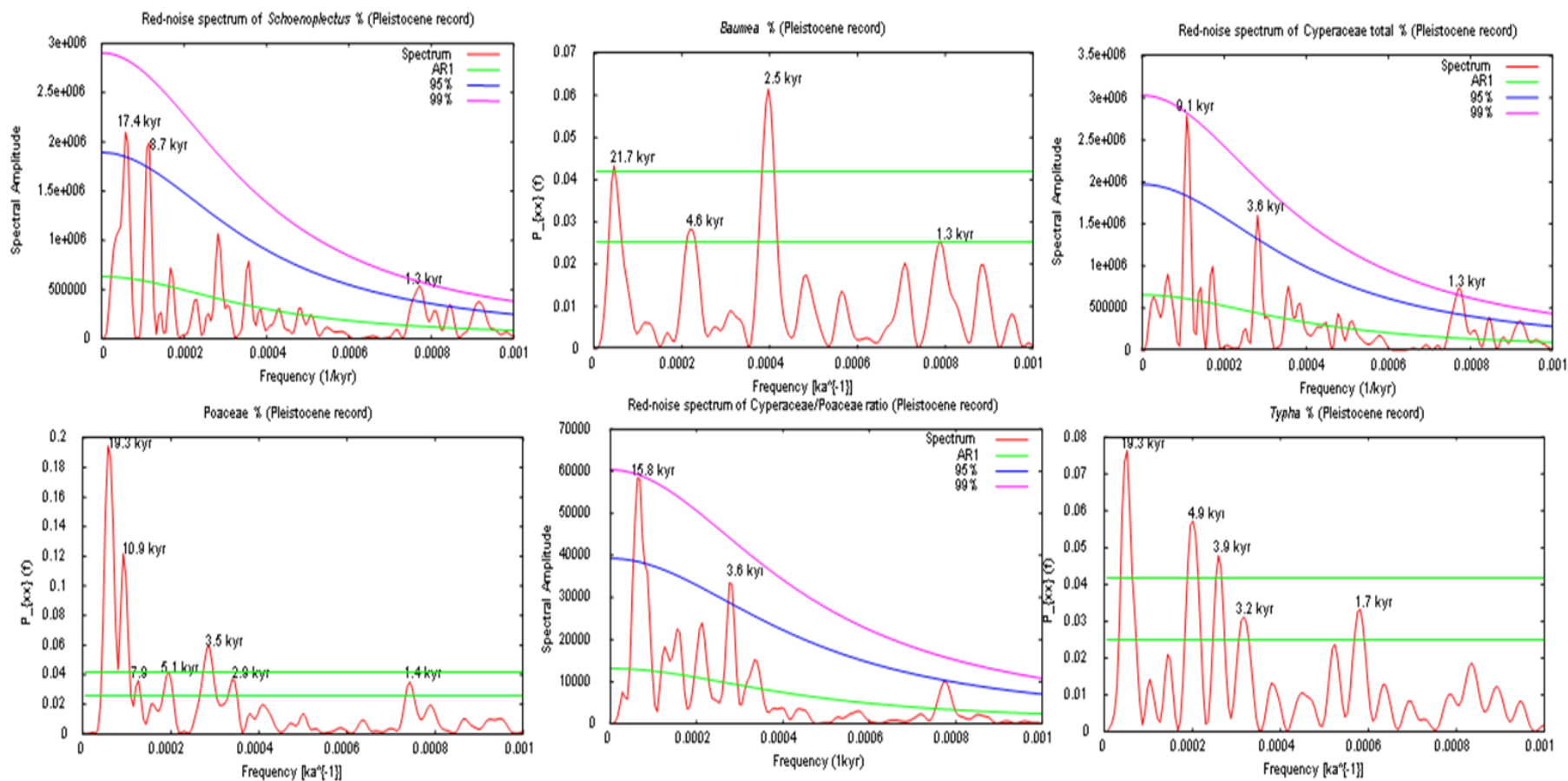


Plate 4.26. Taxon and frequencies noted on graph

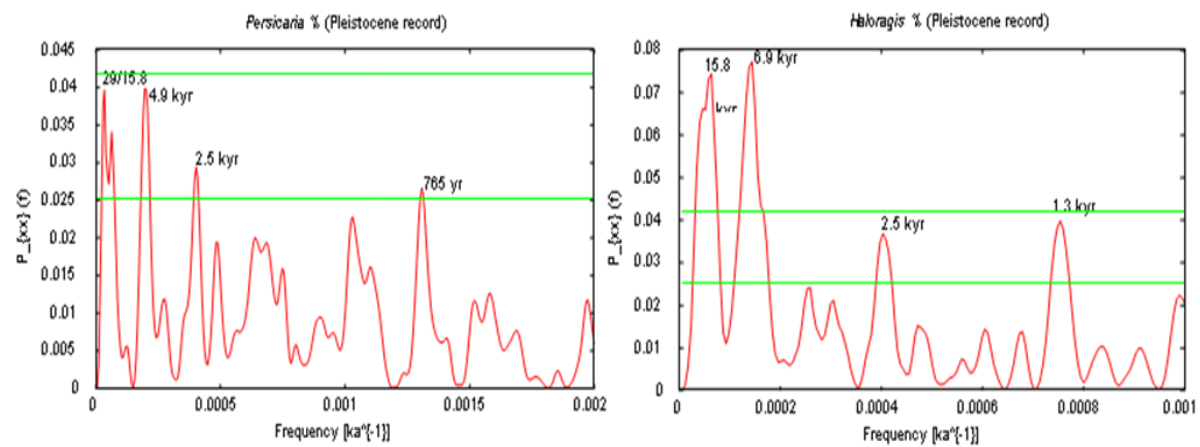


Plate 4.27. Taxon and frequencies noted on graph

Plates 4.28-4.30. Aquatic/swamp (inc. charcoal) influx data Pleistocene sequence (11.8-54 ka)

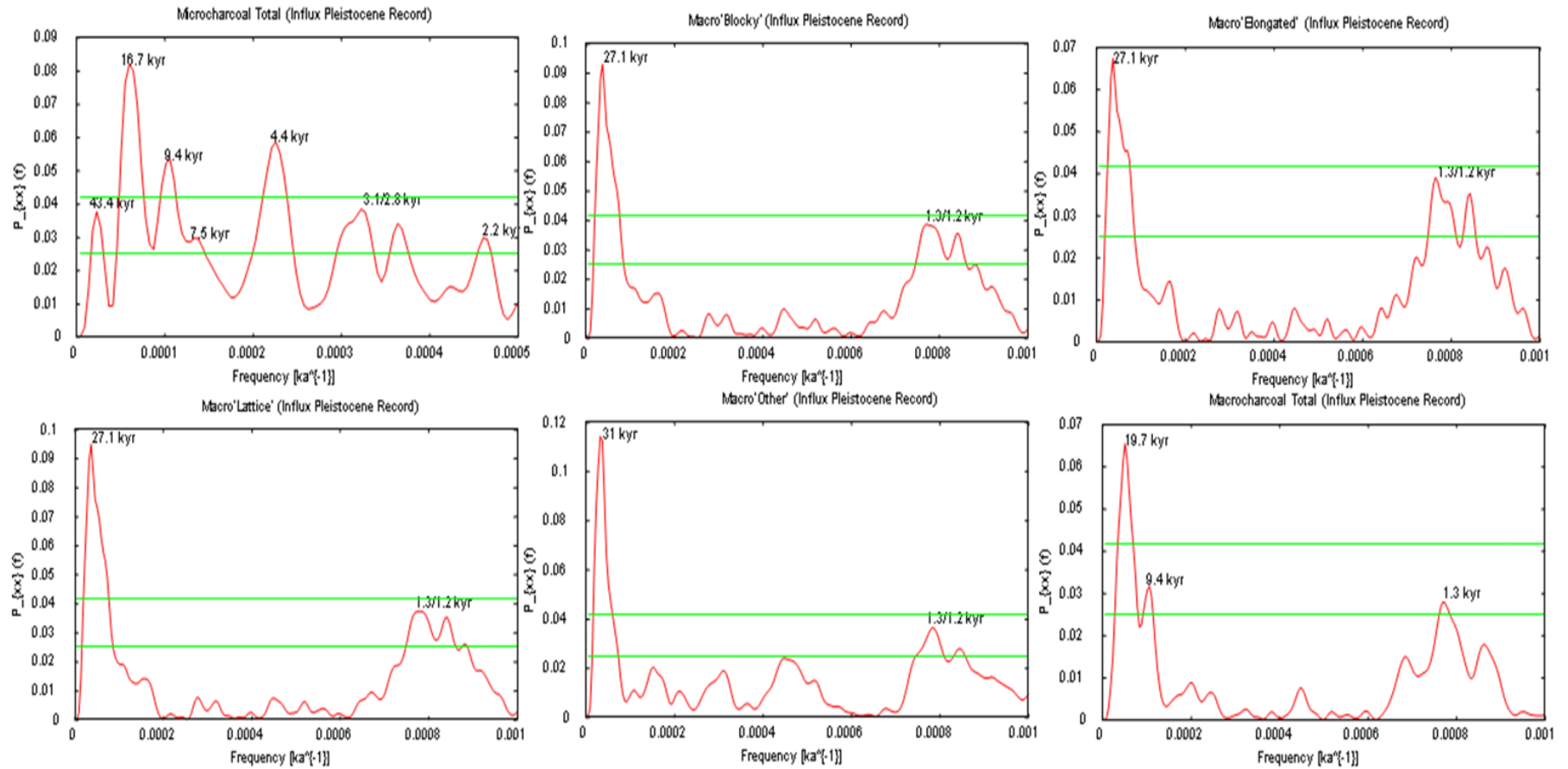


Plate 4.28. Taxon and frequencies noted on graph

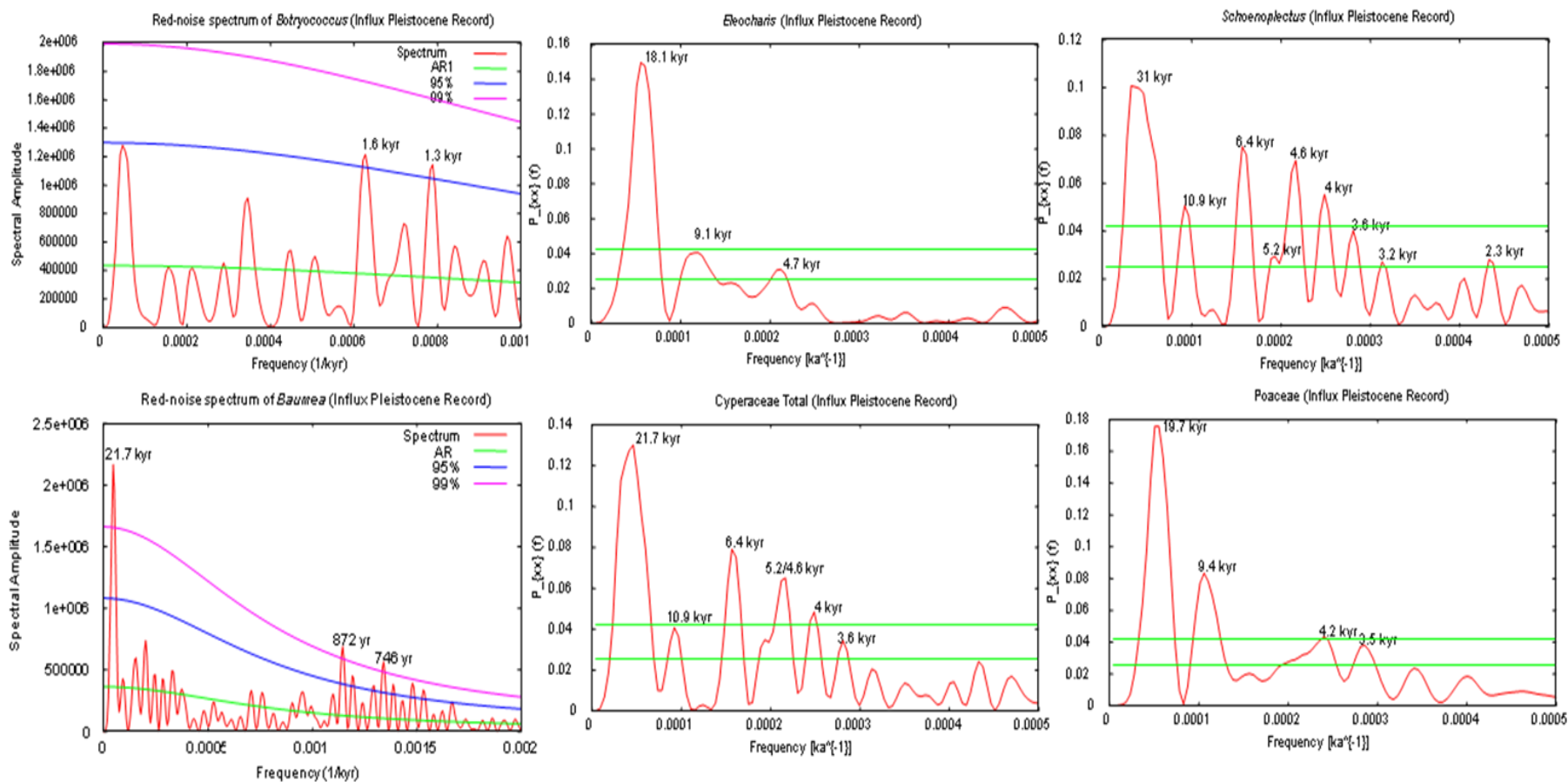


Plate 4.29. Taxon and frequencies noted on graph

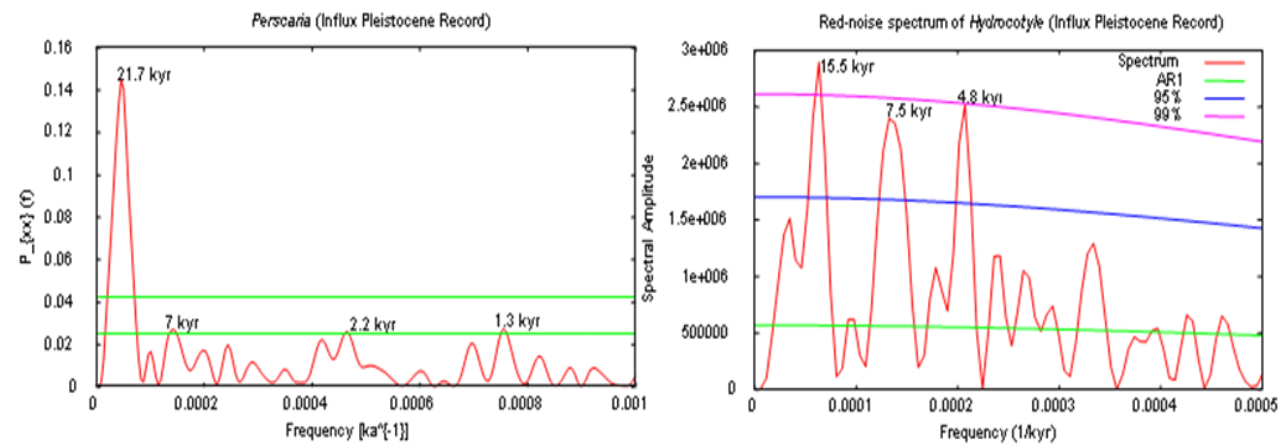


Plate 4.30. Taxon and frequencies noted on graph

Appendix C- Distribution map (*Nymphoides* and *Liparophyllum*) and calibration of ages (Kershaw 1976, 1983a)

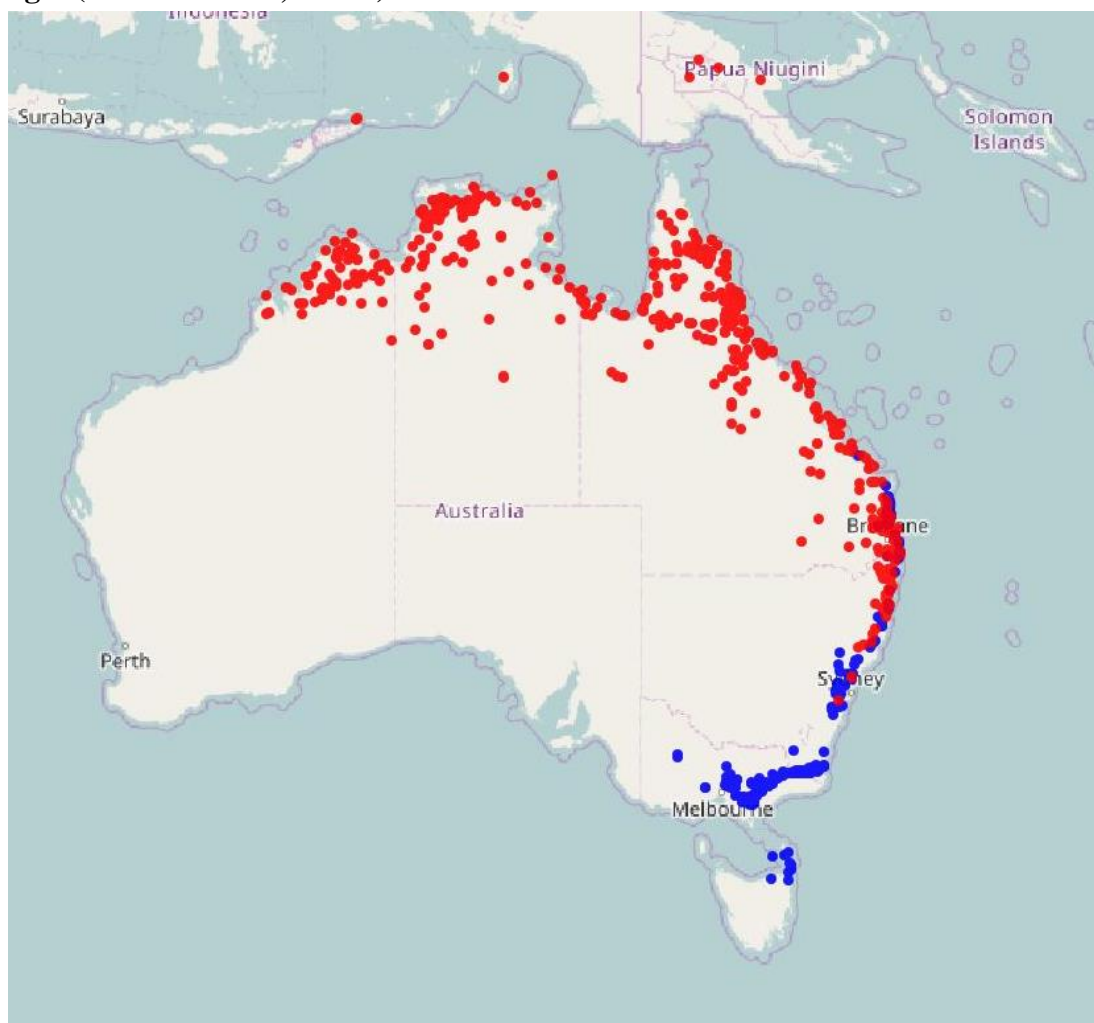


Figure 1. Distribution map of *Nymphoides indica* (red circle) and *Liparophyllum exaltata* (blue circle) in the present-day Australia and nearby (Australia's Virtual Herbarium (2015)).

Table 1. ^{14}C Age and calibrated age for Kershaw (1976, 1983a), '+' ^{14}C Age from core 1 (1976), '*' ^{14}C Age from core 2 (1983a).

Depth	^{14}C Lab code	^{14}C Age	Calibrated Age	1sd
65-80	ANU958+	6850 \pm 90	7649	46
80-100	ANU959+	7090 \pm 100	7867	100
140-160	ANU960+	10390 \pm 130	12159	238
200-220	ANU961+	15510 \pm 210	18732	234
40-45	WK265*	3200 \pm 60	3370	81
60-65	WK266*	4550 \pm 60	5152	109
90-95	WK267*	6410 \pm 70	7300	80
120-125	ANU1538A*	7160 \pm 150	7948	153
120-125	ANU1538B*	6050 \pm 120	6872	158
130-135	ANU1686*	4270 \pm 90	4751	136